

SSR Virtual Abstracts JULY 8–12, 2020



A Sustainable World Through the Science of Reproduction, Fertility, and Development

ABSTRACT INDEX

Categories

- - Contraception......9-14

- - - - - Gene Editing/CRISPR...... 92-39
 - Implantation.....94-105
 - Meiosis 106
 - Oogenesis and Oocyte Maturation...... 107-124
 - Ovarian Dysfunction......125-133
 - Ovary: Corpus Luteum...... 134-144
 - Ovary: Folliculogenesis145–176
 - Parturition/Myometrium 177
 - Placental Development & Function.......... 178-200
 - - Reproductive Aging...... 222-224

| Reproductive Tract: Female |
|--|
| Reproductive Tract: Male |
| Sex Determination and Differentiation |
| Spermatogenesis |
| Stem Cells and iPS Cells |
| Testis 273-278 |
| Trophoblast Differentiation and Function |
| Uterine Biology: Endometrium, Fibroids |

Award Abstracts

| Lalor Foundation Merit Awards |
|--|
| USDA-NIFA-AFRI Merit Awards |
| SSR Trainee Travel Awards |
| The Gates Foundation Poster Award for Research Relevant to Contraceptive Research and Development |
| Trainee Research Award Platform Competition – Pre-Doctoral 354-360 |
| Trainee Research Award Platform Competition – Post-Doctoral 361-369 |
| Trainee Research Award Poster Competition – Pre-Doctoral 370-376 |
| Trainee Research Award Poster Competition – Post-Doctoral 377-384 |
| Best International Awards |

3

2020 Virtual Posters

Comparative Biology/Evolution/Exotic Species

Abstract # 1850

Luteinizing Hormone Receptor Gene Expression in Canine Neoplastic Lymphoma Cells is Upregulated by Treatment with Human Chorionic Gonadotropin. Wanli Li, Michelle Anne Kutzler

Circulating luteinizing hormone (LH) concentrations in gonadectomized dogs can be increased by up to 20 times the concentration occurring in reproductively-intact dogs. Gonadectomized dogs also have a higher relative risk for developing lymphoma compared to intact dogs. Previous research in our laboratory has shown that luteinizing hormone receptors (LHR) are present in circulating canine lymphocytes and the number of T-lymphocytes expressing LHR increases in gonadectomized dogs. The purpose of this study was to determine the effect of an LH agonist on LHR gene expression in canine T-lymphoma cells. We hypothesized that increasing concentrations of human chorionic gonadotropin (hCG) would result in a dose-dependent increase in LHR expression in canine T-lymphoma cells. Immortalized cell lines from three dogs with multicentric T-lymphoma donated from Dr. Takuya Mizuno at Yamaguchi University, Japan were cultured under standard conditions in RPMI 1640 media containing 10% fetal bovine serum, 100 U/mL penicillin, and 100 µg/mL streptomycin. Increasing concentrations (0, 4, 100 and 400 U/mL) of hCG were added to 25 mm2 flasks in triplicate for each cell line (2.5 million cells/flask) and incubated for 72 hours at 37°C in 5% CO2. Following incubation, RNA was isolated from 2.5 million cells using a routine phenol-chloroform extraction and total RNA (1 µg) was reverse transcribed. Real-time PCR was performed in triplicate for each RNA sample to determine gene expression of LHR as well as for four housekeeping genes (GAPDH, 18S, β-actin, β2-microglobulin). The stability of the housekeeping genes was evaluated using BestKeeper software. The delta delta Ct method was used to calculate the relative LHR expression and a oneway ANOVA was used to compare LHR expression between hCG concentrations in each cell line. β2-microglobulin was the only housekeeping gene that was stable in canine T-lymphoma cells at increasing concentrations of hCG. The average coefficient of correlation for β 2-microglobulin with all three cell lines was 0.934 (p<0.01). Additionally, hCG increased LHR gene expression in one of the three canine Tlymphoma cell lines (p<0.005) and there was a trend for an increase in LHR gene expression in the other two cell lines (p=0.06 and p=0.08, respectively). These results may explain the increase in LHR expression in circulating T-lymphocytes from gonadectomized dogs as well as why gonadectomized dogs are at a higher risk for developing lymphoma. Clinical studies are needed to determine if down-regulation of LH secretion in gonadectomized dogs with lymphoma will extend remission times. This

project was supported by the American Kennel Club Canine Health Foundation (grant #02751-A) and International Youth Exchange Foundation of Henan Academy of Agricultural Sciences Fund.

Abstract # 1990

Laparoscopic Collection And In Vitro Maturation Of Oocytes From Common Marmosets. Werner G. Glanzner, Hernan Baldassarre, Karina Gutierrez, Jim Gourdon, Mariana Priotto de Macedo, Naomi Dicks, Luke G. Currin, Abigail Shea, Mitra Cowan, Sonia Do Carmo, Keith K. Murai, Vilceu Bordignon

Suitable animal models are critical for advancing fundamental and translational research in biomedical sciences. Non-human primates are considered an optimal animal model because of several similarities with humans that include their physiology, metabolism, development, reproduction and neuroanatomy, as well as for social and cognitive aspects. In vitro embryo technologies are crucial for developing new animal models of pathophysiology conditions that may not be naturally available. In this study, laparoscopic ovum pick-up (LOPU) was used to collect cumulus-oocyte complexes (COCs) from 10 Common Marmoset (Callithrix jacchus) females with average age of 18 months (range 15-23 months). A total of 18 LOPU procedures were performed under general anesthesia maintained with isoflurane. Prior to LOPU, females were hormonally stimulated with FSH for 4 days. For the LOPUs, two 2.5 mm endoscopy ports were inserted into the abdominal cavity. One port was used for the laparoscope to visualize the ovaries, and the other port was used for the grasping forceps to manipulate the ovaries. All visible follicles were aspirated using a 25G x 1 $\frac{1}{2}$ hypodermic needle, connected to a collection tube and a vacuum pump with the pressure set at 50 mmHg. In total, 726 structures were collected, averaging 40.3 structures per animal/LOPU. After selection to remove those having poor morphology, small size and degenerated, 522 COCs were placed on in vitro maturation (IVM), which represents an average of 29 COCs/animal/LOPU. The COCs were matured in TCM199-based media supplemented with 10 % fetal bovine serum, 0.5 μ g/mL FSH, 0.5 μ g/mL LH, growth factors (10 ng/mL EGF, 20 ng/mL IGF1, 40 ng/mL FGF and 20 ng/mL LIF), 3.05mM Glucose, 1 µg/mL estradiol, 100 µg/mL cysteine, 0.91 mM sodium pyruvate and 20 µg/mL gentamicin. In vitro maturation was performed at 37.5 °C in humidified atmosphere with 5% CO 2 in air. Cumulus cells were removed at 24 h of IVM to evaluated oocyte maturation (presence of the first polar body). Immature oocytes were returned to IVM and re-evaluated for the presence of the first polar body at 40 h. The total number of oocytes with the first polar body at the end of IVM was 284 (54.4%), among which 133 (25.5 %) matured during the first 24 h and 151 (28.9 %) matured between 24 h and 40 h of IVM. These maturation rates are consistent with previous publications where occytes were recovered by using more invasive (laparotomybased) techniques. Our study shows that each LOPU followed by IVM produces in average 15.8 (284/18) meiotically competent oocytes in Common Marmosets, which

highlights the potential of this technology for the creation of animal models for research in this species.

Abstract # 2158

Verification Of Telomere And 18S Primers In A Monochrome Multiplex Qpcr Assay To Determine Relative Telomere Length In Multiple Species Of Birds. Tania Tejakusuma, Patricia Byrne, Thomas Jensen

Being able to estimate the life expectancy of birds is a valuable tool to conservation and breeding programs, not only to know how long a particular bird might live, but also as a measure of overall health. Previous research has shown that in some bird species, life expectancy, age, and stress can be correlated with the relative telomere length (RTL). Developing a standardized assay to measure the RTL across multiple species as a proxy for stress and life expectancy could greatly benefit captive breeding programs. In this study we test a monochrome multiplex qPCR (MMqPCR) SYBR Green assay, which allows for simultaneous amplification of both the telomere and reference primers. In our assay, the reference primers (18S-GC F/R) include long GC-clamps at the 5' ends, resulting in an elevated amplicon T m. This allows for the acquisition of data from both primer sets in the same reaction. It is crucial that the DNA concentration of the two amplification targets are significantly different to assure accurate data acquisition. As the concentrations of telomere and 18S are very similar in our cells, we used low amounts of gDNA (0.25ng/reaction), and a telomere primer only preamplification 95,15m(94,15s;49,15s)2(94,15s;62,10s;74,15s)6 to obtain Cq values of 8-12 for telomere amplicons, and 23-26 for the 18S amplicons in the MMqPCR 95,15m(94,15s;49,15s)2(94,15s;62,10s;74,15s;84,10s;88,15s)40. Although a different reference gene with a higher Cq value would be desirable, the only universal reference we successfully verified across a broad taxonomic range of species is 18S, hence the preamplification PCR. In order to demonstrate the versatility of this tool across a broad taxonomic range, we tested gDNA from packed RBC samples of ten species representing ten orders (Accipitriformes, Anseriformes, Apterygiformes, Columbiformes, Coraciformes, Galliformes, Gruiformes, Passeriformes, Phoenicopteriformes, and Psittaciforkmes). The telomere (telC and telG) and reference primers were tested in triplicate to assess intra-assay variation. We repeated the preamplification and MMqPCR on four plates to asses inter-assay variation and preamplification consistency and reliability. The CV% for the intra-assay technical triplicate Cq values for all the species ranged from 0.16%-3.27% (telC/telG) and 0.06%-1.21% (18S-GC F/R). The CV% for Cq values across the four replicate plates for telC/G ranged from 0.76% to 14.71% and for 18S-GC F/R 0.7% to 3.14%. The four-plate replicate CV% for the calculated DCq across all species ranged from 1.48% to 16.59%. Cq values from three species and one DCq value from one plate replicate was determined to be outliers (whisker-boxplot analysis) and were removed. In this study we demonstrated the use of a MMqPCR assay to measure relative telomere length across a broad taxonomic range. The low interand intra-plate variation in Cq and Δ Cq confirmed that the pre-amplification method is

consistent and repeatable regardless of bird species. The preamplification PCRs are consistent across plates/repeats, however, we did detect outliers, which were all from the same plate. Due to these outliers we recommend repeating preamplification and MMqPCRs on a minimum of three plates. This method will be used to investigate correlations of RTL with age, stress, or overall health.

Abstract # 2161

Maintaining Spermatogonial Stem Cells in Testes Cultured in Vitro Supplemented with Steroids and Gonadotropins. Kelley Kramer, Patricia Byrne, Thomas Jensen

Genetically valuable individuals contribute to population diversity only when they are producing offspring. Sperm and eggs collected during an animal's life can be used in future reproduction; however, techniques for post-mortem recovery of germplasm are not well developed. The restoration of spermatogenesis from testicular tissue collected post-mortem would allow for genetically valuable individuals to contribute to the gene pool after death. We hypothesize that in vitro cultures supplemented with steroids and gonadotropins will support testes tissue survival and spermatogenesis. In this study, adult mice testes were collected post-mortem and cryopreserved for at least 2 months. Mice testes were separated into 2-3mm3 pieces and placed in 22mm wells with 1mL culture media (M199, 10% FBS, 1% Penicillin-Streptomycin). In preliminary trials, testicular tissues were assigned to one of the following treatments: no treatment, 0.5mg testosterone (T), 1mg T, 2mg T, 1ng follicle stimulating hormone/luteinizing hormone (FSH/LH), 3.5ng FSH/LH, 7ng FSH, 0.5mg T and 1ng FSH/LH, 1mg T and 1ng FSH/LH, 2mg T and 1ng FSH/LH, 0.5mg T and 3.5ng FSH/LH, 1mg T and 3.5ng FSH/LH, 2mg T and 3.5ng FSH/LH, 0.5mg T and 7ng FSH/LH, 1mg T and 7ng FSH/LH, 2mg T and 7ng FSH/LH. After 7 days, tissues were dissociated and stained with FITC-conjugated stage specific embryonic antigen (SSEA) antibodies SSEA-1, SSEA-3, and SSEA-4. Propidium iodide was added to determine the percent live cells. Treatment groups containing both T and FSH/LH in high concentrations showed the greatest amount of presumptive germline stem cells. Based on preliminary data, we repeated the study with treatment groups: A: No Treatment (n=2), B: 1mg T and 3.5ng FSH/LH (n=3), C: 2mg T and 3.5ng FSH/LH (n=3), D: 1mg T and 7ng FSH/LH (n=3), and E: 2mg T and 7ng FSH/LH (n=3). Live dead A-E; 12.14%±9.26% (mean±SEM), 2.19%±0.078%, 0.71%±0.056%, 2.33%±47%, 2.30%±0.50%, respectively.SSEA-1 A-E; 0.03%±0, 0.03%±0.0067%, 0.02%±0.0067%, 0.01%±0.0033%, 0.01%±0.0033%, respectively. SSEA-3 A-E; 0.25%±0.04%, 0.35%±0.15%, 0.19%±0.058%, 0.15%±0.013%, 0.11%±0.04%, respectively. SSEA-4 A-E; 0.07%±0.045%, 0.15%±0.048%, 0.09%±0.027%, 0.19%±0.026%, 0.14%±0.06%, respectively. Group C had more SSEA-4 positive cells than group A (p<0.05). Treatments were compared to fresh testicular tissue (n=5); live dead, SSEA 1, SSEA 3, and SSEA 4: 19%±1.07%, 0.03%±0.0024%, 0.09%±0.019%, 0.03%±0.01%, respectively. Fresh tissue had more cell death compared to groups B, C, D, E (p<0.005). Fresh tissues had more SSEA-1 positive cells compared to groups D (p<0.05) and E (p<0.05). Fresh tissues had less SSEA-3 positive cells than groups A (p<0.005), B (p<0.05), C (p<0.05), D (p<0.05). Fresh tissues had less SSEA-4 positive cells than groups B (p<0.05),

C (p<0.05), D (p<0.001), E (p<0.05). Increased number of SSEA positive cells indicate a higher percentage of presumptive germline cells. Ongoing studies are focusing on further refining the culture system to increase the percentage of germline cells and maintaining seminiferous tubule structure and function. The results of this research will lead to in vitro production of sperm from cryopreserved testicular tissue, which could be used in ART. If successful, this project will have a significant impact on captive breeding efforts, especially those aimed at endangered species.

Contraception

Abstract # 1815

Multiple Delivery Of Spermicide/Microbicide LL-37 Peptide, Into The Uterus Or Vagina Does Not Induce Tissue Injury Or Inflammatory Cytokine Production. Seung Gee Lee, Wongsakorn Kiattiburut, Stephanie Burke Schinkel, Ana Vera-Cruz, Guangshun Wang, Jonathan B. Angel, Nongnuj Tanphaichitr

LL-37 is a cathelicidin antimicrobial peptide with known microbicidal action on >40 bacteria and 10 viruses, including those that are involved in sexually transmitted infection (STI) (Tanphaichitr et al., Pharmaceuticals 2016). Recently, we have shown that LL-37 can act as a spermicide to both human and mouse sperm at 10.8 and 3.6 mM, respectively. Transcervical injection of sperm plus 3.6 mM LL-37 into female mice cycling in the estrous phase resulted in no pregnancy (n = 26), whereas 92% of control females (n =26) transcervically injected with sperm alone became pregnant (Srakaew et al., Human Reprod 2014). Before advocating LL-37 as a vaginal multipurpose protection technology (MPT) agent having both contraceptive and microbicidal activity, it is important to demonstrate that multi-administration of LL-37, either transcervical or intravaginal, does not cause adverse effects to the female reproductive tract (FRT) as shown by a lack of both tissue injury and production of inflammatory cytokines/chemokines. LL-37 (36 mM) was transcervically injected into female mice (6-8-week-old) one hour before the expected ovulation time. Vaginal lavages were collected 15 h after LL-37 injection for cytokine/chemokine analysis. The peptide injection and vaginal lavage collection were repeated twice in the next two estrous cycles. Negative controls were females that were injected in parallel with PBS, whereas positive controls were animals injected with VCF (vaginal contraceptive foam, containing 12.5% N-9, available from the counter), which is known to disrupt the integrity of the human vaginal epithelia (Tanphaichitr et al., ibid). Multiple (3X) injections of LL-37, VCF and PBS were also performed intravaginally to represent the potential peptide administration in humans. Before each intravaginal injection of LL-37, VCF or PBS, each female was subcutaneously injected with 2.5 mg depo-provera to thin the vaginal epithelium, so that the effects of LL-37/VCF to the vagina could be assessed under an insulted condition. In both types of injections, the FRT tissues were collected for histology assessment from the females, sacrificed 24 h after the last injection. Our results indicated that there was no obvious FRT tissue injury after multiple administration of LL-37 or VCF in both injection types. Among the cytokines/chemokines (IL-1a, IL-1b, IL-6, IL-10, TNFa, MIP-2, MCP-1) analyzed, there was no significant increase in their production in the females multiply administered with LL-37 (n = 7) over the PBS-injected females (n = 7). In contrast, the VCF-treated females (n = 7)7) showed elevated levels of MCP-1 in both injection types. As well, the reversibility of fecundity of LL-37-treated mice (n = 4) was assessed one week after the third transcervical administration of the peptide. All of these females, as well as PBS-injected females (n = 4), became pregnant upon transcervical injection of sperm from fertile males. In contrast, VCF-treated females (n = 4) showed no pregnancy following parallel

sperm injections. All of these results suggest that LL-37 is safe to be administered in the FRT and it is promising to be developed into an MPT agent. This technology will empower women to protect themselves against unwanted pregnancies and sexually transmitted infections.

Abstract # 1856

Anti-Catsper Monoclonal Antibodies Inhibit Mouse In Vitro Fertilization And Are Non-Hormonal Contraceptive Candidates. Dana Lord, Wiliam Bronkyk, Felipe Navarette, Melissa Paziuk, Isabelle Sansal, Doris Le, Matthew Maderia, Merlit Mathew, Madhavi Kohl, Catherine Venturini, Eric Furfine,

Rationale: There are a dearth of options for non-hormonal contraception for men or women. Men in particular have few contraception options altogether and while hormonal approaches have demonstrated efficacy in men, they are generally not welltolerated in clinical evaluations. Therefore, a non-hormonal approach is necessary for a male contraceptive and a desirable option for female contraception. CatSper is a Ca channel specific to sperm that is required for fertility. Thus, agents blocking CatSper can have contraceptive properties.

Results: Antibodies that bound to the extracellular domains of the four human and mouse CatSper subunits by ELISA were potential CatSper-inhibiting antibodies. Using surface plasmon resonance, separate monoclonal antibodies that specifically and tightly bind each of the four human CatSper subunits with Kd values as low as 20 fM were identified. Some of these antibodies cross-reacted with human, monkey, and mouse CatSper with similar affinity and blocked mouse oocyte fertilization with a IC90 value of approximately 0.5 nM in an IVF study of gametes from CD1 mice. Intraperitoneal administration of anti-CatSper antibodies bind epidydimal sperm in mice in vivo and are present in the reproductive tract at concentrations well above the inhibitory concentrations in the IVF studies.

Conclusions: Monoclonal antibodies that tightly bind human, monkey and mouse CatSper, inhibit mouse IVF, and reach the male reproductive tract after systemic administration are candidates for the development of a non-hormonal contraceptive.

Abstract # 1907

Identification And Prioritization Of Targets And Compounds For Non-Hormonal Contraceptive Development: A Systematic Literature Review. Amelia C. L. Mackenzie, Ashini Fernando, Christopher L. Harmon, Randy M. Stalter, Gregory S. Kopf

Side effects and health risks remain persistent impediments to contraceptive use and continuation, and high rates of unintended pregnancy are a stark reminder of the unmet need for highly-effective contraceptive methods. Although refinements in the last few decades have improved the safety and side effect profile of many methods for women, most still employ biological mechanisms discovered in the 1960s using delivery

systems developed in the 1970s. Men have even fewer options for contraception, and progress towards identifying and developing new male methods has been slow. Because hormonal methods that interfere with the hypothalamic-pituitary-gonadal axis can lead to side effects of concern to many users, there is a need for new nonhormonal contraceptive methods for women and men. We conducted an extensive literature review to identify non-hormonal contraceptive strategies and then evaluated them for potential pharmaceutical research and development (R&D). Our search included a review of English-language, peer-reviewed journal articles encompassing all biomedical disciplines (i.e., via PubMed, Embase, BIOSIS, LILACS, and Web of Science), conference abstracts (e.g., from SSR, ASA, ESHRE, etc.), and patent filings (i.e., via PatSnap and Patent Lens) since 2010. We reviewed over 64,000 titles and over 700 putative targets and compounds. After full text screening, we identified over 100 potential non-hormonal targets and compounds appropriate for inclusion in a more detailed review. The majority of our findings were targets, and about one-fifth were compounds. About 40% could be developed for use by women, 20% for use by men, and 40% for use by either or both. Although about half of targets were involved in more than one reproductive process, the most common was sperm function in the female reproductive tract, followed by sperm maturation; spermatogenesis & spermiogenesis; sperm-egg interaction; oogenesis, folliculogenesis, & oocyte/egg maturation; ovulation; and implantation. We found a similar trend in common reproductive processes among compounds. Targets were from a variety of classes; enzymes, GPCRs, ion channels, and kinases were the most common. Just over half of compounds were small molecules. To evaluate viability of targets and compounds for contraceptive R&D, we developed a risk-based numerical ranking system based on their role in/effect on reproduction; specificity; biomarker availability; social issues associated with modulation; target class and drug-ability (targets only); reference compound availability (targets only); and development stage (compounds only). Approximately 60% of targets and compounds were evaluated as medium-risk, few as low-risk, and about a third as high-risk, and we have identified de-risking measures for each target and compound. Overall, our review and risk evaluation showcase opportunities and challenges associated with the development of non-hormonal methods relevant to reproductive biology research. This work was supported by the Bill & Melinda Gates Foundation (OPP1055878) and the Male Contraceptive Initiative.

Abstract # 2004

Contraceptive Use And Preference Of HIV Infected Pregnant Women Living With HIV Negative Partners In The Central Region Of Cameroon: A Cross Sectional Survey. Martin Kuete, Hilary Christiane Ngueye Sipeuwou, Sean Wang Zhe, Yannick Zomnyate Nyangono, Carrel Raspail Zangue Founou

Evidences in sub-Saharan Africa including Cameroon indicate that most of HIV discordant couples want more children despite their HIV status. Investigating and establishing contraception preferences among HIV infected individuals are

fundamental and crucial to provide effective reproductive healthcare. We performed a cross-sectional study using structural based questionnaire to explore HIV positive pregnant women patterns including their family planning services, their preferences and its use, and their knowledge related to HIV/AIDS. Bivariate and multivariate analyses were conducted to explore associations and predictors of contraception preference and use; all tests were two sided significant at P < 0.05. Overall, 94 HIVpositive pregnant women aged 30.70±5.50 years living with HIV negative partners were from the different areas of the central region of Cameroon. Three-fourths were aware of the effectiveness of modern contraceptives and condoms, and only 28% had experienced modern contraception. 98% preferred to use traditional methods associated with infrequent condoms use. Multiple sociodemographic factors (marital status, group age, educational level, religion, occupation) affected contraceptive method preferences and its use (P < 0.05). These factors are the landmarks to predict discordant couples' behavior in HIV disclosure, discussion and decision making for contraception, preventing mother to-child transmission and HIV negative partner infection (P<0.05). Despite the awareness of participants related both on contraception methods and HIV/AIDS matters, participants faced societal, cultural and demographic barriers to make own decision for contraception use. Promoting effective family planning services and giving the entire range of contraception options may help women living with HIV to choose for effective ones and consequently reduce new cases of HIV infection.

Abstract # 2030

Reproductive Health And Family Planning Services Use Among Married Women In Central China: Does "One Child To Two Child Policy" Relaxation Affect The Population Behavior? Martin Kuete, Fan Yang, Cui Ling Li, Huang Qiao, Hilary Christiane Ngueye Sipeuwou, Xiu Lan Ma, Carrel Raspail Founou Zangue, Hui Ping Zhang

Family planning services use dramatically lowers maternal mortality and disabilities, infant mortality risk, unwanted pregnancies, birth defects, both illegal and unsafe abortions, mother-to-child transmission of human immunodeficiency virus and overall improve women and men sexual and reproductive health. Recently, the Chinese government has launched the two-child policy allowing families to have additional child. The aim of this study was to explore the population interest for family planning services, the unmet needs of reproductive health services and the populations' expectations towards male contraceptive methods. Cross-sectional study using stratified random sampling was conducted in 102 counties of Hubei province of China between august 2014 and July 2016. 17,555 randomized subjects interviewed from rural, transitional, and urban areas were included in the data analysis. Univariate and bivariate statistical analyses were applied to fit the associations between a set of sociodemographic patterns, family planning related factors and contraceptives use. In all tests, a P-value below 0.05 was considered significant. The studied population was disproportionally dominated by Han ethnic individuals (96%). Although 54% resided in

rural area, 34% in urban area, and 12% in urban area; participants were enrolled in a range of prosperous activities found across the surveyed settings. The number of living children per family varied from 0-6 children. Although 81% of population recognized family planning as a shared responsibility, the contraceptive method rates excluding condom were intrauterine devices (IUDs) 76%, 16% tubal ligation, 8% vasectomy, pills 3%, vaginal ring 2%, withdrawal and female awareness based method 1%. 24% had a history of contraceptive failure and the rate of effective contraceptive used after prior failure remained lower 6% (tubal ligation and vasectomy) and 26% IUDs. Among 13% who had never practiced any form of contraceptive, 74% clearly rejected family planning services especially male contraception. Overall, age, gender, education, vulnerable living status, knowledge in family planing services, discussion and making decision with spouse, and gender discrepancies were strongly associated with family planning services use and reproductive health unmet needs (P < 0.001). The decline of contraceptive use roughly varied with sociodemographic and reproductive health features. While the family size is increasing among China's population, family planning services especially vasectomy practice rate is decreasing. More investments taking in account population's expectations are needed to support exiting strategies for the new family planning policy and reproductive health matters in China.

Abstract # 2042

Development of Anti-Follicle Stimulating Hormone Receptor Nanobody as a Contraceptive Prototype in Monkey. Sroisuda Chotimanukul, Kaywalee Chatdarong, Pakpoom Navanukraw, Siwaporn Prachoochote, Natchaya Rasri, Kiattawee Choowongkomon

Population control of monkeys in Thailand is essential for animal welfare, zoonotic prevention and human safety in free-ranging or captive setting, especially when resources are limited. In species in which dominance rank and reproductive success are positively correlated, traits include physical strength, fighting abilities, and body mass are known to be positively related to androgen levels. Novel technique of contraception without interfering androgen level is targeting specific protein at testis that regulate spermatogenesis. Follicle stimulating hormone (FSH) is essential for normal function of Sertoli cells in males which is to support spermatogenesis. The biochemical actions on target tissues are initiated by the interaction of the FSH with FSH receptor (FSHR) in testis. This study aimed to develop anti-FSHR nanobody from the concept of targeting specific protein in monkey testis. The monkey FSHR protein purification was performed by plasmid transformation. The purified FSHR recombinant protein was analysed by Western blot analysis. Finally, the FSHR was concentrated and stored at -80°C. Selection of nanobody repertoire from phage display library was performed. Briefly, specific clones were captured by binding to FSHR and non-specific clones were removed. Phages were amplified by infection and regrowth of phage-producing cells between selection rounds. After selection, individual colonies were tested for FSHR specific binding by enzyme-linked immnosorbent assay (ELISA). The best nanobody

clone was subcultured and purified. The interaction of anti-FSHR nanobody and specific FSHR protein was characterized by surface plasmon resonance (SPR). From this study, anti-FSHR nanobody was purified with the molecular weight of 27 kDa. The result showed high affinity for binding with dissociation constant (KD) = 10.3 × 10-6 M. In conclusion, monkey anti-FSHR nanobody was successfully developed by the technique of phage display. Furthermore, the high-affinity binding between anti-FSHR nanobody and specific FSHR protein was found in vitro. Nevertheless, the efficacy of anti-FSHR nanobody on monkey Sertoli cells should be investigated in a further study.

Developmental Origins of Health and Disease (DOHAD)/Prenatal Programming/Maternal Health

Abstract # 1724

Is the Placenta Necessary for Gestational Diabetes Mellitus Development? Kathryn M. Storey, Sean Pirrone, Kristen Warncke, Barley Kozlowski, Kathleen A. Pennington, Laura C. Schulz

Gestational diabetes mellitus (GDM) is insufficient insulin production and/or signaling during pregnancy and affects ~7% of pregnancies in the United States. Pregnancy is a natural state of insulin resistance and to combat this, the pancreatic islets of Langerhans undergo structural and functional changes such as beta cell proliferation and increasing islet volume. These changes are stimulated through the prolactin receptor by prolactin and placental lactogens from maternal and placental origins, respectively. We have shown that an acute high fat, high sugar diet (HFHS) impairs beta cell proliferation by gestational day 13.5 and leads to severe glucose intolerance in pregnant, but not virgin mice. Here, we examine whether placental signaling is necessary for the development of GDM by using pseudopregnant mice, which have ovarian and pituitary pregnancy hormones through days 10-13 postcoitus, but no placenta. Our hypothesis is that HFHS affects the stimulation of beta cell expansion by the placenta, and that the placenta is therefore necessary for the induction of glucose intolerance by HFHS. The study included three groups: virgin, pregnant and pseudopregnant C57BL/6J females. In each group females were randomly allocated to either control or HFHS beginning one week prior to mating, either to proven C57BL/6J males (pregnant, n = 10 HFHS, 10 control), vasectomized CD-1 males (pseudopregnant, n = 12 HFHS, 10 control) or were not mated (virgin, n = 10 HFHS, 10 control). In addition to plug dates for all mated dams, estrous cycles and uterine weights were used to confirm pseudopregnancies. On pregnancy or pseudopregnancy day 10.5, intraperitoneal glucose tolerance tests were performed on all females. The diet maintained a strong interaction with each pregnancy state, but it had a significantly greater impact on glucose tolerance in pregnant dams than in pseudopregnant or virgin females (p = <0.0001). This suggests the placenta and associated hormones are necessary for HFHS to induce GDM development in dams. Thus, we compared morphology of the placenta in control and HFHS dams by measuring maternal and fetal blood spaces, as well as areas of the labyrinth and junctional zones at gestational day 17.5. No significant differences in blood spaces or placental zone areas were identified (p = >0.05). Our ongoing study aims to quantify beta cell number, mass, and proliferation along with levels of insulin release in each treatment group at gestational day 10.5. These data will provide further valuable information on GDM pathophysiology and lead to future investigation of signaling pathways of beta cell proliferation in normal and diabetic pregnancy.

Sub-optimal Paternal Diet in Mice Alters Fetal Growth and Skeletal Formation In Utero. Hannah L. Morgan, Donna O'Neil, Warwick Dunn, Adam J. Watkins

Studies have shown that the quality and quantity of maternal diet during gestation impacts significantly on offspring long-term ill-health. This maternal programming is mediated in part through perturbed patterns of fetal growth. There is now emerging evidence that poor paternal diet at the time of conception also impacts on the weight of his offspring at birth, increasing the risk of development of cardiovascular and metabolic disorders in adulthood. However, it is unknown whether paternally programmed offspring ill-health also associates with altered patterns of fetal growth and development. The aim of this study was to ascertain how sub-optimal paternal diet (over- and under-nutrition); with/without supplementation of essential vitamins and minerals; impacts male reproductive health and fetal physiology. Male C57/BL6 mice were fed one of five diets [LPD: low-protein (9% casein, 24% sugar, 10% fat), MD-LPD: methyl-donor (including choline chloride, betaine, methionine, folic acid and vitamin B12) supplemented LPD, WD: western diet (19% casein, 21% fat, 34% sugar), MD-WD: methyl-donor supplemented WD or control diet (18% casein, 10% fat, 21% sugar) for at least 8 weeks (n=8/group) before mating with female C57/BL6. One-carbon metabolite levels in male liver and testes tissue were determined by targeted metabolomic analysis using gas chromatography-mass spectrometry. On embryonic day (E)17.5, fetal weights were recorded and whole fetuses, fixed in formalin, were scanned using Skyscan1172 micro-CT scanner to determine skeletal formation (1 fetus per litter, n=8 litters/group). MD-WD males had increased testicular methionine levels compared to WD (p<0.01). Liver methionine, S-adenosylhomocysteine and S-adenosylmethionine were significantly increased in MD-WD compared to WD (p<0.001). WD male livers also demonstrated reduced levels of methionine, S-adenosylhomocysteine and homocysteine compared to LPD (p<0.05). There was no effect of paternal diet on mean litter size or average fetal weight at E17.5. However, the distributions of fetal weight was impacted by sub-optimal paternal diets, with 23% of fetuses from LPD (p=0.032) and 28% from WD (p=0.004) found above the 90th percentile for fetal weight. Placental distributions were also altered by paternal diet, however they showed a different distribution profile to the fetus; with a significant reduction in placentas below the 10th centile in the MD-WD group (0%, p<0.05). No significant difference in bone compositions was found in LPD, MD-LPD or WD fetuses compared to control. However, fetuses from MD-WD males had a significantly reduced low-density (p < 0.05) and high-density (p < 0.01) bone area at E17.5. We have shown that a paternal Western diet altered the one-carbon metabolic status of males, which was not returned to control status with dietary supplementation of methyl-donors. Furthermore, paternal pre-conception diet influenced fetal growth, without any obvious negative ramifications for his fertility. The influence this has on offspring outcome are still not fully understood, thus, more investigations into paternal regulation of fetal development are vital.

Estradiol Stimulates Pregnancy-dependent Hydrogen Sulfide Biosynthesis by ERa/ERβ-Mediated CBS Transcription in Human Uterine Smooth Muscle Cells. Jin Bai, Qian-rong Qi, Yan Li, Georgene Vasquez, Dong-bao Chen

Introduction : Normal pregnancy is featured by significantly increased endogenous estrogens that cause the rise in uterine blood flow for delivering nutrients to the fetus and for providing bidirectional fetal-maternal exchanges of respiratory gases for fetal growth and survival. Our recent novel work has identified that pregnancy-associated uterine vasodilation is linked to local production of a novel uterine artery (UA) vasodilator hydrogen sulfide (H 2 S) by upregulating endothelium and smooth muscle (UASMC) expression of its producing enzyme cystathionine β -synthase (CBS) in vivo. Smooth muscle occupies the majority of the large tube-shaped primary UA and expresses both estrogen receptors ERa and ERB. However, the importance of SM in UA vasodilation has been for the large part neglected. We hypothesized that estrogens stimulate pregnancy-dependent smooth muscle H 2 S production via ER-dependent CBS transcription. Methods : Main UAs were collected from nonpregnnat (NP) and pregnant (P) women for isolating primary human UASMC, named as NP and P hUASMC, respectively. Cells were treated with estradiol (10 nM) with or without ICI 182,780 (1 µM). CBS mRNA and protein were determined by q-PCR and immunoblotting. CBS promoter activation was accessed by luciferase reporter assay using full-length human CBS promoter and its deletion constructs. Estrogen-responsive elements (ERE) were analyzed by bioinformatics. ChIP-qPCR was used to determine ERa and ERB interactions with the EREs on the human CBS promoter in hUASMC. Results : Estradiol stimulated CBS mRNA and protein as well as CBS promoter activity in NP and P hUASMC, but with significantly greater potency in P cells, which was blocked by ICI 182,780. Human CBS promoter contains proximal estrogen-responsive elements (EREs), including 1 aERE (-216/-197) and 5 βEREs that preferentially bind ERa and ERβ, respectively. Luciferase reporter gene expression studies using constructs with human CBS promoter and its 5'-deletions identified the aERE to be responsible for mediating estradiol-stimulated trans -activation of CBS promoter in P-hUASMC. ChIP-qPCR using specific ERa and ERB antibodies demonstrated differential interactions of ERa and ERB with the aERE and BEREs in unstimulated and estradiol-treated NP and P cells; in unstimulated NP and P cells, ERa and ERB interactions with all aERE and BEREs were detected. Treatment with estradiol specifically stimulated the recruitment of ERβ to the aERE in a pregnancy-dependent manner, indicating pregnancy-dependent ERa and ERB homo and hetero dimer formation on the aERE by estrogen stimulation. Conclusion : Estradiol stimulates pregnancy-dependent CBS expression by trans-activating its promoter involving specific ERa and ERβ interactions with the aERE (RO1 HL70562, and R21 HD097498).

Altered Microrna 21 And 374 Expression In The Chorioallantoic Membrane During Placentitis In Mares. Europa Meza Serrano, Rogelio Alonso Morales, Hector Flores Herrera, Sergio Hayen Valles, Ana Delia Rodriguez Cortes, Elizabeth Morales Salinas, Ana Myriam Boeta Acosta

Placental pathologies are multifactorial diseases, being placentitis one of the main pathologies induced by infection and/or tissue damage. Placentitis involves a complex network of pro- and anti-inflammatory mediating molecules which include miRNAs. miRNAs are small noncoding RNAs that work as fine-tune signaling regulators in order to control, prevent or increase inflammatory responses, miRNA 21 have been previously studied in nervous human tissue where it can control the expression of IL-6 and IL-10 in order to regulate the inflammatory response and has been found to be down regulated in various types of cancers, therefore was classified as an oncomir. During recent years, additional roles to miR-21 and miR-374 had been described during hypoxia and, cardiovascular, immunological and developmental diseases in human. However, it is unknow if miRNAs 21 and 374 are involved in placentitis. Therefore, the objective of this study was to determine the expression of miRNAs 21 and 374 during mare placentitis. All experimental procedures using mares were reviewed and approved by the Universidad Nacional Autónoma de México Animal Care and Use Committee. Thoroughbred mares, multiparous, 10 to 20 years old with a body condition score of 3 or 4 on a scale from 1 (thin) to 5 (fat) were used in this study. Gestational age was determined using the day of ovulation as day 0. Blood samples were collected at 8 and 10 months of pregnancy in order to measure by ELISA the concentration of afetoprotein levels, a common marker for placental pathologies. Samples for ARN extraction were collected from blood and the chorioallantoic membrane after birth and classified as healthy or placentitis positive according to the levels of afetoprotein and, a microscopic and macroscopic evaluation of the placenta. miRNA levels were measured by Real-time PCR. Both miRNAs, 21 and 374 were significantly down-regulated in the chorioallantoic membrane from placentitis positive samples when compared to healthy tissue (P<0.05). Both miRNAs were present in blood, however, there was no significant differences between healthy and placentitis positive mares. We conclude that sub-regulation of miRNAs 21 and 374 might be involve in the signaling cascade during the inflammatory response in placental tissue during placentitis in the mare. Nevertheless, its necessary a punctual analysis of both miRNAs behavior during pregnancy to fully understand their role during placentitis. This work was supported by PAPIIT IN-226816 (UNAM-México).

Hydrogen Sulfide (H2S) Stimulates Uterine Artery Vasodilation by Activating Smooth Muscle Calcium-activated Potassium (BKCa) Channels in Women. Yan Li, Qianrong Qi, Jin Bai, Naoto Hoshi, Dongbao Chen

Introduction: Activation of smooth muscle (SM) calcium-activated potassium (BK Ca) channels plays a critical role in pregnancy-associated uterine artery (UA) dilation that is rate-limiting for pregnancy health. Our recent novel work has identified hydrogen sulfide (H 2 S) as a new UA vasodilator, which is augmented in pregnancy by selectively upregulating the expression of its synthesizing enzyme cystathionine β -synthase (CBS) but not cystathionine y-lyase (CSE) in both endothelium and smooth muscle. However, how H 2 S dilates UA is unknown. We hypothesized that H 2 S activates UASMC BK Ca to mediate UA dilation. Methods: Main UA was collected from women undergoing hysterectomy. Primary UASM cells were isolated and studied within 2-3 passages. BK Ca protein was determined by immunofluorescence microscopy and immunoblotting. BK Ca activity was recorded by whole cell and single channel patch clamp. KATP channel activity was determined by whole cell patch clamp with its specific agonist and inhibitor. UA dilation was measured by organ bath studies by using freshly isolated UA rings. Results: Immunoreactive BK Ca β1 subunit was detected in the SM layer of UA and primary UASMC in culture. Outward current was recorded in UASMC by both whole cell and single channel patch clamp techniques; treatment with the specific BK Ca blockers, iberiotoxin (IBTX, 100 nM) or tetraethylammonium (TEA, 1mM), inhibited the outward current, indicative of specific BK Ca channel activity. IBTX inhibited baseline BK Ca channel open probability. K ATP current was not observed by applying either K ATP channel agonist cromakalim (10 μ M) or blocker glibenclamide (10 μ M). H 2 S dosedependently potentiated BK Ca currents and open probability in HUASMC. Ca 2+ blocker nifedipine (5 μ M) and chelator (EGTA, 5 mM) partially inhibited H 2 Spotentiated BK Ca currents. Organ bath studies showed that the H 2 S donor NaHS dose-dependently relaxes phenylephrine (10 µM) pre-constricted UA rings, which was inhibited by TEA but not glibenclamide. Conclusions: H 2 S stimulates Ca 2+ dependent and independent activation of smooth muscle BK Ca channels to contribute to human UA dilation (RO1 HL70562 and R21 HD097498). Key words : H 2 S, BK Ca channels, uterine artery smooth muscle, women

Abstract # 1956

Maternal malnutrition programs postnatal metabolism, adiposity, and pituitary development in beef heifers. Michael C. Satterfield, Kenneth C. Hobbs, Andrew Poletti, Chelsie B. Steinhauser, John M. Long, Tryon A. Wickersham, Jason E. Sawyer, Rodolfo C. Cardoso

Maternal undernutrition during pregnancy followed by ad libitum access to nutrients during postnatal life has been shown to induce postnatal metabolic disruptions in a variety of species. We previously observed that maternal malnutrition during the latter half of pregnancy results in altered fetal pancreatic development and reduced fetal insulin concentrations in heifer (female) calves. Based on these observations we conducted an experiment to evaluate postnatal growth, metabolism, and development of beef heifers exposed to late gestation maternal malnutrition. Pregnancies were generated by embryo transfer of in vitro-produced embryos produced from a single Angus sire sexed to produce female offspring, transferred into virgin dams of similar age, breed type (Brangus), frame score, and body condition. Pregnant dams were moved into individual rationing facilities on gestational day (GD) 130 for 28-d acclimation and were randomly assigned to dietary treatments beginning on GD 158, receiving either 70% nutrient requirements (n=9; restricted) or 100% nutrient requirements (n=9; control). Individual feed intakes were adjusted twice monthly based on predicted pregnancy requirements using mean metabolic body weights (BW). After parturition, calves were maintained on dams grazing improved pastures until 7 months of age, at which time calves were weaned and individually fed ad libitum in a Calan gate facility until slaughter on postnatal day (PND) 485. Calves from restricted dams were lighter than controls (P<0.05) at birth and PND 35 (P<0.01) and tended to be lighter (P=0.052) on PND 70. There was no difference in calf BW at PND 105, 140, 175, 210, 245, 315, 350, 385, 420, 455, or 485. To assess pancreatic function in the pre- and peri-pubertal heifers, glucose tolerance tests were performed on PND 315 and PND 482. Glucose area under the curve was greater (P<0.05) on both PND 315 and PND 482 in calves born to restricted dams than controls. At slaughter, total internal fat was greater (P<0.05) in calves born to restricted dams, while weight of the whole pituitary was lighter (P<0.05). There was no difference (P>0.1) in ribeye are (REA), 12th rib back fat thickness, or weights of the brain, heart, lungs, liver, pancreas, spleen, adrenals, ovaries, uterus, kidneys, rumen, and small intestine. Immunohistochemical staining of the pituitary revealed that heifer calves born to restricted dams had fewer GH-positive cells (somatotrophs) compared to calves born to control fed dams (33% vs 39%; P<0.05). There was no difference between treatments for the percentage of tropic cells staining for ACTH (corticotrophs), LH (gonadotrophs), TSH (thyrotrophs), or PRL (lactotrophs). Results of the present study extend findings from previously conducted research by demonstrating impaired insulin sensitivity in heifer calves born to restricted dams leading to an increased deposition of internal fat. A reduction in the number of GH positive somatotrophs may contribute to the adipogenic phenotype of the calves born to restricted dams due to GH's known anabolic roles in growth, protein synthesis, lipolysis, and maintenance and function of pancreatic islets.

Abstract # 1958

Nutrient Restricted Ewes Demonstrate Thyroid Hormone And Placental Thyroid Hormone Receptor Adaptions Associated With Differential Fetal Phenotypes. Kenneth C. Hobbs, Chelsie B. Steinhauser, Michael C. Satterfield

An appropriate birth weight is essential for neonatal survival and vigor of human and livestock species. Low birth weight is associated with an increased risk of mortality and

comorbidities, such as perinatal issues, metabolic diseases, and infection. Impaired thyroid function and downstream effects are thought to increase risk for potential morbidities in small for gestation age (SGA) offspring. The nutrient restricted (NR) sheep model produces a range of fetal birth weights, resulting from different adaptations in the dam, placenta, and fetus. Therefore, studies were performed to analyze circulating thyroid hormones, placental hormone receptors (THRA, THRB, TSHR), placental thyroid conversion enzymes (DIO2, DIO3), and transporters (SLC16A2, SLC16A10, SLC10A1, SLO4A1) relative to fetal weight from NR dams. Singleton pregnancies were produced with embryo transfer. The control group (n=8) received 100% and the NR group (n=28)received 50% of NRC nutrient requirements starting on gestational day (GD) 35 and continuing until necropsy on GD 135. A surgical placentomectomy was performed to remove one placentome from each ewe on GD 70, which was compared to a second placentome collected at necropsy. Maternal blood was sampled on GDs 35, 70, 105 and 135, and fetal blood was collected at necropsy. The NR fetuses in the top quartile for fetal weight were classified as NR non-SGA (n=7), and NR fetuses in the bottom quartile were classified as NR SGA (n=7). These two groups of differential growth rates were compared with controls. Thyroxine (T4) concentrations in maternal blood were highest in the controls, lowest in the NR SGA group, with the NR non-SGA group being intermediate (P<0.05). Triiodothyronine (T3) and thyroid stimulating hormone (TSH) in maternal blood were higher in the control and NR non-SGA groups than the NR SGA group (P<0.05). T4 and TSH concentrations were highest at GD 35 and decreased throughout gestation. T4 concentrations in the fetal umbilical vein (FUV) were higher in the control group than in the NR non-SGA and NR SGA group (P<0.05) with no differences in FUV T3 concentrations. Placentome expression of THRA and DIO2 mRNA exhibited a GD by treatment interaction (P<0.05) with expression being highest for NR SGA on GD 135 and controls on GD 70, respectively. Placentome expression of DIO3, SLC16A2, SLC16A10, SLC10A1, and SLO4A1 mRNA was higher on GD 135 (P<0.01). Expression of DIO3 mRNA was higher for NR SGA than NR non-SGA (P<0.05). However, THRB mRNA expression was higher in the NR SGA group than controls (P<0.05). TSHR mRNA expression was higher on GD 70 (P<0.0001), and the NR SGA group was lower than the control and NR non-SGA groups (P<0.05). Placentomal TSHR protein localized to maternal and fetal epithelia at GD 70, then to mostly fetal epithelia by GD 135. Collectively, these results demonstrate potential maternal-placental-fetal adaptations to produce NR non-SGA offspring. Future studies are warranted to observe the growth and development of NR non-SGA lambs as well as the function of their hypothalamicpituitary-thyroid axis as they mature.

Nutritionally-induced Perturbation of Uterine Artery Hemodynamics in the Gestating Cow. Jennifer F. Thorson, Riley D. Messman, Caleb O. Lemley, Ligia D. Prezotto

Uterine arteries supply blood to the uteroplacental unit once maternal and fetal tissue interdigitation occurs and is terminated at parturition. Maternal blood delivers nutrients essential for the development of the fetus via the placenta. In order for fetal development to progress, maternal cardiovascular adaptation must occur throughout gestation. Moreover, meal-induced hyperemia of the gastrointestinal tract occurs preand post-prandially as a result of meal anticipation and during digestion and absorption of feed. Therefore, shunting of blood away from the uteroplacental unit as a result of maternal malnutrition (over- or undernutrition) may contribute to maldevelopment of the fetus. Doppler ultrasonography was employed every 28 days from 168 to 280 days of gestation to test the hypothesis that hemodynamics of the uterine artery are altered in response to maternal malnutrition during gestation. Mature Angus cows were fed diets to meet 60 (Underfed; n=7), 100 (Control; n=5), or 140 (Overfed; n=6) percent of gross nutrient recommendations from 28 days of gestation to parturition. Effect of maternal dietary treatment on maternal uterine artery hemodynamics were evaluated by ANOVA. Underfed and Overfed dams had reduced (P≤0.03) uterine artery diameter (0.79±0.04, 0.96±0.04, and 0.82±0.04 cm for Underfed, Control, and Overfed, respectively), area (0.39±0.04, 0.57±0.04, and 0.43±0.03 cm2 for Underfed, Control, and Overfed, respectively), and circumference (2.15±0.11, 2.59±0.12, and 2.21±0.10 cm for Underfed, Control, and Overfed, respectively) when compared to Control. Uterine arterial diameter, area, and circumference are also influenced by side (P<0.0001; ipsilateral or contralateral to fetus) and treatment by side interaction (P≤0.02). These findings demonstrate that parameters of uterine artery dimension are similarly altered by divergent, yet proportional degree of maternal malnutrition. Underfed dams had increased uterine artery systolic velocity to diastolic velocity ratio (P=0.02; 3.8±0.4, 2.3±0.4, and 2.8±0.4 unitless for Underfed, Control, and Overfed, respectively) when compared to Control, a phenomenon associated with poor placental perfusion. Overfed dams had reduced (P<0.03) uterine artery time-averaged peak velocity (71±3, 73±4, and 57±3 cm/s for Underfed, Control, and Overfed, respectively), mean velocity (72±4, 71±5, and 53±5 cm/s for Underfed, Control, and Overfed, respectively), unilateral blood flow (2226±204, 2847±235, and 1512±216 ml/min for Underfed, Control, and Overfed, respectively), and bilateral blood flow (4486±411, 5730±480, and 3011±438 ml/min for Underfed, Control, and Overfed, respectively) when compared to Control and Underfed. Data illustrate overnutrition during gestation has a greater detrimental influence on parameters of uterine artery blood flow velocity and volume than undernutrition, potentially driven by dietary-induced shunting of blood towards the gastrointestinal tract and away from the uteroplacental unit. Dietaryinduced alterations in hemodynamics during gestation have the potential to contribute to increased hepatic metabolism of hormones and metabolites, leading to compromised fetal development and maladaptation to postnatal environment. In conclusion, uterine artery hemodynamic alterations are modified by maternal

malnutrition during gestation, supporting why offspring subject to in utero malnutrition succumb to postnatal maladaptations. This research is supported by Agriculture and Food Research Initiative Competitive Grant no. 2018-67016-27579 from the USDA National Institute of Food and Agriculture.

Abstract # 2147

Gut Microbes Participate in Maternal Metabolic Adaptations to Pregnancy. Erica Yeo, Deborah Sloboda

Maternal pregnancy-induced metabolic adaptations support fetal and placental growth and include decreased maternal insulin sensitivity and a compensatory increase in insulin secretion. Until recently, these changes were thought to be primarily endocrine-mediated. However, the gut microbiota has emerged as a possible modulator of maternal glucose metabolism and may be in part, regulated through the production of bacterial metabolites (short-chain fatty acids, SCFAs). We have previously shown that maternal gut microbial populations change over the course of pregnancy, but the functional impact of this change is unknown. In the current study we therefore investigated whether maternal gut microbiota are necessary for glycemic adaptations to pregnancy using a germ-free (lacking any microbial communities) mouse model. Non-pregnant (NP) and pregnant (gestational day 14.5; GD14.5) specific-pathogen free (SPF; NP, n = 10; GD14.5, n=11) and germ-free (GF; NP, n = 6; GD14.5, n = 5) C57BL/6N female mice received an oral alucose tolerance test (oGTT; 3.5g/kg). Mice were sacrificed post-oGTT and blood, pancreatic tissue and cecal contents were collected. Serum insulin was measured by ELISA. Pancreatic -cell mass was quantified by immunohistochemical staining of insulin (abcam, ab7842) in fixed tissue sections. SCFA in cecal contents was determined by gas-chromatography mass spectrometry (GC-MS). Data were analyzed using a Bonferonni-corrected two-way ANOVA. Pregnant SPF and GF mice had a lower fasting blood glucose than non-pregnant SPF and GF mice (p = 0.0114). Glucose tolerance was similar between SPF and GF mice in both NP and GD14.5 animals. Serum insulin levels increased with pregnancy in SPF mice (p = 0.0095), but not in GF mice, and GF mice had lower serum insulin levels overall compared to SPF mice (p = 0.0087). GF mice demonstrated lower pancreatic β -cell mass compared to SPF mice (p = 0.0421), both in non-pregnant and pregnant states. Pregnant SPF mice had increased butyrate (a SCFA) levels at GD14.5 compared to non-pregnant SPF mice (p = 0.0075). GF non-pregnant and pregnant mice showed nearly undetectable levels of SCFAs. In the absence of gut microbiota, GF mice had lower serum insulin levels compared to pregnant SPF mice, despite similar glucose tolerance, suggesting that GF mice do not appear to make the same pregnancy adaptations as conventional mice. GF mice had fewer pancreatic β -cells and cecal SCFA levels, suggesting that the maternal gut microbiome (including bacterial metabolites) may participate in processes that increase insulin production and/or expand β -cell mass during pregnancy. Importantly, this study may inform interventions in maladaptive metabolic states during pregnancy.

Meconium Does Not Have a Detectable Microbiota Prior to Birth. Katherine M. Kennedy, Max Gerlach, Thomas Adam, Michael G. Surette, Thorsten Braun, Deborah M. Sloboda

A clear relationship exists between the host and residing gut bacteria on metabolism and immunity. When this relationship begins however is unclear; in utero colonization remains a highly contentious topic with studies showing both presence and absence of commensal bacteria in the intrauterine environment. Although numerous studies have reported bacterial DNA in first-pass meconium samples, these samples are collected hours to days after birth. We investigated whether bacteria could be detected in meconium prior to birth. Meconium was collected from 20 fetuses (female n=14, including 2 monochorionic-diamniotic twins) by rectal swab during elective breech Cesarean sections without labour. An additional meconium sample was collected for aerobic and anaerobic culture analysis performed under standard hospital pathology conditions. Antibiotics were given only after sample collection. A sampling negative control was taken by exposing a sterile swab to operating room air during a Cesarean section. Negative controls of DNA extraction reagents without meconium, and PCR amplifications without template DNA, were also generated to control for reagent contamination. Genomic DNA was isolated by phenol-chloroform extraction and the combined V3-V4 region of the 16S rRNA gene was amplified for 30 and 40 PCR cycles. Amplicons were sequenced using the Illumina MiSeq platform (2x150bp). Amplicon Sequence Variants (ASVs) were inferred using DADA2 and taxonomy was assigned using the RDP Classifier against the Silva 132 reference database. Beta diversity was calculated using the Bray Curtis dissimilarity metric in Phyloseg and visualized via Principal Coordinate Analysis (PCoA) ordination. Whole community differences across groups were analyzed using permutational multivariate analysis of variance (PERMANOVA) in the adonis command (vegan). After removing host associated ASVs, the number of ASVs per meconium sample ranged from 2-104 (mean = 16.6, median 13), which was similar to the number of ASVs in sampling negative controls (7 & 21 ASVs). Of the 271 meconium ASVs not detected in negative controls, 226 were present in only one meconium sample and an additional 25 ASVs were present in only two samples. The most prevalent ASV, present in 18 samples belonging to 15 unique fetuses, was the environmental extremophile Acidocella. Although there was a significant difference between meconium samples and negative controls overall (PERMANOVA, R2=0.042, p=0.045), this effect was absent when PCR negative controls were excluded (PERMANOVA, R2=0.023, p=0.34) indicating meconium samples were not distinct from sampling and DNA extraction negative controls. Of the 20 meconium samples cultured, 7 were negative under both aerobic and anaerobic conditions after 120 hours and the remainder were positive for common skin contaminants including Staphylococcus epidermidus and Propionibacterium acnes. In conclusion, we were unable to detect a microbial signature from meconium collected prior to birth that was distinct from

negative controls suggesting that when sampling meconium in a sterile environment, with appropriate controls, the data do not support fetal gut colonization prior to birth.

Abstract # 2285

Steroidogenic Acute Regulatory Protein (Star) RNA Processing Experiences Increased Regulation as Fetal Leydig Cells Mature. Keer Jiang, Anbarasi Kothandapani, Colin R. Jefcoate, Joan S. Jorgensen

During male fetal development, testosterone plays essential roles in the differentiation and maturation of the male reproductive system. While the control of testosterone synthesis is well studied in adult testis, little is known about its regulation in fetal testis. Steroidogenic acute regulatory protein (STAR) protein transfers cholesterol from the cytoplasm to the inner membrane of mitochondria for access to future enzymatic reactions. Classic studies suggest that STAR's function is a critical rate-limiting step in steroidogenesis and its importance is illustrated by sensitive regulation at three levels: 1) transcriptional, 2) RNA processing, and 3) post-translational modification. Our overall goal is to understand the regulation of steroidogenesis within the fetal testis; this study focuses on RNA processing kinetics during testis development. Studies in the MA-10 Leydig cell line reveal that Star transcript kinetics feature delayed splicing and production of two isoforms, of which the longer isoform is highly regulated in terms of RNA decay. Based on our knowledge and given the importance of fetal testosterone, we hypothesize that regulation of Star RNA splicing and turnover is under exquisite control in fetal Leydig cells. To study the changes in Star transcript numbers throughout development, we used copy number RT-qPCR, which can detect and measure accurate numbers of RNA molecules. Our primers were designed to detect primary (p)-, spliced (sp)-, long, and short forms of Star RNA. We harvested mouse testes at embryonic days 11.5, 13 and 16, which correspond to the time of sex determination, the onset of fetal Leydig cell differentiation, and the peak of testosterone synthesis, respectively. We detected both p-RNA and sp-RNA for Star indicating delayed splicing. While both forms increase with development, sp-RNA transcripts accumulate at a more rapid pace, showing increased splicing efficiency overtime. Over the same developmental period, the long isoform of RNA becomes significantly more prevalent than the short isoform, suggesting an increase in RNA turnover regulation. Together, these data highlight dynamic changes of Star RNA with an increasing demand for splicing regulation and precise turnover control as fetal Leydig cells mature in their steroidogenic capacity during testis development. FUNDING NIH R01HD090660

Education/Science Communication/Research Resources

Abstract # 1830

NICHD Strategic Plan: Healthy Pregnancies. Healthy Children. Healthy And Optimal Lives. Travis Kent, Chrisopher Lindsey, Stuart Moss, Susan Taymans, Candace Tingen, Clara Cheng, Daniel Johnston, Lisa Halverson, Louis De Paolo

For more than 50 years, NICHD has been a global leader of research in the field of reproductive health, and our investment in this area has yielded many scientific advances. For example, the field of fertility preservation has greatly expanded in the last few decades, in large part, due to the efforts of NICHD and its grantees. Today the US and global community face an array of challenges in the field of reproductive biology that must be adequately and swiftly addressed. At the same time, exciting technological advances have offered new opportunities to tackle these challenges. For the first time in 20 years, NICHD has undergone a strategic planning process to reevaluate our portfolio and plan future research directions for the institute. Working with institute staff, grantees, advocacy groups, the general public, and other stakeholders, we have identified areas where NICHD can lead research efforts. Here we present the five broad research themes outlined in the strategic plan, as well as the five cross-cutting topics that are woven throughout the research themes. One of these themes, "Promoting Gynecologic, Andrologic, and Reproductive Health," is directly relevant to the attendees of this meeting. In response to this strategic plan, the Fertility and Infertility Branch, Gynecological Health and Disease Branch, and Contraception Research Branch are presenting their updated high program priority areas. These high program priorities not only provide a guide as to the future directions of the respective branches, but also will be one factor in making funding decisions on grant applications. Finally, current Funding Opportunity Announcements administered by the three mentioned reproductive health focused branches will be presented.

Abstract # 2015

Image Feature Detection And Analysis Of Micrographs From Common Cell Culture-Based Functional Assays. Jacob A. O'Brien, Heyam Hayder, Chun Peng

Microscopy is a vital technology in the biological sciences. Many techniques assaying various cellular physiologies heavily rely upon microscopy for data collection; however, analysis can be tedious where only manual methods exist or automated systems are cost-prohibitive. There is a growing community of scientists creating open-source software to fully automate or add computer-assisted analysis to many techniques from single cell analyses like motility or more complex behaviours like angiogenesis. Using the National Institute of Health's ImageJ, we developed two freely available plugins. The first plugin (Cell Concentration Counter) counts cells in phase contrast images taken of a loaded haemocytometer. Traditionally, this is performed using a handheld tally counter and throughput is limited to how quickly cells can be accurately tallied. We

skip this step by counting cells in volume-calibrated images to determine cell concentration. Immediate feedback is given about the distribution of counts, correlating to how well the sample was loaded. Trypan blue stained cells can also be excluded. The end result is a higher throughput in cell counting, decreased variability between experiments, and a reduction of time cells spend outside the incubator. Boyden chamber cell migration and invasion assays are infamous time sinks. A typical experiment may require anywhere from 15 000 to 65 000 cells to be individually counted on a computer. This can take hours to days. Various alternative techniques have been developed to increase throughput by either subsampling or colourimetric correlation to cell number. To avoid these compromises, we developed an ImageJ plugin (Transwell Counter) to quickly (< 1-2 seconds/image) analyze whole membrane images of Boyden chamber-based cell migration and invasion assays. They can be manually adjusted to clean up any false detections, if required, and the output is saved in a commaseparated values (.csv) file. We are currently developing an application using MathWorks MATLAB that is more generalizable and applicable to a wider range of assays, building on what we have learned previously. MATLAB is a relatively new programming language and desktop environment with numerous professionally designed toolkits that are rigorously tested and fully documented. Our new design architecture follows a runtime programmable pipeline of image preparation, feature detection, datafication, statistical analysis, and figure creation. Pipelines are under development to detect cell divisions and quantify cell proliferation from phase contrast images as well as quantification of tube formation networks. The goal is to provide a flexible, modular, and automated quantification tool for a wide range of input images that is open-source and free to use.

Abstract # 2211

Midwifery Students' Pre- and Post-Clinical Placement: Work-life Interface and Effects on Intention to Stay in the Profession: A Pan-Canadian Study. Derek K. Lobb, Farimah Hakem Zadeh, Elena Neiterman, James Chowhan, Jennifer Plenderleith, Johanna Geraci, Isik Zeytinoglu

Facing high attrition rates and a severe shortage of midwives, Canada needs evidence-informed policies to fulfil its goal of providing equitable access to quality primary care and effectively manage its healthcare workforce. For these purposes and funded by CIHR, the Canadian Midwifery Study was undertaken as a mixed-method longitudinal study, conducted by a multi-disciplinary team of researchers, seeking to understand the effects of various individual perceptions and attitudes and provincial employment policies at various career stages on both student- and registered-midwives intention to stay in the midwifery profession. As a part of this study, 456 midwifery students at either pre- or post-clinical placement stages of their educational program responded to two separate online surveys. The data collected through these surveys helped to answer two questions. First, whether there was a significant difference between pre- and post-clinical placement students with regard to their intention to stay in the midwifery profession. Second, whether students experiences at the interface of their study/work and personal lives were associated with their intention to stay in the midwifery profession. For capturing students experiences at the interface of their study/work and personal lives, this survey measured the extent to which students perceived that their midwifery studies/work interfered with their personal lives, their personal lives interfered with their midwifery studies/work, and their midwifery work/studies and personal lives enhanced one another. Regarding the first question, results indicated that post-clinical placement students had significantly lower intention to stay in the midwifery profession compared to pre-clinical placement students. Regarding the second question, the data showed that for pre-clinical placement students, higher personal life interference with midwifery study/work was significantly associated with lower intention to stay in the midwifery profession. For post-clinical placement students, higher midwifery study/work interference with personal life was associated with lower intention to stay in the profession. No significant relationships between work/personal life enhancement and intention to stay were found in pre- or post-clinical placement students. Based on these findings and to help with maintaining positive intentions to stay in the profession, midwifery education programs can benefit from student recruitment approaches that provide individuals with a realistic preview of the time, commitment, workload, and personal involvement required for successful midwifery education and practice before they apply to or enrol in a midwifery program. Furthermore, midwifery education programs can facilitate the development of skills for better management of the boundaries between the various roles students manage related to their studies, professional practices, and personal lives. This research was funded by CIHR Operating Grant MOP 142286.

Endocrine Disrupting Chemicals (EDC)/Toxicology

Abstract # 1639

Essentials Oils: Does "Natural" Mean Risk-Free for Human Health? A Risk Assessment Story Using Reproductive and Developmental Data. Clotilde Maurice, Allison Clark, Saba Berhane, Christopher Rowat

The Chemicals Management Plan (CMP) was launched in 2006 in Canada to merge all federal programs into a single strategy. The CMP is a science-based approach which aims to protect human health and the environment. Under the CMP, Health Canada is evaluating the risks for human health on Terpenes and Terpenoids substances, which are being known as essential oils for the majority of them. They are naturally occurring complex mixtures that are produced by plants and often believed to be safe due to their long history of use and their natural source. This presentation specifically addresses the evaluation of mandarin & tangerine, and turpentine oils by using reproductive and developmental toxicological endpoints. These substances were found to be present in personal care products (e.g., body lotion, shampoos, drugs and natural health products), cleaning products, air fresheners and in food. For the characterization of health effects, preference was given to hazard data on the whole oil itself. In the absence of quality hazard data on the whole oil, hazard data for the main components present in the essential oil were considered to inform the risk assessment. These data were then combined with exposure estimates (e.g. duration of exposure, route of exposure, age of population) to generate scenarios by using the software ConExpo and the Margins of Exposure (MOE) approach for each kind of product in order to determine potential risks to human health. No relevant toxicity data were identified for turpentine oil. As such, the health effects information available for the main component alpha-pinene was considered. A no-observed-adverse-effect-level (NOAEL) of 66 mg/kg bw/day was determined based on a decrease of sperm motility and concentration in adult male rats and mice in 14-week inhalation study at 133 mg/kg bw/day. The MOE between the NOAEL and the estimate of daily exposure for paint thinner and remover, non-medicinal ingredient in topical medicated vapour product and a counterirritant product were inadequate. For mandarin & tangerine oils, because of the total absence of data on the whole oil and main components, an approach by read-across using QSAR Toolbox 4.2 on the main component, gammaterpinene, was taken and alpha-terpinene was identified as analogue. A NOAEL of 30 mg/kg bw/day was determined based a significant increase of fetal anomalies in the skeleton such as shorter ribs and bifurcated basiphenoids, delayed ossification and organ weight observed at 60 mg/kg bw/day in an in utero gavage study. The MOE between the NOAEL and the estimate of daily exposure to mandarin & tangerine oils from a body lotion and dietary supplement were inadequate. Even though the toxicological database for these substances is poor, the available data indicates that exposure to mandarin & tangerine, and turpentine oils, via consumer products may pose a risk to human health. Essential oils are considered "natural" substances, and as such, the perception of safety may be underestimated. As they become more and

more popular in consumer products, toxicological studies should be conducted on whole oils and their main components to guarantee their safety to Canadians.

Abstract # 1645

Low Dose of Tributyltin Exposure for Short Time Impairs Ovarian Reserve and Other Reproductive Features in Female Mice. Eduardo Merlo, Isabela Valim Sarmento, Silvana dos Santos Meyrelles, Elisardo Corral Vasquez, Genoa R. Warner, Andressa Gonsioroski, Kathy De La Torre, Daryl D. Meling, Jodi A. Flaws, Jones Bernardes Graceli

Tributyltin (TBT) is a well-known endocrine disrupting chemical (EDC) associated with metabolic and reproductive dysfunctions. However, few studies have explored the effects of TBT on the ovarian follicular reserve in female mice. The current study evaluated whether an acute and low dose of TBT exposure impairs the ovarian follicular reserve and/or other reproductive parameters in female mice. Further, we also evaluated whether TBT impairs antral follicle growth in vitro. Female C57BL/6 mice were treated daily with vehicle (ethanol 0.4%, control mice, n = 15) or TBT (500 ng/kg/day, TBT mice, n = 15) for 12 days by gavage. The estrous cycles were assessed before and during the exposure time. After euthanasia, the ovaries and uterus were weighed and reproductive tract structural and functional parameters, such as inflammation and oxidative stress markers, were evaluated. For in vitro procedures, untreated mice were euthanized, and their antral follicles were isolated from whole ovaries. The cultured antral follicles were exposed to TBT (0.5, 1, 10, or 100 ng/mL) or DMSO vehicle only for 96h (n = 5 separate culture experiments). The follicle growth was measured during and after exposure. Follicular growth, sex steroid levels, and expression of steroidogenic enzymes and oxidative stress regulators were assessed. Student's t-test was used for statistical evaluations from in vivo data and one-way ANOVA was used for statistical evaluations from in vitro data. To evaluate the relationship between the assessed parameters, Spearman's or Pearson's correlation was used if a non-Gaussian or Gaussian distribution, respectively, was detected. TBT exposure causes improper functioning of the reproductive tract. Specifically, TBT mice presented irregular estrous cyclicity, determined by an increase in time spent in the metestrus-diestrus phase (p < 0.05). TBT exposure also impaired follicular development, causing a reduction in primordial (54%, p < 0.01), primary (33%, p < 0.05), antral (26%, p < 0.01), and total healthy ovarian follicles (29%, p < 0.05), as well as corpora lutea (CL) numbers (28%, p < 0.01) compared to controls. Further, TBT exposure increased cystic ovarian follicle numbers and testosterone levels compared to controls (p < 0.05). In contrast, TBT exposure did not affect progesterone and estrogen levels (p > 0.05). In the uterus was observed atrophy, reduction in endometrial glands number (32%, p < 0.001), low ERa (estrogen receptor alpha) protein expression (27%, p < 0.05), as well as inflammation, and oxidative stress in the TBT mice. Further, strong negative correlations were observed between serum testosterone levels and primordial, primary, and total healthy ovarian follicles (p < 0.05). Interestingly, the TBT exposure did not alter any parameter evaluated in vitro. Collectively, these data suggest that an acute and low dose of TBT exposure

impaired ovarian follicular reserve and other reproductive features in female mice and that the observed effects of TBT on the ovary in vivo are likely indirect. This research was supported by CNPq (#304724/2017-3/ N°12/2017) and FAPES/CNPq (PRONEX 24/2018 / TO #572/2018) and NIH T32 ES 007326. Nothing to Disclose: EM, IVS, SSM, ECV, GRW, AG, KDLT, DDM, JAF, JBG.

Abstract # 1652

Early Life Exposure Of Rats To Organophosphate Flame Retardants Found In Canadian House Dust Causes Reduced Sperm Production And Increased Oxidative Stress. Aimee L. Katen, Abishankari Rajkumar, Trang Luu, Xiaotong Wang, Zixuan Li, Dongwei Yu, Michael G. Wade, Barbara F. Hales, Bernard Robaire

There is growing evidence that environmental toxicants are contributing to the decline in sperm concentrations and fertility observed in men. Organophosphate esters (OPEs) are used widely as flame retardants, plasticizers, and solvents. Despite ubiquitous human exposure, there are only limited data assessing the effects of OPEs on reproductive function. Our aim was to test the effects of the combination of OPEs detected in Canadian house dust on male reproduction. Adult male and female SD rats (n=15/treatment) were administered vehicle or an OPE mixture, low(L), middle(M) or high(H) dose, via the diet for 70 and 30 days, respectively. The diets were designed to deliver mixture doses of 0.48, 1.6 or 48 mg/kg bw/day, approximating 0, 30, 1,000 or 30,000 times the amounts that humans are exposed to via dust. Males and females from the same treatment groups were mated. Female rats continued treatment throughout gestation and lactation. A subset of F1 pups was euthanized on postnatal day (PND) 4 and at weaning on PND 21. The remaining pups were transferred to an OPE-free diet and euthanized on PND 90-100. OPE exposure of F0 males had no significant effects on body weights or weights of reproductive/accessory sex organs. There were no changes in testicular homogenization resistant spermatid/spermatozoa (HRS) spermatid nuclei or sperm numbers in the caput-corpus or cauda epididymidis. There were no effects on sperm motility or number of pups born per litter. There was no effect on anogenital distance in the F1 pups at PND 4, nor on the ages for nipple retention, testis descent, or preputial separation. F1 testis weights were reduced by 10% in the highest dose group at PND 90-100. HRS per testis were significantly reduced in all dose groups (19, 30 and 36% for L, M, and H, respectively). Daily sperm production per testis was reduced by 31 and 36% for M and H doses (p= 0.004, 0.001). There was an increase in sperm transit time in the caput-corpus epididymidis, from 4-days in control to 8-days with H (p= 0.02) in the absence of an effect on caput-corpus epididymidis tissue weights or sperm numbers. There was a 17% decrease in sperm number/g of cauda epididymidis in the H group; however, no effects on cauda epididymidis weights, sperm transit time or sperm motility were noted. Sperm collected from the cauda epididymidis were probed with anti-4hydroxynonenal (4-HNE) by immunofluorescence. Image analysis revealed an increase in corrected total cell fluorescence with M and H (190% and 202% of control, p-values 0.08, 0.05). While exposure of adult males to an environmentally-relevant mixture of

OPEs had no apparent effect on the male reproductive system, exposure of both parents and throughout gestation/lactation clearly impaired sperm production in the F1 generation. Cauda spermatozoa had increased levels of 4HNE, a major product of lipid peroxidation and marker of oxidative stress. These data suggest that exposure to OPEs may contribute to a decline in sperm count and quality. Funded by CIHR and FRQS.

Abstract # 1653

Disruption of Rat Fertility, Pregnancy Outcome, and Multigenerational Inheritance of Hepatic Steatosis by Organotin Exposure in Contaminated Seafood. Jones B. Graceli, Priscila L. Podratz, Eduardo Merlo, Julia F. P. de Araújo, Leandro C. Freitas-Lima, Mércia B. da Costa, Leandro Miranda-Alves

Early life exposure to endocrine-disrupting chemicals (EDCs) is an emerging risk factor for the development of complications later in life and in subsequent generations. We previously showed that exposure to the EDC organotin (OT) present in contaminated seafood resulted in reproductive abnormalities in female rats. However, few studies have explored the effect of OT accumulated in seafood on pregnancy outcomes. This led us to consider the potential effects of OT present in seafood on fertility, pregnancy, the placenta, and the offspring. In this investigation, we assessed if OT present in contaminated seafood exposure resulted in abnormal fertility and pregnancy features, and offspring complications. OT present in contaminated seafood (LNI) was administered daily to female Wistar rats (600 mg day-1 for 15 days via gavage) and their fertility and pregnancy outcomes were assessed. We further assessed fetal liver morphology. All the protocols were approved by the Ethics Committee of Animals of the Federal University of Espírito Santo (N° 01/2017). All data are reported as the mean \pm SEM. The D'Agostino and Pearson omnibus normality tests were to evaluate the data normality. Comparisons between groups were performed using one and two-way ANOVA for Gaussian data (Tukey's multiple comparison test). In addition, for non-Gaussian data, a Kruskal-Wallis test followed by Dunn's multiple comparisons was used to analyze the data. P < 0.05 was regarded as statistically significant. Statistical analyses were performed using GraphPad Prism (version 6.00, La Jolla, CA, USA). LNI exposure caused abnormal fertility, reduced the total number of pups (~50% reduction), and increased serum testosterone levels (\sim 33% increase) compared to controls (n=4-6, p < 0.05). Further, LNI exposure causes irregular morphology in the uterus, with inflammation (~75% increase) and fibrosis (~51.7% increase), leading to a reduction in embryonic implantation compared to controls (~20% reduction, n=4-6, p < 0.05). In pregnant rats, LNI causes abnormal lipid profiles and liver with steatosis features compared to controls (n=4-6, p < 0.05). LNI exposure also causes placental morphophysiology disruption, with high presence of glycogen (~90.16% increase) and inflammatory cells (~68.4% increase), and irregular lipid profile compared to controls (n=4-6, p < 0.05). In addition, LNI exposure increases delivery of high levels of carbohydrate and lipids to the fetus (~16 and 27.5% increase) by increasing in placental nutrient sensor protein expressions (~22% GLUT1, ~40/61% IRβ/mTOR and ~29% Akt increase) compared to controls (n=4-6,

p < 0.05). In both genders of offspring, LNI exposure increased body weight (~14% increase), liver megakaryocyte (~100% increase), lipids accumulation (39% increase) and oxidative stress (~27% increase) levels compared to controls (n=4-6, p < 0.05). Collectively, these data suggest that OT exposure from contaminated seafood in female rats leads to reduced fertility, uterine implantation failure, pregnancy and placental metabolic outcome irregularities, offspring adiposity, liver steatosis, and oxidative stress. Further some of the effects of OT may be as a result of obesogenic and multigenerational effects of OT in adult female rats. Nothing to Disclose: none. Research Support Source: CNPq (#304724/2017-3/ #12/2017) and FAPES/CNPq (PRONEX 24/2018 / #572/2018).

Abstract # 1713

Exposure To Glyphosate Alters The Ovarian Proteome With Differential Effects In Lean And Obese Mice. Bailey C. McGuire, Maria E. Gonzalez-Alvarez, Aileen F. Keating,

Glyphosate (GLY) is an herbicide with high usage in rural and urban environments, and both GLY and the main GLY metabolite have been detected in human urine. Approximately 40% of the United States female population is obese, which results in an increased incidence of reproductive dysfunction and ovarian cancer. We have previously discovered an additive impact of obesity on chemical-induced ovotoxicity, thus, we tested the hypothesis that GLY exposure would alter ovarian endpoints with hyperphagia-induced obesity causing ovarian additive effects. Female non-agouti KK.Cg-a/a mice (designated lean; n=20) and agouti lethal yellow KK.Cg-Ay/J mice (designated obese; n=19) were exposed to saline vehicle control (CT) or GLY (2 mg/kg daily per os) for 70 days ranging from 6 to 16 weeks of age. Ovarian protein was isolated, and LC-MS/MS performed. Comparison between lean CT and lean GLY exposed mice identified 1496 proteins, with 202 increased and 191 decreased (P < 0.05) in abundance due to GLY exposure. PANTHER analysis determined alterations to pathways involved in DNA damage repair, follicle development, and chemical metabolism. Comparison of protein changes occurring between obese CT and obese GLY-exposed mice identified 1522 proteins, with 24 increased and 7 decreased proteins (P < 0.05). PANTHER analysis determined changes to pathways involved in chemical metabolism. This data indicates that GLY impacts the ovarian proteome in both lean and obese mice with a greatly reduced response in the obese mice. This work was supported by R21ES026282 and R21ES026282-S1 from the NIEHS, and the Bailey Career Development award from Iowa State University.

Cadmium Exposure Leads to Features of Polycystic Ovary in Rats. Charles Santos da Costa, Thiago Fernandes de Oliveira, Alessandra Simão Padilha, Jones Bernardes Graceli

Cadmium (Cd) is a pollutant heavy metal and Cd exposure is associated with cardiovascular and metabolic abnormalities. However, few studies have evaluated Cd's toxicologic effect on reproductive function. In this study, we assessed whether Cd exposure results in reproductive abnormalities. Cd was administered to adult female rats (100ppm in drink water for 30 days), mimicking the Cd levels found in exposed human blood, and Cd level accumulated in blood and reproductive tract were evaluated by inductively coupled plasma mass spectrometry (ICPMS). We further assessed the reproductive tract function, inflammation, oxidative stress and fibrosis. All the protocols were approved by the Ethics Committee of Animals of the Federal University of Espírito Santo. All data are reported as the mean ± SEM. Comparisons between the groups were performed using Student's and Mann-Whitney t-tests for Gaussian and non-Gaussian data, respectively. A value of p < 0.05 was regarded as statistically significant. Cd exposure led to increased serum, ovary and uterus Cd levels compared to control rats (784, 2018 and 8841 %, respectively, p<0.05, n=4). An irregular estrous cyclicity, with longer estrous cycle length (~76 %), high basal LH levels (~ 136%) and ovary atrophy were observed in Cd rats (p<0.05, n=5-6). A reduction in ovarian follicular reserve was observed, with low primordial and primary follicles numbers in Cd rats (36 and 39%, p<0.05, n=6). Impairment in ovarian follicular development was observed in Cd rats, with reduction in preantral, antral follicles and corpora lutea numbers (41, 48 and 39 % respectively, p<0.05, n=6). A reduction in the Cd antral follicle granulosa thickness was observed (15 %, p<0.05, n=6). Cd exposure led to uterus atrophy, reduction in the total uterine area and myometrium layer (20 and 31 %, p<0.05 and p<0.001, respectively, n=6). Cd exposure was able to increase ovary inflammation by neutrophil (MPO) and macrophage (NAG) indirect activity (45 and 22 % respectively, p<0.05, n=5). Cd uterine inflammation increased by MPO activity and mast cell number (Alcian blue staining) (10 and 128 % respectively, p<0.05, n=4). High TBARS (the thiobarbituric reactive species), DHE (superoxide anion indicator) and low GSH (reduced glutathione) levels were observed in Cd ovaries compared with control ovaries (34, 176 and 6 % respectively, p<0.05, n=5). An increase in uterine DHE levels were observed in Cd rats (207 %, p<0.05, n=6). Ovarian and uterine fibrosis was observed in Cd rats using a Picrosirius Red staining (15 and 79 % respectively, p<0.05, n=4). Metabolic dysfunctions were observed in Cd rats, with reduction in adiposity and body weight gain (25 and 37 %, p<0.05, n=6). Interesting, an increase in the serum T4, leptin, and insulin and a reduction in the adiponectin levels were observed in Cd rats (25, 43, 37 and 10% respectively, p<0.05, n=6-7). Cd exposure impairs insulin sensitivity and glucose tolerance tests (11 and 12 % respectively, p<0.05, n=8). Thus, these data suggest that Cd exposure led to abnormal reproductive and metabolic features similar to those found in the polycystic ovary syndrome (PCOS) rat models.

Fenhexamid, A Pesticide, Enhanced Breast Cancer Cell Migration And Angiogenesis Via An ER-Dependent And PI3K/AKT Pathway. Ryeo-Eun Go, Kyung-Chul Choi

Fenhexamid (Fen) is a fungicide used to treat the gray mold of fruits and vegetables. Especially, in wine, its residue concentration was detected more than other fungicide of similar effects such as cyprodinil, azoxystrobin and boscalid. In this study, to examine the effects of Fen on breast cancer progression, the ER positive-MCF-7 breast cancer cells and the ER negative-MDA-MB-231 breast cancer cells were employed. The cells were treated with 0.1% DMSO (control), 17β-estradiol (E2; 1x10 -9 M) and Fen (10 -5 -10 -7 M) in the absence or presence of ICI 182,780 (ICI, ER antagonist, 10 -8 M) or Pictilisib (Pic, PI3K inhibitor, 10 -7 M). To confirm the migration of MCF-7 by Fen compared to E2 as a control, wound-healing assay was conducted. In similar, when they were observed by live cell imaging incubator system for 72 h, the scratch area of MCF-7 cells was decreased by E2 or Fen in a time-dependent manner. In migration assay used insert chamber with fibronectin, the MCF-7 cells migrated to the opposite side from the inside of chamber by E2 or Fen at 72 h. The cell migration induced by E2 or Fen was inhibited partially or completely by co-treated with Pic or ICI. In immunofluorescent, E2 and Fen promoted the decrease of E-cadherin (cell adhesion protein), and increase of Ncadherin (cell-cell adhesion protein) in MCF-7 cell at 72 h. In addition, in Western blot, E2 and Fen induced the decrease of cell adhesion related proteins such as E-cadherin and Occludin, while expression of cell migration regulating proteins was not observed in MDA-MB-231 cells. In an angiogenesis assay, E2 and Fen promoted the vessel formation than control for 4 h in HUVEC cells. When HUVEC cells were incubated in conditioned HUVEC media for 4 h, which was incubated in MCF-7 cells treated with the E2 or Fen for 24h, E2 or Fen directly increased the vessel formation in HUVEC cells. In tumor spheroid formation assay, E2 and Fen promoted larger and higher density of the formation of spheroid than the control. These effects were reversed in partially or completely in the presence of Pic or/and ICI. These results imply that Fen may induce breast cancer progression by increasing cell migration and angiogenesis via an ER-dependent and PI3K/AKT pathways.

Abstract # 1743

Effect Of Fludioxonil On Cell Proliferation And Cardiac Differentiation In Mouse Embryonic Stem Cells. Sung-Moo Lee, Kyung-Chul Choi

Fludioxonil is a phenylpyrrole fungicide widely used in agriculture. It is present in many fruits and vegetables, which is harmful to health. In some studies, it has been reported that fludioxonil caused low weight in rats. However, the effect of fludioxonil on cardiac differentiation is not yet understood. Therefore, we evaluated the early developmental toxicity of fludioxonil on cardiac differentiation of mouse embryonic stem cells (mESCs). Firstly, to confirm the effect of fludioxonil on mESCs viability, the water soluble tetrazolium (WST) assay conducted. The mESCs viability significantly decreased under

50% at 10 -5 M fludioxonil, but there was no change in cell morphology by fludioxonil (10 -5-10-9 M). Then, the colony formation assay was performed to confirm the effect of fludioxonil on cell proliferation. Cell proliferation was suppressed by 10-5 M fludioxonil, compared to the control (0.1% DMSO) at 5 days, but it was re-increased at 10 and 15 days. To test embryoid body (EB) formation capacity of mESCs, hanging drop assay was conducted and fludioxonil reduced the EB size at 10 -5 M. In the process of differentiation to cardiomyocytes derived from mESCs, 10 -5 M fludioxonil completely inhibited the beating ratio (the ratio of the number of contracting cells to the number of attached EBs) of cardiomyocytes at early stage of differentiation (day 5), but the beating ratio gradually increased after 5 days at 10 -5 M fludioxonil. It seemed that fludioxonil delayed the differentiation of mESCs to cardiomyocytes at 10-5 M compared to control. These results imply that fludioxonil may have a potential toxicity on the developmental process of mESCs, especially into cardiac lineage. For more information for developmental toxicity of fludioxonil, further studies on the mechanisms of fludioxonil to induce altered cell proliferation and cardiac differentiation of mESCs are needed.

Abstract # 1779

Ovarian Effects Of Perfluorooctanoic Acid Exposure In Lean And Obese Mice. María Estefanía González-Alvarez, Bailey C. McGuire, Aileen F. Keating

Perfluorooctanoic acid (PFOA) is a per and poly-fluoroalkyl substance that persists in the environment due to strong bonds between carbon and fluorine groups. PFOA is classified as a persistent organic pollutant and is widely used in consumer products such as Teflon, textile and paper coating, polishes, lubricants, food packaging, carpets, and firefighting foams. The half-life for human elimination is ~3.8 years. PFOA exposure has reproductive and developmental effects including delayed vaginal opening, subfertility, altered age of menopause onset, diminished ovarian reserve, female reproductive histopathological changes, delayed puberty onset, and decreased ovarian steroid hormone synthesis. In the US, obesity affects 40% of women and 20% of girls, with higher incidence in minority populations. Obesity causes infertility, poor oocyte quality, miscarriage, and offspring defects. We investigated impacts of PFOA exposure on the ovarian proteome and further hypothesized that obesity would increase PFOAinduced ovotoxicity. Female wild type (KK.Cg-a/a; lean) or KK.Cg-Ay/J mice (obese) received saline (CT) or PFOA (2.5 mg/Kg) per os for 15 days beginning at 7 weeks of age. They received water and food ad libitum. Food intake and body weight were monitored twice per week. Euthanasia was performed on the second day of diestrus after completion of dosing. Blood samples and tissues were collected. Progesterone and 17B-Estradiol were quantified by ELISA. There were no effects on food intake, final body weight, steroid hormone level or length spent at different stages of the estrous cycle (P > 0.05). There were also no effects on the weight of uterus, heart, kidney, and spleen, but PFOA exposure increased (P < 0.0001) liver weight regardless of body composition. Ovary weight was decreased (P < 0.05) in lean mice exposed to PFOA,

but not in the obese mice. LC-MS/MS was performed on isolated ovarian protein for proteomic analysis. Comparison between lean CT and lean PFOA-exposed mice revealed that 22 proteins differed due to PFOA exposure (P < 0.01). The cellular pathways identified as being targeted by PFOA included pathways in cancer, estrogen signaling pathway, PI3K-AKT signaling pathway, progesterone-mediated oocyte maturation, metabolic pathways, hepatocellular carcinoma, chemical carcinogenesis, and xenobiotic metabolism. In the obese mice, 28 proteins were altered (P < 0.01) due to PFOA exposure with alterations to chemical metabolism, DNA damage sensing and repair, and reproduction pathways. The data suggest that PFOA exposure alters ovarian proteins that may reduce fecundity in mice. In addition, the findings support that the ovary of obese mice differs in the response to PFOA exposure. Supported by funding from the Iowa State University Bailey Career Development Award to AFK, the Iowa State University Nutritional Sciences Council Martin Fund to AFK, and the Fulbright Foreign Student Program to EGA.

Abstract # 1899

Reproductive And Developmental Toxicity In Fischer Rats Exposed To The Mycotoxin Ochratoxin A In Diet. Anne Marie Gannon, Ivan Curran, Laurie Coady, Steven Bugiel, Don Caldwell, Keri Kwong, Francesco Marchetti, Clotilde Maurice, Peter Pantazopoulos, Genevieve Bondy

Ochratoxin A (OTA) is a mycotoxin produced by Aspergillus and Penicillium molds. In humans, grain-based foods account for the large majority of dietary exposures. Renal toxicity in the proximal tubule is the primary adverse effect of OTA in most animals. Teratogenicity studies show that OTA causes embryotoxicity and gross skeletal and visceral malformations when administered by various routes on specific gestational days. However, the reproductive and developmental effects of continuous low-level exposure to dietary OTA are poorly understood. To address this gap, a one generation reproductive toxicity study was conducted with groups of 16 male and 16 female Fischer rats exposed to 0, 0.026, 0.064, 0.16, 0.4 or 1.0 mg OTA/kg in diet. Dams exposed to 1.0 mg OTA/kg diet had statistically significant F1 pup losses between implantation and PND 4. Preputial separation and vaginal opening were delayed in F1 male and F1 female rats, respectively. Exposure to OTA caused significant negative effects on multiple sperm quality parameters in F1 male rats. In F1 females, changes in total transitional and primary ovarian follicle populations were observed only in the 0.4 mg/kg dose group. Renal lesions were present in F1 male and female rats in the 0.4 and 1.0 mg/kg dose groups. These results indicate that OTA causes post-implantation fetotoxicity. In F1 males and females, pubertal delay and changes in sperm motility or ovarian follicle populations were suggestive of endocrine disruption. Evidence was strongest for an anti-androgenic mode of action in males. Renal lesions were more pronounced in F1 rats than in F0 rats, indicating that the developing kidney was more susceptible to OTA than the adult kidney. Residue analyses confirmed that OTA was present in milk from F0 dams and in plasma, kidneys and testes from F0 and F1 rats.

Concentrations were highest in plasma, since OTA binds strongly to plasma proteins. The accumulation of OTA in testes provided evidence of proximity for adverse effects on spermatogenesis. Collectively, the results confirm that continuous exposure to OTA administered in diet causes renal, reproductive and developmental toxicity in Fischer rats, and that OTA accumulates to a similar extent in renal and reproductive tissues.

Abstract # 1967

Benchmark Dose Analyses Of The High Content Imaging-Based Effects Of Bisphenol A And Its Replacements In Ma-10 Leydig Cells. Abishankari Rajkumar, Trang Luu, Theresa Bock, Barbara Hales, Bernard Robaire

Bisphenol A (BPA) has been used widely in polycarbonate (PC) plastics and epoxy resins. Concern about the potential adverse health effects of BPA have led to an increase in the use of BPA replacements. However, many of these replacements have chemical structures that are similar to BPA and little is known about their safety. The objective of this project was to use high-content imaging to determine the effects of bisphenol A and some of its replacements on MA-10 Leydig cells. Cultured cells were exposed for 48 h to BPA, BPAF, BPF, BPS, BPM or BPTMC (vehicle, 0.001, 0.01, 0.1, 1, 3.2, 5, 10, 20, 50 or 100 µM in 0.5% DMSO). The effects of these chemicals on cell survival and morphometric parameters were determined using cell-permeable fluorescent dyes to assess cell viability, mitochondrial activity, lysosome number, oxidative stress and lipid droplet formation. Benchmark dose (BMD) analyses using BMD Express 2.2 followed by one-way ANOVA with multiple testing correction (Benjamini and Hochberg-FDR; p<0.05) were done to quantitate the effects of BPA and its replacements on these cell parameters. Models that were significant went through BMD analyses with BMR (benchmark response) factor (10%) with selection for best poly model (nested chi square test). Recommended models by analyses based on low Akaike information criterion (AIC) and best fit were selected for BMD value determinations. In vitro exposure to BPA as well as its replacements affected MA-10 Leydig cells to different extents. BPA was the least cytotoxic (BMD=40.2µM), followed by BPAF (BMD=23.4 µM), BPF (BMD=16.5 µM), BPTMC (BMD=7.5 µM) and BPM (BMD=6.9 µM). Exposure to BPS did not produce an interpretable BMD model for cytotoxicity due to poor fit of data with proposed models. However, using a one-way ANOVA the IC 50 value for BPS was 46.2 µM. Interestingly, exposure of MA-10 cells to BPA and BPAF resulted in an increase in lysosomal number (BPA: BMD=4.1 µM; BPAF: BMD=9.8 µM), while exposure to BPTMC resulted in a decrease in lipid droplet formation (BMD=4.4 µM). In contrast, exposure to BPS, BPF and BPM did not significantly affect any morphological parameters. In conclusion, in vitro exposures to BPA and some of its replacements affect MA-10 Leydig cells to different extents and via different pathways. These data suggest that bisphenol exposures may result in chemical-specific pathway alterations. BMD analyses of high content imaging data provide a means to compare structurally similar chemicals effectively; this approach may be useful for prioritizing chemicals for human risk assessment purposes. Supported by CIHR IP3-150711 and McGill University.

Abstract # 2179

Phthalate and Phthalate Metabolite Mixtures Alter Gene Expression in Mouse Neonatal Ovaries. Genoa R. Warner, Jessica S. Yue, Kathy M. De La Torre, Daryl D. Meling, Cassandra E. Atkinson, Jodi A. Flaws

Phthalates are a group of chemicals used as additives in various consumer products, medical equipment, and personal care products. Although phthalates have short biological half-lives, phthalates and their metabolites are consistently detected in humans, indicating widespread and continuous phthalate exposure. Because a wide range of phthalate structures are used in consumer products, mixtures of phthalates and phthalate metabolites are present in the body. Thus, environmentally relevant mixtures of phthalates and phthalate metabolites were investigated to determine the effects of phthalates on the function of the ovary during the sensitive neonatal period of development. Neonatal ovaries from CD-1 mice were cultured with either DMSO (vehicle control) or phthalate mixture (0.1-100 µg/mL) composed of 35% diethyl phthalate (DEP), 21% di(2-ethylhexyl) phthalate (DEHP), 15% dibutyl phthalate (DBP), 15% diisononyl phthalate (DiNP), 8% diisobutyl phthalate (DiBP), and 5% benzylbutyl phthalate (BBzP). In a second experiment, neonatal ovaries were cultured with either DMSO (vehicle control) or a mixture of the major metabolites of the phthalate mixture (0.1-100 µg/mL) composed of 36% monoethyl phthalate (MEP), 19% mono-(2-ethylhexyl) phthalate (MEHP), 15% monobutyl phthalate (MBP), 10% monoisobutyl phthalate (MiBP), 10% mono-isononyl phthalate (MNP), and 8% mono-benzyl phthalate (MBzP). After 96 hours of culture, ovaries were harvested for gene expression analysis for cell-cycle regulators and apoptosis regulators. Phthalate mixture exposure borderline significantly decreased levels of apoptosis regulator Bcl2 (1 µg/mL), whereas exposure to the metabolite mixture borderline increased expression of cell proliferation marker Ki67 (100 µg/mL) and cell cycle regulators Cdkna1 and Ccna2 (100 µg/mL). These data suggest that phthalates alter ovarian gene expression and that phthalates and their metabolites differentially impact the developing ovary. Supported by NIH R01ES028661 and NIH T32FS007326.

Abstract # 2193

Measurements of Mono-n-butyl Phthalate in the Tissues of Adult CD-1 Female Mice after Repeated Oral Administration of Di-n-butyl Phthalate. Estela J. Jauregui, Jasmine Lock, Lindsay Rasmussen, Zelieann R. Craig

Di-n-butyl phthalate (DBP) is used worldwide as a plasticizer or solvent in many consumer goods such as personal care products and medication coatings. Previous studies have estimated that the general population is exposed to 7-10 µg/kg/day of DBP, patients taking medications are exposed to 1-233 µg/kg/day of DBP, and workers in occupational settings are exposed to 0.1-76 µg/kg/day of DBP. In humans and rodents, DBP is rapidly hydrolyzed into its monoester metabolite, mono-butyl phthalate (MBP), by lipases (LpI). MBP is then oxidized and/or glucuronidated in additional

reactions catalyzed by biotransformation enzymes including aldehyde dehydrogenase (Aldh1a1) and UDP glucuronosyltransferase (Ugt1a6a). We have shown that MBP accumulates in serum, liver, and ovary of mice treated with a single high dose of DBP (1000 mg/kg/day). The objective of this study was to quantify the accumulation of MBP and the expression of DBP-metabolizing enzymes after repeated daily exposure to lower levels of DBP. We pipet-fed mice (N=5 per treatment/time point) for 10 consecutive days with tocopherol-stripped corn oil (vehicle) or DBP at 1 (DBP1), 10 (DBP10) or 1000 mg/kg/day (DBP1000) and collected liver, ovary, and serum at 2, 6, 12, and 24 h after the final treatment. Serum, liver, and ovary samples were subjected to liquid chromatography/tandem mass spectroscopy assays. The contralateral ovary from each animal was processed for qPCR analysis to determine the expression of Lpl, Aldh1a1, and Ugt1a6a. In mice treated with vehicle, background MBP levels were detected in serum (0.001 \pm 0.0002 µg/ml) and liver (0.005 \pm 0.012 µg/g), but not in ovaries at the 2 h time point. MBP concentration peaked at 2 h (p<0.05) in serum (DBP10, 0.76±0.10 µg/ml; DBP1000, 75.6±10.7 µg/ml), liver (DBP10, 36.94±3.49 µg/g; DBP1000,1255.9±215.3 µg/g), and ovary (DBP10, 3.82±1.37 µg/g; DBP1000, 1186.8±201.3 μ g/g). MBP levels then gradually decreased until reaching undetectable levels at 24 h after the final dose. Compared to vehicle-treated control ovaries, ovaries from DBPtreated mice had significantly increased expression of Lpl (DBP1000; 1.5-fold) and significantly decreased expression of Ugt1a6a (DBP1, 0.4-fold; DBP10, 0.6-fold) at 6 h (p<0.05). At the 24 h time point, qPCR showed significantly increased expression of Aldh1a1 (DBP1, 2.1-fold; DBP10, 1.8-fold) in DBP-treated ovaries versus controls (p<0.05). In conclusion, we have measured MBP levels and DBP metabolizing enzymes in the tissues of mice after repeated oral exposure of DBP. This study demonstrates that MBP accumulates in the ovary and that DBP exposure modulates the expression of its metabolizing enzymes. Future studies will involve investigating further molecular mechanisms that might be altered by DBP in the ovaries of mice. Supported by NIEHS grant R01026998-01A1 (ZRC).

Abstract # 2246

Environmental Particulate Matter Exposure TO Placental Trophoblast CELLS. Taylor Bruett, Corrine Hanson, Ann Anderson Berry, Tara Nordgren, Sathish kumar Natarajan

Ambient air pollution is an environmental health hazard specifically during pregnancy. Particulate Matter (PM) and ambient black carbon particles were shown to cross the placenta and reach the fetal side of the human placenta suggesting that the placental barrier is inefficient in preventing the particles from crossing the human placental barrier. Ultrafine particles and PM can also escape the maternal lung and increase maternal systemic inflammation, resulting in direct fetal exposure leading to detrimental effects to the placenta and fetal organs. Further, PM exposure to firsttrimester human normal immortalized trophoblast cells (HTR-8 SV) showed increased inflammation, trophoblast cell growth inhibition, and endoplasmic reticulum stress. We also published that increased levels of specialized pro-resolving lipids mediators (SPM) resolvin D1 (RvD1) and RvD2 in the maternal circulation in cases of at-risk deliveries like preterm. Here we hypothesize that supplementation of n-3 fatty acids and generation of n-3 fatty acid-derived SPM can protect against PM-induced placental trophoblast inflammation, ER stress and apoptosis. Methods: HTR-8, a human normal immortalized trophoblast cells and human malignant-derived trophoblast (JEG-3 and JAR) cell lines were treated with different levels of environmental particulate matter isolated in Nebraska for 24 hours. Placental inflammation, apoptosis and ER stress markers were examined. Results . Treatment of placental trophoblast cells with environmental dust exposure for 24 hours did not induces any increase in the levels of percent apoptotic nuclei and caspase 3/7 activity. The protective role for n-3 fatty acid-derived SPMs like RvD1 and RvD2 against PM-induced inflammation and ER stress in placental trophoblasts are currently underway . In conclusion, environmental PM exposure do not induce placental trophoblast apoptosis.

Endocrinology: Reproductive Neuroendocrine

Abstract # 1610

IGSF1 Does Not Regulate FSH Synthesis or Secretion. Emilie Brûlé, Yining Li, Gauthier Schang, Courtney L. Smith, Xiang Zhou, Daniel J. Bernard

Loss of function mutations in the human X-linked immunoglobulin superfamily, member 1 (IGSF1) gene result in central hypothyroidism, often associated with macroorchidism. lgsf1 -deficient mice are also centrally hypothyroid due to impaired thyrotropinreleasing hormone action in the pituitary. The mechanisms underlying macroorchidism are unclear and disputed. IGSF1 was originally characterized as an inhibin B coreceptor. As inhibin B negatively regulates FSH secretion, it was hypothesized that loss of IGSF1 would impair inhibin B action, leading to elevated FSH levels and enhanced Sertoli cell proliferation during development. Yet, in direct contradiction to this model, IGSF1 does not bind inhibin A or B in heterologous binding assays. In addition, inhibin A or B antagonism of FSH synthesis is unperturbed in pituitaries of Igsf1 knockout mice. More recently, IGSF1 was proposed to inhibit activin type IB receptor (ALK4) signaling. As activing stimulate FSH, loss of this inhibition should lead to increased FSH. However, neither humans nor mice with IGSF1-deficiency have elevated FSH, and IGSF1 expression in FSH-producing gonadotrope cells is negligible. Previous methods used to demonstrate IGSF1 regulation of a human FSHB promoter-reporter were conducted in a heterologous system in which such reporters lack activin/ALK4-dependent activity. In our hands, overexpression of IGSF1 in homologous LBT2 gonadotrope-like cells does not impair induction of murine or human Fshb/FSHB promoter-reporters by activin A or of endogenous Fshb mRNA expression by a constitutively active form of ALK4. Finally, IGSF1 and ALK4 do not physically interact. Collectively, the available data fail to support a role for IGSF1 in FSH regulation by inhibins, activins, or otherwise.

Abstract # 1638

GATA2 May Regulate FSH Production In Male Mice Via The BMP Antagonist Gremlin 1. Gauthier Schang, Luisina Ongaro, Émilie Brûlé, Xiang Zhou, Ying Wang, Ulrich Boehm, Frederique Ruf-Zamojski, Nitish Seenarine, Mary Anne Amper, Venugopalan Nair, Yongchao Ge, Stuart C. Sealfon, Daniel J. Bernard

Mammalian reproduction is dependent on follicle-stimulating hormone (FSH) and luteinizing hormone (LH) secreted by pituitary gonadotrope cells. These dimeric glycoproteins share a common a-subunit linked to hormone-specific β-subunits. Expression of the FSHβ subunit (Fshb) depends on the transcription factors FOXL2, SMAD3, and SMAD4. These proteins mediate the actions of the activins or related TGFβ ligands, which stimulate Fshb transcription. Another transcription factor, GATA2, was also implicated in FSH production in male mice, although its mechanisms of action and role in females were not determined. To address these gaps in knowledge, we generated and analyzed gonadotrope-specific Gata2 knockout mice using the Cre-lox system. While conditional knockouts (cKO) males exhibited ~50% reductions in serum FSH and pituitary Fshb mRNA levels relative to controls, FSH production and fertility were normal in gonad-intact cKO females. LH production was unaltered in cKOs of both sexes. Fshb expression was also reduced in male mice in which Gata2 was ablated in adult gonadotropes, ruling out a developmental effect. The male-specific FSH phenotype was reminiscent of that observed in mutant mice expressing a stabilized form of β -catenin in their gonadotropes. In that case, FSH deficiency derived from increased expression or activity of the activin antagonists follistatin and inhibin. These mechanisms did not explain FSH deficiency in Gata2 cKO males; nor did a testicular factor, as FSH deficiency persisted post-castration. RNA-seg analysis of purified gonadotropes from cKO males revealed a profound decrease in expression of gremlin 1 (Grem1), a bone morphogenetic protein (BMP) antagonist. Grem1 is expressed in gonadotropes, but not other cell lineages, in the male mouse pituitary. Both Gata2 and Grem1 mRNA levels were significantly higher in pituitaries of wild-type males relative to females, but both increased significantly following ovariectomy in the latter. In cKO females, post-ovariectomy increases in pituitary Grem1 and Fshb expression were blocked or blunted relative to controls. This suggests that an ovarian factor, perhaps estradiol, may contribute to the sex-specific FSH deficiency in gonad-intact cKO mice. Indeed, exogenous estradiol decreased Gata2 and Grem1 expression levels in castrated wild-type males Collectively, the data suggest that GATA2 promotes Grem1 expression in gonadotropes and that the Gremlin protein potentiates FSH production. The mechanisms of Gremlin action in this context are not yet clear, but may involve potentiation of activin-like and/or attenuation of BMP signaling in gonadotropes.

Abstract # 1726

FSH Synthesis Depends On The Tgfβ Type I Receptors ALK4 And ALK5 In Murine Gonadotropes. Luisina Ongaro Gambino, Xiang Zhou, Gauthier Schang, Ulrich Boehm, Gloria H. Su, Daniel J. Bernard

Follicle-stimulating hormone (FSH) is an essential regulator of mammalian fertility. FSH is a dimeric glycoprotein, composed of an a subunit, which it shares with other glycoprotein hormones, and a hormone-specific FSH β subunit (product of the Fshb gene), which confers biological specificity. FSH is synthesized by pituitary gonadotrope cells in response to gonadotropin-releasing hormone secreted by the hypothalamus and, according to current dogma, by pituitary-derived activin B. Like other TGF β family ligands, activins bind type II and type I serine/threonine receptor kinase complexes. Mice lacking the activin type II receptors, ACVR2A and ACVR2B, in gonadotropes are FSH-deficient. Though these data are consistent with the idea that activins play a necessary role in FSH production in vivo , other TGF β ligands bind these receptors and mice lacking activin B (Inhbb knockouts) have elevated rather than reduced FSH levels. Moreover, bioneutralizing activin A and B antibodies do not affect FSH synthesis in murine pituitary cultures. Therefore, it is presently unclear whether activins or other members of the TGF β family are the main drivers of FSH production in mice. A type I

receptor inhibitor, SB431542, fully suppresses Fshb expression in pituitary cultures, indicating that a TGFB ligand that signals through activin receptor-like kinases (ALK) 4, 5, and 7 is required for FSH production. Activin B signals via ALK4 and ALK7. FSH production is normal in pituitary cultures of mice lacking ALK7. The relative roles of ALK4 and ALK5 in FSH production have not been reported. Here, we used a Cre-lox approach to generate conditional knockout (cKO) mice lacking ALK4 (Acvr1b) and/or ALK5 (Tgfbr1) in gonadotropes. ALK4 cKO mice were fertile and had serum FSH levels similar to those of control mice. As ALK4 is the canonical activin type I receptor, these data are consistent with the emerging concept that activins are not required for FSH production in mice in vivo. In contrast, serum FSH levels were significantly reduced in male and female ALK5 cKOs relative to controls. ALK5 cKO females also had impaired ovarian follicle development and reduced litter sizes. Male and female mice lacking both ALK4 and ALK5 in gonadotropes were FSH-deficient and hypogonadal. Testes weights were reduced by 50% in males and females were sterile. Collectively, these data challenge current dogma by showing that a non-activin TGFB ligand that signals via ALK5 and, to a lesser extent, ALK4 is a main driver of FSH synthesis in mice. Although ALK5 is the canonical TGF β type I receptor, this ligand is unlikely to be a TGF β isoform as gonadotropes do not express the TGF β type II receptor. The identity of the TGFβ ligand driving FSH synthesis and its cell type of origin is currently unresolved.

Abstract # 1758

Metabolism and Reproduction: Gonadotrope Leptin Signals Broadly Influence the Pituitary Transcriptome as Revealed by Single-Cell RNA-Sequencing. Angela K. Odle, Ana Rita Silva Moreira, Alexandra N. Lagasse, Anessa C. Haney, Stephanie D. Byrum, Jordan T. Bird, Nathan L. Avaritt, Ulrich Boehm, Melanie C. MacNicol, Angus M. MacNicol, Gwen V. Childs

Leptin plays an integral role in female reproduction, binding to receptors in the brain, the pituitary, and the ovary to communicate information about the body's nutritional status to this system. Our previous work has investigated the specific role for leptin signaling in the murine female gonadotrope. Using Cre-lox technology, we have determined that Gonadotrope-Lepr-null females (mice lacking leptin receptors specifically on gonadotropes through Gnrhr- driven Cre expression) have a blunted LH surge and a blunted secondary rise in FSH. These females also have a significant decrease in GnRH receptors on the morning of proestrus as well as significant decreases in Fshb mRNA. Therefore, leptin appears to be important for estrous cycle stagedependent regulation of gonadotrope functions in females. Given the onset of Cre expression as early as embryonic day 13, we were curious how this cell population (and other cell populations in the pituitary) may be affected by the loss of the gonadotrope leptin signal early in development. We therefore subjected control and Gonadotrope-Lepr- null female proestrous pituitaries to single-cell RNA-sequencing. A total of 12,400 control cells (from two pools of n=3 pituitaries each) and 13,000 Gon- Lepr- null cells (also two pools, n=3 pituitaries each) were methanol fixed and submitted for single-cell

RNA-sequencing (10x Genomics). An average of 23,568 reads/cell were obtained. Based on expression of key cell lineage markers and hormone genes, 15 pituitary clusters were identified along with 2 small unknown populations in both control and mutant animals. There were 292 total genes significantly changed between the control and Gon-Lepr- null datasets. Out of these, 39 were downregulated and 253 were upregulated. In some cases, the same gene was significantly altered in multiple clusters. The most significantly changed gene out of the dataset was Fshb, which is decreased in Gon-Lepr- null gonadotropes (confirming our earlier data in whole pituitaries). The other most downregulated genes in gonadotropes included secretogranin-encoding genes, as well as Nnat, a gene that is highly expressed in the rat pituitary during development. Also changed in gonadotropes are genes contributing to cellular metabolism as well as a long non-coding RNA highly regulated in the CNS during development. A number of non-gonadotrope populations were also significantly affected by the gonadotrope-Lepr deletion. The second largest transcriptional change in the dataset was a decrease in growth hormone (Gh) mRNA in somatotropes. We also saw a major shift in the distribution of lactotropes in Gon-Leprnull females due largely to a downregulation in genes encoding secretogranins. Our single-cell RNA-seq data indicate that leptin regulates Fshb transcription and/or stability and influences the way gonadotropes develop and package/secrete gonadotropins. In addition, leptin plays a broad role in pituitary development and/or in the maintenance of paracrine signals coming from gonadotropes that influence somatotrope and lactotrope functionality. Future studies will explore pathways that are down or up-regulated in the Lepr- null gonadotrope females and determine how leptin may modulate the development and function of the pituitary gland.

Abstract # 1773

Musashi as a Regulator of Pituitary Gonadotropes: A Single-Cell RNA Sequencing Approach. Ana Rita Silva Moreira, Alexandra N. Lagasse, Anessa C. Haney, Stephanie D. Byrum, Jordan T. Bird, Nathan L. Avaritt, Ulrich Boehm, Michael G. Kharas, Christopher J. Lengner, Melanie C. MacNicol, Angus M. MacNicol, Gwen V. Childs, Angela K. Odle

Reproductive processes are energetically expensive, thus sufficient nutrition is critical for reproduction. Leptin is a crucial mediator of metabolic regulation of the hypothalamicpituitary-gonadal axis. We have previously shown that leptin signals to pituitary gonadotropes to maintain the protein levels of the gonadotropin releasing hormone receptor (GnRHR) in female mice. We established that this occurs at a post-transcriptional level and identified the RNA-binding protein Musashi (MSI) as a potential mediator of this process. We have shown that MSI binds to Gnrhr and inhibits its translation, and that a gonadotrope-specific deletion of Msi1 and Msi2 (Gon-Msi1/2-null) leads to increased GnRHR protein levels. This culminates in dysregulated levels of luteinizing hormone and follicle-stimulating hormone. We have recently identified other gonadotrope and pituitary targets of MSI. We therefore suspected that MSI plays a role in both the maturation of gonadotropes and the normal cyclic regulation of gonadotropes. We hypothesized that the deletion of MSI would lead to downstream effects on (1) the composition of the gonadotrope population and (2) the molecular landscape of these cells. Using adult, diestrous Gon-Msi1/2-null females, we performed single-cell RNA-sequencing on methanol-fixed dispersed pituitary cells. Libraries were made from two control pools and two mutant pools (n=3 pituitaries/pool) using 10x Genomics v3.1 Single-Cell Gene Expression technology. We recovered single-cell mRNA transcript information from 15,614 control pituitary cells and 13,423 Gon-Msi1/2-null cells to a depth of 24,242 reads/cell. We identified differentially expressed genes between control and Gon-Msi1/2-null mice. Our analysis revealed that the Gon-Msi1/2-null gonadotropes have a significant decrease in Msi2 expression (as expected), as well as a significant increase in expression of Tmsb4x (thymosin beta 4 X-linked), a regulator of actin cytoskeleton, which has previously been identified as a high confidence Msi2 target. Additionally, the Gon-Msi1/2-null gonadotropes show a 2-fold increase of Gal (galanin), a modulator of pituitary hormone secretion, possibly underlying the dysregulated gonadotropin production and secretion in these mice. In addition to altering the gene expression profile in gonadotropes, the gonadotrope-specific deletion of Msi surprisingly affected a number of other pituitary cell types. We observed a significant decrease in the expression of Crhbp (corticotropin releasing hormone binding protein) in corticotropes and lactotropes of Gon-Msi1/2-null mice. Conversely, a number of genes were upregulated in non-gonadotrope populations. Of particular interest is the gene coding the a chain of the glycoprotein hormones (Cga), which we have determined to have two MSI-binding elements. Our analysis shows the Cga transcript upregulated in several clusters, including somatotropes and lactotropes. Taken together, our data indicate that MSI influences the molecular landscape of the female gonadotrope, as well as the pituitary as a whole, including progenitor cells. This highlights the high degree of interaction between the different pituitary cell populations. Additionally, we have identified potential gonadotrope MSI target mRNAs, which might give insight to the mechanisms leading to the dysregulated gonadotropin production and secretion seen in Gon-Msi1/2-null females. Future studies will compare pubertal and adult females, as well as females from different estrous cycle stages.

Abstract # 1991

Reduced Endogenous GnRH-II Receptor Expression Leads to Decreased 17β-estradiol Secretion Despite Larger Follicular Diameter in Cyclic Gilts. Caitlin E. Ross, Rebecca A. Cederberg, Fina H. Choat, Dorothy H. Elsken, Scott G. Kurz, Ginger A. Mills, Clay A. Lents, Brett R. White

Pigs are the only livestock species encoding a functional protein for both the second isoform of gonadotropin-releasing hormone (GnRH-II) and its cognate receptor (GnRHR-II). Unlike the classical GnRH system, GnRH-II and GnRHR-II are expressed in reproductive and non-reproductive tissues. To examine the role of GnRH-II and its receptor in reproductive function, we produced a swine line with reduced endogenous levels of

GnRHR-II (GnRHR-II KD). Our laboratory demonstrated that GnRH-II binding to its receptor on Leydig cells stimulates LH-independent testosterone secretion in porcine testes. However, the role of the GnRH-II/GnRHR-II system has not been elucidated in female pigs. Therefore, the objectives of this study were to characterize 17β-estradiol secretion and compare morphometric criteria of mature GnRHR-II KD (n = 4) and littermate control (n = 4) gilts during the follicular phase of the estrous cycle. Prepubertal animals were monitored daily for behavioral estrus beginning at 180 d of age. Once all females exhibited their third behavioral estrus, they were individually fed 15 mg of the progestogen, altrenogest, for 14 consecutive days to synchronize estrus. During this time, indwelling jugular catheters were surgically placed. At 48 h after the final altrenogest feeding, blood samples for 17β-estradiol were collected from each animal every 4 h until 24 h following the onset of estrus (0 h), determined by twice daily estrous detection. Serum was obtained and 17β -estradiol quantified by radioimmunoassay. Animals were euthanized during proestrus (Day 18 to 20) of the following estrous cycle, and body, ovarian, uterine, oviductal, and right kidney weights determined. Next, follicle diameter was measured using calipers and antral follicles (≥ 6 mm) counted. Statistical analyses were performed using the MIXED procedure of SAS. The model for 17β-estradiol concentrations included line, time and line x time as fixed effects, litter as a random effect, and time as the repeated measure (subject = gilt x line). The model for morphometric data included line as a fixed effect and litter as a random effect. During the follicular phase, a tendency for a line x time interaction (P = 0.0745) was detected for 17β-estradiol levels; additionally, circulating 17β-estradiol concentrations tended to be reduced approximately 20% in GnRHR-II KD (18.7 ± 2.5 pg/mL) vs. control $(23.2 \pm 2.5 \text{ pg/mL})$ females (P = 0.0760). Furthermore, total area under the curve (AUC) was lower for GnRHR-II KD females compared to controls (P = 0.05) and AUC at peak 17β -estradiol levels (-44 to -8 h relative to the onset of estrus) tended to be reduced in transgenics (P = 0.0996). Finally, morphometric weights and antral follicle counts were not different between lines (P > 0.10). However, follicles tended to be larger in GnRHR-II KD (7.7 \pm 0.3 mm) than control (6.9 \pm 0.3 mm) females (P = 0.0602). Thus, these data indicate that the GnRH-II/GnRHR-II system regulates 17B-estradiol secretion and follicular dynamics in mammalian females, representing a potential avenue for future reproductive therapies. Supported by USDA/NIFA AFRI (2017-67015-26508) and Hatch Multistate (NEB-26-244) funds. USDA is an equal opportunity provider and employer.

Abstract # 2039

Leptin Transport Across the Blood-Brain Barrier in Postpubertal Heifers Exposed to Nutritional Extremes during the Perinatal Period. Tatiane S. Maia, Meaghan M. O'Neil, Sarah M. West, Rodolfo C. Cardoso, Gary L. Williams

Nutritional programming during pre- and postnatal periods has been shown to have major impacts on the reproductive neuroendocrine axis of female offspring. Previous work in our laboratories has focused on the positive benefits of postnatal nutritional programming to accelerate timing of puberty in heifers. However, the potential negative interactive effects of pre- and postnatal nutrition have not been thoroughly examined. Objectives of the current study were to test the hypothesis that leptin transfer across the blood-brain barrier (BBB) is reduced in heifers subjected to dietary energy excess or deficiency during gestation and coupled with high or low energy diets postnatally. Crossbred heifers (Bos indicus x Bos taurus; n=134) were developed using a 3x2 factorial arrangement of pre- and postnatal dietary treatments. Pregnant Braford and Brangus cows were fed to reach targeted body condition scores (BCS; 1 = emaciated; 9 = morbidly obese) of 7.5-8 (H, obese), 5-5.5 (M, moderate) or 3-3.5 (L; very thin) during the third trimester. Heifer offspring were weaned and fed to gain at either a high (H; 1 kg/d) or low (L, 0.5 kg/d) rate between 4 and 8 months of age, then fed a common diet. A subgroup (n=36) was slaughtered prepubertally at 8 months of age for tissue analysis. Remaining heifers (data 95% complete) reached puberty between 9 and 19 months of age. Those in postnatal L reached puberty approximately 9 wk later (P<0.001) than those in postnatal H groups, and those representing the maternal x postnatal combination LL reached puberty 10.3 and 11.6 wk later (P<0.03) than MH and HH, respectively. Using quantitative rt-PCR, we showed previously that, compared to postnatal M and H, postnatal L heifers exhibit a significant depression (P<0.05 - P<0.01) in mRNA abundance of the leptin receptor (Obr-c) in the choroid plexus. Moreover, the combined maternal/postnatal treatment (LL) suppressed (P<0.057) mRNA abundance of low-density lipoprotein receptor-related protein 1 (LRP1) which affects BBB permeability. Eighteen heifers were selected randomly from LL, HH and MH treatment groups, ovariectomized, and received estradiol replacement following puberty. Cannulas were placed surgically in the third ventricle (IIIV) for CSF collection. The ratio of CSF/plasma leptin at surgery (2.28 ± 0.6) and at least 2 wk postsurgically after a 56-h fast did not differ among LL, MH and HH treatments. Three hourly IV injections of recombinant oleptin (0.2 µg/kg body weight) increased (P<0.001) plasma leptin from an initial baseline of 0.9 ± 0.3 ng/mL to mean peak concentrations of 12.3 ± 3.6 ng/mL within 30 min. This reduced (P<0.002) the CSF/plasma ratio to as low as 0.4, with no detectable transfer of leptin into IIIV CSF over a 5-h period in any group. Data suggest that heifers were able to maintain an equivalent CSF/plasma leptin ratio irrespective of nutritional treatment. Failure to exhibit evidence of active transfer during fasting was unexpected since heightened secretion of GnRH in response to leptin occurs only in the fasted state.

Abstract # 2130

Effects of Prenatal and Postnatal Nutrition on Neuropeptide Y Neuronal Projections to Kisspeptin Neurons in the Arcuate Nucleus of Beef Heifers. Sarah M. West, Sterling H. Fahey, Carson M. Andersen, Thomas H. Welsh, Jr., Gary L. Williams, Rodolfo C. Cardoso

Early life nutrition modulates the development of hypothalamic neurocircuitries controlling GnRH secretion, thus programming puberty in female mammals. Neuropeptide Y (NPY) is an orexigenic peptide involved in the metabolic control of reproduction. The inhibitory effects of NPY on GnRH secretion are mediated directly and indirectly via neurons expressing kisspeptin, a potent GnRH stimulator. Morphological changes in the NPY neurocircuitry can delay puberty and have longterm detrimental effects on reproduction. Therefore, it is critical to understand the effects of early life nutrition on the development and plasticity of the hypothalamic NPY system. Using the bovine model, objectives herein were to test the hypothesis that either maternal obesity or undernutrition during late gestation, in combination with a high or low rate of body weight (BW) gain in heifer offspring during the juvenile period, alters: 1) the expression of kisspeptin neurons in the arcuate nucleus (ARC), and 2) the magnitude of NPY neuronal projections to kisspeptin neurons. Brangus cows (n = 36) bearing female pregnancies were fed to achieve thin (L, n = 12), moderate (M, n = 12), or obese (H, n = 12) body condition (BC) by ~6 mo (second trimester) of gestation and maintained at the target BC until calving. Heifer offspring from each group were then weaned at ~3.5 mo of age and assigned randomly to be fed to achieve a low (L; 0.5 kg/d) or a high rate of BW gain (H; 1 kg/d) until 8 mo of age. This 3×2 factorial design created six combinations of maternal-postnatal nutritional treatments (LL, LH, ML, MH, HL, and HH). At ~14 mo of age, heifers were euthanized and hypothalamic tissue was dissected and processed for double-label immunofluorescence to determine the extent of NPY projections toward kisspeptin neurons. While maternal overnutrition did not impact NPY inputs to kisspeptin neurons, maternal undernutrition reduced (P<0.05) the percentage of kisspeptin neurons highly innervated (-->7 close appositions) by NPY projections in the heifer offspring compared to maternal M and H diets. When combining the effects of maternal and postnatal nutrition, the percentage of kisspeptin neurons highly innervated by NPY fibers was decreased in LH heifers compared to MH (P<0.05) and HH heifers (P=0.09). Moreover, reduced postnatal nutrition resulted in a trend (P=0.1) for a higher percentage of kisspeptin cells receiving NPY contact in the caudal region of the ARC. Preliminary analysis indicates that gestational undernutrition, when combined with adequate postnatal nutrition (LH heifers), results in diminished NPY (inhibitory) inputs to kisspeptin neurons in the ARC. This likely represents a compensatory response during postnatal development to counter the effects of undernutrition in utero and to allow for the pubertal increase in GnRH pulsatile secretion. This premise is supported by the observation that LH heifers attain puberty at a similar age as MH (control) heifers. Additionally, our findings demonstrate that reduced nutrition during juvenile development increases NPY inputs to kisspeptin cells in the caudal ARC, which likely contributes to the well-established effects of postnatal undernutrition delaying puberty in heifers.

Abstract # 2135

Induction of Follicle Wave Emergence with a Physiological Dose of Exogenous Ovine Follicle Stimulating Hormone (oFSH) in Anestrous Ewes. Katherine J. Nason, Zohreh Madiseh, Elodie Cusset, Ashley Eason, Felicia Gauthier, Scot Everson, Cassidy Singh, Mojtaba Rahbar, David Barrett

To date, seasonally anestrous ewes exhibit poor reproductive performance even when using the latest available techniques for out of season breeding protocols. These techniques remain unable to effectively synchronize follicle wave emergence, resulting in lower fertility rates. The objective of this study was to compare the ovarian and behavioural responses, pregnancy, and lambing of seasonally anestrous ewes treated with a CIDR and eCG with either oFSH or vehicle injections on the day before CIDR removal. All experimental procedures were carried out in accordance with the Canadian Council on Animal Care guidelines, with formal approval from the Dalhousie University Committee on Laboratory Animals. Ewes (n=14) received CIDRs (Day -12), two injections of oFSH (oFSH; $0.5 \mu g/kg$ BW per injection; n=7) or vehicle (CON; n=7) on the day before CIDR removal (Day -1), and an eCG injection (500 IU) at the time of CIDR removal (Day 0). The vehicle was BSA, polyvinylpyrrolidone, and saline. Daily ovarian ultrasonography began on Day -1 and twice daily ovarian ultrasonography was done from Day 1 until ovulation was confirmed. A ram was introduced to the ewes to observe estrus every 6 h beginning 24 h after CIDR removal until ewes were unreceptive to the ram. Ultrasonography was done at 7 d, 30 d, and 60 d after ovulation to record CL, embryos, and fetuses. Lambing results were also obtained. Serial blood samples were taken by indwelling jugular catheters every 6 h for 36 h (where time 0 = 1 st s.c. oFSH; 3 mL) to determine the effects of the oFSH treatment on circulating FSH concentrations. Data was analyzed by ANOVA (Two Way; Two Way RM; One Way) and then by Tukey Test. There were no significant differences found between treatments when analyzing reproductive parameters (estrus, ovulation, lambing), mean serum FSH levels and peaks, or follicular dynamics/follicle wave emergence. There was a day effect on daily mean follicle diameter (dMFD; P< 0.001) but there was neither a significant treatment nor interaction effect. Daily MFD increased from Day -1 to Day 2, then decreased from Day 2 to Day 3. All ewes exhibited behavioural estrus and ovulated, however only 13 of 14 ewes were pregnant at both 30 d and 60 d – one CON ewe was not pregnant at 60 d. The oFSH treatment in this study does not appear to effect follicular dynamics or follicle wave emergence, FSH levels, estrus, ovulation, pregnancy, or lambing rate when used in a CIDR-eCG estrus synchronization protocol for seasonally anestrous ewes.

Abstract # 2348

Luteinizing Hormone Secretion In Gnrhr-II Knockdown Boars. Amy T. Desaulniers, Rebecca A. Cederberg, Clay A. Lents, Brett R. White

The second mammalian form of GnRH (GnRH-II) and its receptor (GnRHR-II) are produced in only one livestock species, the pig. Paradoxically, the physiological interaction of GnRH-II with its receptor does not stimulate gonadotropin secretion. Instead, both are abundantly produced within the testis and have been implicated in autocrine/paracrine regulation of steroidogenesis. To further study the role of GnRH-II and its receptor, our laboratory generated a transgenic swine line with ubiquitous knockdown (KD) of GnRHR-II; expression is reduced by 70% within the testes of transgenic males and serum concentrations of 10 gonadal steroids (2 progestogens, 2 estrogens and 6 and rogens) are reduced by 60 - 98%. The objective of this study was to assess luteinizing hormone (LH) secretion in mature GnRHR-II KD (n = 5) and littermate control (n = 5) males via a series of in vivo endocrine trials. In all experiments, blood was collected via indwelling jugular cannulae and serum concentrations of LH were measured via radioimmunoassay. In the first trial, diurnal secretory patterns of LH were assessed by sampling every 15 min for 8 h. There was an effect of time (P = 0.0008) but no effects for line (GnRHR-II KD versus control) or line by time interaction (P > 0.05). Pulse analysis of LH data revealed no differences between lines (P > 0.05); baseline, minimum and maximal concentrations as well as pulse frequency, pulse amplitude, pulse duration and area under the curve were similar between lines (P > 0.05). In the next trial, blood was serially collected prior to and after intravenous treatment with either the agonists D-Ala6 GnRH-I or D-Ala6 GnRH-II (150 ng/kg BW). A time by treatment interaction was detected (P = 0.0004); however, there was no line by time by treatment interaction (P = 0.6654). In both control and transgenic animals treated with D-Ala6 GnRH-I, LH concentrations rose dramatically above baseline within 10 min posttreatment and remained elevated throughout the duration of sampling (270 min). In control and GnRHR-II KD boars treated with D-Ala6 GnRH-II, however, LH levels rose slightly above pretreatment concentrations within 10 min post-treatment and remained elevated for only 40 min before returning to basal levels. In the third trial, blood was serially collected prior to and after intramuscular injection with the GnRHR antagonist, SB-75 (cetrorelix; 10 μ m/kg BW). An effect of time was detected (P < 0.0001) but no effects of line or line by time interaction were evident (P > 0.05). In both transgenic and control males, LH levels were suppressed below baseline concentrations at 2, 2.5, 3, 6, 9 and 24 h post-injection (P < 0.05). Together, these results provide further evidence that GnRH-II and its receptor are not physiological regulators of gonadotropin secretion in mammals; instead, attenuation of gonadal steroidogenesis in transgenic boars is likely due to reduced testicular expression of GnRHR-II. Supported by USDA/NIFA AFRI-ELI predoctoral fellowship (2017-67011-26036; ATD) and AFRI (2017-67015-26508; BRW) funds. USDA is an equal opportunity provider and employer.

Endocrinology: Steroid Hormones and their Receptors

Abstract # 1786

Metabolic Features of Hepatic Steatosis and Insulin Resistance are Alleviated by Nicotinamide Mononucleotide Treatment in a DHT-Induced PCOS Mouse Model. Ali Aflatounian, Melissa C. Edwards, Valentina Rodriguez Paris, Michael J. Bertoldo, Dulama Richani, Blake J. Cochran, William L. Ledger, LindsayE. Wu, Robert B. Gilchrist, Kirsty A. Walters

Nicotinamide adenine dinucleotide (NAD+) plays a key role in energy metabolism. Recent studies have shown that NAD+ precursors, such as nicotinamide mononucleotide (NMN), can have beneficial effects on age related sub-fertility, insulin resistance and liver damage. Polycystic ovary syndrome (PCOS) is a common and complex endocrine disorder, which is defined by the presence of key characteristic reproductive and endocrine defects. PCOS patients also suffer from metabolic features including obesity, insulin resistance, liver steatosis and an increased risk of type 2 diabetes. Although insulin sensitizing agents such as metformin are commonly administered to ameliorate PCOS metabolic traits, there is uncertainty about the effectiveness of metformin in women with PCOS. Therefore, we gimed to assess the efficacy of nicotinamide mononucleotide (NMN), a precursor of NAD+, in treating features of PCOS in a dihydrotestosterone (DHT)-induced PCOS mouse model. Peripubertal female mice were implanted s.c with blank (n=14) or DHT (n=14) implants. After 12 weeks, control and PCOS mice (8/group) were treated with NMN in drinking water while the remaining mice received normal water (NW). All mice were euthanized 8 weeks after administration of NMN/NW. NMN treatment had no beneficial effect on the PCOS reproductive traits of irregular cycles and anovulation. However, oil red O absorption, a marker of liver steatosis, was significantly lower in NMN- versus NW-treated PCOS mice (PCOS+NW: 13.4±2.3; PCOS+NMN: 2.6±1.7; P<0.01). Fasting insulin levels and homeostatic model assessment of insulin resistance (HOMA-IR) were also ameliorated in PCOS+NMN mice compared to PCOS+NW mice (fasting insulin levels: PCOS+NW, 0.85±0.1 ng/mL; PCOS+NMN, 0.52±0.1 ng/mL; P<0.05. HOMA-IR: PCOS+NW, 10.6±1.9; PCOS+NMN, 6.9±0.5; P<0.05). Furthermore, the observed DHT-induced increase in fat pad weight was not observed in inguinal or mesenteric fat pad weights of PCOS+NMN mice (inguinal fat weight: PCOS+NW, 17.1±1 mg/BW; PCOS+NMN, 12.7±1 mg/BW; P<0.001. Mesenteric fat weight: PCOS+NW, 14.1±1 mg/BW; PCOS+NMN, 11.7±1 mg/BW; P<0.041). These findings suggest that boosting NAD+ via NMN administration may represent a novel therapeutic option to target metabolic features of PCOS.

Abstract # 1854

Melatonin Protects The Mouse Testis Against Heat-Induced Damage. Yi Zheng, Pengfei Zhang, Yinghua Lv, Fuyuan Li, Yuwei Qin, Wenxian Zeng

Spermatogenesis, an intricate process occurring in the testis, is responsible for ongoing production of spermatozoa and thus the cornerstone of lifelong male fertility. In the testis, spermatogenesis occurs optimally at a temperature 2–4°C lower than that of the core body. Increased scrotal temperature generates testicular heat stress and later causes testicular atrophy and spermatogenic arrest, resulting in a lower sperm yield and therefore impaired male fertility. Melatonin (N-acetyl-5-methoxytryptamine), a small neuro-hormone synthesized and secreted by the pineal gland and the testis, is widely known as a potent free-radical scavenger; it has been reported that melatonin protects the testis against inflammation and reactive oxygen species generation thereby playing anti-inflammatory, -oxidative and -apoptotic roles in the testis. Nevertheless, the role of melatonin in the testicular response to heat stress has not been studied. Here, by employing a mouse model of testicular hyperthermia, we systematically investigated the testicular response to heat stress as well as the occurrence of autophagy, apoptosis and oxidative stress in the testis. Importantly, we found that pre-treatment with melatonin attenuated heat-induced apoptosis and oxidative stress in the testis. Also, post-treatment with melatonin promoted recovery of the testes from heat-induced damage, probably by maintaining the integrity of the Sertoli cell tight-junction. Thus, we for the first time provide the proof of concept that melatonin can protect the testis against heat-induced damage, supporting the potential future use of melatonin as a therapeutic drug in men for sub/infertility incurred by various testicular hyperthermia factors.

Abstract # 1933

Ovarian Steroid Regulation of Lactic Acid Bacteria and Redox Potential in the Vaginal Environment of Ewe Lambs. Fernando Silveira Mesquita, Amilcar Jardim Matos, Matheus Beltrame Padilha, Maria Eduarda Rodrigues Costa, Jessica Ferreira Rodrigues, Andressa Minozzo Oliveira, Camila Cupper Vieira, Ana Carolina da Rosa, Tiago Gallina Correa, Francielli Weber Santos Cibin, Irina Lubeck, Paulo Bayard Dias Goncalves, Thamiris Vieira Marsico

This study aimed to characterize the vaginal population of lactic acid bacteria (LAB) and local redox potential in response to the exposure to progesterone (P4) in the presence of estradiol benzoate (EB). For this purpose, ten prepubertal, 11-12 months old ewe lambs were randomly selected to receive (Group P4EB; n=5) or not (Group EB; n=5) 30 mg of long-acting injectable P4 (i.m.; Sincrogest, Ouro Fino, Brazil) on Day 0 (D0); on D5 all animals received 500 µg of EB (i.m.; Sincrodiol, Ouro Fino, Brazil). Weight did not vary between groups (P4: 26.4±3.61; P4EB: 28.78±3.61; p=0.65). Vaginal samples were collected (D0, D2 and D7) by a sterile swab, immersed in sterile saline, vortexed for 30 seconds and poured in triplicate on De Man, Rogosa and Sharpe agar. Plates were

incubated in an anaerobic chamber at 37°C for 72 hours when LAB colony-forming units were counted. Three months later, the experiment was repeated with the same animals, and vaginal washings were obtained (D0, D2, and D7) by infusion of 5 ml of sterile saline in the fornix, followed by recovery into a sterile tube, and storage at -20°C. Reactive oxygen species (ROS) content was assessed by incubation of the vaginal washing with 2', 7'-dichlorofluorescein diacetate (DCFDA) dye (i.e., expressed as arbitrary fluorescent units/mg of protein); antioxidant activity was determined by the ferric reducing antioxidant potential (FRAP) assay (i.e., expressed as µg equivalent of ascorbic acid/mg of protein), and the Bradford method was used to determine protein content. LAB and FRAP were log-transformed, whereas ROS and protein data were normally distributed. The effect of group was assessed as repeated measures data using the MIXED procedure. The main effects of group, day, and their interaction were determined by Student's t-test as posthoc analyses. The covariance structure with the lowest Akaike Information Criteria was used for each model. There was no effect of group or group*day interaction on the dependent variables ($p \ge 0.05$). Protein content was not affected by the tested main effects (p≥0.05). Day affected LAB, ROS and FRAP (p=0.01; p=0.0002; p=0.0004). LAB on D7 and D2 were greater than on D0, whereas D2 was not different from D7 (D0: 24.00±5.61; D2: 2829.33±1884.21; D7: 6899.67±3207.49 CFUs). ROS decreased on D2 and D7 in comparison to D0, with D2 not different from D7 (D0: 65.92±7.85; D2: 25.40±4.21; D7: 29.14±5.32 arbitrary fluorescence units/mg of protein). FRAP declined from D0 to D2 and increased from D2 to D7, but it did not vary from D0 to D7 (D0: 63.82±9.81; D2: 34.76±5.30; D7: 88.65±17.82 µg equivalent of ascorbic acid/mg of protein). Our results indicate that P4 does not influence the LAB population and redox potential of the vaginal environment. Despite the confounding effect between EB exposure and day, our data are suggestive of estrogen favoring the growth of the vaginal LAB population, while regulating the redox balance towards an antioxidant environment. Induced vaginal antioxidant potential, which may be due to estrogen-induced epithelium-derived antioxidant activity, may explain reduced vaginal ROS content. Acknowledgments: CAPES (código 001), FAPERGS, CNPg, FINEP.

Abstract # 1979

Protegrin 1 Regulates Porcine Granulosa Cell Proliferation Via The EGFR-ERK Signaling Pathway. Xiaoshu Zhan, Bo Pan, Canying Liu, Bingyun Wang, Julang Li

Antimicrobial peptides (AMPs) are traditionally known to be essential components in host defence via their broad activities against bacteria, fungi, viruses, and protozoa. Their immunomodulatory properties have also recently received considerable attention in mammalian somatic tissues of various species. However, little is known regarding the role of AMPs in the development and maturation of ovarian follicles. Protegrin1 (PG1) is an antimicrobial peptide which is expressed in neutrophils. We report that the PG1 is present in porcine ovarian follicular fluid in a follicular stage-dependent manner. However, RT-PCR analysis showed that the transcript of PG1 was barely detectable in granulosa cell of ovarian follicle, suggesting the PG1 may be derived from blood.

Treatment of granulosa cells with PG1 enhanced cell proliferation in a concentrationdependent manner (p<0.05). RT-PCR analysis revealed that the mitogenic effect of PG1 is accompanied by enhanced expression of cell-cycle progression related genes such as cyclin D1(CCND1), cyclin D2 (CCND2), and cyclin B1 (CCNB1). Additionally, Western blot analysis showed that PG1 increased phosphorylated-/total ERK1/2 ratio. The PG1 proliferation stimulating effect was blocked by pretreatment with U0126, a specific ERK1/2 phosphorylation inhibitor. Consistent with this finding, luciferase reporter assay also showed the activation of ERK1/2 by PG1 compared to controls (p<0.05), suggesting the antimicrobial peptide may regulate granulosa function via this pathway. Furthermore, PG1 increased phosphorylated EGFR while stimulating granulosa cell proliferation. Pretreatment with EGFR kinase inhibitor, AG1478, reversed the PG1 stimulation on both the phosphorylated EGFR and granulosa cell proliferation. Taken together, our data suggests PG1 may regulate granulosa cell proliferation via the EGFR-ERK signalling pathway. Our finding reveals a novel function of PG1 in the ovary, offers insights into the understanding of antimicrobial peptides on ovarian follicular development regulation.

Abstract # 2003

Follicle-Stimulating Hormone (FSH) Does Not Impact RANKL-Induced Osteoclastogenesis. Ziyue (Sabrina) Zhou, Luisina Ongaro, Daniel J. Bernard

Postmenopausal osteoporosis has been attributed to decreased estradiol levels. In the hypothalamic-pituitary-gonadal axis, estradiol synthesis is stimulated by folliclestimulating hormone (FSH). FSH is secreted from the anterior pituitary gland and estradiol feeds back to the hypothalamus and pituitary to suppress FSH production. In postmenopausal women, the loss of estradiol (and inhibin) negative feedback leads to elevated serum FSH levels. It was recently proposed that this increase in FSH also contributes to postmenopausal osteoporosis by stimulating differentiation and activation of bone-resorbing osteoclasts cells. If FSH does indeed have these noncanonical actions in bone, antagonism of FSH might represent an effective preventative measure or treatment for postmenopausal bone loss. Our objectives were to determine whether FSH has direct actions on osteoclast differentiation in vitro and, if so, its mechanism of action. First, a murine leukemic monocyte macrophage cell line, RAW 264.7, was differentiated into osteoclasts by treatment with receptor activator of nuclear factor kappa-B ligand (RANKL, 50 ng/ml) for seven days. As expected, we observed the appearance of osteoclasts, characterized as tartrate-resistant acid phosphatase (TRAP)-positive multinucleated cells. RANKL also induced expression of established osteoclast differentiation markers, including Rank, Trap, cathepsin K (Ctsk), and matrix metalloproteinase-9 (Mmp-9). The mRNA expression of FSH receptor (Fshr), however, was low to undetectable both before and after osteoclast differentiation. Co-treatment of RAW 264.7 cells with FSH (35, 70 and 140 IU/L) and RANKL did not further impact the expression of Rank, Trap, Ctsk, Mmp-9, or Fshr. Second, primary murine monocytes were differentiated into osteoclasts by treatment with RANKL (50

ng/ml) and macrophage colony-stimulating factor (M-CSF, 25 ng/ml) for five days. FSH co-treatment (70 and 140 IU/L) had no impact on the expression of osteoclast markers, and Fshr expression was low to undetectable both before and after osteoclast differentiation, consistent with the results from RAW 264.7 cells. In conclusion, in our hands, FSH does not impact RANKL-induced osteoclast differentiation in immortalized or primary murine monocytes. We are currently assessing whether and how FSH directly regulates bone resorption using a series of genetically-modified mouse strains.

Abstract # 2119

Androgen Increases the Half-life of Its Receptor Through Enhanced Nuclear Retention. Olga Astapova, Christina Seger, Stephen R. Hammes

Androgen plays important roles in both male and female reproduction, but the molecular actions of androgen particularly in female reproductive tissues are not fully understood. We have found that in human and mouse granulosa cells androgen increases the half-life of its own receptor protein by approximately four-fold, leading to significantly higher protein abundance of androgen receptor (AR) in the presence of its ligand. Using well-characterized inhibitors in mechanistic studies of human granulosalike KGN cells, we show that this effect of androgen is not the result of increased AR gene transcription or protein synthesis, nor is it fully explained by reduced proteasome degradation of AR. Activity of cytoplasmic kinases AKT, ERK, FAK or GSK is not involved in this mechanism. Knockdown of PTEN, which contributes to dearadation of cytoplasmic AR, did not diminish AR accumulation in the presence of DHT. Using immunofluorescence cellular localization studies, we show that nuclear AR is selectively protected from degradation in the presence of DHT. When nuclear import of AR is inhibited by knockdown of importin 7, DHT still leads to nuclear accumulation of AR, suggesting importin 7-independent nuclear import of AR in the presence of DHT. Taken together, our data indicate that ligand binding protects granulosa cell AR from degradation by the proteasome by enhancing its nuclear accumulation and/or retention, thereby sequestering AR from the cytoplasm. Further, we replicated these findings in human prostate cells, suggesting that this is a ubiquitous effect of androgen. This phenomenon may have physiological significance through a positive feedback in which androgen induces its own activity in male and female reproductive tissues.

Abstract # 2251

COUP-TFII Negatively Regulates Exosomal VEGF-C Secretion And Lymphangiogenesis In Endometriosis. Wan-Ning Li, Meng-Hsing Wu, Shaw-Jenq Tsai

Endometriosis is one of the most common gynecological disease in women of reproductive age and severely reduces fertility and life quality of affected women. Unfortunately, there is no cure for this disease due to insufficient understanding of the molecular etiology. Chicken ovalbumin upstream promoter transcription factor II (COUP-TFII), also known as nuclear receptor subfamily 2 group F member 2, is an orphan nuclear receptor, which plays a vital role in organogenesis, angiogenesis, energy metabolism and adipogenesis. Recent studies indicate COUP-TFII level is abundant in uterine endometrium but significantly reduced in ectopic endometriotic cells. This study was designed to elucidate the biological function of COUP-TFII in the disease etiology of endometriosis. Total RNA collected from human endometrial stromal cells with or without COUP-TFII knockdown were subjected to microarray analysis and differentially expressed genes were further analyzed by Gene Set Enrichment Analysis and cross-referenced with biological processes from Gene Ontology (GO) database. Results showed genes involved in vasculature development are enriched in COUP-TFII knockdown endometrial stromal cells and VEGF-C is one of the upregulated angiogenic genes under COUP-TFII knockdown. Molecular biological characterization demonstrated that COUP-TFII suppresses VEGF-C expression at the transcriptional level. Further studies showed that knockdown of COUP-TFII increases exosomal VEGF-C secretion and subsequently induces lymphatic endothelial proliferation and cell migration. In vivo study using autotransplanted mouse endometriosis model revealed that VEGF-C is elevated in ectopic endometriotic-like lesion. Accompanied with the elevation of VEGF-C are increased lymphangiogenesis, immune cells infiltration, and retroperitoneal lymph node enlargement, indicating local inflammation. Treatment with selective VEGFR inhibitor, lenvatinib, markedly inhibited lymphatic vessel formation, immune cell infiltration, and lymph node enlargements as well as caused endometriotic lesion regression. To translate this finding to clinical application, we evaluate the exosomal VEGF-C from sera of women with or without endometriosis and found exosomal VEGF-C is a good predictor for endometriosis. Taken all together, our study reveals a novel mechanism contributing to endometriosis progression and provide an alternative strategy for developing new treatment regimens for endometriosis.

Abstract # 2311

Mechanism of Action for Irilone as a Potentiator of Progesterone Receptor Signaling. Julia R. Austin, Jeongho Lee, Brian T. Murphy, Joanna E. Burdette

Regulation of progesterone signaling is important for reproductive function. When progesterone signaling is dysregulated, gynecological diseases can occur, for example endometriosis, uterine fibroids, and endometrial cancer. While these diseases are treated with progestin therapy, progestins can bind to multiple steroid receptors,

exerting side effects of weight gain, immunosuppression, cardiovascular disease, and stroke. Discovering an alternative progestin that is selective for the progesterone receptor (PR) is ideal. One potential source of such an alternative is botanical supplements, which have become increasingly popular among consumers with sales reaching \$8.8 billion in 2018. Although botanical supplements are popular, the chemical structures and biological action of botanical supplements would benefit from deeper scientific investigation. Studies of Trifolium pratense L. (red clover), primarily used for the treatment of menopausal symptoms, has identified phytoestrogen compounds as the chemicals that mitigate those symptoms. Interestingly, irilone, identified from red clover, potentiated progesterone signaling via a progesterone response element luciferase (PRE/Luc) assay. Potentiation is when a compound has no activity by itself but when combined with another molecule, i.e. progesterone, that compound enhances PR activity. Prior to irilone, a natural compound with the ability to potentiate progesterone signaling had not been previously reported. To uncover how irilone is acting, a potentiation PRE/Luc assay was conducted in Ishikawa PR-B and T47D cells. Irilone (10 µM) was combined with various concentrations of progesterone, ranging from 1 nM to 100 nM. In both cell lines, irilone significantly potentiated 5 nM P4. Next, irilone's ability to potentiate PR signaling was measured at an endogenous progesterone responsive gene. In Ishikawa PR-B cells, irilone was able to potentiate the progesterone responsive genes PDK4 and FKBP5 when irilone was combined with the progestin R5020. Since T47D cells contain estrogen receptor (ER) and PR is an ER target gene, irilone increasing total PR levels could be the mechanism of potentiation. To investigate this hypothesis, T47D cells were transfected with an estrogen response element luciferase reporter, and irilone (10 µM) significantly increased luciferase expression, suggesting estrogenic activity. Irilone was then combined with the selective estrogen receptor modulator, tamoxifen, and a PRE/Luc assay was performed with 5 nM P4 in T47D cells. When ER was blocked in T47D cells, irilone still potentiated PR signaling. Western blots were performed for PR degradation to determine if irilone could degrade PR. Irilone by itself and in combination with P4 induced PR expression. When irilone was combined with tamoxifen, PR expression was reduced, and irilone did not stabilize PR expression when combined with P4 and tamoxifen, indicating that irilone's effect on PR expression was through the ER. This indicates that PR degradation is ER regulated but PR gene activation is independent of ER. Irilone potentiating progesterone at progesterone responsive genes is occurring through another mechanism that is ER independent. Since irilone could be enhancing progesterone signaling by affecting post-translational modifications of PR, mass spectrometry will be performed to uncover these changes. Determining how irilone is potentiating progesterone will help us understand PR biology and could be an effective treatment for gynecological diseases.

Environmental Impacts on Reproduction

Abstract # 1744

Treatment Of Mouse Embryonic Stem Cells With Cigarette Smoke Extracts Resulted In The Inhibition Of Neural Differentiation And Their Development. Cho-Won Kim, Kyung-Chul Choi

Maternal smoking during the perinatal period is linked to adverse neonatal outcomes such as low birth weight and birth defects. Numerous studies have shown that cigarette smoke or nicotine exposure has a widespread effect on fetal nerve development. However, there exists a lack of understanding of what specific changes occur at the cellular level on persistent exposure to cigarette smoke during the differentiation of embryonic stem cells (ESCs) into neural cells. We previously investigated the effects of cigarette smoke extract (CSE) and its major component, nicotine, on the neural differentiation of mouse embryonic stem cells (mESCs). Differentiation of mESCs into neural progenitor cells (NPCs) or neural crest cells (NCCs) was induced with chemically defined media, and the cells were continuously exposed to CSE or nicotine during neural differentiation and development. Disturbed balance of the pluripotency state was observed in the NPCs, with consequent inhibition of neurite outgrowth and glial fibrillary acidic protein (GFAP) expression. These inhibitions correlated with the altered expression of proteins involved in the Notch-1 signaling pathways. The migration ability of NCCs was significantly decreased by CSE or nicotine exposure, which was associated with reduced protein expression of migration-related proteins. Taken together, we concluded that CSE and nicotine inhibit differentiation of mESCs into NPCs or NCCs, and may disrupt functional development of neural cells. These results imply that cigarette smoking during the perinatal period potentially inhibits neural differentiation and development of ESCs cells, leading to neonatal abnormal brain development and behavioral abnormalities.

Abstract # 1745

Investigating the effects of Fipronil on Male Fertility. Jeong-Won Bae, Woo-Sung Kwon

Fipronil (FPN) is a widely used phenylpyrazole pesticide for the control of insects and removal of veterinary pet fleas, ticks, etc. Although FPN presents moderate hazards to human health, people are readily exposed in daily life. In 2017, FPN was detected in chicken eggs in Europe and Korea. FPN acts by impairing the central nervous systems of insects by blocking gamma-aminobutyric acid (GABA) and glutamate-activated chloride (GluCI) channels. A previous study demonstrated that GABA and GABA A R are present in spermatozoa and play various roles in the process of sperm capacitation, which is required for fertilization. However, the effects of FPN on mammalian fertility are not yet fully understood. Therefore, the present study was designed to investigate the effects of FPN on spermatozoa. Herein, we treated various concentrations of FPN (0.1, 1, 10, 100, and 300 µM) or a control treatment with ICR mouse spermatozoa. Sperm

motility and motion kinematics were assessed using computer-assisted sperm analysis. Capacitation status was evaluated using combined Hoechst 33258/chlortetracycline fluorescence. Intracellular ATP and LDH generation were also measured. In addition, the PKA activity, protein tyrosine phosphorylation, as well as GABA A R B-3 and GABA A R B-3 pS408/pS409 were evaluated by Western blot analysis. Finally, in vitro fertilization was performed, and the cleavage and blastocyst formation rates were determined. FPN treatment significantly reduced sperm motility and motion kinematic parameters in a dose-dependent manner, whereas the acrosome reaction was enhanced. Intracellular ATP generation was significantly decreased in all treatment groups, and LDH was similar in all treatment compared with the control. Levels of phospho-PKA substrate and phospho-tyrosine substrate were significantly decreased in a dosedependent manner. Meanwhile, there was no difference between control and treatment aroups in the level of GABA A R B-3. Only the ratio of GABA A R B-3 pS408/pS409 was significantly decreased at higher concentrations of FPN (100 and 300 µM). Moreover, cleavage and blastocyst formation rates were also significantly decreased at 10, 100, and 300 µM FPN. Taken together, these data suggest that FPN can directly and indirectly suppress various sperm functions. Therefore, FPN can negatively affect male fertility leading to infertility. From these results, we suggest that the use of FPN as a pesticide requires robust regulation and caution. This work was supported by a National Research Foundation of Korea (NRF) arant funded by the Korea government (Ministry of Science and ICT) (NRF- 2019R1F1A1049216).

Abstract # 1935

Exposure to Concentrated Ambient Fine Particulate Matter (PM2.5) Depletes the Ovarian Follicle Reserve in Apolipoprotein E Null Mice. Ulrike Luderer, Jinhwan Lim, Laura Ortiz, Johnny D. Nguyen, Lisa Liao, Joyce H. Shin, Barrett Allen, David A. Herman, Michael T. Kleinman

Exposure of female mice to polycyclic aromatic hydrocarbons (PAHs) results in destruction of immature primordial and primary follicles. PM2.5 air pollution is rich in PAHs, which are adsorbed onto particle surfaces, but the effects of exposure to ambient PM2.5 on the ovaries have not been investigated. Ovarian follicles progress from a primordial stage through primary, secondary, antral and finally preovulatory stages. The finite pool of primordial follicles constitutes the total ovarian follicle reserve. We hypothesized that exposure to ambient PM2.5 induces DNA damage resulting in apoptotic death of ovarian follicles. 3-month old female Apolipoprotein E (ApoE) null mice were exposed to concentrated ambient PM2.5 or filtered air for 12 weeks, 5 days per week for 4h/day using a Versatile Aerosol Concentration Enrichment System. ApoE null mice have hypercholesterolemia and are predisposed to develop atherosclerotic plaques; these mice were part of a study investigating the ovarian and cardiovascular effects of PM2.5. Mice were euthanized on the day of proestrus of the estrous cycle 24h after the final exposure. One ovary per mouse was processed for follicle counts (N=14-15/group). Primordial and primary follicles were counted blind to treatment in every 4th

20 mm section on a stereology system using the optical fractionator method. Secondary and antral follicles were followed through every section. Primordial and primary follicle numbers were significantly decreased in PM2.5-exposed mice by 40% and 43% (P<0.05, t-test), respectively. Numbers of healthy secondary follicles were significantly decreased by 22% in PM2.5-exposed mice. Antral follicle counts were not significantly affected. We assessed follicular DNA damage by immunostaining for gH2AX, apoptotic death of follicles by immunostaining for activated caspase 3, and recruitment of primordial follicles into the growing pool by immunostaining for the mitosis marker Ki67. The percentages of primary follicles with gH2AX-positive granulosa cells were significantly increased. The percentages of follicles at each stage of development with granulosa cells positive for Ki67 or activated caspase 3 were not significantly different in the ovaries from PM2.5 versus filtered air-exposed mice. In summary, the irreplaceable ovarian follicle reserve was decreased by nearly half in PM2.5-exposed mice, and induction of DNA damage in follicles may play a role in follicle demise. Decreased ovarian reserve leads to premature ovarian failure, which increases the risk for cardiovascular disease in women. Thus, our data provide a potential link between ovarian and cardiovascular effects of exposure to PM2.5. Supported by California Air Resources Board, 16RD005.

Abstract # 1964

Early Impacts Of In Utero Exposure To Ethinylestradiol Or Genistein On Rat Perinatal Testis Development And Germ Cells Transcriptome. Laetitia L. Lecante, Bintou Gaye, Amelie R. Tremblay, Geraldine Delbes

Although the male fertility decline is believed to be partly driven by environmental exposures during critical developmental periods, the underlying molecular mechanisms are still poorly understood. Spermatogenesis is based on the self-renewing reservoir of spermatogonial stem cells (SSCs) established during perinatal life from the differentiation of fetal male germ cells named gonocytes. Studies have shown that fetal exposure to high doses of xenoestrogens can affect testis development, global gene expression and decrease gonocytes number, which could lead to long-term impairment of male fertility. But only very few studies evaluated repercussions of environmentally relevant doses of xenoestrogens and their specific impact on gonocytes transcriptome. We hypothesized that fetal exposure to xenoestrogens could have short term effects on gonocytes transcriptome and affect their differentiation. Germ cell-specific GFP (GCS-EGFP rats) transgenic Sprague Dawley dams were gavaged from gestational days (GD) 13 to 19 with $2 \mu g/kg/d$ of ethinylestradiol (EE2), 10 mg/kg/d of genistein (GE) or vehicle. Sampling was done at GD20 or on post-natal day (PND) 5 (n=4 litter/group/age). Pregnant dams exposed to EE2 gained 10% less weight during treatment compared to controls but none of the treatments affected the number of pups/litter, sex ratio, anogenital distance or progeny body and gonadal weights. Serum was collected from each male and pooled per litter to measure testosterone levels. Only GE significantly decreased circulating testosterone at GD20. At each stage, 2 testes per litter were collected and fixed for histological analyses. Others from that litter were pooled and dissociated to sort gonocytes. Using GCS-EGFP rats allowed to obtain purified gonocytes by fluorescence-activated cell sorting, with more than 90% purity. RNA were extracted from GFP-positive sorted cells and probed on Affymetrix Rat Gene 2.0 ST Arrays. Testicular histology was not altered and further quantification indicated that neither germ nor Sertoli cells densities were altered by treatments at both stages. Nevertheless, analysis of differentially expressed genes (DEG) (p<0.05; fold change 1.5) in GFP-positive cells showed that significant changes in the expression of 116 and 100 transcripts were induced by EE2 and GE respectively at GD20, and 276 and 160 transcripts respectively at PND5. Surprisingly, only about 1% were common between the two stages in each treatment. As well, in each stage, only about 6% were common between treatments suggesting different modes of action. Nevertheless, functional analysis of coding DEG revealed an overrepresentation of olfactory receptor activity in all groups. In parallel, many non-coding RNAs were affected by both treatments, representing more than 40% of DEG at GD20 and around 30% at PND5. Further analyses are ongoing to compare the effects on germ cells transcriptome to the somatic cells ones, using the GFP-negative sorted cells. Our data suggest that despite no immediate toxic effects, fetal exposure to xenoestrogens can modify germ cells transcriptome. The increased number of DEG from GD20 to PND5 while exposure has ended may suggest an imprint of early exposure that may impact their differentiation potentially altering future SSCs. This project is funded by Natural Sciences and Engineering Research Council of Canada.

Abstract # 2011

Whole-Genome Expression Of Ewe Lambs' Ovary, Primordial Follicle And Oocyte Size And Plasma AMH Levels Are Altered By Diet's Protein Level Plus Haemonchus Contortus Infection. Paula Suarez-Henriques, Camila Chaves, Horacio Montenegro, Danielle Gregorio Gomes Caldas, Siu Mui Tsai, Helder Louvandini

In ewes, the manipulation of nutrition can be an efficient management tool to improve ovarian performance. Helminth infection may cause an undesirable delay in puberty manifestation because it demands a higher amount of protein, which is required to repair the damage caused by the parasite in sheep's tissues and building the host's immune response. Helminths become resistant to drug therapy shortly after they are exposed to a new treatment, besides the contamination caused by anthelmintic drugs in ovine products, possibly affecting human health and the environment. We hypothesized that supplementing protein to pubertal females infected with Haemonchus contortus would improve their reproductive and clinical parameters. The objective of this study was to evaluate if reproductive parameters can be incremented with a more sustainable alternative than anthelmintic usage. In our experiment, we used a 2 x 2 factorial model where eighteen Santa Inês ewe lambs (Ovis aries) were treated with one of the two levels of dietetic protein (14% or 20%) for 92 days. After 45 days of being fed this diet, they were infected or not (control group) with 10000 Haemonchus contortus L3 larvae. Following 47 days of infection, the lambs had their left ovaries removed and we examined the ovary's whole gene expression through RNAseq, ovarian morphometrics through histological analysis and AMH plasma levels with an ELISA test, as well as other blood biochemical parameters. There was no statistically significant difference (Anova) related to age nor weight gain among the groups High Protein Infected (n=5), Low Protein Infected (n=5), High Protein Control (n=4) and Low Protein Control(n=4). In the analysis of plasma protein related to diet and infection in factorial Anova, the level of protein in the diet was significant (p=0.02). In Anova factorial analysis, with primordial follicle size as the dependent variable, and infection and diet as categorical factors, the result was significant for the interaction diet*infection (p=0.046) and in the same type of analysis for oocyte size, we found significance for diet (p=0.047). Plasma protein levels were also significantly related to primordial follicle size in multiple regression analysis (b*=0.70; p=0.04). We found a significant relationship between AMH and protein plasma levels in a multiple regression analysis (b*=0.628; p=0.05). The RNA-seq analysis generated a list of 49361 transcripts. Comparisons among High protein control and Low protein control presented 3568 differentially expressed gene transcripts (FDR p-value ≤ 0.05) related to angiogenesis(AMOTL1, MYOF; MYOF_3) fertilization process(OVGP1), follicle-stimulating hormone secretion(INHBA_1; INHBA_4), female gonadal development (FST-3; KIT_4; KITLG_2), steroid hormone synthesis(STAR_1), cell response to starvation(CRTC), chromatin remodeling(SMARCA;ARID1A;PBRM1), histone

methylation/demethylation(EZH2;KDM3;KDM2B;;ASH1L;KMT2C;KMT2B),cell response to nutrients and germ cell development(MTOR).The contrast between High protein infected and High protein control generated 248 differentially expressed genes and the contrast between Low protein infected and Low protein control 3467 differentially expressed genes being those genes in both groups a possible ovarian response to the infection. The analysis intersecting these two lists found 110 genes in common. Based on our results we conclude that supplementing protein had a positive impact on reproductive parameters in pubertal ewes despite being infected by Haemonchus contortus.

Abstract # 2033

Transposable Element Expression In Normal And Stressed Preimplantation Bovine Embryos. Natasha Martin, Reem Sabry, Laura Favetta, Jonathan LaMarre

The genome of virtually every eukaryotic organism contains transposable elements (TEs), which can constitute up to 80% of DNA in some species. One subtype of TE, known as Long Interspersed Element-1 (L1), has been identified as a potential driver of interindividual and interspecies genetic variation and has been the subject of intensive study in different species. L1 and other TEs such as Endogenous retrovirus (ERV) have the ability to change their position within DNA, leading to many potential consequences such as mutations and DNA breaks. Evidence is now emerging to suggest that the over-expression of TEs can lead to many problems with respect to fertility. Additionally, the

expression levels of the TEs and the TEs themselves vary in organisms at different stages of development. Normally, epigenetic factors such as DNA methylation and histone modification inhibit TE expression. However, these factors are removed during gamete and embryo development in a process called reprogramming. Importantly, environmental stressors can alter the transcriptional environment, which may lead to the over-expression of TEs. The current study investigates the hypothesis that environmental stressors cause changes in the expression levels of L1 and other TEs in the developing bovine oocyte and embryo with downstream consequences on fertility. The project aims are to analyze and quantify L1 and other TE expression levels in the maturing bovine oocyte and developing embryo in vitro under normal conditions and when exposed to environmental stressors. Cumulus-oocyte complexes (COCs) were aspirated from bovine ovarian follicles. The oocytes and embryos were collected at different stages of development. RT-qPCR was employed to quantify L1, BovB and ERV1 expression levels within the oocytes and embryos. Surprisingly, expression levels of TEs in metaphase II (MII) oocytes were altered in stressed embryos compared to controls. L1 expression levels in the 2-cell, 4-cell and blastocyst embryo stages are currently under investigation. The present study is directly relevant to the practice of agriculture but is also linked with human health as bovine oocytes and early embryos represent an excellent translational model for early human development. Overall these studies suggest that environmental factors can alter TE expression during early bovine development.

Abstract # 2043

Mycotoxins Induce Differential Autophagy Activation In Bovine Granulosa And Theca Cells. Hilda Morayma Guerrero-Netro, Christopher Alan Price

Mycotoxins commonly observed in animal feed in North America and Europe can have severe negative impacts on fertility. Deoxynivalenol (DON) and its metabolite deepoxy-DON (DOM1) have been shown to increase the rate of apoptosis in bovine granulosa (GC) and theca cells (TC) respectively, with TC being sensitive to low doses of DOM1. Apoptosis is associated with autophagy, which is a cell preservation process where damaged organelles are degraded by autophagosomes in order to avoid apoptosis. The signaling cascade to activate the formation of the autophagosome is through unc51-like autophagy activating kinase 1 (ULK-1) which phosphorylates beclin 1 (BECN1) promoting the recruitment of microtubule-associated protein 1A/1B-light chain 3 (LC3) to the autophagosome membrane. We tested the hypothesis that DON and DOM1 induce autophagy in GC and TC. Bovine granulosa and theca cells from follicles 3-5 mm diameter were placed in serum-free culture and challenged with DON and DOM-1, respectively. LC3 and BECN1 mRNA levels were measured by qPCR. LC3 protein levels were measured by western blot and immunofluorescence. Cell were also challenged with an ULK-1 inhibitor to measure apoptosis by Annexin V flow cytometry. Treatment with mycotoxin resulted in the significant increase of LC3 mRNA abundance at 48h and levels of both forms of protein (LC3-I and LC3_II) increased at 12 h after addition of DON (P<0.05) in GC. However, BECN1 was significantly up-regulated by DON in GC (P<0.05) but not by DOM-1 in TC. Culture with ULK-1 inhibitor significantly increased the proportion of apoptotic GC (P<0.05) but did not affect TC. These data demonstrate that pro-apoptotic mycotoxins induce autophagy in granulosa but not in theca cells; this may explain the sensitivity of theca cells to DOM-1. Supported by PAPIIT RA204518 (UNAM-Mexico) and NSERC (Canada).

Abstract # 2061

Paternal Alcohol Exposure Leads To Altered Sperm Epigenome And Fetal Growth Restriction. Yudhishtar S. Bedi, Tracy M. Clement, Michael C. Golding, Nicole Mehta

To better understand the contribution of paternal preconception alcohol exposure in fetal growth and development, we gave male C57BL/6J mice access to 10% ethanol (w/v) during the first four hours of their dark cycle for ten weeks to recreate a chronic binge exposure model, also known as the Drinking-in-the-Dark model (DID). These mice were then mated to alcohol-naive female mice and pregnancies were terminated at gestational day 16.5 to measure fetal and placental growth parameters. Male reproductive physiology and effects on sperm small non-coding RNA profiles were also assessed. This exposure had no significant effect on male reproductive physiology, sperm count, sperm DNA damage or chromatin integrity. Preconception alcohol exposure did lead to late-term fetal growth restriction and a significant drop in placental efficiency. This was correlated with a shift in the proportion of transfer RNAderived small RNA fragments (tRFs) and Piwi-interacting RNAs (piRNAs), two major classes of small non-coding RNAs present in sperm, as well as an altered enrichment of microRNAs 21, 30 and 142 in alcohol-exposed sperm. These findings suggest that environmental exposures can alter the sperm epigenetic landscape without effecting DNA damage and have robust contributions in fetal growth and development of the offspring.

Abstract # 2166

Systemic Inflammation In Beef Cows Is Associated With Delayed Puberty Attainment And Decreased Androgen Production In Small Follicles. Kerri A. Bochantin, Jessica A. Keane, Alexandria P. Snider, Scott G. Kurz, Jeffrey W. Bergman, Renee M. McFee, Andrea S. Cupp, Jennifer R. Wood

In livestock species, stressors, including inadequate nutrition, heat stress, and subclinical infection, are associated with systemic low-grade inflammation and infertility. Furthermore, increased ovarian inflammation impairs follicle growth and luteal function. When bovine theca cells are treated in vitro with TNFa, a well characterized proinflammatory cytokine, androgen production is decreased. Our hypothesis is that increased circulating TNFa concentrations are positively correlated with other circulating pro-inflammatory cytokines and negatively correlated with androgen concentrations in the follicular fluid of large and small follicles. To test this hypothesis, 34 cows were synchronized with 5ml Prostaglandin F2alpha (PG) 14 days apart and ovariectomized (OVX) 36 hr after last PG. An additional 16 cows were stimulated (six injections 35IU FSH 12 hours apart with PG at last FSH) and OVX 24 hours after PG. At OVX, blood plasma was collected and used for: cytokine array, TNFa ELISA, LPS-binding protein (LBP) ELISA, glucose assay, and insulin ELISA. Dominant (> 7mm) and small (< 5mm) follicular fluid was aspirated from the ovaries and frozen for P4 RIA and A4 ELISA. Cows (n=50) were categorized into upper (n=13) and lower (n=13) quartiles based on circulating TNFa concentrations. In the upper quartile (High-TNFa), there was a 15-fold increase (6988.6±1716.8pg/mL) in plasma TNFa compared to the lower quartile (CTL) (531.3±141.9pg/mL). Furthermore, there were positive correlations between TNFa and other circulating pro- and anti-inflammatory cytokines independent of quartile classification: IFNg (r = 0.65; p = 0.01), IL-13 (r = 0.94, p < 0.0001), IL-1F5 (r = 0.81; p = $(1 - 1)^{-1}$ (0.0004), IP-10 (r = 0.71, p = 0.0065), MIG (r = 0.7, p = 0.01), IL-1b (r = 0.61, p = 0.01) IL-17a (r = 0.58, p = 0.02), IL-21 (r = 0.49, p = 0.08). Thus, High-TNFa cows exhibit a systemic inflammatory response. Body weight, body conditioning score, and age were not different between High-TNFa and CTL cows. There were also no differences in LBP or glucose:insulin ratio, suggesting that the systemic inflammation in the High-TNFa cows was independent of intrinsic metabolic dysfunction or gut LPS leak. Interestingly, if the pubertal classification of a cow was non-cycling (defined in the UNL herd as delayed puberty and decreased reproductive performance), they tended $(c_{2,p} = 0.06)$ to be in the High-TNFa quartile. Furthermore, circulating TNFa concentration was decreased (1723±558.2pg/mL, n = 14; p=0.003) in cows that had a typical pubertal classification compared to non-cycling cows (8036±2510pg/mL, n=7). Follicular fluid androstenedione (A4) concentrations were decreased in follicles (>7mm) from High-TNFa (30.0±15.0ng/mL; n=6, p=0.07) compared to CTL (90.88±21.82ng/mL, n=17) cows. Likewise, A4 concentrations in follicles <5mm, were decreased when collected from High-TNFa (11.27±2.8ng/mL; n=4, p=0.03) compared to CTL cows (36.49±10.26ng/mL; n= 4). These results suggest that cows with delayed attainment of puberty may be more susceptible to environmental stressors resulting in low-grade chronic inflammation later in life. Decreases in androgen production of High TNFa cows suggests that systemic inflammation may be acting at the level of the ovary, causing alterations in steroidogenesis.

Abstract # 2184

Heat Stress Modulates The Inflammatory Response Of Bovine Endometrial Cells To Bacterial Components. Paula C. Molinari, John J. Bromfield

Uterine disease occurs in approximately 40% of postpartum dairy cows. Pathogenic bacteria in the uterus cause inflammation and tissue damage which results in reproductive impairment after the resolution of the disease. Bovine endometrial epithelial (BEND) cells exposed to bacterial components, such as lipopolysaccharide (LPS), increase the secretion of inflammatory cytokines including interleukin (IL)-1β, and

IL-6, and the chemokine IL-8. Heat stress of dairy cows reduces milk production and impairs fertility. Interestingly, the incidence and persistency of uterine disease is increased under heat stress conditions, which is independent of pathogen load in the reproductive tract. Heat stressed cows also display decreased immune function, characterized by reduced neutrophil phagocytosis and oxidative burst. This suggests that heat stress may increase uterine disease incidence by reducing immune function of cows. The effect of heat stress on bovine endometrial cell immune function has yet to be determined. We hypothesized that elevated temperature would alter the capacity of BEND cells to respond to bacterial components compared to cells under thermoneutral conditions. We exposed BEND cells to either medium alone, LPS, or PAM3CSK4 (1, 10, 100, 1000, or 10000 ng/mL) for 24 h at either 38.5°C (thermoneutral) or 41°C (heat stress). Expression of IL6, CXCL8 and HSPA1A was measured by qPCR. Exposure of BEND cells to LPS or PAM3CSK4 increased expression of IL6 and CXCL8 compared to medium alone controls. Interestingly, expression of HSPA1A was decreased in BEND cells exposed to LPS compared to medium alone. As expected, BEND cells cultured at 41°C increased expression of HSPA1A compared to cells cultured at 38.5°C, regardless of exposure to LPS or PAM3CSK4. Exposure of BEND cells to PAM3CSK4 at 41°C increased expression of HSPA1A compared to BEND cells exposed to PAM3CSK4 at 38.5°C, regardless of concentration. A moderate, but significant (P<0.05) increase in IL6 expression was observed in BEND cells exposed to 10 ng/mL of PAM3CSK4 at 41°C compared to cells exposed to PAM3CSK4 at 38.5°C. A similar tendency (P = 0.08) in IL6 expression was observed in BEND cells exposed to 100 or 10,000 ng/mL of PAM3CSK4 at 41°C compared to cells exposed to matching doses at 38.5°C. These data suggest that cellular heat stress can increase the responsiveness of BEND cells to bacterial components. Increased endometrial cell responsiveness to bacterial components due to elevated temperature may be a contributing factor to the development or persistency of uterine disease in heat stressed dairy cows. Further investigation is required to determine the mechanisms by which elevated temperature alters the responsiveness of BEND cells to bacterial components.

Abstract # 2199

Environmental Parameters May Increase Likelihood of Beef Heifers Classified with Earlier or Later Pubertal Attainment. Jessica A. Keane, Sarah R. Nafziger, Jeff W. Bergman, Scott G. Kurz, Alexandria P. Snider, Kerri A. Bochantin, Jennifer R. Wood, Robert A. Cushman, Adam F. Summers, Andrea S. Cupp

We have identified 4 pubertal classifications from 754 heifers born during 2012-2018: 1) Early-greater than 1 ng/ml of progesterone (P4) and continued cyclicity (317±4 days of age (DOA), n=143); 2) Typical (378±2 DOA, n=279) with continued cyclicity; 3) Start-Stop- P4≥1ng/ml at 265±4 but discontinued cyclicity (n=91); and 4) Non-Cycling - no occurrence of P4≥1ng/ml during sampling period (n=98). Heifers that achieved puberty with continued cyclicity had greater reproductive performance (Early and Typical) their first calving season. However, the distribution of heifers classified into each puberty category was different each year. Since genetics and environment impact physiological processes, we hypothesized that environmental factors at certain developmental periods: 1) gestation [July-March]; 2) parturition-weaning [March-October]; 3) weaning-breeding [October-May] would impact heifer classification each year. Environmental parameters (i.e. high temperature, rain-per-day-ratio, snowfall) were averaged each month and compared between years. Each environmental factor was standardized to a z-score identified as high (above the third quartile), average (within the first to third quartile), or low (below the first quartile) each year per animal within the developmental periods. Data were analyzed using z-scores and the GLIMMIX procedure of SAS to determine the impact of environmental parameters during each developmental timepoint on pubertal classifications. During gestation, the years that dams were exposed to high temperatures (high) their offspring were more often classified as Typical (p<0.0001) or Non-Cycling (p<0.0001) while in years dams were exposed to reduced high temperature (low) their offspring was more often classified as Early (p<0.0001) or Start-Stop (p=0.0016). For the weaning-breeding period, heifers classified as Early or Start-Stop were associated with years where there was reduced monthly high temperatures (p<0.04), lower rain-per-day-ratios (p<0.02), and greater monthly snowfall (p=0.001). Conversely, there were greater numbers of heifers classified as Typical or Non-Cycling heifers in years that had a greater rain-per-day-ratio (p<0.001) and reduced monthly snowfall (p=0.002). Taken together our data indicate that classification of heifers reaching 1 ng/ml of progesterone at reduced DOA (Early and Start-Stop) were from dams exposed to reduced high temperatures; whereas, heifers that reached puberty at greater DOA (Typical and Non-Cycling) had dams exposed to hot temperatures (high). After weaning, heifers classified as Early and Start-Stop were more often exposed to environments with reduced rain-per-day-ratios and greater snowfall which may have led to environmental stress inducing puberty. In contrast, females that took longer to become pubertal, Typical and Non-Cycling heifers, were more often classified in years with a greater rain-per-day-ratio and less snowfall. Start-Stop and Non-Cycling classified heifers have reduced reproductive performance in their first year of calving, thus, future research will determine how environmental impacts may interact with genetics and age of dam to affect puberty and subsequent reproductive performance. USDA is an equal opportunity provider and employer.

Abstract # 2238

Dietary Coconut Oil Improves Glucose Tolerance But Increases Theca Androstenedione Production In Response To Chorionic Gonadotropin In Obese Females. Payal A. Shah, Cassandra Skenandore, Camille Goblet, Kadden H. Kothmann, Anne Elizabeth Newell-Fugate

Obese women suffer not only from metabolic syndrome but also hyperandrogenemia. Many obese women struggle to lose weight through lifestyle choices such as a restricted calorie diet and exercise. A promising alternative to weight loss may be use of coconut oil to modulate metabolism and improve hyperandrogenemia in obese females. We hypothesized that female Ossabaw pigs fed a high fat-fructose diet with 9% of calories from coconut oil(COC) as opposed to lard(WSD) would have improvements in glucose tolerance as well as hyperandrogenemia due to decreased RNA transcript expression of steroidogenic enzymes and androstenedione ($\Delta 4$) from theca interna cells. We fed female Ossabaw pigs 2200 kcal of a control(n=6), or 5000 kcal of a lard(WSD; n=5) or coconut oil(COC; n=6) high fat diet for 9 estrous cycles(~ 7.5 months). To suppress folliculogenesis and steroidogenesis we administered of 45 mg orally of a synthetic progestogen (MATRIX [®], Merck Animal Health) per pig per day for 18 days starting at estrus(D1) of C8. On day 17, an intravenous(IV) catheter was placed in each pig. On day 18, while pigs were still on MATRIX, an ACTH stimulation of adrenal steroidogenesis was performed(data not shown). On day 19 chorionic gonadotropin(CG) stimulation of ovarian steroidogenesis was initiated as follows: withdrawal of MATRIX and administration of 7.5 ug/kg dexamethasone IM every 12 hours for 4 days (D 19-D 22). On day 20 at 8:00 AM(T0), blood was drawn and 3000 IU/m 2 CG (Chorulon; Merck Animal Health) was given IV. Fasting blood was collected at: 12, 24, 36, 48, 72, and 96 hours post-CG for serum $\Delta 4$. On day 23, a fasting intravenous glucose tolerance test(IVGTT) was performed. Animals were euthanized and tissue was snap frozen when animals had dominant follicles(5-7 mm) in C 9. gPCR was performed for the following genes in theca interna with GAPDH as a house keeping gene: 17 β HSD2, 17 & HSD3, CYP17 a 1, 3&HSD1. COC females tended to be more glucose tolerant(p = 0.07) and had lower serum insulin concentrations in response to a glucose bolus (p<0.001) than WSD females. There was a trend for WSD females to have higher CYP17 a 1 transcript expression levels in theca interna than control females (p = 0.09), whereas COC females tended to have lower 3BHSD1 transcript expression levels in theca interna than WSD females (p = 0.10). Administration of CG led to progressively increased secretion of and rostenedione in all treatments. Serum $\Delta 4$ for the COC females was higher than the control females 72 hours post-CG, and, unlike the control and WSD females serum $\Delta 4$ in the COC females dropped 96 hours post-CG. These data demonstrate that coconut oil, even as a part of a high fat diet, can improve glucose tolerance. Our findings suggest that coconut oil may affect steroidogenesis in theca interna at the level of 3BHSD1. On-going studies in our lab will assess the effect of insulin and LH on theca interna steroidogenesis in vitro.

Abstract # 2261

Aqueous Extract Of Rhus Trilobata Decreases The Damage Induced By Exposure To Sodium Arsenite In BALB/C Mice. Guillermo Eduardo Cuellar-Nevarez, Lourdes Ballinas-Casarrubias, Miguel Angel Flores-Villalobos, Carmen Gonzalez-Horta, Margarita Levario-Carrillo, Blanca Sanchez-Ramírez

Exposure to arsenic through drinking water is a health problem that could be related to cases of male infertility. Arsenic exposure causes testis damage decreasing steroidogenesis and affecting the spermatic indexes. Previous studies have

demonstrated that Rhus trilobata extracts contain a high level of antioxidants, such as quercetin and gallic acid. This study aimed to analyze whether the aqueous extract of Rhus trilobata stems suppress the damage induced by sodium arsenite in BALB/c mice. Mice were divided into five groups (n = 6): exposed to 7.5 mg/kg/day of sodium arsenite, treated or not with Vitamin C (100 mg/kg/day) or Rhus trilobata extract (200 mg/Kg/day), and controls not exposed treated with Rhus trilobata stems extract or without treatment, these were administrated in drinking water for 35 days. The results showed that the treatment with Vitamin C or with Rhus trilobata extract ameliorated the sperm count and viability, and reduced the percentage of abnormal sperms forms induced by sodium arsenite exposure, mainly abnormal tail. Moreover, Rhus trilobata improved the percentage of sperm head abnormalities concerning the control non exposed. Our results suggest that Rhus trilobata may prevent sperm damage like Vitamin C, and may be useful to improve male reproductive health. Exposure to arsenic in drinking water is a health problem that could be related to cases of male infertility. It has been demonstrated that a significant number of residents in southwest Chihuahua are chronically exposed to arsenic. Previous studies have shown that exposure to arsenic causes a decrease in sperm quantity and quality, in the levels of testosterone and tissue damage of the testicle. Rhus Trilobata is a regional plant of northern Mexico that has been used as a traditional treatment for cancers or leukemia. It has been demonstrated that the aqueous extract of Rhus trilobata has a high level of antioxidants. The aim of present study was to analyze the antioxidant effect of Rhus trilobata in BALB/c mice exposed to sodium arsenite orally. 30 2-month-old BALB/c mice were divided into 5 groups (n = 6): control, exposed to 7.5 mg/kg/day of sodium arsenite, treated or not with 100 mg/kg/day of Vitamin C or 200 mg/Kg/day of Rhus trilobata extract, and not exposed treated with Rhus trilobata extract. All treatments were administrated in drinking water for 35 days. Mice were sacrificed before anesthesia and sperm quality parameters were evaluated. Statistical analysis was performed using the Minitab[™] version 17 software. The results showed that the treatment with Vitamin C or with Rhus trilobata extract ameliorated the sperm count and viability and reduced the percentage of abnormal forms related to the exposure to sodium arsenite, mainly those related to abnormal tail, including the percentage of sperm head abnormalities with respect to the control. Our results suggest that Rhus trilobata may prevent sperm damage in a manner similar to Vitamin C.

Abstract # 2269

Proteomic Identification Of Molecular Pathways And Biomarkers Related To Porcine Seasonal Heat-Induced Infertility In Males. Kankanit Doungkamchan, John J. Parrish, David J. Miller

Although the effects of elevated testicular temperature on spermatogenesis have been studied for many years, the molecular events disturbed by testicular hyperthermia are uncertain. This is particularly important because infertility of a single male can impact hundreds or thousands of females due to artificial insemination. The two-fold purpose of

this study is to identify molecular pathways affected by testicular hyperthermia and develop potential sperm biomarkers to improve detection of reduced fertility. We conducted this study using 3 sibling pairs (n = 3) of boars housed under normal conditions. One boar from each pair was assigned to either control or heat-treated groups. The thermal insult was introduced to the heat-treated boars by applying insulated sacs over the scrotum for 48 hours. The control boars were treated the same except that the sacs lacked insulation. Temperature sensors demonstrated the insulated sacs increased scrotal temperature by 3-4° C. Semen was collected thrice weekly prior to and 2 months following insulation to minimize sperm mixing in the epididymis. Sperm motility was analyzed using CASA. Sperm morphology was analyzed after the samples were fixed and stained with Coomassie Blue G-250. Sperm proteins were extracted with 6M GuHCl prior to insulation and at Days 6, 24 and 60 after insulation was removed. As expected, the percentage of motile sperm and the percentage of progressively motile sperm decreased at Days 6 and 24 (p < 0.05) in boars following removal of insulated sacs. The percentage of morphologically normal sperm was also reduced at Days 6 and 24 (p < 0.05) in the testicular hyperthermia group. Proteins were identified using LC-MS/MS and bioinformatic analysis was completed using MaxQuant and Bioconductor. The analysis was completed using 881 proteins detected in at least 3 or more time points. The majority of proteins identified were catalytic activity proteins (45%), binding proteins (38%), and molecular function regulator proteins (5.5%). Abundance of a flagellar protein required for fertility (TTC29), a mitochondrial protein (AGXT2), and a proteasome protein (PSMD4) was increased in the scrotal insulated group compared to the control; however, Ts translation elongation factor (TSFM) was decreased at day 6 after insulation. Hyaluronan and proteoglycan link protein (HPLN1) and lactate dehydrogenase protein (LCHB) were increased in the heat-treated group compared to the control group at day 60. This study indicated that increased testicular temperature decreased the percentage of motile sperm, induced abnormal morphology, and altered the abundance of sperm proteins involved in flagellar function, metabolism, protein degradation, translation and extracellular matrix function. This project was supported by Aariculture and Food Research Initiative Competitive Grant no. 2019-67030-29244 from the USDA National Institute of Food and Agriculture.

Abstract # 2351

Investigating The Impact Of Chronic Multi-Generational Atrazine Exposure On Female Mouse Fertility. Jessica M. Stringer, Elyse OK Swindells, Amy Winship, Nadeen Zerafa, Deepak Adhikari, Jodi Flaws, Mark Green, Karla Hutt

Atrazine is one of the most widely used herbicides in the world, with 34,500 tonnes sprayed each year in the USA and 3,000 tonnes in Australia. As such, atrazine is a common ground and surface water contaminant and is banned in the European Union. Our research has shown that the female germline is exceedingly sensitive to the exposure to toxicants, at concentrations found in the environment. For the females of many species, perturbations caused by toxicants result not only in reproductive disorders, such as infertility and premature ovarian failure, but also in non-reproductive metabolic and health-related diseases. Of further concern is that these adverse effects can also be passed onto offspring. While accumulating evidence suggests that atrazine can have significant effects on reproductive processes, comprehensive analyses of the impact of environmentally relevant exposures on ovarian function and female fertility, as well as multigenerational effects are lacking. Using environmentally relevant concentrations of atrazine (0.02 ng/ml, a conservative contamination level in Australian waterways) we have continuously exposed female mice, via their drinking water, for three generations. Preliminary data suggests there was no significant difference in whole body or individual organ weights in animals from first, second or third generations (n=10-35 per generation/treatment). Similarly, there was no significant difference in body composition or bone density in third generation female animals. Control and atrazine treated breeding females aged 9-12 weeks (n=5/treatment/generation) produced a single litter, with no significant difference in the days to conception (Control 24.1±3.7, ATZ 24.2±7.2) or litter size (Control 6.2±2.24, ATZ 6.0±2.8). However, super-ovulating 6-month old third generation mice identified a significant reduction in the number of healthy mature MII oocytes (Control 10.6±0.9, n=5, ATZ 4.0±3.8, n=5, P<0.005). These data suggest that while very low doses of atrazine in our waterways may not manifest in obvious metabolic health defects such as obesity, there may be a significant impact on female fertility. To determine if atrazine exposure is associated with reduced ovarian reserve and premature ovarian ageing, follicle populations will be counted and assessed for increased levels of DNA damage and apoptosis. This study represents the first in-depth analysis of the impacts of chronic multi-generational atrazine exposure on female reproductive health. Understanding the effects of pervasive environmental toxicants on the ovary, oocytes, and female fertility is vital, as perturbations can result in reproductive disorders and systemic diseases in current and future generations.

Abstract # 2357

Enrichment Of Maternal Environment Induces A Tolerogenic Response In The Amniotic Fluid And Protects The Offspring Against An Inflammatory Challenge. Julieta A. Schander, Carolina Marvaldi, Fernando Correa, Federico Jensen, Ana Franchi

Maternal lifestyle affects both pregnancy outcome and maternal health. We previously demonstrated that the exposition to an enriched environment (EE), a non-invasive stimulus of the sensory pathway combined with voluntary physical activity, prevented pretern birth induced by the administration of bacterial lipopolysaccharide (LPS) in a mouse model. Furthermore, mothers exposed to EE presented less perinatal death when compared to control environment (CE, standard cages) and EE also reverted some of the deleterious effects of the LPS on the offspring development during the lactation period. The amniotic fluid (AF) exerts several functions during pregnancy. It protects the fetuses by not only cushioning it from outside pressures but also having immunological functions. The aim of the present study was to analyze physiological changes in the AF,

associated to the protective effects of the EE on the offspring exposed to LPS. Furthermore, we aimed to study the offspring metabolism when they reached adulthood.

Animals were housed in EE (or CE) cages during six weeks and then mated with CE males. On day 15 of pregnancy, LPS was administered and 8 hours later, one group of animals was sacrificed to collect amniotic fluid and several cytokines expression and cellular profile by flow cytometry were evaluated. Another group was allowed to came to term and the offspring was housed in CE till adulthood was reached. We found higher levels of IL-10, an anti-inflammatory cytokine, in AF from EE exposed females when compared to controls (p<0.05). It was not modified in any group by LPS treatment. In contrast, LPS induced a significant increase of IL-6 levels (p<0.05) (a proinflammatory cytokine) in AF from both groups. However, it was 3.6 times higher in CE exposed group when compared to EE. Furthermore, IL-22, involved in protective response against inflammation, was significantly increased by LPS in both groups (p<0.05), but it was 6.7 times higher in EE group. We analyzed the presence of B cells in the AF and found a higher percentage of this population in EE exposed mice compared to controls (p<0.05). On adult male offspring, we observed that the maternal enrichment of the environment modulated adipose tissue weight (p<0.05) and that the intrauterine inflammatory environment induced by LPS administration increased cholesterol and triglyceride serum levels. Those changes were not observed in female offspring. Our results suggest that the enrichment of maternal environment modulates the AF components and response to systemic LPS-administration, protecting the offspring. Furthermore, intrauterine environment exerts programming effects on adult offspring metabolism in a sex dependent manner.

Abstract # 2363

The Enrichment Of Maternal Environment Promotes Vascular Remodeling At The Maternal-Fetal Interface During Early Gestation In Mice. Fernanda L. de la Cruz Borthiry, Jimena S. Beltrame, Julieta A. Schander, María L. Ribeiro

First trimester events associated to implantation are crucial for pregnancy success. Defects in these processes have been associated to the onset of many obstetric pathologies. In particularly, failure in vascular remodeling at the maternal-fetal interface affects blood supply to the fetus and increases maternal blood pressure. Therefore, it has been correlated with preeclampsia and intrauterine growth restriction. Maternal lifestyle affects the development of pregnancy outcome. Furthermore, stress and physical activity have shown to improve pregnancy outcome. Furthermore, stress during gestation is associated with preeclampsia, which is linked to defective vascular remodeling at the early placenta. We have previously demonstrated that female mice exposed preconceptionally and during gestation to an enriched environment (EE) present higher reproductive efficiency in day 15 of gestation, compared to females maintained in control environment (CE) (80% vs 40%, p<0.05).

Based on these antecedents, we hypothesized that the EE regulates crucial events at early gestation that finally impact in the reproductive efficiency. Therefore, the aim of the present study was to investigate if EE exposure regulates vascular remodeling at the maternal-fetal interface. Six-week-old female mice were housed in EE or CE cages for six weeks, and then mated with CE fertile males. The EE strategy combines non-invasive stimulus of the sensory pathway with voluntary physical activity. Pregnant mice were sacrificed on day 7 of pregnancy (d7). In one group of animals, the implantation sites were collected to perform PCR, western blot and histological studies. In the other group of females, the uterine arteries were clamped after sacrifice, and the uterine horns and the associated vasculature were extracted to evaluate macrovasculature. We found an increase in the uterine artery cross length in EE females compared to CE females (p<0.05). When we analyzed the microvasculature of the implantation sites, no differences in the number or in the circumference of the vessels were detected. However, the wall:lumen ratio was lower in EE females' vessels, suggesting that EE exposure promotes the vascular remodeling of the implantation sites. Moreover, we observed that NOS activity and iNOS expression were increased in the implantation sites of EE housed females. Also, an increase in PGF 2 a production and in the expression of endoglin and VEGFR-1 was detected in EE group compared to control. No differences in the histological structure of the implantation sites were observed among the groups. Our results demonstrate that preconceptional and conceptional maternal exposure to EE promotes the remodeling of the vessels at the maternal-fetal interfase during early gestation in mice (d7). We propose that the improvement in vascular remodeling might be the cause of the increment in the reproductive efficiency observed in d15 of pregnancy. Therefore, the enrichment of the maternal environment might protect the progression of pregnancy and help to alleviate obstetric complications.

Epigenetic Regulation of Gene Expression

Abstract # 1681

Roles of MEK and SRC Signaling in Pronuclear Formation and Epigenetic Regulation After Fertilization in Mice. Shiho Naruto, Kazunori Magara, Ren Watanabe, Teruhiko Wakayama, Satoshi Kishigami

After fertilization, mammalian oocytes resume meiosis, leading to pronuclear (PN) formation and dynamic reprogramming of both male and female PNs. It has been known that MOS-MAPK pathway negatively regulates PN formation. Recently we found that zygotes treated with a MEK inhibitor, PD0325901 (MEKi) resulted in alterations in pronuclear size and histone modifications as well as earlier pronuclear formation, suggesting that cellular signaling play an important role in chromatin regulation after fertilization. But the other involving signaling factors are largely unknown. In this study, we examined the effects of SRC, MEK and Ribosomal S6 kinase (RSK) inhibitions on pronuclear formation and an epigenetic modification (H3K27me3) using IVF embryos. IVF were performed in HTF medium which contained each specific inhibitor: MEKi, CGP77675 (SRCi) for inhibition of SRC tyrosine kinase family (FYN, YES, SRC), and BI-D1870 (RSKi) for RSK inhibition. First, we found that SRC inhibition caused earlier PN formation although the effect was weaker than MEK and RSK inhibition (pronuclear formation rate 3 h after fertilization: control 15% vs MEKi 80% vs SRCi 35% vs RSKi 95%; P< 0.05). On the other hand, the size of the pronuclei and the level of H3K27me3 are mostly affected by MEK inhibition but not by RSK or Src inhibition (P< 0.01). These data indicate that regulation of PN size and histone modification is exclusively MEK-dependent. Remarkably, MEK showed nuclear localization (MEKnuc) during the one-cell stage, which was inhibited by MEKi but not SRCi or RSKi, suggesting that MEKnuc could be involved in histone modifications. Our data suggest that the MOS/MEK/RSK pathway is involved in regulation of the initiation of pronuclear formation, but MEK is also independently involved in normal chromatin formation in the pronucleus.

Abstract # 1846

Aberrant ERa Binding with Atypical Motif Enrichment and H3K27ac Accumulation Near Altered Uterine Genes in Adult Mice Exposed Neonatally to DES. Wendy N. Jefferson, Tianyuan Wang, Carmen J. Williams

Developmental exposure to the estrogenic chemical diethylstilbestrol (DES) induces extensive alterations in ERa-dependent histone H3K27ac association at enhancers of differentially expressed genes (DEGs) in neonatal uterine tissue. To determine if these features persist in adults, we used a global epigenomic approach. RNA-seq and ChIPseq was performed on mouse uteri collected from adult controls at diestrus (CoD) and estrus (CoE) and adults neonatally exposed to DES, who stay in persistent estrus. There were 4,161 DEGs between CoD and CoE, attributable to estrous cycle changes. Of those, 2,961 (71%) had differential ERa peaks (DERs) or differential H3K27ac peaks (DHRs) associated nearby (±100Kb). However, only 2,288 of these 21,144 DERs and 24,721 DHRs overlapped directly. Metaplots of ERa signal in both CoD in CoE were very similar but the H3K27ac associated with them was much higher when ERa was bound in CoE versus CoD, suggesting other factors play a role in H3K27ac binding. DES-exposed females exhibited three patterns of DEGs determined by EPIG analysis: 1) persistent estrus, where gene expression in DES was similar to CoE (1349 DEGs), 2) hormone insensitive, where gene expression in DES was similar to CoD (2322 DEGs) and 3) aberrant, where gene expression was unlike CoE or CoD (292 DEGs). A large percentage of DEGs in each category had DERs and/or DHRs nearby but less than 10% overlapped. Excessive accumulation of H3K27ac was seen near DEGs in patterns 1 and 3, particularly in up-regulated genes. Analysis of H3K27ac signal at the TSS of DEGs showed large decreases in H3K27ac at down-regulated genes but little difference at up-regulated genes. The most striking finding was increased ERa signal near DEGs in DES-exposed mice compared to CoE or CoD in both up- and down-regulated genes across all three patterns. A comparison of the 3,963 adult DEGs (all three patterns combined) with 4,498 DEGs observed on PND5 between control and DES-exposed mice revealed 2,083 (53%) were persistently altered and 86% of these 2,083 genes had DERs and/or DHRs nearby. In addition, approximately 17% of PND5 DERs and aberrant adult DERs overlap, suggesting a permanent change in ERa association in some locations. To understand differences in ERa binding between adult groups, we performed a motif analysis of ERa binding in CoD, CoE and DES-exposed mice. There were 60 enriched transcription factor binding motifs at ERa peaks in DES-exposed mice that were not found in either CoD or CoE. These data suggest that aberrant ERa and H3K27ac binding associated with aberrant binding of additional transcription factors drives the permanent alteration of gene expression in DES-exposed uteri.

Genome-Wide DNA Methylation Reprogramming In Porcine Primordial Germ Cells. Isabel Gómez-Redondo, Benjamín Planells, Sebastián Cánovas, Elena Ivanova, Gavin Kelsey, Alfonso Gutiérrez-Adán

The dynamics of DNA methylation reprogramming of primordial germ cells (PGCs) has been analyzed in mice, showing genome-wide erasure of DNA methylation and reestablishment of epigenetic marks; however, some retrotransposons elements (IAPs) remained substantially methylated during reprogramming, suggesting a mechanism of transgenerational epigenetic inheritance. In pig, there is scarce information about this process. The objective of this study was to unravel the methylation profile of porcine PGCs during the timing of reprogramming. For this purpose, sows were artificially inseminated and slaughtered at a commercial slaughterhouse 28 (n=2), 32 (n=2), 36 (n=2), 39 (n=2) and 42 (n=2) days later. At each time point, genital ridges were dissected from mesonephros and PGCs were isolated through magnetic activated cell sorting (MACS), using anti-SSEA-1 antibody. The sex of the fetuses was determined by PCR, using genomic DNA extracted from the tail tips. Then, recovered PGCs from 3 male and 3 female fetuses at each day were selected for whole-genome bisulfite sequencing, using an adaptation of the post-bisulfite adaptor tagging method (PBAT). Methylation levels were quantified using Segmonk software by performing an unbiased analysis, and similarly methylated regions (SMRs) were determined by filtering those probes with a difference below 1% in each pairwise comparison for each sex (D28 vs D32, D32 vs D36, D36 vs D39 and D39 vs D42). We observed that some elements (CpGs, promoters, exons, introns, and highly repetitive elements), have a drop of methylation levels starting at day 32, showing the lowest levels on day 36, and recovering it at day 42. However, we found that 1090 regions remained similarly methylated (SMRs) in males and 1015 in females. Repetitive elements (SINE, LINE and LTR) located within the identified SMRs showed a high level of methylation (~60% of elements presented a level of methylation higher than 50% in males, and ~40% in females). LTRs are particularly resistant to demethylation, being ~70% of them highly methylated both in male and female. Interestingly, 10% of the first introns located in these SMRs are also highly methylated, which could imply a regulation of expression of these genes. A detailed analysis allowed to identify several genes which remained highly methylated in one sex, but not in the other, (i.e. BCR, GIT1, DISP3 remain methylated in male PGCs; ERI3, RAB11FIP4, MARK4 in female PGCs). Further investigation is needed to confirm the potential role of these genes in the regulation of sex determination and gonad differentiation. This study reveals the methylation reprogramming profile of porcine PGCs, provides a deeper insight of the implication of epigenetics during sex determination, and identifies some genomic elements that may be candidates for transgenerational inheritance in porcine. Research supported by the Spanish Ministry of Science through BES-2016-077794 predoctoral grant.

Erk1/2 Pathway Modulates H3k4me3 At Promoters Of Lh Regulated Genes During Ovulation. Ejimedo Madogwe, Raj Duggavathi

The preovulatory luteinizing hormone (LH) surge regulates ovulation through a unique gene expression program in granulosa cells of the ovulating follicle. Histone modifications such as trimethylation of lysine 4 of histone 3 (H3K4me3) are associated with gene transcription. The extracellular signal-regulated kinases 1 and 2 (ERK1/2) signaling pathway in granulosa cells has been shown to be essential for LH surgeregulated gene expression. We hypothesized that LH regulates ovulatory genes through H3K4me3 and ERK1/2 modulates the H3K4me3 deposition at LH-regulated genes. First, we collected granulosa cells from immature mice superovulated with eCG and hCG (5 IU, i.p.), before (0h) or 4h after hCG treatment. We profiled the LH-regulated transcriptome using RNA sequencing (n = 3 replicates per timepoint) and found 4873 differentially regulated genes at 4h hCG compared to 0h hCG (FDR < 0.05; log fold change > 1). We then employed chromatin immunoprecipitation and sequencing to explore the H3K4me3 profile prior to (0h) and 4h after hCG treatment (n = 2 replicates per timepoint). There was an increase (from 66.2% to 82.6%) in the number of H3K4me3 peaks at promoter regions at 4h hCG compared to 0h hCG. About a quarter (1198) of the LH-regulated genes, including Pgr, Ptgs2, Star, Tnfaip6, had differential enrichment of H3K4me3 at their promoters. Of these, we found higher mRNA levels as well as higher H3K4me3 deposition at the promoters for 768 genes (including Star and Pgr); while 75 genes showed lower mRNA abundance and lower H3K4me3 enrichment (including Inhbb and Nppc). Next, we analyzed the transcriptome profile of granulosa cells collected at 4h post-hCG from mice treated with vehicle or the MEK inhibitor PD0325901 (n = 3 replicates per group). There were 2504 genes that were differentially regulated in granulosa cells of PD0325901-treated compared to vehicle-treated mice (FDR < 0.05; log fold change > 1). The top LH enriched KEGG pathways identified by EGSEA included ERK1/2 signaling, TNF signaling, VEGF signaling, chemokine signaling, and transcriptional misregulation in cancer; these pathways showed decreased enrichment when ERK1/2 was inhibited (p < 0.05). We found a similar pattern with the top molecular and cellular functions and the top physiological processes including cellular movement and organization, tissue morphology and immune processes, where the LH surge resulted in an enrichment of these functions whereas ERK1/2 inhibition resulted in a decrease. Among the 2504 ERK1/2 dependent genes, 609 genes were LH-regulated genes with differential H3K4me3 deposition at their promoters. We confirmed these results using ChIP-qPCR analysis for important genes regulated during ovulation including Star, Pgr, Ptgs2, Sult1e1, Infaip6, Timp1 and Cyp19a1 (P < 0.05). The pathways enriched among these 609 genes included inflammation, gonadotropin releasing hormone receptor, integrin signaling and interleukin signaling (P < 0.05). These data demonstrate that ERK1/2 inhibition altered the LH-surge regulated genes and pathways as well as H3K4me3 enrichment thereby disrupting ovulatory events. In conclusion, these findings implicate ERK1/2 pathway in modulating H3K4me3 deposition on the LHregulated ovulatory genes in granulosa cells.

Unraveling The Landscape Of Mitochondrial Mtdna Methylation In Bovine Oocytes And Embryos. Camila Bde Lima, Marc-André Sirard

In several mammalian species, accumulation of thousands of mitochondria during oocyte maturation represents an investment of the cell, as it will be able to better support ATP demand until mitochondria replication is reinitiated at morulae stage. The production of ATP occurs essentially through oxidative phosphorylation, which is dependent on mitochondrial DNA. Recently, mtDNA has gained more attention as changes in its structure and sequence were associated with mitochondrial dysfunction and thereby the pathogenesis of metabolic diseases. With the improvement of detection techniques, recent studies proposed that mtDNA is subjected to cytosine methylation, which can influence mitochondrial gene expression and function. Given the relevance of mitochondria for oocyte maturation and formation of the embryo, it is important to comprehend the mtDNA epigenetic dynamics and distribution. For this purpose, GV-stage oocytes were collected from abattoir ovaries or from OPU, and then matured, fertilized and cultured in vitro up to blastocyst stage (Day 7). Methylation profile of mtDNA was characterized by WGBS. Transcription profile was obtained from RNA-Seg data (GEO Series GSE52415). Statistical analysis considered a=5%. Global methylation level of OPU-oocytes is lower when compared to abattoir oocytes (10.09 vs. 16.04%; p<0.000), and this is reflected in the total methylation of derived blastocysts (20.04 vs. 23.55%, respectively; p<0.000). In terms of distribution, the highest methylation levels were found in the regions coding for respiratory chain enzymes (ND1, ND2, ND3, ND4, ND5 and ND6) and ATPases (ATP8 and ATP6) of blastocysts, especially those derived from OPU-oocytes. Further investigation revealed that total methylation level is negatively correlated with expression of mitochondrial genes in OPU samples (r= -0,71 and -0.73; oocytes and blastocysts, respectively), but this strong correlation was not maintained in vitro (r= -0,31 and -0.21, respectively). Average methylation level was also significantly increased in the light strand in all gene regions comparing to the heavy strand of mtDNA, but surprisingly, there was little strand-specific correlation with gene expression in all groups, indicating that methylation of both strands together may be essential for transcriptional machinery recognition and control. These results reinforce the existence of a specific epigenetic regulation of mitochondrial function. With a less methylated mtDNA, oocytes can better support mitochondrial biogenesis during maturation and energy demand postfertilization. On the other hand, although blastocysts have a high energy demand, ATP can be obtained from other sources, allowing for a more restrictive regulation of mitochondrial genes. The high correlation observed between methylation and transcription in OPU oocytes and the derived blastocysts is a quite unique phenomenon, but the loss of such correlation observed in abattoir samples indicates a possible dysregulation in the maturation of mitochondria during maternal-embryo transition. Finally, the comprehension of the profound interaction between mitoepigenetics and metabolism can provide a whole new set of metabolic tools for the improvement of existing culture systems and biomarkers for metabolic diseases.

The Effect Of General Anesthesia On Germ Cells. Margaret Rose McCoy, Lindsey Banks, Melissa Pepling

Halothane was widely used as an anesthetic between 1950 and 1980, including pregnant women undergoing surgery and during birth to relax the uterus and act as an analgesic. However, very limited work has been done to assess the effect of anesthetic exposure on germ cells. There is anecdotal evidence that suggests in utero exposure to general anesthetics may cause cognitive defects in subsequent generations; possibly due to aberrant methylation of the exposed germ cells. A previous mouse study showed that embryonic exposure to halothane anesthesia affected the offspring's cognitive ability to learn. Although this finding was significant, genetic and epigenetic tools were not as powerful as they are today, so no biological mechanism could be determined. When a pregnant woman is exposed to a toxin, such as an anesthetic, three individuals are exposed, herself (F0), her offspring (F1) and her offspring's germ cells (F2). In this study, we are investigating if germ cell exposure to halothane anesthesia has intergenerational cognitive behavioral effects. Gestating female mice were exposed to 1.5% halothane anesthesia for 30 minutes and control mice were exposed to oxygen. The F1 offspring were subjected to three behavioral tests between 10 and 16 weeks of age. The behavioral tests included: the elevated plus maze to test for anxious behavior, social approach to assess sociability, and object placement to test learning and memory test. A subset of the F1 mice were used for gamete collection at 13 weeks of age. Genomic DNA was collected and used for reduced representation bisulfite sequencing to capture the methylome of the exposed gametes. Halothane treated F1 mice were then mated with unexposed mice to produce the F2 generation from both maternal and paternal exposure. The same behavioral tests were repeated with the F2 generation. There was no significant difference between control and halothane treated groups in the F1 generation in the three behavior tests. This was not unexpected as our hypothesis is that the exposure affected the germ cells that give rise to the F2 generation and thus would not affect the F1 generation. For the social approach test, both F1 treatment groups showed preference for the mouse chamber, exhibiting sociability. While not significant, there was a positive trend in which the control group spent more time in the mouse chamber than the halothane group (the trend was more pronounced between male treatment groups), demonstrating that they may be more socially inclined. As for object placement, neither group indicated successful learning or memory. Data analysis is currently underway for methylome results, as well as the F2 behavioral testing, for evaluation of the intergenerational effects of halothane.

Identification of SWI/SNF Chromatin Remodeling Complex GBAF Subunits BRD9 and GLTSCR1 in Porcine Oocytes, Embryos, and Cell Lines. Sarah Innis, Aktan Alpsoy, Jennifer Crodian, Yu-Chun Tseng, Ryan Cabot, Emily Dykhuizen, Birgit Cabot

The mammalian switch/sucrose-non-fermenting (SWI/SNF) chromatin remodeling subcomplexes BAF, PBAF, and GBAF play crucial roles in regulating gene expression and modulating chromatin architecture, among other processes. Each complex contains a central ATPase (BRG1 or BRM) and several accessory BAF (BRM/BRG1 Associated Factor) subunits. A core group of accessory subunits is shared among these complexes, but each complex is distinguishable by the presence of unique constituent accessory subunits. Within the context of porcine early embryonic development, BAF and PBAF subunit localization and expression has been studied under both in vivo and in vitro conditions. However, while GBAF has been identified and characterized in murine and human cell lines, it has not yet been identified in porcine embryos or cell lines. Using immunocytochemistry and confocal microscopy, we identify here the expression and localization of the unique GBAF subunits Bromodomain-containing protein 9 (BRD9) and Glioma tumor suppressor candidate region gene 1 (GLTSCR1) in porcine oocytes and cleavage stage embryos derived from in vitro fertilization. In germinal vesicle stage oocytes, and both four-cell and blastocyst stage embryos, BRD9 and GLTSCR1 signal localization was ubiquitous, with slight enrichment in the nucleus. Using immunoprecipitation enrichment and Western blotting techniques, we also report the identification of GLTSCR1 in porcine trophectoderm and fetal fibroblast cells. Taken together, these results suggest the presence of the SWI/SNF chromatin remodeling subcomplex GBAF in various porcine early development stages and provide a precedent for future investigations into the specific role(s) GBAF may play within critical early development timepoints.

Abstract # 2183

BVDV Infection Epigenetically Alters T-Cell Transcription Factors In Persistently Infected Fetal Spleens. Hanah M. Georges, Hana Van Campen, Thomas R. Hansen

Maternal infection with Bovine Viral Diarrhea Virus (BVDV) has life-long negative effects on progeny. Despite current preventative measures, BVDV continues to be an issue, costing the industry \$1.5 billion annually and producing infected calves that remain the primary reservoirs of the virus. If fetal infection occurs prior to day 120 of gestation, then the fetus becomes persistently infected (PI) and sheds the virus throughout its life. The mechanisms of persistent infection and impact on postnatal health is still not well known. Previous in vivo studies revealed a substantial activation of the PI fetal innate immune response 22 days after maternal infection. The innate immune activation was then followed by an attenuation of both the innate and adaptive immune branches 115 days after maternal infection. It was concluded that attenuation of the immune system was caused by a lack of T-cell response in the fetus, resulting in an inability for T- cells and B-cells to mature properly. In this study, it was hypothesized that T-cell activation and signaling genes were epigenetically altered after fetal infection, thus impairing the expression of key genes of the innate and adaptive immune responses Splenic tissue from PI and control fetuses were collected on day 245 of gestation, 170 days post-maternal infection. DNA was isolated and sent to Zymo Research for reduced representation bisulfite sequencing. Methylation sequencing files were aligned to the bovine ARS-UCD-1.2 genome using the Bismark package, then processed and analyzed using the methylKit R package. Differentially methylated regions (DMR) were selected based on a 25% difference in methylation compared to controls as well as a p-value cutoff of < 0.05. Within these parameters, 2,641 regions were differentially methylated: 1,951 hypermethylated and 691 hypomethylated regions. Results revealed hypermethylation of nuclear factor of activated T cells (NFAT) 1 and 4, while NFAT2 was hypomethylated. Calcium signaling components, calcium release activated calcium channel protein ORAI and calmodulin, were hypomethylated. Additionally, signal transducer guanine nucleotide exchange factor VAV1 was hypermethylated. Calcium regulated NFAT family members consist of NFAT 1,2, and 4. The NFAT family is critical in Tcell activation/anergy as well as cardiac development. NFAT 1 and 4 are associated with T helper (Th) 1 cell differentiation, while NFAT 2 is associated with Th2 cell differentiation. Hypermethylation of NFAT 1 and 4 is likely to shift the Th cell differentiation from Th1 to Th2 cells. An increase in NFAT2 and VAV1 expression due to hypomethylation would promote anergy of T-cells, further exacerbating the shift from Th1 to Th2 cells. This shift of Th cells is associated with T-cell receptor hyper-reactivity and lymphoproliferative disorder. Additionally, the hypomethylation of ORAI and calmodulin may contribute to the Th2 hyper-reactivity by increasing the amount of calcium transported into a cell upon T-cell activation. The observed epigenetic modification of critical T-cell genes may help explain inability of postnatal PI calves to fight secondary infections efficiently, contributing to performance loss and continued BVDV viral shedding. This work is supported by: USDA AFRI NIFA Predoctoral Fellowship 2019-67011-29539/1019321, 2016-38420-25289 and W3112 Project.

Abstract # 2235

A Novel Method for Collection and Preservation of Newborn Screening Specimens at Ambient Temperatures. Neha Nayak, Yolanda Taverner, Jenny Mantyla, Subhendu Das, Xinqiang Li, Nihar Nayak, Zhibing Zhang, Pravansu Mohanty

Newborn screening specimens are collected for nearly every infant born in the US and globally in order to routinely screen for a variety of disease conditions. Testing of these specimens not only yields critical information regarding the risk for inherited conditions, but also represents a unique opportunity to investigate the influences of in utero exposure on newborns and has the potential to provide information critical to understanding the antecedents of both child and adult diseases. Indeed, the use of residual newborn screening specimens in research has generated significant direct public health benefits. These blood specimens are usually obtained on a filter paper

and the unused (residual) portions are stored in biorepositories in unrefrigerated conditions. Although RNA transcripts have been identified from these blood spots, the deterioration of the quality of RNA in these specimens makes them unsuitable for advanced gene expression analysis. In this study, we examined the effect of Upkara Inc.'s proprietary vitrification process on the quality of RNAs recovered from Jurkat T cells and blood spotted on membranes stored at room temperature and at 55 o C for various storage periods. Analysis of RNA integrity, 28S/18S rRNA, and quantitative real-time PCR (qRT-PCR) analysis for representative genes, including GAPDH, IL-10, and vascular endothelial growth factor, revealed persistently high RNA quality from all samples stored at varying temperatures (including samples stored at 55 o C). Thus, we concluded that Upkara Inc's proprietary vitrification process fully preserved RNA quality on membrane spots, even those stored at 55 o C, and provides a reliable method for future collection and preservation of newborn screening specimens at ambient temperatures.

Abstract # 2268

XIST DMR Methylation Levels And Knockdown In Bovine Somatic Cells And SCNT-Derived Embryos. Rafael Vilar Sampaio, Luis Aguila, Jacinthe Therrien, Lawrence Charles Smith

XIST (X-inactive specific transcript) is a long non-coding RNA responsible for the random inactivation of one X chromosome during the development of the female conceptus in placental mammal. During early development in mice, female XX embryos achieve Xchromosome dosage compensation by inactivating exclusively the paternal X chromosome. Apart from XIST expression, other epigenetic mechanisms are involved such as DNA methylation and histone modification. Abnormal X inactivation has been described with assisted reproductive techniques as somatic cell nuclear transfer (SCNT) using both female and male cells. Albeit well characterized in mice, little is known about XIST function in large domestic animals produced in vitro (IVF) and by SCNT. Thus, the overall goal of this work is to investigate the role of XIST during X chromosome inactivation (XCI) in somatic cells and embryos derived by IVF and SCNT. Specifically, we will utilize a small interference RNA (siRNA) approach to investigate the consequence of XIST knockdown in both IVF and SCNT embryo production on XCI and the role of DNA methylation of the XIST differentially methylated region (DMR) and its relationship to the Barr body formation using H3K27me3 immunostaining. We first analyzed the levels of methylation of the XIST DMR in male and female fibroblasts, spermatozoa, oocytes, and embryos at the morula and blastocyst stage. Our results showed that the XIST DMR in sperm, oocytes, and both morula and blastocyst stage embryos were hypomethylated, while the female and male fibroblasts showed around 50% and 92% of methylation, respectively. We then examined the effects of 3 different siRNAs, and obtained a significant downregulation of XIST using fibroblasts. Finally, we performed SCNT using female fibroblast donor cells transfected with the most efficient XIST siRNA (60% reduction of the XIST) and a scramble siRNA as a negative control. After

three replicates, we showed that the blastocyst development rates of SCNT oocytes reconstructed with donor cells were similar among control and XIST knockdown groups (12.3% ±6.4 vs. 12.7% ±6.3, p =0.9), indicating that XIST downregulation in the donor cells does not affect development to the blastocyst stage after SCNT. Further studies are planned to examine the effects of XIST knockdown on its DMR and the patterns of H3K27me3 using male fibroblasts and IVF embryos. These results present a unique opportunity to investigate the epigenetic control of X inactivation in bovine embryos. Financial support from NSERC Canada with Boviteq Inc (LS) and a postdoctoral fellowship from Mitacs/Boviteq (RS).

Fertilization/Egg Activation

Abstract # 1625

Zinc Interacting Protein Profile Changes During In Vitro Capacitation Of Boar Spermatozoa. Michal Zigo, Karl Kerns, Sidhart Sen, Clement Essien, Dong Xu, Peter Sutovsky

Recently discovered zinc signatures in mammalian spermatozoa and their changes during in vitro sperm capacitation (IVC) gave us an impulse to closely study zinc interacting proteins (further zincoproteins) and their changes during IVC. To study the boar sperm zincoproteome, we gently isolated sperm proteins in non-denaturing conditions and performed Immobilized Metal ion (Zn2+) Affinity Chromatography (IMAC) purification. Non-specific binding was checked by performing IMAC after Zn2+ chelation with 50 mM EDTA from both sperm protein extract and the IMAC column. Purified zincoproteins from ejaculated and capacitated spermatozoa were analyzed by quantitative LC-MS. We identified 2,650 zincoproteins, out of which we found 124 zincoproteins to differ in amounts significantly (P<0.05) between ejaculated and capacitated sperm zincoproteomes. By pathway analysis, the significantly different zincoproteins have a function in sperm tail structure (41 %), in the cytoskeleton (33 %), in gamete recognition and binding (23 %) and the rest in energy metabolism. We also analyzed chemical-protein interaction networks of known genes that encode zincoproteins from the STITCH database and compared them to the gene sequences of IMAC-identified zincoproteins. A total of 181 (5.1%) genes were shared between IMAC and STITCH chemical-protein interaction networks. The significantly different zincoproteins between ejaculated and capacitated spermatozoa are prime candidates for processing and regulation during sperm capacitation. The next logical steps will be a prediction of zinc-binding sites by in silico analysis and pathway analysis to determine how these proteins may interplay during capacitation. Supported by USDA-NIFA grants 2013-68004-20364, 2016-67015-24923, 2017-67015-26760 (JT, PS), 2013-68004-20365 (PS), and 2019-67012-29714 (KK), and MU F21C Program (PS). Keywords: Sperm Capacitation, Zincoproteins, Zincoproteome

Abstract # 1669

Unveiling the Proteome of Sperm-Oocyte Plasma Membrane Interaction Using a Porcine Model. Javier I. Vazquez Morales, Trish Berger

The underlying molecular interactions between sperm and oocyte plasma membranes before gamete fusion are poorly understood. Some tetraspanins, ADAM proteins, proteins of the complement system, and the lzumo1/FolR4 pair have been reported to be involved in mammalian fertilization. We hypothesize that there are additional, as yet unknown plasma membrane proteins participating in ligand-receptor interactions between the sperm and oocyte during mammalian fertilization. Affinity chromatography is an unbiased separation technique to enrich proteins interacting with the complementary gamete plasma membrane, facilitating further identification. The current project aims to identify these membrane protein interactions using a porcine model. Sperm and oocyte plasma membrane proteins were isolated through differential centrifugation on a sucrose gradient. Proteins potentially involved in interactions with the complementary gamete plasma membrane were isolated by affinity chromatography using plasma membrane proteins from the complementary gamete covalently attached to polystyrene magnetic beads as the stationary phase. Three separate preparations of oocyte plasma membrane and three separate preparations of sperm plasma membrane were separated by affinity chromatography. Negative controls consisted of co-incubating the stationary phase with plasma membrane proteins from the same gamete. The proteins present in the eluted fractions were trypsinized into peptides and identified by liquid chromatography coupled to a tandem mass spectrometer. The spectral data were analyzed with X!Tandem search engine, validated with Scaffold Proteome Software, and the UNIPROT database. The proteins consistently present across replicates from the eluted fractions were included in the proteomic analysis. Following bioinformatic analysis, 213 proteins from oocyte plasma membrane were identified or predicted as either integral or peripheral proteins with an affinity for the sperm plasma membrane. Analysis of sperm plasma membrane proteins yielded 128 sperm plasma membrane proteins that met similar criteria with an affinity for the oocyte plasma membrane. Some identified proteins were previously reported to be involved in fertilization, such as the tetraspanin CD63, some ADAM proteins including Fertilin beta and Complement C3. Forty-four proteins from the oocyte plasma membrane and 36 from the sperm plasma membrane are presently uncharacterized and potentially involved in fertilization. The present study provides an unbiased approach to identify gamete proteins involved in membrane attachment, binding, and gamete fusion. The analysis of protein-protein predicted interactions derived from the proteomic analysis will contribute to developing strategies to assess the biological relevance of potential interacting pairs in in vitro fertilization. Overall, the present study contributes to expanding our understanding of fertilization. [This work was supported in part by UC-MEXUS, CONACYT, Jastro-Shields Research Awards, MSP 3171 from USDA, a W.K. Kellogg Endowment Fund, and infrastructure support from the UC Davis Animal Science Department.]

Abstract # 1675

Should Heifers Receive Timed Al Later If Using Sex-Sorted Semen? Jaclyn N. Ketchum, Rachael C. Bonacker, Carson M. Andersen, Emily G. Smith, Katy S. Stoecklein, Christine M. Spinka, Jordan M. Thomas

An experiment was designed to evaluate later insemination timepoints when using Split-Time AI, with the hypothesis that later timing of AI may improve estrous response and pregnancy rates when using sex-sorted semen. Estrus was synchronized in 794 heifers across 4 locations with the 14-d CIDR®-PG protocol. Heifers were administered a 1.38 g progesterone insert (CIDR®) on Day 0, which was removed on Day 14. On Day 30, 25 mg dinoprost tromethamine (PG) was administered intramuscularly and estrus detection aids were applied. Split-Time AI was performed based on estrous status. Within location, heifers were blocked based on breed composition, source, sire, RTS, and BW and assigned within block to one of two experimental approaches: Approach 66: heifers that were estrual prior to 66 h after PG administration were inseminated at 66 h, and remaining heifers were inseminated 24 h later (90 h), with 100 µg gonadorelin acetate (GnRH) administered intramuscularly to heifers that were nonestrual by this time; or Approach 72: heifers that were estrual prior to 72 h were inseminated at 72 h, and remaining heifers were inseminated 24 h later (96 h), with GnRH administered to heifers that were nonestrual by this time. Within approach, heifers were preassigned to receive either SexedULTRA 4M[™] sex-sorted or conventional semen. Overall estrous response did not differ between approaches. However, the proportion of heifers that were estrual by the first timepoint (66 h or 72 h following PG administration) was greater (P < 0.0001) with Approach 72 (76%; 302/395) compared to Approach 66 (61%; 242/399). Pregnancy rates to STAI differed (P = 0.0005) between semen type but were not affected by an approach x semen type interaction or by approach. Conventional semen (59%; 240/404) pregnancy rates to STAI were greater than sex-sorted semen (48%; 187/390). Among heifers that were estrual by Timepoint 1, pregnancy rates tended (P = 0.08) to differ between semen type (Conventional: 62% [174/280]; Sexsorted: 55% [146/264]). Pregnancy rates of nonestrual heifers were reduced (P < 0.01) with sex-sorted semen (25%; 15/61) compared to conventional semen (41%; 23/56). In summary, when using sex-sorted or conventional semen for STAI in heifers following the 14-d CIDR®-PG protocol, pregnancy rates did not differ when timing of STAI was delayed by 6 hours. However, the proportion of estrual heifers prior to the first timepoint for STAI was greater when using the later timepoints.

Abstract # 1700

Catsper Regulates Targeting Of Catsper Channel To Sperm Ca2+ Signaling

Nanodomains. Jae Yeon Hwang, Huafeng Wang, Yongdeng Zhang, Joerg Bewersdorf, Jean-Ju Chung

Compartmentalized domains enable specific and fast-triggering downstream signaling events and are common cellular adaptation for effective Ca 2+ signaling in many biological systems. In sperm cells, Ca 2+ signaling mediated by the CatSper Ca 2+ channel is essential for sperm hyperactivated motility and male fertility. Each CatSper channel is a multi-protein complex, and the channel complexes are organized into unique quadrilinear Ca 2+ signaling nanodomains along the sperm tail. How CatSper is assembled and traffic into the uniquely compartmentalized sub-flagellar nanodomains remains largely unknown. Here we identify a novel protein with a conserved membrane trafficking domain associated with CatSper channel. We refer it as CATSPER tau and the protein-encoding gene as Catspert, respectively. Mutant mice studies have revealed that, in the absence of CATSPERt, CatSper subunits interact with each other to form complexes but targeting of the channel complexes to the flagellum is retarded. This results in a severe reduction in each CatSper subunit in the sperm cells, failure to develop hyperactivated motility, and male infertility. We find that CATSPERt compartmentalizes CatSper channel complexes to arrange in the quadrilateral distribution during tail elongation. These findings suggest that CATSPERt is a bona fide targeting protein for the CatSper channel complex to traffic to the flagellar Ca 2+ signaling nanodomains.

Abstract # 1774

A Quantitative Proteomic Investigation of Early Fertilization. Dalen M. Zuidema, Won-Hee Song, Michal Zigo, Peter Sutovsky

Post-fertilization sperm mitophagy is a well-documented early fertilization mechanism which ensures the inheritance of mitochondria from the maternal lineage in many taxa, including mammals. This process of mitochondrial degradation has been shown to be carried out by the ubiquitin proteasome system. In mammals, the ubiquitin-binding proautophagic receptors such as SQSTM1 and GABARAP and the proteasome-interacting ubiquitinated protein dislocase VCP, all contribute to sperm mitophagy. It is hypothesized that other branches of the autophagic pathway and their substrates are involved in sperm mitophagy. The objective of this study is to utilize our novel mammalian cell-free system, in conjunction with mass spectrometry, in order to identify other cofactors and substrate proteins which are involved in sperm mitophagy. Our cellfree system utilizes primed boar spermatozoa co-incubated with porcine oocytes extracts and is able to recapitulate and be used to study early post-fertilization interactions between sperm and ooplasmic proteins. After co-incubation, the sperm and oocyte proteins can be separated based on differential tagging and those oocyte proteins which have bound to the sperm structures can be quantified and identified using MALDI TOF mass spectrometry. We have successfully replicated this process and using a normalized Ttest, have identified 39 proteins of which the quantity was significantly different between control and oocyte extract exposed spermatozoa. Some of these proteins are candidate substrates of oocyte mitochondria-eating proteins, which are degraded during sperm-oocyte extract coincubation, while others are oocytes' own derived mitophagy cofactors which warrant further investigation. We are in process of further studying these individual proteins to better understand their role in mitophagy, utilizing porcine in vitro fertilization (IVF), proteomics, and imaged based flow cytometry to accomplish this validation process. We expect to further validate and understand these presumed pro-autophagic, sperm-bound proteins which are found in higher amounts after exposure to the cell-free system. Research supported by USDA-NIFA grants 2015-67015-23231 and 2019-05318, and MU F21C Program (PS).

The Molecular Characterization Of A Stump-Tailed Sperm Defect In Bovine Spermiogenesis And Mature Spermatozoa. Lauren E. Hamilton, Dietrich Volkmann, Michal Zigo, Filip Tirpak, Jeremy F. Taylor, Robert D. Schnabel, Peter Sutovsky

Cattle and calf production in the United States, which includes the largest fed-cattle industry in the world, had an estimated value of \$50 billion in 2018. Whilst the industry has made substantial progress through the optimization of female reproductive performance, the important role of sire fertility has been largely overlooked. For the cattle industry to further improve economic gains, attention must now be turned to the reproductive management of bulls and the genes impacting variation in male fertility. Our research focuses on phenotyping bovine semen to identify sperm abnormalities and the underlying genetic polymorphisms affecting male fertility. These findings fill further enable testing to improve artificial insemination (AI) sire conception rates. We sequenced the genomes of 85 Holstein, Jersey, Angus and composite breed bulls with differing AI fertilities and phenotyped the semen of these bulls for sperm abnormalities. Within this cohort, a bull producing 100% of sperm with a stumped-tail phenotype was identified and the genome sequence of this bull is being compared to the sequences of the other bulls to identify candidate polymorphisms responsible for this aberrant defect. This rare sterilizing sperm phenotype results in the absence or severe stunting of the sperm tail causing sperm immobility. This bull also had a decreased sperm concentration, possibly due to the severe disorganization of its testes, which had few seminiferous tubules with identifiable lumens. In addition to stumped-tails, other abnormal features of this bull's spermatozoa included knobbed acrosomes, a high prevalence of defective protein aggregates, and aberrant distributions of microtubuleassociated proteins KATNAL2, EML4 and EML5. Work is currently under way to identify and characterize the molecular signatures of this stumped-tail defect in both spermiogenesis and mature spermatozoa, with the overall goal of developing an assay to enable the pre-screening of candidate AI bulls to eliminate the prevalence of causal alleles in AI sires. Supported by NIH 1R01HD084353 (PS, JT, RS), MU F21C Program (PS), and USDA-NIFA grants 2016-67015-24923 and 2017-67015-26760 (JT, RS). In-kind contributions provided by Genex Cooperative and Select Sires Inc.

Abstract # 2164

Artificial Intelligence Analysis of the Mammalian Sperm Zinc Signature Predicts Malefactor Subfertility. Karl Kerns, Skyler Kramer, Michal Zigo, Amanda Minton, Dong Xu, Susanta Behura, Peter Sutovsky

Analysis of both the U.S swine and bovine herds show variation in pregnancy rate is more attributable to male-factor subfertility and infertility than the dam. To date, a limited degree of correlations is observed between conventional semen analysis parameters and actual fertility after standard quality cutoffs are met. Thus, a clear ability to predict male-factor fertility is lacking. Building on our recent discovery of the sperm zinc efflux on the pathway to fertilization competency present in boar, bull, and human spermatozoa published in Nature Communications (DOI:10.1038/s41467-018-04523-y), we hypothesized in vitro capacitation-induced changes to the sperm zinc signature would be indicative of male-factor sub- and infertility. The ongoing fertility trial currently includes 108 boar ejaculates inseminated to over 1,917 sows in a single, fixedtime artificial insemination setting, with pregnancy results ranging from 56.4% - 96.8%. Each ejaculate underwent in vitro capacitation with 10,000 spermatozoa imaged at 0, 1, and 4 hours utilizing high-throughput, image-based flow cytometry. We calculated over 6,550 bioimage values for each of the time points analyzed. Mutual information analysis found 27 sperm bioimage features with scores areater than 0.1 mutually informative to the pregnancy rate. Linear regression analysis was performed on these features and tested with a nested model. ANOVA of the linear regression model identified four features significant with high fertile males within the nested model and eight features for the full model. Next the data was randomly split (4:1) into training and testing sets and classification trees were calculated to predict the pregnancy rates after being discretized into fertile (above 85% pregnancy rates) and subfertile classes (below 80% pregnancy). One tree was trained with 17 features found in traditional semen analysis related strictly to sperm morphology and computer-assisted sperm analysis (CASA) motility outputs, and a separate tree was trained with 170 features related to differences in zinc signature subpopulation changes after in vitro capacitation, significant features found by mutual information analysis, and motility. The traditional semen analysis feature set yielded respective training and testing accuracies of 100% and 53.8%, whereas the later feature set yielded respective training and testing accuracies of 100% and 76.9%. Artificial neural network analysis of zinc, acrosome, and plasma membrane integrity bioimages along with litter size are currently underway. In summary we identified the ability for sperm to transition from a zinc signature 1 and 2 to a capacitated-state signature 3 and 4 along with acrosomal modification and changes to the plasma membrane integrity excels in predictive value of male factor fertility compared to traditional motility and morphology scores alone. Altogether, our findings establish a new paradiam on the role of zinc ions in sperm function and pave the way for accurate sperm biomarker identification of male-factor sub/infertility in future precision agriculture and medicine applications. Supported by the National Institute of Food and Agriculture (NIFA), U.S. Department of Agriculture (USDA) Postdoctoral Fellowship award number 2019-67012-29714 (KK), USDA NIFA grant number 2017-67015-26760 (PS), NIH BD2K Training Grant T32HG009060 (SK), and funding from the MU F21C Program (PS).

The G Protein-coupled Receptor 56 (GPR56) Changes Surface Localization When Mouse Cauda Epididymal Sperm are Incubated in Capacitating and Non-capacitating Conditions. James A. Foster, Lauren A. Bowman, Megan N. Dillon, Christine L. Burke

The G protein-coupled receptor 56 (GPR56) is a member of the adhesion family of GPCRs and is involved in several important developmental processes (e.g. cerebral cortex development) as well as in several pathologies (e.g. polymicrogyria, melanoma). A knockout mouse model has shown that GPR56 is necessary for normal testis development and male fertility and our lab has confirmed and extended these findings. We have found that GPR56 is localized in the acrosome of maturing spermatids in the testis and in cauda epididymal sperm. The goal of this study was to evaluate the localization and cell surface appearance of GPR56 in cauda epididymal sperm and during incubation in capacitating and non-capacitating conditions. The localization of GPR56 and ZP3R, a known acrosomal marker, was determined by immunofluorescence microscopy by fixing sperm immediately following removal from the cauda epididymis (unincubated), and after a 90 minute incubation in capacitating or non-capacitating conditions. A significant majority (85-95%) of sperm that were fixed immediately after removal from the cauda epididymis showed GPR56 staining in a crisp acrosomal crescent pattern which was the same as that seen for ZP3R. Following 90 minutes of incubation in both capacitating and non-capacitating media, GPR56 was localized in several different patterns: 1) the aforementioned crisp acrosomal crescent pattern (<25% of cells), 2) a range of partial acrosomal staining patterns from the crisp acrosomal crescent pattern to smaller round patches over the acrosome (>50% of cells), and 3) smaller speckles over the equatorial region of the head (more variable 10-40% of cells). Since sperm incubation in both capacitating and non-capacitating media showed the same redistribution of GPR56 on the sperm head, GPR56 movement was not dependent on capacitation. This relocation of GPR56 from the acrosomal crescent to a broader distribution on the sperm surface over the equatorial region of the head suggests a role for GPR56 in female reproductive tract events, possibly including capacitation, sperm-oviduct binding, or sperm-egg interactions.

Gene Editing/CRISPR

Abstract # 2208

Pig Androgen Receptor Knockout Fetuses via CRISPR/Cas9 Technology. Kelly A. Zacanti, Insung Park, Joan D. Rowe, Bret R. McNabb, Pablo J. Ross, Elizabeth A. Maga, Trish J. Berger

Androgens are steroid hormones that are involved in the development and maintenance of the male reproductive system via androgen receptors. Knocking out androgen receptor (AR) would render male pigs sterile and is a novel approach to genetic containment. Nonfunctional AR should also eliminate a substrate that causes boar taint, a stale urine and fecal odor and flavor in meat from boars. This study aims to use CRISPR/Cas9 technology to generate pigs with nonfunctional AR. Clustered regularly interspaced palindromic repeats (CRISPR)/Cas9 is an efficient, RNA-guided endonuclease technology that specifically targets and mutates a selected gene of interest. Three guide RNAs (gRNAs) were designed to create mutations in the AR gene. Two gRNAs were designed to target exon 2, while one gRNA was designed to target exon 5. To determine gRNA efficiency, pig parthenotes (one-cell) were electroporated with gRNA and Cas9 or a combination of gRNAs and Cas9. The DNA extracted from individual parthenote blastocysts was amplified by polymerase chain reaction (PCR) and DNA sequences were obtained for the targeted regions. The mutation efficiency of the chosen gRNA or combination of gRNAs was \geq 80%. Zygotes generated by in vitro fertilization (IVF) of in vitro matured oocytes were electroporated with a combination of two gRNAs targeting exon 2 or a single gRNA targeting exon 5. Equal numbers of 2- to 4cell stage embryos targeting exon 2 and exon 5 were transferred into each oviduct of synchronized recipients. At 22 to 24 days post embryo transfer, fetuses were collected. The DNA was extracted from each fetus, amplified by PCR, and sequenced to confirm mutation at the target loci. Survival of the resulting AR exon 2 edited fetuses for 22 to 24 days demonstrated system success. The introduction of equal numbers of embryos targeting exon 2 and exon 5 allows comparison of the viability of different gRNAs. Partial deletion of exon 2 was compatible with fetal viability to 24 days. This project may lead to a novel approach to genetic containment, as well as contribute to the welfare and sustainability of pig production by eliminating boar taint and the need for castration. This project was supported by the Biotechnology Risk Assessment Grants (BRAG) Program, award number 2018-33522-28711 and infrastructure support from the Department of Animal Science, UC Davis.

Generation of a CRISPR/Cas9 Swine Knockout Model to Determine the Role of SSTR2 in the Neuroendocrine Regulation of Reproduction and Growth. R. Blythe Schultz, Yunsheng Li, Malavika K. Adur, ZoëE. Kiefer, Kaitlyn A. Olson, Nicholas K. Gabler, Jason W. Ross

To meet the growing population's demand for high quality animal protein in a sustainable manner, pork producers must increase production and decrease inputs and environmental impact. The use of technology to improve lean tissue growth and feed efficiency in the swine industry is one way to address this challenge. Although improvements in animal husbandry, nutrition and genetic selection programs continue to provide incremental progress, the use of gene editing technologies provides us with novel opportunities for rapid gains in lean tissue accretion and efficiency. Growth efficiency and reproductive performance are physiologically connected. Furthermore, the relationship between the hypothalamic-pituitary-gonadal axis and hypothalamicpituitary-somatotropic axis is acknowledged but poorly understood. Somatostatin (SST) binds to receptors in the anterior pituitary and reduces the production and secretion of growth hormone (GH) by antagonizing GH releasing hormone. Increases in circulating GH improve production and efficiency in many livestock species, including pigs. In order to better understand the neuroendocrine regulation of growth and its effect on reproduction, the objective of this project was to knockout an SST receptor (SSTR) utilizing the CRISPR/Cas9 system. Our hypothesis is that the elimination of one or more SSTRs will reduce SST's negative feedback on GH resulting in measurable improvements in growth efficiency. Porcine fetal fibroblasts were transfected using electroporation with pX330, a plasmid containing the sequence for the Cas9 endonuclease and a guide RNA targeting a locus in exon 2 of SSTR2. Single cell clonal colonies were isolated with cloning cylinders in 10 cm dishes, transferred to individual wells and screened via PCR and Sanger sequencing. Colonies carrying mutations were expanded, verified through sequencing of TA clones, and stored in liquid nitrogen. Somatic cell nuclear transfer followed by surgical embryo transfer was performed using a cell line determined to be modified in a compound heterozygous manner (possessing both a 1 bp and 3 bp deletion in exon 2 of SSTR2). Two male piglets (74-1 and 74-2) were born alive and sequencing data confirmed each pig possessed the expected deletions in the target locus. Based on predicted protein sequence, we expect the 1bp deletion to result in a non-functioning SSTR2 protein. Both pigs were weaned at 21 days of age and weighed 6.31 kg and 8.26 kg, respectively. Early semen collections from 74-2 appear to possess sperm with normal morphology and motility enabling this founder boar to propagate SSTR2 -/- pigs for further characterization. This project was supported by the Lloyd L. Anderson Professorship in Physiology at Iowa State University.

Implantation

Abstract # 1696

A Feedforward Interaction Between GREB1 And Progesterone Receptor Promotes Uterine Receptivity For Embryo Implantation. Sangappa B. Chadchan, Pooja Popli, Eryk Andreas, Denise G. Lanza, Jason D. Heaney, Rainer B. Lanz, Charles E. Foulds, John P. Lydon, Kelle H. Moley, Emily S. Jungheim, Bert W. O'Malley, Ramakrishna Kommagani

Up to 30% of women attempting to conceive experience early miscarriage resulting from the blastocyst failing to implant into the uterus. For an embryo to implant, the uterus must respond to the steroid hormones estrogen and progesterone and become receptive. One key component of receptivity is endometrial stromal cell decidualization. We previously showed that decidualization requires the activity of the progesterone-responsive gene Growth Regulation by Estrogen in Breast Cancer 1 (GREB1). Here, we confirmed that GREB1 is an early progesterone target gene in both human and mouse endometrium. To determine whether GREB1 is required for uterine receptivity, we generated Greb1 knockout mice. Homozygous Greb1 knockout female mice were sub-fertile owing to defective embryo implantation (n=5-6; P ≤0.05; Student's t-test). In a controlled steroid hormone regimen to induce uterine receptivity, estrogen induced epithelial proliferation equivalently in wild-type and Greb1 knockout mice, but progesterone induced less stromal cell proliferation in Greb1 knockout mice than in wild-type mice (n=5-6; $P \leq 0.05$; Student's t-test). Moreover, Greb1 was essential for transcriptional activation of early progesterone target genes such as Areg, Ihh, Calca, and Cyp26a1 (n=5-6; P ≤0.05; Student's t-test) in the mouse endometrium. Finally, we found that GREB1 associated with progesterone receptor on chromatin and is required for progesterone-mediated transcription. Collectively, our data suggest that GREB1 acts as a progesterone receptor cofactor to help orchestrate progesterone-mediated gene expression via a feedforward mechanism. This work may have implications for understanding and treating recurrent pregnancy loss and other endometrial pathologies. This work was supported, in part, by National Institutes of Health/National Institute of Child Health and Human Development grants R01HD065435 and R00HD080742 to RK, R01HD07857 to BWO, and R01HD042311 to JPL; and Washington University School of Medicine start-up funds to RK.

Abstract # 1712

Characterization of LPS-Induced Leukocyte Distribution at the Early Blastocyst Implantation Site of Mice. Bibhash C. Paria, Sourav Panja

Women who have infection are often at a higher risk for early pregnancy loss/defects despite progress in the management and treatment of infection. The reason for this is the lack of clear understanding about how the blastocyst implantation site (BIS) responds to maternal infection. A hallmark of any infection-induced inflammatory response is that it elicits leukocyte migration and the release of many inflammatory

mediators including cytokines from various cell-types. Importance of several of these leukocytes and cytokines are implicated maintaining an optimized balance of immune and inflammatory dynamics at the BIS. However, excessive profusion of leukocytes and their hyperactivity at the BIS may induce an exaggerated inflammatory response that can either support pathogen elimination or cause incidental cell death or tissue damage at the BIS. With a better understanding of this infection-induced exaggerated inflammatory response at the BIS, development of a specific intervention strategy becomes a possibility. In present studies, we have evaluated whether a low dose (1 µg/mice) of lipopolysaccharide (LPS) alters the profile of neutrophil and monocyte subsets of leukocytes at the BIS. The abundances of CD45 + pan-leukocytes, Gr1 + , Ly6G + and MPO + neutrophils, Ly6c + monocytes, F4/80 + and CD206 + positive macrophages and CD11c + positive dendritic cells (DCs) were examined by immunofluorescence staining. On day 6 of pregnancy, BIS of mice injected (ip) with saline had an abundance of CD45 + cells in the uterine muscle layer as well as in the non-proliferating stromal layer that locates above the circular muscle layer. A few CD45 + cells were also evenly distributed throughout the decidua. An analysis of the relative abundance of monocytic and granulocytic myeloid cells within the CD45 + myeloid population revealed the presence of largely monocytic myeloid (CD11c + , F4/80 + and CD206 +) cell populations at the BIS. However, when the day 6 BIS was evaluated following 24 hours after LPS injection (ip), we observed huge infiltration of neutrophil (Gr1 + , Ly6G + and MPO +) subset of leukocytes at the BIS. Majority of neutrophils were located within the uterine non-proliferating stromal region but not in the decidual area. Unexpectedly, injection of LPS compared with its vehicle did not have much of an impact on monocytic myeloid cell populations such as DCs (CD11c +) and macrophages (F4/80 + and CD206 +) at the BIS. These findings show that a hallmark of bacterial response at the BIS is the accumulation of neutrophil within the uterine nonproliferating stromal region. These infection-induced recruited neutrophils could either be involved in enhancing antimicrobial defense or be contributing to immune hyperreactivity leading to hostile inflammation and increased pathology at the BIS. Thus, pertinent future studies in deciphering the process of pathogen-induced neutrophil recruitment and the extend of inflammation that is harmful at the BIS may provide insights for the development of a plausible therapeutic strategy to enhance antimicrobial immune defense or alleviating harmful inflammation at the BIS. This work was supported by a grant from the NIH (1R01HD094946).

Abstract # 1808

Temporal And Spatial Expression Of Adrenomedullin And Its Receptors In The Porcine Uterus And Peri-Implantation Conceptuses. Sudikshya Paudel, Bangmin Liu, Magdalina J. Cummings, Kelsey E. Quinn, Fuller W.Bazer, Robert C. Burghardt, Kathleen M.Caron, Xiaoqiu Wang

Adrenomedullin (ADM) is an evolutionarily conserved multi-functional peptide hormone that regulates implantation, embryo spacing and placentation in humans and rodents.

However, the potential roles of ADM in implantation and placentation in domestic animals, particularly pigs (as litter-bearing species), are not known. This study investigated patterns of expression of ADM mRNA and protein and ADM receptor components that include: calcitonin receptor-like receptor (CALCRL; G proteincoupled receptor bound by ADM), receptor activity modifying protein (RAMP2; dimerized with CALCRL to form ADM 1 receptor), RAMP3 (dimerized with CALCRL to form ADM 2 receptor with lower specificity to ADM) and atypical chemokine receptor 3 (ACKR3; a decoy receptor that serves as a cell-autonomous molecular rheostat to dampen ADM signaling) in porcine uteri and conceptuses (embryonic/fetus and its extra-embryonic membranes) during peri-implantation period of pregnancy when 30-40% of embryonic death loss occurs. Gilts (n=42) that exhibited at least two normal estrous cycles (18-21 days) were bred via artificial insemination at 12 and 24 h after detection of estrus and assigned randomly to be ovariohysterectomized on Day 10, 11, 12, 13, 14, 15, or 16 of pregnancy (n=6 gilts/day; Day 0 is day of onset of estrus). Pregnancy was confirmed by the presence of morphologically normal conceptuses. Each uterine horn was flushed with 20 ml sterile PBS (pH 7.2). Conceptuses had the expected morphological features, from spherical (Days 10 and 11), ovoid and/or tubular (Day 12) to filamentous forms (Days 13 to 16 of pregnancy). Real-time quantitative RT-PCR analyses revealed that ADM mRNA increased (P<0.05) in porcine endometrium and conceptuses between Days 12 and 16 of pregnancy when conceptuses were elongating as compared to Days 10 and 11. Expression of mRNAs for CALCRL and RAMP2 also increased (P<0.05) in the porcine endometrium on Day 13 compared to Days 10 to 12 of pregnancy. Immunohistochemical analyses revealed localization of ADM only to uterine luminal epithelium (LE) of gilts between Days 12 and 16 of pregnancy; whereas CALCRL, RAMP2 and RAMP3 were expressed in uterine LE, glandular epithelium (GE) and stroma between Days 12 and 16 of pregnancy. In porcine conceptuses, expression of ADM, CALCRL, RAMP2 and RAMP3 proteins increased in trophectoderm cells between Days 12 and 16 of pregnancy. Further, in situ hybridization showed that expression of ADM, CALCRL, and RAMP2 mRNAs increased in conceptus trophectoderm between Days 12 and 16 of pregnancy; whereas ACKR3 mRNA increased between Days 13 and 14 of pregnancy, but then decreased to Day 16 of pregnancy. These results indicate that ADM may play functional roles in uterine receptivity as well as survival, growth and development of the porcine conceptus during the peri-implantation period of pregnancy. This research was supported by the Hatch project 1020014 from the USDA National Institute of Food and Agriculture.

Abstract # 1857

Endometrial Epithelial ARID1A Loss Causes Defects of Uterine Receptivity and Endometrial Gland Function. Ryan M.Marquardt, Tae Hoon Kim, Jung-Yoon Yoo, Ho-Geun Yoon, Ripla Arora, Jae-Wook Jeong,

Endometrial receptivity is key to successful pregnancy establishment and is compromised in many women with endometriosis. ARID1A, a SWI/SNF chromatin

remodeling complex subunit, is attenuated in the endometrium of women with endometriosis. Moreover, conditional uterine Arid1a knockout mice are infertile due to endometrial receptivity defects resulting from increased pre-implantation epithelial proliferation. We thus hypothesized that epithelial ARID1A loss compromises fertility by causing a non-receptive state in the endometrium. To examine the effects of endometrial epithelial-specific ARID1A loss, we established a conditional knockout mouse where Arid1a is ablated in the endometrial epithelium (Ltficre/+Arid1af/f). We observed severe subfertility in Ltficre/+Arid1af/f mice in a six-month breeding trial (n=6). Immunohistochemical analysis revealed a failure of embryo implantation and stromal cell decidualization at gestation day (GD) 4.5 (n=3-4), and an artificial decidualization test confirmed the compromised decidual response (n=6) caused by Arid1a loss in the endometrial epithelium. Ltficre/+Arid1af/f mice also exhibited a non-receptive endometrium at pre-implantation stage (GD 3.5) due to increased epithelial proliferation (n=3), and we found significant reduction in expression levels of endometrial gland-related genes including Foxa2 (n=5; p<0.01) and Lif (n=4-5; p<0.05), critical factors for pregnancy establishment. Furthermore, ChIP analysis indicated that ARID1A directly binds the Foxa2 promoter during early pregnancy in wild type mouse uterus (n=5), implying direct transcriptional regulation of Foxa2 by ARID1A. Previous experiments revealed that implantation and decidualization can be rescued in uterine Foxa2 knockout mice by LIF repletion at GD 3.5. However, LIF repletion did not rescue implantation in Ltficre/+Arid1af/f mice, assessed histologically at GD 5.5 (n=3). Despite the failure of LIF to rescue implantation, phospho-STAT3 and EGR1, downstream signaling targets of LIF important for implantation and decidualization, were significantly decreased around Ltficre/+Arid1af/f implantation sites at GD 4.5 based on IHC H-score (n=3; p<0.001). Taken together, these data indicate that loss of preimplantation LIF expression is disrupted by endometrial epithelial Arid1a ablation but is not the sole cause of implantation failure. Our results reveal the importance of epithelial ARID1A in promoting endometrial receptivity by allowing proper implantation and decidualization, regulating epithelial proliferation, and maintaining gland function. Research reported in this publication was supported in part by the Eunice Kennedy Shriver National Institute of Child Health & Human Development of the National Institutes of Health under Award Number R01HD084478 to J.W.J. and T32HD087166 to R.M.M., MSU AgBio Research, and Michigan State University. The content is solely the responsibility of the authors and does not necessarily represent the official views of the National Institutes of Health.

RNA Sequencing Reveals Differential Gene Expression In Porcine And Ovine Conceptus Trophectoderm Cells In Response To Arginine. Xiaoqiu Wang, Sudikshya Paudel, Hongyao Yu, Tianyuan Wang, Fuller W.Bazer, Guoyao Wu, Robert C. Burghardt C.Burghardt, Guang Hu

Hatched ungulate (e.g., pigs, sheep and other ruminants) blastocysts undergo dramatic morphological transitions from spherical to tubular to filamentous forms to conceptuses (embryo/fetus and associated extraembryonic membranes) before implantation. L-Arginine (Arg), a conditionally essential amino acid, is required for this process to activate the mTOR cell signaling pathway to induce proliferation of both porcine and ovine conceptus trophectoderm cells. However, the genomic effects of arainine on trophectoderm cells is unknown. RNA-seg was used for a comparative transcriptome analysis of porcine and ovine trophectoderm cells to further understand effects of Arg on regulation of metabolism in trophectoderm cells. An established porcine trophectoderm (pTr) cell line isolated from Day12 porcine conceptuses, as well as an established ovine trophectoderm (oTr) cell line isolated from Day15 ovine conceptuses were used to determine response to Arg at the physiological concentration of 0.2 mM in a 48 h culture. In pTr cells, a total of 2,723 genes were found to be differentially expressed in response to Arg; 1,482 genes were up-regulated and 1,241 genes were down-regulated compared to the control. In oTr cells, a total of 5,369 genes were altered by Arg treatment for 48 h; 2,819 genes were up-regulated and 2,550 genes were down-regulated compared to the control. Comparison analyses showed that the Arg-treated pTr and oTr transcriptomes share 873 affected genes with 273 genes up-regulated and 342 genes down-regulated. Canonical pathway analyses performed by Ingenuity Pathway Analysis (IPA) software identified the top enriched pathways in both pTr and oTr cells, including: 1) activation of RhoA signaling, integrin signaling, EIF2 signaling, actin cytoskeleton signaling, adrenomedullin signaling, heme biosynthesis II, and Ga12/13 signaling; as well as 2) inhibition of cell cycle G2/M checkpoint regulation, tRNA charging, and p53 signaling. In response to Arg, pathways associated with cholesterol biosynthesis, estrogen-mediated S-phase entry and oxidative phosphorylation were specifically activated in the pTr cells; whereas interferon signaling, ephrin receptor signaling, and sphingosine-1-phosphate signaling pathways were specifically activated in the oTr cells. Furthermore, IPA upstream regulator analyses identified several potential upstream molecular factors involved in Argstimulated proliferation of pTr and/or oTr cells, including PRL, AHR, BRD4, IGF2BP1, KAT6A, SRF, IFNG, OGT, CXCL12, CAB39L, MEIS1, COMMD3-BMI1, TEAD4, RUNX2, and FOXM1. Results from this study of Arg-induced changes in transcriptomes of pTr and oTr cells advance understanding of mechanism responsible for elongation of ovine and porcine conceptuses and enables the rational design of future experiments. This research was supported by the Hatch project 1020014 from the USDA National Institute of Food and Agriculture.

The Autophagy Protein Beclin-1 Is Critical For Endometrial Function In Mice. Pooja Popli, Sangappa Chadchan, Vineet Maurya, Ramakrishna Kommagani

For the uterus to become receptive, endometrial stromal cells must differentiate into decidual cells. One key cellular process in decidualization is the recycling pathway autophagy. Autophagy is upregulated during decidualization, and the autophagy genes ATG16L1 and FIP200 are required for decidualization in both mice and human endometrial stromal cells. Here, we asked whether a key autophagy regulator, Beclin1 (Becn1), is required for uterine receptivity and decidualization. By crossing Beclin1 flox/flox mice with mice expressing Cre recombinase under control of progesterone receptor promoter, we generated Becn1 reproductive tract-specific conditional knockout (Becn1 cKO) mice. Uteri from Becn1 cKO mice contained less of the autophagy marker LC3B-II than uteri from wild-type mice, confirming that deletion of Becn1 impaired autophagosome formation. In six-month breeding trials, Becn1 cKO females delivered no litters, whereas wild-type females delivered an average of 25 litters with 8.2 pups per litter (P ≤0.05; n=4-6; Student's t-test). Although Becn1 cKO females ovulated normally and had normal serum estradiol and progesterone concentrations, they had irregular estrous cycles. Using a controlled steroid hormone regimen to induce uterine receptivity, we found that endometrial stromal cell proliferation was greatly reduced in uteri from Becn1 cKO mice. Additionally, in artificial decidualization experiments, decidualization was greatly impaired in Becn1 cKO mice as evidenced by reduced deciduoma size (n=6) and decreased expression of the decidualization markers Wnt4 and Bmp2 (n=7) ($P \leq 0.05$; n=5-8; Student's t-test). Taken together, our data demonstrate that the autophagy protein Beclin-1 is crucial for uterine receptivity and decidualization. Given these and previous findings indicating the importance of autophagy in human endometrial decidualization, autophagystimulating strategies could be explored as a way to treat women with recurrent pregnancy loss. This work was supported by NIH grants R01HD065435 and R00HD080742 and Washington University School of Medicine start-up funds to Dr. Kommagani.

Abstract # 1950

Can The Er®Map Endometrial Receptivity Study Improve Reproductive Results After Any Previous Implantation Failure In In-Vitro Fertilization Cycles? Silvia Graupiera, Eugeniarocafort Curia, Rebeca Begueriafernandez, Marinamartinez Mena, Ramon Aurellballesteros

Introduction: Repeated failures in in vitro fertilization are a challenge in fertility treatments, especially in cycles with good quality embryos, where the endometrium appears to be the cause of reproductive failure. Targeted diagnostic testing for optimal endometrial evaluation prior to retransfer remains a challenge for assisted reproduction treatments. The ER®map endometrial receptivity test provides information to customize the next embryo transfer to improve reproductive outcomes. Objective: The main

objective is to know if there are differences in the percentage of implantation and pregnancy, after a previous failed embryo transfer cycle with good quality embryos, with a previous endometrial receptivity study using the ER®map test compared to a control group in which no endometrial study was performed prior to a new transfer. Material and methods: Retrospective case-control study at Hospital Quirón Salud Barcelona, including 104 patients who, after a previous failed embryo transfer with good quality embryos, prepare for a new transfer between the periods 2017-2019. With two or more previous failed transfers, all patients underwent a diagnostic hysteroscopy and were asked for lupus anticoagulant, anti-B2-glycoprotein IgG/IgM antibodies, anticardiolipin IaG/IaM antibodies, and hereditary thrombophilia as part of the study of implantation failure. An endometrial biopsy was added to the study group with 55 patients for the analysis of endometrial receptivity using the ER®map test before scheduling a new personalized transfer (pTE) based on the test result. The control group with 49 patients was not performed, and a new transfer was scheduled with a standard protocol (sTE). Results: The results of the endometrial receptivity test in the study group were 63.63% receptive, 36.36% non receptive. The study group presented a higher implantation rate (IR) than the control group (IR 70.91% vs 42.85% p<0.05 Cl 95%), and a higher evolutionary pregnancy rate (PR) in the study group (PR 60% vs 38.77% p<0.05 CI 95%).If we analyze the data according to the number of failed previous transfers, the IR and PR in the study group was higher than the control group (IR 72.22% vs 33.33% NS), (PR 55.55% vs 33.33% NS) after a previous failed transfer; we also obtained better results in the study group (IR 84.21% vs 56% p<0.05 CI 95%), (PR 73.68% vs 48% NS) after two previous failed transfers; results after three or more previous transfers were better in the study group (IR 55.55% vs 27.77% NS), (PR 50% vs 27.77% NS). If we eliminate the embryonic factor analyzing only the results with euploid embryo transfers and/or oocyte donation, the IR was also higher in the study group vs. the control group (IR 71.05% vs. 47.05% NS), (PR 60.53%% vs. 41.17%) respectively. Conclusions: Although the results are not statistically significant, we can affirm that performing an endometrial receptivity study prior to a new transfer in patients with two or more previous failures of in vitro fertilization with good quality embryos improves the rates of implantation and evolutionary pregnancy rates with respect to the control group in which we have not performed the study.

Abstract # 1987

Immunometabolism Regulates the Production of IFNG by Elongating Conceptuses and the Function of Immune Cells in the Endometrium of Pigs. Bryan A. McLendon, Heewon Seo, Avery C. Kramer, Robert Burghardt, Guoyao Wu, Fuller Bazer, Gregory Johnson

Our current understanding of the immunology of pregnancy is that it is a host-graft model in which an immune suppressive state protects the semi-allogeneic conceptus (embryo/fetus and associated placental membranes) from the maternal immune system. This host-graft model of pregnancy may be outdated because evidence is accumulating to indicate that immune responses at the endometrial-placental interface are highly dynamic. Our preliminary studies indicated that porcine conceptuses secrete interferon gamma (IFNG) that recruits activated T cells into the hypoxic endometrium during the peri-implantation period of gestation, and this initiates a controlled inflammatory response that may be essential for tissue remodeling during the initial stages of placentation. However, the mechanisms by which pig conceptuses regulate IFNG production to induce activation of T cells within the hypoxic endometrium remain unknown. Immunometabolism is a growing field of immunology that deals with the metabolic changes that affect immune cell functions. It has been shown that hypoxia leads to enhanced glycolysis in activated immune cells, and hypoxia-induced alycolysis regulates the production of pro-inflammatory cytokines by immune cells at the post-transcriptional level. Therefore, in Study 1, we investigated whether enhanced glycolysis is potentially required for T cell activation within the porcine endometrium during the peri-implantation period of pregnancy. In Study 2, we investigated whether enhanced glycolysis and the generation of metabolic intermediates potentially regulate the post-translational production of IFNG by pig conceptuses. In Study 1, we localized phosphoglycerate dehydrogenase (PHGDH), phosphoserine aminotransferase 1 (PSAT1), and phosphoserine phosphatase (PSPH), enzymes required for serine biosynthesis, to the endometrial luminal epithelium, and hypoxia-inducible factor 1 alpha (HIF1A), as well as glucose 6-phosphate dehydrogenase (G6PDH) and serine hydroxymethyltransferase 2 (SHMT2), enzymes required, respectively, for the pentose phosphate pathway (PPP) and one-carbon metabolism, to proliferating T cells. In Study 2, we observed that elongating porcine conceptuses: 1) express glucose transporters and lactate dehydrogenase A (LDHA), an enzyme that converts pyruvate to lactate, and oxidize glucose to produce CO 2; 2) express glutaminase (GLS), alpha-ketoglutarate dehydrogenase (OGDH), and succinate dehydrogenase (SDHA), enzymes required for synthesis of a-ketoglutarate and succinate; and 3) express IFNG, but levels of IFNG protein sharply decrease on Day 16 of gestation while the mRNA levels remain high, suggesting post-transcriptional regulation of IFNG expression. We hypothesize that in response to a hypoxic environment: 1) proliferating T cells within the porcine endometrium utilize alycolytic branching pathways including the PPP and one-carbon metabolism to support T cell activation; and 2) enhanced glycolysis within conceptuses allows porcine conceptuses to regulate the synthesis of pro-inflammatory IFNG that is secreted into the uterine lumen. This research was supported by Agriculture and Food Research Initiative Competitive Grant no. 2016-67015-24955 from the USDA National Institute of Food and Agriculture.

Abstract # 2017

Role of specific Akt Isoforms during Decidualization Using A PR-Cre Mouse Model. Pascal Adam, François Fabi, Laurence Tardif, Sophie Parent, Eric Asselin

Infertility is a rising problem currently touching 16% of North American couples trying to conceive. To achieve conception, successful implantation is primordial and

necessitates a prepared and receptive endometrium which is dependent of the decidualization process. Under the effect of progesterone and cAMP, endometrial stromal cells undergo phenotypical changes, transitioning from fibroblasts to epitheliallike secretory and glycogen-filled cells. During this process, many signaling factors involved in proliferation and apoptosis are modulated such as the PI3K/Akt pathway. Three isoforms of Akt have been identified and are well recognized to have distinct physiological and pathological roles in different processes. Previously, it has been demonstrated in vitro that expression and activity of specific Akt isoforms are downregulated during decidualization, but little is known about their implication in cell survival, apoptosis and alycogen synthesis in the endometrium. We hypothesize that, for a successful pregnancy, each Akt isoform have specific roles and are differently regulated throughout the decidualization process. Therefore, we developed a unique endometrial-targeted mouse model with simple and combined KO of each Akt isoforms using the PR-Cre mouse model. Using artificial decidualization activation during pseudopregnancy, specific cellular localization, expression and activation of each Akt isoforms and their downstream targets was investigated in order to evaluate the role of PI3K/Akt pathway in this process. Preliminary results suggest that p70S6K activity is regulated by Akt2 and that IkBa is regulated by Akt3 during a non-gestational, progesterone driven context in the endometrium. Moreover, subfertility phenotypes such as variation of the average mouse litter number and absence of decidualization has been observed in Akt1-2 KO, showing redundant roles between those isoforms (Akt1 KO or Akt2 KO mouse showed a more regular phenotype). Further experiments will allow us to understand the precise signaling mechanisms by which this pathway is regulated. We suggest that the PI3K/Akt pathway has an important role in fertility and a better understanding of how this pathway is involved in decidualization could possibly lead to better develop strategies to reduce fertility issues.

Abstract # 2087

Ovine Conceptuses Utilize Specific And Common Cell Adhesion Binding Proteins For Attachment To The Maternal Endometrium During The Early Implantation Period. Yuta Matsuno, Kazuya Kusama, Yoshihito Suda, Kazuhiko Imakawa

Approximately half of embryo fails to proceed during the implantation period. Low implantation rate is a significant factor limiting pregnancy outcome in mammals. Successful pregnancy in ruminants depends on the proper attachment of conceptus to the maternal endometrium, leading to placentation. Although numerous studies suggested that the attachment of conceptus to the maternal endometrium is mediated by implantation specific cell adhesion binding molecules, the investigation of cell adhesion molecules not considered specific to implantation is limited in ruminants. In addition, it remains unclear what proteins related to cell adhesion binding are secreted from conceptuses during the early implantation period. Using proteome and transcriptome analysis with ovine conceptuses and uterine flushings (UFs) from the early implantation period, this study aimed to identify the conceptus-derived proteins functioning as cell adhesion binding. Proteins were extracted from UFs on days of 15

and 17 pregnancy (D15, day 0 = day of estrus, pre-attachment and D17, right after attachment, respectively; day of ovine conceptus attachment to endometrial epithelial cells is initiated on D16-D16.5) and the proteome determined by isobaric tags for relative and absolute quantification (iTRAQ) analysis. The total RNA was extracted from ovine conceptuses on D15, D17, and D21 and the transcriptome determined by RNA-Sequence analysis. To identify the potentially conceptus-derived proteins, we then cross-referenced the proteome data to the transcriptome data from the same stage tissues and used the criteria; proteins from UFs with the abundance score of iTRAQ > 0 and mRNAs from conceptuses with reads per million mapped reads (RPKM) value > 0.1. With this criteria, total 1183 and 1213 conceptus-derived proteins were detected on D15 and D17, respectively. The conceptus-derived proteins were then subjected to Gene Ontology (GO) analysis. The GO analysis revealed that the ontology of cell adhesion molecule binding (GO:0050839) was significantly enriched in the conceptus-derived proteins. The GO analysis also demonstrated that sixty-three proteins were categorized as extracellular region molecule and eight proteins were categorized as cell surface molecule. Among the cell surface molecules, the expression levels of communication network factor 2 (CCN2), collagen alpha-1 (III) (COL3A1), fibrinogen alpha (FGA), fibrinogen beta (FGB), fibrinogen gamma (FGG), fibronectin (FN1), and secreted phosphoprotein 1 (SPP1) were increased in UFs and conceptuses on D17. On the other hand, the expression levels of CD9 molecule (CD9) and epithelial cell adhesion molecule (EPCAM) were decreased in UFs and conceptuses. These results demonstrated that changes in conceptus derived cell adhesion proteins were found as implantation process proceeded and conceptus remodeled cell adhesion binding proteins during the early implantation period. This study suggested that although conceptus implantation to the maternal endometrium is achieved by implantation specific proteins, conceptus implantation may require not only implantation specific proteins but also common cell adhesion binding proteins which have yet been considered as crucial molecule for conceptus implantation. Further functional investigations based on this study may help us to understand the regulation of the implantation. Research was supported by Japan Racing Association grant and Grantin-Aid for Scientific Research (16H02584).

Abstract # 2096

Contribution of lysyl oxidase(LOX) to in vitro decidual differentiation. Min Young Lee, Yeon Jeong Hwang, Yunmi Jeon, Hyo-il Jung, Yong-Pil Cheon

During implantation, differentiation of uterine endometrial stromal cells (ESCs) into decidual cell is critical step for successful embryonic implantation and development. At this time, ESCs are proliferated and differentiated by the ovarian hormones estrogen (E2) and progesterone (P4). Based on the previous our microarry data in pregnant uterus for Bax KO mice, lysyl oxidase(Lox) was identified as a specific gene in pregnant uterus. Lox gene product is a cooper-dependent anmine oxidase, converts the lysine residues of collagen and elastin into aldehydes to form a complex cross-link to

remodel the structure of extracellular matrix (ECM). In this study, we examined the expression of Lox and its possible role during decidualization of ESCs in vitro. During in vitro culture of ESCs and induction for decidualization, the expression of Lox was increased in the mRNA and protein levels. The expression profiles of mRNA and protein of Lox were similar to the degree of decidualization. Decidual differentiation markers, decidaul/trophoblast PRL-related protein (Dtprp) and cytotoxic T-Lymphocyte Associated Antigen 2 Beta (CTLA2b) were increased. By the knock-down down of Lox expression with siRNA, the expressions of those decidual markers were decreased. Those results show that LOX plays a critical roles in decidual cell differentiation. Although further study is needed, the loss of LOX may cause the defects in ECM.

Abstract # 2223

IRX3 Promotes Successful Embryo-Uterine Interactions During Early Embryo Implantation. Ryan M. Brown, Michael P. Mussar, Anqi Fu, Athilakshmi Kannan, Chi-Chung Hui, Indrani Bagchi, Joan S. Jorgensen

Spontaneous abortions have been reported to affect up to 43% of parous women, with over 20% occurring before pregnancy is clinically diagnosed. Establishment of pregnancy is dependent on proper embryo-uterine interactions and implantation. Besides oocyte abnormalities, implantation failure is a major contributor to early pregnancy loss. Previously, we demonstrated that two members of the Iroquois homeobox transcription factor family, IRX3 and IRX5, exhibited distinct and dynamic expression profiles in the developing ovary to promote oocyte and follicle survival. Elimination of each gene independently caused subfertility, but with different breeding pattern outcomes. Irx3 KO (Irx3 LacZ/LacZ) females produced fewer pups throughout their reproductive lifespan which could only be partially explained by poor oocyte guality. Based on prior studies, we hypothesized that IRX3 is expressed in the uterus where it acts to establish functional embryo-uterine interactions. To test this hypothesis, we harvested nonpregnant and pregnant uteri from control and Irx3 KO females to evaluate IRX3 expression profiles and the integrity of early embryo implantation sites. Our results indicate that IRX3 is expressed in the glands of the nonpregnant and pregnant uterus and in the endometrium of the pregnant uterus. Notably, of the days evaluated, IRX3 expression was highest at pregnancy day 5 (D5), which corresponds to a critical window for implantation and remodeling of the vasculature network. Further, histology at D7 showed that while embryos were able to attach to the uterus, implantation sites in Irx3 KO pregnant mice exhibited impaired vascularization. Further analysis of decidua confirmed that markers of vascularization were significantly downregulated in implantation sites from Irx3 KO females compared to WT controls. Altogether, these data suggest that IRX3 promotes fertility via at least two different mechanisms: 1) promoting competent oocytes and 2) facilitating functional embryouterine interactions during implantation. Future research aims to tease apart the roles for IRX3 in the oocyte versus the uterus and the mechanisms by which it promotes early embryo survival and a successful pregnancy outcome. NIHR01HD075079.

Temporal Expression Pattern of HP1 during Mouse Embryo Implantation and Decidualization. Hui Gao, Yichen Wang, Changjun Zhang, Yuanmei Zhang, Honglu Diao

Temporal Expression Pattern of HP1 during Mouse Embryo Implantation and Decidualization Hui Gao 1,2, Yichen Wang 1, 2, Huigi Liao 1, 3, Yuanmei Zhang 1, Changjun Zhang 1, 3, Honglu Diao 1, 2, 3* 1. Reproductive medicine center, Renmin Hospital, Hubei University of Medicine, Shiyan, Hubei 442000, China; 2. Biomedical Research Institute, Hubei University of Medicine, Shiyan, Hubei, 442000, China 3. Hubei Clinical Research Center for Reproductive Medicine, Shiyan, Hubei 442000 P.R. China *Correspondence: Honglu Diao, Email: hldiao1976@hotmail.com Embryo implantation involves the synchronized preparation of a competitive embryo and a receptive uterus; however, it remains largely unknown. The relationship between HP1 (encoded by Cbx gene) and embryo implantation has not been reported. The aim of this project is to examine the uterine expression and regulation of HP1 during pregnancy in mice and its regulation under pseudopregnancy, steroid hormone treatment, and artificial decidualization conditions by Realtime PCR and Immunofluorescence. Our Pre-limited data showed that the expression of HP1 protein increased in the luminal epithelium and decreased in the glandular epithelium during mouse pregnancy Day0.5-4.5, and can be detected on decidual zone on day 4.5. Both estrogen and progesterone could down-regulate the expression of Cbxs mRNA, but Treatment with estrogen receptor inhibitor ICI 182 780 or progesterone inhibitor RU486 partially blocked the downregulation of Cbxs mRNA by estrogen or progesterone respectively. Our Pre-limited data showed that HP1 may play a role in the process of embryo implantation by regulating the uterine receptivity. Estrogen and progesterone down-regulate the expression of HP1 through estrogen receptor or progesterone receptor. Next step, we will identify molecules and proteins that can directly interact with HP1 and downstream signaling pathways affected by Cbxs deletion in mouse in vitro induced decidualization model.

Meiosis

Abstract # 2148

Autophagy And Dynein Regulate Cytoplasmic Microtubule Organizing Centers During Oocyte Meiosis. Daniela Londono Vasquez, Katherine Rodriguez-Lukey, Ahmed Balboula

During oocyte meiosis I (MI), the spindle is assembled centrally prior to its timelymigration towards the cortex. Such central positioning of the spindle is crucial to allow proper kinetochore-microtubule (MT) attachments and to prevent the development of aneuploid eggs. In mitotic cells, spindle positioning relies on centrosome-mediated astral microtubules (MTs). Mammalian oocytes lack classic centrosomes and instead contain numerous MT organizing centers (MTOCs). Using immunocytochemistry and time-lapse confocal microscopy, we identified two different sets of MTOCs: those known to form spindle poles (polar MTOCs; pMTOCs) and those remaining free in the cytoplasm (cytoplasmic MTOCs; cyMTOCs). Using 2-photon laser ablation to deplete cyMTOCs, we revealed two novel functions of cyMTOC-mediated MTs in regulating (1) spindle positioning and (2) timely-spindle migration by anchoring the spindle to the cortex. Interestingly, each oocyte at metaphase I has a variable number of cyMTOCs (ranged from 4 to 11) located at different focal planes. Elevated cyMTOC numbers are associated with poor oocyte quality; however, how the oocyte regulates cyMTOC numbers remains unknown. Here we describe two novel regulators of this function, autophagy and dynein-mediated cyMTOC clustering. In mitotic cells, autophagy plays a key role in controlling centrosome numbers. We investigated the involvement of autophagy in regulating cyMTOC numbers during MI. Autophagy inhibition using 3-Methyladenine significantly increased the number of cyMTOCs, whereas autophagy induction using rapamycin significantly decreased cyMTOC numbers relative to controls. Interestingly, neither drug affected pMTOC numbers, suggesting that autophagy controls cyMTOC numbers during MI through a selective mechanism. Because autophagosome trafficking relies on MT-dependent motor proteins and because cyMTOC-mediated MTs anchor the spindle, we investigated the involvement of a major MT motor protein, dynein, in regulating cyMTOCs. Using immunocytochemistry, we found that dynein localizes to cyMTOCs, pMTOCs and MT connections. Culturing nuclear envelope breakdown oocytes with dynein inhibitors (dynarrestin, Dyn, or dynapyrazole-A, DypA) inhibited dynein-MT binding, decreased the level of autophagy, increased the number and decreased the volume of cyMTOCs relative to DMSO-treated oocytes. Importantly, autophagy induction by rapamycin partially rescued the significant increase of cyMTOC numbers in dynein-inhibited cells, suggesting that dynein regulates cyMTOC numbers through autophagy and, at least, another additional mechanism. Time-lapse tracking of the spindle revealed that dynein inhibition perturbs spindle positioning, induces precocious spindle migration and causes early polar body extrusion compared to controls. These results implicate dynein and autophagy as novel regulators of cyMTOCs, and provide additional evidence that

cyMTOCs are essential for spindle positioning and timely-spindle migration. This research was supported by laboratory start-up funding from the University of Missouri to AZB.

Oogenesis and Oocyte Maturation

Abstract # 1616

Age-dependent Expression of MVH in Murine Primordial Follicles: Implications for its use as a Primordial Follicle Quantification Tool. Alyssa Y. Gonzalez, Nicole Galicia, Isaac Villalpando, Timothy Graham, Kerui Gong, Tom Hartl, Manuel Lopez, Geoffrey Berguig, Sherry Bullens, Shauna Rasmussen, Judith L. Fridovich-Keil, Stuart Bunting, Joseph C. Chen

Identification and quantification of ovarian primordial follicles (PF) is an important, but difficult aspect of studying rodent ovarian biology. This is largely due to the variability and fastidiousness of existing morphological-based counting protocols. Identifying a protein marker of PF would improve our ability to count PF rapidly and reliably. Other published methods, including proliferating cell nuclear antigen (PCNA), have been shown to target both primordial and primary/antral follicles in rats. However, PCNA as a counting tool for mouse ovarian follicles have been shown (by our group and others) to have signal background and specificity issues, ultimately resulting in it being suboptimal for use in mice. Mouse vasa homolog (MVH), a member of the ATP-dependent RNA helicases, has been shown to be a possible marker of PF in mice. However, the pattern of its expression in the aging murine ovary is not well understood. The purpose of the current study was to evaluate the patterns of MVH expression via immunohistochemistry in mouse and rat ovaries. C57BL6 mouse and Sprague Dawley rat formalin fixed, paraffin embedded (FFPE) ovarian tissues were sectioned at 5µm, and 5 serial sections were used for immunohistochemical evaluation. Our results indicate that in the mouse, MVH is detectable in the first, singular pre-granulosa layer of the PF (<25µm and confirmed by morphological analysis to be PF) and does not detect anti-müllerian hormone (AMH)-positive primary, pre-antral, and early antral follicles (shown in adjacent sections). Furthermore, the average number of MVH-positive follicles per section is 10.48 ± 2.6 SEM at 4 weeks of age. That number significantly decreases (P<0.05) by 25 and 48 weeks of age $(2.2 \pm 0.6 \text{ SEM}; 1.32 \pm 0.8 \text{ SEM} \text{ respectively})$ and is undetectable at 72 weeks of age. This pattern of decrease with increasing age is similar to the decrease in AMH levels observed in the serum and ovarian tissue of the mice. In 4-week-old rats, structures histologically confirmed to be rat PF stained positive for MVH with comparable patterns to mouse PF, with no signal in post-primordial, maturing follicles. Similar to mice, there was a significant decrease (P<0.05) in rat MVH-positive PF at 21 and 60 weeks of age. Interestingly, and similar to one previous report, MVH also stains positive in the cytoplasm of a few, select population of pre-antral follicles in both mouse and rat ovaries. Together, our data indicates that the use of MVH could support and extend existing PF counting strategies in murine ovaries. Future studies will address the role of MVH in the limited pre-antral follicles that we observed, and also seek to

determine if comparable homologs of the vasa protein could serve as reliable PF marker in humans and other primates.

Abstract # 1672

FGF2, LIF, And IGF1 (FLI) Supplementation Improves Human Cumulus Cell Expansion During In Vitro Maturation In A Pediatric Population. Luhan T. Zhou, Farners Amargant, Rebecca L. Krisher, Michael Roberts, Randall S. Prather, Lee D. Spate, Ye Yuan, Courtney J. Harris, Jordan H. Machlin, Aminata Bangoura, Erin E. Rowell, Monica M. Laronda, Francesca E. Duncan

Life preserving cancer treatments may threaten reproductive function, and ovarian tissue cryopreservation (OTC) is often the only pretreatment fertility preservation option for pediatric girls. This procedure involves isolating the ovarian cortex from the medulla and cryopreserving cortical strips containing primordial follicles. During the tissue processing, cumulus oocyte complexes (COCs) are released from small antral follicles into the media, which is typically discarded. The recovery and maturation of COCs from this media may provide an additional fertility preservation option for pediatric girls. However, the reproductive potential of COCs from this population is unknown. Therefore, our goal was to determine the characteristics of these COCs and optimize in vitro maturation (IVM) methods. We received media from 37 participants between 0.5 – 22 years old. 53.8% of the participants had received chemotherapy and/or radiation prior to OTC. We recovered intact COCs, as well as denuded and degenerate oocytes. Total yield significantly increased with age (P = 0.0006). While an average of 3.7 ± 5.6 intact COCs were recovered per participant, history of previous treatment was associated with significantly reduced yield (average 0.6 ± 1.4 ; P < 0.0001). COCs in this pediatric cohort contained oocytes with an average diameter of 105.7 ± 1.1 mm. We previously demonstrated that human oocytes in an adult population must be >112mm in diameter to resume meiosis and produce mature gametes. Thus, most oocytes within the pediatric population likely lack meiotic competence. In agricultural species, supplementation of IVM medium with three cytokines (FGF2, LIF, and IGF1; FLI) significantly improves oocyte maturation. Therefore, we examined whether the FLI cocktail could improve maturation parameters of COCs recovered pediatric ovarian tissue. FLI supplementation resulted in an increased percentage of oocytes that reached the mature metaphase II-arrested state (-FLI: 26.3% and +FLI: 31.6%). Moreover, FLI supplementation increased COC expansion by 2.83 fold (P=0.005) relative to untreated controls, which is a known marker of developmental competence. Studies are ongoing to identify FLI-regulated molecular pathways and to evaluate gamete quality.

Carbohydrate Metabolism Characterization of a Novel Two-Step In Vitro Maturation System Reveals Alterations from Cell Specific Roles Within Cumulus-Oocyte-Complex. Nazli Akin, Lucia von Mengden, Anamaria-Cristina Herta, Katy Billooye, Juul van Leersum, Berta Cava Cami, Laura Saucedo-Cuevas, Fabio Klamt, Johan Smitz, Ellen Anckaert

Obtaining competent mature oocytes (MII) from immature oocytes (GV) requires wellorchestrated coordination between the cells of the cumulus-oocyte complex (COC). It is known that COC utilizes carbohydrate metabolism to produce required energy and metabolites for the final maturation. However, the metabolic demands and outputs of the individual cell types within COC are largely unknown. In vitro maturation (IVM) is an assisted reproduction technique with reduced hormone-related side effects, developed mainly for patients with polycystic ovarian syndrome. For IVM, COCs are retrieved from small unprimed follicles. Capacitation (CAPA)-IVM is an optimized IVM system with pre-maturation step added before IVM. C-type natriuretic peptide in the pre-maturation culture inhibits reinitiation of meiosis while promoting oocyte competence. Yet, good quality embryo rates after CAPA-IVM are still lower in number than classical IVF. Carbohydrate metabolism profiles of cell compartments from immature and mature mice COCs have been studied (i) to map the metabolic specificities of each cell type from in vivo matured COCs and (ii) to identify the metabolic deviations in the CAPA-IVM matured COCs. Oocytes and their corresponding cumulus cells (CC) were collected both after pre-maturation (GV) and IVM (MII) steps. In vivo control samples were collected either after only PMSG injection (GV) or both PMSG and hCG injections (MII). Three repeat cultures were performed, and samples were stored in pools of five. Glycolysis, tricarboxylic acid (TCA) cycle and pentose phosphate pathway (PPP) were studied by measuring twenty different enzymes' target molecules and products through colorimetric and fluorometric assays. Gene expression study was performed using QRT-PCR to support metabolomics data (analysis ongoing). Two or three technical repeats were used for each analysis. Student's t-test was used for statistics. The results show that cells of COCs compartmentalize glucose metabolism pathways during final meiotic maturation. Within in vivo COC, during final maturation, glycolysis and TCA activity were increased in the CC, demonstrated by upregulated pyruvate, lactate, citrate and aconitase levels (p-values: between <0.05 and <0.01). CC are most probably producing the intermediates to transfer them to oocytes for further energy production. Oocytes are responsible for performing PPP. We observed increased glycolysis and TCA cycle activity in in vitro CC from immature COC (compared to in vivo) after the prematuration step already, indicated by significantly higher pyruvate, lactate, citrate and alpha-ketoglutarate levels and aconitase and phosphofructokinase activities (p-values: between <0.05 to <0.001). Comparing the final maturation in CAPA-IVM COCs to their in vivo counterparts, the metabolism pattern was opposite and marked by significant decrease in the phosphofructokinase, lactate dehydrogenase and aconitase activities besides lower alpha-ketoglutarate levels (p-values < 0.01). These data demonstrate that

CAPA-IVM CC have the capacity to perform glucose metabolism. However, their metabolism pattern during final maturation is strikingly different compared to in vivo CC. Cumulus cells might be subjected to an early exhaustion caused by culture, which possibly alters their ability of providing for oocytes during final maturation. Thus, the lower embryo quality rates of CAPA-IVM oocytes could be due to altered CC metabolism since oocyte competence depends on intermediates supplied by cumulus cells.

Abstract # 1686

Evaluation Of Aging-Related Alterations In Bovine Oocytes. Maria Soares, Raquel D. Fernandes, Sandra Reis, Ana Paula Sousa, Teresa Almeida-Santos, Joao Ramalho-Santos

Female reproductive aging is a serious issue that, among other issues, involves functional and structural alterations in oocytes that reduce their developmental potential. Studying these aging-related alterations in order to design better therapeutic approach is hindered by the inherent ethical problems of working with human gametes, as well as the limited number of samples. Given that the bovine model is more similar to humans that rodent alternatives this study aimed to characterize both in vitro- and in vivo- induced age-related cow oocyte modifications, that were then compared to an appropriate control group (CTRL). First of all, to determine if our model is a reliable approach to study human oocyte aging, in vitro -induced alterations (IVTA) were compared to a in vivo aged group of bovine oocytes obtained from cows with more advanced age (IVVA), as well as to information reported in the literature regarding the features of human oocyte aging. For this purpose, ooplasm volume (CTRL n=160; IVTA n=84; IVVA n=44) was evaluated under optical microscopy; mitochondrial mass (CTRL n=47; IVTA n=44; IVVA n=10), distribution (CTRL n=47; IVTA n=44), aggregation (CTRL n=47; IVTA=44), activity (CTRL n=47; IVTA=42) and hydrogen peroxide levels (CTRL n=43; IVTA n=47; IVVA n=10) were assessed by fluorescent microscopy using appropriate probes; while mitochondrial DNA content (CTRL n=5; IVTA n=5; IVVA n=3) and the expression of several transcription factors involved in mitochondrial biogenesis (CTRL n=4; IVTA n=3) were monitored by quantitative real-time PCR. Results show that our in vitro approach of inducing aging causes a significant decrease in ooplasm volume (p£0.001), which is in accordance with what has been reported for human oocytes. However, regarding mitochondrial content, mitochondrial distribution (Mitotracker Green) and activity (JC-1), no differences were detected in the in vitro and in vivo aged groups. However, in vitro aged bovine oocytes showed a significantly different aggregation pattern (p=0.001) similar to aging-related alterations in human oocytes that have been previously reported. Indeed, both in vitro aged bovine oocytes and aged human oocytes present lack of granularity, demonstrated by a homogeneous and regular Mitotracker Green staining. Molecular analysis showed no statistical differences in mitochondrial DNA content and mitochondrial biogenesis transcription factors after in vitro aging. Finally, a significant increase in hydrogen

peroxide content (p£0.001) was observed in in vitro aged oocytes using 2',7'-Dichlorofluorescein, in accordance with what was detected in the in vivo aged group of bovine oocytes, and already reported in terms of age-dependent increase of ROS levels in other animal models, such as mice. In conclusion, this work characterizes aging-related alterations in bovine oocytes that validate this model as a reliable in vitro approach for studying human oocyte aging. In the future, this methodology may contribute towards the identification of therapeutic targets that could compensate deleterious age-related changes in mammalian oocytes. Funding: STEM@REST Project (CENTRO-01-0145-FEDER-028871). Additional funding by the European Regional Development Fund(ERDF), through the Centro2020 Programme: project CENTRO-01-0145-FEDER-000012-HealthyAging2020, the COMPETE2020, and the Portuguese national funds via FCT – Fundação para a Ciência e a Tecnologia, I.P.: project POCI-01-0145-FEDER-007440.

Abstract # 1690

Uncovering A TAF4b-Dependent Gene Expression Program Required For Embryonic Oocyte Differentiation. Megan A. Gura, Kimberly A. Seymour, Richard N. Freiman

Proper embryonic female germ cell development is critical for the healthy establishment of the adult ovarian reserve. TBP-Associated Factor 4b (TAF4b) is a subunit of the basal transcription factor TFIID complex, which is required for RNA Polymerase II recruitment in gonadal tissues. Taf4b-deficient female mice are infertile due to several related deficits of embryonic germ cell development including increased chromosome asynapsis, excessive germ cell death, and delayed germ cell cyst breakdown. We have previously demonstrated that Taf4b mRNA and protein expression are nearly exclusive to the germ cells of the embryonic ovary from E9.5 to E18.5 and its expression is directly regulated by STRA8 and DAZL in male meiotic germ cells. Therefore, we hypothesized that TAF4b, as part of germ cell-specific from of TFIID, regulates obgenesis and meiotic gene programs. To elucidate a TAF4b-dependent program of embryonic oocyte development, we performed low-input RNA-sequencing on GFP+ germ cells sorted from Oct4-EGFP transgenic mice that were Taf4b-heterozygous or -deficient at E14.5 and E16.5. To our surprise, gene ontology analysis of our differentially expressed genes (DEGs) showed few germ cell development-related genes deregulated in the absence of TAF4b. Importantly, a few notable genes were down-regulated in the Taf4b-deficient germ cells such as Nobox. Brca2, Rhox10, and Rhox13. There were several unexpected DEGs such as Mtor, Apoe, Clock, and Igf2. Further perplexing from this RNA-seg analysis was the proportion of DEGs on the X chromosome at each time point, especially several members of the MAGE and RHOX gene families. For E14.5 DEGs in the Taf4bdeficient germ cell, there were very few down-regulated genes but many up-regulated genes located on the X chromosome. At E16.5 the trends were precisely the reverse, many down-regulated genes but no up-regulated genes were on the X chromosome. These interesting results implicate an unexpected but important role of TAF4b in regulating gene expression on the X chromosome during oocyte development. We are

currently performing CUT&RUN using mouse embryonic stem cells and sorted embryonic female germ cells to clarify which genes are directly bound by TAF4b. This research may add new dimensionality to the female germ cell transcriptome as we uncover new genes that participate in the healthy development of the ovarian reserve.

Abstract # 1708

Communication with the Soma via Physical Contacts is Required for Acquisition of Oocyte Developmental Potential. Flora Crozet, Christelle Da Silva, Gaëlle Letort, Hugh J. Clarke, Marie-Hélène Verlhac, Marie-Emilie Terret

The quality of the oocyte, the female germ cell, determines the chances of producing a healthy embryo after fertilization. This quality, also called developmental potential, decreases with maternal age, while the age of the mother at first conception increases in our industrial societies. Understanding how the oocyte acquires this capacity has therefore become a public health issue. However, the mechanisms by which this developmental potential is acquired are poorly understood. Prior to division, mammalian oocytes undergo a growth phase in a specialized niche, the follicle, where they increase in volume while accumulating organelles and macromolecules necessary for future meiotic divisions and early embryogenesis. Growing oocytes physically communicate with the somatic follicular cells that enclose them via filopodia-like extensions of the follicular cells, termed transzonal projections (TZPs). To test whether soma-germline communication is required for the oocyte developmental potential, we have sought to reduce these physical contacts. By genetically inactivating the TZP structural component and filopodia inducer, Myosin-X, we reduce TZP density in fully grown oocytes by five-fold. Oocytes that have reduced physical contact with the follicular cells grow to full size and show no morphological defects. However, only half of them are able to complete the subsequent meiotic divisions; the other half arrest at metaphase of first meiotic division (meiosis-I). The conditional deletion of Myosin-X in oocytes does not impair meiotic divisions, confirming that Myosin-X in the granulosa cells is required for the oocyte developmental potential. Live-imaging analysis reveals that the meiosis-I spindles of TZP-deprived oocytes show no alteration in morphogenesis or anchorage to the oocyte cortex, indicating that the molecular basis of the meiotic defect lays elsewhere. Strikingly, however, transcriptomic analysis by RNA-seq of these oocytes at the end of their growth show deregulated expression of multiple genes. Most of the deregulated genes are up-regulated and are enriched in processes linked to translation, encoding ribosomal proteins and enzymes involved in the polyamine metabolism, a pathway known to promote protein synthesis. We propose that the somatic compartment, through TZPs, shapes oocyte quality by remodeling its proteome, and that this is a prerequisite for the successful completion of the meiotic divisions. Interestingly, TZP-number may decrease with maternal age. Our results therefore identify a mechanism, of somatic origin, that may help to explain the increase in meiotic errors during female ageing leading to impaired fertility.

Exploring The Unexpected Cytoplasmic Localization Of The General Transcription Factor TAF4b During Embryonic Oocyte Development. Kimberly M. Abt, Kimberly A. Seymour, Richard N. Freiman

Long-term female fertility depends on the proper establishment of the ovarian reserve that occurs before birth; however, the transcriptional mechanisms that drive this essential process are just coming into focus. Our lab has shown that TBP-Associated Factor 4b (TAF4b), a gonad-enriched subunit of the general transcription factor TFIID complex, is required for female fertility in the mouse and plays an essential role in primordial follicle assembly. Recently, we have demonstrated that TAF4b protein and mRNA are consistently enriched in the germ cells of the embryonic ovary (E9.5-E18.5) and Taf4b mRNA expression significantly increases soon after meiotic initiation (E14.5). This intriguing expression pattern combined with TAF4b's essential role in development led us to investigate how TAF4b expression and/or function is regulated in embryonic germ cells. Previous work demonstrated that nuclear localization of TAF4b is regulated in human B lymphocytes, thus we first examined whether mouse TAF4b is regulated by alterations in its subcellular localization. We harvested ovaries from Oct4-GFP transgenic mice at E14.5 and then used fluorescently activated cell sorting (FACS) to separate the somatic (GFP-) and germ cells (GFP+) populations. We separated each cell population into nuclear and cytoplasmic fractions, and then performed immunoblotting to probe for TAF4b. We also performed immunofluorescence (IF) on ovaries from E13.5 Oct4-GFP mice to visualize TAF4b localization. Using these complementary methods, we interestingly found that TAF4b is predominantly cytoplasmic in E13.5-E14.5 female germ cells. To extend these data, we will present TAF4b localization at later embryonic timepoints (E16.5-E18.5) to determine if TAF4b levels accumulate in the nucleus and/or cytoplasm as germ cell development progresses. This work could potentially challenge the paradigm that TAF4b only acts as a subunit of the general transcription machinery in the nucleus and opens up the possibility of new, undiscovered roles of TAF4b in the cytoplasm of female germ cells. Ultimately, understanding how TAF4b is regulated in the embryonic ovary will help us more precisely elucidate the molecular mechanisms by which TAF4b functions to promote healthy ovarian development and long-term fertility and how its disruption leads to primary ovarian insufficiency (POI).

Abstract # 1824

TGFβ Receptors Localized at Sites of Intercellular Membrane Contact May Mediate GDF9 Signalling from Oocyte to Granulosa Cells. Wusu Wang, Hugh Clarke

Bidirectional signaling and communication between the oocyte and its surrounding granulosa cells is crucial for oocyte and follicular growth. One such signaling interaction depends on the activation by oocyte-produced growth-differentiation factor (GDF) 9, a member of the transforming growth factor (TGF)- β superfamily, of type I-type II TGF β dimeric receptors on the plasma membrane of the granulosa cells. However, the

mechanics of this essential ligand-receptor interaction remain poorly understood. Notably, although freely diffusible GDF9 is biologically active, physiological conditions including the presence of an extracellular matrix often impair the diffusion of growth factors, thus severely limiting their range of activity. During follicular growth, actincontaining filopodia-like structures known as transzonal projections (TZPs) extend from the granulosa cells, pass through zona pellucida - an ECM-like layer that surrounds the oocyte - and attach to oocyte plasma membrane. We speculated that TZPs, which mediate contact-dependent signaling from the granulosa cells to the oocyte, might also mediate the GDF9 signaling in the opposing direction. Using immunostaining and 3D reconstruction of confocal serial sections, we show that ALK4, a type I receptor of GDF9, is abundant at the tips of TZPs where they contact the oocyte plasma membrane. When granulosa cell-oocyte complexes were disaggregated and then reconstructed, ALK4 became localized at the points of contact between the newly generated TZPs and oocyte membrane, implying a mechanistic link between cell contact and ALK4 localization. Moreover, ALK4 co-localized with N-cadherin, which mediates adhesion between the granulosa cells and the oocyte. Strikingly, when follicles were incubated in calcium-free medium for 0.5h to detach the TZPs from the oocyte membrane, as verified by loss of gap junctional communication, ALK4 was lost from the TZP tips; conversely, after they were returned to calcium-containing medium for 24h, ALK4 became reconcentrated at the tips of reattached TZPs. Moreover, the loss of ALK4 from TZP tips was associated with a decrease in the phosphorylation of SMAD3, which transduces GDF9 signaling, and the reconcentration of ALK4 at the tips was associated with restoration of SMAD3 phosphorylation, suggesting that the concentration of ALK4 at the tips of attached TZPs contributes to GDF9 signaling. Our findings identify an unexpected regionalization of the granulosa cell plasma membrane and suggest that direct membrane contact between oocyte and granulosa cells induces ALK4 to become concentrated at tips of TZPs where it mediates GDF9 signaling. Taken together, these results raise the possibility that under physiological conditions, efficient signaling to the granulosa cells by GDF9 and perhaps other oocyte-derived factors requires physical contact between the two cell types. Supported by the Canadian Institutes of Health Research and Wusu Wang is the recipient of scholarship from China Scholarship Council.

Abstract # 1829

Molecular And Cellular Control Of Cumulus Layer Expansion, An Essential Prerequisite For Fertilization. Karen F. Carvalho, Hugh J. Clarke

Oocytes within antral follicles are enclosed by several layers of tightly packed follicular cells known as the cumulus granulosa. In response to the pre-ovulatory surge of luteinizing hormone, which triggers release of epidermal growth factor (EGF)-like peptides by the mural granulosa cells, the cumulus layer undergoes a process termed expansion, in which the cumulus cells both secrete a hyaluronic acid-rich extracellular matrix (ECM) and become displaced away from the oocyte within the ECM. Cumulus

layer expansion is essential for efficient fertilization and disturbances in it can lead to infertility. Expansion requires up-regulation in the cumulus cells of genes regulating production of the extracellular matrix, as well as secretion by the oocyte of members of transforming growth factor β superfamily, but how these cooperate to induce expansion remains unclear. We found that addition of EGF to cumulus-oocyte complexes isolated from antral follicles triggered the development of numerous cytoplasmic protrusions on the leading edge of the migrating cumulus cells. Because the Arp2/3 complex, which promotes the formation of branched-chain actin filaments, directs the formation of cytoplasmic protrusions in other cell types, we tested the effects of CK-666, a specific inhibitor of Arp2/3 activity. CK-666 blocked the development of these protrusions, and also prevented the displacement of the cumulus granulosa cells away from the egg. In contrast, CK-666 did not prevent the EGF-triggered up-regulation of mRNAs whose products are required for deposition of the extracellular matrix. We propose that cumulus layer expansion comprises two linked but independent events: i) production and secretion of ECM by the cumulus cells and ii) active and directed migration of the cumulus cells within the ECM. This model may provide new insight into the origin and treatment of some cases of infertility. Funding: Supported by the Canadian Institutes of Health Research.

Abstract # 1902

Effect Of Carbamazepine At Environmentally Relevant Concentrations On Oocyte Developmental Competence. Dorit Kalo, Alisa Komsky-Elbaz, Zvi Roth

Carbamazepine (CBZ), an anticonvulsant that is mainly used in epilepsy treatment, reduces fertility. The estimated half-life of CBZ is over 130 days in soil and more than 100 days in surface water, making it highly persistent in the environment. CBZ has been detected in crops irrigated with treated wastewater, as well as in the urine of healthy volunteers that consumed vegetables and fruit irrigated with recycled water. Whether the residual concentration of CBZ in food has a negative impact on mammalian oocytes and/or spermatozoa is not clear. Two in-vitro dose-response studies were performed to examine of the effects of CBZ on the spermatozoa and oocyte. In the first study, fresh semen from 3 bulls was subjected during capacitation (4 h) to CBZ (0, 0.001, 0.01, 0.1, 1, 10 or 100 µg/L). The integrity of the plasma membrane, mitochondrial membrane potential, reactive oxygen species (ROS) level and acrosomal membrane integrity were examined by flow cytometry, using spermatozoon-specific kits (IMV Technologies). Statistical analysis was conducted by one-way ANOVA with post-hoc test. CBZ did not affect the proportion of viable spermatozoa; at 0.1 μ g/L, it increased (p < 0.02) the proportion of spermatozoa with high mitochondrial membrane potential relative to the control; at 0.001 μ g/L, it increased (p < 0.01) the proportion of spermatozoa with pseudo-acrosome reaction; at 0.01, 0.1, 1, 10 and 100 µg/L, it increased (p < 0.001) the proportion of spermatozoa exhibiting higher ROS levels than the control. In the second study, cumulus oocyte complexes (COCs; n = 1100) were aspirated from ovaries collected at a local abattoir, and in-vitro matured with CBZ (0,

0.01, 0.1, 1, 10, 50 or 100 μ g/L—the maximum level detected in vivo) for 22 h. At the end of maturation, COCs were fertilized and cultured for 7 days. Embryo kinetics was evaluated using a time-lapse incubator system (24 h/day for 7 days). Blastocysts (n = 96) were subjected to gene-expression analysis (for SOX2, NANOG, OCT4, CCA2, GATA, GDF9 and STAT3) by qPCR. CBZ at 0.01 and 0.1 μ g/L tended (p < 0.07) to decrease the proportion of oocytes that cleaved to 2- to 4-cell-stage embryos. A delay in the first two cleavages was recorded in the 0.1 and 1 μ g/L CBZ-treated oocytes relative to the control group. However, the proportion of oocytes that developed to the blastocyst stage did not differ between groups. On the other hand, alterations in transcript abundance were recorded in blastocysts derived from oocytes treated with 1 μ g/L (STAT3, GATA), 10 μ g/L (GDF9, STAT3) and 100 μ g/L CBZ (CCA2, GDF9, GATA). We conclude that exposure to low levels of CBZ affects, to some extent, both the oocyte and spermatozoa. Moreover, CBZ-induced alterations seem to carry over to the developed embryo. While the current study focuses on CBZ, the effect of its metabolites should also be examined.

Abstract # 1923

The Role Of Janus Kinase 3 (JAK3) In Bovine Ovarian Granulosa Cells. Amir Zareifard, Kalidou Ndiaye

Janus kinase 3 (JAK3) is a member of the membrane-associated non-receptor tyrosine kinase protein family predominantly expressed in hematopoietic cells, and mediates signals initiated by cytokine and growth factor receptors through the JAK/STAT pathway. We have previously identified JAK3 as a differentially expressed gene in granulosa cells (GC) of bovine preovulatory follicles and shown its downregulation in vivo in ovulatory follicles by the endogenous luteinizing hormone (LH) and post-hCG injection. We hypothesize that JAK3 signaling in GC might be potentiated by FSH and would lead to the recruitment and phosphorylation of target proteins, which contribute to the growth of the dominant or preovulatory follicle. The objectives of this study were to analyze the effects of JAK3 inhibition and overexpression in the phosphorylation of target proteins including STAT proteins and newly identified JAK3 binding partners CDKN1B and MAPK8IP3 and define JAK3 function in ovarian GC. GC from slaughterhouse ovaries were used for in vitro experiments and treated with or without FSH and with or without Janex-1, a JAK3 inhibitor. JAK3 regulation by FSH as well as expression and phosphorylation of target genes and proteins were analyzed by RTgPCR and western blotting, respectively. Additionally, an in vivo model was used with GC obtained from small follicles (SF: 2-4 mm), growing dominant follicles at day 5 of the estrous cycle (DF), ovulatory follicles obtained 24 hours following injection of hCG (OF) in order to analyze the regulation of JAK3 targets. We previously reported JAK3 downregulation by hCG in OF as compared to DF and SF. RT-qPCR analyses from this study using in vivo samples showed that other JAK members were differently regulated. JAK1 steady-state mRNA was stronger in OF as compared to SF, DF and CL, while JAK2 expression was stronger in CL as compared to the different groups of follicles (SF, DF,

OF). In contrast, TYK2 expression was weaker in SF as compared to DF, OF and CL but did not change among DF, OF and CL. In vitro experiments revealed that Janex-1 treatment significantly decreased JAK3 expression in GC while FSH tended to increase JAK3 expression. Additionally, steady-state mRNA expression for steroidogenic enzymes CYP19A1 and CYP11A1 as well as proliferation markers PCNA and CCND2 were upregulated in GC with FSH treatment and significantly decreased with Janex-1 treatment as compared to control. Western blot analysis showed that JAK3 overexpression increased STAT3 phosphorylation while Janex-1 treatment reduced STAT3 phosphorylation levels with or without JAK3 overexpression. However, FSH treatment for 4 hours seems to partially rescue STAT3 phosphorylation in Janex-1-treated cells. These results suggest that JAK3 plays a key role in GC proliferation, follicular growth and steroidogenesis likely trough phosphorylation of target proteins.

FG-oocytes showed chromatin condensation in both peri-nucleus and peri-nucleolus, both of which were transcriptionally silent. Mitochondria with high membrane potential were evenly distributed in XX FG-oocytes but concentrated near the nucleus or aggregated in XY FG-oocytes. Intensity of EU labeling was comparable between XX and XY oocytes of 50-59 µm whereas it became significantly weaker in XY oocytes than XX oocytes of 60-69 µm. Three way comparisons of RNA-Seq data in the oocytes of 50-59 µm revealed; (1) 13.8% of X-linked DEGs showed the transcript levels in correspond to the X chromosome dosage; (2) 9 genes on the Y short arm and 2 genes near the distal end of the Y long arm were highly expressed in XY oocytes; and (2) 54 and 39 X-linked and autosomal genes show higher and lower transcript levels, respectively, in XY oocytes compared to XX and XO oocytes. In conclusion, the Y-linked genes are highly expressed and alter the transcript levels of X-linked and autosomal genes in XY oocytes by the mid growth phase, potentially causing precocious decline in transcription and abnormal morphological features in XY FG-oocytes.

Abstract # 2102

Hyaluronic Acid Component Supplementation Increases Perivitelline Space Thickness During in vitro Oocyte Maturation. Kimberly N. Sprungl, Haley A. Arena, Emma C. Hicks, Skyla B. Reynolds, Brian D. Whitaker

The addition of the perivitelline space (PVS) components glucuronic acid and N-acetyl-D-glucosamine (GlcNAc) to the media increase PVS thickness and the amount of hyaluronic acid by the end of oocyte maturation. A decrease in polyspermic penetration and subsequent improvement in embryonic development can be attributed to this increase in PVS thickness. However, it is unknown if the PVS component supplementation has an environmental effect or is acting directly on the PVS. Therefore, the objective of this study was to determine if glucuronic acid and GlcNAc supplementation to the media was incorporated into the oocyte PVS or had alternative beneficial effects in the surrounding environment and granulosa cells. Oocytes (n=180) were supplemented during maturation with 4-methylumbelliferone (MU) (0, 0.125, 0.250, 0.375, 0.500 mM) to determine the minimum concentration of MU (hyaluronic acid synthase inhibitor) that had no effect on oocyte maturation but significantly decreased the PVS thickness. The PVS thickness was determined at the equatorial plane of the oocyte using a micrometer. The addition of 0.250 mM MU was the lowest concentration observed to cause PVS thickness $(3.87 \pm 0.12 \,\mu\text{m})$ to be significantly thinner (P<0.05) without affecting maturation compared to no MU supplementation $(4.33 \pm 0.27 \,\mu\text{m})$. Based on those results, oocytes were supplemented with or without 0.01 mM glucuronic acid and 0.01 mM GlcNAc and with or without 0.250 mM MU then evaluated for the amount of hyaluronic acid (n = 360) present. Hyaluronic acid concentrations were determined using an ELISA method. The amounts of hyaluronic acid/oocyte differed significantly (P<0.05) between each treatment group. Supplementing MU to the media decreased the amount of hyaluronic acid $(1.03 \pm 0.05 \text{ pg/oocyte})$ compared to not supplementing the media with MU (2.16 ± 0.01 pg/oocyte). Supplementing the

maturation media with 0.01 mM glucuronic acid and 0.01 mM GlcNAc increased the amount of hyaluronic acid (4.16 \pm 0.09 pg/oocyte) compared to no supplementation of the PVS components. Adding MU to the PVS component supplemented media decreased the amount of hyaluronic acid (3.91 \pm 0.03 pg/oocyte), but not to the same level as oocytes only supplemented with MU. These results suggest that when hyaluronic acid synthase is inhibited, supplementation of the PVS components are supplemented to the maturation media they improve the PVS thickness through incorporation into the matrix and not by benefiting the surrounding environment.

Abstract # 2150

Metalloproteinase Activity Allows The Oocyte To Detach From The Zona Pellucida At Ovulation. Angus D. Macaulay, Kevin Moore, Jay M. Baltz

Fully grown oocytes are tightly attached to the zona pellucida (ZP) in the follicle. Following ovulation or mechanical isolation, they progressively detach within the first few hours of meiotic maturation. The underlying mechanisms leading to detachment remain unknown. We hypothesized that oolemma-zona release is mediated by a peptidase cleaving ZP proteins that still remain in their transmembrane form, thus attaching the oocyte to the ZP. We therefore sought to determine whether proteinase activity was required for oocyte-ZP detachment and if so, to identify the proteinase. An initial bioinformatics screen was performed, using published RNAseg datasets for mouse oocytes (GSE70116) to reveal oocyte transcripts encoding peptidases as identified in the MEROPS peptidase database. These were further refined using Gene Ontology terms indicating localization in the plasma membrane or extracellular space. This led to the identification of thirty-nine initial candidate extracellular peptidases in oocytes. Small-molecule inhibitors selective for each class of candidates were screened for their ability to prevent oocyte detachment from the ZP using an osmotic shock assay. We found that only inhibition of the metalloproteinases class of peptidases significantly inhibited oocyte-ZP detachment. Oocytes remained strongly attached to the ZP in the presence of the general metalloproteinase inhibitors batimistat or marimistat for at least 24 hours, persisting even through first polar body formation. Oocytes matured in the presence of the inhibitor developed similarly to controls following activation and had comparable egg activation rates. Immunofluorescence imaging using a monoclonal antibody that recognizes an epitope just distal to the putative cleavage site of the ZP3 protein was carried out on maturing oocytes following an incubation in acid Tyrode's solution to remove cleaved ZP protein. Within 1.5 hours following oocyte isolation we observed significant membrane-bound ZP3 signal loss with further progressive loss continuing until four hours of maturation. This loss was prevented by metalloproteinase inhibition. More specific inhibitors were then employed, allowing us to narrow our likely candidates to the M12 family (ADAM and ADAMTS family) of metalloproteinases. An inhibitor reportedly selective for ADAM10, GI254023X, effectively inhibited ZP detachment, provisionally implicating ADAM10, which is highly expressed in oocytes.

We have thus identified the M12 family of metalloproteinases, possibly ADAM10, as likely to be responsible for the detachment of the oolemma from the ZP.

Abstract # 2157

Cumulus-Oocyte Interaction Is Required To Maintain Active Suppression Of Glycine Transport In The Preovulatory Mouse Oocyte. Allison K. Tscherner, Jay M. Baltz

Oocytes and early embryos are highly sensitive to changes in cell volume. It is now understood that cell volume dysregulation was a major cause of developmental arrest that occurred in traditional embryo culture. Early (1- to 2-cell) mouse embryos use a novel mechanism to control cell volume, in which glycine is accumulated intracellularly via the GLYT1 transporter (SLC6A9 protein). While SLC6A9 is expressed and localizes to the membrane of fully-grown oocytes, transport of glycine is absent until this transporter becomes activated by an unknown mechanism. In vivo, GLYT1 activation normally occurs in parallel with release of an oocyte from meiotic arrest that precedes ovulation. It also activates in vitro shortly after oocytes are removed from antral follicles, implying active suppression within follicles. The primary aim of this research is to identify the specific factor(s) responsible for the release of suppression of GLYT1 in oocytes, which are currently not known. To evaluate this, we have established a GLYT1 activity assay based on [3H]glycine uptake and adapted it for single oocyte measurements. Oocytes were cultured within COCs for 4 hours after removal from follicles. We have found for the first time that it is possible to maintain guiescence of GLYT1 in GV oocytes within isolated COCs, in a model where COCs are cultured individually and meiotic arrest is maintained by natriuretic peptide precursor C (NPPC). This suppressive effect is reversed when NPPC is removed. NPPC acts by inducing production of cGMP, which in turn mediates suppression of the oocyte's cAMP-specific phosphodiesterase, PDE3. GLYT1 suppression is similarly maintained when oocyte meiosis is arrested with milrinone, a direct inhibitor of PDE3. However, GLYT1 suppression is maintained only in intact COCs cultured in milrinone, whereas oocytes stripped of cumulus cells maintain meiotic arrest but GLYT1 is activated. Together, these findings indicate that maintaining GLYT1 suppression requires both meiotic arrest and the presence of cumulus cells, though either factor itself is insufficient to maintain active suppression. Finally, since gap junctions between the oocyte and cumulus cells play a major role in the physical association as well as chemical communication between these cells, we impaired gap junctional coupling with specific inhibitors and observed a partial activation of GLYT1 in COCs in the presence of milrinone. Overall, we have shown that the factor maintaining GLYT1 suppression before the resumption of meiosis requires the presence of cumulus cells. GLYT1 quiescence is only maintained under conditions of oocyte meiotic arrest and appears to involve gap junctional communication between cumulus cells and the oocyte. This study highlights the conditions required for glycine transport in vitro and provides insight into the signaling mechanisms likely involved in GLYT1 suppression in ovarian follicles in vivo.

Validation of DAPI/Anti-Iamin A/C Immunofluorescent Labeling Technique for Improved Classification of Meiotic Maturation Stage in Porcine Oocytes. Kadden H. Kothmann, Zheng Shen, Shaodong Guo, Annie E. Newell-Fugate

Use of aceto-orcein staining to visualize the stages of oocyte meiotic maturation is ambiguous as the diplotene stage of meiosis, before germinal vesicle breakdown (GV), cannot be precisely distinguished from the germinal vesicle breakdown (GVBD). An immunofluorescent technique which allows for visualization of both the nuclear membrane and chromatin could increase the precision and accuracy between discernment of the diplotene (GV intact) and post-diplotene (GVBD) stages of meiotic maturation. We chose to utilize a fluorophore-bound antibody to detect lamin proteins on the inner surface of the GV coupled with labeling of the chromatin by 4',6diamidino-2-phenylindole (DAPI) as an alternative approach to aceto-orcein staining. This study compares a DAPI/Anti-Iamin A/C labeling protocol to aceto-orcein staining in porcine oocytes with the following specific objectives: 1) validation of a fluorophorebound anti-lamin antibody in porcine oocytes; 2) comparison of the percent of GVBD classification using each technique; 3) comparison of procedural losses using each technique. Immature porcine oocytes were aspirated from slaughter-house gilt ovarian follicles (3-8 mm in size) using vacuum aspiration, after which those oocytes with at least 2 layers of cumulus cells and homogenous cytoplasm were selected for maturation. Oocytes (n=180) were matured in groups of 40-45 per well in Medium 199 in 4 well IVF plates (NUNC, Thermofisher). Replicates (n=3) of oocytes were divided into two groups: aceto-orcein and DAPI/Anti-Iamin A/C. Aceto-orcein stained oocytes were mounted on slides, fixed for 48 hours in an aceto-alcohol fixative followed by staining with acetoorcein. DAPI/Anti-lamin A/C oocytes were exposed to Triton-X and Tween 20 detergents, 2% BSA blocking buffer, and Alexa Fluor 488-labeled mouse anti-lamin A/C (Cell Signaling Technology), then mounted on a slide with DAPI-containing mountant (Cell Signaling Technology). For the DAPI/Anti-Iamin A/C technique, meiotic stage was classified from morphologic observation of chromatin material (DAPI, blue) and germinal vesicle (anti-lamin, green) under a fluorescent confocal microscope at 200x magnification. Aceto-orcein staining classification was performed using bright field microscopy at 400x. Procedural losses for each technique were calculated by dividing the initial number of oocytes allocated to a given technique by the final number found on the slide. Although not significant, the DAPI/Anti-lamin A/C technique experienced less oocyte loss than the aceto-orcein stain $(7.9\% \pm 3.7 \text{ vs.} 32.8\% \pm 13.8, p = 0.2)$. Additionally, despite not reaching the criteria for statistical significance, the DAPI/Antilamin A/C technique yielded fewer un-identified oocytes $(3.95\% \pm 3.95 \text{ vs.} 35.82\% \pm 3.95\% \pm 3.9$ 22.78, p = 0.19). It was easier to qualitatively identify the GVBD using the DAPI/Anti-lamin A/C technique than the aceto-orcein staining. The anti-lamin A/C antibody had crossreactivity with a protein on the cell membrane, which occurred predominantly in the condensed chromatin and telophase stages (91.67%). We anticipate that increased numbers of repetitions will decrease the variability within each technique and improve

our ability to discern true differences between these two techniques for assessment of meiotic maturation in porcine oocytes.

Abstract # 2248

Validation of Methods to Determine ATP Quantity and Mitochondrial DNA Copy Number from a Single Oocyte. Casey C. Read, Emma A. Hessock, Emma J. Horn, Samantha R. Roberts, Sarah E. Moorey

To complete meiotic maturation, be fertilized, and support early embryonic development the oocyte must achieve metabolic maturation. Metabolic maturation involves obtaining the necessary energy stockpiles and mitochondria number to support these downstream developmental processes. Oocytes primarily produce energy via oxidative phosphorylation while cumulus cells possess high glycolytic activity. This metabolic dichotomy results in the transport of metabolic products like ATP, pyruvate, and NADH from the cumulus cells to support the oxidative phosphorylation of the oocyte. This intricate relationship remains to be completely elucidated because previous studies have not related individual oocyte ATP concentration with that oocyte's mitochondria number or cumulus cell glycolytic activity. Our lab has developed a system that allows us to obtain ATP and mitochondrial DNA copy number from a single oocyte. These values can then be assessed concurrently with measures of glycolytic activity in the cumulus cells to holistically visualize the metabolic activity of the cumulus-oocyte complex. We hypothesized that careful division of sinale oocyte samples would enable multiple metabolic measurements. Our objective was to validate and utilize the ability to measure mitochondrial DNA copy number and ATP concentration in single oocytes to better understand their relationship within the oocyte. We aspirated cumulus-oocyte complexes from 3-8mm follicles of Bos taurus, abattoir derived ovaries. Cumulus-oocyte complexes were washed with TCM-199 media before morphologically ideal cumulus-oocyte complexes were transferred into individual 20 µl microdrops of 1X Trypsin. Cumulus cells were manually removed by repeated pipetting, and denuded oocytes were washed twice in 1x PBS. Both cell types were individually snap frozen in liquid nitrogen. Initially, we validated whether the values of nanograms of total DNA and ATP levels were comparable in whole oocytes and oocyte fractions. Four oocytes were combined and the equivalents of two whole oocytes, two half oocytes, and four quarter oocytes were quantified for DNA concentration and assayed for ATP levels. The values for the half oocytes were multiplied by two and the values for the quarter oocytes were multiplied by four to represent whole oocyte equivalents. ANOVA was performed on the values and no significant difference was observed in the whole oocyte equivalent DNA and ATP levels obtained from either oocyte fraction (p>0.40 and p>0.75, respectively). We then performed an experiment to relate oocyte ATP concentration with mitochondria number within germinal vesicle stage oocytes (n=32.) We utilized $\frac{1}{4}$ oocyte equivalents to perform duplicate measures of ATP concentration and mitochondrial DNA copy number from single oocyte samples. We used a commercial ATP assay kit to quantify

ATP concentration and performed qPCR of the COX1 gene to quantify mitochondrial DNA copy number. Linear regression was performed, and for each increase in one mitochondrial DNA copy number within the oocyte there was a 0.33 pMol increase in oocyte ATP concentration. While the results were not significant (p=0.11), they confirmed the feasibility of our objective. The ability to obtain multiple metabolic measures from a single oocyte has incredible implications for future studies in our lab and others that seek to further elucidate the complex metabolic interactions found within cumulus-oocyte-complexes.

Abstract # 2252

Aging of Pig Oocytes Initiates Apoptosis. Haley A. Arena, Emma C. Hicks, Kimberly N. Sprungl, Skyla B. Reynolds, Brian D. Whitaker

Oocytes that experience prolonged aging, or are not fertilized during the optimal time window, potentially have decreased occurrences of successful fertilization and embryonic development. Trichostatin A (TSA) inhibits germinal vesicle breakdown and was used to stimulate aging by delaying oocyte maturation. The objective of this study was to determine the effects of aging on the initiation of apoptosis in in vitro matured pig oocytes. Oocytes (n=1453) were matured with or without TSA (100 ng/mL) for 24 (short OMI) or 48 h (long OMI) followed by an additional 16 h maturation (OMII) without TSA. Oocytes were used after OMI or OMII for either Annexin V (n=453), mitochondria membrane potential (n=405), Caspase 3 (n=403), or TUNEL (n=192) assays. Based on the Annexin V assay, oocytes matured through OMII with a short OMI and TSA supplemented had a significantly greater (P < 0.05) percent of annexin V positive oocytes $(38.3 \pm 0.17\%)$ than the other treatments. Oocytes matured through OMI with a short OMI and TSA supplemented ($9.1 \pm 0.17\%$), through OMII with a short OMI and TSA supplemented (10.0 \pm 0.16%), and at the end of long OMI and no TSA supplemented $(6.5 \pm 0.16\%)$ had significantly greater (P < 0.05) percent of propidium iodide positive oocytes than the other treatments. Oocytes matured through OMI with a short OMI and TSA supplemented $(7.3 \pm 0.15\%)$, through OMII with a long OMI and TSA supplemented $(10 \pm 0.16\%)$, and no TSA supplemented $(8.1 \pm 0.15\%)$ had significantly greater (P < 0.05) percent positive oocytes for both annexin V and propidium iodide than the other treatments. The mitochondria membrane potential of oocytes matured through OMI (5.87 ± 6.44) and through OMII (7.14 ± 5.41) with a long OMI and no TSA supplemented had a significantly greater (P < 0.05) percent of intact mitochondrial membranes than the other treatments. Results from the TUNEL assay indicate oocytes matured through OMII with a short OMI and TSA supplemented $(23.8 \pm 2.99\%)$ and through OMI with a long OMI and TSA supplemented $(24.3 \pm 1.11\%)$ had significantly greater (P < 0.05) percent of oocytes with fragmented DNA than the other treatments, except for the oocytes matured through OMII with a long OMI and TSA supplemented $(35.0 \pm 3.55\%)$, which was significantly areater (P < 0.05) than all other treatments. This study demonstrates that by the end of maturation in the aged oocyte, early stages of cellular apoptosis could be triggered.

Loss Of Cnotél Impairs Inosine RNA Modifications In Mouse Oocytes. Pavla Brachova, Nehemiah S. Alvarez, Lane K. Christenson

Oocyte meiotic maturation is regulated by a balance of RNA storage and translational activity. Through a process that is incompletely understood, a stock of maternal mRNA undergoes translational activation, followed by deadenylation and mRNA decay, facilitating maternal mRNA clearance. After translational activation, transcripts become deadenylated by the CCR4-NOT complex through a translationally coupled mechanism. Knockout of Cnot6l, a component of the CCR4-NOT complex, results in mRNA decay defects during MI entry. Knockout of Btg4, another component of the CCR4-NOT complex, results in mRNA decay defects in the early embryo. Our previous work in oocytes, as well as published work from others, established that inosine RNA modifications can impact mRNA stability through a translation mechanism. Since the Cnot6I and Btg4 knockout mice result in over-translation and stabilization of mRNA, we hypothesized that in these mutant backgrounds, we would observe an increase in inosine modifications in mRNA. To test this, we used a computational approach to identify inosine RNA modifications in total and polysomal RNA-seq data during meiotic maturation (GV, MI, and MII stages, n=2/stage) in wild-type, Cnot6l-/-, and Btg4-/- mice. Surprisingly, we observed strong defects in inosine modifications in oocytes from Cnot6l-/-, but not in Btg4-/- mice. Among common transcripts, inosine modifications were significantly reduced in Cnot6l-/- GV oocytes (WT=1249±232, Cnot6l-/-=91±27, Btg4-/-=1161±110, p<0.05 one-way ANOVA). Additionally, sequencing of the polysomeassociated RNA revealed clearance of inosine modified mRNA (GV=1666±30; MI=850.5±5.5; MII=709.5±6.5; p<0.05 one-way ANOVA). Efficiency of inosine RNA modifications also decreased at these stages (GV=83%, MI=38%, and MII=32%). Our results suggest a novel connection between the components of the deadenylation and inosine RNA modification machinery during oocyte maturation.

Ovarian Dysfunction

Abstract # 1689

Iodoacetic Acid Affects Estrous Cyclicity, Ovarian Gene Expression, and Hormone Levels in Mice. Andressa V. Gonsioroski, Liying Gao, Daryl D. Meling, Michael Plewa, Jodi A. Flaws

The disinfection of drinking water was a major public health achievement of the last century, greatly reducing the incidence of waterborne diseases. However, the reaction between disinfectants and organic/inorganic matter in water generates water disinfection byproducts (DBPs). Iodoacetic acid (IAA) is one DBP that has been shown to be an ovarian toxicant in vitro, but its effects on the ovaries in vivo are not well known. This study determined whether IAA exposure affects estrous cyclicity, the levels of reproductive hormones, and ovarian expression of genes related to apoptosis, the cell cycle, steroidogenesis, estrogen receptors, and oxidative stress in mice. Adult CD-1 mice were dosed with only water or with IAA (0, 0.5, 10, 100, and 500 mg/L) in the drinking water for 35 days and estrous cyclicity was monitored for the final 14 days of dosing. After dosing, ovaries were collected for analysis of expression of apoptotic factors (Bax, Bok, Aimf1, Bcl2 and Bcl2110), cell cycle regulators (Ccna2, Ccne1, Ccnb1, Ccnd2, Cdk4, and Cdkn1a), steroidogenic factors (Star, Cyp11a1, Cyp17a1, Cyp19a1, Hsd17b1, and Hsd3b1), estrogen receptors (Esr1 and Esr2), and oxidative stress markers (Sod1, Cat, Gpx, Gsr, and Nrf2). In addition, sera were collected to measure pregnenolone, androstenedione, testosterone, estradiol, inhibin-B, and follicle stimulating hormone (FSH) levels. IAA exposure (500 mg/L) decreased the time that the mice spent in proestrus compared to control. Further, IAA exposure decreased expression of the pro-apoptotic factor Bok (100 and 500 mg/L), the cell cycle regulator Ccnd2 (500 mg/L), and borderline decreased expression of the anti-apoptotic factor Bcl2l10 (10 mg/L), the pro-apoptotic factor Aimf1 (0.5 mg/L), and the steroidogenic factor Cyp19a1 (10 and 500 mg/L) compared to control. In contrast, IAA exposure increased expression of the pro-apoptotic factors Bax and Aimf1 (500 mg/L), the antiapoptotic factor Bcl2l10 (500 mg/L), the cell cycle regulators Ccna2, Ccnb1, Ccne1, and Cdk4 (500 mg/L), and the estrogen receptor Esr1 (500 mg/L) compared to control. Moreover, IAA exposure decreased expression of Cat and Sod1 (0.5 mg/L), and increased expression of Cat (500 mg/L), Gpx (10 mg/L), and Nrf2 (500 mg/L). IAA exposure did not affect expression of Star, Cyp11a1, Cyp17a1, Hsd17b1, Hsd3b1, Esr2, and Gsr compared to control. Further, IAA exposure decreased estradiol levels (500 mg/L), but did not alter pregnenolone, androstenedione, testosterone, inhibin-B, and FSH levels compared to control. Collectively, these data show that IAA exposure alters estrous cyclicity, ovarian gene expression, and estradiol levels in mice. Supported by NIH R21 ES028963 and NIH T32 ES007326.

The PARP Inhibitor, Olaparib, Blocks Intrinsic DNA Repair In Oocytes And Depletes The Ovarian Reserve In Mice: Implications For Fertility. Amy Winship, Meaghan Griffiths, Urooza Sarma, Kelly Phillips, Karla Hutt

Introduction: The ovary contains a finite number of oocytes stored within primordial follicles, which give rise to all mature ovulatory oocytes. They are highly sensitive to DNA damaging insults, like cytotoxic cancer treatments. Members of the poly(ADP-ribose) polymerase (PARP) enzymes are central to the repair of single-strand DNA breaks. PARP inhibitors have shown promising clinical efficacy in reducing tumour burden, by blocking DNA repair capacity. Olaparib is a PARP1/2 inhibitor recently FDA approved for treatment of BRCA1 and BRCA2 mutation carriers with metastatic breast cancer. Despite this, there is no preclinical or clinical information regarding the potential impacts of olaparib on the ovary or female fertility. Unfortunately, it may be many years before clinical data on fertility outcomes for women treated with PARP inhibitors becomes available, highlighting the importance of rigorous preclinical research using animal models to establish the potential for new cancer therapies to affect the ovary in humans. We aimed to comprehensively determine the impact of olaparib alone, or following chemotherapy, on the ovary in mice. Methods: On day (d)0, adult female mice (n=5-8/treatment group) were administered a single intraperitoneal dose of cyclophosphamide (75mg/kg/body weight), doxorubicin (10mg/kg), carboplatin (80mg/kg), paclitaxel (7.5mg/kg), or vehicle control. From d1-d28, mice were administered subcutaneous olaparib (50mg/kg), or vehicle control. This regimen is proven to reduce tumour burden in preclinical mouse studies and is also physiologically relevant for women. Vaginal smears were performed to monitor estrous. At 24h after final treatment, ovaries were harvested for follicle enumeration and immunohistochemical analysis of primordial follicle remnants (FOXL2 expressing granulosa cells), DNA damage (yH2AX) and analysis of apoptosis (TUNEL). Serum anti-Müllerian hormone (AMH) concentrations were measured by ELISA. Results: Olaparib significantly depleted primordial follicles by 46% versus control (p<0.01), but had no impacts on other follicle classes, serum AMH, corpora lutea number (indicative of ovulation), or estrous cycling. Primordial follicle remnants were rarely detected in control ovaries, but were significantly elevated in ovaries from mice treated with olaparib alone (p<0.05). Similarly, DNA damage denoted by yH2AX foci, was completely undetectable in primordial follicles of control animals, but was observed in \sim 11% of surviving primordial follicle oocytes in mice treated with olaparib alone. Discussion: These observations suggest that functional PARPs are essential for primordial follicle oocyte maintenance and survival and that inhibition of intrinsic DNA repair mechanisms may be a cause of primordial follicle loss. Importantly, diminished ovarian reserve can result in premature ovarian insufficiency and infertility. Notably, the extent of follicle depletion might be enhanced in BRCA1 and BRCA2 mutation carriers, and this is the subject of current investigations. Together, our data suggest that fertility preservation options should be considered for young women prior to olaparib treatment, and that human studies of this issue should be prioritised.

Examining The Effects Of Obesity On Circulating Prolactin And The Ovarian Proteome In Hyperphagia-Induced Obese Mice. Crystal M. Roach, Kendra L. Clark, Aileen F. Keating

Obesity is a metabolic syndrome that affects approximately 93.3 million U.S. adults, with increased incidence in African American (\sim 46.8%) and Hispanic populations (\sim 47.0%). Comparably, obesity affects approximately 18.5% of children, with higher prevalence also in African American (22.0%) and Hispanic (25.8%) ethnicities. Reproductive health is compromised in obese women, such that research has shown a decline in conception and implantation, fecundity, infertility, poor oocyte quality, birth defects, miscarriage, polycystic ovarian syndrome (PCOS), and ovarian cancer. Previous studies by our group have discovered that obesity alters ovarian insulin signaling, folliculogenesis, and steroidogenic signaling in female mice. Recent research suggests that prolactin (PRL) promotes insulin sensitivity and may play a key role in inducing hyperphagia resulting in obesity-driven metabolic changes. Utilizing a hyperphagic mouse model, we hypothesized that dysregulation of proteins involved in metabolic and ovarian pathways will ensue in proteomes of obese mice along with increases in PRL. Female wild-type non-agouti (a/a; n = 10; designated lean) and agouti lethal yellow (KK.Cg-Ay/J; n = 10; designated obese) were fed a standard chow diet ad libitum, until 10 weeks of age. Serum PRL levels (pg/mL) were analyzed by a solid phase enzyme-linked immunosorbent assay (ELISA). Ovarian protein extracts (50 µg/ul) were analyzed by LC-MS/MS and gene ontology (GO) analysis was performed with PANTHER 14.1 Classification System to identify biological processes altered. Serum PRL levels were numerically but not statistically decreased (P = 0.17) in obese relative to lean mice. In lean and obese mice, 1,400 and 1,411 ovarian proteins were detected, respectively. Among the treatment comparison, 34 ovarian proteins were deemed to be differentially abundant (P < 0.05; log2fc>±0.1) with 20 increased and 14 decreased. Forty-two biological processes were identified with a 39.4-fold enrichment associated with metabolic processes related to cellular and hormonal proteins. This data supports the hypothesis that obesity alters the ovarian proteome potentially contributing to reproductive dysfunction. This project was funded by the Bailey Career Development Award from Iowa State University.

Abstract # 1843

High-Refined Carbohydrate Diet Induced A Disruption Of The Reproductive Function In Female Rats. Oscar Mauricio Santamaria Niño, Charles Santos da costa, Eduardo Merlo, Jones Bernardes Graceli

Obesity is a growing epidemic in the world and impacts all functions of the body, including reproduction. An increase of consumption of diet containing fat or refined carbohydrate contributes to obesity and related diseases. Although studies have shown the obesity effect induced by high fat diet in reproduction, no reproductive data are

available in obesity animals as result of fed high-refined carbohydrate-containing (HC) diet. In this study, we assessed whether HC diet results in reproductive abnormalities. Adult female Wistar rats were fed regular chow (Socil, CON) or HC diet for 15 days. The HC diet was composed of 45% condensed milk, 10% refined sugar, and 45% chow diet. The macronutrient composition of the chow diet (4.0 kcal/g) was 65.8% carbohydrate, 3.1% fat, and 31.1% protein; the HC diet (4.4 kcal/g) was 74.2% carbohydrate, 5.8% fat, and 20% protein. It is important to note that HC diet contains at least 30% refined sugars, mostly sucrose. We further assessed the reproductive tract function, inflammation, oxidative stress, fibrosis and metabolic parameters. All the protocols were approved by the Ethics Committee of Animals of the Federal University of Espírito Santo. All data are reported as the mean ± SEM. Comparisons between the groups were performed using Student's and Mann-Whitney t-tests for Gaussian and non-Gaussian data, respectively. A value of p < 0.05 was regarded as statistically significant. HC diet led to increased body weight and adiposity compared with CON rats (p<0.05, n=10). An irregular estrous cyclicity, with longer estrous cycle length (54 %), tendency to increase basal LH, FSH and estrogen levels were observed in HC rats 30 and 48 % respectively (p=0.09, p=0.05 and p=0.05, respectively, n=10). A reduction in ovarian follicular reserve was observed, with low primordial and primary follicles numbers in HC rats compared with CON rats 30 and 15 % respectively (p<0.05, n=6). Impairment in ovarian follicular development was observed in HC rats, with reduction in preantral, antral follicles and corpora lutea numbers 15 and 25 % (p<0.05, n=6). HC diet led to uterus atrophy, reduction in the endometrium and myometrium area and uterine gland numbers (10% p<0.05 and 12% p<0.001, respectively, n=6).

HC diet was able to increase ovary and uterus inflammation by increase mast cells number (Alcian blue staining, 52 and 46 % respectively, p<0.05, n=6). Imbalance in oxidative stress was observed in reproductive tract in HC rats, with increase in TBARS 86 % respectively, p<0.05, n=5 (the thiobarbituric reactive species) and DHE uterine (superoxide anion indicator) 23 % respectively, p<0.05, n=5). Ovarian and uterine fibrosis was observed in HC rats using a Picrosirius Red staining (32 and 30 %, respectively, p<0.05, n=5). Other metabolic dysfunctions were observed in fat HC rats, with abnormal serum lipid profile impairment in insulin sensitivity and glucose tolerance tests, an increase in the serum leptin and a reduction in the adiponectin levels 33 and 53 % respectively (p<0.05, n=6). Thus, these data suggest that HC diet is responsible to abnormal reproductive and metabolic functions in female rats.

Abstract # 1944

Testosterone Induces Proliferation Of Ovarian Stroma By Upregulation Of Cell Cycles And Growth Factors. Myoungseok Han, Yeon Jean Cho, Juhwa Baek, Seung Bin Park

This study aims to investigate that testosterone would be able to proliferate the stromal cells in ovary and it would be explicable for the ovarian enlargement of polycystic ovary syndrome. Immunochemical expression of Ki 67 were quantified from ICR mice

ovaries treated with intraperitoneal injection of testosterone (100mg/kg). The expressions of cell cycle regulating genes and growth factors (GDF9 and BMP15) were quantified by quantitative PCR from the cultured ovary stromal cells.. Apoptosis related protein (Caspase-9, Caspase-3 and Bcl-2) and cell signaling molecules (pRb, E2F1, p27 and p21) were measured by western blot as well. Testosterone induced higher Ki-67 expressions in both primary and secondary follicles significantly. BMP15 and GDF9 expressions were higher in the testosterone treated cells. Caspases and bcl-2 expressions were lower in the testosterone treated cells as well. Those events were controlled through the cell signaling molecules that were fit for the cell proliferation. In conclusion, this study showed that testosterone induced the cell proliferations in ovary and the cell cycle controlling would be another therapeutic option for polycystic ovary syndrome.

Abstract # 2098

Increased Adiposity And Circulating Glucose Promote Pro-Inflammatory Signaling In The Cumulus Oocyte Complex Of TLR4-Hyporesponsive Mice Fed A High Fat/High Sugar Diet. Alison F. Ermisch, Katie L. Bidne, Jennifer R. Wood

Oocyte maturation, both cytoplasmic and meiotic, is essential for fertilization and normal embryonic development. Multiple studies show that obesity reduces oocyte quality due, in part, to abnormal cytoplasmic maturation. Obesity is a multi-faceted phenotype characterized by insulin resistance and increased circulating proinflammatory cytokines. One source of inflammation is accumulation of excess adipose tissue. The other is loosening of intestinal epithelium tight junctions allowing endotoxin leak from the gut into circulation. To discriminate between adipose- and endotoxindependent effects of systemic inflammation on oocyte quality, we used C3H/HeJ mice, which contain a mutation in TLR4 and are hyporesponsive to lipopolysaccharide (LPS). Our hypothesis is that consumption of a high fat/high sugar western diet (WD) by female C3H/HeJ mice induces cumulus cell inflammation and impaired oocyte quality in the absence of TLR4 signaling. To test this hypothesis, 8-week old C3H/HeJ mice were randomly placed on a normal control diet (ND) or the WD in addition to 20% sucrose water. After four weeks, females were superovulated using 5IU each of PMSG and hCG and cumulus oocyte complexes were collected 16-18h post-hCG. Final body weight was higher (P<0.001) in WD (27.40±0.79g) than ND females (18.98±0.33g), with an increase in percent body fat (29.06±1.20%, 15.11±0.66%, respectively). Fasting glucose was also higher (P<0.01) in WD compared to ND females (127.9±6.1 mg/dL, 97.9±6.9 mg/dL, respectively), suggesting development of insulin resistance in WD females. A NanoString nCounter metabolism panel, which measures the abundance of 748 genes related to metabolic processes and immunometabolism, was performed using RNA from isolated cumulus cells. The majority of mRNAs with increased abundance (> 2-fold) were genes involved in cytokine and chemokine signaling (Alox15, Alox5, Csf3r, Il2ra, Itgam, Itgb2), TLR signaling (Tlr4, Itgam, Itgb2, Ctss, Ly86, Cd14), and NFkB signaling (Bcl2a1a, Tlr4, Cd14). Furthermore, cell type profiling indicated increases (P<0.01) in B-

cells and macrophages, in addition to increases in genes involved in T-cell receptor signaling (Ptprc, Cd28, Cd274) and antigen presentation (Tlr4, Cd14, Cybb, H2-Eb1, H2-Aa). Unexpectedly, there was no evidence of altered fatty acid or glucose metabolism. There were also no differences in the number of oocytes ovulated per female or percentage of degenerate oocytes between ND and WD females. Similarly, there was no difference in the percentage of spindle abnormalities in mature oocytes from ND (14%) and WD (9%) females. Using C3H/HeJ mice, we have developed a novel model that essentially eliminates pro-inflammatory contribution of circulating endotoxins, which characteristically leak from the gut in the context of obesity. Our data showed that consumption of a high fat/high sugar diet and concomitant increase in adiposity induced systemic inflammation independent of LPS-mediated TLR4 signaling. Differential gene expression in cumulus cells from WD mice indicates localized inflammation within the cumulus oocyte complex. We did not detect differences in the percentage of degenerate ovulated oocytes or spindle abnormalities, suggesting cumulus cell inflammation alters oocyte cytoplasmic maturation. Taken together, we have identified cumulus cell and oocyte phenotypes that are likely driven by increased adiposity and high circulating glucose.

Abstract # 2117

Identification Of Biomarkers In Urine And Saliva For Gilts With High Litter Size Potential. Lauren Fletcher, Nadeem Akhtar, Mohsen Jafarikia, Brian P. Sullivan, Brent DeVries, Victoria Stewart, Nicole Gregory, Rupasri Mandal, David Wishart, Lee-Anne Huber, Julang Li

Selection of gilts with high reproductive potential is an essential step in the management of a pork operation as selected gilts represent the future breeding stock of the herd. Current gilt selection protocols utilize phenotypic and genetic measures to identify the gilts of highest reproductive potential. However, these protocols are not highly efficient due to the low heritability of many reproductive performance traits, leading to the selection of more gilts than required, high culling rates, and profit losses. The metabolomic profile has emerged as a unique chemical signature that reflects the genetics, microbiome, physiology and environmental experiences of an organism of interest. Biofluids, such as urine and saliva, can be collected easily through non-invasive methods and contain this metabolomic profile. We hypothesized that through metabolomic analysis of biofluids (urine and saliva) collected from sows with known reproductive potential, biomarkers indicative of high reproductive potential could be identified and utilized to make the on-farm selection of gilts for the breeding stock more efficient. Urine and saliva samples from sows with high litter size (mean litter size of ≥ 16) and low litter size (mean litter size of ≤ 12) were collected 4-7 days after weaning (beginning of estrus) and analyzed for metabolites and steroid hormones using DI/LC-MS/MS and LC-MS/MS techniques, respectively. Of the 187 saliva metabolites analyzed, sphingomyelin C 20:2, hexadecanoyl-L carnitine and phosphatidylcholine diacyl C 20:0 were found to be significantly higher (p < 0.05) in the low litter size groups (n = 21) when

compared to the high litter size groups (n = 18). Of the 9 steroid hormones analyzed in urine, 17-hydroxyprogesterone was found to be at significantly higher levels (p < 0.05) in the high litter group (n = 16) compared to the low litter group (n = 18). Additionally, the urine hormone ratios of androstenedione:testosterone and

androstenedione:dehydroepiandrosterone were found to be significantly higher (p < 0.05) in the low litter size group (n = 18) when compared to the high litter size group (n = 16). Our findings reveal metabolite and steroid hormone differences between the high and low sow litter size groups. This lays the foundation of biomarker identification for gilt selection. Further validation will be performed to make conclusions regarding how reflective these biomarkers are of litter size. A prediction study involving the analysis of biofluid samples from non-pregnant gilts is underway to determine if levels of the biomarkers identified in this study are indicative of future reproductive potential.

Abstract # 2118

Platelet Rich Plasma (PRP) Treatment During Transplantation Of Ovarian Tissue Performed On A Rat Model - Evaluation Of AMHR And AMHR2 Mrna Expression. Anna Niwinska, Ricardo Faundez, Jaroslaw Kaczynski, Slawomir Gizinski, Katarzyna Siewruk, Zdzisław Gajewski, Ewa Kautz

Ovarian tissue transplantation seems to be a crucial fertility preserving option for some cancer survivals like young girls or women who are rejecting other options due to ethical concerns. Low effectivity and "burn-out" effect caused by time needed for neovascularization are still the main limitations of autotransplantation method. The aim of this study was to reveal a potential treatment of PRP on vitrified and transplanted ovarian tissue to maintain natural follicle reserve in rat model. Female WAG rats (n=18) in dioestrus phase underwent the standard ovariectomy. Gonads were vitrified with DMSO, ethylene glycol and sucrose solution and stored in liquid nitrogen for 30 days according to the protocol. Subsequently, warming solution with PRP was used in treated ovaries group (right side) while control ovaries (left) were moistened in sterile NaCl. After autotransplantation animals were divided into 3 groups (n=6 each group) and sacrificed on 2nd, 7th and 30th day postoperative. All samples were collected for histological analysis and for mRNA expression evaluation. Total primordial, primary and antral follicles number was counted. Afterwards we determined anti-Mullerian hormone and its receptor (AMH and AMHR2) expression in all samples. AMH together with AMHR2 have shown significant increased mRNA expression in treated groups in contrast to control groups (AMH :P=0,013; AMHR2 P= 0,012; unpaired t-test). In group "2" (2days after transplantation) difference between treated and control group was statistically significant in AMH expression (P=0,034) but non-significant in AMHR2 expression (P=0.064). In group "7" (7 says after transplant) AMH expression differed non-significantly (P=0,189), and AMHr2 expression was highly significantly different (P=0,002). Histological analysis of the preserved material stays in accordance with molecular analysis and confirms influence of the PRP on the transplanted ovaries. The data indicate favourable effect of PRP on follicles preservation in transplanted ovarian tissue which is

reflected in decreased "burn-out" effect especially in groups 2 and 7 days after after surgery. These findings correlate to previous data which present improved steroidogenic activity in all groups treated with PRP. Research supported by KNOW2018/CB/ESR5/7

Abstract # 2160

Clinical Insights from Ongoing Interventional Trials of Myo-inositol in Polycystic Ovarian Syndrome Across Varied Clinical Conditions: Systematic Review and Meta Analysis. Nitin Lad, Neha Lad

Introduction Published evidence demonstrates role of myo-inositol (MI) therapy in PCOS. We aim to identify and analyze trials across global registries to gain insights for the evolving role of MI in PCOS in varied clinical conditions including comorbidities Methods and Analysis We reviewed the contemporary protocols of the ongoing trials actively recruiting patients, through the WHO-ICTRP (www.who.int/ictrp/search/en) registry database. Latest evaluation was on January 6, 2020 with key word 'myoinositol', for the trials initiated over last 8 years (2012-2019). Two researchers independently extracted outcomes, SPSS was used for statistical analysis Results We evaluated clinical parameters to improve PCOS in association with other clinical conditions including metabolic syndrome, obesity, women undergoing ART procedures; across seven trials, cumulatively enrolling 654 patients; with trials being conducted in Belgium (2), India (2) and one each in Italy, Iran and Lebanon. The study designs varied from open label, double blind to quadruple comparing IM with metformin, rosuvastatin, clomiphene, D- chiro-inositol, folic acid, liraglutide, in monotherapy and combinations. Mean number of participants being enrolled is 93 (SD \pm 46, maximum 164, minimum 40, range 124, 95% CI 50 to 136). The trials evaluate the ovulatory dysfunction, menstrual frequency, variability of cycle length, lipid profile, glycemic indices, fertilisation rate, oocyte yield Discussion The present snapshot of worldwide ongoing clinical trials of myo-inositol provides useful information for planning futuristic clinical programs. Comparative assessment helps incorporate findings of ongoing trials, across various parameters in diverse clinical conditions with PCOS into decision models

Abstract # 2243

Anti-Mullerian Hormone Concentrations During Pubertal Attainment May Contribute To Altered Puberty And Predict Reproductive Performance In Heifers. Courtney M. Sutton, Shelby A. Springman, Jessica A. Keane, Sarah R. Nafziger, Alexandria P. Snider, Jeff W. Bergman, Scott G. Kurz, John S. Davis, Andrea S. Cupp

Our long-term goal is to develop markers identifying heifers that should be culled due to predicted reduced reproductive performance. Heifers that achieve earlier puberty are more likely to become pregnant, have a calf in the first 21 days of calving, and remain in the herd. Predicting when heifers will achieve puberty is difficult because there are

no inexpensive, easily administered methods, including known reproductive markers that accurately predict age at puberty or reproductive longevity in heifers. Anti-Mullerian hormone (AMH) is an indicator of antral follicle counts and follicle reserve. However, elevated AMH concentrations arrest follicle development and may inhibit development of ovulatory follicles. During puberty attainment, AMH concentrations are elevated and then become reduced after puberty is achieved. Therefore, our hypothesis was AMH patterns in blood plasma may be used as a marker to determine heifer pubertal attainment. Heifers from the UNL research herd were classified into four different puberty groups based on a SAS program developed to determine when heifers attain >1ng/ml progesterone (P4) and continue to cycle. Heifers were bled weekly from weaning (October) until the end of breeding (May). A total of 754 heifers born during 2012-2018 were classified: 1) Early- greater than 1 ng/ml P4 and continued cyclicity (317±4 days of age (DOA), n=143); 2) Typical- (378±2 DOA, n=279) with continued cyclicity; 3) Start-Stop- P4≥1ng/ml at 265±4 but discontinued cyclicity (n=91); and 4) Non-Cycling - no occurrence of $P4\geq 1$ ng/ml during sampling period (n=98). Heifers achieving puberty with continued cyclicity (Early and Typical) had greater reproductive performance their first calving season. AMH concentrations were determined in blood plasma samples from a sub-set of heifers in each pubertal classification (approximately 10/pubertal classification from 2015-2018) at: 1) prior to P4>1ng/ml (pre-puberty); 2) P4>1ng/ml (puberty); 3) one month after P4>1ng/ml (postpuberty) and at serial blood collection (one year of age; OYA). Non-cycling females did not achieve >1ng/ml P4 throughout the collection period so samples were collected at similar time points as Typical heifers. Concentrations of AMH were analyzed using a nonparametric test in SAS and were different by pubertal group over time (p<0.001). Plasma samples at each collection point tended to differ (p=0.08). Prepuberty AMH concentrations were bi-modal with Early/Start-Stop heifers having greater and Typical/Non-Cycling having reduced AMH concentrations in plasma. At postpuberty to OYA, Non-Cycling Heifers increased AMH concentrations to Start-Stop levels and Early heifers had decreased AMH concentrations to that of Typical heifers. At OYA Non-Cycling females from the sub-sample heifers had reduced percentage of reproductive tract score 5 (p<0.05) and reduced total P4 from puberty to OYA (p<0.05) than Typical, Early and Start-Stop indicating reduced reproductive maturity. Furthermore, Start-Stop and Non-Cycling heifers from previous data have reduced response to prostaglandin prior to breeding, and Non-Cycling heifers had reduced numbers of calves in the first 21 days of calving. Thus, AMH concentrations pre-pubertal to OYA may predict delayed or altered pubertal attainment allowing for selection of females with greater reproductive performance.

Ovary: Corpus Luteum

Abstract # 1807

Vaspin And Receptor GRP78 Expression In Corpus Luteum During Estrous Cycle In Polish Large White Pigs And In Vitro Effect Of Vaspin On Luteinisation. Patrycja Kurowska, Ewa Mlyczyńska, Monika Dawid, Małgorzata Grzesiak, Joelle Dupont, Agnieszka Rak

Vaspin is an adipose tissues hormone – adipokine, which is involved in the development of obesity, insulin resistance or pathogenesis of inflammatory reactions in the body. It is well known fact that adipokines are correlated with obesity, led to female infertility. Our previous results showed vaspin expression and stimulatory effect on steroid synthesis and proliferation by activation of GRP78 receptor in porcine ovarian follicles. In the present study we focused on vaspin expression and role in corpus luteum (CL). CL is a transient endocrine gland and it formation and limited lifespan is critical for estrus periodicity and consequently normal fertility. Regression of CL is initiated by prostaglandin F2 alpha (PGF2a), which by activating phospholipase C, inhibits progesterone (P4) synthesis and leads to apoptosis of luteolytic cells. Whereas, prostaglandin E2 (PGE2) is involved in maintaining the hormonal function of CL. The aim of the study was to examine vaspin and GRP78 mRNA and protein expression in CLs during the estrous phases and next in vitro impact of vaspin on CL function including signaling pathways, steroidogenesis, prostaglandin secretion, proliferation and apoptosis.

CLs were collected from Large White sows during the early (CL1), middle (CL2) and late (CL3) luteal phase, then mRNA, protein level and immunolocalisation of vaspin/GRP78 were determined by real time PCR, Western Blot and immunohistochemistry, respectively. Next, CL2 cells were in vitro treated with vaspin at 1 ng/ml for 1, 5, 15, 30, 45 and 60 minutes and then effect on MAP3/1 and PKA kinases phosphorylation was measured by Western blot. Additionally, CL2 cells were treated with vaspin at 0.01-100 ng/ml for 24 hours and then P4, estradiol (E2), PGE2/PGF2a secretion and protein expression of HSD3B, CYP19A1 PTGER1, PTGFR were study by ELISA and Western blot, respectively. Moreover, vaspin effect on CL2 cells proliferation was measured by Alamar blue assay after 24, 48 and 72 hours, while apoptosis by Caspase-Glo 3/7 Assay. Statistical analyses were performed by Graph Pad Prism 5 software and the data were analyzed using a one-way ANOVA (Tukey's honest significant difference test). Our results documented, dependent on estrous cycle phase both vaspin and GRP78 expression: mRNA and protein level was higher in CL2/3 than CL1 (n=10, p<0.05). Strong signal of vaspin/GRP78 were detected in the cytoplasm of large CL cells. Vaspin at time-depend manner stimulated MAP3/1 and PKA kinases phosphorylation (n=3, p<0.05). Additionally, vaspin increased significantly both P4, E2 secretion and HSD3B, CYP19A1 expression (n=4, p<0.05). Furthermore, vaspin increased PGE2/PGF2a secretion and receptors PTGER1/PTGFR expression ratio (n=4, p<0.05). Finally, vaspin stimulated cell proliferation and decreased apoptosis in CL2 cells after 24 hours of incubation (n=3, p<0.05). The present study provides evidence that vaspin/GRP78 are

dynamically expressed in CL cells during the estrus cycle in pigs. Moreover, vaspin by effect on CL cells physiology: kinases phosphorylation, hormones secretion as well proliferation and apoptosis is a new local luteinisation player in female fertility. Supported by National Science Centre, Poland project PRELUDIUM no 2018/31/N/NZ9/00959.

Abstract # 1910

Assessment of Corpus Luteum Function After Single Doxorubicin Treatment. Christian LAndersen, Rachel Byun, Zidao Wang, Yuehuna Li, Xiaoqin Ye

A unique side effect of concern from cancer therapy in millions of premenopausal cancer patients is fertility impairment. Oncofertility has recently been developed to address future reproductive health of these cancer patients. One aspect of oncofertility is understanding the gonadotoxicity of cancer therapy, including chemotherapy. Within the ovary, much of the research on chemotherapeutic drugs centers on their gonadotoxicity in the primordial follicles. However, there is little research on any effects of chemotherapeutic drugs on the corpus luteum. The corpus luteum is the main site for producing progesterone, which is critical for supporting early pregnancy in mammals. To fill this knowledge gap, we hypothesized that chemotherapeutic drugs could have adverse effects on the corpus luteum. To test this hypothesis, we use C57BL/6J mice as an in vivo model and doxorubicin (DOX) as a representative chemotherapeutic drug. Since a corpus luteum normally develops from an ovulated follicle, and mating activity is often associated with ovulation in female mice, we detect mating activity by the presence of a vaginal plug and treat the mated mice via intraperitoneal injection on post coitus day 0.5 (D0.5) with 100 µl of DOX (10 mg/kg, n=11) or 1xPBS vehicle (n=9). Serum and ovaries are collected on D3.5 when the corpus luteum is fully functional and serum progesterone level has reached a plateau during early pregnancy. Preliminary data collected so far indicate 3/5 (60%) of DOX-treated mice but 0/6 (0%) of vehicle control mice have progesterone deficiency. Progesterone steroidogenesis starts from the substrate cholesterol, which is transported from the outer to inner mitochondrial membrane by steroidogenic acute regulatory protein (StAR) for conversion to pregnenolone by P450SCC/CYP11A1, and further conversion of pregnenolone to progesterone by 3β -hydroxysteroid dehydrogenase (3β -HSD) in the smooth endoplasmic reticulum. Preliminary data show an accumulation of lipid droplets, reservoirs for cholesterol, in the DOX-treated corpus luteum, suggesting that DOX may not affect the availability of the substrate cholesterol for progesterone steroidogenesis. We have utilized a proprietary bioinformatics pipeline to analyze the size and number of lipid droplets in a maturing corpus luteum. Utilizing similar pipelines, we hope to characterize important corpus luteum protein expression to understand the effects of DOX on corpus luteum function. We will determine the expression of StAR, CYP11A1, and 3β -HSD, as well as cell proliferation and apoptosis in the corpus luteum, to understand the molecular and cellular mechanisms of DOX-induced progesterone deficiency.

Crucial Roles For Glycolysis And De Novo Lipogenesis For Proper Luteal Steroidogenesis. Emilia Przygrodzka, Fatema Bhinderwala, Pan Zhang, Xiaoying Hou, Robert Powers, John S. Davis

Production of progesterone by the corpus luteum (CL) is fundamental for establishment and maintenance of pregnancy. Luteinizing hormone (LH) is crucial for the formation, function and maintenance of the CL, but the cellular metabolic changes induced by LH are unclear. In the present study, highly steroidogenic small luteal cells (SLC) were isolated from bovine CL and treated them with LH (10 ng/ml) for 10, 30, 60 and 240 minutes. Additionally, SLC were incubated with C13-labaled glucose in the absence (control) or presence of LH for 1 and 4h. Cells and post-incubation media were harvested to determine metabolomic changes using GC/MS and LC/MS/MS platforms as well as NMR. Metabolomic changes were verified using Seahorse analysis. Selected metabolic pathways were inhibited in order to determine their relevance to LHstimulated production of progesterone. Finally, the effects of LH and the PKA activator Forskolin (FSK; 10 µM) were examined on phosphorylation of enzymes involved in de novo lipogenesis. Metabolomics data and results of Seahorse analysis were analyzed using Welch's two-sample t-test and t-student test, respectively. Results of western blots and progesterone assay were analyzed using one-way ANOVA with Dunnett's post hoc test. Mass spectrometry revealed an elevated (P<0.05) concentrations of progesterone and CAMP in cells and media post-LH treatment. The content of lanosterol and squalene, a cholesterol precursors, was increased (P<0.05) in cells treated with LH indicating on de novo lipogenesis. Isocaproate, a product of CYP11A1, increased and cholesterol levels decreased (P<0.05) confirming cholesterol utilization for steroidogenesis. Glucose and other carbohydrates were significantly lower (P<0.05) in cells and media after LH treatment. Simultaneously, lactate and metabolites of the pentose phosphate pathway (PPP) were increased (P<0.05) and pyruvate was depleted (P<0.05). Longer (4h) incubation with LH elevated (P<0.05) concentration of lysophospholipids in cells extracts. Experiments with C13-labeled glucose confirmed changes in the glycolytic pathway, de novo lipogenesis and PPP in cells cultured with LH. Additionally, changes in metabolites of hexosamine biosynthesis pathway were observed in cells treated with LH. Seahorse analysis confirmed enhanced glycolytic capacity (P<0.05) of cells incubated with LH. Both LH and FSK enhanced (P<0.05) phosphorylation of ATP citrate lyase (ACLY) and inhibited (P<0.05) phosphorylation of acetyl-CoA carboxylase 1, enzymes responsible for lipid synthesis. The stimulatory effects of LH on progesterone production were prevented by inhibitors of ACLY or other enzymes involved in the TCA cycle or glycolysis (P<0.05). LH enhances glucose metabolism in small luteal cells leading to its utilization in different metabolic pathways associated with ATP production, synthesis of nucleotides, glycosylation of proteins and de novo synthesis of fatty acids, which constitute important sources of energy and cofactors required for maintenance of steroidogenic capacity in luteal cells. Support: NIFA USDA 2017-67015-26450, VA and NIH R01HD092263.

Identification of FOS/AP-1's Downstream Genes and Functions in Human Luteinized Granulosa Cells by High-throughput RNA Sequencing and Bioinformatics Analyses. Yohan Choi, Jmaes A. Akin, Thomas E. Curry Jr., Misung Jo

FOS, a subunit of activator protein-1 (AP-1) transcription factor, controls various cellular events by stimulating or suppressing the expression of numerous genes. Previously, we have reported that hCG increases the expression of FOS and its heterodimeric binding partners JUN, JUNB, and JUND in ovulatory follicles of normally cycling women and in primary human granulosa-lutein cell cultures (hGLCs), suggesting that the FOS/AP-1 is necessary for the ovulatory process. To determine the specific functions of the FOS/AP-1, the present study took advantage of high-throughput RNA sequencing (RNA-seq) and bioinformatics analyses using hGLCs treated with or without a selective FOS/AP-1 inhibitor T-5224 in the presence of hCG for 12 hours when the FOS/AP-1 levels are highest in hGLCs. Based on the research criterion false discovery rate (FDR) < 0.01 and |fold change | > 2, a total of 2295 genes were identified as differentially expressed genes (DEGs; 938 genes upregulated and 1357 genes downregulated by the addition of T-5224). The quantitative PCR analysis was performed to validate differential expression profiles of 18 selected DEGs (downregulated: EGLN3, HILPDA, HAS2, RASD1, ID2, SLC2A1, FGF12, PTX3, SOX9; upregulated: JUN, JUND, AREG, EREG, PTGS2, HSPA5, DUSP6, FOSB, INHBA). The KEGG mapping tool grouped the 2295 DEGs into several cellular pathways (e.g., CAMP-PKA, MAPK, PI3K-AKT, cytokine, chemokine, Wnt, hypoxia/angiogenesis, cell cycle, glycolysis/gluconeogenesis, and sterol biosynthesis). To further verify the roles of the FOS/AP-1 in human periovulatory granulosa cells, the effect of T-5224 on cell viability and cellular glycolysis was examined by the MTS assay and the Seahorse glycolysis stress test, respectively. hCG significantly increased both cellular metabolic and glycolytic activities; however, these stimulatory effects of hCG were markedly attenuated by T-5224 in hGLCs. These results suggest that the FOS/AP-1 plays an essential role in the ovulatory process by coordinating various cellular events during the periovulatory period in the human ovary. Supported by P01HD71875, R03HD088866, and R01HD096077.

Abstract # 2006

The Impact Of Pregnancy On The Transcriptome Of The Bovine CL: Insights From Combining Two Independent Experiments. Megan A. Mezera, Camilla H K Hughes, Joy L. Pate, Milo C. Wiltbank

The corpus luteum (CL) is vital for pregnancy maintenance in cattle, yet luteal function during maternal recognition of pregnancy (MRP) is not fully understood. Two independent RNAseq experiments were performed to characterize the luteal transcriptome during MRP and were subsequently evaluated to identify key regulators of luteal maintenance. In dataset 1, CL from pregnant, nonlactating cattle on days 14 and 20 were compared (n=4). Among 16875 genes identified, 305 were differentially

abundant (DA; false discovery rate adjusted P-Value: Q<0.05). In dataset 2, CL from multiparous lactating Holstein cattle on day 20 of pregnancy (n=5) were compared to CL from non-bred animals on day 20 in which luteolysis had not begun (n=6), as confirmed by bihourly measurement of plasma PGF metabolite and progesterone on days 18-21. In dataset 2, among 13986 genes, 93 were DA (Q<0.05). There were 10672 mRNA common to both datasets, yet only 20 genes were commonly DA (Q<0.05). Of these 20, all were in greater abundance on day 20 of pregnancy and 17 were classical interferon stimulated genes (ISG). Two of the 3 remaining mRNA encode latent transforming growth factor beta (TGFB) binding proteins (LTBP1 and LTBP2). These molecules are regulators of TGFB activation and extracellular matrix stability. Using a less conservative approach, which relied on the independence of the datasets (therefore omitting false discovery rate correction), 37 transcripts were altered in the same direction on day 20 (P<0.01) in both datasets. Many of these are regulators of immune response, balancing inflammation, cellular proliferation, apoptosis, and matrix remodeling. In a third approach to integrate these datasets, pathway analysis was performed on each dataset separately (included transcripts with Q<0.10) and commonalities among the pathways, rather than genes themselves, were identified. Unsurprisingly, this approach highlighted interferon related pathways, as well as a potentially novel pathway involving retinoic acid signaling in early pregnancy. Many transcripts changed in only one of the datasets, with dataset 1 containing 285 unique DA mRNA (Q<0.05), and dataset 2 with 73. Altered transcripts unique to dataset 1 indicate regulation of the complement system and mitochondrial function, whereas those unique to dataset 2 indicated regulation of the extracellular matrix and IGF binding proteins. While the differences in experimental design prevent conclusive interpretations of transcripts uniquely different in one dataset, the combination of independent analyses revealed transcripts that were differentially abundant in both datasets, greatly increasing the confidence with which conclusions can be drawn regarding maintenance of the CL in early pregnancy. This analysis highlighted the upregulation of luteal ISGs during maternal recognition of pregnancy, allowed identification of novel molecules, the latent TGFB binding proteins, and revealed common pathways that are likely regulated in the CL of pregnancy, despite differences in transcripts from the two datasets that are components of those pathways. Funding: dataset 1 - Agriculture and Food Research Initiative Competitive Grant no. 2016-67015-24900 from the USDA NIFA to JLP, USDA NIFA predoctoral fellowship no. 2017-67011-26062 to CHKH; dataset 2- BARD-US Israel grant IS-4799-15, WI Experiment Station Hatch Project WIS01240.

Form Of Supplemental Selenium Affects Steroidogenesis By The Early Luteal Phase Corpus Luteum In Beef Cattle. Sarah NCarr, Benjamin R. Crites, Yang Jia, Charles H. Hamilton, James C. Matthews, Phillip J. Bridges

In forage-grazing cattle, selenium (Se) -deficient soils necessitate supplementation of this dietary trace mineral. Mineral mixes are commonly formulated with an inorganic form of Se (sodium selenite). However, organic forms occur naturally in forages. We have investigated the effect of supplementing cattle with a vitamin-mineral mix containing sodium selenite (ISe; Prince Agri Products, Inc. Quincy, IL), an organic form (OSe; SEL-PLEX, Alltech, Inc., Nicholasville, KY), or an isomolar 1:1 mix of ISe and OSe (MIX), and demonstrated that the MIX form (versus OSe or ISe alone) increases early luteal phase systemic progesterone (P4), which advances embryonic development. Our objective was to investigate the mechanism responsible for this MIXinduced increase in P4. Ten, non-lactating three-year-old Angus-cross cows were randomly selected from established, Se form-specific cowherds. Cows were subject to a 45-day depletion period (Se-free mineral mix), followed by a 45-day repletion (35 ppm ISe/cow/day) to return total blood Se in all cows to physiologically adequate concentrations. Following repletion, cows received at least 90 days of individual access to a vitamin-mineral mix formulated with 35 ppm Se as either ISe or MIX (n=5/TRT), then were observed for estrus (Day 0). On Days 5, 6, and 7 post-estrus, the diameter of the CL and serum P4 was determined. On Day 7, CL were collected from each cow. Half of each CL was used to determine the effect of selected agonists on the release of P4 by luteal cells in vitro; the remainder was used for the quantification of levels of selected mRNA transcripts by RT-PCR. In vitro, the effect of treatment was analyzed using a split-plot design for repeated measures with form of Se as the main-plot and agonist (LH, PGE2, and hCG) as the sub-plot factors. After 24 h of culture, form of Se did not affect P4 by LH- or PGE2-treated luteal cells. However, P4 was greater (P < 0.05) in media retrieved from hCG-treated luteal cells collected from ISe-versus MIX-cows, suggesting an effect of form of Se on small luteal cells. The effect of Se treatment on concentration of mRNA transcripts in the CL was analyzed by ANOVA, using the PROC GLM function of SAS. Form of Se did not (P > 0.05) affect the abundance of key steroidogenic mRNAs (Star, Cyp11a1, Hsd3b1, Ptgs2 and Ptges). However, the expression of mRNA encoding the low-density lipoprotein receptor (Ldlr) was increased (P < 0.05) in MIX versus ISe cows, suggesting that the MIX-induced increase in systemic P4 involves, in part, stimulation of cholesterol uptake. Interestingly, the content of mRNA encoding the nuclear progesterone receptor (Pgr, P < 0.05), but not the membrane components (Pgrmc1 and Pgrmc2) was decreased in CL from MIX versus ISe cows, suggesting down-regulation of PGR-mediated events in those animals. Overall, it appears that the MIX-induced increase in early luteal phase P4 is not directly mediated by an increase in the expression of key steroidogenic transcripts, but by an increase in cholesterol uptake, through at least the LDLR.

Influence Of Dietary Manganese Supplementation On Transcript And Protein

Abundance In The Corpus Luteum Of Swine. Jamie M. Studer, Zoe E. Kiefer, Aileen F. Keating, Lance H. Baumgard, Kristin M. Olsen, Zachary Rambo, Mark E. Wilson, Christof Rapp, Jason W. Ross

The establishment and maintenance of pregnancy in pigs is dependent on the formation of functional corpora lutea (CL). Manganese (Mn) is potentially critical for CL function as it is a cofactor for the antioxidant enzyme Mn superoxide dismutase (Mn-SOD) and enzymes involved in cholesterol synthesis. Previously we have shown luteal Mn content increased and luteal progesterone (P 4) concentration decreased in the CL of gilts fed Availa-Mn. Importantly, serum P 4 increased from D0 (estrus onset) through D12, as expected, but P 4 abundance in circulation was not affected by dietary Mn source (P = 0.75). We hypothesized that a more bioavailable Mn source (resulting in increased luteal Mn content) would alter the luteal proteome and abundance of mRNA associated with steroid biogenesis during the mid-luteal phase of the estrous cycle. Post-pubertal gilts (n = 32) were assigned to one of four gestation diets. The control diet (CON) contained 20 ppm of supplemental Mn in the form of Mn-sulfate. Three additional diets included 20 (TRT1), 40 (TRT2), or 60 (TRT3) ppm of supplemental Mn in the form of a Mn amino-acid complex (Availa-Mn; Zinpro Corporation) in place of Mn-sulfate. Dietary treatment began at estrus synchronization and continued through D12 of the subsequent estrous cycle when gilts were euthanized and tissues were collected. Protein and total RNA extracts from the CL (n = 4 CLs per animal) were used for proteomic analysis via liquid-chromatography with tandem mass-spectrometry (LC-MS/MS) to assess global protein abundance and quantitative real-time PCR to assess specific mRNA abundance, respectively. Compared to CON, 123, 293, and 345 proteins were differentially abundant (P<0.05) in TRT1, TRT2, and TRT3, respectively. KEGG pathway analysis revealed proteins involved in P 4 signaling (membrane-associated P 4 receptor component 2) and cholesterol synthesis and transport (HMG-CoA reductase, mevalonate kinase, diphosphomevalonate decarboxylase, squalene, 7dehydrocholesterol reductase, low-density lipoprotein receptor) were downregulated in Availa-Mn treatments compared to CON. Quantitative real-time PCR revealed relative transcript abundance of genes encoding steroidogenic enzymes (CYP11A1 and STAR) were decreased in TRT2 compared to CON (P = 0.02), but TRT1 and TRT3 were not affected ($P \ge 0.3$). Collectively, this data supports our hypothesis that dietary Mn source affects Mn accumulation in the CL and may influence luteal function by altering key protein and transcript abundances.

Form Of Dietary Selenium Affects Mrna Encoding Cholesterol Biosynthesis And Immune Response Elements In The Early Luteal Phase Bovine Corpus Luteum. Benjamin R. Crites, Sarah N. Carr, Charles H. Hamilton, James Matthews, Walter R. Burris, Phillip Bridges

Widespread regions of the southeast United States have soils deficient in selenium (Se), necessitating Se supplementation to grazing cattle. Adequate dietary Se is required for optimal immune function, growth, and fertility. In forages, Se is predominantly found in an organic form (OSe), which increases bioavailability; however, an inorganic form (ISe) is typically found in commercial supplements. We previously reported that supplementation with an isomolar 1:1 mix (MIX) of ISe (sodium selenite, Prince Se Concentrate; Prince Agri Products, Inc., Quincy, IL) and OSe (SEL-PLEX, Alltech Inc., Nicholasville, KY) increases early luteal phase concentrations of progesterone (P4) above that in cows on ISe or OSe alone. Increased early luteal phase P4 advances embryonic development. The objective of this study was to investigate the effect of form of supplemental Se on the transcriptome of the bovine corpus luteum (CL) with a goal of elucidating form of Se-regulated luteal processes affecting fertility. Three-yearold Angus-cross cows were assigned to receive a basal mineral mix containing 35 ppm Se/day as either ISe (n=5) or MIX (n=5). Cows underwent a 45-day depletion period (Sefree), followed by a 45-day repletion (35 ppm ISe/cow/day) to return total blood Se to physiologically adequate concentrations. Following repletion, cows received at least 90 days of supplementation (ISe or MIX), then were treated with PGF2a to synchronize estrus (Day 0). On Days 5, 6 and 7, diameter of the CL and systemic P4 was determined. On Day 7, CL were recovered, total RNA isolated, and the effect of treatment on the luteal transcriptome evaluated after hybridization to bovine gene 1.0 ST arrays (Affymetrix, Inc., Santa Clara, CA). The level of expression of mRNA transcripts in each CL was subjected to one-way ANOVA (Partek Genomic Suite) to determine treatment effects. Microarray analysis indicated a total of 887 transcripts were differentially expressed and functionally annotated, with 425 and 464 up- and down-regulated (P<0.05) in MIX vs. ISe cows. Bioinformatic analysis (Ingenuity Pathway Analysis) revealed the top treatment-affected canonical pathways included four specific to cholesterol biosynthesis and three involved in inflammatory responses. Results from the microarray analysis were corroborated by targeted RT-PCR of key transcripts associated with these pathways. MIX-supplemented cows had increased (P<0.05) mRNA abundance of transcripts regulating cholesterol biosynthesis including Dhcr7, Dhcr24, and Cyp51a1 (fold changes of 1.65, 1.48, and 1.40, respectively), suggesting the increase in P4 observed in MIX-treated cows is, in part, due to increased availability of cholesterol in luteal cells. Additionally, MIX-supplemented cows had greater (P<0.05) CL content of several immune-response transcripts including C1qc, Fas, IIr8b, and II1r1 (fold changes of 2.30, 1.74, 1.66, and 1.63, respectively). Interestingly, mRNA encoding Srebf1 was increased in MIX-cows (1.32-fold, P<0.05), which increases cholesterol synthesis and stimulates II1B, linking effects of treatment on cholesterol biosynthesis and immune function. Overall, our results suggest that the MIX-induced increase in early luteal phase

P4 is due to an increase in cholesterol availability, and that the form of dietary Se affects immune function of the CL.

Abstract # 2131

Transcriptome Analysis of Caprine Abnormally Regressing and Normal Cycling Corpora Lutea on Day 5 of the Estrous Cycle. William B. Foxworth, Scott Horner, Louis Nuti, Alphina Ho-Watson, Islyn Gilmore, Katherine Gutierrez, Shaye Lewis, Seungchan Kim, Gary Newton

Progesterone secretion by the caprine corpus luteum (CL) is essential for the establishment and maintenance of pregnancy and required throughout gestation. Estrus/ovulation synchronization programs employed for artificial reproduction technologies in goats is a widely used practice. However, when synchronization schemes are utilized, 20 – 60 % of those does short-cycle because the CL abnormally regresses by Day 5. This decreases the efficiency of artificial insemination programs where fertilization occurs but the short cycle results in early embryonic loss. Furthermore, recipients with early regressing CL are not suitable for embryo transfer protocols. Therefore, this study was conducted to characterize the transcriptomic profiles, using RNA-sequencing (RNAseg), of the abnormal regressing versus normal cycling Day 5 CL (late metestrus, n=3 / group) in the goat. The RNAseq data were first subject to differential expression analysis, followed by pathway analyses utilizing gene ontology (GO) and Kyoto Encyclopedia of Genes and Genomes (KEGG) databases. Of the 33,433 genes analyzed, we identified 1,516 genes differentially expressed between abnormally regressed and normal cycling caprine CL with statistical significance (adjusted p value < 0.05 and log2 fold change > 1). Specifically, 932 genes were upregulated and 584 genes downregulated. Gene Ontology (GO) over-representation analysis revealed 374 GO Biological Process (BP) terms significantly enriched (Padj < 0.05) while KEGG enrichment analysis indicated only two pathways, steroid biosynthesis and terpenoid backbone biosynthesis, even at lowered statistical significance (Padj < 0.1). Among the GO BP terms with significance were those involved in response to altered oxygen levels, including hypoxia, and regulation of chemotaxis. The differential expression analysis revealed a significantly decreased expression of superoxide dismutase 1 (SOD1, Padi < 0.05) which in tandem with increased reactive oxygen species (ROS) exerts a luteolytic effect. This study provides initial insights into the transcriptomic attributes of the abnormally regressing caprine CL during late metestrus, resulting in its demise.

MiR-1246 Is The Most Abundant Mirna In Luteal Extracellular Vesicles And It Regulates T Cell Transcripts Associated With Their Activation. Martyna Lupicka, Joy L. Pate

Extracellular vesicles (EV) are cup-shaped, membranous structures that contain specific cargo used for cell-to-cell communication. Previously, we showed that bovine luteal EV regulate cytokine production in monocytes and T cells. We also characterized miRNA cargo of luteal EV using Next Generation Sequencing (NGS), and it revealed that miR-1246 was the most abundant miRNA regardless of the functional status of the corpus luteum (CL). Ingenuity Pathway Analysis (IPA) of 2377 predicted miR-1246 targets (determined with TargetScan algorithm) showed potential regulation of mRNA associated with NF-KB signaling and proliferation (p<0.05). Therefore, we hypothesized that miR-1246 affects T cell activation. To determine real targets of miR-1246 in bovine T cells, a miRNA pull-down assay was performed. Biotin-labeled miR-1246 mimic was transfected into cultured bovine peripheral blood T cells (n=6). Cells were then treated with PMA (phorbol 12-myristate-13-acetate) and ionomycin to increase expression of genes associated with cell activation. After treatment, miR-1246, together with its bound targets, were isolated using streptavidin-coated beads. Pulled-down targets were sequenced using NGS. Overall, the analysis revealed 37 transcripts that were different (P<0.05) or tended to be different (P<0.08) from negative control pull-down, among which 7 were also predicted miR-1246 targets. Among these identified transcripts, genes associated with cell cycle, such as cAMP regulated phosphoprotein 19 (ARPP19), cell division cycle 27 protein (CDC27) and PWWP domain containing 2A protein (PWWP2A), and genes associated with NFKB signaling, such as nuclear receptor coactivator 3 (NCOA3) were identified. Pathway analysis of pulled-down targets showed involvement of these transcripts in pathways associated with RXR activation, which among other functions also induces cell cycle progression and proliferation. To further test the hypothesis, cell cycle progression was measured in activated T cells transfected with miR-1246 mimics (n=2). After transfection with mimic, 8% of cells progressed to S or G2/M phase, whereas, cell cycle progression occurred in 12% of control cells. In summary, miR-1246 that is shuttled via luteal EV may regulate T cell activation in the CL through inhibition of translation of mRNA associated with cell cycle regulation. In our previous studies, luteal EV induced increased production of proinflammatory cytokines by T cells, but luteal cell-induced proliferation is limited, perhaps, because miR-1246 controls cell cycle progression and resident T cell survival during their activation. This project was supported by Agriculture and Food Research Initiative Competitive Grant no. 2016-67015-24900 from the USDA National Institute of Food and Agriculture.

Pro-inflammatory Immune Cell Derived Cytokines (TNFa, IL1a, IL1β, IL17) Aid in Luteal Regression by Triggering Downstream Signaling Pathways and Decreasing LH-stimulated Progesterone Production. Corrine F. Monaco, Emilia Przygrodzka, Xiaoying Hou, John S. Davis

Luteal regression is mediated by various factors, including prostaglandin F2a (PGF2a), which inhibits progesterone production by the corpus luteum. Importantly, studies have shown that progesterone serves as a luteal survival factor. Furthermore, previous studies document a rapid elevation of the transcripts for some proinflammatory cytokines including TNFa, IL1B, IL1a, IL17, and IL33 in luteal tissue during induced luteolysis. However, it remains unclear how these cytokines contribute to luteal regression. The aim of the present study was to determine: (1) the cytokines produced by activated PBMCs; (2) the effect of activated bovine peripheral blood mononuclear cells (PBMCs) on progesterone production; (3) the effect of selected cytokines on production of progesterone and (4) signaling pathways evoked by these cytokines. In order to identify which cytokines were produced by PBMCs, media from those samples was collected and analyzed by cytokine array. Luteal cells were isolated from the mature corpus luteum and pre-incubated with control or Concanavalin A (ConA)-activated PBMCs overnight, followed by LH treatment (10 ng/mL) for 4 hours. Luteal cells were then pretreated overnight with identified cytokines (IL1β, 10ng/mL; TNFa, 10ng/mL; IL17a, 10ng/mL; IL-1a, 10ng/mL) alone or in combination with each other or with PGF2a (100 nM). Following incubation, cells were treated with LH for 4 hours. Progesterone in culture media was measured by ELISA. Additionally, western blot analysis was used to determine time- and dose- dependent effects of IL1a, IL1B, and IL17, and TNFa on the phosphorylation of kinases (SAPK/JNK, p38MAPK) and their downstream transcription factors (NFKB, cJUN). Statistical analysis was done using student's t-test or one-way ANOVA followed by Bonferroni post hoc test. Incubation of luteal cells with activated PBMCs inhibited LH-stimulated progesterone production (P<0.05). Activated PBMCs produced more cytokines; the cytokine array identified elevated content of IL1a, IL1 β , and IL17 by up to 2.5-, 2-, and 9.5-fold, respectively. Overnight incubation of luteal cells with IL1a, TNFa, and PGF2a decreased LH-stimulated production of progesterone (P<0.05). Western blot analyses indicated that IL1 β , IL17, and TNFa enhanced phosphorylation of SAPK/JNK (Thr183/Tyr185), and p38MAPK (Thr180/Tyr182). Both pathways can contribute to prostaglandin synthesis and reduced progesterone. Cytokine treatment also enhanced phosphorylation of downstream transcription factors, NFkB (Ser536), cJUN (Ser63). These results indicate that cytokines released by activated immune cells (IL1a, IL1β, TNFa, and IL17) can reduce LH-stimulated progesterone secretion by luteal cells. Further mechanistic studies are needed to elucidate how pro-inflammatory cytokines act on cell survival, and whether they adversely affect luteal endothelial cells.

Ovary: Folliculogenesis

Abstract # 1667

Differential Expression of Alternatively Spliced Disabled-1 (DAB-1) Isoform in Granulosa Cells. Marianne Descarreaux, Jacques G. Lussier, Kalidou Ndiaye

Disabled-1 (DAB1) is a cytosolic adaptor protein that is essential for signal transduction of the apolipoprotein E receptor 2 (ApoER2 also known as LRP8; low-density lipoprotein receptor-related protein 8) membrane receptor following binding of its extracellular ligand Reelin. Binding of Reelin to ApoER2 induces tyrosine phosphorylation of DAB1, which is required for migration and differentiation of neurons during brain development in vertebrates. We previously showed that ApoER2 was differentially expressed in granulosa cells (GC) of bovine dominant or preovulatory follicles and that Reelin is expressed in the theca layer, suggesting that signaling through Reelin-ApoER2-DAB1 contributes to the growth of the dominant or preovulatory follicle. The objective of this study was to investigate DAB1 expression and function in GC of bovine follicles since its expression has not been demonstrated in mammalian GC. Characterization of the DAB1 mRNA isoform expressed in bovine GC was compared to the canonical DAB1 mRNA expressed in the brain cortex. Expression and regulation of DAB1 was analyzed by RT-qPCR in GC obtained from small follicles (SF: 2-4 mm in diameter), growing dominant follicles (DF) at day 5 of the estrous cycle, ovulatory follicles (OF) obtained at 0, 6, 12, 18 and 24 hours following injection of hCG (OF) and corpus luteum (CL) at day 5. Characterization of DAB1 mRNA expressed in GC differed from the canonical brain isoform. The bovine DAB1 gene consists of 17 exons. In the brain DAB1 isoform, exons 10 and 11 are spliced out with the stop codon located within exon 16. In GC, exons 7, 8 and 16 are spliced out whereas 14 amino acids (aa) are expressed by exon 17, which also contains the stop codon for this isoform. The brain-DAB1 mRNA codes for 555 aa (59.7 kDa), that include five tyrosine residues (Y185, Y198, Y200, Y220 and Y232) corresponding to two consensus Src family kinase recognition sites (YQxI: Y185 and Y198) and two consensus Abl/Crk recognition sites (YxVP: Y220 and Y232). The DAB1-granulosa cells mRNA codes for 536 aa (58.1 kDa), with only two tyrosine residues (YxVP: Y185 and Y197). Furthermore, the Y185 site is modified compared to the brain isoform from a YQxI to a YxVP site that results in two consensus Abl/Crk recognition sites. RT-qPCR showed strongest expression of DAB1steady-state mRNA in GC of DF when compared to SF, OF and CL (P < 0.0001). The expression level of DAB1 mRNA in DF is 2.5 fold stronger compared to SF, 7.2 fold stronger compared to OF, and 5.5 fold stronger compared to CL (P < 0.05). These results provide for the first time the characterization of DAB1 isoform in GC in mammals, and demonstrate its strongest mRNA expression in the growing dominant or preovulatory follicle. These observations support a physiologically relevant role for the GC-DAB1 isoform in transducing the ApoER2/LRP8 membrane receptor signal. This work represents the first step in understanding the role of the GC-DAB1 isoform in transducing the ApoER2/LRP8 signal in GC of the growing dominant or preovulatory follicle.

Function Of Ankyrin-Repeat And SOCS-Box Protein 9 (ASB9) In Bovine Ovarian Granulosa Cells. Soma Nosrat Pour, Kalidou Ndiaye

Ankyrin-repeat and SOCS-box protein 9 (ASB9) is a member of the large SOCS-box containing proteins family and acts as a specific substrate recognition component of E3 ubiquitin ligases in the process of ubiquitination and proteasomal degradation. We previously reported ASB9 as a differentially expressed gene in granulosg cells (GC) of ovulatory follicles following luteinizing hormone (LH) surge or hCG injection. We also identified ASB9 binding partners in GC including tumor necrosis factor alpha-induced protein 6 (TNFAIP6/TSG6), hypoxia-inducible factor 1 alpha (HIF1A), thousand and one amino acid (TAO) kinase 1, a MAP3K, and protease-activated receptor 1 (PAR1). Results from this previous work suggest that ASB9 could affect signaling pathways regulating GC proliferation and function by targeting and modulating binding partners. The current study aimed to further investigate the role of ASB9 in GC, to determine whether induction of ASB9 by LH/hCG in the ovulatory follicle is necessary for the recruitment and ubiquitination of target proteins and to decipher ASB9 mechanism of action in GC. GC were obtained from follicles at different developmental stages: small follicles (SF), dominant follicles (DF), ovulatory follicles (OF), and corpus luteum at day 5 of the oestrous cycle (CL). In addition to this in vivo model, an in vitro model of cultured GC was used along with the CRISPR/Cas9 approach and the pQE overexpression system, respectively, to inhibit and overexpress ASB9 in GC. Regulation of ASB9 as well as its targets was analyzed from in vivo and in vitro experiments. Western blot analyses demonstrated ASB9 induction by hCG from 12h post-hCG through 24h. RT-qPCR analyses using in vivo samples showed greater expression of PAR 1 mRNA in DF as compared to OF while TNFAIP6 and TAOK1 are induced in OF by hCG. Inhibition of ASB9 via CRISPR/Cas9 was confirmed by RT-gPCR and resulted in a significant increase in PAR1, PCNA, and CCND2 steady-state mRNA expression and increased GC proliferation. Western blot analyses showed an increase in ERK1/2 phosphorylation level following ASB9 inhibition. Moreover, western blot analyses using in vivo samples showed significant decrease of pERK1/2 in OF, which is concomitant with induction of ASB9 suggesting that ASB9 reduces ERK1/2 phosphorylation. These results provide strong evidence that ASB9 could be a regulator of GC activity and function by taraetina specific proteins that affect MAPK signaling, therefore limiting GC proliferation and contributing to GC differentiation into luteal cells. This work was supported by a Discovery grant of the National Sciences and Engineering Research Council of Canada (RGPIN#04516 to KN).

Functional Effects of Tribbles Homolog 2 (TRIB2) in Ovarian Granulosa Cells. Aly Warma, Jacques G. Lussier, Kalidou Ndiaye

The family of Tribbles (TRIB) proteins is composed of TRIB1, TRIB2 and TRIB3, which are part of the superfamily of serine/threonine kinase proteins and the pseudokinase family of proteins. We previously reported that TRIB2 is differentially expressed and downregulated by LH/hCG in granulosa cells (GC) of bovine ovulatory follicles. This study aimed to further investigate TRIB2 function and binding partners in GC of bovine follicles. Granulosa cells were obtained from follicles at different developmental stages: small follicles (SF; 2-4 mm in diameter), dominant follicles (DF) at day 5 of the oestrous cycle, ovulatory follicles (OF) obtained at 0, 6, 12, 18 and 24h after human chorionic gonadotropin (hCG) injection, and corpus luteum (CL) at day 5 of the oestrous cycle. In addition to this in vivo model, an in vitro model of cultured transfected GC was used for functional studies using the CRISPR/Cas9 approach or an overexpression system, to inhibit or overexpress TRIB2, respectively. The yeast two-hybrid approach was used to identify TRIB2 partners in CG. RT-qPCR analyses showed greatest expression of TRIB2 mRNA in GC of DF and weakest expression in OF (P<0.0001). A significant decline in TRIB2 mRNA expression was observed at 6h post-hCG through 24h post-hCG as compared to 0h (P<0.001). In vitro studies showed that FSH stimulates TRIB2 mRNA expression (P<0.05) while inhibition of TRIB2 increased GC proliferation and CYP19A1 mRNA expression (P<0.05). Western blot analyses showed reduction in ERK1/2 (MAPK3/1) and p38MAPK (MAPK14) phosphorylation levels following TRIB2 inhibition, while TRIB2 overexpression increased p-ERK1/2 and p-p38MAPK. Yeast two-hybrid screening analyses showed that TRIB2 interacts with protein binding partners such as INPPL1, CALM1, RAB14, SCD, SDHB, NT5E and INHBA. Further analyses showed that TRIB2 manipulation (inhibition or overexpression) leads to significant changes in protein partners expression. INPPL1 and INHBA mRNA were significantly decreased in TRIB2inhibited GC and significantly increased in TRIB2-overexpressed GC. CALM1 mRNA was also increased following TRIB2 overexpression while NT5E was increased following TRIB2 inhibition. These results provide evidence that TRIB2 modulates MAPK signaling in GC. Thus, TRIB2 could act as a regulator of GC proliferation and function as well as a regulator of target genes, and could affect steroidogenesis during follicular development. This work was supported by a Discovery grant from the National Sciences and Engineering Research Council of Canada (RGPIN#04516 to KN).

Chlamydia Infects The Ovary, Elicits An Immune Response And Depletes The Ovarian Reserve In Mice. Urooza C. Sarma, Alison J. Carey, Kenneth Beagley, Karla J. Hutt

Chlamydia trachomatis is the most common sexually transmitted infection worldwide and can cause severe damage to the Fallopian tubes, often resulting in complete infertility. Recent studies indicate significantly increased miscarriage rates and time to natural conception, along with poor IVF outcomes in women seropositive for Chlamydia but in the absence of tubal pathology, suggesting that that fertility may be compromised by mechanisms that extend beyond fallopian tube scarring. In this study, we used a well-characterised mouse model to investigate the hypothesis that Chlamydia can infect and damage the ovary. Chlamydial DNA was detected in ovaries at 6 and 35 days post infection (pi) using qPCR and inclusion bodies were localised within macrophages in the ovarian stroma using immunofluorescence. Chlamydial infection was associated with an increase in the expression of mRNA for CXCL16 and IFNy, suggesting the induction of a pro-inflammatory immune response within the ovary, which persists at least up to 35 days pi. Significantly greater numbers of immune cells including macrophages, NK cells and CD4+ /CD+ cells in the ovary 35 days pi, suggesting a localised ovarian inflammatory response to chlamydial infection, parallels this. Strikingly, the number of ovarian follicles was significantly reduced 35 days following a single infection compared to uninfected controls (p<0.05, n=4-5

mice/group) and the extent of follicle depletion was greater following a second infection (p<0.05, n=4-5 mice/group). Two infections was also associated with changes to the overall ovarian morphology and increased apoptosis and fibrosis in the ovary (p<0.05, n=5/group), consistent with activation of a prolonged inflammatory response. Collectively, these observations demonstrate that Chlamydia can penetrate the ovary, deplete the ovarian reserve and compromise ovarian function, and suggest that the ovary may act as a potential reservoir of infection. Ovarian follicles are essential for female fertility because they secrete hormones and contain oocytes. Follicles cannot be replaced once lost from the ovary. Thus, our data suggests that damage to the ovary caused by Chlamydia is permanent and may underlie some cases of unexplained infertility and poor IVF outcome in women.

Abstract # 1822

Androgen-Induced Mir-143-3p Promotes ERK5-Mediated Granulosa Cell Proliferation. Toru Hasegawa, Reza Salehi, Brandon A. Wyse, Stewart Russell, Bo Pan, Sahar Jahangiri, Andree Gauthier-Fisher, Julang Li, Clifford L. Librach, Hisashi Masuyama, Benjamin K T Sang

Polycystic ovarian syndrome (PCOS) is associated with hyperandrogenemia and ovarian stage-specific follicular growth arrest. Several microRNAs (miRNAs), include mir378-5p, regulate granulosa cell proliferation and aromatase expression, and follicular growth. While it is well established that miRNA regulate mRNA translation by binding to the 3` UTR of target gene in the cytoplasm. Recent studies have shown that these regulatory molecules could also increase transcription of target genes through binding and activating of their target promoters or enhancers in the nucleus. In prostate cancer cells, miR373 activates both of E-cadherin and cold-shock domain-containing protein 2 gene transcription. However less is known about the possible role of nuclear miRNA in granulosa cell fate regulation and follicular growth. Although extracellular vesicles (EV) facilitate intercellular cross-talk carrying miRNAs as cargo, among other biomolecules, the role of EV associated miRNAs in the regulation of granulosa cell function and ovarian pathophysiology of PCOS are unknown. The objectives of the present studies were to determine: (i) whether EV-derived miRNAs are differentially expressed in follicular fluid (FF) from human PCOS subjects; (ii) if these responses are vesicle-specific; (iii) if and how miR-143-3p regulates the granulosa cell proliferation. Microvesicles, exosomes and EV-depleted FF were isolated from FF of individual mature follicles of 35 subjects with and without PCOS (according to the Rotterdam criteria. miRNAs in the EV were extracted and sequenced, using libraries constructed with the Small RNA Library Prep Kit (Norgen) and the NextSeg 550. The differentially up- or down-regulated miRNAs appeared to be vesicle type-specific: (i) microvesicles (13 miRNAs): e.g. miR-140-3p and miR-200a-3p, respectively; (ii) exosomes (19 miRNAs): e.g. miR-424-3p and miR-99a-3p, respectively; (iii) EV-depleted FF (5 miRNAs): e.g. miR-4657-5p and miR-1181-3p, respectively; (iv) miRNAs present in both EVs and EV-depleted FF (21 miRNAs): e.g. miR-143-3p and miR-182-3p, respectively. miR-143-3p was selected for further investigation

based on its potential function and target gene (ERK5). To determine the influence of androgen on granulosa cell miR-143-3p content and possible downstream responses, aranulosa cells isolated from immature female rats were cultured ± 1 uM dihydrotestosterone (DHT) for 3, 6, 12, 24, 36, 48 hours. DHT treatment increased both primary and mature miR-143-3p content (12h), ERK5 mRNA abundance (24h) and protein content (36h). Subcellular localization of miR-143-3p indicates that miR-143-3p content increased in the nucleus at 6h post-DHT treatment, suggesting the nuclear translocation of the miRNA may be an early event in androgen-induced up-regulation of granulosa cell ERK5 expression. Collectively, our results support the hypothesis that dysregulation in miRNA expression and intracellular localization lead to altered granulosa cell proliferation, follicular growth arrest and anovulation in PCOS. Specifically, DHT increases ERK5 content by reinforcing miR-143-3p synthesis and nuclear transport for ERK5 transcription. Currently, we are testing (i) the binding of miR-143-3p with ERK5 promoter site; (ii) whether and how androgen regulates miR-143-3p synthesis; and (iii) whether this mechanism is follicular stage-dependent (Supported by CIHR grant, The Lalor Foundation and Mitacs Postdoctoral Fellowship).

Abstract # 1848

Characterization Of The Effects Of Immune Checkpoint Inhibitor Pembrolizumab On Juvenile Ovarian Follicles. Pauline C Xu, Yi Luan, Maya Eldani, So-Youn Kim

Background : The five-year survival rate of cancer patients has improved over the last thirty years. The survival rate of pediatric cancers in particular has reached almost 90%, and many young cancer survivors go on to live generally normal lives due to life-saving treatments. Although advances in cancer therapies such as chemotherapy and radiation therapy have increased survival rate, these therapies also result in long-term adverse health effects. One of the most serious side effects is the off-target effect on germ cells, as it causes the loss of primordial follicles that make up the ovarian reserve, which is defined as all follicles in the ovary available for future fertility and endocrine support for women. This results in premature ovarian insufficiency, which clinically presents as endocrine dysfunction and infertility. Recently, immunotherapy has been recommended for cancer patients due to its specificity and relative safety by selfdefense treatment. Pembrolizumab (KEYTRUDA), which targets programmed cell death protein 1 (PD-1), has been approved by the Food and Drug Administration for use in pediatric patients with relapsed or refractory classical Hodgkin lymphoma. However, there is no information regarding the effects of pembrolizumab on the germ cells of pediatric patients. Hypothesis: Since PD-1 is known to be involved in the activation of Tcell-mediated immune responses against tumor cells, we hypothesized that pembrolizumab would not exert significant effects on ovarian follicles. Experimental Design: CD-1 IGS female mice were injected subcutaneously once with the mouse equivalent dose of the maximum human pediatric dose of pembrolizumab on postnatal day 13. The mice were later euthanized at either 24 hours post-injection or 7 days post-injection. Control mice of the same age were euthanized at both time points.

Ovaries were serially sectioned, and every other slide stained with hematoxylin and eosin to perform follicle counting and analyze gross morphological consequences. In addition, immunofluorescence assays were performed to confirm the functionality of each cell type. Result s: While there were no gross significant changes in the ovarian histology in the 24 hours post-injection group, the results from the 7 days post-injection ovaries were prominent. We noted a decrease in the number of primordial follicles, but the numbers of other follicle types appeared to be like those in the control ovaries. In addition, there was an increase in the number of apoptotic granulosa cells in antral follicles of ovaries from 7 days post-injection mice. Conclusions: Pembrolizumab as an immune checkpoint inhibitor affects ovarian follicles. These data suggest that further investigation is needed to elucidate the mechanism by which primordial follicles are lost due to pembrolizumab as well as the potential non-canonical role of PD-1 in the ovary. Funding Resources: Dr. Kim's Startup Package and 1R01HD096042 (Development of Mechanism-Based Ovarian Reserve Protecting Adjuvant Therapies Against Gonadotoxic Therapeutic Agents).

Abstract # 1903

Jagged-Notch Signaling Between the Oocyte and Granulosa Cells is Active during Follicular Growth. Herthana Kandasamy, Hugh Clarke

Oocyte and follicular development depend on bi-directional communication between the oocyte and neighbouring somatic granulosa cells. The specific pathways that mediate this crucial communication are, however, only partly understood. The Jagged-Notch pathway is a highly conserved signaling pathway, where membrane-bound Jagged binds to membrane-bound Notch, triggering cleavage of Notch, releasing its intracellular domain, which migrates to the cytoplasm and ultimately to the nucleus. Previous studies have shown that Jagged-Notch signaling is required for the formation of primordial follicles. We hypothesize that it may also act later; specifically, to regulate growth of the oocyte or follicle. RT-PCR confirmed that Jagged1 mRNA is expressed at all stages of oocyte growth. Conversely, using an antibody specific for cleaved Notch2, immunofluorescence of granulosa cell-oocyte complexes (GOCs) isolated at mid- and late follicular growth revealed strong cytoplasmic staining in the granulosa cells. This suggests that oocyte-derived Jagged1 activates granulosa cell-derived Notch2 throughout growth. Unexpectedly, anti-Jagged1 immunoblotting of oocytes revealed a band at ~20 kDa instead of the predicted 150 kDa. To identify the origin of the ~20kDa band, oocytes were incubated either as intact GOCs or in the absence of granulosa cells. Whereas the ~20 kDa band was retained by oocytes incubated as GOCs, the 150 kDa band appeared in oocytes incubated without granulosa cells. This suggests that activation of Jagged-Notch signaling in the ovarian follicle leads not only to cleavage of the Notch receptor in the granulosa cells, but also to cleavage of the Jagged ligand in the oocyte. The sole site of physical contact between the oocyte and granulosa cells is at the tips of specialized filopodia, termed transzonal projections (TZPs), that extend from the granulosa cells to the oocyte. To test whether the ~20 kDa band depended on

intercellular contact, we incubated cumulus-cell oocyte complexes (COCs) with epidermal growth factor (EGF), which triggers retraction of TZPs and thus loss of granulosa cell-oocyte contact. Following an 8-hour incubation in the presence of EGF, the 150 kDa Jagged1 species became detectable. These results suggest that activation of Jagged-Notch signaling in the ovarian follicle is dependent on the presence of TZPs, leading to cleavage of the Jagged ligand in the oocyte. Future work will address the potential role of the Jagged cleavage product. Understanding cell communication pathways such as Notch signaling could help us better understand the mechanisms involved in the healthy development of the ovarian follicle.

Abstract # 1905

The Long-Term Treatment With A Low Dose Cisplatin Induces Oocyte Death In Primordial Follicles. Maya Eldani, Yi Luan, Pauline Xu, Wend Ouedraogo, So-youn Kim

Background: Melatonin is reported to be a protectant of cisplatin-induced ovotoxicity and decrease the side effects of the chemotherapeutic drug. The mechanism by which melatonin exerted its effects was stated to be the activation of ovarian follicles with the long-term treatment of a low dose of cisplatin in the mouse. In this study, we investigated whether the consequence by cisplatin on the ovarian follicles is different dependent on chemotherapeutic dose and schedule. We further tested the efficacy of melatonin as a protectant for primordial follicles against cisplatin.

Question: (1) Does a high dosage (5mg/kg) of cisplatin lead to apoptosis, while a low dosage of cisplatin (2mg/kg) leads to activation of follicles? (2) Does melatonin protect ovarian follicles from toxicity by cisplatin? Experimental design: Six-week-old CD1 female mice (n=35) were intraperitoneally (i.p.) injected in vivo with DPBS, 2 mg/kg or 5mg/kg cisplatin for 15 days to assess the effect of cisplatin. In addition, melatonin (30mg/kg) was co-injected with 2 mg/kg cisplatin to test the protective efficacy of melatonin. To examine the direct effect, we cultured postnatal day 5 (PD5) mouse ovaries in vitro with DPBS, 4 mM cisplatin, 1 mM cisplatin with the combination of 6hydroxymelatonin, a metabolite of melatonin. H&E staining, follicle counting with serial sections, western blotting, and immunofluorescence assays were performed. Transmission electron microscopy (TEM) was used to take a closer look at ovarian follicles. Results: Our results showed that either high dose or long-term treatment with a low dose of cisplatin decreased total numbers of each class of follicles - primordial, primary, secondary and antral follicles - in the mouse ovaries. In addition, cisplatin with the combination of melatonin did not show any significant difference in follicle numbers in comparison with ovaries treated with cisplatin alone, suggesting that melatonin does not have any efficacy as a protectant of primordial follicles against cisplatin. Although cisplatin increased p-AKT and p-PTEN signals in a whole ovary, the signals were not present in oocytes of primordial follicles. Furthermore, in vitro studies using PD5 mouse ovaries confirmed that cisplatin induces oocyte death, especially in primordial follicles and granulosa cells within growing follicles. Our observations using transmission electron

microscopy (TEM) supported that cisplatin induces damage of intra-organelles inside of primordial follicles, especially the mitochondria and nucleus of oocytes. Conclusion/discussion: Our results indicate that the effect of cisplatin on the loss of follicles in the mouse ovary is the same between the high dose of injection and the long-term treatment with a low dose of it. Moreover, results indicate melatonin does not have any efficacy for protecting primordial follicles against cisplatin-induced ovotoxicity. Therefore, we conclude that fertoprotectants against cisplatin should target molecules that control the apoptotic pathway in the oocyte of primordial follicles. Funding Resources: Dr. Kim's Startup Package and 1R01HD096042 (Development of Mechanism-Based Ovarian Reserve Protecting Adjuvant Therapies Against Gonadotoxic Therapeutic Agents).

Abstract # 1934

Small RNA Sequencing Reveals Distinct Nuclear Micrornas In Granulosa Cells During Ovarian Follicle Growth. Derek Toms, Bo Pan, Yinshan Bai, Julang Li

Nuclear small RNAs have emerged as an important subset of non-coding RNA species that are capable of regulating gene expression. One class of small RNAs, microRNA (miRNA) has been extensively shown to control development of the ovarian follicle via canonical targeting and translational repression. Increased detection sensitivity and genetic studies have revealed non-canonical roles for small RNAs including as RNA-DNA transcriptional scaffolds and as mediators of metabolic stress. Whether these molecules reside in the nucleus or cytoplasm is a necessary first step to begin understanding their function, yet little has been done to study the "small RNAome" at a subcellular level in granulosa cells. We hypothesized that the subcellular distribution of miRNA and other small RNA would change during the development of the ovarian follicle and may be reflective of their function. Using cell fractionation and high throughput sequencing, we surveyed the cytoplasmic and nuclear small RNA found in the granulosa cells of the pig ovarian antral follicle at two stages of antral growth (n = 4 x 4 = 16). Bioinformatics analysis revealed a diverse network of small RNA including miRNA and small nucleolar (sno)RNA that differed in their subcellular distribution. Seven miRNA had significant changes to their subcellular distribution during follicle growth, including several previously shown to affect granulosa cell function. The small nucleolar RNA (snoRNA) SNORA73, known to be involved in steroid synthesis, was also found to be highly enriched in the cytoplasm, suggesting an as-yet uninvestigated role for snoRNA species in ovarian function. Leveraging reads from all samples, we were also able to identify three novel pig miRNAs expressed in granulosa cells. Taken together, these data suggest that small RNA trafficking within the cell may regulate granulosa cell function through a variety of mechanisms. Our data and analysis is provided as a freely available survey of the subcellular small RNAome in pig granulosa cells and we anticipate that it will be a valuable resource for others studying the role of small RNA in the ovary. Increasing granularity in small RNA profiling, including from single cells, will

continue to increase our understanding of the complex role these molecules play in ovarian granulosa cells and on fertility.

Abstract # 1939

MicroRNA-574 Regulated ERK1/2 Phosphorylation And Estradiol Production Via Targeting TIMP3. Bo Pan, Xiaoshu Zhan, Julang Li

Estradiol is one of the key steroid ovarian hormones that not only plays a vital role in ovarian follicular development but is also associated with many reproductive disorders. Our primary study revealed that miR-574 expression decreased in porcine granulosa cells during development from small to large follicles, and this is accompanied by an increase in ERK1/2 phosphorylation. Since it has been well established that the ERK1/2 activity is tightly associated with granulosa cell functions including ovarian hormone production, we next investigated if this miRNA is involved in the regulation of estradiol production in granulosa cells. It was found that overexpression of miR-574 decreased phosphorylated ERK1/2 without affecting the level of ERK1/2 protein. On the contrast, down-regulation of miR-574 increased phosphorylated ERK1/2 level (P<0.05) and decreased estradiol level in granulosa cells. To identify the potential mechanism involved in the miR-574 regulatory effect, in silico screening was performed which revealed a potential binding site on the 3'UTR region of the tissue inhibitor of metalloproteinase 3 (TIMP3). Our gain- and loss- of function experiments, and luciferase reporter assay confirmed that TIMP3 is indeed the target of miR-574 in granulosa cells. Furthermore, downregulation of TIMP3 using siRNA resulted in a decrease of phosphorylated ERK1/2, and an increase of estradiol production while the addition of recombinant TIMP3 increased phosphorylated ERK1/2 level and decreased estradiol production. Thus, our results suggest that miR-574 may stimulate estradiol production via its targeted downregulation of TIMP3, and subsequently pERK1/2. This finding contributes to our understanding of the regulation of ovarian steroid hormone by miRNA.

Abstract # 1955

MiR-21 Enhances Estradiol Production by Inhibiting WT1 Expression in Porcine Granulosa Cells. Renée E. Hilker, Bo Pan, Xiaoshu Zhan, Julang Li

MicroRNAs (miRNAs) are noncoding small RNAs that play important roles in a variety of physiological events including ovarian follicular development. Within the antral follicle, transition of proliferative granulosa cells to differentiated, estradiol-producing granulosa cells is critical for proper oocyte maturation and subsequent fertility performance. However, how granulosa cell differentiation and steroidogenesis is regulated by miRNAs are not fully understood. We reported that microRNA 21 (miR-21) significantly increased in granulosa cells isolated from large-size follicles (3-6 mm in diameter) compared to those from small-size follicles (1-3 mm in diameter). To further investigate the function of

miR-21, porcine granulosa cells were transfected with miR-21 mimic (gain-of-function) or miR-21 targeted siRNA (loss-of-function). We found a knockdown of miR-21 resulted in a decrease in FSHR, LHR, CYP11A1, and aromatase mRNA, which was accompanied with a decreased estradiol level in the culture supernatant. In addition, Wilms Tumor 1 transcription factor (WT1) at the mRNA and protein level increased in the miR-21 knockdown group. On the contrary, the over-expression of miR-21 increased FSHR, LHR, aromatase mRNA and estradiol production while WT1 was downregulated at both mRNA and protein level. WT1 was previously shown to negatively regulate estradiol production by inhibiting FSHR expression. To verify this role of WT1 in our granulosa cell model, we transfected porcine aranulosa cells with siRNA targeted to WT1 and observed an increase in FSHR, LHR, aromatase and estradiol production. We thus hypothesized that miR-21 promotes estradiol production via inhibiting WT1 expression. Using the microRNA prediction software RNAhybrid, we found a potential miR-21 binding site in the 3' untranslated region (UTR) of the WT1 transcript. A dual luciferase reporter assay with the wild type and mutated putative miR-21 binding site was performed. There was a significant decrease in luciferase activity in the wild type miR-21 binding site group compared to the mutated miR-21 and the control (no miR-21). Our results suggest that miR-21 increases estradiol production via targeting the 3'UTR of the WT1 transcript. To our knowledge, this is the first report on the role of miR-21 in estradiol production and its regulation on WT1 expression. Our study provides insights into the regulation of granulosa cell differentiation and steroidogenesis and may have implications in ovarian disorders.

Abstract # 1984

Evidence And Effects of O-GlcNAcylation In Granulosa Cells Of Bovine Antral Follicles. Abigail M. Maucieri, David H. Townson

Glucose is widely recognized as the preferred energy substrate for metabolism by granulosa cells (GCs). Yet in most cells, 2-5% of glucose is shunted through the Hexosamine Biosynthesis Pathway (HBP) for O-linked N-acetylglucosaminylation (O-GlcNAcylation). O-GlcNAcylation is an evolutionarily-conserved, post-translational process that modifies serine and threonine residues on a variety of proteins. O-GlcNAcylation is also considered a nutrient sensor that can regulate cellular processes such as metabolism, signal transduction, and proliferation. In this respect, O-GlcNAcylation may be similar to, and possibly mediates, AMP-activated protein kinase (AMPK) signaling and its nutrient-sensing actions. However, the occurrence of O-GlcNAcylation and its relative importance to GC function has not been determined. Here, we characterized relative O-GlcNAcylation in bovine GCs from small and large antral follicles and determined its effects on GC proliferation. Bovine ovary pairs morphologically staged to the mid-to-late estrous period were used. Granulosa cells and follicular fluid were aspirated from small (3-5mm) and large (>10mm) follicles. Freshly isolated GCs of small follicles exhibited greater immunodetectable O-GlcNAcylation and the O-GlcNAcylation enzyme, O-GlcNAc transferase (OGT)

expression than large follicles (P<0.05, n=7 ovary pairs). Glucose and lactate concentrations from these same follicles had less glucose (0.4mM vs 2.2 mM, P<0.05) and more lactate (33.3mM vs 9.6mM, P<0.05) in small follicles compared to large follicles, respectively. Steroid profiles showed an estradiol to progesterone ratio >1 in 6/7 small follicle pools and in all 7 large follicles, indicative of healthy, estrogen-active follicles. Culture of GCs revealed that inhibition of the HBP via the glutamine fructose-6phosphate aminotransferase (GFAT) inhibitor, DON (50µM), impaired O-GlcNAcylation for small follicles (P<0.05) and, to a lesser extent, large follicles (P<0.1, n=3 independent expts.). DON also prevented GC proliferation, regardless of follicle size (P<0.05, n=4). Similarly, direct inhibition of O-GlcNAcylation via the OGT inhibitor, OSMI-1 (50µM), reduced O-GlcNAcylation in GCs of both follicle sizes, but only prevented proliferation of GCs from small follicles (P<0.05, n=3). Augmentation of O-GlcNAcylation via the O-GICNAcase (OGA) inhibitor, Thiamet-G (2.5uM), occurred in GCs from both follicle sizes (P<0.05, n=3), but had no effect on GC proliferation for either follicle size (P>0.05, n=3). In these latter experiments, GC proliferation was evaluated by both MTS assay and immunodetection of Ki-67. Lastly, the use of the AMPK activator, Metformin (10 mM), revealed that while AMPK activation inhibited GC proliferation from small follicles (P<0.05, n=4) as anticipated, it had no effect on O-GlcNAcylation (P>0.05 n=3). The results indicate: 1) O-GlcNAcylation occurs in GCs of bovine antral follicles, 2) Changes in O-GlcNAcylation are associated with alterations of alucose and lactate within the follicle, 3) Disruption of O-GlcNAcylation impairs GC proliferation, and 4) AMPK activation does not affect O-GlcNAcylation. In conclusion, the HBP and O-GlcNAcylation in GCs constitute an alternative, potential nutrient-sensing pathway to influence GC function and folliculogenesis in the bovine ovary. This work was supported in part by USDA Hatch Funds and USDA Multistate Project NE-1727. The authors also thank Drs. George Perry and Jerica Rich of South Dakota State University for their gracious work quantifying the steroids in these follicles.

Abstract # 2051

Androgen-Induced, Exosome-Mediated mir-379-5p Release Promotes Granulosa Cell Proliferation And Ovarian Inflammation In Pre-Antral Follicles Of PCOS Subjects. Reza Salehi, Brandon A. Wyse, Atefeh Abedini, Bo Pan, Toru Hasegawa, Yunping Xue, Yoko Urata, Jose L. Vinas, Alexey Gutsol, Sahar Jahangiri, Kai Xue, Kevin Burns, Barbara Vanderhyden, Julang Li, Dylan Clifford Burger, Clifford L. Librach, Benjamin K. Tsang

Polycystic ovarian syndrome (PCOS) accounts for 75% of anovulatory infertility and is associated with antral follicle growth arrest, minimal granulosa cell (GC) proliferation and hyperandrogenemia. MicroRNAs (miRNAs) suppress target gene expression through binding to 3'UTR. Follicular fluid extracellular vesicles, including exosomes (sEV) and microvesicles (IEV), facilitate inter-cellular cross-talk across the follicular antrum by selective packaging and transferring miRNAs from donor to recipient cells. However, the roles of exosome secretion in determining the cellular content and function of miRNAs in exosome-secreting and -receiving cells remain unclear. Our objectives were

to determine: (i) if androgen (5a-dihydrotestosterone, DHT) regulates cellular and extracellular content of mir-379-5p in granulosa cells; (ii) the function of mir-379-5p in the ovarian follicle in vitro and vivo; (iii) the role of GC-derived mir-379-5p in macrophage polarization; (iv) whether mir-375-5p-induced M1 polarization regulates GC proliferation and estradiol synthesis, and (v) whether this process is follicular stage-specific. Androgenized rats (DHT-treated) exhibited lower GC mir-379-5p but higher phosphoinositide-dependent kinase-1 (PDK1) content and proliferation. DHT reduced GC mir-379-5p content by increasing its exosomal release in pre-antral follicle (PAF) but not in antral follicle (AF) in vitro. Studies with miRNA-3'UTR binding assays and interrogation with miRNA mimic and inhibitor confirmed PDK1 is a mir-379-5p target. Inhibition of exosome release in PAF GC increased cellular mir-379-5p content and reduced PDK1 and proliferation in the presence of DHT, suggesting androgen-induced exosomal mir-379-5p release regulates GC PDK1 content. Ovarian mir-379-5p overexpression (ovarian intrabursal injection of lentivirus containing mir-379-5p) reduces ovarian growth (length and weight) and suppresses follicular growth by reducing PAF number in both control and androgenized rats. Compared with follicular fluids from human non-PCOS subjects, follicular fluid in human PCOS subjects exhibits high freetestosterone levels, lower exosomal mir-379-5p content and higher M1/M2 macrophage ratio, supporting the concept that PCOS is an inflammatory response, but whether androgen alters ovarian macrophage function is unknown. Studies with human macrophage-GC co-cultures confirmed that macrophages engulf GC-derived exosomal mir-379-5p. Transfection of macrophages with mir-379-5p mimic reduced the cellular content of PDK1 and induced M0-M1polarization, whereas its inhibitor polarized M0 towards M2, suggesting PI3K/Akt signaling pathway regulates macrophage polarization and inflammatory response. To investigate if mir-375-5p-induced M1 polarization suppresses GC proliferation and estradiol synthesis, pre- and antral follicle GC were treated with conditioned media from macrophages transfected by mir-375-5p mimic (CM-mimic) or inhibitor (CM-inhibitor). CM-mimic increases aromatase protein content without affecting proliferation in PAF GC, and reduces aromatase and proliferation in AF GC, responses reversible by CM-inhibitor. These findings suggest a follicular stage-specific response of GC to changes in the ovarian immunity induced by mir-379-5p. Taken together, our findings suggest that mir-379-5p inhibits PDK1-mediated GC proliferation, and androgen-induced mir-379-5p exosomal release from GCs removes its inhibitory action on PDK1; a survival mechanism specific for PAF GC. Uptake of GC-derived exosomal mir-379-5p by macrophages induces M1 polarization, a process which suppresses AF-specific GC estrogen biosynthesis and proliferation, two ovarian characteristics observed in human PCOS subjects (Supported by a grant from CIHR, the Lalor Foundation and Mitacs Postdoctoral Fellowship).

Hypo-glycosylated hFSH21 has Greater Bioactivity than Fully Glycosylated hFSH24 in Primary Porcine Granulosa Cells. Haley R. Blum, Aixin Liang, Michele R. Plewes, Guohua Hua, Xiaoying Hou, Pan Zhang, Emilia Przygrodzka, Jitu George, Kendra Clark, Jeffrey V. May, George Bousfield, John S. Davis

Follicle stimulating hormone (FSH) is an important regulator of several biological processes in humans, and plays a major role in maintaining natural menstrual cyclicity and fertility in females. The FSH receptor (FSHR) is a G-protein coupled receptor located on ovarian granulosa cells. The binding of FSH to the FSHR stimulates the cAMP-protein kinase A (PKA) signaling pathway, thereby regulating follicle growth, steroidogenesis, and oocyte maturation. Previous studies have reported hypo- and fully glycosylated FSH to occur naturally in humans. These alycoforms exist in changing ratios over a woman's lifespan and exhibit differing bioactivities in KGN cells and preantral follicles, as well as in vivo, in FSHB knockout mice. However, the precise cellular and molecular effects of FSH glycoforms have not been documented in primary granulosa cells. Porcine granulosa cells were cultured and subsequently treated with concentrations of FSH glycan variants ranging from 0-100 ng/mL. Data analysis was performed using GraphPad Prism 8.0 software and included Student's t-test or one-way ANOVA followed by either Tukey's or Bonferroni's post hoc test. Quantification of cAMP assays indicated that hypo-glycosylated hFSH 21 was significantly more effective at stimulating cAMP accumulation than fully glycosylated hFSH24. At 100 ng/mL, hFSH21 was able to stimulate a 21.8-fold increase in cAMP accumulation (p< 0.01) compared to controls, whereas hFSH24 treatment was much less effective, producing an 8.3-fold increase (p < p0.01). Western blot analysis indicated that phosphorylation of several downstream signaling elements, including PKA substrates, CREB, and b-Catenin, were induced to a greater extent by hypo-glycosylated hFSH21 than fully glycosylated hFSH24. For instance, 30 ng/mL of hFSH21 stimulated a 10.7-fold increase in phosphorylated CREB, while hFSH24 only stimulated a 3.2-fold increase. Additionally, progesterone production was significantly greater in cells treated with hypo-glycosylated hFSH21 compared to fully glycosylated hFSH24. Compared to fully glycosylated hFSH, hypo-glycosylated FSH also induced higher levels of transcripts for several steroidogenic genes, including STAR and 3bHSD, as indicated by quantitative real time PCR. Our results demonstrate that hypo-glycosylated hFSH21 exhibits higher bioactivity than fully glycosylated hFSH24 in primary cultures of porcine granulosa cells, and furthers our understanding of the differing effects of FSH glycoforms upon granulosa cells. Support: NIH P01 AG029531, VA 101 BX004272, Kansas INBRE P20 GM103418

Ad Libitum Feeding in Broiler Breeder Hens Alters Gene Expression in Granulosa Cells of Prehierarchal Follicles. Laurie Francoeur, Claire S. Stephens, Patricia A. Johnson

Broiler breeds of chickens are selected for fast growth and feed efficiency, while laying breeds are selected for optimal egg production. This selective breeding has resulted in suboptimal egg production in broiler breeder hens. The reproductive phenotype is exacerbated in hens fed ad libitum (FF) and this leads to excessive and disorganized follicular growth. One strategy used to improve broiler breeder hen reproductive efficiency is restricted feeding (RF), which results in an ovarian phenotype more like the laying hen. It is not known what factors translate level of dietary intake to follicle selection and growth. We have previously studied the liver transcriptome of FF broiler breeder hens and shown that increased feed intake overstimulates GH/IGF-I signaling and lipogenesis compared to RF hens, likely contributing to the reproductive dysfunction in FF hens. In the current project, we investigated transcriptional differences at the ovarian level between FF and RF broiler breeder hens. Broiler breeder hens (n=32) were raised according to commercial guidelines until 28 weeks of age. Birds were then randomly assigned to FF (n=16) or RF (n=16) for 6 weeks and egg production was monitored daily. Following dietary treatment, birds were euthanized, and ovarian weight, liver weight, fat pad weight, and follicle numbers were collected. The RF group had a higher egg/hen/day rate than the FF group throughout the treatment (p=0.001). Body weight (BW) (p<0.001), fat pad weight/BW (p<0.001), and liver weight/BW (p<0.001) were higher, and ovary weight/BW (p=0.101) tended to be higher in FF individuals compared to RF individuals. At the ovarian level, FF hens had significantly more preovulatory follicles (p=0.002) compared to RF hens. Granulosa cells from growing 6-8 mm follicles from FF (n=2) and RF (n=3) hens were collected, RNA was extracted, and samples processed for RNA-sequencing on Illumina NextSeg 500. Differential expression analysis was conducted from RNA-sequencing data using DESeq2. This analysis found 350 differentially expressed genes, of which 207 were upregulated and 143 were downregulated in FF hens compared to RF hens. Of the differentially expressed genes, several genes known to play a role in follicle development were shown to be upregulated in FF hens including INHA, INHBB, STAR, and CYP11A1. INHA and INHBB are both subunits of Inhibin B, a known regulator of FSH and therefore, possibly involved in follicle selection. Both STAR and CYP11A1 are critical factors in steroidogenesis, a defining characteristic of follicle selection at the 6-8 mm follicle stage. In addition to differences in body parameters, FF broiler breeder hens differed at an ovarian transcriptional level compared to the RF counterparts, resulting in a decreased egg laying efficiency rate. Several genes involved in follicle selection were upregulated in prehierarchal follicles of FF hens, suggesting an ovarian effect of dietary treatment at early stages in follicle development.

This project was supported by Agriculture and Food Research Initiative Competitive Grant no. 2017-67015-26453 from the USDA National Institute of Food and Agriculture and Multistate Funding from USDA/NIFA.

Abstract # 2067

Characterization of Carbohydrate Metabolism in In Vitro Grown and Matured Mouse Antral Follicles: a Baseline for Culture Optimization Strategies. Anamaria-Cristina Herta, Lucia von Mengden, Nazli Akin, Katy Billooye, Juul van Leersum, Berta Cava Cami, Laura Saucedo-Cuevas, Fabio Klamt, Johan Smitz, Ellen Anckaert

Establishing a robust human follicle culture system for oncofertility patients is challenging since donor tissue is scarce and often of suboptimal quality. Therefore, data generated from animal models are important for understanding the biological mechanisms regulating follicle and oocyte growth. The culture system developed in our lab supports in vitro growth of prepubertal mouse secondary follicles up to mature oocytes. Despite good maturation rates, lower developmental competence compared to in vivo oocytes suggests that further optimization is needed.

Tracking the metabolic changes triggered by meiotic maturation in follicles could indicate possible strategies to improve our culture system and identify metabolic markers of oocyte quality. In this study, the carbohydrate metabolism profiles are compared between in vitro cultured (10 days) antral follicles and their in vivo superovulated age-matched controls, during the final maturation. Several key players involved in glycolysis, tricarboxylic acid (TCA) cycle, pentose phosphate pathway (PPP) and the antioxidant capacity were measured by enzymatic assays with spectrophotometric detection in oocytes, cumulus cells (CC) and granulosa cells (GC). GC from in vivo ovulated follicles were not included. Pools of 5 oocytes and corresponding somatic cells were separately collected for testing, from 3 independent experiments. Statistical analysis was performed via t-test and results were considered significant when p<0.05.

The results highlight several differences between in vivo and in vitro metabolic trends. Within in vivo follicles, GV to MII transition triggered a metabolic boost in CC. Significant increases were detected in glycolysis and PPP key enzymes and intermediates (p<0.05). A rise in aconitase activity (p<0.05) and citrate levels (p<0.01) indicates TCA cycle upregulation. Additionally, higher total antioxidant capacity (p<0.05) and small molecule antioxidant capacity (p<0.01) in CC suggest enhanced protection against oxidative damage. Products of glycolysis and TCA cycle are most likely transferred to the oocyte for anabolic processes and further energy production. After ovulation, the only significant change detected in in vivo oocytes was increased nicotinamide adenine dinucleotide phosphate (NADP) levels that can be due to a higher rate of reduced-NADP recycling. For in vitro grown oocytes, no significant differences were observed in any of the metabolic pathways following meiotic maturation. In vitro differentiated CC and their controls revealed distinct metabolic profiles during this final

stage. Unlike the in vivo counterparts, the significant metabolic upregulations in the in vitro CC were limited only to aconitase, lactate dehydrogenase and glutathione-s-transferase activity. During in vitro oocyte maturation, GC showed increased glucose-6-phosphate dehydrogenase activity (p<0.05) suggesting PPP upregulation. No changes were detected in glycolysis and TCA. Furthermore, gene expression study was performed to verify these findings at transcriptomic level (data analysis ongoing).

Through a complete evaluation of enzyme activity and intermediates levels, this study reveals that suboptimal culture conditions, leading to low oocyte quality, are reflected in the altered metabolic pattern in the in vitro CCs. Deeper understanding of the follicular metabolic requirements is essential for the further fine-tuning of the follicle culture system. Additionally, the metabolic status of the somatic cells within the follicles could be used as an indirect evaluation of oocyte quality.

Abstract # 2076

Does Maternal High Fat Diet Alter The Ovarian Reserve In Female Mouse Offspring? Meaghan J. Griffiths, Urooza Sarma, Jessica M. Stringer, Luise A. Cullen-McEwen, Gessica Goncalves, John F. Bertram, Amy L. Winship, Karla J. Hutt

Background: Obesity contributes to adverse pregnancy events. Obese pregnant women have increased rates of early pregnancy loss and congenital abnormalities. Moreover, a high fat diet prior to conception in mice contributes to fetal growth abnormalities and developmental delay. Such abnormalities may arise from oocyte defects, including epigenetic reprogramming alterations, oxidative stress and meiotic abnormalities. Existing literature suggests a decrease in the finite ovarian reserve of primordial follicles in adult mice exposed to a high fat diet (HFD). In this study, we aimed to determine if combined maternal (preconception), gestational and lactational exposure to a HFD altered follicle number in offspring. Materials and Methods: C57BL/6 dams were fed ad libitum a normal fat diet (NFD; 6% fat, SF04-057, Specialty Feeds, WA, Australia) or high fat diet (HFD; 22% fat, SF00-219, Specialty Feeds, WA, Australia) for 6 weeks prior to mating, gestation and lactation. Pups were maintained on the mother's diet until weaning at post-natal day (PN)21, at which time they were either culled (n=6-8 animals/group) or placed on normal chow and subsequently culled at 4 (n=4 animals/group) or 6 weeks of age (n=3 animals/group). One ovary per mouse per litter was utilised for follicle counts using design-based stereology. Growing follicles and corpora lutea were assessed by light microscopy. In the contralateral ovary, histological markers of DNA damage (yH2AX), follicular atresia (TUNEL) and oocyte quality (Stella) were assessed (n=3-4/group). Data are mean ± standard error of the mean. Statistical analysis was performed using unpaired t-test or one-way ANOVA, with significance considered p<0.05. Results: At PN21, exposure to HFD throughout development and weaning yielded no significant differences in primordial (NFD 1968±31, HFD 1241±743), primary (NFD 691±134, HFD 594±303) or growing follicle (NFD 633±38, HFD 525±72) numbers. At 6 weeks of age, primordial (NFD 1516±308, HFD 1339±311), primary (NFD

975±127, HFD 647±139) and growing follicle (NFD 222±34, HFD 177±21) numbers remained similar in the two groups. HFD exposure led to an increased proportion of TUNEL-positive dying follicles (NFD 7.5±0.9%, HFD 27±10%, p=0.06) at PN21. At 6 weeks of age, there were no differences in follicle death between groups (NFD 32±11%, HFD 25±5%). Localisation patterns of DNA double strand breaks (yH2AX) and Stella were similar between all diet and age groups. Conclusions: Preliminary data suggest exposure to a high fat diet throughout development until weaning yields no effect on follicle numbers, but follicular atresia may be increased. Previous studies demonstrate a decrease in ovarian reserve in offspring aged 15 weeks, exposed to high fat diet throughout development. Therefore, the age groups assessed in the current study may be too early to observe any follicle number differences. Further analysis will determine if these HFD-exposed offspring are able to enter puberty as normal by assessing corpora lutea number at 4 weeks of age.

Abstract # 2094

Single-Cell Transcriptomic Interrogation of Primordial to Primary Follicle Transition in the Human Ovary. Katarzyna J. Szymanska, Xiujuan Tan, Nur-Taz Rahman, Kutluk Oktay

Primordial to primary follicle transition represents the dormant oocyte's entry into the growth phase. This process provides a source of fertilizable ova, determining both female fertility and natural menopause. Previous studies linked the mammalian primordial follicle activation to several signaling pathways, including the PTEN/PI3K/AKT/FOXO3, mTOR and Hippo pathways, and the expression of several oocyte-specific genes. However, mechanisms regulating the timing and trigger of primordial follicle growth initiation remain poorly understood. To better delineate the signaling pathways that are involved in human primordial follicle activation, we developed a single-cell RNA-sequencing approach from laser-captured oocytes. Single primordial (n=7) and primary (n=7) oocytes were laser-captured from 5 organ donor ovaries (age range 17-35 years). From each oocyte, RNA was extracted, reverse transcribed, and amplified using Smart-seq2 protocol. Libraries were prepared with Illumina Nextera XT Library Prep Kit, and their quality was assessed by Agilent Bioanalyzer using High Sensitivity DNA Assay. Sequencing was performed on the Illumina HiSeq4000 with 100bp, paired-end configuration, and obtained a read depth of 26.2M on average per oocyte with good read quality (Phredscore = 37). Reads were aligned by the STAR method to human hg38 RefSeq Transcripts with an average mapping rate of 89.5%. Differentially expressed genes (DEGs) were analyzed using Partek Flow after fragments/kb/million-reads (FPKM) normalization. Further DEG analysis and pathway analysis were done on Qlucore and Ingenuity Pathway Analysis (IPA) software, respectively. We identified 196 DEGs (114 upregulated, and 82 downregulated) in primary compared to primordial follicle oocytes ($p \le 0.05, -2 \le$ fold change (FC) ≤ 2). Upregulated genes included translocase of inner mitochondrial membrane 29 (Timm29 , FC = 7.88), kelch domain containing 8B (Klhdc8b, FC = 4.85), and heat shock protein family A (Hsp70) member 2 (Hspa2, FC = 4). Among the downregulated genes were

interferon-induced transmembrane protein 1 (Ifitm1, FC = -4.85), olfactory receptor family 7 subfamily E member 24 (Or7e24, FC = -4.56), ribosomal protein lateral stalk subunit P1 (Rplp1, FC = -4.35) and \$100 calcium-binding protein A6 (\$100a6, FC = -3.27). IPA identified enrichment for pathways regulating cellular development, growth, and cell cycle progression. Top canonical pathways, novel to primordial follicle growth, included activation of the Sirtuin Signaling Pathway (p = 3.39E-04), Integrin Linked Kinase Pathway (p = 4.53E-03), Thrombopoietin Signaling (p = 1.33E-02), Platelet-Derived Growth Factor Signaling Pathway (p = 2.28E-02), and inhibition of The Peroxisome Proliferator-Activated Receptor Signaling (p = 9.96E-04). IPA Upstream Analysis predicted PI3K and Akt pathways to be upregulated (p = 1.57E-2 and p = 1.22E-02), corroborating the pre-existing knowledge and validating our analysis. We identified novel molecular pathways related to human primordial to primary follicle transition using single-cell RNA sequencing. The interrogation of these pathways may lead to treatments to combat premature ovarian insufficiency, and age-induced infertility, as well as novel contraceptive and fertility preservation approaches.

Abstract # 2100

Possible Roles Of Estrogen Receptors Mediated Regulation In Follicle Growth And Differentiation. Hee-Seon Yang, Eun-Kyoung Choi, Young-Jin Son, Chongsuk Ryou, Yong-Pil Cheon

Ovary works as an endocrine organ and gonad for oogenesis. Estrogen is secreted from granulosa cell and works as autocrine, paracrine, and hormone. Estrogen is the ligand for estrogen receptor alpha (ERa, Esr1) and beta (ER β , Esr2). In the different cell types of the ovary, two different ER proteins are differentially localized. ERa is localized in theca/interstitial cell and ERB is localized in granulosa cell. ERa is known as required for ovulation and ERB is known as required for antrum formation and preovulatory follicle. However, so far, the role of estrogen is controversy in folliculogenesis in some parts. In this study, we investigated the role of estrogen receptor on folliculogenesis based on estrogen receptor alpha knockout mice (ERaKO) and ER specific antagonists. A 3-D in vitro culture method was employed in this study. The media level of 17b-estradiol was continuously during growing phase in both WT and ERaKO containing 17b-estradiol, PHTPP, or not in media. Progesterone levels were increased during growth phase in control and PHTPP treated WT and ERaKO, but decreased in 17b-estradiol treated WT. Follicle size was bigger in estradiol treated groups than ERaKO mice. ICI 182,780 inhibited the follicle growth in both WT and ERaKO. The expression level of Insl3 mRNA was significantly in ligand free culture condition in ERaKO than WT, but estradiol inhibit the expression of it in ERaKO mice. On the other hand, PHTPP induced the expression of Insl2 mRNA in WT but not in ERaKO. In the case of Cyp17a1, the expression level was also similarly highly induced by PHTPP in WT without estradiol. In the case of no estradiol, it was expressed only at WT. In the case of Fshr mRNA, its expression was induced by estradiol only in ERaKO. In the case of Cyp19a1, its expression was independent to estradiol but induced by PHTPP in WT without 17b-estradiol. Ptx3 mRNA expression was very high in ERaKO without 17b-estradiol. 17b-estradiol did not induced the expression of Ptx3 in this culture model. Ptgs2 mRNA expression was induced by estradiol in ERaKO but not in WT. Infaip6 mRNA expression was also induced by estradiol in ERaKO but PHTPP induced its expression in WT without 17b-estradiol. These results suggest that estrogen receptors might effect on the growth of follicles, differentiation of granulosa and theca cells in the manner of its receptor dependent or independent manners. In addition, it means that the expression of genes which are involved in GC differentiation are not under the same hormonal condition for their expression. Key words: estrogen receptors, folliculogenesis, ER specific antagonist, PHTPP, ERaKO Acknowledgement: This research was supported by a grant of the Korea Health Technology R&D Project

through the Korea Health Industry Development Institute (KHIDI), funded by the Ministry of Health & Welfare, Republic of Korea (grant number: H16C1085).

Abstract # 2112

YAP/TAZ-TEAD Interaction is Critical for the LH-Induced Ovulatory Cascade in Bovine Granulosa Cells. Esdras Correa dos Santos, Ariane Lalonde-Larue, Marcos Henrique Barreta, Alfredo Quites Antoniazzi, Paulo Bayard Dias Gonçalves, Valério Marques Portela, Gustavo Zamberlam

The ovulatory process required for normal fertility is initiated by a surge of LH that acts upon its receptors on granulosa cells (GC) to culminate with the rupture of the ovarian follicle that leads to the release of an oocyte into the oviduct for fertilization. This cascade, however, requires the activation of EGF receptor (EGFR) which consequently activates ERK1/2 and AKT signaling and stimulates the expression of critical genes not only for ovulation but also for luteinization, cumulus expansion and oocyte maturation. Interestingly, there is evidence in tumor cells that the Hippo signaling effectors, YAP and TAZ, can modulate the EGFR-ERK and AKT signaling by their binding to transcription factors of the TEAD family. In addition, it has been demonstrated recently that Hippo effectors interact with EGFR to regulate granulosa cell function during follicle development and ovulation in rodents; nevertheless, it has not been demonstrated how important is the binding of YAP/TAZ to TEAD transcription factors to the LH-induced signaling in preovulatory granulosa cells of monovulatory species as the cow. Therefore, the main objective of the present study was to elucidate the Hippo pathway effectors roles in the bovine preovulatory cascade. For this, we first employed a short-term bovine GC culture system in which cells respond to LH with rapid and transient increases in mRNA levels of critical preovulatory genes. First, cells were pre-treated with verteporfin (VP; a small molecule inhibitor that interferes with YAP/TAZ binding to TEADs) and challenged with LH. VP inhibited the expression of several key preovulatory genes required for LH-induced signaling, including EGFR (P<0.05). To explore whether Hippo effectors inhibition affects the EGFR-downstream signaling, we then challenged VP pretreated cells with EGF. The results indicated that VP downregulated basal and EGFinduced EGFR expression and therefore EGF was not capable of activating ERK1/2 nor AKT (P<0.05), consequently VP also blunted the expression of important genes dependent on EGFR activation (P<0.05). To better elucidate the contribution of these in vitro findings to the physiology of ovulation, we then performed an in vivo experiment using an ultrasound-guided follicle injection system. For this, VP doses or control vehicle were intrafollicularly injected in preovulatory follicles and cows (n=8 per treatment) were treated with GnRH intramuscularly. The results indicated that the intrafollicular injection of VP inhibited GnRH-induced ovulation in cattle in a dose-dependent manner (P<0.05). To our knowledge, this is the first study indicating that the roles of Hippo effectors are critical to the ovulatory process in monovulatory species. These findings may lead us to better understand ovulatory disorders and how to improve ovulatory

efficiency not only in monovulatory species of agricultural importance as the cow but also in women.

Abstract # 2113

PI3K Signaling Promotes Establishment of the Ovarian Reserve. Joshua Burton, Amanda Luke, Melissa Pepling

Cell signaling mediated by the KIT receptor is critical for many aspects of oogenesis. KIT is known to mediate the proliferation and migration of primordial germ cells, as well as the survival, growth, and maturation of ovarian follicles. We have previously shown that blocking KIT in mouse ovary organ culture reduces cyst breakdown and primordial follicle formation, while activating KIT promotes cyst breakdown and primordial follicle formation. To investigate the mechanism by which KIT regulates these processes, we modulated the activity of two downstream signaling cascades: the phosphoinositide 3kinase (PI3K) and the mitogen-activated protein kinase (MAPK) pathways. E17.5 ovaries were cultured for five days with a daily dose of media supplemented with either 25µM of LY294002 (a PI3K inhibitor), 10µM of U0126 (a MEK inhibitor), or DMSO vehicle controls of 0.1% or 0.05% respectively ($n \ge 21$ ovaries per group). After culture, ovaries were immunolabeled with a germ cell marker for confocal imaging and histological assessment. Oocytes in ovaries treated with LY294002 were noticeably smaller than those in the control cohort with average diameters of 15.31µm and 22.44µm respectively. Additionally, a significantly higher proportion of oocytes in treated ovaries remained in cysts and development appeared to be arrested at the primordial follicle stage. In contrast, no significant differences in oocyte size, cyst breakdown, or follicle development were observed in ovaries treated with U0126 when compared to control ovaries. Given these observations, we deduce that KIT may be signaling through the PI3K pathway to promote oocyte growth, cyst breakdown, and early follicular development in mice. However, further work is required to confirm that KIT specifically induces PI3K signaling to promote these developmental processes, and to identify specific target genes. These observations are important as they point to the potential molecular mechanisms that regulate oocyte development and may serve to better elucidate the etiology of reproductive disorders like primary ovarian insufficiency.

Abstract # 2127

Lipids Involved In Pro And Anti-Inflammatory Responses Are Altered In Follicular Fluid And Plasma Of Cows Administered A Low Dose FSH Treatment And May Be Used As Markers Of Ovulation In Beef Cows. Alexandria P. Snider, Renata S. Gomes, Adam F. Summers, Mohamed A. Abedal-Majed, Sarah C. Tenley, Renee M. McFee, Jennifer R. Wood, John S. Davis, Andrea S. Cupp

Superovulation procedures using Follicle Stimulating Hormone (FSH) in cattle promote development of a larger cohort of follicles to increase number of oocytes collected for

assisted reproductive technologies. These procedures are used if there are problems associated with ovulation since anovulation is a major factor affecting female fertility. Ovulation has been demonstrated to be an inflammatory process. Thus, our hypothesis was that treatment of cows with a low-dose-FSH protocol (35 IU FSH every 12 hours for 3.5 days plus prostaglandin at last and 12 hours after last FSH; FSHLow) would increase follicular fluid (FF) pro-inflammatory lipid markers compared to unstimulated controls; and blood plasma lipid markers compared to early or late luteal phase unstimulated controls. Follicular fluid from unstimulated samples was collected prior to and 24 hours after FSHLow. Blood plasma was collected from the same unstimulated cows (n=11) at D7-early luteal control, D15-late luteal control and 24 hours after FSHLow. Lipid compounds (863) were identified via UPLC-MS Analysis (CSH PhenylHexyl method) with 124 lipid compounds annotated utilizing XCMS software package in R. Analysis of variance (AOV) function was used for each lipid compound and p-values were adjusted using the Bonferroni-Hochberg method (p.adjust function) to determine differences in FF and plasma samples in non-stimulated controls and FSHLow-stimulated cows. There were 29 annotated lipid compounds different (p<0.05) in FF. Seventeen are involved in anti-inflammatory responses with ten of them decreased (p<0.05; e.g. HODE cholesteryl ester, C18–02:0 PC) FSHLow compared to control cows. Twelve of the 29 lipids are associated with pro-inflammatory responses with six of them increased (p<0.05) in FSHLow compared to Controls. Of these six lipids, LysoPC(20:4) and Glycerophosphocholine are involved in cytokine signaling; PE(P-36:2) and SM(d18:1/16:0) stimulate macrophage recruitment; Docosahexaenoyl PAF C-16 stimulates leukocyte localization; and Sodium Glycochenodeoxycholate increases signaling through the NFkB pathway (p < 0.05). In blood plasma, 16 lipid markers associated with anti-inflammatory and 16 associated with pro-inflammatory responses were altered in cows after FSHLow compared to Day 7 and 15 controls. A greater number of lipid markers associated with anti-inflammatory response were decreased (13; p<0.05; e.g. Oleamide, CE(15:2)) than increased (7; p<0.05; e.g. PC(38:2), PC(38:1)) in FSHLow compared to D15 controls indicating a shift from anti- to pro-inflammatory processes. Seven lipids associated with pro-inflammatory response were increased (p<0.05) in plasma after FSHLow compared to D15 controls. These pro-inflammatory lipids are involved with cytokine signaling (LysoPC(18:3) and TGs) and TLR2 receptor function (diacylglycerols). Overall, lipid markers decreased or elevated in FF were found to have a similar profile in blood plasma suggesting that collection of either would be reflective of lipid content in the ovarian follicle or circulating blood plasma. Taken together, these results indicate that FSHLow stimulation increases pro-inflammatory lipids in FF and blood plasma over that of controls and these lipids amplify different aspects of the inflammatory process. Furthermore, these lipid markers could be utilized to better understand females with anovulation or other problems with the ovulatory process resulting in female infertility.

Impact Of Chemotherapy Exposure On PI3K And Hippo Signaling Pathways Prior To Ovarian Tissue Cryopreservation In Pre-Pubertal And Young Adult Patients. Melody Devos, Paula Diaz Vidal, Isabelle Demeestere

Oncology progresses have improved overall cancer patients survival but therapeutic regimen can damage the ovarian reserve leading to infertility. Among the fertility preservation options, ovarian cortex banking appears to be an attractive alternative for women who cannot postpone their treatment or have already started chemotherapy and is the only available option for pre-pubertal girls. Although previous studies showed that first-line chemotherapy may induce follicular damage, little is known about the impact on the signaling pathways governing the ovarian follicular pool in human. Deciphering the signaling modifications among patients exposed or not to chemotherapy is critical to have a better understanding of the processes involved in the follicular depletion. Moreover, only few studies on cryopreserved tissue were conducted in child whereas follicles distribution differs compared to post-pubertal women. Cryopreserved ovarian cortical tissues from young adult (16-27 years old) and pre-pubertal (3-5 years old) cancer patients were thawed and cultured in vitro for 24 hours after size homogenization. Patients who received chemotherapeutic treatment before the cryopreservation were compared to non-exposed patients. PI3K/AKT/mTOR and Hippo pathways, as well as follicles and stroma survival, were assessed among the different groups at thawing and after the culture. At thawing, DNA damage analyses showed that chemotherapeutic treatment prior to cryopreservation was specifically deleterious on quiescent follicles of adult and pre-pubertal patients. Surprisingly, prepubertal treated tissue contained an oocyte-specific staining of DNA damages while adult treated patients showed granulosa cells death. After one day of culture, apoptosis was observed in the stroma but healthy follicles were observed in all conditions. However, dying follicles were observed after 24 hours of culture in prepubertal and adult cortex that was previously exposed to chemotherapy while not in the unexposed groups. Protein analysis showed a higher expression of PI3K and Hippo proteins among all groups at thawing compared to cultured groups while difference was observed between pre-pubertal and adults cortex. At thawing, cortical tissue exposed to chemotherapy before the cryopreservation procedure have a higher expression of phosphorylated forms of AKT and RPS6 compared to untreated groups, whatever the age. Our results highlight the involvement of the age and the previous chemotherapeutic treatment prior to the cryopreservation in the regulation of the signaling pathways regulating follicular activation, growth and survival.

Single-Cell RNA Sequencing Of Neonatal Ovaries Reveals Distinct Inhibitory Gene Signatures Of Mullerian Inhibiting Substance (MIS/AMH) In Ovarian Cell Types: A Novel Insight Into The Mechanisms Of Regulation Of The Ovarian Reserve. Marie-Charlotte Meinsohn, Hatice D. Saatcioglu, Wesley Samore, LiHua Zhang, Motohiro Kano, Lina Wei, Yi Li, Nicholas Nagykery, Mary E.Morris Sabatini, Bernardo Sabatini, Esther Oliva, Patricia K. Donahoe, David Pépin

Women are born with a limited number of primordial follicles. Their activation is an irreversible process that leads to either ovulation or atresia. The mechanisms involved in long-term primordial follicles quiescence and subsequent activation remain unclear. Mullerian inhibiting substance (MIS/AMH), produced by the granulosa cells of growing follicles, regulates ovarian reserve maintenance by providing negative feedback to primordial follicle activation. We have previously shown that administration of exogenous MIS in mice resulted in a complete arrest of folliculogenesis and loss of cyclicity. We hypothesized that MIS inhibits folliculogenesis by imposing a quiescent state on granulosa cells, thereby inhibiting their differentiation. We first confirmed expression of the MIS receptor, Misr2, in pregranulosa cells, granulosa cells, and ovarian surface epithelium (OSE) in mouse, rat, and human ovaries by in situ hybridization (RNAish). Mice and rats were injected with AAV9-MIS (or vector control) to deliver MIS continuously from postnatal day 1 (PND1) through PND6. At PND6, the MIS-treated ovaries were significantly smaller, and had significantly fewer growing primary and secondary follicles. To elucidate the mechanisms of action of MIS on granulosa cells and characterize its non-cell autonomous effects on the diverse cell types of the ovary, we performed single-cell RNA sequencing (inDROP) of MIS-treated and control mice ovaries at PND6. We catalogued a single cell atlas of the normal mouse ovary along with gene expression signatures uniquely associated with cell autonomous and non-cell autonomous MIS responses. In cells with high Misr2 expression (granulosa, OSE) we identified a common canonical MIS signature (Smad6, Id3, Igfbp5), which was associated with cell-cycle repression. Furthermore, we identified unique cell-specific gene signatures induced by MIS in the OSE, ovarian stroma, oocytes, and granulosa cells. Key genes within each MIS signature were validated by RNAish and qPCR. In aranulosa cells, Kctd14, Tmem184a, Slc18a2, and Nr5a2 were downregulated by MIS. In OSE, MIS regulated the expression of the progenitor markers Aldh1a1 and Lgr5, and was accompanied by an inhibition of proliferation. Finally, in stromal cells, Ptch1 and Ltbp2 were significantly downregulated and Kcnk3 upregulated by MIS, and those changes were accompanied by repression of proliferation and tissue remodeling. Conversely, oocyte transcriptome was only modestly affected by MIS treatment, suggesting the inhibition of folliculogenesis is primarily driven by inhibition of granulosa cell differentiation. By comparing gene expression in quiescent and activated follicles in the control ovaries to that of granulosa cells treated by MIS we defined a common quiescent gene signature in granulosa cells involving important pathways of stemness, immediate-early genes, and cytokine signaling. Importantly, we could recapitulate the inhibition of primordial follicle activation in exvivo ovarian cultures, and primordial

follicle in vitro cultures, by treatment with recombinant MIS. These studies support the view that MIS inhibits cell growth of multiple cell types in the ovary, and imposes a quiescent cell state in the granulosa cells of both primordial and preantral follicles leading to inhibition of preantral follicle progression, and profound suppression of ovarian activity.

Abstract # 2192

D-cloprostenol on Induction and Synchronization of Ovulation in Pluriparous Sows. Ciro Alexandre A. Torres, Domingos Lollobrigida Souza Netto, Jurandy Mauro Penitente Filho, Celina Alves de Oliveira, Vivian Angélico Pereira Alfradique, Danielle Estanislau Coelho Silva, Andréia Ferreira Machado, José Domingos Guimarães

In pig farms, one of the focuses is the manipulation of the estrous cycle and ovulation aiming for reproductive and productive efficiency in order to reduce the costs with the number of artificial inseminations and/ow development piglets, among others. This experiment was designed to evaluate the use of d-Cloprostenol (Prostaglandin F2a Analog - PGF2a) in synchronization and ovulation induction in pluriparous sows. One hundred and twenty females of commercial lineage, between the 3rd and 6th parturition order and after weaning, were randomly distributed as follows: 1) Control, (n = 42) 2 mL saline (0.9% NaCl) administered at estrus detection; 2) Treatment 0h (n = 44), administration of 0.150 mg d-Cloprostenol at estrus detection; and 3) Treatment 24h (n = 39) administration of 0.150 mg d-Cloprostenol 24 h after estrus detection. From estrus detection, follicular monitoring was performed every 8 hours by transabdominal ultrasound examination. Ovulation data parameters were evaluated in a block design (GLM procedure), the onset of ovulation for treatments was evaluated by survival analysis (LIFETEST procedure) and the equality over treatments was tested by Log-Rank and Wilcoxon tests. Significance level adopted was a = 0.05. The application of PGF2a did not affect the ovarian response with no difference (P>0.05) between the onset (0h = 41.5 ± 1.5 ; $24h = 41.8 \pm 1.6$ and Control = 41.3 ± 1.5), end of ovulation (0h = 45.6 ± 1.6 ; 24h= 44.9 ± 1.5 and Control = 45.9 ± 1.6), total ovulation time (0h = 4.2 ± 0.8 ; 24h = 3.1 ± 0.7 and Control = 4.6 ± 0.7) and the likelihood of the onset or end of ovulation. All treatments showed similar results for the onset and end of ovulation, consequently total ovulation time. This may be related to the fast metabolism of PGF2a in the lungs, where 99% is inactivated by the first passage. As swine do not have very functional sweat glands, the main form of heat lost under thermal stress (ambient temperature above 20° C) is to increase the respiratory rate. Two hours after d-Cloprostenol injection, the ambient temperature (°C), exceeded thermoneutrality, remaining for nine hours above the acceptable limit. This increase in temperature affects the respiratory rate of sows and consequently speeds up degradation of the analogue, even with a half-life of approximately 3 hours. The increased respirations combined with the immaturity of the pre-ovulatory follicle wall, impairs the action of prostaglandins in increasing intrafollicular pressure and the synthesis of collagenolytic and proteolytics enzymes. This

study, demonstrates that PGF2a did not synchronize or induce ovulation, at time 0 and 24 hours after estrus detection

Abstract # 2194

Androgens Modulate the Expression of Genes Associated with the Hippo Pathway in the Mouse Ovary; Implications for PCOS. Thomas I R Hopkins, Iain Dunlop, Stephen Franks, Kate Hardy

The Hippo signalling pathway is a key regulator of organ size, through control of cell proliferation and apoptosis. Ovarian Hippo signalling has been implicated in control of follicle development. This pathway is associated with the promotion of downstream growth factors associated with follicle growth. Polycystic ovary syndrome (PCOS) is a very common endocrine disorder, causing anovulatory infertility in women. PCOS is associated with elevated androgen levels and aberrant follicle development. This study aimed to examine the role of Hippo signalling in androgen-mediated growth and development of mouse preantral follicles. Follicles were isolated from PND16 (C57BL/6) mouse ovaries and treated in vitro with dihydrotestosterone (DHT) (10nM) for 72HR. DHTtreated follicles demonstrated a significant increase in growth at all time points with a significantly larger overall diameter when compared to controls (24HR $p\leq0.001$, 48HR p<0.0001, 72HR p<0.01, n=23). The DHT-exposed follicles demonstrated significant changes in a number of Hippo pathway genes and downstream targets. Among Hippo pathway genes, there was an increase in Yap1 ($p\leq 0.05$, n=9), Lats2 ($p\leq 0.01$, n=9), Lats1 ($p\leq0.05$, n=9), Stk3 ($p\leq0.05$, n=9) and Stk4 ($p\leq0.05$, n=9). Notably, further analysis showed there was an increase in gene expression of downstream targets of the Hippo signalling pathway; Connective Tissue Growth Factor (Ctgf) (p≤0.0001, n=9); AXL Receptor Tyrosine Kinase (Axl) (p≤0.01, n=8) and Cysteine-rich angiogenic inducer 61 (Cyr61) ($p \le 0.05$, n=7). The results demonstrate a clear alteration in Hippo signalling in response to DHT. Since PCOS is associated with ovarian hyperandrogenism, we suggest that androgen -related perturbations in hippo signalling and its regulation may lead to the abnormalities in follicle development that are observed in PCOS.

Abstract # 2196

Epidermal Growth Factor (EGF) and EGF+ Kit Ligand or Leukemia Inhibitory Factor Enhances Survival and Growth of Bovine Multilayer Follicles in 3D Matrix-free Culture System. Wilson P. Simmons, Shaina L. Jachter, Vanessa Peixoto De Souza, Jing Xu, Charles Estill

To facilitate further studies on theca-granulosa cell and oocyte interactions in growing preantral follicles of ruminant species, the goal of this study was to characterize the impact of epidermal growth factor (EGF) supplementation alone, or in the presence of kit ligand (KITLG) or leukemia inhibitory factor (LIF), on survival and growth of bovine

(Bos taurus) multilayer preantral follicles. Ovaries from dairy-breed female cows (Jersey and Holstein; n=12) were collected by left paralumbar laparotomy ovariectomy two days following prostaglandin-induced luteal regression. Healthy multilayer follicles were mechanically isolated, randomly divided between groups (~15 follicles/cow, at least 4 follicles/treatment group) and placed into ultra-low attachment plates for matrix-free 3dimensional (3D) culture in serum-free media containing follicle stimulating hormone (100 ng/ml) and insulin (10 µg/ml). A subset of follicles received EGF (10 ng/ml) at the start of culture, and follicles receiving EGF were supplemented additionally with LIF (50 ng/ml) or KITLG (50 ng/ml). After 5 days of culture, luteinizing hormone was added to the culture media (100 ng/ml). Images of follicles were captured throughout culture to visualize antral formation and measure follicle diameter up to 21 days. Follicle survival and classes of antrum formation were analyzed by Generalized Linear Models function of SAS. The impacts of treatments on discrete variables were analyzed by Linear Models, and Mixed Model were used to observe impact of treatments on follicle growth by treatment and day. Pairwise comparisons were conducted by Least Squares Means. Addition of EGF dramatically increased the numbers of follicles surviving to form an antrum (29% vs 95.7%, p<0.0001). Follicles cultured in the presence of EGF were 1.3-1.4fold larger in diameter than controls (p<0.0004), and those cultured in the presence of EGF+KITLG formed an antrum slightly earlier than those with EGF alone (p<0.09). Follicles were further classified by speed of antrum formation (fast, 1-5 days; slow, 6-19 days; no antrum, but survived up to 21 days). EGF alone did not impact growth of fast follicles, but fast antrum follicles cultured with either EGF+KITLG or EGF+LIF did not survive past culture day 2 and formed smaller antrums on day 1 (p<0.04, 0.01). In contrast, slow grow follicles cultured in the presence of EGF were larger than controls (p<0.0001), and those cultured with EGF+KITLG and EGF+LIF were larger at the end of culture (p<0.005, p<0.06 vs EGF). Surviving no antrum follicles were also larger at the end of culture with EGF than controls (p<0.0001). All classes of follicles cultured in presence of EGF alone produced significant amounts of androstenedione, indicating presence of intact theca layer contributing to steroidogenesis. In conclusion, KITLG and LIF may be detrimental to fast developing bovine small antral follicles. EGF promotes survival and arowth of slower developing bovine multilayer and small antral follicles. These data suggest further investigation into factors induced by EGF, KITLG and LIF in bovine multilayer follicles to determine other factors critical to folliculogenesis in cattle. This work was supported, in part, by the USDA National Institute of Food and Agriculture, Hatch/Multi State project #1017763 (CVB).

Abstract # 2204

Effects of FSH and IGF-1 on AMH mRNA Expression in Granulosa Cells of Small Follicles in the Hen. Deena M. Scoville, Laurie Francoeur, Patricia A. Johnson

The laying hen has a high reproductive efficiency, laying approximately one egg per day. In order to maintain this level of productivity throughout her reproductive lifetime, ovarian follicle development must be regulated through a series of coordinated events. Follicle stimulating hormone (FSH) and insulin-like growth factor 1 (IGF-1) are known to be important regulators of follicle development. IGF-1 has been found to act synergistically with gonadotropins to increase cell proliferation and FSH receptor (FSHR) in mammalian granulosa cells. Anti-mullerian hormone (AMH) is known to inhibit follicle recruitment in both mammalian and avian species. In the chicken, AMH is mainly expressed in granulosa cells of smaller follicles and expression decreases with increasing follicle size. It has been proposed that AMH is important in keeping granulosa cells in an undifferentiated state. At the 3-5 mm follicle stage in hens, granulosa cells remain undifferentiated and express abundant AMH. We hypothesized that FSH may inhibit AMH expression and that the effect would be potentiated with IGF-1 in 3-5 mm follicles. Granulosa cells from 3-5 mm follicles from commercial Single-comb White Leghorn hens (n=7 cultures) were removed and pooled according to follicle size. Approximately 1.6-2 million cells were plated in 6-well culture plates and allowed to arow in Medium 199 + 0.1% BSA + 5% FBS for 24 hours. Cells were then cultured in serum-free media with treatments for an additional 24 hours. Following a 24 hour treatment, cells were collected for RNA extraction and RNA was reverse transcribed into cDNA for downstream RT-qPCR. AMH and FSHR mRNA expression were measured using RT-qPCR and normalized to 18S. In Experiment 1, we tested the effect of ovine FSH (0, 10, 25, 100 ng/ml) on AMH and FSHR mRNA expression. FSH at all doses decreased AMH mRNA expression in granulosa cells from 3-5 mm follicles (p=0.0004). FSHR mRNA expression was not affected by FSH treatment (p=0.85). In Experiment 2, we cultured granulosa cells similarly, using the optimal dose of FSH (0, 10 ng/ml) from Experiment 1 and cultured cells in the presence or absence of recombinant human IGF-1 (0, 10, 100 ng/ml). We found that FSH decreased AMH mRNA expression in granulosa cells from 3-5 mm follicles (p<0.0001), and IGF-1 treatment showed no additional effect on mRNA expression. Treatment of FSH as well as IGF-1 had no effect on FSHR expression in the granulosa cells (p=0.89). In summary, FSH decreased AMH mRNA expression in granulosa cells from 3-5 mm follicles, although IGF-1 did not potentiate the effect of FSH. Future studies will investigate whether FSH has a direct effect on AMH gene transcription or affects other pathways associated with follicle selection. This project was supported by Agriculture and Food Research Initiative Competitive Grant no. 2017-67015-26453 from the USDA National Institute of Food and Agriculture and Multistate Funding from USDA/NIFA.

Abstract # 2231

Transcriptional Profiles In Cumulus-Oocyte Complexes Reveal New Genes Associated With Successful Embryo Development. Bailey N. Walker, Fernando H. Biase

During folliculogenesis, oocytes and cumulus cells undergo many morphological and physiological changes. Within this unique microsystem, named cumulus oocyte complex (COC), there is complex bidirectional exchange of signals between the two cell types. Moreover, there is a quantitative relationship between transcripts present in the oocyte and the surrounding cumulus cells. While there is strong evidence that the

cells influence each other's transcriptional activity, little is known of the mechanisms and genomic rules that govern these interactions at the transcriptional level. Our goal was to infer the differences in gene regulatory networks between oocytes and surrounding cumulus cells in fully grown versus growing phase oocytes. Using cow ovaries from an abattoir, we collected COCs from follicles ranging from 3 to 8 mm in diameter. COCs were incubated in the supravital stain Brilliant Cresyl Blue (BCB) as a means of separating oocytes based on growth phase. Fully grown oocytes remained stained and were categorized as BCB+, whereas oocytes in the growing phase were colorless and were categorized as BCB-. Immediately following the classification, we separated the cumulus cells from the oocytes and generated single-cell RNA-seg data for oocytes and RNA-seq data for the corresponding surrounding cumulus cells. In total, we produced sequencing data for 26 pairs of oocytes and corresponding cumulus cells (BCB+ n=13, BCB- n=13). We detected 2,214 and 2,237 genes to be exclusively expressed in oocytes and cumulus cells, respectively; and 10,383 genes were expressed in both oocytes and cumulus cells. Differential gene expression analysis revealed one long non-coding RNA (ENSBTAG0000053835) to be differentially expressed when comparing BCB+ to BCB- oocytes at FDR<0.1. Moreover, there were 13 genes, (ANXA1, B3GALT4, CPAMD8, DKK3, FLNB, KBTBD11, KRT8, KYAT1, PRICKLE1, RGS2, SLC7A5, STUM, SVIL) differentially expressed within cumulus cells surrounding oocytes labeled as BCB+ or BCB- (FDR<0.1). Next, we interrogated whether gene coexpression differed depending on BCB status. In oocytes, we determined 35 differential connections composed of 44 genes. The gene OXT emerged as a hub with 22 differential connections. In cumulus cells, there were 1057 differential connections containing 472 genes. The genes, AK5, GSTA3, andTMEM59L emerged with the greatest number of differential coexpression with 103, 93 and 67 connections, respectively. Of the 472 genes, we identified enrichment (FDR<0.01) for the following biological processes: protein-coupled receptor signaling pathway (fold change (FC)=3.9), protein-coupled receptor signaling pathway (FC=3.9), negative regulation of cell proliferation (FC=2.9), and negative regulation of Wnt signaling pathway (FC=7.7). In conclusion, there was relatively no difference between expression patterns associated with oocytes relative to BCB status. However, there were significant differences in expression patterns associated with BCB status within the corresponding cumulus cells. Collectively, the results confirm minor changes in growing oocytes within late tertiary follicles. More importantly, we detected biologically relevant changes of gene transcript abundance in cumulus cells that are likely to be critical for successful embryo development.

Abstract # 2242

Culture with Isoproterenol and Gonadotropins Restores Aspects of Steroidogenesis in Photoregressed Ovaries. Amanda A. Macias, Lauren K. Delhousay, Kelly A. Young

Adrenergic activation in the ovary is involved in the secretion of sex steroids as well as folliculogenesis. Culture of ovaries with isoproterenol, a β -adrenergic receptor agonist, increases follicle stimulating hormone receptor and progesterone production, and in

vivo exposure to isoproterenol can also increase androgen secretion. While the role for adrenergic stimulation in active and neonatal ovaries has been examined, the impact of adrenergic activity in the return to function of photoregressed ovaries in seasonallybreeding animals is not fully understood. In photoperiodic Siberian hamsters (Phodopus sungous), exposure to long photoperiods (>12 hours of light per day) stimulates and maintains ovarian function, whereas exposure to short photoperiods (<12h light/day) induces reduction in antral follicle formation, ovulation, and plasma estradiol concentrations. We hypothesized that stimulating photoregressed ovaries in vitro with isoproterenol with or without gonadotropins would potentially recapitulate aspects of photostimulated recrudescence as opposed to untreated ovaries; specifically impacting estradiol production as well as the expression of genes associated with the return of folliculogenesis and steroidogenesis. Adult female Siberian hamsters were exposed to short day (8L:16D) photoperiods for 16 weeks to induce gonadal regression. Isolated ovaries were then cultured for 10 days in one of four treatment groups: standard media (no treatment, NT); gonadotropins (follicle stimulating hormone and luteinizing hormone, GT); isoproterenol (20 micromolar, ISO); or isoproterenol plus gonadotropins (ISO+GT). While there were no significant differences among the groups for uterine or pre-culture ovarian masses, indicating that all groups showed similar levels of reproductive regression, ovaries cultured in ISO+GT showed a significant increase in mass post-culture as compared to all other treatments. Media concentrations of estradiol were significantly increased in the ISO+GT groups as compared to all other treatment groups. Culture with GT, ISO, or ISO+GT, increased total media prostaglandins, as compared to NT individuals. Ovarian expression of steroidogenic acute regulatory protein (Star), 3β-hydroxysteroid dehydrogenase (3βHsd) and growth and differentiation factor-9 (Gdf-9) mRNA, assessed using real time PCR, was increased in the ISO and ISO+GT groups, whereas cyclooxygenase-2 (Cox-2) mRNA increased in GT, ISO, and ISO+GT groups as compared to NT. Estrogen receptor 1 (Esr1) mRNA expression increased in the ISO+GT group as compared to all other groups, whereas expression of Esr2 mRNA did not differ significantly across treatments. Culture with isoproterenol stimulated expression of genes involved with both steroidogenesis and folliculogenesis, along with increasing estradiol production and prostaglandins, critical for multiple aspects of ovarian function. Culture with ISO, regardless of GT exposure, increased mRNA expression of early steroidogenic enzymes (Star and 3BHsd) along with folliculogenic factors (Gdf-9 and Cox-2). In contrast, only the combination of ISO+GT increased Esr1 mRNA, ovarian mass, and media concentrations of estradiol and prostaglandins. These data suggest that photoregressed ovaries are able to respond to β-adrenergic stimulation alone, particularly in aspects of steroidogenesis; however, the additional stimulation of gonadotropins is needed to restore actual production of estradiol and ovarian growth. While β-adrenergic stimulation advanced some aspects of recrudescence, gonadotropins as well as exposure to additional factors are likely necessary to fully restore function in photoregressed ovaries.

Protective Effect Of Humanin Against Oxidative Stress In Granulosa Cells. Julia Gaetana Conte, María Sol Gosso, Mercedes Imsen, Adriana Seilicovich, Marina Cinthia Peluffo, Gabriela Alejandra Jaita

Humanin (HN) exerts a cytoprotective action in the presence of pro-oxidative agents in several tissues. Recently, we demonstrated the expression of HN in the ovary of prepuberal and adult rats. Also, we showed a differential location dependent on the follicular stage. In the present study, our aim was to evaluate the anti-apoptotic action of HN, as a cytoprotective mechanism against oxidative stress in granulosa cells. To explore this aim, we examined the effect of HN on apoptosis in granulosa cells from ovaries of prepuberal and adult rats incubated in a pro-oxidative environment. Thus, we incubated each ovary from prepuberal or adult rats with HN (1µM) for 30 min and H2O2 (150 µM) for further 1 or 2 h, respectively. Contralateral ovaries from rats of each treatment were used as respective controls. We determined the number of TUNEL positive granulosa cells per follicle. In prepuberal ovaries, we observed that HN decreased the number of TUNEL positive granulosa cells per follicle induced by H202 (C: 3.8 vs HN: 3.0 ns.; C: 1.7 vs H202: 5.7 p<0.05; H202: 8.8 vs H202+HN: 6.0 p<0.05. Student'st test). In adult rats, HN decreased the number of TUNEL positive granulosa cells per follicle induced by H202 (C: 8.7 vs HN: 9.3 ns.; C: 8.8 vs H202: 46.8 p<0.05; H202: 26.2 vs H202+HN: 16.0 p=0.0581. Student's t test).

In addition, we previously reported that inhibition of endogenous HN increases apoptosis in human granulosa-like tumor cell line (KGN). Also, we demonstrated that HN decreases ROS production in KGN cells exposed to pro-oxidative environment. In this study, we also evaluated the anti-apoptotic effect of HN against oxidative stress in KGN. To explore this aim, we assessed the percentage of TUNEL positive KGN cells incubated with HN (1 μ M) for 30 min and H2O2 (150 μ M) for further 1 h. Our results demonstrated that HN decreased the percentage of KGN TUNEL positive cells induced by H2O2 (C: 0.2, HN: 0.5, H2O2: 1.5, H2O2+HN: 0.5, *p<0.01 vs respective control without H2O2, Λ p<0.01 vs. respective control without HN. χ 2 test).

To conclude, our results suggest that HN exerts a cytoprotective role against oxidative stress on granulosa cells probably through an anti-apoptotic mechanism.

Parturition/Myometrium

Abstract # 2356

Cannabinoid Receptor 1 (CB1) Signaling Participates In The Triggering Of Preterm Birth Induced By LPS. Carolina Marvaldi, Julieta Aylen Schander, Julieta Aisemberg, Ana Maria Franchi, Manuel Luis Wolfson

Endocannabinoid system (ECs) is one of several signaling pathways implicated in maternal-fetal interface, and endocannabinoids are involved in different aspects of physiopathology of reproduction. Preterm birth (PTB) is the leading cause of mortality and morbidity in neonates. It is well known that premature deliveries are mainly associated with infectious process. In mice, it has been shown that one of the major causes of PTB is premature decidual senescence, which becomes more aggravated by an inflammatory stimulus. Our group developed a murine model of preterm labor, consisting of two injections of bacterial lipopolysaccharide (LPS), that produces an 85% of PTB in BALB/c mice. The aim of the present work was to evaluate if the ECs participates in LPS-induced preterm labor. For this purpose, we administrated two doses of bacterial lipopolysaccharide (LPS, 10ug/g of weight and 3h later 20ug/g of weigh respectively) on day 15 of pregnancy to CD1-wild type mice (CB1-WT) and CD1-knock out mice for the cannabinoid receptor 1 (CB1-KO). We found that CB1-KO mice show lower PTB percentage than CB1-WT mice (60% CB1-KO vs 81% CB1-WT). To dilucidated this protective effect of the absence of CB1 on the triggering of PTB, we first studied different inflammatory mediators in decidua 5h after the second dose of LPS. We observed that LPS receptor, TLR-4, protein levels were diminished in LPS treated mice (p<0.05) while CD14 (its co-activator protein) levels were augmented (p<0.05). We analyzed COX-2 protein levels because it is a proinflammatory protein involved in prostaglandins production that preceded PTB and found that were increased in LPStreated mice. The same response pattern was observed both in CB1-WT and CB1-KO mice. As decidual cells undergo progressive senescence as labor approaches, we decided to evaluate decidual protein expression of y-H2AX, an indicator of higher levels of DNA damage after LPS administration. We did not observed differences between CB1-WT and CB1-KO mice nor LPS treated mice. Considering the cross-talk between senescence and autophagy and that it has been reported that disruption of autophagy balance (either increase or decrease) can lead to PTB, we also evaluated decidual protein expression of LC3b II, a marker of autophagy. We observed that CB1-KO mice presented lower decidual protein levels of LC3b II when compared to CB1-WT (p<0.05) in both LPS and control groups. In summary, our results indicate that cannabinoid receptor 1 is involved in the triggering of LPS-induced preterm birth, showing differences in the autophagic flux between WT and CB1-KO mice.

Placental Development & Function

Abstract # 1660

The Use of Placental Pathology To Examine Differential Adverse Pregnancy Outcomes Following IVF And Oocyte Donation. Erika Mery, Sonia Dancey, Ashley Esteves, Dina El, Shannon Bainbridge

Introduction: Infertility among North American women lies between 11-16%, resulting in Introduction: Infertility among North American women lies between 11-16%, resulting in increased use of in vitro fertilization (IVF) and oocyte donation (OD). Unfortunately, these therapies are associated with increased risk of placenta-mediated diseases. To date, a comprehensive analysis of the types of placental disease associated with assisted reproductive technologies (ART) has not been conducted. Considering the difference in genetic complements in IVF vs OD, with OD as a complete maternal-fetal genetic mismatch, we hypothesize that immune-driven forms of placental disease are more prevalent in OD-derived pregnancies.

Methods: A retrospective study of placenta pathology findings from 121 women who conceived using IVF or OD was conducted on specimens from the Children's Hospital of Eastern Ontario (Ottawa) between 2012-2018. Cases with singleton, twin or triplet gestation and a diagnosis of a placenta-mediated disease (intrauterine growth restriction, preeclampsia, HELLP syndrome or gestational hypertension) were included. Cases with gestational diabetes, intrauterine fetal demise or severe preterm birth (<28 weeks) were excluded. Archived histopathology samples were examined by a perinatal pathologist, blinded to the ART used and pregnancy outcome, using a validated synoptic data collection tool to assess presence, absence and severity of 30 distinct placental lesions. Data are presented as mean number of lesions ± standard deviation ranging from 0-5 for lesion categories and 0-30 for overall pathology. Odds ratios (OR) and t-tests with 95% confidence intervals were calculated.

Results: Of the 121 participants, 34 used OD (28%) and 87 used IVF (72%). OD conceptions demonstrated a higher degree of overall placenta pathology (4.71±1.70 vs 4.59±2.23 lesions, p<0.005), with enrichments in lesions consistent with maternal vascular malperfusion (MVM) (2.62±1.23 vs 2.18±1.43 lesions; p<0.05) and chronic inflammation (1.35±1.47 vs 0.89±1.06 lesions, p<0.05). Cases with OD conception were also more likely to demonstrate more than 2 MVM (65%±0.49 vs 42%±0.50;OR= 2.48 [1.09-5.64]) or inflammatory (18%±0.39 vs 9%±0.31;OR= 14.83 [1.66-132.21]) lesions. Conversely, cases of IVF conception were far more likely to demonstrate minimal placenta pathology (<2 placental lesions total;2%±0.17 vs 21%±0.4;OR=8.61 [1.10-67.27]).

Conclusion: Our results show that OD, compared to IVF, is associated with an overall increase in placental pathology findings, with enrichments in lesions of malperfusion and chronic inflammation. The increased presence of these lesions in placentas from OD pregnancies support the hypothesis of heightened maternal-fetal interface immune

disturbance, or allograft-like rejection, in cases of complete maternal-fetal genetic mismatch.

Abstract # 1663

Does Placental Tissue Sampling Site Affect Placental Protein Expression Outcomes? Diana M.Encalada, Jayasri Basu, Yingyi Wu, Sara Oraee, Aruna Mishra, Magdy Mikhail

Introduction: In studies investigating the expression patterns of placental proteins, tissue samples from a single site are normally taken. The objective of this study was to ascertain whether placental tissue sampling site influences placental protein expression outcomes. Two robust placental proteins involved in placental angiogenesis and development were selected for the study, vascular endothelial growth factor (VEGF)165 and VEGF165b.

Methods: In this IRB approved study, term delivered placentas from women with uncomplicated pregnancy was collected. The procedure was: placental membranes were removed; photograph of the fetal side was taken (with a paper ruler placed at the bottom of each placenta to record placental dimension; and to demarcate the insertion point); placenta was flipped from left to right to expose the maternal side; and photographed again. Each placenta was then visually dissected into four quadrants (Qs), designating North-East as Q1, South-East as Q2, South-West as Q3 and North-West as Q4. A section from each quadrant was removed, thoroughly washed to remove blood and dissected under normal saline to isolate chorionic villi (CV). A few pieces of CV from each quadrant were placed in separate tubes pre-labeled with placental ID and quadrant number. Tubes were stored at -800C until analysis. Monoclonal antibody based ELISA kits: DY293B and DY3045 from R&D Systems, Minneapolis, MN were used for analysis. ANOVA and Pearson's correlation were used for statistical analysis. P<0.05 was considered significant.

Results: 26 term delivered normal placentas were analyzed. The average distribution of VEGF165 protein in the quadrants was: Q1: 237.63 + 84.53; Q2: 274.36 + 99.85; Q3: 260.12 + 87.33 and Q4: 266.43 + 90.94, respectively. The average distribution of VEGF165b protein in the quadrants was: Q1: 469.49 + 352.99; Q2: 468.80 + 386.82; Q3: 465.67 + 348.36 and Q4: 448.95 + 362.22, respectively. The results revealed that there was no significant difference in the expression of VEGF165 (p=0.505) or VEGF 165b protein (p=0.997) between the four quadrants. However, the two proteins were found to be significantly correlated (r2 = +0.527, p=0.0001). Scatterplot data showed that placental weight was highest when VEGF165 protein was between 200 to 300 pg/100 mg tissue, and VEGF165b protein was <1000 pg/100 mg tissue. Higher levels of VEGF165b protein negatively impacted placental weight. Positive correlations were seen between placental weight (r2=+0.792, p=0.0001). Significant positive correlations were seen between seen between placental weight and newborn weight (r2=+0.792, p=0.0001). Significant positive correlations were seen between placental weight and distance between the insertion point and two

quadrants: Q3 (r2 = +0.563, p=0.003) and Q4 (r2 = +0.481, p= 0.013) only; but not for the other two quadrants.

Conclusions: In term delivered normal placentas, tissue sampling site had no bearing on the expression patterns of placental VEGF165 and VEGF165b proteins. The proteins were equally expressed throughout the placentas and were significantly correlated. The findings of significant positive correlations between placental weight and the distance between the insertion point and Quadrant 3 and 4 perhaps suggest that orientation of the placenta within the uterus may have some effect on placental growth.

Abstract # 1721

Paternal Diet-Induced Obesity Induces Hypoxia and Sex-Specific Changes in MicroRNAs that Regulate Implantation and Early Placentation. Patrycja A. Jazwiec, Violet S. Patterson, Deborah M. Sloboda

The prevalence of obesity has dramatically increased in recent years. While it is well established that maternal obesity impacts her child's health later in life, the paternal influence is largely underappreciated. Using a mouse model of paternal high fat (HF) diet-induced obesity, we have demonstrated that paternal obesity induced hypoxia and altered angiogenesis in mid-gestational and term placentae. Placental microRNAs (miRNAs) regulate decidualization, implantation, as well as angiogenesis and vasculogenesis. While we have demonstrated impairments in placental vascular development associated with paternal obesity, the signaling pathways are unclear. Therefore, we investigated whether key placental miRNAs involved in hypoxia signaling pathways were altered in placentae sired by obese fathers. C57BL/6J male mice were randomized to receive either a standard control diet (CON; 17% kcal fat) or a high fat diet (HF; 60% kcal fat) for 10 weeks. Male mice were then time-mated with control-fed C57BL/6J female mice to generate CON and paternal HF pregnancies. Placentae were collected at mid-gestation (embryonic day (E) 14.5). Relative levels of 84 miRNAs were measured in male and female CON (n = 4/sex) and paternal HF (n = 4/sex) placentae using the miScript® miRNA PCR Array (Qiagen). Significance was assessed by 2-way ANOVA with Bonferroni's post-hoc, where appropriate. In total, 18 miRNAs were altered due to paternal HF diet-induced obesity. Relative expression of miRNAs involved in implantation and/or decidualization, miR-let-7a-5p, miR-let-7b-5p, miR-let-7g-5p, miR-101a-3p, and miR-199a-5p (pDiet < 0.05), were increased in paternal HF placentae. Transcript levels of miRNAs shown to regulate cell migration, invasion, and angiogenesis, including miR-103-3p, miR-107-3p, miR-130a-3p, miR-130b-3p, miR-148b-3p, miR-15a-5p, miR-31-5p, and miR-324-5p, were increased in paternal HF placentae (pdiet < 0.05). Expression of miR-491-5p and miR-504-5p was increased in paternal HF placentae (pDiet < 0.05); these miRNAs are suggested to supress cell proliferation and/or invasion. Female placentae sired by HF males had increased let-7e-5p (pDiet < 0.05, pSex < 0.05, pInt <0.05; p < 0.05), let-7f-5p (pDiet < 0.05, pSex < 0.05, pInt < 0.05; p < 0.05), and let-7i-5p (pDiet < 0.05, p < 0.05) expression. Our data suggest that paternal HF diet-induced

obesity upregulates expression of miRNAs regulating processes essential for proper placentation in mid-gestational placentae. Further studies will investigate whether these placental changes are accompanied by alterations in implantation and early placentation.

Abstract # 1733

GDF-8 Up-Regulates Human Trophoblast Invasion By Increasing Its Antagonist Follistatin-Like 3 Expression Through Activating Smad3 Signaling Downstream Of ALK5. Jiamin Xie

We previously demonstrated that follistatin-like 3 (FSTL3), an important antagonist of TGF- β superfamily, increased invasion and migration of trophoblast and its potential effects on preeclampsia using human trophoblast cell lines, but the underlying regulatory mechanism is unknown. Interestingly, our recent findings elucidate that growth differentiation factor 8 (GDF-8), one member of the TGF- β superfamily which can be antagonized by FSTL-3, can promote trophoblast invasion through up-regulating the expression of FSTL-3, confirmed in human extravillous cytotrophoblast (EVT) cells lines and primary EVT cells from human first-trimester placenta. Moreover, using the siRNA knockdown technique, we find that the effects of GDF-8 on FSTL-3 expression and trophoblast invasion are via the transforming growth factor β receptor I (ALK5) then subsequent activation of SMAD3. Overall, our studies discover that the GDF-8 and its antagonist FSTL-3 can both increase trophoblast invasion, which is a novel molecular functional modality important for the understanding of early developments and functions of trophoblast.

Abstract # 1760

Single Cell Interrogation Of The Uterine-Placental Interface. Regan L. Scott, Ashish Jain, Khursheed Iqbal, Geetu Tuteja, Michael J. Soares

During a healthy pregnancy, a special lineage of placental cells, referred to as invasive trophoblast cells, exit the placenta and invade into the uterus where they restructure the uterine parenchyma and facilitate remodeling of spiral arteries. Invasive trophoblast cells help anchor the placenta, modulate immune cell populations, and facilitate nutrient delivery to the fetus. These trophoblast-directed uterine modifications are essential for a healthy pregnancy. Insufficient trophoblast invasion and abnormal cross-talk at the uterine-placental interface are major contributors to obstetrical complications such as early pregnancy loss, preeclampsia, intrauterine growth restriction, and pre-term birth. In humans, these events transpire during early gestation, thus their investigation represents a significant ethical challenge. In vitro analyses can provide insights into trophoblast cell potential but fall short as tools to understand the physiology of the invasive trophoblast cell lineage. Implementation of in vivo models to test hypotheses regarding mechanisms underlying the development and function of the invasive trophoblast cell lineage are essential to advance the field. Rodents exhibit

hemochorial placentation similar to humans. While the mouse displays shallow trophoblast invasion, the rat exhibits deep intrauterine trophoblast invasion and extensive uterine spiral artery remodeling, comparable to what is observed in the human. In this study, we sought to phenotype cells at the uterine-placental interface of the rat with the goal of identifying conserved candidate regulators of the invasive trophoblast cell lineage. Single-cell RNA sequencing (scRNA-seq) and single-cell assay for transposase-accessible chromatin sequencing (scATAC-seq) were used to interrogate cells at the uterine-placental interface on gestation days 15.5 and 19.5 of the Holtzman Sprague-Dawley rat. Single cell suspensions were prepared by enzymatic digestion of the uterine-placental interface. Single cell libraries were then constructed using the 10X Genomics platform and sequenced with an Illumina NovaSeg 6000 system. Computational analysis with the Cellranger pipeline led to the identification a number of unique cell clusters defined by their transcript profiles, including invasive trophoblast cells (e.g. Prl5a1, Prl7b1, Tpbpa, Plac1, Tfap2c, Igf2, Cdkn1c, Tfpi), endothelial (e.g. Egfl7, Adgrl4, Rasip1, Sox17, Nos3), vascular smooth muscle (e.g. Acta2, Myl9, TagIn, Myh11), natural killer (e.g. Nkg7, Prf1, Gzmb, Gzmm), and macrophage (e.g. Fcgr3a, Lyz2, Aif1, Tyrobp, Cybb) cell clusters. A prominent subset of rat invasive trophoblast cell transcripts is conserved in the invasive extravillous trophoblast cell lineage of first trimester human placenta (e.g. lgf2, Cdkn1c, Tfpi, Ascl2, Mmp12, Cited2, etc). Nuclei were also isolated from the single cell preparations of the uterine-placental interface, libraries prepared, and sequenced. Analysis with the Cellranger-ATAC pipeline identified unique clusters based on chromatin accessibility, including invasive trophoblast, endothelial cell, vascular smooth muscle, natural killer cell, and macrophage clusters. ASCL2, AP1, TFAP2C, and ATF1 DNA binding motifs were most abundant in accessible regions of the invasive trophoblast cell clusters. These findings provide a foundational dataset to identify and interrogate key conserved regulatory mechanisms essential for development and function of an important compartment within the hemochorial placentation site that is essential for a healthy pregnancy. (Supported by HD020676, HD096083, HD099638; Pew Charitable Trust, Sosland Foundation)

Abstract # 1782

Adrenomedullin Is A Critical Regulator Of Placental And Fetal Development. Marija Kuna, Khursheed Iqbal, Kelly Gorman, Keisuke Kozai, Masanaga Muto, Kathleen M. Caron, Michael J. Soares

Adrenomedullin (ADM) is a peptide hormone with a broad spectrum of actions on vascular smooth muscle, endothelial cells, and immune cells. These ADM cellular targets are prominent constituents of the uterine-placental interface that undergo structural and functional transformation during the course of gestation. Trophoblast cells are viewed as primary engineers of pregnancy-dependent uterine transformation. Impaired placentation and compromised trophoblast cell function is a common denominator of the "Great Obstetrical Syndromes", such as early pregnancy loss,

preeclampsia, intrauterine growth restriction, and pre-term birth. ADM is produced by trophoblast cells at the uterine-placental interface and possesses modulatory actions on the uterine vasculature and resident immune cell populations that promote fetal development. Deficits in circulating maternal ADM have been linked to preeclampsia. Animal models can be effective tools in elucidating the pathophysiology of pregnancy. Mutant Adm mouse models have provided considerable insight into the role of ADM in the biology of pregnancy. Unlike the mouse, the rat exhibits deep hemochorial placentation, which also occurs in the human. To explore the physiological role of ADM signaling at the uterine-placental interface, we generated and characterized an Adm mutant rat model using Crispr-Cas9 -mediated genome editing. Crispr RNAs were designed to target Exon 2 of the Adm gene. Cas9 proteins along with an Adm targeted Crispr RNA:transactivator RNA complex were electroporated into embryonic day 0.5 rat zygotes and transferred into the oviducts of appropriately-timed pseudopregnant female rats. A founder offspring possessing a 206 bp deletion spanning part of Exon 2 (the first coding exon), the Exon 2-Intron 2 boundary, and 121 bp into Intron 2 was identified via PCR screening and confirmed by genomic DNA sequencing. The deletion resulted in an out-of-frame mutation and the appearance of a premature Stop codon and a predicted protein product containing only the first four amino acids of ADM. The founder Adm mutant rat was mated with a wild-type rat in order to confirm germline transmission and to generate heterozygous pups. Adm heterozygous males and females were fertile; however, Adm heterozygous intercrosses did not generate live Adm null rats. Timed Adm heterozygous intercrosses were euthanized at various stages of gestation to determine the onset of demise. Adm null fetal-placental sites were viable at gestation day (gd) 13.5, some were dying on gd 15.5, and all were dead and resorbing by gd 18.5. Fetal and placental growth restriction were evident on gd 13.5. On gd 15.5 some Adm null placentas exhibited prominent hemorrhagic regions, whereas both hemorrhage and edema were evident in some gd15.5 Adm null fetuses. These phenotypic observations in the Adm null rat model resemble earlier descriptions of ADM deficiency in the mouse. Our results indicate that ADM serves as a critical regulator of placental and fetal development. This new Adm mutant rat model will be used to investigate roles for ADM in the regulation of vascular smooth muscle, endothelial cells, and immune cells at the uterine-placental interface. (Supported by postdoctoral support provided by P20 GM103418 and the American Heart Association, NIH grants: HD020676, HD060860, HD099638 and Sosland Foundation)

Abstract # 1833

Phosphate Regulation Pathways are Present in the Ovine Conceptus, Endometrium and Placentome. Claire Stenhouse, Katherine M. Halloran, Makenzie G. Newton, Larry J. Suva, Fuller W. Bazer

Phosphate is the most abundant anion in humans comprising approximately 1% of total body weight. Around 80% of phosphate present in the fetal skeleton at the end of

gestation crosses the placenta. Phosphate is essential for bone development and growth however, little is known regarding the mechanisms of placental phosphate transport during pregnancy. This study sought to identify phosphate regulatory pathways in the ovine endometrium and placentome throughout gestation. Suffolk ewes were bred with fertile rams upon visual detection of estrus (Day 0). On Days 9, 12, 17, 30, 70, 90, 110 and 125 of pregnancy (n=4-18/Day), ewes were euthanized and hysterectomized. On Days 9, 12 and 17, the lumen of the uterine horns were flushed with PBS to recover conceptuses. On Day 17, conceptus tissue was frozen in liquid nitrogen. On the other days of pregnancy, following separation of the endometrium from the chorioallantois, sections of placentomes and endometria were frozen in liquid nitrogen. Inorganic phosphate was detected spectrophotometrically in allantoic and amniotic fluid, and homogenised placentomes and endometria. The expression of mRNAs for sodium-dependent phosphate transporters (SLC20A1 and SLC20A2) and components of klotho signalling (FGF21, FGF23, FGFR1, KL and KLB) were quantified by qPCR. Klotho proteins are essential for fibroblast growth factor receptor action, with FGF23 as an important phosphaturic hormone. Concentrations of phosphate were greater in placentomes than endometria at Days 30 and 110 (P<0.05). In contrast, concentrations of phosphate in endometria were greater than those in placentae at Day 125 of pregnancy (P<0.001). Endometrial phosphate concentration was lower at Day 30 when compared with both Days 9 and 12 (P<0.05). Phosphate in placentomes was lowest on Day 125 (P<0.001) and total phosphate was greater in allantoic fluid associated with female compared to male fetuses at Day 125 (P<0.05). The expression of all candidate mRNAs was detected in both placentomes and endometria, except for KLB which was only expressed in placentomes. Day 17 conceptuses express SLC20A1, SLC20A2, KLB, and FGFR1 mRNAs. Endometrial expression of FGFR1 (P<0.001) and FGF21 (P<0.05) mRNAs was highest at Day 30, as was expression of KL mRNA (Days 30 and 110) (P<0.001). Stable endometrial expression of FGF23, SLC20A1 and SLC20A2 mRNAs was observed throughout gestation. Expression of KLB (P=0.06) and FGF21 (P<0.05) mRNAs increased in placentomes between Days 110 and 125. Expression of FGF23 mRNA increased with advancing gestational day (P<0.01) in placentomes. Expression of FGFR1 mRNA in placentomes was lowest at Day 90, before increasing to Day 125 (P=0.05) of pregnancy. In contrast, SLC20A1 mRNA expression peaked at Day 30, before decreasing to Day 110 (P<0.001). These results indicate that phosphate and its transporters have dynamic expression throughout gestation, suggesting an important role for multiple phosphate regulatory pathways throughout gestation. Temporal expression profiles support a role for phosphate in sheep during the peri-implantation period and in later stages of gestation. This research was supported by Agriculture and Food Research Initiative Competitive Grant 2016-67015-24958 from the USDA National Institute of Food and Agriculture.

Abstract # 1839

Single-Cell RNA-Seq Reveals The Diversity Of Trophoblast Subtypes And Patterns Of Differentiation In The Bovine Placenta. Eleanore V. O'Neil, M. Sofia Ortega, Thomas E. Spencer

Establishment of pregnancy in cattle involves growth and elongation of the mononuclear trophoblast cells (MTC) that secrete interferon tau (IFNT) for pregnancy recognition on day 15, which is followed by differentiation of trophoblast giant binucleate cells (BNC) beginning on day 17 and placentation. By day 60, the bovine placenta contains vascularized placentomes formed by interdigitation of cotyledons with caruncles of the endometrium. The chorion of the cotyledonary villi contain MTC and multinucleated syncytia, which are formed by partial fusion of the LE and BNC and are supported by fetal stromal cells. Current evidence supports the hypothesis that pregnancy loss during the first month in cattle is caused by inadequate placental development. However, little is known about trophoblast differentiation and placentation in cattle. Heifers were bred and collected on days 17, 24, 30, and 50 of gestation (n = 3-4 heifers per day). The chorioallantois was carefully removed and gently digested with enzymes (0.125% trypsin, 0.05% type IV collagenase, and 0.04% DNAse in DMEM/F12 medium) to isolate trophoblast cells. Single cells were subjected to analysis using 10x Genomics platform and sequenced (scRNA-seq). Bases with high quality (Q > 30) were estimated to be 97% of the unique molecular identity counts. After data filtration, 56,657 single cells were assigned to 22 clusters by shared nearest neighbor and t-distributed stochastic neighbor embedding (t-SNE) methods across the four timepoints. Gene expression of cell markers was used to identify cell clusters as trophoblast cells, stromal cells, BNC, blood cells, and macrophages. Interestingly, the proportion of cell identities changed across the timepoints. On days 17, 30, and 50, approximately half or more of the cells were trophoblast cells, while 72% of the day 24 placenta cells had a stromal cell identity, as indicated by their expression of vimentin (VIM), and extracellular matrix proteins including collagens, actins, and tubulins. On days 17 and 24, IFNT2 and IFNT3 was abundant in MTC, but negligible in day 30 and 50 placentae. The BNC populations, identified by expression of the marker gene chorionic somatomammotropin hormone 2 (CSH2), accounted for only 3% of the cells on day 17 but increased to 17% by day 50. Several pregnancy-associated glycoproteins (PAG) were expressed and showed differential expression in MTC and BNC. For example, PAG7 was almost exclusively expressed in BNC across all four days. Macrophages, demarcated by expression of cluster of differentiation (CD) CD14 and CD68, were almost absent on days 17 and 24 (< 0.5% total cells), but made up 3% of the cells in day 30 and 50 placentae. These results document bovine placental trophoblast differentiation at single-cell resolution and advance our understanding of bovine placentation during the establishment of pregnancy. Supported by USDA National Institute of Food and Agriculture grants 2016-67015-24741 and 2019-67015-28998.

Abstract # 1888

Palmitic Acid Activates NLRP3 Inflamassome And Placental Inflammation, Resulting In The Induction Of Pregnancy Complication In Mice. Sayaka Shimazaki, Michiya Sano, Hisataka Iwata, Takehito Kuwayama, Koumei Shirasuna

In recent years, the incidence of obesity rate has been increasing around the world. Although obesity is a mild chronic systemic inflammation, it has become a global problem as a cause of various lifestyle-related diseases. The incidence of maternal obesity has recently been on the rise around the world due to the modern lifestyle and obesity is a major risk factor in pregnancy complications such as gestational diabetes, spontaneous miscarriage, intrauterine growth restriction, and preeclampsia. Pregnant women with obesity are associated with elevated serum levels of pro-inflammatory cytokines such as interleukin (IL)-1β, IL-6, IL-8, and tumor necrosis factor-a, and free fat acids especially palmitic acid (PA) compared to pregnant women with normal weight. Recently, there have been numerous reports of NLRP3 inflammasome mechanisms that control sterile inflammation involved in various lifestyle-related diseases including obesity, diabetes, pregnancy complications. Therefore, we hypothesized that higher levels of PA induce NLRP3 inflammasome activation and placental inflammation, resulting in pregnancy complications. We investigated the effect of PA on the activation of NLRP3 inflammasome and inflammatory responses in a human Sw.71 trophoblast cell line. PA stimulated caspase-1 activation and markedly increased interleukin IL-1ß secretion in Sw.71 cells. NLRP3 and caspase-1 knockout (KO) using a CRISPR/Cas9 system in Sw.71 cells suppressed IL-1 β secretion, which was stimulated by PA. In addition, PA-induced IL-1 β secretion was depended on reactive oxygen species (ROS) generation. These results indicated that PA stimulate IL-1b secretion depending on NLRP3 inflammasome in trophoblast cells. Next, we examined the effect of PA on NLRP3 inflammasome during pregnancy in vivo. PA solutions were administered intravenously into pregnant mice on day 12 of gestation. Maternal body weight was significantly decreased and absorption rates were significantly higher in PA-injected mice. The administration of PA significantly increased IL-1ß protein and the mRNA expression of NLRP3 inflammasome components (NLRP3, ASC, and caspase-1) within the placenta. Simultaneously, the number of macrophages/monocytes and neutrophils, together with the mRNA expression of these chemokines increased significantly in the placentas of PA-treated mice. To examine the role of NLRP3 inflammasome for accumulation of immune cells by PA, PA was intraperitoneally administered to wild-type (WT) mice and NLRP3- KO mice, then peritoneal immune cells (PEC) were collected. Using flowcytometric analysis, the number of immune cells such as macrophages (CD45 + CD11b + cells) and neutrophils (CD45 + Ly6G + cells) were significantly lower in NLRP3-KO mice compared to WT mice. Therefore, we investigate the effect of PA in macrophages using THP-1 cells (macrophage/monocyte cell line) in vitro considering that macrophages was accumulated in the placenta by PA administration. Generally, ASC assembles into a large protein complex, which is termed "speck-like formation" after inflammasome activation. A core component of the inflammasome pathway, ASC, was found to form ASC speck upon PA treatment of THP-1 cells. In addition,

treatment with PA induced IL-1 β secretion in normal THP-1 cells, and this PA-induced IL-1 β secretion was significantly suppressed in NLRP3-knockout THP-1 cells.Transient high level exposure to PA in pregnant mice activated NLPR3 inflammasome and induced placental inflammation, resulting in the increased absorption.

Abstract # 1890

S100A9 Induces IL-1β And Seng Secretion Via NLRP3 Inflammasome Activation And Involves In Developing Preeclampsia. Michiya Sano, Yuka oogaki, Ayae Ozeki, Tadayoshi Karasawa, Masafumi Takahashi, Hironori Takahashi, Akihide Ohkuchi, Hisataka Iwata, Takehito Kuwayama, Koumei Shirasuna

Preeclampsia (PE) is a pregnancy-specific hypertensive syndrome and pathophysiological changes of PE include inflammation and immune cell activation. The increases in inflammatory cytokines [interleukin (IL)- 1ß, IL-6, and IL-8] and antiangiogenic factors [soluble fms-like tyrosine kinase (sFlt1) and soluble Endoglin (sEng)] are associated with the pathological features of PE. However, the detail mechanisms of PE remain unclear. Recently, the inflammasome mechanism controlling sterile inflammation has received attention, which is mediated through the NLRP3 inflammasome, composed of NLRP3, ASC and caspase-1. NLRP3 inflammasome regulates IL-1 β secretion and involves in the development of various life-style diseases. On the other hand, \$100A9 (a calcium-binding protein) plays an essential role in the regulation of inflammatory and immune response. For example, \$100A9 is expressed higher in inflammatory tissues including the placenta of habitual abortion patients. In the present study, we hypothesized that \$100A9 induces inflammatory responses via NLRP3 inflammasome activation in human placenta, resulting in the occurrence of PE. Sera and placental tissues were collected from normal pregnant (NP) women and PE patients. The serum concentrations of \$100A9, sFlt1 and sEng were higher in PE patients than in NP women. S100A9 and IL-1 β secretion as well as S100A9 mRNA expression in PE placentas were higher compared to NP placentas. In placenta tissues, treatment with \$100A9 increased IL-1β and sEng secretion and treatment with MCC950 (NLRP3-specific inhibitor) suppressed \$100A9-induced IL-1ß and sEng secretion. Then, we checked the effect of \$100A9 on NLRP3 inflammasome using trophoblast cells (Sw.71) and human umbilical vein endothelial cells (HUVEC). \$100A9 increased ASC speck-like formation, caspase-1 activation and IL-1ß secretion in Sw.71. Treatment with MCC950 or Caspase-1 Inhibitor and gene knockout of NLRP3 or caspase-1 in Sw.71 resulted in the reduction of \$100A9-induced IL-1ß secretion, indicating \$100A9 increased IL-1ß secretion via NLRP3 inflammasome. Also, \$100A9 increased matrix metalloproteinase 14 (MMP14, the cleavage enzyme of sEng) and Kruppel-like factor 6 (KLF6, the transcription factor of MMP14) mRNA expression and sEng secretion in Sw.71 and HUVEC. Genetic inhibition (siRNA of NLRP3) and treatment with MCC950 suppressed mRNA expression of KLF6 and MMP14 and sEng secretion stimulated by \$100A9, indicating \$100A9 activates KLF6-MMP14 and increases sEng secretion via NLRP3 inflammasome. To clarify the effects of \$100A9 during pregnancy in vivo, we administered \$100A9 intravenously into pregnant

mice on pregnant day (PD) 15 and 16. Maternal body and fetal weights were significantly decreased in \$100A9-injected mice. In addition, direct injection of \$100A9 to murine placenta accumulated neutrophils (CD45+Ly6G+cells). To investigate long-term effects of \$100A9 during pregnancy, \$100A9 were injected intraperitoneally every day from PD8 to 17. Maternal blood pressure was significantly elevated by injection of \$100A9. These results suggest \$100A9 increases IL-1β and sEng secretions via NLRP3 inflammasome activation in placentas. Moreover, \$100A9 induces neutrophils accumulation in placenta, decreases fetal weights and elevates maternal blood pressure in pregnant mice, suggesting the involvement of \$100A9 in pathogenesis of PE.

Abstract # 1900

The Impact of Paternal Diet on Late Gestation Fetal Growth and Placental Gene Expression. Afsaneh Khoshkerdar, Hannah Morgan, Adam J. Watkins

Placental function and blood flow are central regulator of fetal growth and are controlled by numerous pathways including the renin-angiotensin system (RAS), apoptosis and 1-Carbon metabolism. DOHaD theory states that maternal intrauterine environment is of upmost importance in fetal development and fetal growth is a significant indicator of long-term offspring health therefore understanding placental function maybe important. There is now growing evidence linking paternal diet with impaired fetal growth and adult offspring cardiometabolic ill-health. However, the underlying mechanisms linking paternal diet and fetal development are poorly defined. The aim of this study was to address the impact of paternal diet on fetal growth and the placental expression of multiple renin-angiotensin system (RAS), 1-Carbon metabolism and apoptosis pathway genes., known to be involved in placental blood flow and fetal growth. Male C57/BL6J mice were fed one of five diets; low protein (LPD(9% casein, 24% sugar, 10% fat), western diet (19% casein, 21% fat, 34% sugar)), diets supplemented with methyl-donors (MD-LPD and MD-WD) or an isocaloric control diet (18% casein, 10% fat, 21%sugar) for at least 8 weeks). Males were mated with virgin 8-12-week-old females C57BL/6J mice, which were maintained on standard rodent chow. Pregnancy were allowed to progress to embryonic day 17.5 before the dam was euthanized and the fetal and placental tissues weighted and collected. Placentas were snap frozen for analysis od RAS, 1-Carbon metabolism and apoptosis gene expression using RT-qPCR. Paternal diet did not significantly alter mean fetal weights, litter size, placental weight or fetal/placental ratio. However, analysis of placental RAS including Ace, Ace2, Agtr1a, Agtr1b, Ren1, one-carbon metabolism genes including Dhfr, Mat2a, Mat2b, Mthfr and Mtr and apoptosis genes including the pro-apoptotic regulators Bad, Bax and Fas and the anti-apoptotic Bcl2 genes revealed significantly decreased expression of in placentas derived from WD and MD-WD males when compared to NPD males. Interestingly, supplementation of the LPD and WD with methyl donors had no additional effect on gene expression. The current study provide evidence that paternal LPD and WD (with or without methyl donors) had no effect on male fertility or late gestation fetal growth. Also, placentas from WD and MD-WD fed males displayed reduced expression of RAS, apoptosis and 1-carbon metabolism genes when compared to other groups. Interestingly, supplementation of the LPD and WD with methyl donors had no additional effect on gene expression. Further studies are required to define the impact of these changes on placental function, fetal growth and offspring health.

Abstract # 1904

Glutaminolysis Drives TCA Cycle Anaplerosis through Oxidative and Reductive Pathways to Support Nucleotide and Lipid Biosynthesis in Pig Conceptuses. Heewon Seo, Avery C. Kramer, Bryan A. Mclendon, Robert C. Burghardt, Guoyao Wu, Fuller W. Bazer, Greg A. Johnson

During the peri-implantation period, pig conceptuses (embryo and placental membranes) rapidly elongate from spherical to tubular to filamentous forms. This elongation requires that trophectoderm (Tr) cells expend significant amounts of energy to undergo timely and extensive proliferation. Therefore, optimal utilization of multiple biosynthetic pathways is likely an essential aspect of early conceptus development and survival. Our preliminary studies indicated that the endometrium of pigs transports glucose into the uterine lumen. Elongating and proliferating conceptuses then potentially act, in a manner similar to cancer cells, to direct the carbon, generated from glucose, away from the tricarboxylic acid (TCA) cycle for utilization in branching pathways of glycolysis, including the pentose phosphate pathway, one-carbon metabolism, and hexosamine biosynthesis. The result is limited availability of pyruvate for maintaining the TCA cycle within mitochondria. Proliferating cells can replenish TCA cycle metabolites via a process known as anaplerosis to convert glutamine into TCA cycle metabolites other than acetyl-CoA. Glutamine can be converted into glutamate and then alpha- ketoglutarate (a-KG), a TCA cycle intermediate, through the enzymes glutaminase (GLS), glutamate dehydrogenase (GLUD), and aminotransferases. Our preliminary results indicated that the conceptus Tr of pigs utilizes the GLS-phosphoserine transaminase 1 (PSAT1) glutaminolysis pathway to metabolically support proliferation for elongation. In this study, we examined whether glutaminolysis-derived a-KG is utilized through oxidative and/or reductive pathways to support nucleotide and lipid biosynthesis in pig conceptuses. We determined that porcine conceptuses: 1) utilize a-KG for nucleotide biosynthesis because alpha-ketoglutarate dehydrogenase (OGDH) and succinate dehydrogenase (SDHA), mitochondrial enzymes that convert a-KG to succinate and succinate to fumarate, are highly expressed in the Tr on Day 15 of pregnancy, which is coincident with increased expression of GLS and PSAT1; and 2) utilize glutamine for lipid biosynthesis because isocitrate dehydrogenase 1, NADP+ soluble (IDH1), a cytosolic enzyme that converts a-KG to isocitrate, is highly expressed in

the Tr of Day 14 conceptuses, and 14 C-lipids were formed in the conceptuses cultured with [U- 14 C]glutamine. We conclude that glutamine within the uterine lumen provides an alternate carbon source to maintain TCA cycle flux and provide biosynthetic precursors for the synthesis of nucleotides and lipids in porcine conceptuses. Our results provide new insights into how porcine conceptuses metabolically support rapid cell proliferation and migration at a time when they are elongating, have not yet established a placental connection to the uterus, and are dependent upon limited nutrients within the uterine lumen. This research was supported by Agriculture and Food Research Initiative Competitive Grant no. 2018-67015-28093 from the USDA National Institute of Food and Agriculture.

Abstract # 1974

Umbilical Cord Entanglement In Monochorionic-Monoamniotic Twin Gestation. Frederick U. Eruo, Sr, Christopher DeVries, Kaitlyn Marie Bates

Introduction : Twin-to-twin transfusion syndrome (TTTS) is a complication unique to monochorionic twin pregnancies in which each fetus receives a disproportionate amount of blood flow due to placental vascular abnormalities. Failure to manage TTTS appropriately may result in significant morbidity and mortality. Management of TTTS includes expectant management, serial amniocentesis/amnioreduction, fetoscopic laser ablation of the placental anastomoses, fetoscopic septostomy (intentionally drilling holes through the separating membranes) and in rare cases selective fetal reduction may be performed. Septostomy, intentional or iatrogenic, leads to monochorionic-monoamniotic gestation. Disruption of the membranes separating both twins is an attempt to allow even or fairly equal distribution of amniotic fluid between the two gestational sacs. Possible/potential complications of fetoscopic septostomy include but not exclusive: chprioamnionitis, preterm delivery, preterm premature rupture of membranes (PPROM), pseudoamniotic band syndrome (PABS), cord entanglement and intrauterine fetal death (IUFD). Case Presentation : A 24-year-old G2P1001 with no significant past medical history presented to prenatal care following diagnosis of spontaneous monochorionic/diamniotic pregnancy. She followed closely with maternal fetal medicine, and at 19 weeks gestation was determined to be developing TTTS. A therapeutic laser ablation was performed at a different institution. During the procedure, the intertwin membrane separating the amniotic sacs was inadvertently disrupted, effectively creating a monochorionic/monoamniotic gestation. In-house antepartum monitoring was initiated at 26 weeks gestation when the patient chose to be admitted into the hospital. We had planned to admit her earlier but she declined. Growth ultrasound was performed every two weeks while she was admitted for signs of worsening TTTS. At 30w5d gestation, the patient awoke from sleep complaining of sharp abdominal pain and vaginal bleeding. The decision to proceed with primary cesarean delivery was made due to concern for preterm labor and/or placental abruption. Upon rupture of membranes, frank blood-stained fluid was encountered. Significant umbilical cord entanglement was observed, including two

true knots in baby A's cord. The patient did well post-operatively and was discharged home on POD#3. The infants did well and were discharged home on corrected gestational age 35w6d. Discussion : Although not a preferred mode of management of TTTS, septostomy may be performed intentionally for the treatment of TTTS. latrogenic septostomy may occur during fetoscopic laser ablation of the placental anastomoses due to trocar site injury, laser photocoagulation, mechanical injury from the laser tip, etc. Umbilical cord entanglement is a known complication of congenital monochorionic and monoamniotic pregnancies. This case shows that cord entanglement can also be observed in pregnancies in which disruption of the dividing membrane occurs during septostomy. Preterm labor and placental abruption are also known complications of multifetal gestations. This case demonstrates some of the complications associated with multiple pregnancies in general and in-utero procedures in multiple pregnancies. It also highlights morbidity of laser ablation therapy. With both fetuses surviving, this is an acceptable risk worthy of consideration in the management of TTTs. Valuable ultrasonographic and intra-operative photos are also presented and add to value of case discussion.

Abstract # 1989

Iatrogentic Monochorionic-Monoamniotic Twin Gestation. Kaitlyn Bates, Christopher DeVries, Frederick Eruo

Introduction : Twin-to-twin transfusion syndrome (TTTS) is a complication unique to monochorionic twin pregnancies in which each fetus receives a disproportionate amount of blood flow due to placental vascular abnormalities. Failure to manage TTTS appropriately may result in significant morbidity and mortality. Management of TTTS includes expectant management, serial amniocentesis/amnioreduction, fetoscopic laser ablation of the placental anastomoses, fetoscopic septostomy (intentionally drilling holes through the separating membranes) and in rare cases selective fetal reduction may be performed. Septostomy, intentional or iatrogenic, leads to monochorionic-monoamniotic gestation. Disruption of the membranes separating both twins is an attempt to allow even or fairly equal distribution of amniotic fluid between the two gestational sacs. Possible/potential complications of fetoscopic septostomy include but not exclusive: chprioamnionitis, preterm delivery, preterm premature rupture of membranes (PPROM), pseudoamniotic band syndrome (PABS), cord entanglement and intrauterine fetal death (IUFD). Case Presentation : A 24-year-old G2P1001 with no significant past medical history presented to prenatal care following diagnosis of spontaneous monochorionic/diamniotic pregnancy. She followed closely with maternal fetal medicine, and at 19 weeks gestation was determined to be developing TTTS. A therapeutic laser ablation was performed at a different institution. During the procedure, the intertwin membrane separating the amniotic sacs was inadvertently disrupted, effectively creating a monochorionic/monoamniotic gestation. In-house antepartum monitoring was initiated at 26 weeks gestation when the patient chose to be admitted into the hospital. We had planned to admit her earlier but she

declined. Growth ultrasound was performed every two weeks while she was admitted for signs of worsening TTTS. At 30w5d gestation, the patient awoke from sleep complaining of sharp abdominal pain and vaginal bleeding. The decision to proceed with primary cesarean delivery was made due to concern for preterm labor and/or placental abruption. Upon rupture of membranes, frank blood-stained fluid was encountered. Significant umbilical cord entanglement was observed, including two true knots in baby A's cord. The patient did well post-operatively and was discharged home on POD#3. The infants did well and were discharged home on corrected gestational age 35w6d. Discussion : Although not a preferred mode of management of TTTS, septostomy may be performed intentionally for the treatment of TTTS. latrogenic septostomy may occur during fetoscopic laser ablation of the placental anastomoses due to trocar site injury, laser photocoagulation, mechanical injury from the laser tip, etc. Umbilical cord entanglement is a known complication of congenital monochorionic and monoamniotic pregnancies. This case shows that cord entanglement can also be observed in pregnancies in which disruption of the dividing membrane occurs in an iatrogenic septostomy. Preterm labor and placental abruption are also known complications of multifetal gestations. This case demonstrates some of the complications associated with multiple pregnancies in general and in-utero procedures in multiple pregnancies. It also highlights morbidity of laser ablation therapy. With both fetuses surviving, this is an acceptable risk worthy of consideration in the management of TTTs. Valuable ultrasonographic and intra-operative photos are also presented and add to value of case discussion.

Abstract # 2016

Presence Of Clock Genes In Equine Full-Term Placenta. Agata M. Parsons Aubone, Christian M. Bisiau, Patrick M. McCue, Gerrit J. Bouma

Mammals have a circadian rhythm which is synchronized by a master clock located in the hypothalamic suprachiasmatic nucleus (SCN). The SCN regulates additional clocks located in peripheral tissues, including some involved in endocrine or reproductive functions. Studies in humans and mice report that molecular clocks also exist in the placenta. However, little is known about the presence of "Clock genes" in equine placenta. Pregnancy length in mares varies and shows fluctuations in hormone concentrations throughout pregnancy. We postulate that similar to humans and mice, "Clock genes" are present in the horse placentas. Our goal was to determine if relative levels were different between placentas associated with male and female fetuses or correlated with gestational length. Placenta tissue samples were obtained from twenty pregnant mares following normal unassisted foaling by vaginal delivery. Placental biopsy samples were collected from four different areas; uterine body, pregnant horn, none pregnant horn and cervical star. From each area one section was immediately fixed overnight in 4% paraformaldehyde (PFA) and a second section was snap frozen in liquid nitrogen and stored at -80 C until processed. We used PCR and immunofluorescence to study the presence of Circadian Locomotor Output Cycles

Kaput (CLOCK), Brain and Muscle Arnt-Like 1 (BMAL1), Period1 (PER1), Period2 (PER2), Cryptochrome 1 (CRY1) and Cryptochrome 2 (CRY2) in full-term mare placentas. "Clock genes" were present in horse all placentas. Student T-test analysis was performed to determine difference between female and male placentas, revealing lower relative levels of CRY2 and CLOCK in placentas associated with male fetuses. A Pearson correlation analysis showed no association between relative levels of "Clock genes" and gestational length. To determine cellular localization, immunofluorescence was used on horse full-term placenta. BMAL1 and CLOCK were detected in the fetal trophoblast cells, and in both cases, staining appeared to be within the cytoplasm. In conclusion, "Clock genes" are present in term equine placentas, and possibly play a role in sex-different regulation of placental function and pregnancy.

Abstract # 2048

Anti-D Immune Globulin Prophylaxis in the First Trimester. Kaitlyn Bates, Christopher DeVries, Frederick Eruo

Introduction : Rhesus D Incompatibility during pregnancy occurs when a mother is rhesus negative (Rh-) and the fetus is rhesus positive (Rh+). Rh refers to the D antigen of the rhesus factor blood system, and positive denotes its presence on erythrocytes versus negative which denotes its absence. A patient with Rh- blood type will inherently have IgM antibodies to the D antigen, but if exposed to the antigen she would become alloimmunized and produce IgG antibodies. The IgG antibodies can cross the placenta, and in the case of Rh incompatibility, attack fetal erythrocytes leading to severe hemolytic disease of the fetus and newborn. The most common exposure of Rhmothers to Rh+ blood is transplacental feto-maternal hemorrhage, typically during a delivery. Other causes of transplacental hemorrhage include ectopic pregnancy, antenatal hemorrhage, abruptio placenta, and maternal abdominal trauma. Antepartum alloimmunization can occur, but prophylaxis with Rhogam (anti-D immune globulin) can prevent majority of the cases of alloimmunization. Case : A 26 year-old G1P0000 with no pertinent past medical history presents with complaints of vaginal bleeding and spotting. Dating by her last menstrual period indicates she is 8 weeks and 3 days gestation. Her blood type is O negative and her antibody screen is negative for serum antibodies. Patient received an injection of 300 microarams of Rhogam and was instructed to receive this dose again at twenty-eight weeks gestation – usual prophylaxis dose. Discussion : Current recommendations for antepartum Rhogam administration to Rh- mothers include 300 micrograms at 28 weeks gestation, however, events like invasive diagnostic procedures (chorionic villus sampling, amniocentesis, etc), abdominal trauma, and vaginal bleeding would warrant Rhogam administration. The recommendations for care of women in their first trimester who experience bleeding or abdominal trauma are less clear. There are conflicting recommendations for administering Rhogam to Rh- women with a threatened abortion in the first trimester. Furthermore, if one is to administer Rhogam, there is debate about whether one would use 300 micrograms or a smaller dose. The D antigen appears on red blood cells at day

38 of gestation. At 12 weeks gestation, there is about 1.5ml of fetal red blood cells which is enough to incite alloimmunization in the mother. Due to the limited fetal blood volume, debate exists as to whether the full 300 micrograms of Rhogam, which is enough to neutralize exposure up to 30ml of fetal Rh+ blood, is necessary or if a smaller dose, such as 50 micrograms would be enough for alloimmunization prophylaxis.

Abstract # 2064

Spatial And Temporal Dynamics Of FGL2 Expression Reveal Immunoregulatory Function Essential To The Establishment And Outcome Of Pregnancy. Pascale Robineau-Charette, Brendan Kelly, Shannon A. Bainbridge, Barbara C. Vanderhyden

Fibrinogen-like protein 2 (FGL2) is a known immunomodulator and prothrombinase, previously suggested to be involved in the immune balance of the maternal-fetal interface that is crucial to reproductive success. The female reproductive tract is the site of several key events that require careful endocrine and immunological regulation, from ovulation to pre-implantation embryo transport and placentation. We mapped spatial and temporal dynamics of FGL2 expression through murine reproductive tissues, which revealed remarkable cell type specificity hinting at precise function. We carefully examined several parameters of reproductive performance in our Fgl2 knockout (ko) and overexpressing (tg) mouse colonies. Fgl2 ko females produced only half as many pups as their wild-type (wt) counterparts, due to smaller and less frequent litters. Interestingly, this phenotype was rescued in Fgl2 tg X Fgl2 ko mating pairs, despite the presence of only one overexpressing allele. We observed equal rates of embryo resorption in all three genotypes, suggesting a defect in Fgl2 ko ovarian or oviductal (pre-implantation) function. In the ovary, FGL2 is expressed in the stroma and theca cell layer of follicles, and intensity of expression peaks 8 hours after hCG injection in a superovulation cycle. Strong expression is acquired by some cumulus granulosa cells shortly before ovulation and persisting in cumulus-oocyte complexes (COCs) found in the oviduct, suggesting a role in ovulation and in luteinization. Fgl2 ko and Fgl2 tg animals however had a normal ovulation efficiency, as measured by the number of COCs retrieved after superovulation. Fgl2 ko and wt ovaries showed equivalent numbers of functional corpora lutea, demonstrating normal luteinization. In the oviduct, FGL2 expression is restricted to secretory cells of the epithelium, whose frequency increase from the fimbrial to the isthmal end. We detected FGL2 in the culture medium of OVE4, primary oviductal epithelial cells, confirming its secretion into oviductal fluid, where it likely contributes to the immunosuppressive environment conducive to fertilization and to tolerance of paternal/fetal antigens. Single-nuclei RNA sequencing of the ovary, ampulla and isthmus at different timepoints after superovulation will reveal differential immune dynamics between Fql2 wt and ko animals, to identify mechanistic actions of FGL2 in these tissues. Despite being born at rates comparable to wt mice, Fal2 to pups are significantly smaller than their wt and ko counterparts, at birth and at weaning, indicating a probable deficient placental function. Interestingly, we found that women with high placental FGL2 expression tend to be affected by an

immunological subtype of preeclampsia, characterized by chronic inflammatory placental lesions and small for gestational age infants. Our histological examination of term placentas from Fgl2 tg animals will confirm correlative evidence, in the human placenta, of FGL2's role as an immunoregulator at the maternal-fetal interface. Overall, this work supports the hypothesis that FGL2 is secreted throughout the female reproductive tract at precise stages of the estrous cycle, and in the developing placenta, as a physiological attempt to maintain the careful immune equilibrium required for the successful establishment and maintenance of pregnancy.

Abstract # 2124

Porcine Conceptus Expression of Interferon Deltas and Gamma During Early Pregnancy. Destiny NJohns, Carol G. Lucas, Paula R. Chen, Lee D. Spate, Caroline A. Pfeiffer, Raissa F. Cecil, Shelbi D. Perry, Kristin M. Whitworth, Kevin D. Wells, Thomas E. Spencer, Randall S. Prather, Rodney D. Geisert

Establishment and maintenance of pregnancy in the pig requires a complex process that relies on adequate communication between the conceptus and maternal uterine endometrium. Directly before the time of attachment to the uterine surface epithelium, the conceptuses undergo a dramatic morphological change to rapidly elongate throughout the uterine horn between days 10 and 12 of pregnancy. During this time, the conceptuses produce and secrete estrogens, interleukin 1 beta 2, prostaglandins and other biological factors into the uterine lumen that allow the uterine epithelium to become receptive to the attaching conceptuses as well as promote proper conceptus development. Following elongation, the conceptus is known to secrete two different types of interferons between days 12 and 20 of pregnancy. The pig conceptus is unique from other mammals in that it secretes both type I (interferon delta, IFND) and type II (interferon gamma, IFNG) interferons during the peri-implantation period. The objective of the present study was to elucidate conceptus mRNA expression patterns of IFNDs and IFNG on days 14, 17 and 30 of pregnancy. Based on genomic database predictions, there are 11 IFND genes. Because a number of the IFND genes are highly homologous, three unique primer sets were designed to target three groupings of the 11 different IFND genes based on their high similarity to each other. The primer set for Group 1 amplified sequence for IFND1 and IFND2; the primer set for Group 2 amplified sequence for IFND3, IFND4, and IFND10; the primer set for Group 3 amplified sequence for IFND5, IFND6, IFND7, IFND8, IFND9, and IFND11. One primer set was designed to target IFNG which is synthesized from a single gene. IFNG expression was detected on days 14 and 17 of pregnancy but not day 30. Group 1 expression was detected on days 14, 17, and 30 of pregnancy. Group 2 expression was only detected on day 30 of pregnancy. Group 3 expression was not detected across days 14, 17, or 30 of pregnancy. Although previous studies indicated that pig conceptuses produce IFND, we have established that of the 11 IFND family members in the current database, up to five of them appear to be expressed by the conceptus during early pregnancy. Additionally, CRISPR/Cas9 gene editing was utilized in porcine fetal

fibroblast cells to create a loss of function edit in exon 1 of the IFNG gene. Sanger sequencing of individual colonies confirmed a 202 base pair bi-allelic mutation including the start codon located in exon 1 which will be used to identify the biological role of conceptus derived interferons in early pregnancy. Research supported by USDA NIFA grant 2017-12211054.

Abstract # 2139

The Distinct Microbial Ecology Of The Bovine Placenta At Parturition. Gwendolynn L. Hummel, Kelly L. Woodruff, Kathy J. Austin, Travis L. Smith, Hannah C. Cunningham-Hollinger

Recent investigations into the human placental microbiome have led to the discovery of a unique microbial composition within the fetal membranes at parturition. We hypothesize that a similarly unique microbiome exists in the bovine placenta, and that this microbial source has direct implications regarding the development and health of the rumen microbiome of the calf. Our objective was to characterize the microbial populations isolated from three tissues of the bovine chorioallantois including the cotyledon (COT), intercotyledonary membrane of the chorion (ICM), and allantois (AL). The placentas of University of Wyoming multiparous beef cows (n = 10) were collected at parturition, and samples from each tissue of interest were dissected from defined sites along the gravid horn or uterine body. Microbial DNA was isolated and purified with the QIAmp DNA Stool MiniKit (Qiagen) for amplicon 16S rRNA sequencing and analyzed with QIIME2. Alpha and beta diversity were both analyzed by tissue type. Alpha diversity was not significant in evenness (P = 0.517) or richness (P = 0.717), indicating that no differences exist in the number or balance of amplicon sequence variants detected between fetal membranes. However, investigations into beta diversity indicate there is a significant difference between the ICM and AL (P = 0.006), but there was no detected difference between the ICM and COT, or COT and AL ($P \ge$ 0.159). These differences in beta diversity between the chorion and allantois indicate that specific microbial abundances differ between these two tissues. Furthermore, these data may suggest unique microbiome differences between tissue type by highlighting key microbial taxa influential to the maintenance and health of the placenta, as well as those that carry the potential to influence colonization of the calf's microbiome.

Abstract # 2156.

Prostaglandin E2 Is Decreased In Pregnant Cows During Active Placentation. Sydney T. Reese, Gessica A. Franco, Ramiro V. Oliveira Filho, Ky G. Pohler

Relatively little is known about the causes or mechanisms associated with late embryonic mortality, most of which occurs around the time of placentation in the cow. Previous studies have indicated that Prostaglandin E2 (PGE) may have luteal protective functions and the PGE receptors are upregulated prior to day 50 of pregnancy. The objective of the study was to evaluate PGE secretion during active placentation from day 29 to 38 in pregnant cows that maintained pregnancy or experienced LEM. Nonlactating cows were artificially inseminated to high fertility bulls or sham inseminated (control; n = 4) with heat treated semen at day 0. Control cows received a CIDR at day 17, which was replaced with a new CIDR at day 27, to maintain elevated circulating progesterone concentrations. Pregnancy diagnosis was performed at day 29 via ultrasound. Pregnant cows (n = 8) and control cows (n = 4) underwent coccygeal vein cannulation at day 29. A polyethylene catheter (BD Intramedic) was inserted 65 cm into the caudal vena cava via the coccygeal vein of all cows for sampling of utero/ovarian drainage. Blood samples were collected every 6 hours until day 38. Final pregnancy diagnosis was performed at day 70 of gestation. Cows diagnosed as pregnant at day 29 but non pregnant at day 70 based on absence of a fetus with a viable heartbeat were considered to have undergone late embryonic mortality (LEM; n = 4). Serum concentrations of PGE were measured with a validated commercial ELISA (Cayman Chemical). Data were analyzed using repeated measures in SAS 9.4. Interestingly, cows that maintained pregnancy (PREG; n = 4) had decreased PGE concentrations compared to LEM and control cows (P < 0.05) throughout the study period. Concentrations of PGE did not differ between control and EM cows on days 29 to 38 of gestation (P > 0.1). Concentrations of PGE peaked in LEM cows between days 31 and 35 (range: 15.88 – 22.03 pg/mL) while PREG cows maintained decreased concentrations (range: 6.54 – 8.63 pg/mL). Concentrations of PGE did not fluctuate significantly within individual animals during the trial period and no significant pulses were observed. Previous data from our lab has indicated differences in the timing of prostaglandin F2a (PGF2a) pulses between cows that maintained pregnancy and those that undergo LEM. Combined with the present data, prior to day 35 of gestation, LEM cows had a greater PGE:PGF2a ratios compared to PREG cows (P < 0.05). These PGE data provide a novel indication of endocrine prostaglandin alterations in incidences of late embryonic mortality in cattle. This project was supported by Agriculture and Food Research Initiative Competitive Grant no. 2017-67015-26457 from the USDA National Institute of Food and Agriculture.

Abstract # 2205

Maternal Iron Deficiency Elicits Changes In Placental Development and Alters Fetal Growth Trajectories. Hannah Roberts, Andrew G. Woodman, Stephane L. Bourque, Stephen J. Renaud

Iron is an essential mineral that is required for oxygen transport, DNA synthesis and repair, and as a cofactor for various cellular processes. Iron deficiency is the most common nutritional deficiency worldwide and pregnant women are one of the populations most at risk. Iron deficiency during pregnancy poses major health concerns for the developing baby, including fetal growth restriction and long-term health complications. Maternal iron deficiency may indirectly impair fetal growth through changes in the structure and function of the placenta, however, the effect of iron deficiency on the placenta is not well understood. This project aims to establish a model of iron deficiency in pregnant rats and investigate the resulting changes in placental development and fetal growth. We hypothesize that maternal iron deficiency during pregnancy will result in decreased fetal growth, increased placental size and increased expression of nutrient transporters in placental tissue. Pregnant Sprague-Dawley rats were fed either a low iron (10 mg iron/kg) or iron-replete (37 mg iron/kg) diet starting two weeks before pregnancy. Dams were euthanized and conceptuses were dissected at either gestational day 13.5 or 18.5. Dam and fetal hemoglobin concentration and body weight were measured. Placentas were weighed, cryosectioned and stained with hematoxylin and eosin to assess the crosssectional areas of the labyrinth and junctional zones (anatomical units of the rodent placenta). Comprehensive transcriptome profiling of gestational day 18.5 placentas collected from iron-replete or iron-deficient dams was conducted using Clariom S microarray, which was statistically analyzed using the empirical Bayes method and validated using quantitative RT-PCR. Compared to controls, iron deficiency reduced maternal hemoglobin throughout pregnancy, including a 44% reduction on gestational day 18.5 (n=8 dams, P<0.0001). Fetal hemoglobin was also reduced in iron deficiency on gestational day 18.5 by 45% (n=18 fetuses, P<0.0001). Iron deficiency caused a 12% (n=34, P=0.0004) reduction in total fetal body weight and reduced fetal liver weight by 16% (n=30 fetuses, P<0.0001) compared to controls. There was no change in fetal brain, heart or kidney weight. Interestingly, relative placental size was increased in iron deficiency by 32% (n=30 placentas per group, P<0.0001), including a 27% (n=7, P=0.007) increase in junctional zone area and no change in labyrinth zone area. DNA microarray analysis revealed 48 transcripts changed at least 2-fold (n=4 dams, P<0.05) in placentas from maternal iron deficiency compared to controls. Some of the most upregulated transcripts included those involved in immunomodulation and extracellular matrix remodeling, including Alox15 (18.8-fold increase) and Mmp10 (2.6-fold increase). Downregulated transcripts included those encoding hormones (Prl3a1; 4.8-fold decrease) and lipid transport (Apoa1; 4.1-fold decrease). In conclusion, maternal iron deficiency caused maternal and fetal anemia, and was associated with decreased fetal weight, increased placental growth on gestational day 18.5, specifically in the junctional zone, and altered expression of genes associated with immunomodulation, matrix remodeling, and lipid transport. As the placenta forms the interface between a mother and baby, changes in placental development may yield new diagnostic indices of fetal distress in iron-deficient pregnancies, facilitating earlier interventions and improved fetal outcomes.

Abstract # 2207

Effect Of Bovine Trophoblast Cell Derived Extracellular Vesicles On Gene Expression Profiles Of Immune Cells. Ana C. Silva, Kira P. Morgado, Christopher J. Davies, Irina A. Polejaeva, Anhong Zhou, Heloisa M. Rutigliano

Placenta-derived extracellular vesicles (EVs) play a role in the communication between the placenta and maternal immune cells possibly leading to regulation of maternal Tcell signaling components. An abnormal maternal tolerance towards the conceptus has been associated to clinical conditions such as implantation failure and recurrent pregnancy loss. The specific mechanisms by which this tolerance is acquired remain unclear. The hypothesis of this study was that trophoblast-derived EVs modulate gene expression of immune cells. Ten placentas were collected at a local abattoir and enzymatically digested. Isolated trophoblast cells were cultured for approximately 10 days with their supernatants being collected every 72 hours. Extracellular vesicles were isolated by differential centrifugation and characterized by scanning electron microscopy, dynamic light scattering and Raman spectroscopy. Scanning electron microscopy and dynamic light scattering analysis confirmed the isolation of EVs. Raman spectroscopy demonstrated that trophoblast-derived EVs have a unique biochemical fingerprint compared with peripheral blood mononuclear cell-derived EVs. Peripheral blood mononuclear cells were collected from non-pregnant lactating Holstein cows. The following leukocyte populations were stained with monoclonal antibodies and sorted by flow cytometry: CD4 + CD25 + T lymphocytes, CD4 + CD25 - T lymphocytes, CD8 + T lymphocytes, gamma delta T cells, and macrophages. The isolated placental EVs were then, added on the culture of CD4 + CD25 + T lymphocytes, CD4 + CD25 - T lymphocytes, CD8 + T lymphocytes, gamma delta T cells, and macrophages for 48 hours. In order to identify the genes modulated by trophoblast-derived EVs, gene expression of immune cells cultured with and without trophoblast EVs was assessed by microfluidic chip real time RT-PCR. Messenger RNA expression data were analyzed by the Delta Delta Ct method using the average of the housekeeping genes GAPDH and ACTB for normalization using the Fluidigm Real-Time PCR Analysis Software. These experiments were replicated three times using immune cells from three different nonpregnant cows at similar stages of lactation. Gene expression data were analyzed by the mixed procedure of SAS as a randomized block design, where cow is the block, the experimental unit is the cell culture well (n=12). A strong effect of trophoblast-derived EVs on the gene expression profiles of immune cells was detected. The different immune cell populations analyzed responded differently to trophoblast EVs. Both CD4 + CD25 + and CD4 + CD25 - T cell populations had the greatest numbers of significantly regulated transcripts for GMCSF, GATA3, FOXP3, CD28, IL10, TNF among others. Treatment with trophoblast-derived EVs also caused the modulation of C D28, FOXP3 and GATA3 in CD8 + cells, while EVs changed the expression profiles of interleukin (IL) 17, IL13, IL12 and IL6 in macrophages. In conclusion, the overall gene expression profile indicates that trophoblast-derived EVs regulate immune cell activity.

Abstract # 2310

NK Cells Orchestrate Angiogenesis. Katharine Wolf, Sylvia Schneiderman, Valerie Riehl, Mahmood Bilal, Svetlana Dambaeva, Kenneth Beaman

Embryo implantation in the uterus requires both angiogenesis and immunosuppression. Targeted RNA sequencing of uterine NK (UNK) cell subpopulations identified that tissue resident NK (trNK) cells are enriched for proangiogenic genes, while cytotoxicity factors are enriched in conventional NK (cNK) cells. However, the mechanism for uNK- or trNKmediated uterine angiogenesis is unknown. Ephrin-B2 is a mediator of VEGF-driven angiogenesis and arterial development throughout life. Levels of ephrin-B2 and its ligand EphB4 are dynamic during placental development, and have been detected on uterine granulocytes. However, these ephrin-B2-expressing granulocytes have not been confirmed as uNK cells. We hypothesized that uNK cells express ephrin-B2 and that this protein is necessary for uterine angiogenesis. NK cells were isolated from the uterus (uNK) and spleen (sNK) of mice. Isolated NK cells were characterized for the expression of ephrin-B2 by immunofluorescence (IF), flow cytometry, and qRT-PCR. By flow cytometry, ephrin-B2 is expressed by a significant proportion of uNK cells (79.2%, ± 5.1%) compared to sNK cells ($29.7\% \pm 9.0\%$) (p=0.0027). qRT-PCR for confirms that uNK cells, but not sNK cells, express Efnb2 (values expressed as fold change from positive control endothelial cells: UNK cells 0.46 ± 0.13 ; sNK cells 0.02 ± 0.01 ; p=0.0157). In agreement with previous studies, UNK cells expressed less Ifng than sNK cells (fold change from positive control male sNK cells: uNK cells 0.20 ± 0.07; female sNK cells 1.0 ± 0.14). Primary mouse endothelial cells (ECs) were co-cultured with uNK or sNK cells. While sNK co-cultures led to the death of ECs, uNK cell co-cultures promoted tubule formation similar to VEGF. However, this effect was blocked when uNK cells were first incubated with an ephrin-B2 blocking antibody. Our data show that uterine NK cells express ephrin-B2 and that this receptor appears necessary for uterine angiogenesis. This describes a previously unsuspected cellular receptor of uNK cells and is, to our knowledge, among the first data suggesting a mechanism underlying uterine angiogenesis.

Abstract # 2355

Cell Proliferation And Death In Placenta Associated With Fetal Growth Restriction.

Anaclara Marino, Carolina Marvaldi, Julieta Aylen Schander, Manuel Luis Wolfson, Ana Maria Franchi, Julieta Aisemberg

Intrauterine growth restriction (IUGR) is a condition whereby a fetus is unable to achieve its genetically determined potential size. Prenatal stress is one of the causes that alter the intrauterine environment, which affects the normal development and function of the placenta, and the fetal growth. Furthermore, IUGR is associated with placental dysfunction, where altered trophoblast cells turnover and function contribute to reduced feto-placental growth. The balance between placental cell proliferation and death is a key point during the development of the fetus. The aim of this work was to study the differences in cell proliferation, apoptosis and autophagy in placental tissue in normal and IUGR placentas. The IUGR mouse model used was animals treated with a synthetic glucocorticoid during late pregnancy to cause growth restriction. Pregnant BALB/c mice received 8 mg/kg (s.c.) of dexamethasone between days 14 and 15 of pregnancy. The control group was sham-treated with saline. Prenatal glucocorticoid treatment not only induced fetal growth restriction but also decreased placental weight. Placental tissue from pregnant animals was dissected on gestational days 15 to 18 and processed for Western Blot and RT-qPCR analysis. The results were analyzed with a one-way ANOVA and Tukey test (p<0,05). Mice with IUGR presented higher placental levels of mRNA of PCNA on day 16 and lower Bcl2 protein levels on day 15 (p<0.05) compared with control groups. In addition, regarding cell proliferation, there were lower mRNA levels of Cyclin B1 and p57 cell cycle inhibitor on day 16. We found higher protein levels of LC3B-II (p<0,05) on day 18 placentas compared with controls groups. There were no significant changes in mTOR, Bax, Fas and Fas ligand, Cyclin D3 or in the p16 cell cycle inhibitor between studied groups. Therefore, during the day 15 and 16, the mechanism of cell proliferation and apoptosis were altered in IUGR placentas. In term placentas the autophagy increases. In conclusion, IUGR induced by prenatal dexamethasone treatment produces alterations on placental markers expression associated to cell proliferation, cell death and autophagy.

Preimplantation Embryo Development

Abstract # 1671

Effect Of Brd4 Inhibitor (+)-JQ1 Treatment Timing On Preimplantation Development In Mice. Sachi Matsumoto, Ren Watanabe, Kazuki Mochizuki, Satoshi Kishigami

Bromodomain-containing protein 4 (Brd4), a transcriptional coactivator, is expressed throughout murine preimplantation development and is essential for the development of inner cell mass (ICM) of blastocyst. However, it is not clear yet exactly when the Brd4 function is required during preimplantation development. In this study, we examined the effect of Brd4 inhibitor (+)-JQ1 treatment timing on preimplantation development. IVF and in vitro culture were performed using oocytes and sperms from ICR mice. Brd4 inhibition was carried out at the specified timings, 0, 24, 30h after insemination by transferring embryos to culture medium containing 500 nM (+)-JQ1. Embryos treated with (+)JQ1 from the 1-cell stage (0 h) developed significantly reduced incidence of blastocysts (cont 85% vs (+)-JQ1 73%; P<0.05) with normal morphology and a decreased number of Nanog-positive cells (cont 8±3.2 vs (+)-JQ1 6±2.4), consistent with previous studies. Unexpectedly, Brd4 inhibition from the early 2-cell stage (24 h), severely reduced incidence of blastocyst (cont 85% vs (+)-JQ1 57%; P<0.05) with the normal number of Nanog-positive cells but a higher frequency of loss of polar trophectoderm in those blastocysts (cont 0% vs (+)-JQ1 0h 8% vs (+)-JQ1 24h 34%, respectively; P<0.05). Interestingly, Brd4 inhibition from the late 2-cell stage (30 h) showed a normal blastocyst rate with much weaker phenotypes. Further, a lower or partial expression of pERM, a marker of cell polarity of trophectoderm (TE), were often observed in (+)-JQ1-treated embryos after compaction depending on timing of (+)-JQ1-treatment. Embryos treated with (+)-JQ1 from early 2-cell stage also often had loss of outside cells with nuclear localization of YAP. Thus, sudden inhibition of Brd4 during the 2-cell stage led to a more serious disturbance in a developmental program including TE development, first suggesting that study functioning of Brd4 during the 1- to 2-cell stages is required for normal establishment of their cell polarity in addition to ICM development.

Abstract # 1687

Disruption Of Hippo Signalling Pathway During Bovine Preimplantation Embryo Development. Jyoti Sharma, Pavneesh Madan

Blastocyst formation is an important milestone during preimplantation embryo development. Trophectoderm (TE) and inner cell mass (ICM) are the two distinct cell lineages established during the blastocyst formation. Hippo signaling pathway is proven to be responsible for lineage segregation during the formation of a blastocyst during mouse embryogenesis. Even though, our lab has recently established the presence of Hippo signaling pathway components in bovine embryos, the role of these components in bovine embryos still remains unknown. Thus, the aim of present study was to establish the role of Hippo signaling pathway components during early bovine embryogenesis, using chemical inhibition. For the present study, the bovine zygotes were produced using standard In-vitro fertilization and culture protocols. These zygotes were then segregated into control, vehicle and treatment groups. The treatment groups comprised of 0.5, 1, 5 and 5.5 µM of either Atorvastatin or Cerivastatin. Thee embryos were then harvested at 2-cell, 8-cell and blastocyst stages. The difference in the mRNA expression of Hippo signaling pathway components was observed in between single 'control' and 'treated' embryos at 2-cell, 8-cell and blastocyst stages, by using digital droplet PCR. Laser confocal microscopy was used to observe the differences in the TE/ICM ratio using differential staining and the differences in protein localization of the Hippo signaling pathway components. A significant decrease in blastocyst rate was observed in between the control group (39.5%) and Atorvastatin (20%) or Cerivastatin (13.8%) treatment groups. There was also a significant decrease in the total cell count in between the control (112.5 cells) and Cerivastatin (76 cells) treatment groups (0.5 µM). Following treatment with Cerivastatin (0.5 µM), TAZ (Transcriptional co-activator with PDZ binding domain) was absent from the nucleus as compared to the control blastocyst in which TAZ was predominantly expressed inside the nucleus. Similarly, YAP1 (Yes Associated Protein 1) was expressed in the nucleus in both control and vehicle treatment groups, whereas it was absent from the nucleus in the Cerivastatin treatment group (0.5 μ M). p-YAP was present in the nucleus for both the control and vehicle blastocysts, however p-YAP presence could not be detected within the nucleus of treated blastocysts. Inhibitory effects of Statin (Atorvastatin/Cerivastatin) treatments on YAP1/TAZ and p-YAP, suggests that they are potent inhibitors of the downstream effectors of Hippo signaling pathway. However, in the control and Cerivastatin treatment groups, no such effect of Cerivastatin treatment was observed on the protein localization of MST1 and 2 (Mammalian Sterile Twenty Like 1 and 2) and the upstream regulators of Hippo signaling pathway. These results indicate that Statins act on YAP1/TAZ, independent of MST1/2 protein kinase (upstream effectors of signaling pathway), suggesting that some alternate cell signaling pathway(s) to be involved in the regulation of Hippo signaling components. Delineation of Hippo signaling pathway components will help in ascertaining the mechanism of blastocyst formation and the application of the acquired knowledge will help in the production healthy bovine embryos.

Abstract # 1688

Does Global miRNA Expression In The Spent Media Change During Early Embryo Development? Paul Del Rio, Pavneesh Madan

Distinct miRNA populations have been detected in the spent media of in-vitro cultured embryos. However, profiling has only been conducted in spent media cultured with blastocyst-stage embryos. Therefore, the aim of the study was to globally profile the extracellular miRNA population throughout the pre-implantation period in bovine embryos using a heterologous miRNA microarray. To achieve this, cumulus oocyte complexes were aspirated from abattoir obtained ovaries, in-vitro matured, fertilized, and cultured (in groups of 20) under standard laboratory procedures to the 2-cell, 8cell, or blastocyst stage of development. At each of these time points, 25 µl of spent invitro culture media was collected, pooled to 300 μ l, and processed for total RNA extraction using a RNeasy mini kit. In total, 3 biological replicates of total RNA were processed from each morphological stage. Additionally, in-vitro culture media, which never came in contact with any embryos, were processed for total RNA extraction to serve as negative control. Frozen total RNA samples were hybridized on a GeneChip miRNA 4.0 array, consisting of 2500 miRNA probes based on mirBase release 20 (www.mirbase.org). Pre-processing was done in Affymetrix Transcriptome Analysis Console software and comparative analysis was carried out between spent media samples and control using fold-change and independent T-test. Probe-sets with a fold change of ≤ -2 or ≥ 2 (p-value < 0.05), a false detection rate of < 0.05, and a detectable above background value of < 0.05 were analyzed. Three miRNAs (bta-miR-39, bta-miR-122, bta-miR-106b) were uniquely up-regulated in 2-cell spent media. Nineteen miRNAs (bta-miR-320a, bta-miR-24-3p, bta-miR-17-5p, bta-miR-423-5p, bta-miR-193-5p, bta-miR-346, bta-miR-371, bta-let-7b-5p, bta-miR-191, bta-miR-125a, bta-miR-378, bta-miR-361,bta-miR-26, bta-miR-20a, bta-miR-151-5p, bta-miR-182, bta-miR-30d, bta-miR-155, bta-miR-342) were upregulated in blastocyst stage spent media. Four miRNAs (bta-miR-149-3p, bta-miR-1246, bta-miR-92a, bta-miR-450b) were differentially expressed in the spent media of 2 or more stages. In total, 26 miRNAs were found to be differently expressed in the spent media of bovine embryos. To the best of our knowledge, this study is the first to characterize the global miRNA expression in the spent media throughout the pre-implantation developmental period. The miRNAs identified in the study, through pathway enrichment analysis and experimental validation, may contribute to the growing body of evidence supporting the use of miRNAs as biomarkers of normal and aberrant pre-implantation embryo development using noninvasive assessment methods.

Abstract # 1705

Effect Of The Coculture Of Porcine Luteal Cells And Cumulus-Oocyte Complexes On The Blastocyst Development And Gene Expression. Gabriela Maia Teplitz, Marc-André Sirard, Daniel Marcelo Lombardo

The coculture with somatic cells is an alternative to improve suboptimal in vitro culture conditions. In the pig, in vitro fertilization (IVF) is related to poor male pronuclear formation and high rates of polyspermy, and in vitro embryo development is still an inefficient biotechnology. In the present study, we investigated the effects of a coculture system of porcine luteal cells during in vitro maturation (IVM) on blastocyst development and gene expression. The cumulus-oocyte complexes were matured in vitro in supplemented TCM199 with human menopausal gonadotrophin (control) and in coculture with porcine luteal cells from passage 1 (PLC-1). IVF was performed for 4 h with frozen-thawed boar semen in 100 µL-drop of modified Tris-buffered medium (20 denuded oocytes per drop, 1.5x106 spermatozoa/mL). Presumptive zygotes were

washed and cultured in porcine zygote medium at 39°C, 7 % O2, 5 % CO2, and humidity for 7 days. The coculture with PLC-1 significantly increased the blastocyst rate (blastocyst/cleavage) (control: 14.4%; PLC-1 21.2%; Fisher's test p<0.05). Gene expression changes were measured with a porcine embryo-specific microarray in four pools of ten blastocysts of each treatment and confirmed by RT-qPCR on six candidate genes. Transcriptome analysis in the PLC-1 versus control groups revealed differences for 530 transcripts in the PLC-1 group (333 downregulated, 197 upregulated); (symmetrical fold-change > 1.2, p< 0.05) The global transcription pattern of embryos developing after coculture exhibited overall downregulation of gene expression. Following global gene expression pattern analysis, genes associated with lipid metabolism, mitochondrial function, endoplasmic reticulum stress, and apoptosis were found downregulated, and genes associated with cell cycle and proliferation were found upregulated. Canonical pathway and cellular function analysis by Ingenuity Pathway (IPA) revealed that differential expression transcripts were associated with the sirtuin signaling pathway (p = 6,23E-06 and z-score = -0,72); oxidative phosphorylation pathway (p= 2,48E-04 and z-score= 0.63); Chemoquine signaling (p= 4,44E-04 and zscore= 0,707) and Ephrin receptor signaling (p= 1E-03 and z-score= 0,707). To conclude, the results of the present study demonstrate that a coculture system with PLC-1 during IVM has a lasting effect on the embryo until the blastocyst stage modifying the gene expression, with a positive effect on the embryo development rates. Our model could be an alternative to replace the conventional maturation medium with gonadotrophins with higher rates of embryo development, a key issue in the pig.

Abstract # 1746

Distinct Activity Profiles Of Autophagy Between In Vitro And In Vivo Fertilized Embryos During Preimplantation Development In Mice. Saya Kanie, Ren Watanabe, Satoshi Kishigami

While in vivo fertilized preimplantation embryos develop well, in vitro fertilized (IVF) ones still show a limited developmental potential. In this study, in order to clarify how in vitro and in vivo fertilization affect physiological state of embryos during preimplantation development, we focused on their autophagy activities since autophagy activity is reported as an indicator of developmental potential of mouse preimplantation embryos. For live-cell imaging of autophagy activity, we applied DAPGreen (Wako), a fluorescence dye for monitoring autophagy activity in live cells. IVF embryos were produced by normal IVF procedure using ICR strain mice, and in vivo fertilized (IVv) embryos were produced by mating and then recovered at the 2-cell stage by flushing oviducts. Each embryo was stained with DAPGreen (Wako). As a result of time-lapse imaging from the 2-cell stage to the blastocyst stage, it was revealed that the activity of IVv embryos at the 2-cell stage was higher than that of IVF embryos. In contrast, after the morula stage, IVF embryos showed higher autophagy activity than IVv embryos, suggesting that IVv and IVF embryos exhibit distinct profiles in autophagy activity during preimplantation development. Next, we cultured IVF embryos in the absence of BSA to

cause higher autophagy activity of IVF embryos at the 2-cell stage but did not mitigate the abnormally high autophagy activity at the morula stage and failed to improve the embryonic development. Our results suggest that the autophagy activity profiles differ between IVv and IVF embryos through preimplantation development and are regulatable depending on medium components. This finding could be applied to improve the birth rate of IVF embryos by optimizing the culture conditions with monitoring autophagy activity.

Abstract # 1761

Expression Of Ubiquitinases In Bovine Embryos In Response To Ultraviolet-Induced DNA Damage. Zigomar da Silva, VitorBraga Rissi, Daniele Missio, Julia Koch, Werner Giehl Glanzner, Paulo Bayard Dias Gonçalves, Vilceu Bordignon

DNA damage repair enables normal genome replication, segregation, integrity preservation and cell division. DNA damage can result from both endogenous and exogenous factors. DNA double-strand breaks (DSBs) are the most harmful genotoxic lesions because of the risk for creating DNA mutations and segregation of abnormal genomes. In response to DSBs, cells activate a DNA damage response (DDR), which promote DNA repair by activating two main pathways, the homologous recombination (HR) pathway and the non-homologous end-joining (NHEJ) pathway. The engagement and repair activity of each pathway depends on several factors including the cell cycle stage when DSBs occurred. Blastomeres in early developing embryos seem to repair DSBs mainly through the HR pathway, which is likely due to their relative long Sphases compared to the G1-phases. DDR involves several post-translational modifications, such as phosphorylation and ubiquitylation of proteins. Phosphorylation of the serine 139 in the C-terminal domain of the histone H2AX (yH2AX) is a hallmark for DSBs sites. H2AX phosphorylation expands through chromatin near DSBs sites forming yH2AX foci, which anchor the accumulation of DNA repair proteins. Ubiquitylation contributes to the formation of DSBs foci by regulating chromatin accessibility and recruitment of DDR effectors. However, the role of ubiquitinases in the regulation of DDR in early developing embryos is not well understood. The aim of this study was to assess the abundance of transcripts for the ubiquitinases RNF4, RNF8, RNF20, RNF40, RNF126, RNF168, RNF 169, HERC2, TRIM 28, TRIM77, UBE2N, UIMC1 and BRCC3 in control and ultraviolet(UV)-treated bovine embryos. First, zygotes were exposed to UV radiation for 0, 10, 20 or 30 seconds and development to the blastocyst stage was evaluated. Blastocyst formation was significantly reduced by 10, 20 and 30 seconds exposure to UV, which confirmed the induction of DNA damage. Second, mRNA abundance was compared between control and UV-exposed embryos (for 10 seconds) at days 3, 5 and 7 of development. In control embryos, RNF8, RNF20, RNF40, RNF168, RNF169 and TRIM77 mRNA decreased from day 3 to day 7, which suggests these ubiquitinases might play a role during oogenesis and early embryo stages. On the other hand, HERC2 and TRIM28 mRNA increased from day 3 to day 7, while UBE2N, UIMC1, BRCC3, RNF4 and RNF126 mRNA levels tended to decrease from day 3 to day 5 and then increase from day 5 to

day 7, which suggests these ubiquitinases may have a more important role in developing embryos at post-genome activation stages. In addition, we observed an upregulation of RAD51 mRNA and a downregulation of 53BP1 mRNA in UV-irradiated embryos, which suggests that bovine embryos mainly activate the HR pathway to repair damaged DNA. Finally, we observed that mRNA levels of the HERC2, RNF126 and RNF20 ubiquitinases were downregulated in UV-treated embryos at day 7 of development. Given their known roles on DDR in somatic cells, it is possible that RNF20, RNF126 and HERC2 favor the activation of HR pathway in detriment of the NHEJ pathway to promote DSBs repair in early developing embryos. (Supported by CNPq, CAPES and NSERC).

Abstract # 1762

Effect Of High Level Of NEFAs On The Transcriptomes And Epigenomes Of Porcine In Vitro Fertilized Blastocysts. Meihong Shi, Marc-André Sirard

High levels of non-esterified fatty acids (NEFAs) are known to have negative impacts on granulosa cell proliferation and follicular health in several species. Similar research in porcine is scared and the effect of high level of NEFAs effect on porcine blastocyst remains unclear. This study is aiming to explore the mechanism of abnormal NEFAs level on the porcine early embryo development on transcriptomic and epigenetic level. In addition to 1% porcine follicular fluid in control group, a combination of 468 µM palmitic acid, 194 µM stearic acid, and 534 µM oleic acid was supplemented to North Carolina State University (NCSU)-23 maturation medium to achieve a high level of NEFAs during in vitro maturation. Matured oocytes were in vitro fertilized and expanded blastocysts were collected to complete the transcriptomic and epigenetic analysis. There was no significant difference in cleavage rate between two groups, but the blastocyst rate of high level of NEFAs group was significantly decreased compared to the control group (P=0.0044). Transcriptomic microarray data showed there were 280 up-regulated probes and 239 down-regulated probes with P-value >0.05, symmetrical fold-change >1.2 or <-1.2. Ingenuity Pathway Analysis (IPA) of transcriptomic data showed that canonical pathways associated inflammatory process and upstream regulators related to inflammation, embryonic development and gene expression were highlighted. Moreover, NetworkAnalyst analysis indicated that fatty acid, prolactin and folate metabolism besides apoptosis were also involved. Protein-protein interactions analysis showed Cullin 1 (CUL1) and Jun Proto-Oncogene, AP-1 Transcription Factor Subunit (JUN) were the most significantly regulated hub genes. DNA methylation array analysis found 52884 and 52169 probes within known genes above the background in Control and NEFA groups respectively. The limma analysis indicates that 80 regions are hypermethylated in blastocyst of control, compared to 46 hyper-methylated regions of NEFA. IPA analysis of the gene regions where the methylation changes were observed showed that lipid metabolism, cell proliferation, and inflammation pathway were targeted canonical pathways. Tumor Protein P53 (TP53) and CCAAT Enhancer Binding Protein Beta (CEBPB) were identified as potential regulators responsible for the changes.

Therefore, our conclusion is that the high NEFA level was involved in regulating the cell functions, inflammatory response, and metabolism signaling to alter the genes expression and affect the DNA methylation information of blastocysts which could further impact the quality of embryos.

Abstract # 1767

Inhibition of Mitochondrial SHMT2 Translation in Ovine Conceptuses During the Peri-Implantation Period of Pregnancy Increases Embryonic Mortality. Nirvay Sah, Claire Stenhouse, Katherine M. Halloran, Robyn M. Moses, Heewon Seo, Gregory A. Johnson, Guoyao Wu, Fuller W. Bazer

The intracellular transfer of 1-carbon units, commonly known as one-carbon metabolism, is critical for cellular functions, growth, and proliferation. Formate is the active carbon donor in one-carbon metabolism. Formate is generated from serine via a series of mitochondrial reactions initiated by serine hydroxymethyltransferase 2 (SHMT2) and transported to the cytoplasm where it is used for biosynthesis of purine, thymidine, and s-adenosylmethionine, a methyl donor for epigenetic modifications of gene expression. Ovine conceptuses are metabolically active during the peri-implantation period of pregnancy and have high levels of cellular proliferation with abundant expression of SHMT2 protein in trophectoderm cells. In this study, a morpholino antisense oligonucleotide (MAO) was used to knock-down translation of SHMT2 mRNA in ovine conceptuses, and effects on conceptus growth and development during the periimplantation period of pregnancy were assessed. Suffolk ewes (n=20) were synchronized and bred with fertile rams when detected in estrus (Day 0) and 12h and 24h later. The ewes were assigned randomly (n=10 per group) to receive 100 nmol of either a control morpholino (CONT-MAO) or a SHMT2 morpholino (SHMT2-MAO) into the lumen of the uterine horn ipsilateral to a functional corpus luteum on Day 11 postmating. The uterine horns were flushed with 15 ml phosphate buffered saline to recover conceptuses on either Day 16 or 18 post-mating (n=5 per treatment). The pregnancy rate (Days 16 and 18 combined) was lower in ewes treated with SHMT2-MAO as compared to CONT-MAO ewes (30% vs 70%, p =0.07) with no effect of day of gestation. Amino acids in uterine flushes and maternal plasma were analyzed using highperformance liquid chromatography. There was no significant effect of treatment on total recoverable amino acids in uterine flushes; however, the abundance of Asp, Asn, His, Tyr, Phe, Ile, Orn, and Lys increased (p < 0.05) between Days 16 and 18 of pregnancy. There was no effect of treatment, gestational day or their interaction on amino acids in plasma from pregnant ewes, except for glycine. Glycine was the most abundant amino acid in the plasma of pregnant ewes and the concentration of glycine increased (p <0.05) from 248.7 to 454.7 nmol/ml between Days 16 and 18 of pregnancy. Concentrations of arginine in the plasma of SHMT2-MAO treated ewes were lower (p < 0.05) than for CONT-MAO treated ewes on Day 16 post-mating for pregnant and non-pregnant ewes, and total recoverable arginine in uterine flushes from SHMT2-MAO treated ewes was also less than for CONT-MAO ewes. The decreases

of arginine in uterine flushes and maternal plasma of SHMT2-MAO treated ewes on Days 16 and 18 of pregnancy suggest that conceptuses from SHMT2-MAO treated ewes have increased demands for arginine to support conceptus development. These results indicate that knockdown of SHMT2 protein decreases pregnancy rate and concentrations of arginine in maternal plasma and uterine flushes and that SHMT2 may be crucial for conceptus survival during the peri-implantation period of pregnancy. This project was supported by Agriculture and Food Research Initiative Competitive Grant no. 2018-67015-28093 from the USDA National Institute of Food and Agriculture.

Abstract # 1805

Paternal Diet Alters Pre-Implantation Embryo Development and Metabolism in Mice. Hannah L. Morgan, Nader Eid, Adam J. Watkins

Poor parental nutrition during pre-conception periods has been shown to impact embryonic development, fetal growth and alter disease risk of the offspring. The influence of paternal well-being on fetal development and offspring health is beginning to gain more research focus, and emerging evidence has linked sub-optimal paternal diet at the time of conception to poorer offspring outcome. However, the mechanisms that define this development trajectory are still not fully understood. This study aimed to determine how paternal diet (over- and under-nutrition) impacts early blastocyst formation and whether dietary vitamin and mineral supplementation can negate any detrimental effects.

Male C57/BL6 mice were fed one of five diets; low protein diet (LPD (9% casein, 24% sugar, 10% fat)), western diet (WD (19% casein, 21% fat, 34% sugar)), diets supplemented with methyl-donors (MD-LPD and MD-WD) or an isocaloric control diet (18% casein, 10% fat, 21% sugar) for at least 8 weeks (n=8/group). Chow fed female C57/BL6 mice (n=4-5) were mated with these males and on embryonic day 1.5, embryos were flushed from the oviduct and cultured individually (n=17-36) in EmbryoMax® KSOM media at 37°C, 5% CO2, using Embryoscope time-lapse imaging. To define the connection between paternal diet and pre-implantation development, stud male testis gene expression was examined via microarray (n=8 males per group).

Paternal diet did not alter fundamental fertility, as indicated by no significant difference in the number of embryos flushed per female. Embryos from the LPD, WD, MD-LPD and MD-WD fathers displayed advanced rates of preimplantation development when compared to embryos derived from control males. WD embryos had a significantly shortened cell cycle length at the 4-cell stage (11±0.1 vs 12±0.3 hours; p<0.05), when compared to control embryos. However, there was no differences in cleavage synchronicity or in the percentage of embryos achieving successful blastulation between treatment groups. MD-WD embryos demonstrated a significantly reduced time to the start of blastulation ($42\pm0.7 \text{ vs } 47\pm1.1 \text{ hours}$; p<0.01) and, the length of blastulation was significantly increased in embryos from WD males compared to LPD ($15\pm0.6 \text{ vs } 11\pm0.9$; p<0.05). Male testis transcriptome data identified that WD, MD-LPD and MD-WD had a significant downregulation of biological process such as the cell cycle; with changes in cyclin-dependant kinase (Cdk6), transcription factor (E2f2) and retinoblastoma-like protein (Rbl2) gene expression, and embryonic development; which included changes to homeobox protein (Hoxb4, Hoxb7 and Hoxb13) gene expression (FDR<0.05)

These findings suggest that paternal sub-optimal diet alters the trajectories of embryo development at these early stages, and this could negatively impact fetal development later in gestation. Furthermore, we have provided evidence these embryo development changes could be influenced by a dysregulation of key developmental genes originating in the testis.

Abstract # 1863

A Paternal Carry-Over Effect Of Atrazine- And DACT-Treated Spermatozoa On Preimplantation Embryo Transcriptome. Alisa Komsky-Elbaz, Dorit Kalo, Zvi Roth

The herbicide atrazine (ATZ) and its major metabolite diaminochlorotriazine (DACT) are considered ubiquitous environmental contaminants. In-vitro exposure of bovine spermatozoa to ATZ/DACT has been documented to impair plasma, acrosome and mitochondrial membrane integrity; however, the consequences are less known. A sequential set of experiments (Exp.1–4) was performed to examine the effect of ATZ/DACT on spermatozoa's DNA integrity, fertilization competence, embryo development and transcriptome profile. Exp.1: bovine spermatozoa were exposed to ATZ (0.1 or 1 µM) or DACT (1 or 10 µM) during in-vitro capacitation (4 h) and used for invitro fertilization with untreated bovine oocytes. ATZ/DACT reduced the proportion of embryos that cleaved to the 2- to 4-cell stage relative to the control (P < 0.005), but not the proportion of embryos developing to the blastocyst stage, most likely because fertilization was performed with unaffected spermatozoa. Exp.2: to confirm this assumption, spermatozoa were separated into annexin V+ (AV+) and annexin V- (AV-), using the annexin-V micro-bead kit, and then evaluated for DNA fragmentation (acridine orange dye). ATZ/DACT increased the proportion of cells with fragmented DNA (P < 0.0001), in correlation with AV+ (P < 0.0001). Fertilization with AV+ spermatozoa resulted in the absence of blastocyst formation compared to 23.5% for AVspermatozoa. Accordingly, further fertilization was performed only with the AVsubgroup. Cleavage rates were significantly lower in ATZ/DACT groups than in controls (59.8 and 65.3 vs. 78.7%, respectively; P < 0.005). Surprisingly, the proportion of developed blastocysts did not differ between groups. Exp.3: to exclude the effect of ATZ/DACT on the acrosome, found in our previous study, intracytoplasmic sperm injection was performed with control (AV+, AV-) and DACT-exposed (AV+, AV-) spermatozoa. The proportion of cleaved oocytes did not differ between groups and

blastocyst formation tended to be higher for AV- vs. AV+ in both control and DACT groups (P < 0.1 and 0.07, respectively), suggesting that acrosome reaction, rather than DNA fragmentation, underlies the reduced cleavage recorded in Exp.2. Using a timelapse incubator system, we examined the morphokinetics of cleaving embryos. A delay in the second cleavage was recorded in the DACT AV+ compared to DACT AV- group (P < 0.06). This might explain, in part, the reduced blastocyst formation. Exp.4: Transcriptomic analysis of blastocysts was performed (Affymetrix). About 139 and 230 differentially expressed genes were recorded in blastocysts derived from ATZ- and DACT-exposed spermatozoa, respectively, relative to controls. In particular, alterations were found in genes involved in pregnancy (IFNT2, IFNT3, IGFBF5), in-utero embryonic development (YBX3, ANKRD11, PDGFRA, VIM), pluripotency (MYF5), apoptosis (THEM4, BCAD29, EIF2AK2), and methylation and acetylation (H2B, RAB27B, H4, HIST1H1C, LOC616868). In summary, this is the first exploration of a deleterious carry-over effect of ATZ/DACT from the spermatozoa to the developing embryo, expressed by altered second-cleavage morphokinetics and transcriptomic profiles of the developed blastocysts. Further examination should evaluate the implantation competence of embryos derived from spermatozoa exposed to ATZ/DACT.

Abstract # 1931

Porcine Conceptuses Utilize the Polyol Pathway and Fructose-Driven Glycolysis (Fructolysis) to Support Development during the Peri-Implantation Period of Pregnancy. Avery C. Kramer, Heewon Seo, Bryan A. McLendon, Robert C. Burghardt, Guoyao Wu, Fuller W. Bazer, Greg A. Johnson

During the peri-implantation period of gestation, porcine conceptuses (embryo and associated placental membranes) undergo elongation, a process requiring extensive cell proliferation and migration, and nutrients to support these events. The hexose sugars, glucose and fructose are present in the porcine conceptus and endometrium, with fructose being the most abundant hexose sugar. Our preliminary studies suggest that in response to hypoxia, the endometrium of pigs transports glucose into the uterine lumen where the conceptus trophectoderm (Tr) directs the majority of glucose carbons away from the TCA cycle and into aerobic glycolysis for use in the pentose phosphate pathway, one-carbon metabolism, and the hexosamine biosynthetic pathway to fulfill the metabolic demands for cell proliferation. This enhanced glycolytic metabolism to form lactate deprives the environment of sufficient amounts of pyruvate to support the TCA cycle. In response, Tr cells perform glutaminolysis that converts glutamine into aketoglutarate (a-KG), a TCA cycle intermediate, to maintain TCA cycle flux. A result of an active TCA cycle is the generation of ATP and citrate that inhibits a glycolytic enzyme phosphofructokinase (PFK) and, therefore, inhibits continued glycolysis. This inhibition can be circumvented via activation of the polyol pathway to synthesize fructose from glucose. Fructolysis, which refers to the partial catabolism of fructose to pyruvate, lactate and ribose, can then continue to provide the glycolytic intermediates required for conceptus elongation. Therefore, we collected porcine conceptus tissues on Days 11, 13, 15, and 16 of pregnancy and performed real-time PCR, Western blot, and immunohistochemistry to determine expression of enzymes required for the polyol pathway and fructose-driven glycolysis. We also collected elongating conceptus tissues from Days 14 and 16 of pregnancy, incubated these tissues with 14 C-fructose, and measured the 14 CO 2 released from the conceptuses to determine if porcine conceptuses directly metabolize fructose. Results demonstrated that the Tr of Day 15 conceptuses: 1) expresses aldose reductase (AKR1B1) and sorbitol dehydrogenase (SORD), enzymes required for the polyol pathway, suggesting active conversion of alucose to fructose; 2) expresses ketohexokinase (KHK), an enzyme required for fructolysis; and 3) metabolize fructose as they elongate, indicating that conceptus Tr can utilize fructolysis during the peri-implantation period. Our results demonstrate that the Tr of porcine conceptuses: 1) utilizes the polyol pathway to convert glucose into fructose; 2) directly metabolizes fructose; and 3) utilizes fructolysis to maintain pyruvate and ribose fluxes in an environment lacking active PFK. This project was supported by Agriculture and Food Research Initiative Competitive Grant no. 2018-67015-28093 from the USDA National Institute of Food and Agriculture.

Abstract # 1941

Utilization of Serine, Glycine, and Hexose Sugars by the Ovine Conceptus During in-vitro Culture for One-Carbon Metabolism. Katherine M. Halloran, Claire Stenhouse, Robyn M. Moses, Nirvay Sah, Avery Kramer, Guoyao Wu, Fuller W. Bazer

Hexose sugars (fructose and glucose) and amino acids (AA) are nutrients transported into the uterine lumen as components of histotroph during the peri-implantation period of pregnancy in ugulates. Fructose, glucose, and serine transporters are expressed by uterine luminal epithelia, as are enzymes that convert hexose sugars to serine. The trophectoderm also expresses transporters for the uptake of serine and enzymes that convert serine to glycine for entry into one-carbon metabolism. One-carbon metabolism is important for proliferating trophectoderm cells as it produces formate used to yield purines and thymidine -the backbone units of RNA and DNA. We hypothesize that fructose is utilized in serinogenesis for one-carbon metabolism, which is required for rapid proliferation of trophectoderm cells of elongating ovine conceptuses. Suffolk ewes were bred with fertile rams upon detection of estrus (Day 0), and on Day 17 of pregnancy, ewes (n=5) were euthanized and hysterectomized. The lumen of the uterine horns were flushed with 15mL of phosphate buffered saline to recover conceptuses and uterine flushing. Sections of endometrium were frozen in liquid nitrogen and stored at -80 o C or fixed in 4% paraformaldehyde. Conceptuses were washed with Krebs-Henseleit Bicarbonate (KHB) buffer prior to culture with KHB+2mM [U-13 C]-serine (hereafter referred to as KHB+serine), and then cultured at 37 o C for 2h in differing combinations of: 6mM glycine, 4mM glucose, 4mM fructose, and KHB+serine. Medium without conceptus tissue (blank medium) was also assayed. Homogenates (culture medium plus lysate of conceptus tissue), medium following culture of

conceptus tissue, and blank medium were assayed for AA using high-performance liquid chromatography. Concentrations of AA in blank medium were determined and subtracted. Net concentrations of serine in culture medium per gram tissue were less than those for serine in blank medium, indicating serine uptake by conceptus tissue. However, when glycine was not present in the culture medium, conceptuses converted serine and hexose sugars into glycine and released it into the medium. Interestingly, concentrations of tryptophan were less in culture medium than blank medium, suggesting some interaction involving serine interconversion to tryptophan and its uptake by conceptus tissue. For concentrations of AA in conceptus tissue, the concentrations of AA in culture medium plus tissue lysate, minus blank medium, was expressed per gram of tissue. Conceptuses incorporated glycine and hexose sugars in the medium into significant amounts of serine, but in the absence of glycine, conceptuses converted serine and hexose sugars into glycine. Samples will be analyzed for [U-13 C]-formate to assess contributions of serine-derived carbon into the tetrahydrofolate cycle in the presence of fructose, glucose, or fructose plus glucose. Collectively, these results indicate that serine is extensively utilized, along with fructose and glucose, to contribute to both the glycine pool and one-carbon metabolism in conceptus tissue. This study highlights the importance of serine, glycine, fructose, and glucose metabolism to support proliferation and elongation of trophectoderm during the peri-implantation period of pregnancy. This project was supported by Agriculture and Food Research Initiative Competitive Grant 2018-67015-28093 from the USDA National Institute of Food and Agriculture.

Abstract # 1981

SWI/SNF -ARID1A And The Hippo Signaling Effector YAP1 Co-Localize During The Morula-To-Blastocyst Transition In Mouse Preimplantation Embryos. Chad Sdriscoll, Mohamed Ashry, Catherine Awilson, Jasong Knott

Early embryo development is dependent upon large-scale changes in chromatin structure which alter gene expression. Changes in chromatin availability are carried out by multi-subunit proteins collectively known as chromatin remodeling complexes. The SWI/SNF chromatin remodeling complex is a key regulator of development and disease. Loss of function studies in mice demonstrated that various SWI/SNF subunits are required during preimplantation development. Notably, work in our laboratory established that Brahma-related gene 1 (BRG1), a catalytic subunit of SWI/SNF complexes, is required for proper trophoblast lineage specification in blastocysts. For instance, we showed that BRG1 is required for the repression of pluripotency genes and activation of trophoblast linage genes. Recent studies in other cellular contexts found that the AT-rich interactive domain-containing protein 1A (ARID1A), a core SWI/SNF subunit, physically interacts with Yes-associated protein 1 (YAP1) to regulate gene expression. YAP1 plays a pivotal role in trophoblast lineage development by functioning as a key effector of the hippo signaling pathway. YAP1 along with Tea domain transcription factor 4 (TEAD4) upregulate trophoblast-specific genes while simultaneously repressing the pluripotency gene SRY-box 2 (Sox2). We hypothesize that ARID1A collaborates with YAP1 to alter chromatin structure at lineage-specific genes. As a first step to test this, we performed confocal immunofluorescence experiments in mouse preimplantation embryos during the morula-to-blastocyst transition. We found that ARID1A was ubiquitously expressed at the morula and blastocyst stages, localizing to the nuclei. In contrast and consistent with previous studies, YAP1 localized only to the nuclei of outside cells in morulae and blastocysts. In a second set of experiments we used a proximity ligation assay (PLA) to determine if YAP1 and ARID1A physically interact in the outer cells during blastocyst formation. This analysis revealed a modicum of ARID1A-YAP interactions in the outside cells of morulae which became highly enriched in the trophoblast lineage during blastocyst formation (n= 3 replicates, n=5 embryos/stage). In summary, our findings indicate that YAP1 and ARID1A may form a regulatory complex to regulate trophoblast lineage gene expression during early development. Future studies will utilize a combination of functional approaches, RNA sequencing, chromatin immunoprecipitation (ChIP) analysis, and chromatin remodeling assays to elucidate the functional relevance of ARID1A-YAP interactions in early mouse embryos. (Research was supported by NIH-HD095371, Michigan state university AgBioResearch).

Abstract # 2029

Morphokinetic Observation On The Preimplantation Development Of In Vitro Fertilized Mouse Embryos Using A Time-Lapse Incubator. Hiroyuki Watanabe, Hiroshi Suzuki

Since the first success of in vitro fertilization (IVF) in mice in 1968, components of culture medium as well as procedures of IVF have been substantially modified and improved. Recently, time-lapse incubator has been diffused especially in the field of human infertility treatment, and it has become possible to consecutive observation of culturing embryos. Time-lapse observation has advanced the understanding of the morphologic mechanisms of fertilization, development, and behavior of early embryos. In this study, preimplantation development of mouse oocytes fertilized in vitro was continuously assessed using a time-lapse incubator.

IVF zygotes were produced by spermatozoa and oocytes derived from ICR strain in a conventional CO2 incubator. At 6 h after insemination, the zygotes were cultured in a time-lapse incubator for 114 h at 37°C under different gas phases (High O2: 5% CO2 in air, or Low O2: 5% CO2, 5% O2, 90% N2). Time-lapse images of the developing embryos were captured at 15 min intervals. As a control, some zygotes were cultured in a conventional CO2 incubator (5% CO2 in air), and the embryonic development was observed every 24 h.

Developmental rates of embryos, cultured in a time-lapse incubator under the High O2 condition, to the 4-cell and morula stages at 48 and 72 h after insemination were 88.9% (845/951) and 61.8% (588/951), respectively. When the embryos were cultured under the LowO2 condition, the rates of embryonic development to the 4-cell and morula stages were 97.0% (288/297) and 78.1% (232/297), respectively. These

differences were significantly different at P<0.05. Similarly, the developmental rates to the blastocyst stage at 96 and 120 h after insemination were significantly higher in embryos cultured in the Low O2 condition (93.6 and 97.0%) in comparison with those of the High O2 condition (77.1 and 88.1%). When the embryos were cultured in a conventional CO2 incubator, 79.0% (79/100), 71.0% (71/100) and 84.0% (84/100) of them developed to the 4-cell, morula and blastocyst stages at 48, 72 and 96 h after insemination, respectively. The developmental rate to the 4-cell stage was significantly lower than that cultured in a time-lapse incubator under the High O2 condition. Under the time-lapse observation, compaction of mouse embryos began around 8-cell stage, and then the connection among the blastomeres loosened temporarily along with the further cleavage. Finally, the embryos were fully compacted at the 16-cell stage or later. There was no difference in the timing for initiation and completion of compaction between the High O2 and Low O2 conditions. The average values were 59.1 and 69.6 h after insemination for initiation and completion of compaction, respectively. Although more than 90% of embryos were compacting or compacted at 72 h after insemination, about 30% of them did not complete compaction yet. Thus, it is not appropriate to assess the developmental potential of in vitro fertilized eggs by developmental rate to morula at 72 h after insemination in classical microscopic observation.

Abstract # 2050

Ovine Conceptuses Utilize Fructose As A Substrate For The Pentose Phosphate Pathway During The Peri-Implantation Of Pregnancy. Robyn M. Moses, Avery Kramer, Claire Stenhouse, Katherine M. Halloran, Nirvay Sah, Heewon Seo, Gregory A. Johnson, Guoyao Wu, Fuller W. Bazer

Development of conceptuses (embryo and associated extra-embryonic membranes) in all species requires nutrients, such as glucose, to be metabolized to biomolecules essential for basic cellular processes such as proliferation, migration, and differentiation. Prior to implantation, the sheep conceptus elongates to increase surface area for contact with the maternal endometrium. Glucose has been considered to be the preferred substrate for enzymes serving many metabolic pathways. However, fructose has not been studied extensively despite being significantly more abundant than glucose in the uterine flushings and allantoic fluid of ungulates due to the conversion of glucose to fructose by the placenta. Our laboratory has demonstrated that in the absence of glucose, the ovine conceptus can use fructose in glycolytic reactions. We hypothesize that the ovine conceptus can metabolize fructose via the pentose phosphate pathway to generate NADPH and synthesize ribose for the formation of nucleotides for DNA synthesis. Suffolk ewes were bred to fertile rams in six groups of four ewes each on Day (D) 0 of estrus. On D16 of gestation, ewes were euthanized and hysterectomized. Conceptus tissue was flushed from the uterine horns in 15 ml sterile phosphate buffered saline and stored in 10 ml RPMI 1640 + glutamate media until used. Conceptus tissues were washed in Krebs-Henseleit bicarbonate (KHB) buffer, pooled

within group, thoroughly minced and mixed to ensure homogeneity. Then 20 mg of conceptus tissue were cultured in KHB buffer with either unlabeled glucose (4 mM), fructose (4 mM), or glucose plus fructose (4 mM each) and specifically labeled [1-14 C]glucose, [6-14 C]glucose, [1-14 C]fructose, or [6-14 C]fructose. At the end of culture, the 14 CO 2 produced by the conceptuses was measured by a liquid scintillation counter. Carbon contribution to the pentose phosphate pathway was determined as a difference between 14 CO 2 production from [1-14 C]glucose and that from [6-14 C]glucose, or as a difference between 14 CO 2 production from [1-14 C]fructose and that from [6-14 C]fructose. Conceptus tissue cultured with unlabeled alucose and fructose plus 14 C-glucose produced more CO 2 than 14 C-glucose and unlabeled glucose. Results from 14 C-fructose and unlabeled fructose in culture medium revealed that fructose was metabolized via the pentose phosphate pathway and, in the absence of glucose, produced more 14 CO 2 than cultures treated with 14 C-fructose with unlabeled glucose and fructose. These results indicate that in the absence of glucose, fructose can be metabolized via the pentose phosphate pathway, but the ovine conceptus preferentially uses glucose for that pathway when both glucose and fructose are present in equimolar concentrations. Because the concentration of fructose is about 10 to 30 times that of glucose in the allantoic fluid of sheep, fructose likely plays an important role in providing the fetuses with NADPH and ribose for biosynthetic pathways. This research was supported by Agriculture and Food Research Initiative Competitive Grant no. 2018-67015-28093 from the USDA National Institute of Food and Agriculture.

Abstract # 2122

Alternative Splicing Events During The Transition From Maternal To Embryonic Control In Mice. Isabel Gómez-Redondo, Alfonso Gutiérrez-Adán

Oocyte to embryo transition involves a dramatic reprogramming of gene expression and conversion of a differentiated transcriptionally guiescent oocyte to totipotent blastomeres. During this event, maternal mRNAs are degraded, and the embryo starts generating its own transcripts, taking control of its gene expression program. Alternative splicing (AS) is an essential mechanism that allows the generation of multiple transcripts and protein variants, or isoforms, from a single gene, and must be tightly regulated during early development. However, the precise timing of developmental splicing switches and the underlying regulatory mechanisms are poorly understood. Different studies have shown that promiscuous transcription lacking 3' processing or splicing occurs specifically at the zygote stage in minor zygotic genome activation (ZGA), and that transposons and intronless genes are over-represented during early 2-cell stage in mice; suggesting absence of spliceosome functionality. However, it is unknown the role of splicing in major ZGA. To elucidate these AS dynamics, we carried out RNA-seq analyses using pools of 150 oocytes from 3-months-old mice, and pools of 100 late 2-cell stage embryos (12h after the first cleavage and the beginning of the ZGA). Alternative splicing was assessed using vast-tools software, determining the levels of inclusion of

each transcript, and keeping solely those events that passed the standard quality filter in both analyses. With these data, we categorized the intron retention (IR) and exon skipping events, and the differential usage of 5' and 3' splice sites for each group. Gene Ontology enrichment was performed with DAVID software v6.8. Repetitive elements annotation was obtained from RepeatMasker 4.1.0. Firstly, we analyzed the gene expression pattern of the late 2-cell embryos, being those highly expressed (first quartile) enriched in key processes for the cell, as the rRNA and mRNA processing, mRNA splicing, and the ribosome biogenesis and assembly. We then characterized the inclusion of 31,281 introns in both groups, being 1,410 significantly more retained in the oocyte (Δ PSI >10%), and 2,499 in the 2-cell embryos. Regarding exon skipping, 1,826 and 969 events were upregulated in the oocyte and in the late 2-cell stage embryos, respectively. In the case of differential usage of 5' and 3' splice sites, the usage of the canonical splice site was similar in both cases. We characterized the expression of SINEs, LINEs and LTRs within genes that showed intron retention in the oocytes, obtaining expression of transposable elements in more than 50% of those genes. In the late 2-cell embryos, the expression was even higher, detecting overlapping SINEs, LINEs and LTRs in 86.2%, 75.3 and 76% of the genes with intron retention, respectively. Remarkably, ERVL-LTR type transposons were significantly enriched (p<0.00001) in all genes showing intron retention. This strongly suggests that unlike what happens in minor ZGA, the spliceosome is functional during major ZGA and transposable elements and retention of intronic sequences seem to be regulating gene expression during the oocyte-to-embryo transition, playing a functional role in major ZGA. Research supported by the Spanish Ministry of Science through BES-2016-077794 predoctoral grant.

Abstract # 2146

Effects of WNT5A on the Developmental Competency of Bovine Embryos Produced in Vitro. Surawich Jeensuk, PeterJ. Hansen

WNT signaling is important for regulation of many developmental processes including during the preimplantation period. In the cow, the most abundant WNT gene expressed in the endometrium during the preimplantation period is WNT5A. Nonetheless, the role of this WNT in regulation of the preimplantation embryo is unknown. The objective was to determine the effects of WNT5A on development of bovine embryos produced in vitro. We hypothesized that WNT5A enhances the capability of embryos to become blastocysts and alters the numbers of trophectoderm (TE) and inner cell mass (ICM) cells in the blastocyst. Ovaries from a slaughterhouse were used to obtain oocytes. Oocytes were fertilized using conventional semen. Presumptive zygotes (n=3009; n=14 replicates) were divided into 4 groups and cultured in synthetic oviductal fluid – bovine embryo 2 for 7.5 days. On Day 5 of development, embryos were treated with recombinant human/mouse WNT5A (Gln38-Lys380; 100% identical with bovine) at 0, 50, 100, or 200 ng/ml. Each treatment contained the same amount of carrier solution. For a subset of 5 replicates, an additional treatment of 400 ng/ml WNT5A was included (n=238 presumptive zygotes). The number of embryos becoming blastocysts in each group was

evaluated on day 7.5. A subset of blastocysts (n=88; 0 to 200 ng/ml only) was labeled with primary antibody against CDX2 and Hoechst 33342 to determine number of total cells (Hoecsht), trophectoderm (TE) cells (anti-CDX2) and inner cell mass (ICM) cells (total minus TE). The percent of presumptive zygotes that cleaved was not different between groups. The percent of cleaved embryos developing to the blastocyst stage was higher (P=0.02) for 200 ng/ml (50.5±2.2%) than for 0 (41.6±2.1%), 50 (44.8±2.2%), or 100 ng/ml (42.7±2.1%). Similar results were found when examining the percent of presumptive zygotes becoming blastocysts. There was no effect of 400 ng/ml WNT5A on development, however. For the 5 replicates with 400 ng/mL WNT5A, the percent of cleaved embryos becoming blastocysts was 37.7±4.8% for 400 ng/mL vs 38.9±4.8% for 0 ng/ml. Blastocysts from the 200 ng/mL group had an increased (P=0.01) number of ICM (54.2±3.0 vs 48.0±3.0, 42.1±3.3, or 46.0±2.8 for 0, 50, or 100 ng/mL, respectively) and a lower TE:ICM ratio compared to the other groups. Results indicate that WNT5A can enhance competence of embryos to become blastocysts and increase blastocyst ICM cell number at a narrow range of concentrations, with 200 ng/mL being stimulatory. Work is consistent with a possible role for WNT5A signaling in development of the bovine embryo. Research support: USDA-AFRI 2017-67015-26452.

Abstract # 2178

Association of IRF7 and BOLA variants with Early Embryo Mortality Pregnancies in Holstein cows. Carolina L. Gonzalez-Berrios, Courtney F. Pierce, Jeanette V. Bishop, Hana Van Campen, Thomas R. Hansen, Milton G. Thomas

Identifying single nucleotide polymorphisms (SNPs) linked to disruption in maternalconceptus crosstalk can assist with genetic improvement of fertility traits in Holstein cows. It was hypothesized that early embryo mortality (EM) conceptuses are associated with intragenic SNPs that impair maternal-conceptus communication during maternal recognition of pregnancy. Cows were randomly selected and sorted into artificially inseminated (AI; n=15) or controls on day 16 of the estrous cycle (EC; n=7). Al pregnant cows were re-sorted by conceptus morphology at day 16 of pregnancy: EM (n=6) were pink, red, opaque and/or restricted in elongation and normal (N) conceptuses (n=9) were translucent and elongated. RNA was extracted from conceptus and endometrial tissue and submitted to RNA-Seg analysis. Sequences were aligned to ARS-UCD 1.2 bovine assembly, trimmed and processed for SNP discovery using CLC Genomics Workbench. Resulting documents for only N and EM conceptuses were divided for allelic frequencies of 1.00 and merged to find in-common or unique SNPs. Unique EM conceptus SNPs were submitted into STRING and KEGG to identify gene clusters in key biological pathways. Genes were evaluated for raw mRNA counts (RNA-Seq), type of SNP variant and loci relevance (CattleQTLdb) to fertility traits. A total of 352 SNPs were in-common between EM and N conceptuses and 155 for N and 468 for EM were unique. Using these data, KEGG identified three key biological pathways (P<0.001) for unique EM SNPs: viral myocarditis, graft-versus-host disease and allograft rejection. Within these pathways, two non-synonymous SNPs were selected within previously

identified quantitative trait loci for cow conception rate and daughter pregnancy rate. A T/A SNP (chromosome 23; exon 3, rs449657233; Phe to Tyr) was observed in the BOLA gene, which is the bovine equivalent of human major histocompatibility complex I and may cause immunosuppression for maternal-fetal tolerance during early pregnancy. Whereas a C/G SNP (chromosome 29, exon 8, rs383424307; Leu to Val) was observed in the IRF7 gene and was associated with physiological activities of type I interferons such as interferon tau (IFNT) known as the signal for maternal recognition in ruminants. IRF7 mRNA raw counts were higher (P<0.04), while BOLA mRNA raw counts tended (P<0.059) to be higher in EM compared to N conceptuses. These two SNPs and transcriptome responses in EM conceptuses may be associated with increased gene expression and warrant further study. We reported that IFNT mRNA transcript raw counts were greater (P<0.0001) in N than EM conceptuses. While, IFN gene 15 (ISG15) mRNA raw counts were greater (P<0.003) in N and tended (P<0.09) to be greater in EM compared to EC endometrium. Presence of unique SNPs associated with upregulation of IRF7 and BOLA mRNA may reflect a hyperstimulation of type I IFN pathways to induce IFNT production and conceptus protection, eventually failing during EM pregnancies. Further analyses of these genetic markers, especially in-context of consequences of amino acids changes for EM pregnancies may help reveal candidate genes and causal mutations that may be essential for embryo survival, maternal-conceptus crosstalk and pregnancy in lactating Holstein cows. USDA-AFRI-NNF 2016-38420-25289 and Zoetis, Inc.

Abstract # 2224

Abnormal Gene Expression And Methylation Patterns Of X-Chromosome and KCNQ1 Imprinted Loci During Early Development Of Haploid Androgenetic Bovine Embryos. Luis Aguila, Jacinthe Therrien, Lawrence C. Smith

Uniparental haploid embryos are unique models to investigate parental-specific contributions of genomic imprinting to early development. Our previous studies with bovine uniparental zygotes have indicated that, in comparison to haploid parthenogenetic counterparts, haploid androgenetic embryos (hAE) carrying an Xchromosome show poor development beyond the morula stage, suggesting that the paternal genome is developmentally disadvantaged to support the initial differentiation events necessary for early embryonic development. We hypothesize that parental-specific epigenetic dimorphisms between the maternally- and the paternallyinherited genome are at the core of such developmental restrictions. To further investigate the causes of such parental-specific dimorphism, in vitro matured oocytes were fertilized and enucleated to obtain haploid androgenones, which were compared to diploid and haploid parthenogenetic counterparts. We evaluated blastocyst development, pronuclear formation, karyotype, blastocyst quality, gene expression of X-linked genes (XIST, PGK1, HPRT) and imprinted KCNQ1OT1-control region, and the methylation patterns of the differentially methylated regions (DMRs) controling the imprinted expression of XIST and KCNQ1OT1 genes. Our results showed that pronuclear formation was similar among groups and, although all groups cleaved

efficiently (>65%), further preimplantatory developmental was severely affected in haploid embryos (15% and 4% for parthenates and androgenates, respectively), compared to diploid counterparts (>25%). Blastocyst quality, according morphological parameters and cell number was also affected in haploid embryos (40-60 cells/blastocyst) compared to control groups (>100 cells/blastocyst). The karyotypic analysis revealed that hAE had stable karyotypes compared to control parthenogenetic groups. In addition, hAE exhibited a significant 2-fold increase of XIST transcripts. In the case of the PGK1 transcript, hAE only showed significant differences with male embryos, and there were no differences among HPRT expression levels. KNCQ10T1 and maternally expressed genes (CDKN1C, PHLDA2, and TSSC4) also were upregulated in hAE compared to the diploids. Finally, the analysis of methylation marks showed that hAE had altered patterns in both the KNCQ1OT1 and XIST DMRs. In conclusion, we demonstrate that hAE show dysregulated gene expression and altered methylation patterns, suggesting that epigenetic constrains may be involved in the poor development of androgenetic embryos beyond transcriptional activation. Further experiments are being performed to identify the molecular mechanisms involved in the development restriction of bovine hAE.

Abstract # 2245

A New System for Evaluating Protein Interactions in Blastocysts Using the IMARIS Program. Lyda Y. Parra-Forero, Rachel Braz-Arcanjo, María I. Hernández-Ochoa, Jodi A. Flaws, Romana A. Nowak

The blastocyst undergoes cell differentiation and guarantees its survival through activation and inactivation of multiple proteins and transcription factors. For decades, blastocyst differentiation has been assessed by considering only activation and inhibition of proteins, but not their interactions. However, with the advent of computational biology new theories on blastocyst cell differentiation have emerged. In this study, we propose a new method to evaluate protein interactions in blastocysts. The expression of three pluripotency markers, GATA6, OCT4 and CDX2 was assessed in expanded blastocysts from female CD-1 mice. Micrographs were captured by confocal microscopy, and then digitized with the IMARIS program to obtain topographic maps in 2D and 3D by means of quantification of central fluorescence by voxel. We performed analyses, including comparison of the maximum intensity projection, quantitative intensity level in different blastocyst sites, and the uniformity of fluorescence intensity at a specific site. The data showed that each assessed protein in the expanded blastocyst had different intensity patterns. Surprisingly, we found markers that were considered specific for inner cell mass cell (ICM) within trophoblast cells in different proportions (mean ± standard error of the mean (Voxels number)). ICM: GATA6= 183x10 3 ± 35x10 3 , OCT4= 110x10 3 ± 54x10 3 and CDX2= 78x10 3 ± 36x10 3 while in the trophoblast we founded: GATA6= $76x10.3 \pm 47x10.3$, OCT4= $55x10.3 \pm$ 22x10 3 and CDX2= 144x10 3 ± 45x10 3. These results allow us to conclude that there are various patterns of GATA6, OCT4 and CDX2 expression, which involve a dynamic of

unknown expression in the cells of the ICM and the trophoblast. These preliminary results provide evidence supporting that the IMARIS program may be used to study protein interactions in the blastocyst. Due to the large number of variables detected by the IMARIS program, our laboratory continues evaluating algorithms to establish a quantitative score that correlates the dynamics of protein expression with its biological function

Abstract # 2250

Choline Chloride And An Inhibitor Of Choline Kinase A Alter The Phenotype Of Bovine Blastocysts. Eliab Estrada-Cortes, Yao Xiao, Mohammad-Zaman Nouri, Nancy D. Denslow, Peter J. Hansen

Addition of choline chloride (ChCl) to culture medium of bovine embryos produced in vitro programmed development of resultant calves after embryo transfer by increasing birth and weaning weight. Choline is a precursor for phosphatidylcholine (PC), the major phospholipid of cell membranes. Abundance of specific phospholipids may alter membrane lipid composition and cell function. The objective was to determine whether addition of choline chloride or choline kinase a inhibitor (CHKa; first enzyme in the pathway to synthesize PC from ChCI) to culture medium alters the phenotype of in vitroproduced blastocysts. In Experiment 1 (n=15 replicates 240 per treatment), presumptive zygotes (PZ) were incubated in BBH7 culture medium with 0.0, 0.004, 1.3, or 1.8 mM ChCl (treatments were isotonic). Concentrations of ChCl approximated free choline (0.004 mM) and total choline in plasma of cows at week 1 postpartum (1.30 mM) and total choline in plasma of cows fed rumen-protected choline (1.8 mM). Cleavage and blastocyst rate were evaluated at days 3 and 7.5 post insemination, respectively. Blastocysts (n=99) were used to evaluate lipid droplet content by measuring fluorescence of Nile Red and to evaluate blastocyst cell number (n=204) by accounting nuclei labeled with propidium iodide. Pools of 10 blastocysts (n=22) were evaluated by LC MS/MS using a targeted method for 1127 lipid species (n= 490 detected) which identified 15 major subgroups. Cleavage rate (%) for 0.0, 0.004, 1.3, or 1.8 mM ChCl, respectively, was 78.2±1.8, 77.8±1.8, 76.5±1.9 and 78.5±1.8 (P=0.7725); blastocyst rate (%) was 36.2±2.7, 43.8±2.8, 39.8±2.8, and 39.8±2.8 (P=0.0626); blastocyst cell number was 121.7±5.2, 140.2±4.5, 121.2±4.8, and 127.1±6.1 (P=0.008); and lipid droplet content (fluorescence intensity) was 409.1±54.3, 542.3±62.3, 651.3±54.3 and 583.9±55.0 (P=0.0139). For lipid subgroups that were statistically different among treatments, total concentrations (µM) of triacylglycerols were 117.8±14.3, 47.3±14.3, 86.8±12.7, and 89.2±12.7 μM (P=0.0304) and lysophosphatidylethanolamines were 0.149±0.004, 0.159±0.004, 0.165±0.003, and 0.171±0.003 µM (P=0.0050). In Experiment 2 (n=5), PZ were incubated in BBH7 with 0.0, 5.0, 10.0, or 20 µM CHKa inhibitor to evaluate lipid content (n=172). Cleavage rate was 81.3±2.5, 81.4±2.5, 82.0±2.4 and 82.6±2.4 (P=0.9568); blastocyst rate was 50.4±5.1, 43.7±5.0, 47.2±5.1 and 49.4±5.1 (P=0.3591); and lipid content was 38.3±2.2, 33.7±2.2, 31.6±2.2 and 29.3±2.2 (P=0.0381) for 0.0, 5.0, 10.0, or 20 µM CHKa, respectively. In conclusion, addition of ChCl or an inhibitor of CHKa to culture

medium alter the phenotype of in vitro-produced blastocysts. ChCl increased blastocyst cell number, lipid droplet content, and altered lipid composition of blastocysts in a concentration-dependent manner. CHKa inhibitor reduced lipid content (Support: Larson Endowment and Balchem).

Abstract # 2360

Knockdown of cd26 by siRNA Injection During Porcine Preimplantation Embryonic Development. Mi-Ryung Park, Tae-Uk Kwak, Yeongi Kim, In-Sul Hwang

CD26 (Dipeptidyl peptidase IV/DPP-4) is a 110 kDa cell surface alycoprotein that belongs to the serine protease family and is expressed on a variety of tissues, including T lymphocytes, endothelial cells, and epithelial cells. It is composed of a short cytoplasmic domain, a transmembrane region, and an extracellular domain with dipeptidyl peptidase IV activity. The present study aimed to investigate the effect of CD26 in porcine parthenogenetic embryos. We attempted CD26 downregulation of porcine embryos by siRNA, and evaluated CD26 related suppression of developmental competencies. Of 17,663 transcripts evaluated by transcriptome resequencing, 579 genes were differentially expressed between treatment and control embryos at the blastocyst stage (P<0.05). Of these 579 genes, 306 were more highly expressed in CD26 siRNA injected blastocysts, whereas 273 were downregulated. Among these 576 genes, some showed either highly significant decrease or increase in gene expression in the CD26 treated blastocysts. These genes involved in heat shock protein, cell cycle molecule, ATP synthesis, apoptosis, mitochondria metabolism, transport and transcription. Our results indicated that CD26 is an important factor for the regulation of development of porcine embryos.

Reproductive Aging

Abstract # 1973

Inflammation Contributes To Follicle Depletion During Maternal Ageing In Mice. Carolina Lliberos, Seng H. Liew, Ashley Mansell, Karla Hutt

Female reproductive ageing is characterised by a progressive decline in oocyte number and quality, leading to the loss of ovarian function, cycle irregularity, infertility and eventually menopause. The mechanisms that underlie the natural depletion of follicles throughout reproductive life are poorly characterised. In this study, we investigated the hypothesis that inflammation contributes to the loss of follicles as females age. We first determined follicle numbers and characterised the systemic and local ovarian inflammatory phenotype in C57/BI6 mice at 2, 6, 12 and 18-months of age. This period of time spans the onset of sexual maturity to the end of female fertility in mice. We observed that the decrease in follicle numbers over the reproductive lifespan was associated with an increase in the serum concentration and intra-ovarian mRNA and protein levels of pro-inflammatory cytokines IL-1a/β, TNF-a, IL-6, IL-18, and inflammasome proteins ASC and NLRP3. To gain further insight into the possible role of the NLRP3 inflammasome in follicle depletion, we compared follicle numbers in wild type (WT), nlrp3 -/- and asc -/- mice (n=3-6/genotype). We found that the primordial follicle reserves were elevated in aged asc -/- and nlrp3 -/- mice relative to agematched WT mice (WT= 191±62 vs asc -/- = 1122±493, p =0.0130; vs nlrp3 -/- = 700±220, p =0.0195). The number of primary and growing follicles, as well as corpora lutea, were also significantly higher in inflammasome-deficient mice. Consistent with follicle data, serum AMH levels were significantly increased in 12-month-old asc -/- compared to WT mice (WT= 9.27 ± 1.04 vs asc -/- = 16.08 ± 1.33 , p = 0.0022). Notably, expression levels of major pro-inflammatory cytokines within the ovary (e.g. Infa, II1a and II1b) were significantly lower in aged asc -/- mice compared to WT (Infa: WT= 2.02±0.14 vs asc -/- $= 0.87 \pm 0.23$, p = 0.0087). A significant decrease was also observed in the serum levels of several inflammatory cytokines in asc -/- mice relative to age-matched WT mice (TNF-a: WT= 10.96 \pm 5.02 vs asc -/- = 0.47 \pm 0.47, p =0.0281). These data suggest that inflammation contributes to the age-associated depletion of follicles and raises the possibility that ovarian ageing could be delayed, and fertility prolonged, by suppressing inflammatory processes in the ovary.

Abstract # 2037

Epigenetic Drivers of Ovarian Germ Cell Niche Aging. John S. Davis, David L. Klinkebiel, Jitu W. George, Barbara A. Weaver, Xiaoying Hou

The ovary is uniquely situated as both a reproductive organ and an endocrine gland. Granulosa cells (GC) engender a paracrine milieu creating a nurturing germ cell niche. Advanced age is correlated with decreased expression of DNMT1 a DNA methylase, and global DNA demethylation. Conversely DNMT3 another DNA methylase is overexpressed leading to promoter CpG islands hypermethylation. It was the objective of these studies to better understand if ovarian germ cell niche epigenetic profile, at specific loci correlates with chronological aging and altered GC pathway function. GCs were obtained from in vitro fertilization (IVF) patients (with informed consent) following oocyte retrieval. Six patients in each of four groups of ≤32 yr and >39 yr and oocyte yields <7 and >16 oocytes were studied. GC genomic DNA methylation was measured with the Illumina Infinium Human Methylation EPIC BeadChip (850K). Following principle component analyses two patients from each group were excluded. 562 differentially methylated DNA regions (DMR) with decreased and 45 regions with increased methylation were detected in gene promoters defined by -2,500 to +2,500 relative to the transcription start in the patients of advanced reproductive age compared to the younger patients (P<0.0001). DMR of genes that were shared by all patients in either of the two age groups had a role among others in proliferation/apoptosis. Predicted activation of immune cell pathways and proinflammatory pathways were most prominent in advanced age patients, whereas apoptosis pathways were decreased as discussed below. RNA seq was used to explore this further comparing only young (n=4) and advanced age patients (n=4) who were high responders. MEIS1 a transcriptional activator of PAX1/BMP/TGFbeta pathways which is expressed at all stages of follicular development was tightly correlated with a specific locus (R2 > 0.97). Pyrosequencing confirmed MEIS1 was less methylated in GCs of older patients [MEIS1(Pyro) Locus chr2:66437739: % methylation, 24 ± 3.1 vs 14 ± 1.5 in GCs of young vs older patients, n=6, P < 0.001] and following Ingenuity Pathway Analyses its relative expression was reported as 4.42-fold. Likewise, AKAP2 which plays a role in PKA pathway showed a 2.11-fold increase in the advanced age group. EREG or Epiregulin, an EGF family member which binds to EGFR and is important in GC FSH response was elevated 2.12-fold. Both IL8 and IL1B expression were 3.50 and 3.09-fold higher respectively in older patients and are both implicated in premature ovarian insufficiency. For example, IL1 deficient mice have a prolonged ovarian life span. FAM65C relative expression (augments FSH signaling and marker for age) was increased four-fold compared to younger patients. Conversely expression of tumor suppressor gene RHOBTB3 was reduced (0.51 fold) again pointing to an antiapoptotic effect. Despite no significant difference in methylation, there was a severe suppression of anti mullerian hormone AMH expression in the advanced age group, despite no difference in oocyte production. For high responders age related demethylation of these genes had no negative consequence on oocyte production in the age range studied but may become an important modifier in advanced reproductive aging. Support: Olson Center for Women's Health.

Codon Identity In Human Oocytes Reveals Age-Associated Defects in mRNA Decay. Nehemiah S. Alvarez, Pavla Brachova, Lane K. Christenson

Codon composition of mRNA is an emerging factor that affects both translational efficiency and mRNA stability. Codons that facilitate rapid translation promote mRNA stability and are considered optimal, while codons that slow translational efficiency destabilize mRNA, and considered non-optimal. We assessed the codon composition of mRNA in human germinal vesicle (GV) oocytes and metaphase II (MII) eggs from women of young (YNG, <30 yrs) and advanced maternal age (AMA, ≥40 yrs) to examine the relationship between codon composition and mRNA stability. We observed that non-optimal codons are enriched at the 5' end of the coding region in human oocyte and egg transcripts. In AMA samples, we observed a global increase of codon stability during the GV-to-MII transition. Among the transcripts that were commonly expressed in YNG and AMA, transcripts with non-optimal codons were retained in AMA oocytes, but degraded in YNG oocytes. Furthermore, an analysis of protein mass spec data during the human GV-to-MII transition of YNG women revealed that transcripts enriched in non optimal codons resulted in early peptide truncations. Our data indicates that maternal aging causes defects in translation, which result in increased translational efficiency and the retention of maternal mRNA that are degraded in YNG oocytes. These results are important because they show that analyzing the relationship of codon composition to mRNA stability can illuminate the quality of the translational program in cells. In the case of oocytes, defects in translation can alter the RNA decay pathways and result in incorrect maternal mRNA dosage, which may negatively impact embryonic development.

Reproductive Cancers

Abstract # 1837

Plasma Gelsolin: A Mediator Of Ovarian Cancer Chemoresistance And An Inhibitor Of CD8+ T-cell Function. Meshach Asare-Werehene, Laudine Communal, Hideaki Tsuyoshi, Huilin Zhang, Euridice Carmona, Anne-Marie Mes-Masson, Yoshio Yoshida, Dylan Burger, Benjamin K. Tsang

Ovarian Cancer (OVCA) is the leading cause of death in gynecologic cancer. Although combined surgical debulking and chemotherapy is an important treatment strategy, chemoresistance remains a major challenge for long term therapeutic success. Tumor-derived soluble factors down-regulate immune cells which influence the responsiveness of cancer cells to chemotherapy. Although exosomes are involved in cell-cell communications, their role in chemoresistance in OVCA is unclear. We have previously shown that increased gelsolin (GSN) overexpression in gynecologic cancers is significantly associated with chemoresistance, poor prognosis and cancer deaths; however, whether these effects are associated with the secreted plasma gelsolin (pGSN) or the cytosolic gelsolin (cGSN) Isoform, is unknown. Here, we hypothesize that exosomal pGSN derived from chemoresistant OVCA cells confers resistance in chemosensitive OVCA cells, regulate glutathione (GSH) production and suppresses the anti-tumor functions of CD8+ T-cells. The overall objective is to determine if and how OVCA cell-T cell interactions regulate chemosensitivity and how deregulation of these interactions modulate tumor microenvironment (TME) and tumor chemosensitivity. Clinical and in-vitro studies with OVCA cell lines of various histologic subtypes [high arade serous (HGS), endometroid and clear cell], human peripheral CD8+ T-cells, OVCA patient tissue microarray (TMA; Centre hospitalier de l'Université de Montréal; n=208), OVCA tissues (University of Fukui Hospital; n=95) and OVCA TCGA datasets (n=1,259) were used. T-cell and OVCA cells cultures/co-cultures, gain- and loss-infunctions studies, extracellular vesicle dynamics, apoptosis, cytokine and immune profiling and protein expression were assessed with standard molecular and cellular techniques to determine the mechanisms involved in pGSN-mediated immune suppression and OVCA chemoresistance. We have shown that increased expression of tissue pGSN is significantly associated with advanced tumor stage (p<0.01), poor survival (p<0.01), chemoresistance (p<0.01) and suboptimal residual disease (p<0.05). Elevated pGSN levels diminish the favorable prognostic impact of infiltrated CD8+T on patient survival (p=0.02). Our interrogation of OVCA TCGA datasets revealed that patients with increased pGSN mRNA expression had shortened progression-free and overall survival compared with patients expressing lower amount regardless of the chemotherapeutic agent. pGSN secreted and transported via exosomes, up-regulates HIF-1a-mediated pGSN expression in chemoresistant OVCA cells in an autocrine manner and confers cisplatin resistance in otherwise chemosensitive OVCA cells. Exosomal pGSN activated the Nuclear factor erythroid 2-related factor 2 (NRF2) pathway leading to increased production of GSH, a response attenuated cisplatininduced death. In chemosensitive condition, exosomal pGSN secretion is low hence

allowing an optimal CD8+ T-cell function. This resulted in optimal IFNY secretion, STAT1 phosphorylation in the OVCA cells, reduced GSH production and increased CDDP-induced apoptosis. In the chemoresistant condition, increased exosomal pGSN secretion by OVCA cells induced caspase-8/3-dependent apoptosis in CD8+ T-cells. IFNY secretion was therefore reduced, a response that resulted in high GSH production and CDDP resistance in OVCA cells. These findings suggest that pGSN may play a role in immune-modulation and chemoresistance in OVCA, providing novel insights into the coldness (poor immune infiltration and function) of OVCA and suggesting an efficient alternative therapy. (Supported by grants from the Canadian Institutes of Health Research, Ovarian Cancer Canada and the Mitacs Globalink Award).

Abstract # 1969

Characterizing Abnormal Cell Populations Using Single Cell RNA-Seq In Adult Uterine Endometrium From Neonatally DES-Exposed Mice. Elizabeth Padilla-Banks, Wendy N. Jefferson, Alisa A. Suen, Brian Papas, Xin Xu, Carmen J. Williams

Exposing mice to the synthetic estrogen diethylstilbestrol (DES 1 mg/kg) from neonatal days 1 to 5 results in a high incidence of uterine cancer in adult mice. Our laboratory previously identified abnormal uterine epithelial cell populations in DES-exposed mice. Aberrant expression of Krt14, Trp63 and Six1 within these cells may contribute to abnormal endometrial tissue differentiation and the development of cancer. The goal of the current study was to characterize these abnormal cell populations and their gene signatures. To do this we isolated single cells from 12 month-old adult mouse endometrium and performed single cell RNA-sequencing (scRNAseq) to identify subpopulations and characterize gene expression differences in cells from DES-exposed mice compared to controls (CON). We successfully sequenced >10,000 cells for both CON and DES. Using t-SNE plots we identify clusters of the most typical cell types found in uterine tissues. Heat maps of all uterine cell types revealed distinct differences between cells from CON and DES-exposed mice. In particular, mesothelial cells and epithelial cells clustered independently based on treatment group due to dramatic changes in transcriptional profiles. There was also a striking lack of stromal cells isolated from the DES-exposed mice. Aberrant expression of Krt14, Trp63 and Six1 was found in the cell cluster identified as epithelial cells. Cluster analysis of epithelial cells alone revealed a distinct subcluster enriched for Krt14, Trp63 and Six1; this cluster represented basal cells. There were also Six1+ epithelial subclusters that were outside of the basal cell cluster and characterized by high Olfm4, Prap1, and Upk1a. Glandular epithelial cells also clustered into a separate subcluster of CON cells but were not found in DESexposed cells. The glandular epithelial cells were characterized by high Foxa2, Prss28, Prss29, Spink2 and Ttr. Although several clusters of DES-exposed epithelial cells expressed Foxa2, no other gland markers were observed in these clusters, suggesting lack of normal glands in DES-exposed mice. Potential stem cell populations were also found in both CON and DES groups, characterized by high levels of Aldh1a1, Lgr5, Wnt7a and Msx1. Cancer markers were observed in several subclusters in cells from DES-exposed

mice and included Jag2, Hprt, Olfm4 and Aurka. Analysis of the GO categories for genes expressed in these cell subclusters revealed pathways related to regulation of cell migration and vasculature development. Future experiments using this method will help elucidate specific genes changes involved in the formation of the abnormal basal cell phenotype and determine markers of abnormal cell differentiation that may lead to the development of cancer.

Abstract # 2025

MiR-10a Overexpression And Chemoresistance In Ovarian Clear Cell Carcinoma. Kaitlyn E. Collins, Xiyin Wang, Kenneth P. Nephew, Chad J.Creighton, Devin E. Jones, Shannon M. Hawkins

Ovarian cancer is the fifth leading cause of cancer-related death in US women. The most common cause of death in women with ovarian cancer is chemoresistant disease. Ovarian clear cell carcinoma (OCCC) is the histological subtype with the highest rate of chemoresistance, leading to decreased survival rates, even compared to the more common high-grade serous carcinoma. Endometriosis, a chronic inflammatory condition where endometrial-like tissue grows outside of the uterus, is a significant risk factor and precursor lesion for OCCC. To study the molecular contributions, poly-A-RNA sequencing was performed on OCCC from women with concurrent endometriosis. Because miRNAs are known to be differentially expressed in both ovarian cancer and endometriosis and regulate large gene networks and signaling pathways, small-RNA sequencing was also performed, allowing miRNA:mRNA target integration. Analysis of sequencing identified 4799 dysregulated genes (2223 up, 2576 down; P<0.01, log2fold change > ± 1) and 66 differentially expressed miRNAs (19) up, 47 down; P<0.05, fold change > ± 1.2) in OCCC compared to endometrioma. MiR-10a was identified as the most abundant dysregulated miRNA and 11-fold overexpressed in OCCC. Overexpression of miR-10a plays a role in chemoresistance and poor survival in other cancers, including breast and cervical cancer. Importantly, expression of miR-10a was 3-fold higher in a platinum-resistant A2780 cell line compared to the non-platinum-resistant A2780 line. In vitro carboplatin-chemoresistance testing with human OCCC cell lines identified a positive correlation of half maximal inhibitory concentration (IC50) of carboplatin and basal miR-10a expression [R2=0.70]. Lentiviral transduction systems were used to overexpress miR-10a in multiple OCCC cell lines with low basal expression. Overexpression of miR-10a increased carboplatin IC50 to resistant concentrations in the SMOV-2 OCCC cell line. MiRNA;mRNA target integration analysis of predicted miR-10a target genes, which are downregulated in human OCCC with concurrent endometriosis, revealed target genes that may be involved in the mechanism of OCCC chemoresistance. Understanding the role of miR-10a and its target genes in OCCC chemoresistance is critical to solving a significant clinical problem. This work was supported by a predoctoral training fellowship through the Cancer Biology Training Program.

Regulation of Cellular Communication Network Factor 1 (CCN1) by Signal Transducer and Activator of Transcription 3 (STAT3) and Calcium in Ovarian Adenocarcinoma (OVCAR8) Cells. Sarah M. Piet, Paul C. Tsang, Sarah R. Walker

Within the ovary, angiogenesis is not only integral to the formation of the corpus luteum and follicular development, but it is also a hallmark of tumorigenesis and tumor progression in ovarian cancers. Formerly known as Cysteine rich 61-Connective tissue growth factor-Nephroblastoma overexpressed 1 or cysteine-rich 61 (CYR61), CCN1 promotes angiogenesis and is associated with various pathologies including cancer. However, among the key angiogenic factors within the ovary, the regulation of CCN1 remains not well characterized. In the present study, our objective was to determine the roles of STAT3 and calcium in the regulation of CCN1 in OVCAR8 cells. In several ovarian cancer cell lines, including OVCAR8, STAT3 activity is elevated and is capable of promoting angiogenesis. To ascertain the possibility of STAT3 promoting angiogenesis via the regulation of CCN1, STAT3 activity was manipulated using a STAT3 silencing (si)RNA construct. After a 48-hour incubation with the siRNA, the cells were serumstarved for 4 hours and analyzed via quantitative polymerase chain reaction (qPCR). Treatment of cells with the STAT3 siRNA resulted in a 2-fold increase (p < 0.05; n = 6) in CCN1 expression over the cells treated with the control siRNA. Contrary to this result, the endogenously high STAT3 activity in OVCAR8 cells, i.e., in the absence of siRNA, inhibited CCN1 expression (p<0.05, n=3). Interestingly, even in this high STAT3 environment, the addition of a calcium ionophore (0.1, 0.5, 1uM) increased CCN1 expression in OVCAR8 cells (p<0.05; n=3). And, when OVCAR8 cells were incubated for 48 hours with STAT3 siRNA prior to treatment with the calcium ionophore (0.1, 0.5, 1uM) for 2 hours, CCN1 expression increased by 2-fold (p<0.05; n=3). Based on these results, a direct interplay between STAT3 and calcium signaling is unclear. Currently, we have begun to investigate cyclic adenosine monophosphate response element binding protein (CREB) as a potential link between these two signaling pathways. Given that CREB was shown to regulate CCN1 via calcium signaling in lymphoma cells, whether it has similar actions in OVCAR8 cells needed to be verified. Addition of a calcium ionophore (0.1, 0.5, 1uM), alone, increased CREB expression (p<0.05; n=3) in OVAR8 cells. Further, incubation with CREB siRNA for 48 hours, followed by a 2-hour treatment with a calcium ionophore (0.1, 0.5, 1uM), resulted in a 2-fold decrease in CCN1 expression (p<0.05; n=3) in cells with lowered CREB levels. Since low or high STAT3 levels did not affect the ability of calcium to increase CCN1 expression, perhaps the inhibition of CCN1 by STAT3 may be mediated through its interactions with CREB within the CCN1 gene. Further studies are needed. In summary, OVCAR8 cells express CCN1 and its regulation involves STAT3, calcium, and CREB. However, whether or not there is crosstalk between these pathways in the regulation of CCN1 remains to be determined.

Reproductive Technologies/ART/SCNT

Abstract 1619

Oocyte Recovery from Slaughterhouse Collected Ovaries in Goat, Sheep and Swine and their Quality Assessment. Mahipal Singh, Wesley Spratling, Sahraoui Aoued, Olabisi J. Ojo, Abdelmoneim Younis, Eugene Amoah

In vitro embryo production (IVEP) is an assisted reproductive technology that allows offspring to be produced from non-fertile, pre-pubertal, pregnant, lactating, and even dead or slaughtered animals. The core of this technology is availability of the "oocyte", a female gamete that supports fusion of sperm or somatic cell that subsequently develops into embryos and results in live birth. However, the availability of oocytes for in vitro fertilization is a major hindrance since only one or two oocytes are produced in each reproductive cycle. Procuring oocytes from slaughtered animals is an alternate approach which can provide oocytes year round for almost no cost for IVEP that can be transferred in surrogate animals in any season and enhance animal production operations. Therefore, the objective of this study was to assess the rate of recovery and the quality of oocytes from slaughtered animal ovaries in three livestock species i.e. pigs, goat and sheep. Intact ovaries were procured from FVSU slaughterhouse. The oocytes with their attached cumulus cells were carefully recovered from each of the ovaries in buffered media by slicing with a blade. The recovered oocytes were counted and visualized individually under inverted microscope. Each of the oocytes was assigned a grade as A (excellent), B (good) or C (poor) to assess their quality, based on the number of cumulus cell layers around them. Mean ± SD of oocytes recovered from ovaries was 57±2.83; 18.5±4.95 and 12±0.0 for pigs, goat and sheep, respectively. Mean ± SD of A, B and C grades was 10.5±3.54, 13.5±6.36 and 33±7.07 for pigs; 2.5±2.12, 10±2.83 and 6±4.24 for goats, and 4±2.83, 5.5±0.71 and 2.5±2.12 for sheep, respectively. In conclusion, good quality oocytes can be easily recovered from slaughtered animals that can be used to enhance reproductive efficiency, genetic improvement, and cloning of animals.

Abstract # 1649

Seasonally Anestrous Ewe Hormonal Response to CIDR-eCG and Estradiol-17β or Estradiol Cypionate. Zohreh Dehghani Madiseh, Lanna Roberta Yzaura Trucolo, Rojman Khomayezi, Bayode Makanjuola, Meleigha Payne, Katharine Laura McQueen, Brittany Marie Thibault, Melissa Stella Mammoliti, David M.W Barrett

Ewe reproductive output is low in seasonal anestrous even with controlled breeding strategies. The CIDR-estradiol-17β (E2)-eCG protocol improved anestrous ewe reproductive output. Previously we compared estradiol cypionate (ECP) effects with E2 in this protocol and found that anestrous ewe ovarian response differed between ECP and E2 groups; here we report on hormones. Ewes received CIDRs (Day -12), ECP (350µg (ECP350; n=4) or 70µg (ECP70; n=5)) or E2 (350µg; n=5) on Day -6, and eCG (500 IU) at CIDR removal (Day 0). Blood samples were collected on Day -7, and from Day -6 every 6 h for 48 h and 18 h after eCG every 3 h for 72 h. Two Way RM/One Way ANOVA and Tukey test were used. For mean serum E2 (pg/mL) and LH/FSH (ng/mL)

concentrations during 48 h after E2/ECP, there was a time and interaction effect for all hormones and treatment effect for E2 (P<0.05). Mean FSH concentrations decreased from 0 to 6 h and increased from 12 to 42 h after E2/ECP (P<0.05); LH concentrations did not change. Mean E2 concentrations peaked at 6 h after E2/ECP (P<0.001) and were only different between ECP350 (24.5±4.3) and ECP70 (5.6±3.4) groups (P<0.05). Mean E2 concentrations at 6 h after E2/ECP were higher (P<0.001) in E2 (127.9±8.1) than ECP350 (25.2±10.7) and ECP70 (8.3±8.1) groups. Mean E2 concentrations at 18 and 24 h after E2/ECP were higher (P<0.05) in ECP350 (18 h:48.5±10.7; 24 h:39.6±9.0) than ECP70 (18 h:8.0; 24 h:6.4 ±8.1) and E2 (18 h:4.7; 24 h:2.8 ±8.1) groups. Mean FSH and LH concentrations at 0 and 24 h after E2/ECP were respectively higher (P<0.001) in ECP350 (FSH:2.07±0.14; LH:4.21±0.58) than ECP70 (FSH:1.24±0.12; LH:0.13±0.52) and E2 (FSH:1.26±0.12; LH:0.12±0.52) groups. Mean FSH concentrations at 48 h after E2/ECP were lower (P<0.01) in ECP350 (0.70±0.14) than E2 (1.52±0.12) group. The interval from E2/ECP to peak E2 concentrations in E2 was shorter (P<0.05) than ECP350 (6.0±0.0 h vs. 19.5±2.9 h) group. The interval from eCG to the preovulatory LH surge peak and first FSH rise was shorter in ECP350 than ECP70 group (32.0±2.6 vs. 49.0±6.1 h and 32.0±2.0 vs. 46.5±5.1 h respectively; P<0.05); preovulatory LH surge synchrony was similar. Maybe ECP cannot replace E2 in the CIDR-E2-eCG anestrous ewe synchronization program.

Abstract # 1683

Is Sperm Functionality Affected In Patients With Male Infertility Of Unknown Origin? Maria Inês Cristo, Andreia Silva, Renata S. Tavares, Ana Paula Sousa, Mariana Moura-Ramos, Teresa Almeida-Santos, Sandra Amaral, Joao Ramalho-Santos

Although a couple problem, the contribution of different genders in human Infertility varies, with male factor being responsible for nearly 50% of cases. Yet, in half no cause

can be identified, leading to the so-called male infertility of unknown origin, that can be further divided in idiopathic (ID) and unexplained male infertility (UMI). These subtypes only differ in terms of seminal analysis: normal in UMI and having at least one altered parameter in ID. This analysis, although a cornerstone for male infertility diagnosis, is however limited in the prediction of sperm functionality and fertilization capacity. Together with the lack of characterization and the contradictions in the literature regarding male Infertility of unknown origin, this suggests the need of including more reliable functional aspects in seminal analysis. For this purpose, well-characterized groups of patients, including samples from healthy donors (CTRL group), idiopathic (ID aroup) and unexplained patients (UMI group). These samples were evaluated for viability (CTRL n=107; ID n=50; UMI n=23), motility (CTRL n=107; ID n=50; UMI n=23), morphology (CTRL n=99; ID n=37; UMI n=17) and chromatin status (CTRL n=106; ID n=49; UMI n=23), according to the World Health Organization guidelines. Acrosome integrity (CTRL n=100; ID n=40; UMI n=23) was assessed by fluorescence (PSA-FITC) and capacitation status (CTRL n=81; ID n=37; UMI n=18) by immunocytochemistry (phosphotyrosines). Mitochondrial membrane potential (MMP; CTRL n=11; ID n=3; UMI n=4) and reactive oxygen species levels (CTRL n=9; ID n=3; UMI n=4) were assessed by flow-cytometry with the fluorescent probes JC-1 and MitoSOX-Red, respectively. For fertility outcomes (CTRL n=17; ID n=10; UMI n=4), fertilization and embryo development rates were determined. The psychological profile of our patients, regarding the levels of anxiety and depression (CTRL n=62; ID n=40; UMI n=15), was assessed with the Hospital Anxiety and Depression Scale (HADS). Our results show that the ID group has sperm with lower viability, motility, normal morphology, acrosome integrity ($p \pm 0.001$) as well as worse chromatin status (p£0.05), when compared to both control and UMI patients. A decrease in the percentage of capacitated sperm cells (p£0.001) and sperm MMP $(p \pm 0.05)$ was also observed in ID patients, when compared to the CTRL group. Regarding reactive oxygen species levels, fertility outcomes and psychological symptoms of anxiety and depression, no significant differences were observed among groups. Overall, for almost all parameters evaluated the same pattern was found, with the ID group presenting the worse results in several functional aspects, therefore revealing a compromised functionality at several levels. However, the UMI group had very similar results to that of the control group, rising a new challenge that is to understand how these two groups vary at a functional level. Proteomic studies are currently underway in order to begin addressing this issue. Funding: This work was financed by the European Regional Development Fund (ERDF), through the COMPETE 2020 Operational Programme for Competitiveness and Internationalisation and Portuguese national funds via FCT - Fundação para a Ciência e a Tecnologia under the projects POCI 01 0145 FEDER 028599 (INFERT 2 EXPLAIN) and UIDB/04539/2020.

The GDF9:BMP15 Heterodimer Cumulin Improves Oocyte Developmental Competence And Alters Cumulus Cell Protein Expression Of Mouse COCs Matured In Vitro. Dulama Richani, Anne Poljak, David A. Skerrett-Byrne, Baily Wang, William A. Stocker, Craig Harrison, Brett Nixon, Robert B. Gilchrist

Growth differentiation factor 9 (GDF9) and bone morphogenetic protein 15 (BMP15) are co-expressed exclusively by oocytes throughout most of folliculogenesis and are central regulators of ovarian function. Although both growth factors exist as homodimers, recent evidence suggests that the GDF9:BMP15 heterodimer, known as cumulin, may be physiologically important in mono-ovular mammals. We have previously demonstrated that in-house produced cumulin significantly increases blastocyst yield from porcine cumulus-oocyte complexes (COCs) undergoing in vitro maturation (IVM), highlighting the potential of cumulin to improve treatment of female infertility. In this study, we aimed to assess the effect of cumulin on mouse oocyte developmental competence and characterize its downstream targets in mouse COCs. COCs collected from 28-day old C57BI/6 mice following 46 h eCG priming underwent 17 h of IVM \pm 20 ng/mL of pro-cumulin (n= 3-4 biological replicates per experiment). Following IVM, COCs were either fertilized for embryo development assessment, or oocytes and cumulus cells were separated and used for proteomic analysis. Relative to untreated controls, oocytes matured in the presence of cumulin yielded significantly higher total blastocyst rates (56.9 ±6.1% vs 78.8 ±7.6%) and hatching blastocyst rates (43.1 ±4.0% vs 65.4 ±5.6%) six days post-fertilisation (178-180 COCs per treatment; p<0.05, unpaired t-tests). Using LC-MS/MS, comparative proteomic profiling of oocytes and cumulus cells following IVM ± cumulin was performed. A total of 2366 cumulus cell and 1208 oocyte proteins were identified. In cumulus cells, 91 proteins were identified as being differentially expressed between control and cumulin-treated cumulus cells, whilst in oocytes 13 proteins were differentially expressed (fold change of ≤ -1.2 or ≥ 1.2 ; $p \le 0.05$ Mascot search engine and Scaffold comparative analysis software). Application of STRING and Gene Ontology bioinformatics tools to the differentially regulated proteins in cumulus cells revealed that cumulin induced a decrease in proteins localised to the mitochondrion, most of which are involved in oxidative phosphorylation, thus suggesting that cumulin exerts an effect on cumulus cell mitochondrial function. Cumulin significantly increased the abundance of cumulus cell proteins involved in mRNA synthesis yet decreased proteins associated with translation. Furthermore, cumulin significantly downregulated proteins involved in the estrogen signaling pathway. Taken together, these data demonstrate that cumulin enhances mouse oocyte developmental competence during IVM, likely by altering the function of the oocyte's surrounding support cells, the cumulus cells. Characterizing cumulin and its mechanism of action will enhance our understanding of ovarian and oocyte function and may contribute to transforming the way oocytes are matured in vitro for infertility treatment.

Evaluation of the 7 & 7 Synch and 7-Day CO-Synch + CIDR Protocols For Synchronization Of Estrus Among Beef Cows Prior To Fixed-Time Artificial Insemination With Conventional Or Sex-Sorted Semen. Carson M. Andersen, Rachael C. Bonacker, Emily G. Smith, Jordan M. Thomas

Background :An experiment was designed to compare the recently developed 7 & 7 Synch and 7-Day CO-Synch + CIDR protocols for synchronization of estrus among beef cows prior to fixed-time artificial insemination with conventional or sex-sorted semen. We hypothesized that 7 & 7 Synch would result in increased estrous response among cows prior to FTAI as well as greater pregnancy rates to FTAI.

Methods: Bos taurus suckled beef cows (n=868) in six locations were blocked based on age and days postpartum (DPP) and randomly assigned to protocol and semen type. Cows treated with the 7-Day CO-Synch + CIDR protocol (n = 429) received administration of gonadotropin-releasing hormone (GnRH; 100 mg gonadorelin) and insertion of a 1.38 g intravaginal progesterone releasing insert (CIDR) on day -10, and administration of prostaglandin F2a(PG; 500 mg cloprostenol) and removal of CIDR on day -3. Cows treated with 7 & 7 Synch (n = 439) received administration of PG and insertion of CIDR on day -17, administration of GnRH on day -10, and administration of PG and removal of CIDR on day -3. Estrus detection aids (Estrotect[™]) were applied to all cows on day -3, and estrous response was recorded at FTAI on day 0. Cows received FTAI at 66 h after CIDR removal with either conventional (20 x 106cells per unit) or sexsorted (4 x 106cells per unit; SexedULTRA 4M[™]) frozen-thawed semen.

Results: Greater estrous response (p = 0.02) prior to FTAI was observed among cows treated with 7 & 7 Synch (85%; 371/439) compared to 7-Day CO-Synch + CIDR (73%; 313/429). Estrous response was affected by a protocol x DPP interaction (p < 0.0001), with 7 & 7 Synch resulting in a greater increase in estrous response among cows with greater DPP. Sex-sorted semen resulted in lower (p = 0.0003) pregnancy rates to FTAI. However, irrespective of semen type, greater (p = 0.01) pregnancy rates to FTAI were obtained among cows treated with 7 & 7 Synch (conventional semen: 73% [162/222]; sex-sorted semen: 53% [114/217]) compared to 7-d CO-Synch + CIDR (conventional semen: 60% [130/216]; sex-sorted semen: 43% [91/213]).

Conclusion: Results support the hypothesis that 7 & 7 Synch results in greater estrous response and pregnancy rates to FTAI among beef cows when using sex-sorted or conventional semen.

Royal Jelly Produced By Apis Mellifera Can Successfully Synchronize The Estrous Cycle Of Goats. Ninel Castro-Chavez, Javier Gutiérrez-Molotla, Alberto Balcazar-Sanchez

Reproductive management strategies in goats are based on the use of hormones and social factors. The main hormonal protocols are based on intravaginal devices such as CIDR that contain progesterone; however, these protocols may have negative side effects on the follicle development. A possible alternative to the use of progesterone is royal jelly (RJ). RJ is a natural honeybee product produced by the hypopharyngeal gland of young worker bees (Apis mellifera). RJ has been widely used as a method to improve fertility in humans, quail and rabbits. In ewes, a 12-day treatment with progesterone and eCG, plus an intramuscular injection of 500mg of RJ significantly increased conception rates. Nevertheless, its effects have never been assessed in goats. Therefore, the objective of this study was to evaluate the effects of RJ contained in intravaginal devices onsynchronization and fertility rate in goats. A total of 16 primiparous goats from 1 - 1.5 years old were randomly distributed in 2 groups, CIDR or RJ. Estrous synchronization was performed with a CIDR (0.3 g of natural progesterone) or and intravaginal device containing 10g of RJ for 6 days. One day before the withdrawal of both devices, both groups received 200 UI of eCG and 5mg of PGF2a. Natural mattings were given once females showed signs of estrous and the diagnosis of pregnancy was performed by ultrasonography at day 40 post matting. Estradiol, progesterone and testosterone were measured in serum by ELISA. No statistically significant differences were found in serum concentrations of progesterone, estradiol and testosterone between both groups. The group synchronized with RJ had statistically significantly higher number of natural mattings and marked signs of estrous (P<0.05). However, no differences were detected in pregnancy rates. These data demonstrated that RJ can synchronize the estrous cycle of goats as successfully as a CIDR device.

Abstract # 1825

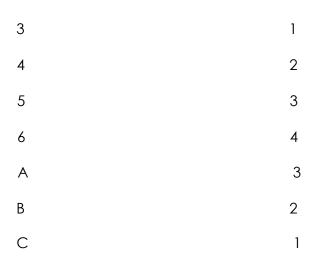
Relative Contribution Of The Components Of Embryo Grading Systems. Michael G. Collins, Aiicia L. Broussard, Cynthia Hudson, Timothy Sharp, Kathryn J. Go

Background: The grading of human embryos infers qualitative likelihood of resulting in pregnancy and live birth from evaluating morphologic features. Common grading systems categorize blastocysts by alphanumeric grades based on the degree of expansion, (i.e., expanding, expanded, hatching, hatched; 3, 4, 5 or 6, respectively), and the appearance of the Inner Cell Mass (ICM) and Trophectoderm (TE) (Good, Fair, Poor; A, B, C, respectively). In clinical embryology, these systems inform the transfer of one blastocyst versus another but cannot be applied to quantitative statistical analyses of blastocyst development over time. The TMRW Embryo Scoring System (TESS) was developed to convert categorical embryo grades into discrete numerical embryo scores. This report describes the application of TESS to the analysis of blastocyst

expansion, ICM quality and Trophectoderm quality to evaluate the relative contribution of each to development over a 24-hour culture interval.

Materials and Methods: One Hundred and Seventy-Seven (177) frozen human blastocysts were thawed and graded using the Gardner or similar scale. The blastocysts were cultured overnight at 37OC in 6% CO2. A second round of grading was performed after ~20 hours of culture. The embryo grades for each time point were converted to numerical scores using the following model:

Alphanumeric grade component Score points awarded



For instance, a 6AA embryo received a score of 10 (4+3+3), and a 3CC received a 3 (1+1+1). A degenerated blastocyst was scored 0.01, and a collapsed blastocyst that could not be graded was scored 0.5 indicating that it was viable with potentially compromised membranes. The collective grades were analyzed in addition to each individual morphologic component (degree of expansion, ICM and TE appearance) using ANOVA with repeated measures to detect any statistically significant change in grades after culture that reflects continued development.

Results: Analysis of the combined scores revealed a statistically significant increase in TESS following ~20 hrs. of culture (Mean±SE; TESS at thaw, 5.085±0.220; TESS after culture, 6.410±0.208; p<0.001). The results of the individual component analyses are presented in Table 1. Only the degree of expansion increased significantly after embryo culture.

Table 1. Mean TESS (±SE) component at thaw and following culture

| Component | No. of Blastocysts | Mean (±SE) at Thaw | Mean (±SE) |
|---------------|--------------------|--------------------|------------|
| after Culture | | | |

| Degree of expansion | 177 | 1.599±0.077a | 2.636±0.092b |
|------------------------|-----|--------------|--------------|
| ICM appearance | 177 | 1.944±0.075 | 1.952±0.070 |
| TE appearance | 177 | 1.808±0.070 | 1.901±0.070 |

a,bMean ±SE with different superscripts within rows are statistically different (P<0.05, ANOVA with repeated measures)

Conclusions: The subjective grading of blastocyst morphology and conversion of those grades to numerical scores allow the detection of statistically significant development after ~20 hrs. of culture. The contributor to this development was identified as an increase in the degree of expansion. Further investigation is required to determine if these results have clinical relevance and to evaluate the contribution of each grading component to the overall score.

Abstract # 1986

The Filopodia Marker MYO10 Reveals A Novel Method For The Assessment Of Granulosa Cell Function And Quality Of Human Growing Follicles. Sofia Granados Aparici, Togas Tulandi, William Buckett, Weon-Young Son, Grace Younes, Jin-Tae Chung, Shaoguang Jin, Hugh J. Clarke, Alexander Volodarsky-Perel

Therapeutic advances over the recent decades have dramatically increased the number of childhood cancer survivors. This success has focused attention on posttreatment quality of life, including fertility, which is frequently compromised by the therapeutic interventions. Currently, cryopreservation of ovarian tissue is the only option available to pre-pubertal girls. However, the effects of cryopreservation on subsequent oocyte and follicular growth remain little understood, due in large part to a lack of knowledge of the early stages in humans. Beginning early during growth, bi-directional signaling between the oocyte and the follicular granulosa cells that surround it regulate oocyte and follicular development. This essential signaling occurs via specialized actin-rich filopodia that project from the granulosa cells to the oocyte membrane. In view of their essential role during folliculogenesis, these intercellular bridges may be a valuable marker of granulosa cell function and follicle quality. We analyzed the morphology of granulosa cell filopodia, as well as the distribution of a protein (MYO10) implicated in the formation of canonical filopodia, in human follicles at early stages of growth. Fresh ovarian tissue was prospectively collected from patients who underwent ovarian surgery. Frozen ovarian tissue was donated by patients who underwent ovarian tissue cryopreservation due to malignant disease. Follicles from primordial to secondary stages were stained using the F-actin binding protein, phalloidin, and anti-MYO10. Confocal microscopy was used to image equatorial optical sections of each follicle. MYO10 expression in the granulosa cells was quantified using Image J. 180 follicles were analyzed and comparisons made between age range (22-30 vs 35-40 years) and fresh vs frozen-thawed follicles. In primordial follicles, actin was present in the oocyte cortex as well as in the squamous adjacent granulosa cells. However, although no filopodia were detectable, some MYO10 foci were present at the interface with the oocyte plasma membrane. As follicles transitioned to the primary stage, filopodia were seen to project from some granulosa cells to the oocyte. This was accompanied by an increase in the number of MYO10 foci. By the late primary stage, a rich network of filopodia extended from the granulosa cells to the oocyte through a visible zona pellucida, named transzonal projections (TZPs). Correspondingly, many MYO10 foci marked the TZP body. Interestingly, whereas some TZPs reached the oocyte plasma membrane others penetrated and connected each other deep into the oocyte. In follicles obtained from 22- to 30-year old women but not in those of 35- 40-year old women, a positive correlation was observed between the distribution of MYO10 in granulosa cells and oocyte diameter. In frozen-thawed follicles from 22- to 30-year old women, this correlation was no longer observed. Strikingly, large MYO10 aggregates in the oocyte cytoplasm were observed and significantly increased in frozen-thawed when compared to fresh follicles. These data suggests a significant impact of age and cryopreservation on the ability of granulosa cells to modulate filopodia formation. Additionally, it identifies a method of molecularly assessing follicle function and quality that may be useful to develop and improve the existing ovarian cryopreservation methods for pre and post-pubertal patients.

Abstract # 2063

Standardization of Powder Chicken Egg-yolk Concentrations With Tris Buffer for Liquid Storage of Rooster Semen. Balogun Adedeji Suleimon, Ranjna S. Cheema

Heat treatment is suspected to denature protein content of powder eggs and consequently reduce nutrient composition of powder egg-yolk, one of the important ingredients for semen preservation. An experiment was therefore conducted to evaluate appropriate concentration of powdered egg yolk require for formulating Tris egg-yolk poultry semen extender for liquid storage of poultry semen. Tris buffer 7.2 pH was prepared by adding 3.785g and 2.115g to 100ml of double distilled water. Powder chicken egg-yolk (PCEY) of 10%, 15%, 20% and 25% concentrations were dissolved separately in it, constituting four treatments. Each solution was spin for 2min. Ejaculate semen from five roosters were collected, pooled and evaluated for mass activities and motility. Semen and extenders were maintained at 37oC before dilution. Pooled semen was divided into four portions. Extenders were diluted separately with each portion at

ratio of 1:2 (semen: extender). Diluted semen were evaluated for microscopic semen quality such as progressive motility, viability, membrane and acrosome integrity at different periods of 0, 24h, 48h and 72h of preservation. The experiment consists of three trials and experimental design used was completely randomized design. All data collected was subject to analysis of variance using SPSS software statistical package, means were separated with Duncan multiple range test. The result of the effect of different concentration of PCEY on rooster semen revealed no significant (P>0.05) different among treatments at 0h in all the parameters assessed. However, at 24h, 15% concentration was significantly higher (P<0.05) than other treatments in most parameters such as; motility (81.67%), viability (88.00%), membrane integrity (79.33%) and acrosome integrity (86.67%). Although was statistically (P>0.05) similar to 20% concentration in viability (88.33%) and acrosome integrity (81.67%). Similar trend was also observed for 48hrs. While at 72h, 15% PCEY was significantly (P<0.05) higher and above average in motility (55.00%) viability (69.33%) and membrane integrity (58.33%) compare to its counterparts (10, 20 and 25%) concentrations. This experiment revealed that 15% PCEY concentration is sufficient to formulate tris egg-yolk poultry semen extender for optimum semen quality. Furthermore it was evident from our observations that 10, 20 and 25% PCEY diluted with semen rapidly form gelatinous substance before 72hs evaluation period. Conclusively, we observed that below and above 15% Powder egg-yolk concentration may not significantly favour sperm cells protection for longer duration nor optimized metabolic activities of rooster sperm during liquid storage of semen.

Abstract # 2162

Excessive FSH Doses During Superovulation Decrease Oocyte Recovery In Women And Adversely Impacts Ovarian Function In Cattle. Zaramasina L. Clark, Kaitlin R. Karl, Meghan L. Ruebel, Fermin Jimenez-Krassel, Janet L. H. Ireland, Robert J. Tempelman, Mili Thakur, Richard E. Leach, Emily Gibbings, Oliver Chen, Rebecca L. Herzog, Sarah M. Huffman, Keith E. Latham, James J. Ireland

High doses of gonadotropins during assisted reproductive technology (ART) cycles cause oocyte and embryo wastage and decrease live birth rates. These observations support the hypothesis that excessive FSH doses during superovulation adversely affect ovarian function. To test this hypothesis, we present data from one study in women (Study 1), and two studies in heifers (Study 2 & 3). Study 2 & 3 used 11-12 month-old heifers with a low antral follicle count (<10 follicles ≥3mm diameter, index for small ovarian reserve). In Study 1, data from >650,000 ART cycles were used to investigate the relationship between total FSH dose and the number of oocytes retrieved (index for ovarian function). Results showed, irrespective of patient age, BMI or infertility diagnosis, total FSH dose during ART was negatively correlated with the number of oocytes retrieved (P<0.0001). In Study 2, heifers (N=9) were treated twice daily for four days with either 35IU, 70IU (industry standard), 140IU, or 210IU Folltropin-V injections beginning on Day 1 of a synchronized estrous cycle. Ovulation was induced with 2,500IU hCG 12h

after the final Folltropin-V injection. Indices of ovarian function, including the development of ovulatory-sized (>10mm) follicles, corpora lutea (CL) and ovulation rate were assessed using daily ultrasonography. Circulating anti-Müllerian hormone (AMH), progesterone and estradiol concentrations were measured from serum collected every 12h during Folltropin-V treatment, at hCG administration, 24h post-hCG and every 48h for nine days post-hCG. Although the 210IU Folltropin-V dose did not alter (P>0.05) ovulatory follicle number, progesterone or AMH concentrations compared with lower doses, circulating estradiol concentrations and ovulation rate were reduced (P<0.05). Thus, the 210IU Folltropin-V dose was considered detrimental to ovarian function. Study 3 evaluated the effects of the 210IU (N=6 heifers) compared with the 70IU (N=7 heifers) Folltropin-V doses on the follicular microenvironment. Heifers were treated with 70IU or 210IU as described in Study 2, except they were euthanized 12h after the last Folltropin-V injection (no hCG was administered), and ovaries were removed. Follicular fluid was aspirated from ovulatory-sized follicles and concentrations of progesterone, estradiol and oxytocin were measured. Cumulus cell morphology (compact vs expanded) was determined for 5-15 cumulus-oocyte complexes (COC)/heifer. Results showed a high proportion (70±4%) of COC from the 210IU group were prematurely expanded, while all COC from the 70IU group were compact. In addition, follicles containing expanded COC had >4-fold higher (P<0.0001) progesterone and oxytocin concentrations and decreased (P<0.05) estradiol concentrations and estradiol:progesterone ratios compared with the non-expanded COC from the 70IU group. These combined results support the conclusion that excessive FSH doses may induce premature COC expansion and premature luteinization of ovulatory follicles, which may be detrimental to ovarian function, oocyte quality and recovery, and pregnancy outcomes. This project was supported by an award to JJI and KEL from the NIH-USDA Dual Purpose Program by Agriculture and Food Research Initiative Competitive Grant no 2017-67015-26084 from the USDA National Institute of Food and Agriculture, and in part by a grant from the NIH, Eunice Kennedy Shriver National Institute of Child Health and Human Development (T32HD087166).

Abstract # 2163

Exogenic Human Muscle Lineage Development In MYF5/MYOD/MYF6-Null Pig Embryos Complemented With Human iPS Cells. Geunho Maeng, Satyabrata Das, Sarah M. Greising, Wuming Gong, Daniel J. Garry, Mary G. Garry

Embryo complementation has been proposed as a method to produce humanized organs from animals to supplement the lack of organ donors for patients with irreversible injuries or terminal diseases. Here, we investigated the possibility of human muscle development in pig embryos by injecting gene edited hiPSCs into the skeletal muscle deficient pig embryos. The skeletal muscle deficient pig embryos were generated by SCNT using MYF5/MYOD/MYF6 -null fibroblasts, which were edited using CRISPR/Cas9. Using morphological and molecular techniques, we observed an absence of skeletal muscle at E27. We hypothesized that this lack of skeletal muscle could be restored by complementation with wild type cloned blastomeres or human iPS cells. Using SCNT and blastocyst complementation techniques, a total of 221 MYF5/MYOD/MYF6 -null pig embryos were injected with the GFP-labeled WT blastomeres at E4 and then surgically transferred into synchronized gilts. At E116, the gilts delivered chimeric piglets, which displayed a normal skeletal muscle phenotype and ambulation. Next, a total of 557 MYF5/MYOD/MYF6 -null pig embryos were injected with cGFP labeled gene edited-hiPSCs at E4. These pig-human chimeric embryos were transferred into six synchronized gilts and 20 embryos were harvested at early stages of gestation (E20 or E27). We observed the ALU expression relative to WT controls in 15 of these pia-human chimeric embryos. Using immunohistochemistry, the cGFP expression was observed throughout the myotome, and the cGFP signal was co-localized with the myogenic transcription factor, MYOD. The human MYF5 and MYOD transcripts, which were absent in the mutant embryo, were present in the limb and body wall of pighuman chimeric embryos using aRT-PCR. Our data support the feasibility of the generation of these interspecies chimeras, which will serve as a novel model for translational research or one day as a source for xenotransplantation.

Abstract # 2170

Medroxyprogesterone Acetate Vs GnRH antagonist for Prevention of Premature LH Surge in Primary and Secondary Infertility Patients undergoing IVF cycles: Multi Centric Study. Ashish Kale, Ashwini Kale, Ekika Singh

Introduction GnRh antagonists for preventing surge during controlled ovarian hyperstimulation is used widely. However, usage of Medroxy Progesterone Acetate (MPA) oral route with decreased incidence of ovarian hyperstimulation syndrome has increased. With the advancement of assisted reproductive techniques many couples with primary or secondary infertility are successfully getting pregnant. Common methods of stimulating ovaries include administration of exogenous gonadotropins and GnRH antagonist such as cetrorelix. The controlled ovarian stimulation is one of the most important and crucial step; premature LH surge is prevented by judicious use of GnRH antagonists and agonists Methods We conducted a comparative study, in different ART centers. Infertile women between age of 25-30 years were included. History included, time since marriage, frequency of intercourse, menstrual history, menstrual irregularity. Inclusion criteria included, women in the age of 25-30 years, primary or secondary infertility, antral follicular count of 8 -15, AMH 2 to 3.2 ng/ml. (n=300, divided into 150 each) Group A received GnRh antagonist (Cetrotide) 0.25 daily when follicular diameter reached 12-13 mm. Stimulation started with recombinant FSH150 IU to 225 IU based on anti-mullerian hormone (AMH) and antral follicle count (AFC). Follicular monitoring on 5th day of stimulation using transvaginal ultrasound, repeated alternate day. Trigger with recombinant hCG 250 IU when leading follicles reached 18 to 20 mm Group B received MPA10 mg OD 2nd day of cycle Results There was no incidence of pre-mature LH Surge as LH suppression was consistently maintained in case group. Number of oocytes retrieved, gonadotrophin requirement was comparable in both

groups, number of mature oocytes significantly higher in case group. Number and grading of embryos obtained were statistically insignificant. Mean age in group A was 27.12+/- 1.12 years as Vs mean age in group B 27.32 +/- 1.64 years. No significant difference in mean age of both groups (p=0.128). Minimum duration of infertility was 16 months, maximum was 8.3 years. Mean duration of infertility in Group A was 6.88 years Vs mean duration of infertility was 7.02 years (Group B). Mean duration of infertility was comparable in both groups (p=0.147 NS). Group A out of 150 cases 112 (74.66%) were of primary infertility whereas 38 (25.33%) were secondary infertility. Mean numbers of mature follicles higher in group B (p< 0.0001). Mean number of retrieved oocytes in aroup A and aroup B was 8.98 +/- 0.78 and 9.12 +/- 0.81 (p=0.12 NS). Number of embryos was 5.98 + -0.68 Vs 6.14 + -0.70 in Group A and Group B respectively. (p=0.03) NS). Pregnancy was 37.33 % in group A and 30.66 % in group B Discussion MPA when used in donor stimulation protocol is good alternative to GnRH antagonist which yields good number of mature oocytes leading to good quality embryos hence reducing cost and dose of gonadotropins required. When used in properly selected patients the outcome is comparable to any standard gonadotropins stimulation cycle Conclusion MPA with stimulation protocol is better alternative, prevents premature LH surge with more mature oocytes leading to good quality embryos, reducing cost and better compliance

Production of Minimized Transgenic Pig for Biomedical Research. In-Sul Hwang, Mi-Ryung Park, Hae-Sun Lee, Tae-Uk Kwak, Seongsoo Hwang

For xenotransplantation research, the size of organ from donor pig must be considered firstly before conducting to transplant into non-human primate recipient. Also in pig breeding and feeding, minimized pig have great benefits compared to wild type pig because of whole body size. There are many ways to reduce and minimize the size of pig like breeding but, it takes very long time with many generations. In the present study, we developed a minimized pig in short time by somatic cell nuclear transfer method using genetically modified somatic cells(GH-R). Then, the characteristics of minimized cloned-piglet was analyzed. Briefly, on day 126 of gestation, 4 transgenic piglets were delivered and only 1 piglet (265g) was succeeded to be alive. Although we took care of this piglet comprehensively within special incubator, the piglets showed a symptom like circling behavior. Therefore, the piglet was sacrificed and histopathological analysis was conducted to find out lesions. Results of histopathological tests showed that demineralization and vacuolation in the white matter of cerebellum was observed. And necrosis and calcium sedimentation were observed in some areas of the cerebrum and cerebellum. Based on the histopathological findings, the neurological symptoms of the piglet were caused by demineralization and vacuolation in the cerebellum. Additionally, necrosis lesions in cerebral parenchyma and calcium sedimentation was observed in cerebellum and cerebrum parenchyma.



Survival Rates Of Vitrified-Warmed Pig Oocytes By Hand-Made Device. In-Sul Hwang, Ji-Hyun Lim, Young-Ji Kim, Sung Woo Kim

To cryopreserve pig oocytes, specially developed commercial devices are very useful for a survival and development of oocytes after vitrification and warming. However, the commercial device for vitrification is quite expensive and difficult to reuse. In the present study, we designed and made simple device for vitrification using disposable laboratory ware such as inoculation loop and cell strainer. Briefly, the inoculation loop was cut into around 10 cm with ring part and nylon mesh was detached from cell strainer. The nylon mesh was attach to ring part of inoculation loop. After vitrification and warming, the survival rates were analyzed regarding the pore size of nylon mesh. In results, 40 µm-sized (75.0%) nylon meshed showed higher survival rates compared to 70 µm-sized (63.3%) nylon mesh while comparable with Cryotop (78.3%). Our result demonstrated that the 40 µm-sized nylon mesh could be useful to cryopreserve oocyte in pig.

Reproductive Tract: Female

Abstract # 1810

Optimization of Sperm-Oviduct Binding Model for In-Vitro Assessment of Buffalo Sperm Fertility. Mohamed M. M.El-Sokary, Sally Ibrahim, Al-shimaa Al-H.H. El-Naby, A.S.A. Sosa, Karima Gh. M.Mahmoud, M.F. Nawito

Successful fertilization is the final step and the capstone of the fertile sperm. For this, the sperm must overcome many obstacles, which face its journey inside female genital tract. One of the most determinant events is the sperm binding with oviduct, which select only sperms with highest reproductive potentials. So far, the molecular aspect concerning interaction of sperm with oviductal cell is still not well understood. The current study aimed (I) to mimic in vivo milieu, via establishing an in vitro paradiam to examine sperm fertility, and (II) to investigate molecular changes that associate with interaction of sperm with oviductal cell. Therefore, two experiments were done. In the 1st experiment, the epithelia cells from different segments of oviducts (isthmus, ampulla, and infundibulum) were dissected and incubated for 90 min at 39°C to form spherical aggregates (100-150 µm). In the 2nd one, straw of buffalo semen were allowed to bind with the previous aggregates (n=20 aggregates) in different media; TALP or TCM199 separately, for 1 h at 39°C. Images of sperm binding were captured, using a Zeiss Axioskop microscope. Furthermore, different segments for both experiments were collected before and after sperm binding and kept at -80°C, for total RNA isolation and gRT-PCR of candidate genes, then data analysis was done using two-way ANOVA. We found that, the highest aggregate yields were retrieved from isthmus followed by ampulla, and then infundibulum. Moreover, TALP medium promoted the formation of higher aggregates yield. Additionally, the sperm expressed higher affinity to bind oviduct cells compared to TCM. Additionally, frozen semen from Baladi breed bind to oviduct explant significantly higher than cross breed does. The binding of sperm to oviductal epithelial cells revealed profound (P<0.001) alterations in the expression profile of IL10, TGFB1, STAT1, and JAK2 mRNAs. Furthermore, these changes were significantly (P<0.001) different among different segments of oviduct. The relative abundance of IL10 mRNA was significantly (P<0.001) increased after sperm binding in TCM media. While, in TALP media IL10 was significantly (P<0.001) decrease after sperm binding with oviductal cells. On the other hand, the expression profile of STAT1 mRNA was shown a clear (P<0.001) inhibition after sperm binding in both media (TCM&TALP). Taken together, our findings indicated that isthmus segment in TALP media showed the highest binding affinity to sperm. Additionally, molecular investigation revealed the success of our in vitro model for simulation in vivo milieu, and subsequently might be used as a simple and effective tool for assessment male fertility in vitro.

Uterine Gland Development and Foxa2 Immunolocalization in Gilts at Postnatal 14 Affected by Lactocrine Deficiency from Birth. Nina E. Paranjpe, Teh-Yuan Ho, Anne A. Wiley, William T. Olivier, Jeremy R. Miles, Clay A. Lents, Frank F. Bartol, Carol A. Bagnell

Bioactive factors of maternal origin present in colostrum are delivered into the neonatal circulation via a lactocrine mechanism and affect patterns of uterine development in swine with lasting consequences. Imposition of a lactocrine null condition by experimental milk replacer feeding for two days from birth (postnatal day = PND 0) altered uterine gene expression patterns globally by PND 2 and inhibited uterine gland development by PND 14. Colostrum consumption can be measured in nursing gilts by monitoring neonatal serum immunoglobin immunocrit ratio (iCrit). Lactocrine deficiency, defined as low iCrit at birth, altered uterine development by PND 14 as reflected by reduced glandular epithelial (GE) and stromal cell proliferation. Lactocrine deficiency from birth impairs lifetime fecundity in adults, indicated by reduced live litter size. Here, objectives were to determine effects lactocrine deficiency from birth on endometrial morphology, uterine gland development and forkhead homeobox A2 (FOXA2) immunostaining patterns on PND 14. FOXA2, a transcription factor essential for the differentiation and development of uterine glands, marks uterine GE cells in humans, mice and sheep, but has not been reported in pigs. In this study crossbred gilts were assigned to low (n = 12) or high (n =10) iCrit groups based on iCrit ratio values determined on PND 0. Serum iCrit ratios were greater (P<0.01) in high (12.04 ± 0.27 relative units) versus low (1.92 ± 0.27 relative units) iCrit groups, indicating a difference in colostrum consumption between groups of approximately 6-fold at birth. Endometrial development was quantified histomorphometrically and FOXA2 expression localized in uterine GE cells immunohistochemically in a subset of high versus low iCrit gilts (6 litter-matched gilts per group) on PND14 when uterine tissues were collected. Neither birth weights, PND 14 body weights, ovary weights nor uterine weights differed between groups. However, both the number of GE cells/mm2 (P<0.05) and, to a lesser extent, endometrial thickness (P<0.08) were reduced in low as compared to high iCrit gilts. Uterine gland penetration depth did not differ between the two groups. Immunoreactive FOXA2 protein was localized consistently and uniquely in GE cells of both low and high iCrit gilts at PND14. The increased number of uterine GE cells/mm2 in high iCrit gilts indicated an overall increase in FOXA2 expression. Results indicate that lactocrine deficiency from birth alters endometrial development resulting in fewer GE cells and an associated decrease in overall expression of FOXA2. Reduction in endometrial FOXA2 expression may contribute to alterations in neonatal lactocrine programing of uterine tissues. Results reinforce the idea that lactocrine deficiency in nursing gilts, maintained under normal husbandry conditions, affects patterns of neonatal uterine endometrial development. Such changes in the neonatal uterine organizational program can affect fecundity in adulthood. [Support: USDA-NIFA 2013-67016-20523; USDA is an equal opportunity employer]

Cystic Ovary Disease Impacts Gamete/Embryo Transport And Its Cholinergic Regulation. Deirdre Scully, Deirdre Campion, Fiona Mccartney, Sven Reese, Sabine Kölle

Cystic ovary disease (COD) is a common cause of subfertility in humans and animals. The effect of COD on the function of the oviduct – especially on the transport of the oocyte and the early embyo - is largely unknown. Therefore, the aim of this study was to investigate transport function and the influence of the cholinergic system in oviducts affected by COD. Oviducts were excised from cows affected by COD (n=29) as well as from healthy cows in mid diestrus (n=20) immediately after slaughter. A unique digital live cell imaging (LCI) system established in our lab was used to capture real time videos of ciliary beat and particle transport speed under near in vivo conditions. For ciliary beat frequency (CBF), the differences in grayscale of beating cilia were transformed into frequencies using ImageJ® and AutoSignal®. For particle transport speed (PTS), polystyrene beads were added to the buffer media and were automatically tracked using ImagePro®. Additionally, smooth muscle contraction and epithelial ion transport were investigated using organ baths and Ussing chambers. Our results showed that PTS was significantly decreased in oviducts from cows affected by COD as compared to controls (p=0.01, Unpaired Student t-test). Further to that, in healthy control cows, PTS was consistently increased in the oviduct ipsilateral to ovulation as compared to the contralateral oviduct (p=0.03, Paired Student t-test). This was not the case in cows affected by COD (p=0.47, Paired Student t-test). Reduced PTS in oviducts from cows with COD was not due to changes in CBF. Although smooth muscle contraction was similar in oviducts from healthy and COD cows, the contractile response (mN) to the cholinomimetic drug carbachol (10 - 7 - 10 - 4 M) was significantly reduced in COD as compared to the controls (p<0.0001, non-linear regression "best fit" analysis). Carbachol-induced active ion transport in the oviductal epithelium of COD cows, which was measured by the change in short circuit current (μ A/cm 2), was significantly decreased as compared to controls (p=0.03, Unpaired t test of area under the curve (AUC)). These results suggest, for the first time, that oviductal transport is compromised in COD. Decreased cholinergic regulation of tubal contractions and fluid formation could have detrimental consequences for the transport and nutrition of the gametes and the early embryo in the oviduct. This knowledge is pivotal to establish novel therapeutic concepts for successful treatment of infertility in individuals affected by COD.

Spatiotemporal transcriptional dynamics of the cycling mouse oviduct. Elle C.Roberson, Riddhiman K. Garge, Ngan Kim Tran, Harrison Mark, Anna Battenhouse, Edward M. Marcotte, John B.Wallingford

The oviduct, like other female reproductive organs, responds to the steroid hormones produced during the estrous cycle, and this cyclical responsiveness is important for female fertility. Further, while the oviduct is a critical site for female fertility, how oviduct physiology is regulated at the genetic, molecular, and cellular level remains fairly mysterious. We set out to understand the underlying global transcriptional response to the steroid hormone secretion by performing RNAseg of the mouse oviduct at each stage of the estrous cycle. In addition, as the oviduct displays intriguing cellular patterning across the anteroposterior axis – at the anterior end (near the ovary), multiciliated cells are enriched while at the posterior end (near the uterus), secretory cells abound – we performed RNAseg on anterior and posterior portions of the oviduct. We have identified over 2,000 differentially expressed genes along the anteroposterior axis, and less than 100 differentially expressed genes across the estrous cycle. Genes enriched in the anterior are mainly responsible for multiciliated cell formation and homeostasis, while genes enriched in the posterior represent secretory transport genes and developmental signaling pathways. The developmental genes enriched in the posterior include Hox genes, FGF signaling, and noncanonical Wht signaling. Interestingly, across the estrous cycle most of the differentially expressed genes are ribosomal protein genes. We are currently investigating ribosome biogenesis across the estrous cycle of the mouse oviduct.

Abstract # 2128

Maternal And Ovarian Impacts Of Chronic Glyphosate Exposure. Shanthi Ganesan, Bailey C. McGuire, Aileen Keating

Glyphosate (GLY) accounts for 50% of total herbicide used in the U.S. and GLY is also used in urban environments for weed control. Human exposure is supported by urinary GLY detection. Reproductive impacts of GLY exposure demonstrated include reduced 17ß-estradiol, increased progesterone and granulosa cell growth inhibition. Additionally, shortened gestational length was associated with urinary GLY levels in women. This study tested the hypothesis that chronic GLY exposure pre-conceptionally would affect both maternal physiology and impair female fertility. Mice (C57BL/6; n = 10 per treatment) were exposed to saline vehicle control (CT) or GLY (2 mg/kg) daily (5 days/week) for twenty weeks. Following exposure, females were housed with unexposed males and the appearance of vaginal plugs monitored. Cohort 1 mice completed three rounds of pregnancy, while Cohort 2 mice were euthanized at gestation day 14 to establish maternal effects mid-pregnancy with age-matched CT or GLY-exposed non-pregnant mice included. Body and organ weights were recorded, and serum was collected at euthanasia. Ovarian samples were processed for histological and proteomic (LC-MS/MS) analysis. Serum 17B-estradiol and progesterone were measured via ELISA. In Cohort 1, there were no overt impact of GLY exposure on pregnancy outcomes, offspring weight or offspring anogenital difference. Pregnancy success in CT mice was 40%, 42% and 33% while in the GLY-exposed mice it was 55%, 58% and 8.3% in rounds 1, 2 and 3, respectively. Additionally, there was 33% maternal demise recorded in GLY-exposed pregnant relative to CT pregnant mice throughout the study. Ovarian proteomic analysis in mice after three pregnancies revealed longterm alterations (P < 0.05) to the ovarian proteome. In addition, GLY increased (P = 0.08) 17ß-estradiol, reduced (P < 0.05) secondary follicle number, and had no impact (P >(0.05) on progesterone. In cohort 2 mice, pregnancy increased liver (P < 0.05) and ovarian (P < 0.07) weight in both CT and GLY-exposed mice. In addition, spleen weight was lower (P < 0.05) in GLY relative to CT non-pregnant mice but increased (P < 0.05) in GLY-exposed but not CT mice during pregnancy. Pregnancy increased (P < 0.05) 17Bestradiol in CT-treated mice but this pregnancy effect was absent in the GLY-exposed mice. Progesterone was increased (P < 0.05) due to pregnancy with no effect of GLY exposure. The ovarian proteome differed (P < 0.05) between pregnant and nonpregnant mice and GLY exposure also altered (P < 0.05) the ovarian proteome in both pregnant and non-pregnant mice. Taken together, these data support maternal impacts of GLY exposure that could negatively impair fertility and pregnancy outcomes. In addition, persistent histological, proteomic and endocrine changes were observed in GLY-exposed females. This study was supported by R21 ES026282 from the National Institute of Environmental Health Sciences.

Abstract # 2174

Fresh, But Not Frozen-Thawed, Semen Induces Netosis In Jenny Polymorphonuclear Cells In A Concentration And Time Dependent Manner. Yentel Mateo-Otero, Fabiola Zambrano, Jaime Catalán, Marc Yeste, Jordi Miró, Beatriz Fernandez-Fuertes

In several species, acute endometritis driven by the recruitment of polymorphonuclear cells (PMNs) occurs in response to semen. Release of DNA from PMNs to form neutrophil extracellular traps (NETs) is stimulated by bull, stallion and human sperm, leading to their entrapment. In mares, this endometrial inflammatory response is more dramatic when exposed to frozen-thawed semen, in comparison to fresh semen. While there is no such evidence of this phenomenon occurring in jenny donkeys, artificial insemination (AI) with frozen semen leads to very poor pregnancy rates. Based on these data, we hypothesised that: 1) NETosis in response to semen also occurs in donkeys; and 2) frozen-thawed semen induces more NETosis than fresh semen in this species. In Experiment 1, PMNs from jennies (n=4) were isolated by centrifugation of whole blood through a density gradient. After confirming the presence of >90% PMNs by flow cytometry, cells were incubated in the presence or absence (control) of fresh sperm (1:1, 1:2 or 1:5 PMN:sperm ratios) from one jackass. After 2h or 4h incubation, cells were fixed, stained with Sytox, and the percentage of PMNs that underwent NETosis was determined. Although NETosis increased in all groups from 2 to 4h, more PMNs had

reacted in the 1:2 and 1:5 groups, but not in the 1:1, compared to the control (2h control: 27 ± 8.6% vs. 1:2: 47 ± 8.7% and 1:5: 59 ± 8.4%; P≤0.05; 4h control: 50 ± 4.4% vs. 1:2: 89 ± 3.6% and 1:5: 92 ± 3.6%; P≤0.05). No differences were observed in the percentage of reacted PMNs between the 1:2 and 1:5 groups. According to these results, in Experiment 2, PMNs (n=3 jennies) were incubated for 2h in the presence or absence (control) of 1:5 fresh or frozen-thawed semen from the same jackass (n=3). Surprisingly, exposure to fresh semen induced higher NETosis than incubation with frozen-thawed semen (78 ± 5.7% vs. 23 ± 2.4%, respectively; P≤0.01). In addition, no differences were observed between the frozen-thawed group in comparison to the control ($23 \pm 2.4\%$ vs. $31 \pm 3.7\%$, respectively; P>0.05). In conclusion: 1) both incubation time and fresh sperm concentration positively correlate with the percentage of jenny PMNs that release NETs, however, 2) frozen-thawed semen does not elicit this response. Because samples were prepared following the steps normally used to produce commercial fresh and frozen semen doses, seminal plasma was more diluted in the frozen-thawed samples in comparison to the fresh samples. In addition, a higher percentage of motile sperm were observed in the fresh than in the frozen-thawed semen samples (as one would expect). Thus, these two factors could explained the differences in NETosis reported in the present study. Future experiments will address these observations in order to elucidate the role that NETs play in donkey reproductive physiology. This work was supported by EU Horizon 2020 Marie Skłodowska-Curie (No 792212).

Abstract # 2201

Characterization Of Putative Biomarkers In Sows With Elevated Risk For Pelvic Organ Prolapse During Late Gestation. Zoe Ekiefer, Jamiem Studer, Amanda Lchipman, Jasonw Ross

Within the past 10 years, the incidence of pelvic organ prolapses (POP) has been increasing in the U.S. swine herd and continues to increase year-over-year. In a survey of the U.S. swine industry, we have recently demonstrated that POP contributes to approximately 21% of sow deaths annually. We have previously developed and tested a perineal scoring system that effectively identified sows for differing risk of POP during late gestation. Further, we have also demonstrated that sows differing in perinealscores demonstrated differences in their vaginal microbiomes and both circulating lymphocytes and monocytes were reduced in sows with elevated risk for POP compared to those with minimal risk. We hypothesized that sows differing in perineal score (and as a result differing in risk of POP) during late gestation will also exhibit differences in serum factors associated with inflammation and/or infection. The objective of our study was to characterize potential inflammation biomarkers (haptoglobin, c-reactive protein (CRP), lipopolysaccharide binding protein (LBP), and tumor necrosis factor alpha (TNFA)) to determine their association with POP risk in sows during late gestation. Perineal scoring was conducted during late gestation (approximately days 107-116) on two commercial sow farms, and blood samples were

collected from a subset of sows scoring a perineal score 1 (PS1) or perineal score 3 (PS3) at the time of scoring. In assignment of perineal scores, PS1 presumes little to no risk of prolapse, and has none of the following: protrusion, vulva swelling, and swelling of the perineal region. A PS2 presumes moderate risk of prolapse, and has only a few of the following: protrusion, vulva swelling, and swelling of the perineal region. By comparison a PS3 presumes high risk of prolapse, and has all of the following: protrusion, vulva swelling, and significant swelling of the perineal region. Perineal scores (PS) were assigned to sows (n = 2865) which were subsequently monitored for POP occurrence. At the time of scoring, blood samples were collected and used for serum and plasma isolation on a subset of sows identified as PS3 along with parity-matched sows that scored PS1. Pelvic organ prolapses occurred in 1.0, 2.7, and 23.4% of PS1, PS2, and PS3 sows, respectively. Circulating haptoglobin was not different (P = 0.35) between PS1 and PS3 whereas C-reactive protein was 24.6% greater (P = 0.02) in PS3 sows compared to P\$1. Furthermore, serum TNFA was not different (P = 0.85) between P\$1 and P\$3 although circulating LBP increased 24.9% (P = 0.04) in PS3 sows compared to PS1 sows. This evidence supports, in part, our hypothesis that biomarkers of inflammation are differentially abundant in serum of sows differing in PS and risk for POP. This project was supported by the National Pork Board and the Foundation for Food and Agriculture Research.

Reproductive Tract: Male

Abstract # 1699

Localization And Expression Of The Vacuolar Atpase And Cytokeratin 5 In The Epididymis Of Korean Native Black Goats. Bongki Kim, Yu-Da Jeong, Sung-Woo Kim

The unique luminal environment in the epididymis that is regulated by intercellular communication networks among epididymal epithelial cells, is necessary for sperm maturation and storage. To characterize the differentiation of epididymal epithelial cells, we examined the localization and expression of H + pumping vacuolar ATPase and cytokeratin 5 in the immature and mature epididymis of goat, expressed in clear and basal cells, respectively. Epididymides were obtained from goats at 1, 2, and 12 months of age. Immunofluorescence labeling was performed, and the localization and expression patterns of V-ATPase and KRT5 were observed using confocal microscopy. At postnatal month 1 (PNM1), the localization of clear cells commenced migration from the cauda toward the caput. Although at PNM2, V-ATPase was similarly expressed in the epididymis as PNM1, V-ATPase is localized in the epithelial cells of the basal region as well as in luminal epithelial cells of the cauda epididymis. In adult goats, two types of V-ATPase positive epithelial cells were observed. One type was present at the entire epididymis with goblet-shaped morphology except for cauda region, and the second type was located at the basal region of the entire epididymis with a dome-shaped morphology. On the other hand, the basal cells with varied shapes such as columnar, projection, and round types were detected in the immatured epididymis but only dome-shaped basal cells located at the base of the epithelium were observed in the matured epididymis. In summary, 1) both clear and basal cells progressively initiates in a retrograde manner from the cauda to the caput epididymis. 2) Clear cells disappear from the cauda region after puberty and only maintain in the caput and corpus regions at the adult epididymis. 3) Interestingly, in the goat epididymis, both V-ATPase and KRT5 were co-expressed in differentiated basal cells that were located at the base of the epithelium. These results suggest that the specific distribution and localization of the epithelial cells could be necessary for establishing an optimal luminal environment for sperm maturation and storage in the goat epididymis.

Abstract # 1740

Quercetin Enhances Induced Acrosome Reaction with Calcium and Calcium Ionophore A23187 in Boar Fresh Spermatozoa. Reza Rajabi-Toustani, Kotono Nakamura, Kazuki Hano, Mohammad Roostaei-Ali Mehr, Quzi SharminAkter, Tatsuya Matsubara, Masaki Takasu

Acrosome reaction is membrane fusion between the outer acrosomal membrane and the plasma membran, followed by vesiculation and exocytosis of the contents of the acrosomal cap. As a prerequisite for normal fertilization, the content of the acrosome is released during the acrosome reaction, which is triggered by the zona pellucida. Calcium ionophore A23187 induces Ca2+ influx, thereby triggering the acrosome reaction. In several domesticated species were reported that there is a relation between the efficacy of a sperm population to undergo the acrosome reaction and male fertilizing potential. Quercetin is a plant flavonol from the flavonoid group of polyphenols and widely distributed in plants and vegetables. It is widely known as potent natural antioxidant and scavenger of reactive oxygen species (ROS) and nitric oxide and can act in the treatment of male infertility by decreasing of H2O2 level, chelation of divalent cations and inhibition of lipoxy radical formation. It could improve sperm parameters and change the expression of CatSper 2, 4 genes in aging male mice. It was reported that CatSper channel mediates progesterone-induced Ca2+ influx, indicating a role in hyperactivation and acrosome reaction in human spermatozoa. The purpose of this study was the effect of different concentrations of guercetin on inducibility of acrosome reaction in the presence of calcium and calcium ionophore in boar fresh spermatozoa. Semen was collected from three mature fertile Landrace boars by the gloved-hand method, diluted with Beltsville Thawing extender and stored at 17 °C up to 3 days. It was washed and incubated with different concentrations of quercitin (0, 50, 100, 200 µM) at 37 °C for 20 minutes. Acrosome reaction induced with incubation of spermatozoa with calcium and calcium ionophore A23187 or DMSO (control) for 10 minutes. At 0, 5 and 10 minutes of incubation, spermatozoa were fixed with 2% paraformaldehyde and stained with fluorescein isothiocyanate peanut agglutinin (FITC-PNA). Following an incubation of 5 minutes at 37 °C, 10,000 gated events were recorded using BD FACSCanto™ II flow cytometer and were analyzed in FlowJo software (Version 10; FlowJo, LLC). Results were presented as the mean ± SEM. All data analyses were performed using a statistical software program (GraphPad Prism Version 8.0; San Diego, CA, U.S.A.). In treatments incubated with DMSO (control) there was not any significant main effect of quercetin, time, and interaction of guercetin and time (P > 0.05), while treatments incubated with calcium ionophore A23187 were significantly affected (P < 0.05). After 5 minutes incubation with calcium ionophore A23187, treatment with 200 µM guercetin showed the highest percentage of acrosome reaction and significant difference with other treatments (P <0.05). After 10 minutes incubation with calcium ionophore A23187, the results revealed that treatment with 50 µM guercetin had the highest percentage of acrosome reaction in comparison to the other treatments (P < 0.05). Overall, preincubation of spermatozoa with quercetin had enhancement effect on acrosome reaction but the effect of high concentration of quercetin dropped with the passing of time.

Abstract # 1776

Na, K-ATPase a4 Controls Glucose Uptake in Sperm via the Sodium Glucose Cotransporter. September Numata, Gustavo Blanco, Gladis Sanchez, Jeffrey McDermott, Kristen Schwingen, Amrita Mitra

Despite the prevalence of male factor infertility, one third of cases are classified as idiopathic, seemingly due to a lack of understanding of the mechanisms underlying

sperm function. We have previously shown that the testis specific Na, K-ATPase a4 isoform (ATP1A4), an ion transporter that exchanges Na + and K + across the sperm flagellar membrane, is essential for male fertility. Thus, deletion of the ATP1A4 gene in mice results in complete male infertility, due to impaired sperm motility and capacitation. Here, we investigated the mechanisms by which ATP1A4 supports sperm function. We found that sperm from ATP1A4 knockout mice have reduced glucose uptake and ATP levels compared to wild type mice. This suggested the presence of sodium glucose cotransporters (SGLTs) in sperm. We confirmed the expression of SGLT by PCR and immunoblot analysis; and identified SGLT-1 as the SGLT isoform expressed in sperm. Inhibition of SGLT1 with the SGLT inhibitors phloretin and phlorizin reduced glucose uptake and total motility of sperm. Altogether, these results display the presence of a Na + -dependent transport of glucose in sperm and suggest that, by maintaining the transmembrane Na + gradient, ATP1A4 is involved in sperm glucose uptake via SGLT-1. [Supported by NIH R01 HD080423]

Abstract # 1885

Utility of PSP94/PSA as a Marker for Differentiating Between Benign Prostatic Hyperplasia and Prostate Cancer Amongst Lower Urinary Tract Symptoms patients: A Pilot Study. Dhanashree D. Jagtap, Bhalchandra J. Kulkarni, Smita D. Mahale, Prakash Pawar, Bhushan Patil, Ajit Sawant, Sujata Patwardhan, Mukund Andankar

Serum PSA (Prostate Specific antigen) is used worldwide for diagnosis of prostate cancer (PCa). PSA is sensitive but lacks specificity for PCa as serum PSA increases in benign prostatic hyperplasia (BPH) and prostatitis. PSP94 (Prostate Secretory Protein 94 amino acids) is synthesized and secreted by the epithelial cells of the prostate. Serum PSP94 levels are found to be lower in PCa patients as compared to BPH cases. The study aimed to test whether ratio of PSP94 and PSA can differentiate between PCa and BPH patients than PSA or PSP94 alone. The objectives were to measure the levels of serum PSP94 using in house developed ELISA in lower urinary tract symptoms (LUTS) patients with prostate pathophysiology and to ascertain whether serum PSP94/PSA ratio has a diagnostic potential to differentiate between BPH and PCa. Further also to check whether serum PSP94/PSA could aid the clinicians in reducing the number of prostate biopsies in LUTS patients with PSA values between 4-20 ng/ml. LUTS patients were consented and recruited as study participants. 5ml blood was collected and used for estimating their serum PSA and PSP94 levels and PSP94/PSA ratio was determined to check the utility of PSP94/PSA ratio as a diagnostic indicator for differential diagnosis of PCa/BPH. 571 LUTS patients from three municipal hospitals in Mumbai, Maharashtra, India were enrolled based on their International Prostate Symptoms Score (IPSS), digital rectal examination (DRE) and ultrasonography (USG) as study participants. 58.7% of the patients had moderate IPSS and 36.5% had severe IPSS. Grade I DRE was found in 44.6% patients while 55.4% had DRE ranging from grade II-IV. Majority had prostate volume between 20-50cc (60.4%) and 30% patients had prostate volume between 52-100cc. Serum PSA and PSP94 was estimated in 533 study participants. Normal PSA values (< 4.0

ng/ml) were found in 376 (70.5%) subjects and 135 (25.3%) subjects had PSA values between 4-20 ng/ml while 22 subjects (4.2%) had PSA values >20 ng/ml. PSP94 median values were found to be 23, 34.3 and 48 (ng/ml) for PSA < 4 ng, 4-20 and >20 ng/ml respectively. In LUTS patients with normal PSA (> 4ng/ml), median PSP94/PSA ratio was 20.26, for PSA between 4.1-20 ng/ml the PSP94/PSA ratio was 4.1 and ratio was 0.87 for PSA values >20 ng/ml. For patients with >20 ng/ml PSA, PSP94/PSA ratio did not miss any prostate cancer cases. Out of 135 patients with PSA between 4-20 ng/ml, 64 prostate biopsies were done. For this group of patients, the PSP94/PSA ratio cutoff of <5.29 showed 100% specificity with 43.3% sensitivity. Biopsy correlation in LUTS patients with PSA 4-20 ng/ml showed that based on PSA data alone, 100% prostate biopsies were required while when PSP94/PSA ratio cutoff of <5.29 was used, 41% biopsies confirmed negative. Results indicate that ratio of serum PSP94/PSA could be useful to prevent ~40% biopsies in patients with prostate pathophysiology in the PSA range of 4-20 ng/ml.

Abstract # 1951

Epididymal Basal Cells Expressing LGR5 Are Multipotent Adult Stem Cells. Laurie Pinel, Daniel Cyr

The epididymal epithelium is pseudostratified and comprised of various cell types including principal, clear, narrow and basal cells. Basal cells share common properties of adult stem cells. They can differentiate into principal and clear cells in vivo, form organoids, self-renew, and differentiate in vitro. The characteristics of basal cells support the notion that these serve as a stem cell population residing at the base of the epididymal epithelium. However, there is currently no method to specifically identify epididymal stem cells. The present objective is to identify a specific marker of this population of stem cells in the epididymis. Leucine-rich repeat-containing G-protein coupled receptor 5 (LGR5) is a seven-transmembrane G-coupled receptor. It shares homology with two members of the LGR family, LGR4 and LGR6; all three proteins are receptors for R-Spondin growth factors, which modulate Wnt/Spondin signaling. LGR5 is a well-established marker of adult stem cells in a variety of tissues. We developed epididymal basal cell-derived organoids as a means to investigate epididymal stem cell differentiation. LGR5 was overexpressed in isolated basal cells of the rat epididymis and localized to the plasma membrane of basal cell-derived organoids. Its expression decreased as organoids differentiated. LGR5, 4 and 6 transcripts were expressed throughout the epididymis during postnatal development. LGR5 and LGR6 mRNA levels decrease during postnatal development while LGR4 mRNA levels remained constant. LGR5 was immunolocalized to undifferentiated columnar cells of the epididymis as early as PND7. However, as the epithelium differentiated, LGR5 became associated with basal cells. In the adult epididymis, LGR5 was localized primarily to basal cells, although weak staining was observed in narrow cells. Co-localization of LGR5 with the basal cell marker TP63 in the adult epididymis indicated the existence of at least 3 basal cell subtypes: LGR5 + /TP63 - , LGR5 + /TP63 + and LGR5 - /TP63 + . Together these data demonstrate that LGR5 is expressed in basal stem cells of the epididymis and that these cells have the ability to form organoids in vitro. Supported by CIHR, CIRD and the Canada Research Chairs Program.

Abstract # 1954

Na,K-ATPase a4 Undergoes Phosphorylation During Sperm Capacitation. Kristen M. Schwingen, Gustavo Blanco

Na,K-ATPase a4 (ATP1A4) is an integral plasma membrane protein responsible for the exchange of Na + and K + between the cell and its environment. ATP1A4 is only found in male germ cells of the testes and is highly expressed in spermatozoa, where its function is necessary for sperm motility and capacitation. We have previously shown that ATP1A4 activity is upregulated in rat sperm during capacitation in vitro . Here, using immunoprecipitation and immunoblot analysis, we found differences in the levels of ATP1A4 phosphorylation when rat sperm was incubated in non-capacitated and capacitated conditions. Specifically, ATP1A4 phosphorylation of Tyrosine residues increased and Serine/Threonine phosphorylation remained constant. However, the pattern of ATP1A4 phosphorylation differs between both conditions. These results were confirmed using tandem mass spectrometry (MS/MS). These data show that ATP1A4 is post-translationally modified and is subjected to a complex pattern of phosphorylation. This regulatory mechanism may be adjusting ATP1A4 activity to the functional needs of the male gamete.

Abstract # 2259

CRISPR/Cas9-Mediated Genome-Edited Mice Reveal 10 Testis-Enriched Genes Are Dispensable For Male Fecundity. Soojin Park, Keisuke Shimada, Yoshitaka Fujihara, Zoulan Xu, Kentaro Shimada, Tamara Larasati, Putri Pratiwi, Ryanm Matzuk, Darius Jdevlin, Zhifeng Yu, Thomas Xgarcia, Martinm Matzuk, Masahito Ikawa

As the world population continues to increase to unsustainable levels, the importance of birth control and the development of new contraceptives are emerging. To date, male contraceptive options have been lagging behind those available to women, and those few options available are not satisfactory to everyone. To solve this problem, we have been searching for new candidate target proteins for non-hormonal contraceptives. Testis-specific proteins are appealing targets for male contraceptives because they are more likely to be involved in male reproduction and their targeting by small molecules is predicted to have no on-target harmful effects on other organs. Using in silico analysis, we identified that Erich2, Glt6d1, Prss58, Slfnl1, Sppl2c, Stpg3, Tex33 and Tex36 are testis-abundant in both mouse and human. 4930402F06Rik and 4930568D16Rik, paralogs of Glt6d1 in mice but not human, were also included to eliminate the potential for compensation. We generated knockout (KO) mouse lines of all listed genes using the CRISPR/Cas9 system. Analysis of all of the KO mouse lines revealed that they are male fertile with no observable defects in reproductive organs, suggesting that these 10 genes are not individually required for male fertility. Further studies are needed to uncover protein function(s), but in vivo functional screening using the CRISPR/Cas9 system is a fast and accurate way to find genes essential for male fertility, which may apply to other studies. In this study, although we could not find any potential protein targets for non-hormonal male contraceptives, our findings help to streamline efforts to find essential genes.

Abstract # 2354

Sperm Motility And Actin Polymerization Are Regulated By Extruded cAMP Through MRP4 in Bovines. Nicolás Chiarante, Carlos Agustín Isidro Alonso, Raquel Lottero, Camila Arroyo Salvo, Jessica Plaza, Eugenia Bogetti, Carlos Davio, Marcelo Miragaya, Silvina Perez Martinez

Capacitation is a key process involved in the acquisition of sperm fertilizing competence. The importance of cAMP during capacitation has led us to study the role of this nucleotide as an extracellular stimulus, as well as the multidrug resistanceassociated protein 4 transporter (MRP4) that extrudes cAMP from cells. Our group previously described that MRP4 mediates cAMP efflux in bovine spermatozoa and that extracellular cAMP triggers events associated to capacitation. In this work, we deepen the study of the role of MRP4 in the acquisition of sperm fertilizing ability using MK571, an MRP4 inhibitor. We evaluated capacitation by LPC-induced acrosome reaction and the ability of sperm to be released from oviductal epithelia. Both events were decreased when the MRP4 inhibitor (50 μ M) was added (p<0.05). Immunofluorescence evidenced that MRP4 is localized in the acrosomal and post-acrosomal regions, and mid-piece of the flagellum at 15 min capacitation time. After 45 min, the protein was mainly located in the acrosome, and few sperm labelled in the post-acrosomal region and the mid-piece were observed. As a result of MRP4 localization in the flagellum, we investigated its involvement in motility in spermatozoa incubated during 15 min in capacitating conditions (CAP). After a 15 min incubation with MK571, a decrease in total sperm motility (TM) was observed. Also, MK571 significantly decreased progressive motility (PM), as well as kinematic parameters such as, VCL, VAP, ALH and BCF. Interestingly, the addition of non-permeable cAMP not only rescued MK571 effect but also increased the percentage of TM, PM and VCL, VSL, VAP, STR and ALH with respect to CAP values. Furthermore, the incubation with cAMP alone produced an increase of TM and PM similar to the MK571+cAMP condition. Since actin cytoskeleton plays essential roles in the regulation of sperm motility, we investigated if MRP4 activity might affect actin polymerization (F-actin). An increase in F-actin (assessed by Alexa 488phalloidin) was observed in spermatozoa after a 15 min incubation in CAP with respect to non-capacitating condition (NC). This increase was detected in sperm's heads as well as in their tails. When MRP4 was inhibited, F-actin decreased, in a process that was reverted with extracellular CAMP 10 nM. In addition, the incubation of CAMP alone

increased F-actin levels both in CAP and NC conditions. Finally, we assessed if cAMPinduced actin polymerization could be mediated by the protein kinase A (PKA). No Factin was detected after cAMP addition when different PKA inhibitors such as H89 (50 μ M), KT5720 (100 nM) and Rp cAMPs (1 mM) were employed. In conclusion, our results support the importance of cAMP efflux through MRP4 in sperm capacitation and suggest its involvement in the regulation of actin polymerization and sperm motility. In addition, the hypothesis of the role of extruded cAMP in an autocrine/paracrine fashion in bovine sperm is reinforced in this work.

Abstract # 2367

Anandamide Regulates Signaling Pathways Associated To Bovine Sperm Motility Through GPR55 Receptor Activation. Raquel M. Lottero Leconte, Camila Arroyo Salvo, Eugenia Bogetti, Nicolás Chiriante, Jessica Plaza, Marcelo Miragaya, Silvina Perez Martinez

The endocannabinoid system (ECS) is an evolutionarily conserved system and has been detected in most reproductive tissues and fluids. ECS is composed of the metabolizing enzymes, the cannabinoid (CBs and TRPVs) receptors and the endocannabinoids. Anandamide (AEA) is the major endocannabinoid and plays a crucial role in sperm function. In addition, AEA is present in uterine and oviductal fluids, and in this sense, spermatozoa are exposed to AEA when they swim through the female's reproductive tract which might affect their sperm fertilizing ability. Previously, we found in bovines that AEA is involved in sperm capacitation by activation of CB1 and TRPV1, but not CB2 receptors. Furthermore, we recently characterized in bull spermatozoa a novel cannabinoid receptor, G protein-coupled receptor 55 (GPR55), which is also modulated by AEA. The weight of evidence points to GPR55 as a receptor that is activated by certain cannabinoid ligands, such as AEA, and by the bioactive lipid I-alysophosphatidylinsoitol (LPI). GPR55 is coupled to different G proteins that activate a widespread of signaling cascades that include cAMP/PKA and PLC/PKC pathways. We demonstrated that GPR55 is localized in the equatorial segment and in the flagellum of capacitated spermatozoa. Also, the activation of GPR55 by AEA is involved in the regulation of sperm motility in bull spermatozoa. In this work, we aimed to study the possible molecular pathways triggered by the activation of GPR55 involved in the regulation of sperm motility. First, we confirmed the participation of GPR55 in sperm motility by using different pharmacological tools. Results of computer-assisted sperm analysis supported that the increase of progressive motility by AEA 1 nM and Met-AEA 1.4 nM (a non-hydrolysable analogue of AEA) was reverted by 10 µM CID16020046, a selective GPR55 antagonist (p<0.05). In order to evaluate the molecular pathway involved in GPR55 activation, we measured protein kinase A (PKA) activity by determination of phosphorylated PKA substrates by Western blot. The incubation of spermatozoa with AEA during 45 min produced an increase of phosphorylated PKA substrates which was decreased by the presence of GPR55 antagonist (p<0.05). The same effect was observed when phosphorylated PKC substrates were measured in the

presence of AEA and/or CID16020046 (p<0.05). On the other hand, the incubation with AM251 (0.2 μ M), a synthetic analogue of LPI, produced an increase of phosphorylated PKC substrates but it had no effect on PKA activity. Then, we analyzed the involvement of PKA and/or PKC activations in sperm motility modulated by AEA. The incubation with H89 (50 μ M) or Gö6983 (10 μ M) (PKA and PKC inhibitors, respectively) decreased progressive motility induced by the endocannabinoid. These results suggest that the activation of GPR55 involves PKA and PKC pathways and support the role of AEA in sperm motility in bovines.

Sex Determination and Differentiation

Abstract # 1949

Functional Characterization Of Cyp19a1(Aromatase) In Sexual Differentiation In Chicken (Gallus Gallus) Embryonic Development. Kai Jin

Cyp19a1 (cytochrome P450 family 19 sub family A number 1, Aromatase) is the vital enzyme as a crucial regulator in sexual differentiation in vertebrates by initiation and maintained the estradiols synthesis. Here we described the expression pattern of Cyp19a1 and its function role in chicken embryonic gonads development. Results showed that Cyp19a1 exhibited female sexual dimorphic expression pattern in embryonic gonads early at day 5.5(HH 28) and robustly expression in cytoplasm at ovary medulla. Most importantly, we ectopically delivered the AI (Aromatase inhibitor) or E2(Estradiol) to chicken embryo induced gonadal sex-reversal characterized. To further explore the role of the Cyp19a1 in chicken embryonic sex differentiation, we successfully developed an effective interfere and overexpression method in chicken (Gallus gallus) using the embryonic intravascular injection. The interfere and overexpression of Cyp19a1 analyses provide solid evidence that Cyp19a1 is both necessary and sufficient to initiate female development in chicken (Gallus gallus) embryonic via lentivirus-mediated RNAi and over-expression systems. Collectively, this work demonstrate that Cyp19a1 is a crucial sex-differentiation gene in embryonic development, which provides a foundation for understanding the mechanism of sex determination in chicken (Gallus gallus).

Spermatogenesis

Abstract # 1684

Increased Ros Production By Sertoli Cells, Testicular Germ Cells And Epididymal Epithelial Cells Are Associated With Subfertility Of Arsa Null Mice. Nongnuj Tanphaichitr, Arpornrad Saewu, Kessiri Kongmanas, Wongsakorn Kiattiburut, Mark A. Baker, Kym F. Faull, Dylan Burger

Arylsulfatase A (ARSA) with its co-enzyme, saposin B, desulfates sulfoglycolipids including sulfogalactosylglycerolipid (SGG), selectively expressed in testicular germ cells (TGCs) and sperm and with relevance in spermatogenesis and sperm fertilizing ability. In testes, ARSA activity is highest in Sertoli cells (Tanphaichitr et al., Prog Lipid Res 2018). Herein we demonstrated that ARSA and saposin B together with SGG were localized in Sertoli cell lysosomes. Since Sertoli cells do not have enzymes to synthesize SGG, this SGG was presumably from residual bodies and apoptotic TGCs phagocytosed by Sertoli cells. Following SGG desulfation by ARSA, galactosylglycerolipid generated would be degalactosylated by galactosylceramidase, present in Sertoli cell lysosomes, to become palmitylpalmitoylglycerol, the SGG backbone neutral lipid, which could

traffic to TGCs to initiate SGG biosynthesis. We have been using Arsa-/- mice to study the role of ARSA in male reproduction and have described their subfertility at the advancing age (>5 months). Eight-month-old Arsa-/- mice show significant decreases in spermatogenesis, sperm fertilizing ability, and litter sizes upon mating with fertile females, compared with age-matched wild types (WTs). High levels of TGCs are also abnormally present in the epididymal lumen. Uniquely, Sertoli cell lysosomes in Arsa-/- mice at 5 months of age and older are obviously swollen with SGG accumulation, typical of lysosomal storage disorder (Xu et al., J Lipid Res 2011). Herein, we demonstrated by mass-spectrometry analyses that SGG levels in Sertoli cells of 8-month-old Arsa-/- were twice those in WT Sertoli cells. Since various cells exhibiting LSD are associated with oxidative stress, we determined superoxide levels in Sertoli cells from 5- and 8-month-old Arsa-/- and WT mice by quantifying 2-hydroxyethidium generated after cell incubation with dihydroethidium. Our results revealed a trend in increasing superoxide levels in Arsa-/- Sertoli cells at both ages, but the increases were not significantly different from the WT levels. However, by using Amplex Red assay, we found that levels of H2O2 generated by Arsa-/- Sertoli cells from 5-month-old and 8-month-old males were 2.5X and 2.1X of those produced by counterpart WT Sertoli cells (P=0.0005 and 0.01, respectively). The released H2O2 could be self-damaging to Sertoli cells and deleterious to TGCs present in adluminal compartments between Sertoli cells. In fact, the number of Sertoli cells isolated from 8-month-old Arsa-/- mice was one half of that isolated from age-matched WTs, and Arsa-/- Sertoli cells had a 62% apoptosis rate compared with 19% of the WT after 4 days in culture. Similarly, the number of TGCs isolated from 8-month-old Arsa-/- mice was 50% of the WT value. Furthermore, TGCs and the epididymis of Arsa-/- mice at both 5 and 8 months of gae produced significantly higher superoxide levels than the WT counterparts. All of the increases in ROS production in the reproductive system of Arsa-/- mice are likely a factor that contributes to their subfertility at advancing ages. Overall, our results indicate the significance of ARSA and SGG homeostasis in male reproduction.

Dynamic Changes of TDP-43 from Germ Cell Development to Epididymal Sperm Maturation. Lyndzi M. Miller, Prabhakara P. Reddi

TAR DNA-binding protein of 43 kDa (TDP-43) is a ubiquitously expressed and evolutionarily conserved protein. TDP-43 has several functions which include gene transcription, mRNA splicing and stability, transposon silencing, and micro RNA biogenesis. TDP-43 is implicated in many neurodegenerative disorders including ALS. Using genetic mouse models, we demonstrated that TDP-43 is essential for spermatogenesis and male fertility. We also showed that sperm from infertile men contain aberrant forms of TDP-43. One in six couples worldwide struggle with infertility with male factor accounting for half the cases, highlighting the importance of better understanding the mechanisms regulating spermatogenesis. The goal of the present study was to evaluate the dynamic changes of TDP-43 expression in the testis through sperm maturation in the epididymis. Previous work demonstrated that TDP-43 is expressed in the intermediate spermatogonia, abundantly expressed in spermatocytes (except leptotene and zygotene spermatocytes), and at a low level in step 1-6 round spermatids. In the present work, indirect immunofluorescence showed that TDP-43 is expressed in the equatorial segment of caudal sperm; however, TDP-43 is not expressed in Step 16 testicular spermatids. We hypothesize that sperm reacquire TDP-43 during transit through the epididymis. CD1 and C57/B6 mouse testis and caudal sperm were collected and immunoblots were performed using antibodies that recognize N- and Cterminal epitopes of TDP-43. We observed identical patterns of TDP-43 immunoreactivity between the CD1 and C57-B6 background mice. The testes samples (n=12) showed TDP-43 bands at 43 kDa (the expected size for a 414aa protein). In contrast, the caudal sperm samples (n=22) displayed a prominent TDP-43 band at ~55 kDa. We find this

difference interesting and predict that protein dimerization and/or post-translational modifications account for the 55 kDa TDP-43 band. Further, an approximately 35kDa cleaved product of TDP-43 was present in both samples. Interestingly, the 35kDa band showed reciprocal reactivity with N- and C-terminal recognizing antibodies in testis and caudal sperm. We hypothesize that these dynamic changes in TDP-43 species indicate differences in functional requirement of this protein in germ cells versus epididymal sperm. Overall, TDP-43 is critical for male fertility and may become a useful biomarker in the andrology clinic.

Abstract # 1754

Loss Of TDP-43 In Sertoli Cells Leads To Failure Of Spermatogenesis In Mice. Helena D. Zomer, Jeremy Rayl, Prabhakara P. Reddi

Infertility affects 15% of human couples and approximately 30 to 40% of the occurrences are due to the male factor. In most cases of male infertility, the underlying pathogenesis is idiopathic. The TAR DNA binding Protein of 43 kD (TDP-43) is an evolutionarily conserved, ubiquitously expressed transcription factor and RNA-binding protein with major human health relevance. It has been previously shown to be present in Sertoli and germ cells of the testis, and its aberrant expression was reported in the sperm of infertile men. Sertoli cells play a key role in spermatogenesis by offering physical and nutritional support to the male germ cells. Thus, the aim of this study was to investigate the requirement of TDP-43 in Sertoli cells. Conditional knockout (cKO) of TDP-43 in mouse Sertoli cells using the Amh-cre deleter strain caused failure of spermatogenesis and male infertility. The cKO mice showed decreased testis weight from as early as postnatal day (PND) 12, which persisted to adult age, and a 5-fold reduction in sperm count. Histopathological analysis revealed seminiferous tubules with a decreased diameter and multiple degenerating alterations, including loss of germ cell layers, presence of vacuoles, and sloughing of round spermatids, suggesting loss of contact with Sertoli cells. Using a biotin tracer, we found that the blood-testis-barrier (BTB) was disrupted in 28.5% of tubule cross-sections at PND 24 and 42.7% at PND 90 in TDP-43 cKO mice. Investigation of the junction proteins by immunohistochemistry showed that the expression of connexin-43 (gap junction) and N-cadherin (ectoplasmic specialization) was altered in 73.7 ± 15.1 SD and $56.25\% \pm 25.6$ SD of the tubules, respectively. Quantitative real-time PCR showed overexpression of candidate genes involved in the formation and/or maintenance of Sertoli cell junctions (N-cadherin, Gja1/connexin-43, claudin-11, and occludin) as well as in the phagocytic pathway (Elmo1, Rac1, Tyro3, and Bai1). Finally, Oil Red O lipid staining showed a decrease in the number of tubule cross-sections containing lipid droplets in Sertoli cells and in the tubule lumen of cKO mice. Given that Sertoli cytoplasmic lipid droplets result from the phagocytosis of residual bodies and apoptotic germ cells, the data indicate inefficient phagocytosis. Overall, our findings suggest that TDP-43 is required in Sertoli cells for the completion of spermatogenesis, formation and maintenance of the BTB, and phagocytosis, thus indicating an essential role for TDP-43 in male fertility.

The Atypical Centriole of Spermatozoa: A Molecular Basis for Basal Sliding and Asymmetric Flagellar Beating. Sushil Khanal, Kebron Assefa, Abigail Royfman, Emily Lili Fishman, Mohamad Baker Nawras, Katerina Turner, Matthew Robert Stolsavljevic, Puneet Sindhwani, Tomer Avidor Reiss

Sperm cells have two centrioles, microtubule based sub cellular structure that form centrosomes and cilia. The centrioles are named based on their relative location: the proximal centriole and the distal centriole. We discovered in human and other mammals that the spermatozoon distal centriole (SDC) is remodeled during spermiogenesis to have an atypical structure and it functions in the zygote as expected from a centriole (Fishman et. al., 2018). The SDC in human consists of doublet microtubules splayed outward making a funnel shape structure, instead of triplet microtubules and barrel shaped structure found in the typical centriole. Importantly, the SDC consists of a unique organization of centriole lumen proteins, POC1B, POC5, and CETN1 into two main rod structures, which we refer as SDC rods. The SDC rods flank the microtubule. The mechanistic detail forming the atypical centriole and its role remains an enigma. Recently, we identified a novel SDC rod protein, FAM161A. In vitro, FAM161A binds to microtubules and SDC rod proteins (POC1B and POC5). In the spermatozoon, FAM161A appears to localize between the microtubules and POC1B or POC5, suggesting that FAM161A functions as a linker between the microtubules and rods. In vivo, FAM161A have a unique localization during spermiogenesis. In the round spermatid stage of human, bovine, and rabbit, centriole remodeling initiates with the enrichment of POC1B, POC5, and CETN1 and their elongation in both proximal and distal centrioles. In the same stage, FAM161A localizes only in a unique plate like structure close to proximal centriole. Later, in the elongated spermatid stage, the FAM161A incorporates into the centrioles. This timing of incorporation suggests that the FAM161A function in centriole remodeling after the rods have already started to form. In the spermatozoon, the protein organization of the SDC rod has left-right asymmetry. The position of left and right rod has distinct position in straight and curved sperm tail, suggesting that the rods are sliding up and down during flagellar beating. This is the first direct evidence that the asymmetric flagellar beating during sperm movement is accompanied with the centriole internal movement. Altogether, this study gives a novel insight to the sperm atypical centriole formation and suggests that centriole sperm are atypical to allow centriole movement which may control sperm movement. This work is supported by grant HD092700 from Eunice Kennedy Shriver National Institute of Child Health & Human Development (NICHD).

The Effect Of Carnitine And Hypotaurine On The Cryopreservation Of Jeju Horse Semen. Sung Woo Kim, Sang Min Shin, Kwang-yun Shin, Jae Young Lee, Chan-Lan Kim, Yeoung-Gyu Ko,

The Jeju horse has been used for more than 700 years as a draft animal in agriculture with a small size but strong in physical ability. However, the number of Jeju horses is now dropped to 5 thousand. The cryopreservation of semen is essential to preserve the originality of Jeju horse. The 6 animals were used to increase the freezing property of the semen with INRA Freeze and KTM diluent that was supplemented with carnitine, glutathione, and hypotaurine. After collection with artificial vagina, fresh semen was diluted with INRA 96 diluent at the ration of 1:3 to 1:4 and cooled to 17 °C for 30min, and centrifuged at 600g for 10min. The 150~200 x 10 6 /ml cells were re-diluted with freezing diluents at 25 °C and cooled to 5°C for 2-3 hours. The cooled diluent was packed into a 0.5ml straws, with exposure to the vaper of LN2 with 5cm height from the surface, and plunged into the LN2. The percentage of motile sperm of 1mM carnitine and 1mM hypotaurine in INRA freeze diluent was higher than control groups, carnitine, glutathione or hypotaurine (71.3±4.6 vs 55.2±6.1, 60.1±4.6, 63.2±2.3 64±5.1, p<0.05). With KTM diluent, the similar results could be found but the viability of all treatments was lower than INRA freeze (57.3±3.2 vs 48.1±4.3, 41.2±3.2, 47.3±3.5, 46.2±4.6). These results show that the additive effects of carnitine and hypotaurine improve sperm viability which was protected from ROS during freezing procedures.

Abstract # 2145

Role of the Bovine PRAMEY Protein in Sperm Function. Chandlar H. Kern, Wansheng Liu

The purpose of this study was to determine whether the Y-linked PRAME (PRAMEY) protein plays a role during bovine sperm capacitation and acrosome reaction (AR). Freshly ejaculated sperm was collected from normal Holstein AI bulls (n=5) at 3 different time points - for biological and technical replicates. PRAMEY localization was observed by western blot (WB) and immunofluorescent (IF) staining on sperm samples with the following treatments: A. 0 hr. control, B. 5 hr. control, C. capacitated and AR, D. capacitated and non-AR, E. capacitated and AR with PRAMEY antibody, F. capacitated and AR with Rabbit IgG, G. capacitated and non- AR with PRAMEY antibody, and H. capacitated and non- AR with Rabbit IgG. Sperm (1x108) were incubated at 37 o C with 5% CO 2 and humidity to induce capacitation and the acrosome reaction for 4 hrs. and 1 hr., respectively. Treatment A had no incubation time, treatment B was incubated for 5 hrs. in PBS, and treatments C-H were treated to induce capacitation using an SP-TALP buffer and heparin. Treatments C, E, and F were then incubated with an SP-TALP buffer and Lysophosphatidylcholine (LPC) to induce the AR, while treatments D, G, and H were incubated in SP-TALP only during that time. WB analysis indicated that three PRAMEY isoforms (58, 30, and 13 kDa) were detected in the current experiments. The 30 kDa isoform was moderately to highly expressed in all treatments except in the AR sperm. The 13 kDa isoform was detected in the 5 hr. control and non-AR samples, but not in the 0 hr. control, suggesting that the 13 kDa isoform appears after sperm have went through the hyperactivation process of capacitation, and that the 13 kDa isoform could be the active PRAMEY isoform for sperm motility. Furthermore, the PRAMEY isoforms (58, 30, and 13 kDa) were not detected in the AR sperm (C, E, and F treatments) except for treatment (E) where the 58 kDa isoform is rescued due to the addition of PRAMEY antibody during the AR process. These results prompt us to hypothesize that PRAMEY is released during the acrosome reaction. To test our hypothesis, IF staining with PRAMEY-specific antibody was performed on fixed sperm from all eight treatments. A typical acrosome-enriched PRAMEY staining pattern was observed in sperm from all non-AR treatments (A, B, D, G, H), whereas little to no PRAMEY staining was observed in the acrosome region of the AR sperm (C, E, F treatments), supporting our hypothesis. In conclusion, our preliminary data demonstrated that the 13 kDa PRAMEY isoform may play a role in sperm motility during capacitation, and the 58 and 30 kDa PRAMEY is involved in the acrosome reaction.

Abstract # 2154

N- linked Glycosylation Supports the Cross Talk of Sertoli cells and Germ cells during Spermatogenesis in Mammals. Barnali Biswas, Krupanshi Brahmbhatt, Rupashree Salvi, Pamela Stanley

Complex and hybrid N-alycan synthesis are initiated by N-acetylalucosaminyltransferase I (GICNACT-I or MGAT1). N- glycans are differentially expressed in germ cells during spermatogenesis in the mouse. We have generated the first conditional deletion of complex N-glycans in Spermatogonia (Sg) and revealed a germ-cell autonomous defect in spermatogenesis. Conditional deletion of Mgat1 in spermatogonia (Mgat1 cKO) causes reduced ERK1/2 signaling and the formation of multinucleated cells (MNC). We showed that MALDI imaging MS (MALDI-IMS) glycomics of N-glycans released from testis sections revealed only oligomannosyl N-glycans in Mgat1 cKO germ cells. To determine in which germ cells MGAT1 is essential for spermatogenesis, we investigated Mgat1 cKO males that also expressed a Mgat1- HA transgene under the control of a germ cell-specific promoter - Stra8 in spermatogonia, Ldhc in spermatocytes and Prm1 in spermatids. Transgenic males expressing Mgat1 -HA in each germ cell type were fertile and both males and females transmitted each transgene. When Stra8 - Mgat1 -HA was expressed in Mgat1 cKO males, spermatogenesis was rescued based on the morphology of testis sections, the N-glycans of basigin, lectin histochemistry, MALDI-IMS and fertility. However, Ldhc-Mgat1 -HA (spermatocytes) rescued 0 of 7 Mgat1 cKO males, and Prm1 - Mgat1 - HA (spermatids) did not rescue fertility in 6 Mgat1 cKO males. Therefore, MGAT1 must be expressed in spermatogonia for spermatogenesis to proceed. Within the testis microenvironment, the presence of extracellular matrix proteins, cell surface receptors and interactions between testicular cells are mediated by glycan binding and recognition reactions. Changes in glycosylation during spermatogenesis occur and affect all of these associated adhesion and regulatory functions. One objective of

these study is to create a two dimensional co-culture model for Sertoli cells (TM4) and N glycosylation deficient germ cells (GC1) and demonstrate the functionality by the formation of tight junctions as shown by the dysregulation of tight junction proteins and decreased transepithelial electrical resistance. We have reported earlier that the glycoprotein Basigin is a major carrier of complex N glycans in germ cells expressed mostly in spermatogonia for spermatogenesis to proceed. Whole body deletion of basigin also caused syncytia formation similar to Mgat1 knock out testis. We hypothesize that basigin interacts with Monocarboxylate transporters (MCT1 and MCT4 in testis) to locate them properly in the membrane of spermatogenic cells and that this may enable germ cells to utilize lactate as an energy substrate. An important observation by dysregulating the glycan portion of basigin utilizing different N glycosylation deficient cell lines (Lec1- Mgat1 deficient, Lec5- Mgat5 deficient) has an effect on the interaction of basigin with monocarboxylate transporters in the cell membrane. By Orbitrap LC-MS studies we identified key membrane proteins that bind to basigin. This study will provide important insights into why Complex N glycans are required and multiple aspects of Basigin during Spermatogenesis.

Abstract # 2172

TDP-43 Is Required For The Completion Of Meiotic Prophase I In Male Mice. Prabhakara P. Reddi, Yiding Xu, Chintan Patel, Huanyu Qiao, Jeremy M. Rayl, Katie Campbell, Kathryn Storey, Lyndzi Miller, Madeline Timken

TAR DNA-binding protein 43 (TDP-43) is a multi-functional DNA/RNA binding protein that has been shown to regulate gene transcription, mRNA splicing and stability, RNA translocation, and miRNA biogenesis. TDP-43 is evolutionarily conserved and ubiquitously expressed; conventional knockout leads to embryonic lethality. TDP-43 was shown to be aberrantly expressed in the motor neurons of patients with amyotrophic lateral sclerosis (ALS) and frontotemporal lobar degeneration (FTLD). Prior to the above finding, we cloned TDP-43 as a transcription factor that binds to the promoter of the Acrv1 gene, which codes for the acrosomal protein SP-10. Mutation of TDP-43 sites in the Acrv1 promoter led to premature transcription of a reporter gene in spermatocytes; further work tied TDP-43 as a repressor of Acrv1 gene in vivo. Our work also showed that TDP-43 is aberrantly expressed in the sperm and germ cells of infertile men. TDP-43 is expressed in the germ cells and somatic cells of the testis. TDP-43 is first expressed in the nuclei of Type B/Intermediate spermatogonia and peaks in preleptotene spermatocytes. TDP-43 associates with premeiotic chromosomes, dissociates at leptonema to early pachynema, but reappears at mid-pachynema, and peaks at diplonema. We hypothesized that TDP-43 would be critical for spermatogenesis and male fertility. To address, we generated TDP-43 male germ cell-specific conditional knockout (cKO) mice (using Stra8-iCre). In these mice, most spermatocytes either arrest or go to apoptosis at mid-pachynema, suggesting a role for TDP-43 in meiosis. Retinoic Acid (RA) signaling has been shown to play a pivotal role in entry into meiosis; however, the target of RA, Stra8 (stimulated by RA), is expressed normally in the preleptotene

spermatocytes of the cKO mice. This suggested that TDP-43 plays a role in meiosis downstream of RA signaling. Severe synaptic defects are observed in spermatocytes lacking TDP-43. Structured illumination microscopy (SIM) showed that loss of TDP-43 causes non-homologous chromosome synapsis in pachytene spermatocytes. Gammahistone 2AX (g-H2AX) staining indicated meiotic silencing of unsynapsed chromatin (MSUC), which represents failures in synapsis of autosomal chromosomes. To begin to find causative factors, we investigated the effect of TDP-43 KO on the expression of genes important for meiosis: Spo11, Mei1, Dmc1, Msh4, Prdm9, Sycp1, Sycp2, Sycp3, Hormad1, Hormad2, Rec8, Rad21L, and SCC3. cKO mice at postnatal day 12 and day 15 were analyzed to capture the direct effect of TDP-43 on target gene expression. We found a decrease in all genes, from -1.9 fold change to -28.3 fold change at day 12 and -2.5 to -26.0 fold change at day 15. Greatest decreases occurred in Prdm9, Spo11, and Sycp2 at day 12 and in Spo11, Msh4, and Sycp2 at day 15. Collectively, these data suggest that TDP-43 is required for normal synapsis of mouse spermatocytes and for proper spermatogenesis. Future studies will focus on the mechanism by which TDP-43 regulates genes critical for meiotic progression. Our studies will have implications on understanding idiopathic male infertility and its treatment.

Abstract # 2234

Deletion Of The Pramel1 Gene Leads To Germ Cell Reduction And Subfertility In Male Mice. Mingyao Yang, Jon Oatley, Wansheng Liu

Prame-like 1 (Pramel1) is a member of the Prame gene family which is one of the most amplified gene families in the mouse genome. The PRAMEL1 protein is localized in the nucleus and cytoplasm of germ cells in testis. The objective of this study was to characterize the role of PRAMEL1 during spermatogenesis by a gene knockout (KO) approach. We reported here the generation of a global Pramel1 KO mouse by CRISPR/Cas9. To evaluate the fertility of the KO males, 7 mutant males were paired with 7 wildtype (WT) females in a breeding test starting at the age of 2 months and ending at 8 months. Compared to WT males, the litter size in the Pramel1 KO males was significantly decreased by 17.45% (P<0.01), suggesting that the Pramel1 KO males are subfertile. A time-course study on developing and mature Pramel1KO testes at postnatal day 7 (P7), P14, P21, P35, P60, P120 and P365 (n=3-5) was performed. Sperm count at the age of 2, 4 and 12 months indicated that there was a significant decrease in sperm production at 4 month (19.41%, P<0.01) and 1 year old (43.02%, P<0.01) testes in the KO mice, but there was no statistical difference between the Pramel1 KO and WT testes at 2 month old (P>0.05). Consistent with the decrease in sperm count, the testicle size of the KO males is reduced by 8.57% (P<0.01) at 4 month and 30.67% (P<0.01) at 1year-old. TUNEL assay revealed a higher rate of apoptotic germ cells in the Pramel1 KO testes observed as early as P7 (P<0.05). Furthermore, loss of germ cells was observed in H&E staining in a small portion (2.07%) of the seminiferous tubules, with a Sertoli cell only (SCO) phenotype, at P21 (P<0.05). The percentage of SCO tubules was gradually increased during testis development and reached to 29.57% at 1 year old, which was

significantly higher than that of WT males (P<0.05). IF staining with germ cell-specific markers (TRA98 and DDX4) and a Sertoli cell-specific marker (SOX9) further confirmed that germ cells were lost in the SCO tubules, while the number of Sertoli cells was not affected by the Pramel1 deletion. In summary, our preliminary data suggest that Pramel1 plays an essential role in spermatogenesis and male fertility, and the Pramel1 KO mice is a valuable model for studying the functional role of the Prame gene family during spermatogenesis.

Stem Cells and iPS Cells

Abstract # 1670

Understanding The Role Of WNT Receptor FZD5 In Maintaining The Self-Renewal Of Endometrial Mesenchymal Stem-Like Cells. Tianqi LI, RWS Chan, EHY Ng, WSB Yeung, RHW Li, PCN Chiu

Human endometrium is a dynamic tissue which undergoes cyclical regeneration under the regulation of sex steroids. The existence of endometrial mesenchymal stem-like cells (eMSCs) can contribute to this remarkable regenerative capacity. Our group recently demonstrated that myometrial cells can activate WNT/B-catenin signaling via WNT5A to maintain the self-renewal capacity of eMSCs [1]. However, there is limited knowledge on the WNT5A-responsive stem cells in the niche. WNT ligands operate by binding to products of the frizzled (FZD) family and co-receptor low density lipoprotein receptorrelated protein 5 (LRP5) which activates WNT signaling pathways. In this study, we examined the protein and gene expression of frizzled receptors that have been reported to interact with WNT5A in three subpopulations of endometrial stromal cells: unfractionated stromal cells, progenitor cells (CD140b+CD146-) and eMSCs (CD140b+CD146+ cells). We further evaluated the importance of the WNT-FZD interaction in eMSCs proliferation and self-renewal. Full thickness endometrial tissues were obtained from women undergoing hysterectomy. Single cell suspension was obtained by enzymatically digestion and red blood cells and leukocytes were removed by ficoll-paque and CD45 dynabeads, respectively. EMSCs isolated by sequential beading with magnetic beads coated with anti-CD140b and anti-CD146 antibodies. EMSCs were co-cultured with myometrial cells at a ratio of 1:90 or with WNT5-A conditioned medium (CM) for 15 days. Clonogenicity and the phenotypic expression of eMSCs were determined by counting the colonies and analyzing the co-expression of CD140b and CD146 (eMSC markers) by flow cytometry. The gene and protein expression of Frizzled receptors in stromal subpopulations were assessed by qPCR and immunofluorescence, respectively. Assessment of subpopulations revealed a significantly higher level of FZD5 gene in eMSCs when compared to unfractionated stromal and progenitor cells (n = 12, P < 0.05). EMSCs abundantly express FZD5 protein $(97.6 \pm 1.24\%, n = 5)$. FZD5 is a classic receptor of WNT5A and has been reported to activate both WNT/β-catenin dependent (canonical) and independent (noncanonical) signaling [2]. Addition of neutralizing anti-FZD5 antibody reduced the stimulatory effect of co-cultured myometrial cells or WNT5A CM on clonogenicity (n = 5, P < 0.05) and expression of active β -catenin in eMSCs (n = 5, P<0.01). Moreover, the expression of FZD5 protein in eMSC was knocked down using FZD5-siRNA. The treatment reduced the myometrial cell or WNT5A CM induction of TCF/LEF luciferase activity when compared to control siRNA (n = 6, P < 0.05). In conclusion, our findings suggest that myometrial-secreted WNT5A interact with FZD5 to modulate the self-renewal of eMSCs by the activation of Wnt/ β -catenin pathway. 1. Cao, M., et al., Stem cells , 2019. 37(11). 2. Kumawat, K. et al., Cellular and molecular life sciences, 2016. 73(3).

C1EIP Functions As An Activator Of ENO1 To Promote Chicken PGC Formation Via The Inhibition Of Notch Signaling Pathway. Kai Jin, Qisheng Zuo

The production of germ cells, especially primordial germ cells (PGCs), is important for avian stem cells and reproduction biology. However, key factors involved in the regulation of PGCs remain unknown. Here, we identified a PGC-related marker gene: C1EIP, whose activation and expression are regulated by transcription factor STAT3, histone acetylation, and promoter methylation. The C1EIP regulates PGC formation by mediating the expression of PGC-associated genes, such as CVH and CKIT. Knockout of C1EIP during the embryonic development reduced PGC generation efficiency both in vitro and in ovo. Conversely, overexpression of C1EIP increased the formation efficiency in vitro. C1EIP encodes a cytoplasmic protein that interacts with ENO1 in the cytoplasm and then ENO1 transfer to MBP1 impress Myc expression in nucleus via inhibits the Notch signaling pathway to positively regulates PGC generation. Collectively, our findings demonstrated C1EIP as a novel gene involved in PGC formation, whose gene product regulates embryonic stem cell differentiation through the interaction with ENO1 and the subsequent inhibition of Notch signaling pathway via the impression of Myc.

Abstract # 1886

Optimization of Acrosome Staining of Korean Chikso spermatozoa with CBB solution. Jae Young Lee, Chan-Lan Kim, Yeoung-Gyu Ko, Sung Woo Kim

The acrosome reaction is two different membrane fusion that enables sperm to penetrate the zona pellucida and fertilize an egg. These processes end the enzymes releasing into out-side environment nearby cumulus-oocyte complex. Many different protocols have been developed to detect the acrosome status of sperm to judge the fertilizing ability of target sperm. To develop efficient protocols of acrosome status in Chikso (Korean native cattle) sperm, two fixatives (methanol and paraformaldehyde) were compared with control (no fixative). Also 0.01, 0.08, 0.25 and 0.5% Coomassie Brilliant Blue (CBB) solutions were tested with different times. The acrosome reaction of Chikso spermatozoa was induced by theophylline in BO medium. Differential interface contrast in the bright field microscope used for judging efficient protocols. These results demonstrate that 0.1~0.25% of CBB solution could be used for bovine spermatozoa without fixatives. The methanol and paraformaldehyde fixation showed weak staining pattern in the acrosomes of sperm heads. The staining time was variable between 5 and 30 seconds. With exposure time in CBB solution, washing steps in water is not needed to remove the overstaining pattern in the head. Therefore, the semen smears that were exposured in 1% CBB solution for 10-30 seconds without fixing step is the choice of acrosome staining in chikso spermatozoa.

The Effect of collagen types on the growth of chicken PGC. Sung Woo Kim, Jae Young Lee, Chan-Lan Kim, Yeoung-Gyu Ko

Primordial germ cells of chicken lines are valuable genetic materials to restore endangered birds for the future. Especially for the case of a female bird, PGCs are indispensable cells because of the inability of freezing eggs and secure the genetic reservoir of the chicken industry. However, PGC culture in vitro is not easy to maintain for expansion of cell numbers due to specialized growth factors from feeder cells, and additives are needed. During culture, the PGC should be regularly dispersed and maintained its originality. In some cases, the divide and expanded PGCs form cell clumps in the bottom of culture dish, and their PGC properties should be checked for future uses. This study sought to establish an expandable culture system with Cellmatrix collagen type 1-A and I-P. Total number of PGC that cultured with stroma cells in primitive gonads for 5-7 days increased 8-12 times. The 1~2% collagen I-P type suspended PGCs were the most suitable culture system for maintaining PGC morphology for more than 1 month. After long term culture, PGC was recovered by gentle mixing with 0.3% collagenase solution for 20min. During culture, collagen treated cells had no direct contacts with PGCs and antigenicity of SSEA-1 also reconfirmed PGC origin. In summary, the collagen type I-P 3D culture system can be used for the expansion of chicken PGCs in suspension, which is available for long term culture.

Abstract # 2369

Effect of Serum and Serum-Free Supplementation on Equine Mesenchymal Stromal Cells During In-Vitro Culture. Saba Oji, Sahar Mehrpouyan, Thomas Koch, Pavneesh Madan

Mesenchymal Stromal Cells (MSCs) are multipotent stromal cells that have a unique potential for application in disease treatment, cell therapy, and biotechnology. In order to culture the MSCs, serum-containing medium is used to provide various growth factors and hormones that assist these cells to grow properly. However, the exact effect of the serum on these cells is not well understood. Additionally, there are a few downsides to the usage of serum in the media, such as the high cost, batch-to-batch variation, limited availability, and the unwanted effects of serum on the cellular function and growth. To combat this, this study aimed to utilize metabolomics to distinguish the global metabolite changes in the cell culture media of equine undifferentiated cordblood (CB) derived MSCs that are cultured in serum and serum-free medium. We first compared the metabolomic profiling of early passage with the late passage of CB MSCs in the normal expansion media with 10% fetal bovine serum (FBS) supplementation. Out of the 127-metabolite detected, we found two metabolites from two different metabolite groups to significantly differ between the two groups. These include organic acid (P < 0.05) and amino acid (P < 0.05). The organic acid plays a role in one pathway in the early group, and it plays in nine different pathways in the late group. Although, this metabolite showed to have a common role in one metabolite

pathway in both the early and late groups. In contrast, the amino acid only seems to be important in one pathway. We then examined the metabolomic differences between CB-MSCs cultured under normal serum-supplemented expansion media (10% FBS) with the commercially available serum-free media over a 24hr period up to 72hrs. Overall, we found 10 metabolites to be significantly (P < 0.05) different between the serum and serum-free groups. These can be categorized into hexane, hydroxy acid, organic nitrogen, acetyl-carnitine, biogenic amines (2), amino acids (2), and glycerophospholipids (2). We further looked into the role of each of these metabolites in the quantitative enrichment analysis for serum and serum-free groups. In the serum group, we found that only hexane, hydroxy acid, and one of the glycerophospholipids played a role in six different pathways. In comparison, in the serum-free group acylcarnitine was the only metabolite that played a role in one pathway. When looking at the metabolites that played a role in both serum and serum-free groups, organic nitrogen and one of the amino acids were involved in nine pathways presented in either of the groups. In addition to the nine pathways, organic nitrogen showed to be an important metabolite for two pathways in both serum and serum-free group. Our study suggests that even though only a few metabolites significantly differ from the early and late stages of MSCs culture, the pathway analysis varies in each time point. In addition, we found that due to the diverse metabolomic profiling and pathway analysis, the serum-free alternative is not an effective alternative to FBS use for equine CB-MSCs.

Testis

Abstract # 1747

Sub-optimal Paternal Diet Influences Testicular Morphology and Global Gene Expression Patterns in Mice. Nader Eid, HannahL Morgan, Christiana Gavriel, Marcos Castellanos Uribe, Iqbal Khan, Adam J. Watkins

Background: There is growing evidence that poor paternal diet adversely affects sperm quality, with consequent impacts on embryonic development and long-term offspring health. It is conceivable that any changes to sperm quality may be a result of underlying alterations to the testicular environment itself, characterised by changes in morphology and global gene expression profiles. Materials and methods: To better understand the impact of diet on male testicular morphology and reproductive fitness, we fed C57BL/6 male mice either a control diet (18% protein, 10% fat, 21% sugar; CD), isocaloric low protein diet (9% protein, 10% fat, 24% sugar; LPD), LPD supplemented with methyl donors (betaine, choline chloride, folic acid, methionine, Vitamin B12; MD-LPD), a high fat, high sugar 'Western diet' (19% protein, 21% fat, 34% sugar; WD), or a WD supplemented with methyl donors (MD-WD) for at least 7 weeks. Testes were collected and processed for either morphological assessment (histology) or gene expression (microarray) analysis. Results: No significant differences were observed in stud male body weights during the feeding regimen, or in organ/body weight ratios for testes, livers, and gonadal fat between treatment groups at the time of sacrifice. Analysis of testicular morphology revealed no significant differences in mean total seminiferous tubule area, total perimeter, luminal area, or area of the tubule epithelium between the aroups. However, abnormalities such as loss of tubular epithelium, tubular vacuolisation and basal membrane separation were observed more frequently in testes exposed to the WD and MD-WD when compared to the other treatment groups. Microarray analysis revealed that WD had the largest effect on testicular gene expression when compared to the CD testes with 134 genes being upregulated while 269 genes being downregulated (fold change = 1.1, +FDR, $p \le 0.05$). Preliminary pathway analysis suggests that LPD upregulated genes involved in prenatal lethality, a process downregulated by MD-LPD compared to the CD group. Furthermore, both WD and MD-WD downregulated genes involved in embryonic organ development while MD-WD upregulated genes influencing abnormal cell cycle compared to CD. Further biological processes influenced by the treatment groups included gametogenesis, abnormal testis morphology, embryo lethality, abnormal mitochondrial physiology, abnormal parathyroid hormone synthesis, in addition to abnormal triglyceride and calcium level regulation. Conclusions: These data provide insight into testicular morphology and global gene expression patterns in response to poor paternal diet with and without vitamin and mineral supplementation. Ongoing research aims to validate testicular gene expression profiles and investigate underlying molecular and cellular pathways linking paternal diet with sperm quality.

Antioxidant Administration Causes Dynamic Changes In The Testis Transcriptome Of An Obese Mouse Model. Taylor Pini, Mary Haywood, Blair McCallie, William Schoolcraft, Mandy Katz-Jaffe

Obesity is a growing epidemic, with potential fertility consequences for the reproductive age male. Grossly elevated body mass results in inflammation and oxidative stress, previously observed locally in the testes, with potentially important impacts on reproductive function. Given this link between obesity and oxidative stress, we investigated the impact of oral antioxidant administration on the transcriptome of the testis and pre-implantation embryo development in a male diet-induced obesity mouse model. Obesity was induced in C57BL/6 male mice (n = 12) by feeding a western diet (42.7% carbohydrate, 42.0% fat as percentage of kcal) for 10 weeks. Mice were maintained on the western diet and had ad libitum access to water (control, n = 6) or 1% (w/v) acai in water (Euterpe oleracea, ORAC > 200,000, n = 6) for a further 10 weeks. Males were mated to hormonally primed C57BL/6 females and zygotes were cultured in vitro until the blastocyst stage. At sacrifice, total RNA was isolated from one testis per male and used for library preparation (TruSeq Total RNA Library Prep Kit, Illumina). Samples were sequenced on an Illumina NovaSeq 6000 (2x150). Reads were trimmed for quality using Trimmomatic and mapped to GRCm38 using GSNAP. Reads were counted using featureCounts and differential expression analyzed using edgeR. Acai administration did not impact the number of zygotes, embryo survival from day 2 to the blastocyst stage or on-time development on days 3 through 5. With an expression cutoff of > 5 counts per million (CPM) in all samples, we identified 147 differentially expressed genes (FDR \leq 5%; p < 0.05), of which 146 had decreased expression in the testis. Administration of the potent dietary antioxidant acai lead to decreased expression of negative regulators of cell proliferation (Cdkn1c, Filip11, p < 0.0001), immune mediators (Ccl27a, Cd59a, Cytl1, Defb33, Ifi209, Nlrc4, Carlr, Ltbp1, p < 0.0005), lipid metabolism genes (Acot12, Adipog, p < 0.00003), ribosomal elements and testis/sperm enriched genes (Glipr111, Kcnmb2, Meig1, Tnp1, p < 0.0005). Ingenuity Pathway Analysis generated "oxidative phosphorylation" (p = 1.3E-8) as a top hit, due to a number of mitochondrial electron transport chain subunits showing decreased expression in the testis following antioxidant treatment. Subunits of mitochondrial complexes I (Ndufa3, Ndufb1, Ndufs4, Ndufs6b, p < 0.0004), III (Uqcrq, Uqcr10, p < 0.0004), IV (Cox7b, p = 0.0002) and V (Atp5md, Atp5me, Atp5mf, Atp5mpl, p < 0.0004) were impacted, as well as mitochondrial biogenesis chaperones (Pet100, Timm8b, p < 1000.0002) and Dnajc15 (p = 3.6E-5), a negative regulator of ATP production. Overall, these results suggest that in the context of obesity, antioxidant administration causes dynamic changes in the testis transcriptome, particularly impacting the mitochondria. Future studies will aim to uncover potential mechanisms linking this antioxidant to mitochondrial biogenesis and oxidative phosphorylation efficiency within the testes. As no alterations to pre-implantation embryo development were observed, we hypothesize that any phenotypic impact of obesity and subsequent improvements with antioxidant treatment may manifest later in offspring development.

Identification of a Germ Cell-Specific Mouse Intraflagellar Transport 172 Isoform and Purification of C-Terminus Full-Length Protein for Generation of Specific Antibodies. Neha Nayak, Qi Zhou, Yi Tian Yap, Zhibing Zhang

Intraflagellar transport (IFT) is a conserved bi-directional cargo transport system essential for the assembly and maintenance of most eukaryotic cilia and flagella. Thus far, twenty two IFT components have been identified, with six of them forming the IFT-A complex, which is believed to be linked to retrograde transport, while the remaining components form the IFT-B complex, which is believed to be essential for anterograde transport. IFT172 is a component of the IFT-B complex and global disruption of the gene in mice caused typical phenotypes of ciliopathy. Using western blot analyses and two antibodies against the N-terminus of the full length mouse IFT172, a full length 172 kDa protein was detected in most somatic tissues, including the brain, lung, and liver. However, in addition to the 172 kDa protein, a smaller protein (IFT172-t) with a molecular weight between 110 kDa to 130 kDa was detected only in mouse testis. Furthermore, a new Ift172 transcript (Ift172-t) has been characterized using RACE experiments. This new transcript matches a recently reported mouse Ift172 isoform in NCBI. In the Ift172-t, there is a twenty one nucleotide insertion which corresponds to a unique ten amino acid sequence followed by a stop code with a predicted 110 kDa protein. To further characterize the mouse Ift172 gene, a peptide containing the ten amino acids was used to immunize rabbits to generate the specific antibodies against IFT172-t. To generate specific antibodies against the full length IFT172, the cDNA encoding Cterminus of the full length mouse IFT172 was amplified by RT-PCR and cloned into a bacteria expression vector pET28A. The plasmid was transformed into BL21 bacteria to express C-IFT172-His fusion protein with IPTG induction. The expressed fusion protein was purified using the Ni agarose beads and rabbits were immunized with the purified C-IFT172-His protein. These antibodies will specifically cross-react with the two IFT172 proteins and allow us to investigate their distinct functions.

Abstract # 2072

Reproductive Impact of Low NAD+ Levels Typical of the Aging Male. Ralph G. Meyer, Abram Bochinclonny, Cedric Mannie, Corey A. Swanson, Sierra Lopez, Miles Wandersee, Mirella L. Meyer-Ficca

Paternal age is positively correlated with reduced sperm chromatin quality and higher numbers of DNA strand breaks which can negatively affect pregnancy outcome and child development. There is a normal aging-related decline of NAD levels in humans that may provide a plausible explanation for reduced sperm quality in aging men, but this hypothesis has been difficult to test due to the absence of suitable laboratory animal models. To address this problem, we developed a transgenic mouse with inducible overexpression of the enzyme hACMSD, which leads to an acquired dependency of the animals on dietary intake of vitamin B3 (niacin) as a metabolic precursor for NAD synthesis (ANDY mouse, Cell Reports, 2018), similar to humans. Dietary niacin restriction of ANDY mice led to reduced NAD levels that we were able to adjust to defined levels, including those typical of aging humans and mice. In addition, ANDY mice with ACMSD overexpression had elevated levels of acetyl-CoA, which is also typical of aging individuals. Oxidized NAD (NAD +) levels were strongly lowered, while reduced NAD (NADH/H +) remained nearly unchanged. This resulted in altered hepatic redox status in niacin-deficient ANDY mice. Concomitantly, the ratio of lactate to pyruvate interconversion, which is facilitated by the NAD-dependent enzymatic activity of lactate dehydrogenase, shifted significantly towards increased lactate levels. The shifted NAD+/NADH redox state also caused increased blood lactate formation upon pyruvate administration. In the testis, niacin deficiency of ANDY mice resulted in defects of postmeiotic sperm chromatin remodeling. Reminiscent of defects in aging males, niacin deficiency resulted in incomplete histone-to-protamine exchange, abnormal head morphology, and low DNA integrity with DNA fragmentation in sperm. Steadystate levels of testicular poly(ADP-ribose), which is formed by poly(ADP-ribose) polymerases (PARP1, PARP2) by cleaving NAD in response to DNA strand breaks in spermatocytes and spermatids, were diminished compared to controls. Sperm DNA showed elevated levels of 8-oxoquanine as an indicator of elevated oxidative stress. Niacin-, and hence NAD-deficient male ANDY mice had reduced fertility where numbers of live offspring were reduced to ~30% of controls. Returning ANDY mice to a defined control diet containing 30 mg/kg of niacin completely reversed niacin- and hence NAD-deficiency in ANDY mice. In conclusion, our data suggest that sinking levels of NAD + contributes to poor sperm chromatin quality and overall reproductive decline of aging males.

Abstract # 2169

Dynamic Regulation of Apoptosis in Male Sexual Development and Cancer Therapy-Induced Infertility. Kaitlyn A. Webster, Cameron S. Fraser, Kristopher A. Sarosiek

Due to advances in pediatric cancer therapies, long-term survival is anticipated for 80% of patients. However, radiation or chemotherapy-induced infertility is commonly observed in pediatric cancer survivors. Age at treatment, sex and pubertal status influence risk of permanent infertility, suggesting that vulnerability of reproductive tissues is dynamic and an important determinant of therapy sensitivity. Using BH3 profiling – an assay that measures a cell's propensity to induce intrinsic apoptosis in response to prodeath peptides – we previously found that apoptosis is dynamically regulated across mammalian cell types and ages, with tissues typically being highly primed for apoptosis in neonates/juveniles but resistant in adults. It is unclear how apoptosis is regulated throughout developing reproductive systems, and how this impacts cancer therapy sensitivity. Importantly, embryonic sex differentiation, pituitary morphogenesis, and germ cell attrition are known to be cell death-dependent processes. We sought to characterize the role and regulation of intrinsic apoptosis in reproductive development, and impacts of excessive or insufficient apoptosis on male fertility. We assessed death

vulnerability at the single-cell level in reproductive tissues from embryos to adults, finding that germ cells in pre-pubertal mice are highly primed to undergo apoptosis and that this sensitivity is reduced after puberty in males but not females (N=3 per age; P<0.0001). To test functional relevance of these findings, we exposed pre- and postpubertal males to 6-8 Gy testicular irradiation to model clinical exposure to radiation therapy, which is known to cause infertility in patients. Testicular apoptosis was 6x greater in irradiated juveniles vs. adults (N=6, P<0.0001), as measured by an enzymatic Cleaved Caspase-3 activation assay. Surprisingly, we found that pre-pubertal irradiated males exhibited testicular regeneration by 2 months post-treatment and could sire viable offspring. In contrast, despite reduced levels of post-treatment apoptosis, postpubertally irradiated males showed testicular degeneration beginning at and continuing after 2 months, and failed to produce offspring despite making sperm (N=4). To investigate the potential for preventing radiation-induced infertility by blocking apoptosis, we studied reproductive development in male mice carrying a null mutation in the pro-apoptotic gene Bax, which were previously shown to exhibit male-specific infertility. We observed that apoptotic priming was, paradoxically, increased in Bax -/testes, which also misexpressed PLZF, a marker of undifferentiated spermatogonia. Thus, we hypothesize that differentiation state of spermatogenic cells may explain the apoptotic vulnerability or resistance characterized in our previous analyses. Furthermore, we have made the novel finding that suppression of apoptosis in the Bax -/- males also results in pituitary hormone signaling defects, abnormal Müllerian duct regression, and aberrant WNT/β-Catenin signaling, which we believe underlie male infertility in this model. Our studies reveal age-dependent dynamic regulation of apoptosis in male sex differentiation and spermatogenesis, and elucidate developmental pathways that can be modulated to prevent therapy-induced infertility. Overall, the insights gained here may inform new treatments or treatment modulators that prevent reproductive toxicity, or restore spermatogenesis in infertile males.

Abstract # 2216

Testis Development and Fetal Leydig Cell Differentiation Dictate Differential Accumulation of Steroidogenic Genes. Anbarasi Kothandapani, Eowyn Yangyang Lin, Joan S. Jorgensen

Sex-specific characteristics of the male fetus depend on testis-derived hormone production during a critical window of time during development. Fetal Leydig cells within the testis are the sole source of androgens that promote male sex differentiation. The aim of this study is to establish the spatiotemporal profile of steroidogenic genes to define the time frame and testicular microenvironments that regulate androgen synthesis. We used copy number qPCR to measure absolute transcript numbers of steroidogenic genes over time within the whole testis. Although fetal Leydig cells do not differentiate until ~embryonic day 13 (E13), steroidogenic genes, Star , Cyp11a1 , Cyp17a1 and Hsd3b were detected as early as E11.5, the onset of sex differentiation,

and they all shared the same timing for onset, peak (E16) and decline of transcript levels. Direct comparisons of transcript copy number among steroidogenic genes revealed that there are profound differences in the magnitude of change over time. Between sex determination and the peak of testosterone synthesis (E11.5 and E16), for example, there is a 35-fold increase in Star versus over 1,700-fold increase in Cyp17a1 transcripts suggesting significant differences in RNA accumulation or stability. To understand individual cell contributions to the overall outcome of the whole population of cells, we performed single-molecule fluorescent in situ hybridization (smFISH) for Star and Cyp17a1. As expected, we detected spliced transcripts at gene loci within the nucleus and mRNA molecules in the cytoplasm, indicating active transcription and RNA processing for both genes. Differences in transcripts could be visualized by the observation that a majority of cells exhibited accumulation of spRNA molecules at both alleles of Cyp17a1 but only one locus of Star. In general, transcripts were detected at gene loci and as message in the cytoplasm in three distinct patterns: 1) predominant expression at loci 2) appearance at loci and in cytoplasm, and 3) diminished detection at the loci with increased accumulation in the cytoplasm. This asymmetric apportioning could be stochastic or arise from differences in local signaling and cell cycle. Single cell transcript quantification is underway to investigate whether underlying patterns emerge to differentiate Star versus Cyp17a1 transcript accumulation and whether individual fetal Leydig cell transcript production efficiency relates to its microenvironmental niche. Altogether, we find that steroidogenic gene transcription profiles in the developing testis are dynamic and highly heterogenous depending on their location within the testis. FUNDING NIH R01HD090660 (JSJ) and R01HD090660-02S1 (AK)

Trophoblast Differentiation and Function

Abstract # 1622

AKT1 Is An Intrinsic Regulator Of The Uterine-Placental Interface. Keisuke Kozai, Mae-Lan Winchester, Regan L. Scott, Masanaga Muto, Khursheed Iqbal, Michael J. Soares

The hemochorial placenta is an extraembryonic structure essential for normal fetal development. Multiple lineages of trophoblast cells contribute to the placenta, including cells with specialized properties to invade and transform the uterus and others that regulate the flow of nutrients to the fetus. These specialized cell populations are compartmentalized within the placenta. In the rat, invasive trophoblast cells arise from the junctional zone, whereas trophoblast regulating nutrient flow to the fetus are situated in the labyrinth zone. Deep intrauterine trophoblast invasion is similar in rat and human placentation and its disruption is associated with obstetrical complications. Molecular mechanisms controlling placental development are not well understood. The phosphatidylinositol 3-kinase/AKT pathway regulates many cellular processes, including proliferation, differentiation, and migration. AKT1 is a serine/threonine kinase implicated in fetal, placental, and postnatal growth. In this study, we investigated roles for AKT1 in placental development using a genome-edited/loss-of-function rat model. Crispr/Cas9 editing of the Akt1 gene yielded a germline mutation consisting of a 1332 bp deletion spanning Exons 4 to 7, resulting in a frameshift, a premature stop codon, and disruption of the kinase domain of the AKT1 protein. Both heterozygous and homozygous Akt1 mutant rats were viable and fertile. Null rats were devoid of AKT1 and showed placental, fetal, and postnatal growth restriction. Closer examination of Akt1 null placentas showed deficits in both junctional zone and labyrinth zone arowth. Junctional zones of wild type and Akt1 null placentation sites were interrogated by RNA-sequencing (RNA-seq) and for their production of invasive trophoblast cells entering the uterine compartment adjacent to the placenta. RNA-seq analysis showed robust differences in the transcriptomes of wild type versus Akt1 null junctional zones. Akt1 null junctional zones exhibited upregulation of transcripts encoding proteins contributing to signal transduction pathways, including Ccn3, Erbb3, Grb7, Ifitm1, and II1r2, and a cell cycle inhibitor (Plk2); and a significant downregulation of transcripts encoding extracellular matrix proteins and integrins (e.g. Lama3, Itgax), cathepsins (e.g. Ctsm, Ctsll3), and cell cycle regulators (e.g. E2f1, Aurkb, Ccne1, Cdc6, Ccnd1, Cdk1). Intrauterine trophoblast cell invasion was monitored by cytokeratin immunohistochemistry and measurement of transcripts specific to the invasive trophoblast cell lineage. Cytokeratin-positive invasive trophoblast cells were significantly diminished in AKT1 deficient placentation sites and expression of transcripts specific to the invasive trophoblast cell lineage (Prl5a1, Prl6a1, Prl7b1, Taf7l, Ceacam11, Ghrh, Mmp15, Galnt6, Lamb1, and Peg3) were significantly decreased at the AKT1 deficient uterine-placental interface. We also found that AKT1 deficiency impaired pregnancydependent adaptations to hypoxia (10.5% oxygen). In summary, AKT1 is an intrinsic regulator of placental development. AKT1 contributes to the formation of the placental-fetal interface and possesses a fundamental role in establishing the uterineplacental interface. These intrinsic actions of AKT1 ensure the requisite plasticity for placental adaptations to physiological stressors. Identification of AKT1 substrates should represent a strategy for elucidating key elements within molecular pathways controlling placental development. (Supported by AHA fellowships to KK and MM, NIH grants HD020676; HD079363, HD099638, and the Sosland Foundation)

Abstract # 1715

ASCL2 is Essential for Differentiation and Function of Extravillous Trophoblast Cells during Human Placental Development. Mariyan J. Jeyarajah, Stephen J. Renaud

Placental maldevelopment is a leading cause of sickness and death among mothers and babies. Thus, understanding placental development is clinically important. Trophoblasts form the epithelial component of the placenta, and they perform functions vital for placental function and pregnancy outcome. There are various sublineages of trophoblasts, and they are all derived from differentiation of trophoblast stem (TS) cells. One sub-type, termed extravillous trophoblasts (EVTs), is responsible for invading into the decidua and remodeling maternal arteries to ensure adequate blood flow reaches the placenta. Insufficient EVT development results in poor blood flow to the placenta, and is associated with serious obstetrical complications that jeopardize health and survival of mother and baby. Mice lacking the transcription factor Achaete-Scute Family bHLH Transcription Factor 2 (ASCL2) fail to form cells that populate the junctional zone (the murine equivalent of human EVTs). However, the role of ASCL2 in human EVT development is unclear. In this study, we test the hypothesis that ASCL2 is a critical regulator of EVT development. Our objectives included: (i) characterizing expression and localization of ASCL2 in human placenta and TS cells, and (ii) generating ASCL2-deficient TS cells to determine its role in EVT development. In 10-week human placenta, ASCL2 was expressed exclusively in EVTs, as determined by in situ hybridization. Using quantitative RT-PCR, we found that human TS cells induced to differentiate toward EVTs displayed a 6-fold upregulation of ASCL2, when compared to undifferentiated cells (N=3, P<0.05). Lentivirus-mediated knockdown of ASCL2 utilizing two distinct short hairpin RNAs (shRNAs; ASCL2-KD1 and ASCL2-KD2) resulted in a 76% and 59% decrease in ASCL2 (N=3, P<0.05). ASCL2-deficient TS cells exhibited poor EVT differentiation, including failure to undergo morphological changes consistent with EVTs, and reduced expression of three EVT markers: HLAG, MMP2, and ITGA1 (70%, 73%, and 77% decreased expression in ASCL2-KD1 compared to control cells, N=3, P<0.05). Consistent with an essential role of ASCL2 for EVT differentiation, ASCL2-KD1 cells exhibited a 54% decreased capacity to invade Matrigel compared to controls (N=3, P<0.05). In silico analysis of the ASCL2 promoter revealed a consensus binding site of a well-known trophoblast differentiation marker, glial cells missing-1 (GCM1). Using chromatin immunoprecipitation, we identified strong binding of GCM1 to the ASCL2 promoter. Moreover, knockdown of GCM1 resulted in 85% decreased expression of ASCL2 compared to controls (N=3, P<0.05). Collectively, our results show that ASCL2 is highly expressed in EVTs and is required for proper EVT differentiation and function.

GCM1 binds upstream of ASCL2 and regulates development of EVTs. This research will reveal fundamental mechanisms by which ASCL2 regulates EVT differentiation and will lead to new insights into the complexities of placental development.

Abstract # 1718

Transcription Factor AP2 Gamma (TFAP2C) And Hippo Signaling Converge To Regulate Cdx2 Expression In Early Mouse Embryos. Mohamed Ashry, Chad S. Driscoll, Catherine A. Wilson, Jason G. Knott

Mammalian reproduction is contingent on the formation of the trophoblast lineage, which supports the growth and function of the placenta. This lineage is established during the window of preimplantation embryo development and represents the first differentiation event in the life cycle of placental mammals. Failure to accurately establish the trophoblast lineage has major consequences, including developmental arrest prior to the blastocyst stage, implantation failure, early miscarriage, and placental abnormalities. We previously discovered a novel and critical role for transcription factor AP-2gamma (TFAP2C) in triggering and regulating key events that underlie trophoblast lineage formation in mouse preimplantation embryos. These include cell polarization, position-dependent HIPPO signaling, and regulation of caudal type homeobox 2 (Cdx2) expression. However, the precise mechanism by which TFAP2C regulates trophoblast-specific genes such as Cdx2 is not well established. We hypothesize that TFAP2C forms a regulatory complex with Tea domain transcription factor 4 (TEAD4) and the HIPPO signaling protein, Yes-associated protein (YAP1) to regulate Cdx2 expression. To test this hypothesis, we executed a series of experiments using mouse preimplantation embryos. In the first experiment we evaluated the global expression and colocalization of TFAP2C, TEAD4 and YAP1 in morula and blastocyst stage embryos by immunofluorescence staining (n= 3 replicates, 5 embryos/stage). This experiment served as a quality control for the specificity of the primary antibodies used in experiment 2. In a second experiment, we performed a proximity ligation assay (PLA) in morulae and blastocysts to define potential physical interactions between TFAP2C-TEAD4 and TFAP2C-YAP1 during the morula-to-blastocyst transition (n=3 replicates, 5 embryos/stage/interaction). In a third experiment we used the pharmacological inhibitor Y-27632 (Sigma, SCM075) to disrupt ROCK kinase signaling and activate hippo signaling in the outside cells of morulae. The effects on YAP1 nuclear localization and Ifap2c, Tead4, and Cdx2 expression were evaluated. In experiment 1, results confirmed previously published findings and demonstrated that the primary antibodies were specific for each target protein in the nucleus. For example, TFAP2C was ubiquitously expressed at the morula stage and became restricted to the trophoblast cells at the blastocyst stage. YAP1 was restricted to the outer cells in morulae and trophoblast cells in blastocysts, while TEAD4 was localized to both the trophoblast cells and inner cell mass (ICM). PLA studies revealed potential physical interactions between TFAP2C-TEAD4, as well as TFAP2C-YAP1 in the outside nuclei of morulae and blastocysts. Interestingly, the interaction significantly increased during the morula-to-blastocyst

transition. In the last experiment, 8-cell embryos cultured in the presence of 0, 10, 20, or 50 µm Y-27632 responded in a dose dependent manner and arrested at the morula stage. YAP1 was excluded from the nucleus and Cdx2 expression was downregulated. Interestingly, Tfap2c and Tead4 expression and localization was unaffected by the treatment, indicating that Cdx2 expression requires a functional YAP1-TEAD4-TFAP2C complex. In summary, these results suggest that TFAP2C regulates Cdx2 by forming a regulatory complex with TEAD4 and YAP1. Ongoing functional studies are dissecting the biological relevance of these protein interactions in early mouse embryos. (Research was supported by NIH-HD095371 and MSU AgBioResearch).

Abstract # 1783

Direct Conversion Of BMP4-Primed Pluripotent Stem Cells Into Trophoblast Stem Cells. Toshihiko Ezashi, Chuyu Hayashi, Jie Zhou, Andreip Alexenko, Yuchen Tian, Laurac Schulz, Danny Jschust, R. Michael Roberts

Human trophoblast stem cells (TSC) will provide invaluable cell models to recapitulate early stage trophoblast differentiation and to study placental diseases, such as preeclampsia, that have their origins in early pregnancy. Human TSC were first derived from human blastocysts and first trimester placental villous tissue by Okae et al. 2018, who utilized collagen IV as a substratum and a novel culture medium (trophoblast stem cell medium; TSCM). However, in order to circumvent the use of human embryos and fetal placentae as a source of TSC and to provide cell lines representing specific placental disease states that are diagnosed in later pregnant stages, there remains a need to generate TSC lines from both existing embryonic stem cell (ESC) lines and induced pluripotent stem cells (iPSC). Generally trans-differentiation from pluripotent stem cells into TSC has not been successful, but recent reports indicate that such a lineage transition can be achieved by using ESC held in an enhanced state of pluripotency. In 2015, our group showed that ESC and iPSC could be converted to an enhanced state of differentiation potential by exposing them to BMP4 for 24 h and, after dispersion with trypsin, selecting colonies by growth on a gelatin substratum. These cells could be directed along the three main germ line lineages and also readily differentiated to trophoblast. Here we report that such BMP4-primed H1 ESC (H1-BP) and iPSC (iPSC-BP) can be converted to TSC by simply switching the culture medium from one routinely used for pluripotent cells to the TSCM established by Okae et al. The H1-BP and iPSC-BP colonies were dispersed with trypsin, and 10 4 cells plated onto collagen IV-coated 35mm-dishes in TSCM. The passaged cells showed a gradual change in morphology, and, by day 6, areas containing cells with an epithelial-like morphology became visible. Other regions were occupied by cells with a more elongated "spiky" morphology. By dissecting out areas of TSC-like cells over the next 2-3 rounds of passage, homogeneous TSC-like cultures could be selected. These putative TSC retained their TSC-like morphologies and demonstrated continuous self-renewal and similar population doubling time (~20 h) to previously described TSC over 12 passages (1: 4, every four days). Immunofluorescent staining of fixed cells revealed

ubiquitous and abundant expression of the markers GATA3, KRT7, TP63 and TEAD4. Semi-quantitative RT-PCR detected mRNA for ITGA6, GATA3, LRP5, FGFR2, TP63, and KRT7 and other trophoblast markers at levels similar to those assessed in TSC controls. After the cells had been injected subcutaneously into the flanks of NOD/SCID immunodeficient mice, the transplanted cells formed ~5-mm lesions by day 8 close to the injection site. The histological and immunohistochemical features of these tumors and whether they release the hormone hCG are currently under investigation. These data suggest that both BMP4-primed ESC and iPSC can be readily converted to TSC status. They provide a new avenue to explore the features of normal and diseased trophoblast in vitro. Supported by NIH R01HD094937.

Abstract # 1860

NOTUM-dependent Modulation of WNT Signaling in Extravillous Trophoblast Cell Lineage Development. Vinay Shukla, Kaela M. Varberg, Marija Kuna, Khursheed Iqbal, Michael J. Soares

The hemochorial placenta develops through tightly regulated expansion and differentiation of trophoblast stem (TS) cells. Effective strategies for the isolation and propagation of human TS cells were recently determined. Human TS cells can differentiate into extravillous trophoblast (EVT) cells and syncytiotrophoblast. EVT cells are specialized cells that invade into the uterus and remodel the uterine vasculature facilitating the redirection of maternal nutrients to the developing fetus. Disruptions in EVT cell lineage determination, expansion, and differentiation are associated with numerous obstetrical complications, such as early pregnancy failure, preeclampsia, intrauterine growth restriction, preterm birth, and stillbirth. Here, we investigate canonical WNT signaling in the regulation of human TS cell differentiation into EVT cells. EVT cell differentiation is accompanied by extensive cell elongation and spreading and the upregulation of transcripts indicative of the EVT cell fate (e.g. HLAG, MMP2, etc). Initially, canonical WNT signaling was assessed by the accumulation of beta-catenin (CTNNB1) in stem cell versus EVT cell nuclei. CTNNB1 was abundant in stem cell nuclei but not in EVT nuclei, suggesting that WNT signaling was downregulated during EVT cell development. Consistent with these observations, we found that addition of a potent WNT activator, CHIR99021 (a GSK3B inhibitor), inhibited differentiation of TS cells into EVT cells. We next interrogated human TS cells in stem and EVT differentiation states for expression of components of the WNT signaling pathway with the goal of identifying potential endogenous regulators of WNT signaling. We observed the downregulation of several transcripts encoding proteins driving WNT signaling and the upregulation of other transcripts encoding proteins inhibiting WNT signaling. Among the upregulated transcripts, NOTUM expression was striking in terms of both magnitude of the increase and overall expression level. NOTUM antagonizes WNT signaling by facilitating the depalmitoleoylation of WNT proteins, which impair their binding to frizzled receptors. We hypothesized that NOTUM is required to repress WNT signaling during human EVT cell differentiation. A loss-of-function strategy using NOTUM short hairpin RNAs

demonstrated that the differentiation-dependent increase in NOTUM expression was essential for EVT cell differentiation. Knockdown of NOTUM inhibited both morphological and molecular indices of EVT cell development. Disruption of NOTUM also enhanced the abundance of active CTNNB1 in the nucleus and LEF1 transcript levels. We further demonstrated that NOTUM expression is tightly controlled by WNT signaling. A role for NOTUM in regulating the invasive trophoblast cell lineage is speciesrestricted. The rat, which exhibits deep hemochorial placentation similar to the human, does not express NOTUM in any trophoblast cell lineage. Overall, our findings indicate that canonical WNT signaling is essential for maintaining human trophoblast stemness and prevention of human TS cell differentiation. NOTUM is an important contributor to the downregulation WNT signaling and is essential to human EVT cell differentiation. Although, NOTUM may not be a conserved regulator of the invasive trophoblast cell lineage, roles for WNT in trophoblast stemness and WNT repression in trophoblast cell differentiation may be conserved. [Supported by KUMC Biomedical Research Training Program (VS); F32HD096809 (KMV), GM103418 (MK); NIH grants HD020676, HD099638; Sosland Foundation)

Abstract # 1869

Neuropeptide Y Inhibits Trophoblast Migration, Invasion, And Proliferation Via NPY Receptor 1. Heyam Hayder, Jacob O'Brien, Caroline Dunk, Jelena Brkic, Stephen Lye, Chun Peng

Neuropeptide Y (NPY) is a neurotransmitter and neurohormone abundantly expressed in the brain. Its actions in humans are mediated by five G-protein coupled receptors (NPY1R-NPY5R). During pregnancy, NPY is also produced in the placenta but little is known about its role in placental development. To investigate the role of NPY in placenta, we used immortalized trophoblast cell lines to examine cell proliferation, migration, and invasion after NPY overexpression or knockdown. We found that NPY overexpression decreased migration, invasion and proliferation of HTR8/SVneo and Swan71 cells while silencing it with siRNA increased their motility and proliferation rate. The inhibitory effect of NPY on cell migration and invasion was specific to the full length NPY (1-36 amino acids), an NPY receptor 1 (NPY1R) agonist but not to the truncated NPY (3-36 amino acids), an NPY2R agonist. Moreover, NPY effect on migration and proliferation was attenuated when cells were treated with an NPY1R-specific inhibitor and not with NPY2R-specific inhibitor. Using immunohistochemistry, we detected NPY and NPY1R in placenta of early pregnancy which decreased to undetectable levels in the 2 nd trimester. Finally, using a floating first trimester villous model, we found that knockdown of NPY expression or inhibition of NPY1R signaling resulted in significant cytotrophoblast proliferation and mesenchymal sprouting. Together, these findings suggest that the NPY-NPY1R signaling pathway negatively regulates trophoblast migration, invasion, and proliferation and contributes to the control of early placental development (This research was supported by CIHR).

Single Cell Multi-Omics Of Peri-Implantation Stage Human Embryos Reveals Similarities Between Early Trophoblast Differentiation And Neuronal Behavior. Deirdre M. Logsdon, Hao Ming, Jiangwen Sun, William B. Schoolcraft, Rebecca L. Krisher, Zongliang Jiang, Ye Yuan

Molecular events associated with successful human implantation are poorly understood due to technical and ethical constraints. Here, we performed single-cell whole genome bisulfite sequencing (scWGBS) on three classes of human trophoblast cells (TB) (cytoTB, syncytioTB, and migratory TB) obtained from peri-implantation stage human embryos cultured to embryonic day (D) 8, D10, and D12 as described earlier for single cell RNA sequencing (scRNA-seq) experiments (PMID: 31636193). In brief, embryos were treated with trypsin. Small, round cells were inferred to be mononucleated cytoTB, the multinucleated syncytioTB were identified as irregular shaped structures significantly larger than the cytoTB, and the migratory TB were recognized as seemingly moving away from the main body of the embryo and collected prior to complete dissociation. Ninety-six samples were sequenced and approximately 25 million 150 bp paired-end reads per sample were obtained. In total, we captured approximately 20 million CpG sites with 66% total coverage of all CpG sites in the human genome. Global DNA methylation of cytoTB increased from D8 to D10 and maintained relatively constant to D12. These changes were consistent with results obtained by immunofluorescence staining for 5methylcytosine on whole embryos. SyncytioTB had a lower, and migratory TB a similar global methylation level compared to cytoTB. The global hypomethylation of DNA in syncytioTB may be correlated with the significantly reduced (p < p(0.001) DNMT3A expression and increased (p < 0.0001) TET1 expression compared to migratory TB revealed by scRNA-seq. We then identified differentially methylated regions within each cell type and noted a large number of significantly hypomethylated pathways (p < 0.0001) in both syncytioTB and migratory TB linked to neuronal behavior, such as axonal guidance signaling, CREB signaling in neurons, GABA receptor signaling, endocannabinoid neuronal synapse pathway, synaptic long term depression, and ephrin receptor signaling. This suggests the critical role of DNA methylation in regulating the invasive nature of syncytioTB and migratory TB by activating machinery traditionally found in neurons. In addition, expression of many genes in these hypomethylated pathways was upregulated similarly in syncytioTB and migratoryTB compared to cytoTB as confirmed by our scRNA-seq data. For example, axonal guidance signaling related genes BMP1, GNA11, PRKAG2, PRKCZ, and WNT11 were upregulated in both cell types compared to cytoTB (P < 0.002).

Interestingly, a subset of genes in the pathway was only significantly upregulated (p < 0.05) in either syncytioTB (ABL1, EPHA2, PRKAR2A) or migratory TB (AKT1, BAIAP2, GNA12, GNB1, MAP2K2, MYL9, PLXNB2, PLXND1, RTN4R, SEMA4B, WNT5A). This suggests that though DNA methylation may play an important role in guiding both syncytioTB and migratory TB differentiation, downstream regulatory mechanisms may vary between

cell types. In summary, we describe global DNA methylation dynamics of trophoblast differentiation during human implantation. By applying a multi-omics approach, our data suggest that DNA methylation is an important driving force for directing TB lineage emergence during implantation and that there are analogies between early trophoblast differentiation and neuronal behavior. This research was funded by Colorado Center for Reproductive Medicine and approved by Western Institutional Review Board (Study no: 1179872).

Abstract # 2108

miR-218-5p Promotes Endovascular Trophoblasts Differentiation In Part Via The Activation Of The NF-kb Pathway. Yanan Shan, Jelena Brkic, Jacob O'Brien, Caroline Dunk, Heyam Hayder, Stephen Lye, Chun Peng

miR-218-5p promotes endovascular trophoblasts differentiation in part via the activation of the NF- k B Pathway Yanan Shan 1, Jelena Brkic 1, Jacob O'Brien 1, Caroline Dunk 2 , Heyam Hayder 1, Stephen Lye 2, and Chun Peng 1 1. Department of Biology, York University, Toronto, ON M3J 1P3, Canada 2. Lunenfeld-Tanenbaum Research Institute, Mount Sinai Hospital, Toronto, ON M5T 3H7, Canada During placenta development, the endovascular trophoblasts (enEVTs) invade into uterine spiral arteries and help to transform them into the high flow, low resistant blood vessels. Recently, we demonstrated that miR-218-5p promotes enEVT differentiation, invasion, and spiral artery remodeling (Brkic et al., 2018. Mol Ther 26: 2198-2205). Gene Ontology analysis of cDNA microarray with mir-218 (the precursor of miR-218-5p)-overexpressing cells revealed that the NF-kB pathway is one of the most affected pathways. These findings suggested that the NF-kB pathway plays a role in mediating the effects of miR-218-5p on enEVT differentiation. To test this hypothesis, we first measured cytosolic and nuclear fractions of p65 and p50, two members of the NF-kB family, in control and mir-218overexpressing HTR-8/SVneo cells. We found that miR-218-5p overexpression resulted in the accumulation of p65 and p50 in the nucleus, confirming the activation of this pathway. Using bioinformatics tools, we identified 3 potential binding sites of miR-218-5p in the 3'UTR of NLRC5, an inhibitor of the NF-kB pathway. Real-time PCR and Western blotting revealed that stable overexpression of mir-218 or transient transfection of miR-218-5p both reduced the mRNA and protein levels of NLRC5. Luciferase reporter assays also confirmed the interaction between miR-218-5p and the 3'UTR of NLRC5. Furthermore, knockdown of NLRC5 in HTR-8/SVneo cells increased cell migration, invasion, the formation of the endothelial-like networks, and expression of enEVT markers, VE-cadherin and NCAM. Conversely, overexpression of NLRC5 reduced the stimulatory effect of miR-218-5p on cell invasion and formation of endothelial-like networks. Finally, inhibition of the NF-kB pathway using ACHP strongly suppressed the ability of mir-218 to induce cell invasion and network formation. These findings suggest that miR-218-5p inhibits NLRC5, leading to the subsequent activation of NF-kB, and that activation of the NF-kB pathway mediates, in part, the stimulatory effect of miR-218-5p

on enEVT differentiation (Supported by CIHR). Key Words: enEVT, miR-218-5p, NLRC5, NF-kB, invasion

Abstract # 2136

Characterizing the Role of OVOL1 in Placental Trophoblast Cell Proliferation. Maram B. Albakri, Gargi Jaju, Stephen J. Renaud, Patrick Lajoie

The placenta supports exchange of nutrients and gases between maternal and fetal blood throughout pregnancy. Trophoblasts are the parenchymal cells of the placenta and perform the vast majority of its functions. There are many different types of trophoblasts, all of which are derived from stem cells called cytotrophoblasts (CTs). The balance between CT proliferation and differentiation is fundamentally important for controlling placental growth, development, and function. OVO-like 1 (OVOL1) is a transcription factor expressed in many epithelial lineages, and we have recently found that it is expressed in human CT cells. It interacts with enzymes called histone deacetylases (HDACs) and has been implicated as a repressor of cell proliferation. The molecular mechanisms through which OVOL1 represses cell proliferation, and whether it exerts this function in CTs, is unknown. We hypothesize that OVOL1 interacts with specific HDACs to repress CT proliferation. Since the pathways regulating cell proliferation are highly conserved between humans and yeast, we initially used yeast (S. cerevisiae) to investigate mechanisms through which OVOL1 regulates this process. OVOL1 was ectopically expressed in wild-type yeast or yeast lacking specific HDACs, and cell growth assays were performed. Furthermore, to delineate which regions within OVOL1 are important for mediating cell growth, yeast were transfected with OVOL1 possessing: (1) a mutation in the zinc finger region to prevent OVOL1 from binding to DNA, or (2) a deletion of the first 15 amino acids within the N-terminus (SNAG domain), to prevent OVOL1 from binding to HDACs. In subsequent experiments, we ectopically expressed OVOL1 into a human CT cell-line (BeWo). Ectopic expression of OVOL1 in yeast caused a significant growth defect compared to control ($P \le 0.01$). Wild type yeast cells showed a significant decrease in survival when OVOL1 was expressed, close to a 15% reduction in viability. There was a 4-fold increase in OVOL1 expression in yeast expressing both wild type and mutant OVOL1. The growth defect was not evident when cells were transfected with mutant versions of OVOL1, and was rescued in yeast lacking class II HDACs (P ≤ 0.001). Ectopic expression of OVOL1 in BeWo CTs caused a 16-fold, and 8-fold increase in expression of ERVFRD1, and CGB respectively, which are genes involved in CT differentiation. Our yeast findings demonstrate that OVOL1 is able to represses cell proliferation. The DNA binding domain and N-terminal SNAG domain were both required for OVOL1 to exert its anti-proliferation effect. We also found that class II HDACs were required for OVOL1 to mediate growth arrest. The combination of both yeast and mammalian models provide a new experimental platform to better characterize the mechanisms by which OVOL1 functions to repress trophoblast cell proliferation, and provide new insights into the complexities of placental development.

Abstract # 2142

Anti-Coagulation Factor Contributions To Placental And Fetal Development. Ross McNally, Masanaga Muto, Khursheed Iqbal, Regan Scott, Vinay Shukla, Michael Soares

During gestation in many mammalian species trophoblast cells are directly bathed in maternal blood. It is this hemochorial placentation that is responsible for the intimate communication between both maternal and fetal compartments. One such placentamediated event involves trophoblast cell transformation of the uterus; wherein invasive trophoblast cells migrate from the placenta and restructure the maternal vasculature thus providing adequate blood flow to the developing fetus. Aberrant trophoblast cell development and function lead to obstetrical complications that are associated with coagulopathies. Trophoblast cells can regulate thrombotic activity through the production of anti-coagulation factors, including tissue factor pathway inhibitor (TFPI) and thrombomodulin (THBD). In mice, loss of TFPI or THBD results in prenatal lethality. Disruption of mouse Tfpi or Thbd genes is associated with anomalous placentation, which was viewed as a contributor to the in-utero demise. Mouse models do not adequately mirror the deep intrauterine trophoblast invasion observed in human and rat placentation. Consequently, in this study we examine the biology of TFPI and THBD in the rat. TFPI and THBD are differentially expressed in compartments of the placentation site over the course of gestation. To investigate the physiological roles of these anticoagulation factors we utilized CRISPR/Cas9 genome editing to establish loss-offunction rat models for TFPI and THBD. Exon 4 of the Tfpi gene and Exon 1 of the Thbd gene were independently targeted in separate experiments. CRISPR/Cas9 reagents were microinjected into embryonic day 0.5 rat zygotes. The zygotes were then transferred into the oviducts of appropriately timed pseudopregnant female rats. Offspring were screened by PCR and mutations confirmed by genomic DNA sequencing. Two mutant Tfpi rat founders were generated: i) 636-bp deletion including all of Exon 4 (Tfpi-K1), which encodes Kunitz domain 1; and ii) 1-bp insertion within Exon 4 (Tfpi1bp); whereas, one mutant Thbd rat founder was produced containing a 1316 bp deletion of Exon 1. Mutations were effectively transmitted through the germline. Heterozygous males and females with any of the Tfpi or Thbd mutations were fertile. However, heterozygous intercrosses for Tfpi-K1, Tfpi1bp, or Thbd rat strains did not yield viable homozygous mutant offspring. Timed heterozygous intercrosses were euthanized at various stages of gestation to determine the onset of in-utero demise. Tfpi-K1 and Ifpi1bp phenotypes were indistinguishable. At gestation day (gd) 11.5 Tfpi null mutants were visibly growth restricted and possessed anemic yolk sacs. All homozygous Tfpi mutants were dead by gd 13.5. Thbd null mutants exhibited growth restriction by gd 10.5 and were dead by gd 12.5. Rat TFPI deficiency exhibited a uniform prenatal death at midgestation, which contrasts with the reported heterogenous phenotypes associated with mouse TFPI deficiency. Rat and mouse THBD deficiency exhibited similar phenotypes. In summary, we have successfully generated rat models possessing global disruption of Tfpi and Thbd loci. Although, the midgestation lethality of homozygous Tfpi and Thbd rat mutants precludes examining their impact on the uterine-placental interface of late gestation, roles for TFPI and THBD in early

placentation events are actively being pursued. (Supported by NIH grants HD020676, HD079363, HD099638; and the Sosland Foundation).

Abstract # 2171

KDM1A Regulates Genes Important for Trophoblast Cell Development and is Necessary for Sheep Conceptus Elongation in vivo. Gerrit J. Bouma, Asghar Ali, Taylor Hord, Russel V. Anthony, Quinton A. Winger

A proper functioning placenta is critical for pregnancy, fetal growth and development and postnatal health. Recently we demonstrated that histone lysine demethylase KDM1A binds to androgen receptor (AR) in human and sheep trophoblast cells and targets the same promoter region of vascular endothelial growth factor A (<i>VEGFA</i>). In the current study we hypothesized that KDM1A regulates expression of genes important for early placental development, and is necessary for sheep conceptus elongation. Using CRISPR-Cas 9 based genome editing and ACH-3P trophoblast cells, we demonstrate that KDM1A knockout (KDM1A KO) leads to significant (P < 0.05) reductions in AR, VEGFA, high mobility group AT-hook 1 (HMGA1) and MYC protooncogene (cMYC), all factors important for cell proliferation and trophoblast cell development. Moreover, KDM1A KO ACH-3P cells had significant (P < 0.05) lower levels of pluripotency factors and let-7 miRNA regulators LIN28A and LIN28B, and significantly (P < 0.05) increased let-7miRNAs (let-7a, b, c, d, e, g) compared to scramble control (SC). Finally, an in vivo experiment was conducted to demonstrate a role for KDM1A in placental development, using the sheep as a model. Day 9 hatched blastocysts were flushed and infected with a Lenti-CRISPRv2 KDM1A target construct (n=4) to knockout KDM1A specifically in the trophectoderm, or with SC (n=5). Infected embryos were transferred to recipient ewes and embryos were collected at gestational day 16. Data suggests that KDM1A KO in trophoblast cells is necessary for conceptus elongation. Current experiments are ongoing to determine the effects of KDM1A knockdown using shRNA lentiviral target vectors on conceptus elongation and pregnancy. Collectively these results indicate that KDM1A plays a central role in regulating genes necessary for trophoblast cell proliferation. This project was supported by Agriculture and Food Research Initiative Competitive Grant no. 2019-67015-29000 from the USDA National Institute of Food and Agriculture.

Abstract # 2241

Glutamine Stimulates Ovine Trophectoderm Cell Proliferation And Migration Via Hexosamine-TSC2-MTOR Cell Signaling Pathway. Bangmin Liu, Robert C. Burghardt, Guoyao Wu, Fuller W. Bazer, Xiaoqiu Wang

Histotroph is required for survival and development of conceptuses (embryo and extraembryonic membranes) during the peri-implantation period of pregnancy in mammals. In sheep, the maternal to fetal flux of glutamine (Gln) was greatest among all amino acids, particularly between Days 13 and 16 of pregnancy when conceptuses are rapidly elongating. Explant cultures of ovine conceptuses were used to demonstrate increases in protein synthesis and activation of MTOR cell signaling pathway by Gln. However, the roles of GIn on activation of MTOR cell signaling and trophectoderm cell behavior are unknown. In this study, we used primary ovine trophectoderm (oTr) cells isolated from Day 15 conceptuses to test the hypothesis that GIn activates MTOR cell signaling via production of hexosamine, thereby stimulating proliferation and migration of oTr cells in a dose-dependent manner with maximum stimulation at 0.5 mM (P<0.05). Gln also increased (P<0.05) intracellular concentrations of glucosamine-6-phosphate (GlcN-6-P), the precursor of UDP-N-acetylalucosamine (UDP-GlcNAc). Inhibition of glutamine-fructose-6-phosphate transaminase 1 (GFPT1; the rate-limiting enzyme in the formation of hexosamine products) with $2 \mu M$ azaserine decreased (P<0.05) the ability of GIn to stimulate proliferation of oTr cells and synthesis of GIcN-6-P. Further, migration of oTr cells in a scratch wound assay increased (P<0.05) in response to Gln at 12 h. Quantitative immunofluorescence analyses revealed that GIn stimulated (P<0.05) the phosphorylation of TSC2 after 30 min; whereas the phosphorylation of MTOR started to increase (P<0.05) at 1 h in response to GIn, and increased progressively at 24, 48 and 96 h. Those effects were abrogated (P<0.05) by inhibition of GFPT1. Collectively, these results demonstrated important roles for GIn that are mediated via the hexosamine biosynthesis pathway to increase activation of TSC2-MTOR cell signaling cascade that induces proliferation and migration of oTr cells. This research was support by the Hatch project 1020014 from the USDA National Institute of Food and Agriculture.

Abstract # 2274

Identification Of Bovine T Cell Populations Involved In Placental Growth And Development. Kelsy A. Leppo, Preston A, Collins, Kira P. Morgado, Ana C. Silva, Aaron J. Thomas, Heloisa M. Rutigliano

Development of a conceptus depends on appropriate communication between placental cells and the maternal immune system. The outermost layer of the placenta is composed by trophoblast cells which are in intimate contact with the maternal endometrial tissue. In humans and mice, CD4+CD25+ and gamma/delta T lymphocytes are associated with normal placental function. It is currently unknown if T cells support placental development during the bovine pregnancy. The objective of this study was to determine whether T cell populations are responsible for fostering placental development during the bovine pregnancy. We hypothesize that CD4+CD25+ and gamma/delta T cells will promote trophoblast cell growth and proliferation and modulate trophoblast gene expression. Peripheral blood was collected from three cows at 160-180 days of gestation and three non-pregnant cows. Mononuclear cells were isolated, and T cell populations were sorted by flow cytometry: CD8+, CD4+, CD4+CD25+, CD24+CD25-, and gamma/delta T cells. After culture of each T cell population for 48 hours, supernatant was collected and frozen at -20°C. Placental samples were collected from a local abattoir, enzymatically digested, and trophoblast cells cultured in a 96-well plate for 24 hours. Trophoblast cells (2,500) were cultured with 50 L of T cell conditioned media and 50 L of fresh culture media for 48 hours. Controls wells were treated with 100 L of unconditioned media. This experiment was replicated four times using trophoblast cells isolated from four individual placentas. Cell proliferation and apoptosis assays were conducted immediately after treatment. Trophoblast cells were also frozen at -80°C for later gene expression analysis. Gene expression analyses were conducted based on a panel of 70 genes related to trophoblast cell growth and development using Fluidigm Real-Time PCR system. Messenger RNA expression data were analyzed by the Delta Delta Ct method using the average of the housekeeping genes GAPDH and ACTB for normalization. Data were analyzed by the mixed command of SPSS where the experimental unit is the cell culture well (n=24). The interaction between T cell population and pregnancy status was included in the model. Proliferation and apoptosis results showed no effect of treatment in growth or viability of trophoblast cells. A T cell population effect was not observed on the expression of the genes investigated. A significant effect of pregnancy status on the expression of LIFR, IGF1R, GDF9, FGF2, COL2A1 and RSPO3 was observed. T cell supernant from non-pregnant cows downregulated the expression of GDF9, FGF2, COL2A1, RSPO3 in trophoblast cells compared to unconditioned media, while T cell supernatant from pregnant cows upregulated trophoblast expression of LIFR and IGF1R. In this study, we show that T cell supernatant from pregnant animals can modulate gene expression of trophoblast cells.

Abstract # 2336

Effect of Hypoxia on Trophoblast Cell Fusion of Human Placental BeWo Cells. Adam K. Jaremek, Mariyan J. Jeyarajah, Gargi Jaju Bhattad, Stephen J. Renaud

Preeclampsia is the most common complication during pregnancy, presenting as hypertension and vascular damage in mothers that can progress to organ failure, stroke, and death. There is no known cure except removal of the placenta, the temporary organ supporting fetal growth. During placental development, cytotrophoblast (CT) stem cells differentiate and fuse to form a multinucleated syncytiotrophoblast (ST) layer, and impaired ST formation is implicated in the etiology of preeclampsia. Also, preeclamptic placentas are often associated with hypoxia, or insufficient oxygen (O2). Hypoxia triggers activation of the transcription factor hypoxiainducible factor (HIF), which elicits adaptive cellular responses by altering expression of genes that affect cell proliferation, differentiation, and metabolism. Although past studies suggest that hypoxia can inhibit ST formation, the underlying mechanisms are not well understood. Therefore, we hypothesize that hypoxia-induced HIF signaling represses transcription of genes resulting in impaired ST formation. Cells of the CT cellline BeWo were induced to differentiate into ST in vitro using 8-Bromo-cAMP for 24 and 48 h under hypoxic (0.5% O2) and normoxic (20% O2) conditions. Using quantitative real-time PCR, we found that cells induced to differentiate under hypoxic conditions for 24 h showed decreased transcript levels of ST markers (3.1-, 4.6-, and 17.7-fold

decreased ERVFRD-1, OVOL1, and CGB expression respectively, N=3, P<0.05) when compared to cells cultured under normoxic conditions for 24 h. Moreover, using immunofluorescence to quantify the percentage of cells that formed ST, we observed a 30% decrease in ST formation for cells exposed to hypoxic versus normoxic conditions for 48 h (N=3, P<0.05). This suggests that hypoxia-induced HIF signaling represses transcription of genes resulting in impaired ST formation. Future research will provide insight into how hypoxia-HIF signaling regulates ST formation and may open doors to test whether targeted inhibition of HIF binding sites could rescue ST formation and placental function in preeclamptic pregnancies.

Uterine Biology: Endometrium, Fibroids

Abstract # 1731

Effects of Cylotraxin-b Treatment on Endometriotic lesion survival in an immunocompromised mouse model. Anna Leonova, Warren Foster, Sarah Scattolon, Kathleen Delaney

Objective: Brain-derived neurotropic factor (BDNF) and its high-affinity receptor neurotrophic tyrosine receptor kinase 2 (NTRK2) are over-expressed in women with endometriosis compared to symptomatic controls. Moreover, plasma levels of BDNF are greater in women with endometriosis compared to controls and plasma BDNF levels are associated with endometriosis associated pelvic pain. Therefore, we investigated the effects of increasing cyclotraxin-b (a NTRK2 antagonist) doses on endometriotic lesion survival and volume in an immunocompromised mouse model of endometriosis. Materials and Methods: Endometrial cells isolated from endometrial lesions of women undergoing laparoscopy for excision of endometriosis were surgically implanted into immunocompromised mice. Animals were treated by intraperitoneal injection with 100µL phosphate buffered saline (vehicle control), cyclotraxin-b (2.5, 5.0, 7.5 mg/kg weight/day), or 0.04 mg/kg/day Letrozol for 4 weeks. The number and volume of endometriotic implants were measured at study termination. Implants were collected for routine histology and immunohistochemistry. All major organs were weighed and collected for routine histology. Design: A pre-clinical study using a mouse xenograft model of endometriosis. Results: Preliminary data revealed that treatments had no effect on body weight of animals as well as on the absolute and relative weight of major organs. There was a dose dependent reduction in endometriotic lesion number and volume. The mean (±SD) number of endometriotic lesions was lower in animals in the high group (n = 0.6 ± 0.5), than the medium (n = 1.3 ± 0.5), and low-dose cyclotraxin-b group (n = 1.5 ± 0.5). The mean (\pm SD) volume of endometriotic lesions was also lower in animals in the high group (0.3 ± 0.5) , than the medium (0.7 ± 0.5) , low-dose cyclotraxin-b group (1.4 ± 1.2) as well as letrozole treated group (0.4 ± 0.7) . Histological abnormalities were found in the liver and kidney of animals from high-dose (7.5mg/kg/day) treatment group. Conclusion: Preliminary results suggested that highdose of cyclotraxin-b treatment was more effective than Letrozole in reducing lesion

size. Our results also suggest that cyclotraxin-b treatment did not induce any serious offtarget effects. Key words: Endometriosis, BDNF, Cyclotraxin-b

Abstract # 1870

Gelatin Hydrogel Platforms to Model the Endometrium and Trophoblast Invasion in Three-Dimensions. Samantha G. Zambuto, Ishita Jain, Ioana Pintescu, Gregory H. Underhill, Kathryn B.H.Clancy, Brendan A.C. Harley

As the site of blastocyst implantation, the endometrium plays a critical role in female reproductive health and pregnancy. Despite the importance of this tissue, few models of the endometrium exist and those that do lack the complexity necessary to recapitulate relevant endometrial features (e.g., stratified three-dimensional structure, presence of an endometrial perivascular niche, ability to monitor trophoblast invasion) and cannot be used to explore dynamic processes such as tissue remodeling, angiogenesis, and invasion. The use of biomaterial-based models allows us to mimic native tissue architecture and heterogenous populations of cells in three-dimensional platforms. We describe the use of methacrylamide-functionalized gelatin (GeIMA) hydrogels to model endometrial function and trophoblast invasion in three-dimensions. The endometrial perivascular niche plays an important role in endometrial function and has implications in pregnancy disorders, including the hypertensive pregnancy disorder preeclampsia which has been linked to insufficient trophoblast invasion and remodeling of maternal spiral arteries in the uterus. To better understand endometrial angiogenesis and vascular remodeling, we model the hormone-responsive endometrial perivascular niche by co-culturing human primary endometrial endothelial microvascular cells and human endometrial stromal cells with or without decidualization hormones (0.5 mM 8bromo-cAMP + 1 µM medroxyprogesterone acetate). Capturing cyclic hormonal stimulation in the endometrium is relevant to modeling endometrial remodeling and growth during the menstrual cycle. We chose to mimic decidualization of endometrial stromal cells to mimic the menstrual cycle phase during which a blastocyst would implant. We show decidualization of endometrial stromal cells in co-culture by a characteristic morphological rounding and a decrease in expression of CD10. Trophoblast cells from the invading blastocyst first come into contact with the endometrial luminal epithelium. As a model of the endometrial epithelium, we cultured primary endometrial epithelial cells on top of GelMA hydrogels. We employed microarray technology to determine which extracellular matrix protein combinations (collagen I + collagen III, collagen IV + tenascin C) facilitate improved epithelial cell attachment. Incorporation of a basement membrane layer underlying epithelial cells will allow us to optimize epithelial monolayer formation overlaying our hydrogels to recapitulate the native stratified structure of the tissue. We employ three-dimensional trophoblast spheroid invasion assays consisting of HTR-8/SVneo trophoblast spheroids embedded in GelMA hydrogels that can be used to quantify invasion and cell viability so we can better understand what drives and constrains trophoblast invasion. We chose to study cues from the maternal-fetal interface to understand cellular crosstalk

between cells from the endometrium and trophoblast cells, specifically how markers of maternal stress influence trophoblast invasion. We demonstrate differences in invasion in the presence of biomolecules from the maternal-fetal interface (epidermal growth factor, transforming growth factor β 1, and the stress hormone cortisol). Ongoing efforts include the development of a stratified endometrial tri-culture consisting of our endometrial perivascular niche and overlaid epithelial culture and quantification of trophoblast invasion in the presence of the endometrial perivascular niche. The platforms we have developed will provide adaptable systems for modeling additional dynamic processes associated with female reproductive health and pregnancy (e.g., endometriosis, pregnancy disorders).

Abstract # 1926

Evaluation Of Changes In Gene Expression On The Equine Endometrium During Early Pregnancy Compared To Non-Pregnant Mares During Diestrus. Alejandro Esteller-Vico, Pouya Dini, Blaire Arney, Kirsten Scoggin, Ted Kalbfleisch, Barry A. Ball

Early pregnancy in the mare is a critical period of interactions between the embryo and the endometrium that results in the extension of lifespan of the corpus luteum through maternal recognition of pregnancy. To date, little is known about the changes in gene expression in the equine endometrium as a result of the interaction with the early embryo. Our hypothesis was that there are changes in the equine endometrium related to maternal recognition of pregnancy as early as day 12. The objectives of this study were to determine differences in endometrial gene expression during early pregnancy in the mare. Thirty mares were divided into two groups, pregnant (P) and non-pregnant (NP). Furthermore, these groups were divided in 3 subgroups according to the sampling times. The first subgroup at day 12 post ovulation (pregnant n=5 and non-pregnant n=5), subgroup 2 at day 14 (P n=5 and NP n=5) and subgroup 3 at 16 days (P n=5 and NP n=5). For each time point, an endometrial biopsy was collected from the base of the uterine horn. All samples were preserved in RNAlater. Additionally, blood samples were collected daily for progesterone analysis. RNA was isolated from equine endometria and submitted for RNA sequencing. The libraries were sequenced on a HiSeq2000 using a TruSeq SBS sequencing kit version 3, generating an average of 12.3x106 stranded 150bp paired-end reads per sample. RNAseq reads were trimmed using Trim-Galore (v0.6.4), mapped to the reference genome (EqCab 3.0) using STAR (v2.7.2a), and annotated by Cufflinks (v2.2.1). Gene expression analyses were performed using an empirical analysis of DGE and a false discovery rate correction (significance set at FDR <0.1). For progesterone concentrations, there were no differences between pregnant and non-pregnant at day 12 and 14, but progesterone was significantly lower in nonpregnant mares at day 16 compared to pregnant mares. When comparing day 12 pregnant to non-pregnant endometria, we found four significant differentially expressed genes, 3 upregulated (SLC36A2, GM2A and LCN2) and one downregulated (ENSECAG16428). At day 14 day there were 10 significant differentially expressed genes, 9 of them upregulated (CTSE, SLC36A2, ACTC1, SLITRK6, MYH11, FGF9, ACTG2, HSPB8,

and KCNN2) and one downregulated (KRT4). Finally, at day 16 there were 132 differentially expressed genes with 83 upregulated and 49 downregulated. Of these 132 genes SLC15A1, DKK1, SLC36A2, ARMC12, HAL, ATF5, KCNN2, SLC1A1, DPYSL5 and TSC22D3 were the most highly upregulated and SPLA2, STMN2, CDH17, ADAMTS18, TNC, LTF, MXRA5, PENK, S100A2, PHLDA1 were the most highly downregulated. The large number of differently expressed genes at day 16 might be the results of an already low progesterone environment in the non-pregnant mares; however, the small number of differentially expressed genes found at the 12 and 14 might be related to the early interactions between embryo and the equine endometrium. Among these differentially expressed genes, SLC36A2 was significantly upregulated in all time points. Supported by the Gluck Equine Research Foundation and the Albert G. Clay Endowment of the University of Kentucky.

Abstract # 1930

Endometrial Transcriptome Of Cows That Fail To Become Pregnant Following Uterine Infection. Mackenzie J. Dickson, Jeanette V. Bishop, Thomas R. Hansen, I Martin Sheldon, John J. Bromfield

Uterine infection occurs in up to 40% of dairy cows postpartum and is associated with infertility, even after the infection resolves. Embryo transfer to recipient cows that had a uterine infection are less likely to establish pregnancy compared to healthy embryorecipients, suggesting that the endometrium contributes to post-infection infertility. Previous research by colleagues used RNAseq to identify 459 differentially expressed genes in the endometrium of healthy pregnant cows at day 16 of gestation compared to healthy cycling cows that were never bred. Here, we examined the endometrial transcriptome of cows that failed to become pregnant after uterine infection, compared to post-infection cows that were pregnant at day 16 of gestation. We hypothesized that the endometrial transcriptome of pregnant cows would be different than that of cows which were not pregnant, and secondly that the post-infection endometrial transcriptome would be different between cows that failed to become pregnant and healthy cycling cows that were never bred. Non-lactating Holstein cows were inseminated 130 days after an intrauterine infusion of endometrial pathogenic bacteria. All cows responded to estrous synchronization and 50% of cows were pregnant at day 16. Intercaruncular endometrial tissue was processed for RNAseq and cows were categorized as pregnant if an embryo was recovered (n=3) or nonpregnant (n=4) if no embryo or interferon-tau was detected in uterine fluid. A total of 171 differentially expressed genes were identified in the post-infection endometrium of pregnant cows compared to non-pregnant cows using a false discovery rate of P< 0.05. Of these, 140 genes were upregulated and 31 were downregulated in pregnant cows compared to non-pregnant cows. Upregulated genes in pregnant cows included RSAD2, MX2, IFIT1, BST2, USP18, and MX1, while downregulated genes included FAM135B, FLRT1, MEF2B, RBFOX1, LILRA6, and MUC5B. As expected, the canonical pathways altered in pregnant cows included interferon signaling, activation of

interferon regulatory factors by cytosolic pattern recognition receptors, and role of pattern recognition receptors in recognition of bacteria and viruses. The predicted upstream regulators of differentially expressed genes included interferon lambda 1, interferon alpha 2, prolactin, interferon alpha, and interferon regulatory factor 7. Seventy-five (44%) of the differentially expressed genes were also identified in the previous study comparing pregnant and cycling endometrium of healthy cows, while 96 genes were unique to the post-infection model. These unique differentially expressed genes may be indicative of differences in the endometrium between healthy and postinfection cow pregnancies. All 31 overexpressed genes in the non-pregnant postinfection cows were not upregulated in the endometrium of healthy cycling cows and may be mechanistically associated with the post-infection endometrium. Further comparison of the endometrial transcriptome of non-pregnant post-infection cows with healthy cycling cows could provide mechanistic insights into how the endometrium contributes to post-infection infertility in cattle. This work is supported by NICHD R01HD084316.

Abstract # 1936

Decreased Endogenous CBS-H2S in the Secretory Phase Contributes to Decidualization in Human Endometrial Stromal Cells. Qianrong Qi, Jin Bai, Yan Li, Joshua Makhoul, Dongbao Chen

Introduction: Human endometrial stromal cells (ESCs) proliferate in the proliferative phase, undergo spontaneous decidualization for preparing endometrium to be receptive for embryo implantation in the secretory phase. Endogenous hydrogen sulfide (H 2 S) synthesized from L-cysteine by cystathionine- β -synthase (CBS) and cystathionine-y-lyase (CSE) is a multifaceted biogas with many biological functions including stimulating cell proliferation. However, it is unknown if H 2 S plays a role in ESC proliferation and decidualization. Objective: To test a hypothesis that endometrial H 2 S biosynthesis undergoes cyclic changes during the menstrual cycle to regulate ESC proliferation and decidualization. Methods: Endometria from premenopausal (proliferative and secretory phase) non-pregnant and pregnant women (n=4-8/group) were collected. Primary endometrial stromal cells (ESC) were isolated and cultured. Cultured cells were treated with a H 2 S donor NaHS (100 μ M), estradiol (10 nM E 2 B), progesterone (1 µM P4), or P4 (1 µM) and dibutyryl-cAMP (1 mM db-cAMP) for up to 8 days. Vehicle (0.1% ethanol) was used as a control. Endogenous CBS in ESC was knockout by using the human CBS sgRNA CRISPR/Cas9 All-in-One Lentivector. Cells morphology was monitored and photographed every other day. Cell proliferation was determined by the CCK8 assay. Levels of mRNA were determined by qPCR and protein was determined by immunoblotting; H 2 S production was determined by the methylene blue assay. Results: Levels of CBS (but not CSE) mRNA and protein and H 2 S production were lower in endometria from the secretory phase than that in the proliferative and pregnancy in women. Baseline CBS and CSE and decidualization markers, i.e., insulin-like growth factor binding protein 1 (IGFBP-1) and prolactin (PRL),

were unchanged during culture. H 2 S donor NaHS and E 2 β promoted timedependent ESC proliferation with elevated CBS mRNA and protein expression, without altering morphology and IGFBP1 and PRL mRNA expression. P4 and P4/db-cAMP inhibited ESC proliferation, CBS mRNA and protein expression and H 2 S production; however, these P4 treatments stimulated time-dependent increases in IGFBP1 and PRL mRNA and ESC transformation into an epithelial phenotype, indicative of ESC decidualization. CBS knockout attenuated E 2 β - and H 2 S- stimulated ESC proliferation, but enhanced IGFBP1 and PRL expression and cell morphology transformation. Conclusion: CBS-H 2 S production displays cyclic changes in the menstrual cycle, which is downregulated in the secretory phase. Decidualization of ESC in vitro is associated with decrease CBS-H 2 S signaling and CBS knockout promoted ESC decidualization in vitro. Endogenous CBS-H 2 S is important for ESC decidualization (AHA 20POST35090000, RO1 HL70562, and R21 HD097498).

Abstract # 2083

RNA-Sequencing Based Analysis Of Bovine Endometrium During The Maternal Recognition Of Pregnancy. Bindu Adhikari, Chin N. Lee, Vedbar S. Khadka, Youping Deng, Rajesh Jha, Birendra Mishra

Background: Reproductive efficiency is crucial to the production of food animals, and the overall profitability of the farm. The majority of pregnancy losses occur in the first month, especially around Day-19 of gestation, mainly due to the inability of the uterus to support conceptus growth or abnormal development of conceptus. As Day 15-17 is a critical period for the maternal recognition and establishment of pregnancy, we hypothesize that RNA-Sequencing based analysis of bovine endometrial tissues during the peri-implantation period (Day-16 of gestation) will reveal important genes and biological pathways required for the conceptus growth and development.

Methods: Grass-fed Angus cows (2-3 years old) were used for sampling. The estrous cycles of cows (n=21) were synchronized using intramuscular injection of a Prostaglandin F2 alpha (on Day-1 and -11). Fifteen cows were bred after detecting the estrus. Endometrial samples were collected at Day-16 of gestation (pregnant), estrous cycle (cyclic) and absence of conceptus (nonpregnant) cows (n=6/group). Total RNAs were isolated and were subjected to high-throughput RNA-sequencing (n=4/group). The genes with at least two-fold change, and Benjamini and Hochberg p-value <= 0.05 were considered as differentially expressed.

Results: About 107 genes (pregnant vs cyclic), and 98 genes (pregnant vs Nonpregnant) were differentially expressed in the pregnant endometrium. The most highly upregulated genes in the pregnant endometrium (vs cyclic) were MRS2, CST6, FOS, VLDLR, ISG15, IF16, MX2, C15H11orf34 and EIF3M. The most highly upregulated genes in the pregnant endometrium (vs nonpregnant) were ISG15, IF16, PENK, PRSS22, MS4A8, CLDN4, C15H11orf34, MRS2, TINAGL1 and R3HDM1. Gene ontology analysis revealed that the biological process related to type-1 interferon signaling (MX1, MX2, IF16, IRF1 and ISG15), immune response (IL23A, RSAD2) and extracellular matrix organization (COL1A1, COL1A2, COL3A1 and TIMP2) were significantly enriched in the pregnant endometrium. Ion transporters (SLC34A2, SLC2A1, SLC16A11, SLC16A4 and ATP1B1), platelets derived factors, telomerase activity (HMBOX1, and TERF1) and ATPase activities (P2RX6 and DNAJB1) were significantly enriched as molecular functions, and endoplasmic reticulum lumen (WNT5B, IL23A1, PENK, TNC, SPARCL1 and B2M) was the most significantly enriched cellular component. In the nonpregnant endometrium, negative regulator of hydrolase, dephosphorylation and phosphatase, death-inducing signaling complex and apoptosis were significantly enriched. Ingenuity canonical pathways analysis revealed that interferon signaling, hepatic stellate cell activation, oxidative phosphorylation, GP6 signaling, coenzyme A Biosynthesis, and sirtuin signaling were the highly enriched pathways.

Conclusions: The presence of an embryo induces the endometrial transcripts related to endometrial remodeling, immune response, nutrients and ion transporters, and relevant signaling pathways. Further, in absence of the embryo, these transcripts are downregulated in the endometrium. This study provides a comprehensive dataset of transcripts changes associated with maternal recognition of pregnancy, which can further be linked with the specific functions of the identified genes.

This work was supported by the Hawaiian Dept. of Agriculture to BM.

Abstract # 2099

Differentially Expressed Mirna And Kinases In Eutopic Stromal Cells Promote To Inflammation In Endometriosis. Indrajit Chowdhury, Saswati Banerjee, Adel Driss, Wei Xu, Ceana Nezhat, Neil Sidell, Robert N. Taylor, Winston E. Thompson

Endometriosis is a benign estrogen dependent gynecological disorder affecting 5-15% of women of reproductive age. It causes a wide range of symptoms including mild to severe pelvic pain and infertility. Current FDA-approved hormonal therapies are often of limited efficacy and counterproductive to fertility, and cause systemic side effects due to suppression of endogenous steroid hormone production. These presents significant challenges in terms of management of endometriosis. Moreover, despite decades of research, there are no sufficiently sensitive and specific signs and symptoms nor blood tests for the clinical confirmation of endometriosis, which hampers prompt diagnosis and treatment. microRNA (miRNA), a class of small non-coding RNAs are emerge as a post-transcriptional regulator of protein expressions and have been shown to be involved in the pathogenesis of several diseases. The pleiotropic nature of this class of nonprotein-coding RNAs make them particularly attractive drug targets for diseases with a multifactorial origin and no current effective treatments. Therefore, in the current studies we examined the expression patterns of miRNAs in primary cultures of normal endometrial stromal cells (NESC) and cells derived from eutopic endometrium of endometriosis subjects (EESC). Endometrial biopsies and eutopic implants from women undergoing laparoscopic surgery for chronic pelvic pain were

collected, followed by NESCs and EESCs were cultured, and total RNA was extracted. Using NanoString nCounter-based assays and semi-quantitative RT-PCR analysis we have identified levels of several anti-inflammatory and anti-angiogenic miRNAs that are lower in EESC compared to NESC. Furthermore, pro-survival and differentiation signaling pathways were analyzed using western blots. The analyses of these signaling pathways suggest that the serine/threonine protein kinase B (PKB/AKT), extracellular signalregulated kinases (ERK) and prohibitin expressions are significantly higher in EESCs compared to NESCs. These findings demonstrate lower anti-inflammatory and antiangiogenic miRNA production in EESC compared to NESC under basal conditions, and higher expression of kinase signaling pathways are constitutively activated in endometriosis. Therefore, a better understanding of the molecular activity of these miRNA and kinases, including the specific extracellular compounds that lead to their activation in EESCs specifically should facilitate their improvement and could potentially lead to new, non-hormonal anti-inflammatory and anti-angiogenic treatments of endometriosis. GRANT SUPPORT Nothing to Disclose: IC; SB; AD; WX; CN; NS, RNT, WET. Sources of Research Support: This study was supported in part by National Institutes of Health Grants 1SC3 GM113751, U01 HD66439, 1R01HD057235, U54 CA118948, HD41749, \$21MD000101 and G12-MD007602. This investigation was conducted in a facility constructed with support from Research Facilities Improvement Grant #C06 RR018386 from NIH/NCRR.

Abstract # 2167

Regulation Of Foxa2 In The Uterus Of Conditional Akt Isoforms Mouse KO During The Estrous Cycle. Nicolas Thibodeau, Pascal Adam, Dadou L. Lokengo, Eric Asselin

Many important endometrial activities are important for embryo implantation in the receptive uterus throughout successful pregnancy such as cell survival and apoptosis. A key pathway involved in those processes during gestation is the PI3K/Akt pathway. Protein kinase Akt is present in 3 different isoforms and their specific roles in the endometrium is still not fully understood. We have shown different expression of Akt isoforms during the different phases of the estrous cycle in the uterus indicating that they might be involved in the preparation of the endometrium for successful implantation. Foxa2 has been shown to be important in the process of decidualization and for embryo implantation. Akt pathway can regulate Foxa2, but how Akt isoforms specifically regulate Foxa2 in the uterus is still unknown. The aim of this study was to determine the role and expression of Foxa2 during the estrous cycle and to show which Akt isoform regulates Foxa2 expression. The hypothesis is that Akt isoforms are important to regulate endometrial functions and that their dysregulation can cause fertilityrelated issues and/or infertility. Using PR-Cre mice and Flox Akt mice for each isoform, we developed endometrial-targeted knockout Akt isoform mice (single, double and triple KO). Our preliminary results showed a decrease of fertility (reduced number of pups) in absence of one or more Akt isoforms. Using immunohistochemistry, we showed that Foxa2 protein is overexpressed in endometrial glands of Akt 1-3 KO mice at diestrus.

Interestingly in Akt 2-3 KO mice, Foxa2 is expressed in a shading manner in the endometrium: Foxa2 showed a strong expression in endometrial glands close to the myometrium and expression is gradually fading in glands close to endometrial lumen. A similar fading pattern of Progesterone Receptor (PR) expression was observed in Akt 2-3 KO mice. The results demonstrate that specific Akt isoforms KO affect spatial and temporal expression of Foxa2 in endometrium. We suggest that progesterone could also be involved in this process. Therefore, Akt pathway play a crucial role in fertility and further analyses will be required to determine how upstream and downstream Akt effectors are specifically involved in the control of endometrial functions.

Abstract # 2200

The Development of a Novel Nonhuman Primate Endometrial Epithelial Organoid Cell Culture Model to Study Uterine Gland Function. Harriet C. Fitzgerald, Ov D. Slayden, Addie Luo, Constantine Simintiras, Pramod Dhakal, Clayton Mitchell, Thomas E. Spencer

The human endometrium is highly dynamic, undergoing complete remodelling during a woman's menstrual cycle to prepare for possible pregnancy. The upper layer of the endometrium, the functionalis, is shed and reformed each month, while the inner layer, the basalis, remains and is a possible source of stem cells for the proceeding regenerative, proliferative phase. Recent studies have revealed that uterine glands and be inference their secretions are essential for pregnancy establishment. Investigating aland function in vivo and obtaining endometrial biopsies which contain both the functionalis and basalis from patients without uterine pathologies is difficult. Fortunately, rhesus macaques (Macaca mulatta) have a similar menstrual cycle and a comparatively similar uterus to humans. As such, macaques present as a useful model for studying the intrinsic differences and actions of uterine glands from different regions of the endometrium, which aids in our understanding of early pregnancy establishment. For the first time, endometrial epithelial organoids (EEO) were established from both the endometrial functionalis and basalis, collected from a macaque. EEO were formed using an established protocol used in human EEOs and within 24 hours of tissue isolation, EEO began forming. After passaging, macaque EEO were grown for 4 days in organoid expansion medium and then treated with estradiol-17b (E2) for 2 days and then either nothing (Control) or E2 and medroxyprogesterone acetate (MPA) for a further 6 days (n=3 replicates per animal). Real-time qPCR analysis found that both the basalis and functionalis derived EEO expressed the glandular epithelial cell marker FOXA2 and that this expression was not significantly altered by hormone treatment. This was in accordance with immunofluorescence analysis of macaque endometrial tissue which found that glands of both the basalis and functionalis were positive for FOXA2. PGR was significantly increased by E2 treatment and decreased by E2+MPA treatment in basalis derived EEO but increased by E2+MPA treatment in functionalis derived EEO. Progesterone responsive genes SPP1 and PAEP were increased by E2+MPA in functionalis derived EEO but not in basalis derived EEO. These results suggest that macaque derived EEO have a similar expression signature to that of human EEO but

that there are some differences in those derived from the basalis compared to the functionalis. This highlights that the EEO derived from macaque can serve as an important alternative to the use of human endometrium and will further our understanding of uterine gland function in the whole endometrium. Supported by NIH Grants R01 HD096266, R21 HD087589 and P510D011092 (ONPRC).

Abstract # 2202

Quantity of Macrophages in Endometriotic Lesions May Depend on Lesion Type in Women with Endometriosis. Morgan Martin, Anna Leonova, Nicholas A. Leyland, Warren G. Foster, Jocelyn M. Wessels

Endometriosis is a chronic, estrogen-dependent and inflammatory gynecological condition for which there is no cure. It is characterized by growth of endometrial glands and stroma outside the uterus, and women with endometriosis often suffer debilitating pelvic pain and infertility. Endometriosis occurs in up to 10% of women, and several physiological pathways including angiogenesis, cellular proliferation, adhesion, inflammation, neurogenesis, and apoptosis are reported to be perturbed by the disease. Macrophages are phagocytic innate immune cells that can influence each of these pathways and are suspected to contribute to the pathophysiology of endometriosis. Therefore in our retrospective study we accessed paraffin-embedded endometrial biopsies and ectopic lesions to localize and quantify macrophages by immunohistochemistry in women with (N=5; stage 3/4) and without (N=6) endometriosis. We did not find a significant difference in the number of macrophages in the eutopic endometrium of cycle-stage matched women with and without endometriosis. Similarly, there was no difference in the number of macrophages identified in the eutopic and ectopic endometrium of women with this disease. However, when the number of macrophages was compared between lesion types (ovarian cyst, deep-infiltrating endometriosis, peritoneal endometriosis), ovarian cysts tended to have more macrophages than the other lesion types grouped together, although the relationship did not attain statistical significance. Taken together, results suggest macrophages are present in the eutopic and ectopic endometrium, and the quantity of macrophages present may be dependent on the type of endometriotic lesion.

Abstract # 2240

Amiloride-Sensitive Epithelial Sodium Channel Receptor (ENaC): Is It Involved With Maternal Recognition of Pregnancy (MRP) In Mares? Casie S. Bass, Michelle L. DeBoer, Rachel Hau, Olivia Fischer, Brooke Grube, Alyssa Decorah

While the maternal recognition of pregnancy (MRP) signal is understood in many mammals, the process in its entirety remains to be explained in the equine species. During early pregnancy, the equine conceptus hovers around one location for several minutes before passing on to the next area of the uterus, termed "migration." And

while some researchers have postulated the diffusion of a MRP signaling molecule during conceptus migration, the theory has minimal supporting evidence. Though importance of conceptus mobility has been recognized by several research teams, the interaction between conceptus and endometrium remains a mystery. And while the binding of signaling molecules to corresponding receptors possessed by target cells is the most well understood method of cellular communication, the last few decades have resulted in the recognition of mechanotransduction to elicit changes by cells. A cellular mechanism that may be involved in the mare MRP process is the amiloridesensitive epithelium sodium channel (ENaC); inhibition or knockdown of ENaC in the murine species leads to complete embryo implantation failure. ENaC has been identified and is necessary for correct function in the equine kidneys and laminar structures within the hoof. For the first time, we recently reported ENaC protein was immunodetected in mare endometrial samples. The objective of the project was to determine whether progesterone (P4) and/or ENaC localization and concentrations were changed when mares had an intrauterine device (IUD) inserted on the day of ovulation (d0). In the current project, nine mares of various breeds were used in a crossover design and administered ReguMate for 14 days to synchronize the estrous cycle. On d0, each mare had either manual stretching of the cervix and an IUD inserted (treatment group), or had the cervix manually stretched but no IUD inserted (placebo group). Endometrial biopsies for ENaC localization and quantification, and blood collections for progesterone (P4) hormone analysis were collected on d0, d5, d15, and d20 of the estrous cycle. Results include the localization of ENaC protein to both mare luminal epithelium and uterine glands. There was no significant difference in P4 concentrations between IUD-treated and placebo-treated mares; however, there was a significant difference in P4 concentrations between days of the estrous cycle. In addition, gPCR conditions for ENaC have been optimized and differential expressions are being quantified by both qPCR and IHC. These data indicate that ENaC is present within the mare uterus and may, similarly to other mammalian species, be involved with the MRP process in the mare.

2020 Trainee Awards

Lalor Foundation Merit Award Recipients

Abstract # 2142

Anti-Coagulation Factor Contributions To Placental And Fetal Development. Ross McNally, University of Kansas Medical Center, USA

During gestation in many mammalian species trophoblast cells are directly bathed in maternal blood. It is this hemochorial placentation that is responsible for the intimate communication between both maternal and fetal compartments. One such placenta-mediated event involves trophoblast cell transformation of the uterus; wherein invasive trophoblast cells migrate from the placenta and restructure the maternal vasculature thus providing adequate blood flow to the developing fetus. Aberrant trophoblast cell development and function lead to obstetrical complications that are associated with coagulopathies. Trophoblast cells can regulate thrombotic activity through the production of anti-coagulation factors, including tissue factor pathway inhibitor (TFPI) and thrombomodulin (THBD). In mice, loss of TFPI or THBD results in prenatal lethality. Disruption of mouse Tfpi or Thbd genes is associated with anomalous placentation, which was viewed as a contributor to the in-utero demise. Mouse models do not adequately mirror the deep intrauterine trophoblast invasion observed in human and rat placentation. Consequently, in this study we examine the biology of TFPI and THBD in the rat. TFPI and THBD are differentially expressed in compartments of the placentation site over the course of gestation. To investigate the physiological roles of these anti-coagulation factors we utilized CRISPR/Cas9 genome editing to establish loss-of-function rat models for TFPI and THBD. Exon 4 of the Tfpi gene and Exon 1 of the Thbd gene were independently targeted in separate experiments. CRISPR/Cas9 reagents were microinjected into embryonic day 0.5 rat zygotes. The zygotes were then transferred into the oviducts of appropriately timed pseudopregnant female rats. Offspring were screened by PCR and mutations confirmed by genomic DNA sequencing. Two mutant Tfpi rat founders were generated: i) 636-bp deletion including all of Exon 4 (Tfpi-K1), which encodes Kunitz domain 1; and ii) 1-bp insertion within Exon 4 (Tfpi1bp); whereas, one mutant Thbd rat founder was produced containing a 1316 bp deletion of Exon 1. Mutations were effectively transmitted through the germline. Heterozygous males and females with any of the Tfpi or Thbd mutations were fertile. However, heterozygous intercrosses for

Tfpi-K1, Tfpi1bp, or Thbd rat strains did not yield viable homozygous mutant offspring. Timed heterozygous intercrosses were euthanized at various stages of gestation to determine the onset of in-utero demise. Tfpi-K1 and Tfpi1bp phenotypes were indistinguishable. At gestation day (gd) 11.5 Tfpi null mutants were visibly growth restricted and possessed anemic yolk sacs. All homozygous Tfpi mutants were dead by gd 13.5. Thbd null mutants exhibited growth restriction by gd 10.5 and were dead by gd 12.5. Rat TFPI deficiency exhibited a uniform prenatal death at midgestation, which contrasts with the reported heterogenous phenotypes associated with mouse TFPI deficiency. Rat and mouse THBD deficiency exhibited similar phenotypes. In summary, we have successfully generated rat models possessing global disruption of Tfpi and Thbd loci. Although, the midgestation lethality of homozygous Tfpi and Thbd rat mutants precludes examining their impact on the uterine-placental interface of late gestation, roles for TFPI and THBD in early placentation events are actively being pursued. (Supported by NIH grants HD020676, HD079363, HD099638; and the Sosland Foundation).

Abstract # 2064

Spatial And Temporal Dynamics Of FGL2 Expression Reveal Immunoregulatory Function Essential To The Establishment And Outcome Of Pregnancy. Pascale Robineau-Charette, Ottawa Hospital Research Institute, USA

Fibrinogen-like protein 2 (FGL2) is a known immunomodulator and prothrombinase, previously suggested to be involved in the immune balance of the maternal-fetal interface that is crucial to reproductive success. The female reproductive tract is the site of several key events that require careful endocrine and immunological regulation, from ovulation to pre-implantation embryo transport and placentation. We mapped spatial and temporal dynamics of FGL2 expression through murine reproductive tissues, which revealed remarkable cell type specificity hinting at precise function. We carefully examined several parameters of reproductive performance in our Fgl2 knockout (ko) and overexpressing (tg) mouse colonies. Fgl2 ko females produced only half as many pups as their wild-type (wt) counterparts, due to smaller and less frequent litters. Interestingly, this phenotype was rescued in Fgl2 tg X Fgl2 ko mating pairs, despite the presence of only one overexpressing allele. We observed equal rates of embryo resorption in all three genotypes, suggesting a defect in Fgl2 ko ovarian or oviductal (pre-implantation) function. In the ovary, FGL2 is expressed in the stroma and theca cell layer of follicles, and intensity of expression peaks 8 hours after hCG injection in a superovulation cycle. Strong

expression is acquired by some cumulus granulosa cells shortly before ovulation and persisting in cumulus-oocyte complexes (COCs) found in the oviduct, suggesting a role in ovulation and in luteinization. Fgl2 ko and Fgl2 tg animals however had a normal ovulation efficiency, as measured by the number of COCs retrieved after superovulation. Fgl2 ko and wt ovaries showed equivalent numbers of functional corpora lutea, demonstrating normal luteinization. In the oviduct, FGL2 expression is restricted to secretory cells of the epithelium, whose frequency increase from the fimbrial to the isthmal end. We detected FGL2 in the culture medium of OVE4, primary oviductal epithelial cells, confirming its secretion into oviductal fluid, where it likely contributes to the immunosuppressive environment conducive to fertilization and to tolerance of paternal/fetal antigens. Single-nuclei RNA sequencing of the ovary, ampulla and isthmus at different timepoints after superovulation will reveal differential immune dynamics between Fal2 wt and ko animals, to identify mechanistic actions of FGL2 in these tissues. Despite being born at rates comparable to wt mice, Fgl2 to pups are significantly smaller than their wt and ko counterparts, at birth and at weaning, indicating a probable deficient placental function. Interestingly, we found that women with high placental FGL2 expression tend to be affected by an immunological subtype of preeclampsia, characterized by chronic inflammatory placental lesions and small for gestational age infants. Our histological examination of term placentas from Fgl2 tg animals will confirm correlative evidence, in the human placenta, of FGL2's role as an immunoregulator at the maternal-fetal interface. Overall, this work supports the hypothesis that FGL2 is secreted throughout the female reproductive tract at precise stages of the estrous cycle, and in the developing placenta, as a physiological attempt to maintain the careful immune equilibrium required for the successful establishment and maintenance of pregnancy.

Abstract # 1760

Single Cell Interrogation Of The Uterine-Placental Interface. Regan L. Scott, University of Kansas Medical Center, USA

During a healthy pregnancy, a special lineage of placental cells, referred to as invasive trophoblast cells, exit the placenta and invade into the uterus where they restructure the uterine parenchyma and facilitate remodeling of spiral arteries. Invasive trophoblast cells help anchor the placenta, modulate immune cell populations, and facilitate nutrient delivery to the fetus. These trophoblastdirected uterine modifications are essential for a healthy pregnancy. Insufficient trophoblast invasion and abnormal cross-talk at the uterine-placental interface are major contributors to obstetrical complications such as early pregnancy loss, preeclampsia, intrauterine growth restriction, and pre-term birth. In humans, these events transpire during early gestation, thus their investigation represents a significant ethical challenge. In vitro analyses can provide insights into trophoblast cell potential but fall short as tools to understand the physiology of the invasive trophoblast cell lineage. Implementation of in vivo models to test hypotheses regarding mechanisms underlying the development and function of the invasive trophoblast cell lineage are essential to advance the field. Rodents exhibit hemochorial placentation similar to humans. While the mouse displays shallow trophoblast invasion, the rat exhibits deep intrauterine trophoblast invasion and extensive uterine spiral artery remodeling, comparable to what is observed in the human. In this study, we sought to phenotype cells at the uterine-placental interface of the rat with the goal of identifying conserved candidate regulators of the invasive trophoblast cell lineage. Single-cell RNA sequencing (scRNA-seq) and single-cell assay for transposase-accessible chromatin sequencing (scATAC-seq) were used to interrogate cells at the uterine-placental interface on gestation days 15.5 and 19.5 of the Holtzman Sprague-Dawley rat. Single cell suspensions were prepared by enzymatic digestion of the uterine-placental interface. Single cell libraries were then constructed using the 10X Genomics platform and sequenced with an Illumina NovaSeg 6000 system. Computational analysis with the Cellranger pipeline led to the identification a number of unique cell clusters defined by their transcript profiles, including invasive trophoblast cells (e.g. Prl5a1, Prl7b1, Tpbpa, Plac1, Tfap2c, Igf2, Cdkn1c, Tfpi), endothelial (e.g.Egfl7, Adgrl4, Rasip1, Sox17, Nos3), vascular smooth muscle (e.g. Acta2, Myl9, TagIn, Myh11), natural killer (e.g. Nka7, Prf1, Gzmb, Gzmm), and macrophage (e.g. Fcgr3a, Lyz2, Aif1, Tyrobp, Cybb) cell clusters. A prominent subset of rat invasive trophoblast cell transcripts is conserved in the invasive extravillous trophoblast cell lineage of first trimester human placenta (e.g. lgf2, Cdkn1c, Tfpi, Ascl2, Mmp12, Cited2, etc). Nuclei were also isolated from the single cell preparations of the uterineplacental interface, libraries prepared, and sequenced. Analysis with the Cellranger-ATAC pipeline identified unique clusters based on chromatin accessibility, including invasive trophoblast, endothelial cell, vascular smooth muscle, natural killer cell, and macrophage clusters. ASCL2, AP1, TFAP2C, and ATF1 DNA binding motifs were most abundant in accessible regions of the invasive trophoblast cell clusters. These findings provide a foundational dataset to identify and interrogate key conserved regulatory mechanisms essential for development and function of an important compartment within the hemochorial placentation site that is essential for a healthy pregnancy.

(Supported by HD020676, HD096083, HD099638; Pew Charitable Trust, Sosland Foundation)

Abstract # 1788

Chlamydia Infects The Ovary, Elicits An Immune Response And Depletes The Ovarian Reserve In Mice. Urooza Sarma, Monash University, Australia

Chlamydia trachomatis is the most common sexually transmitted infection worldwide and can cause severe damage to the Fallopian tubes, often resulting in complete infertility. Recent studies indicate significantly increased miscarriage rates and time to natural conception, along with poor IVF outcomes in women seropositive for Chlamydia but in the absence of tubal pathology, suggesting that that fertility may be compromised by mechanisms that extend beyond fallopian tube scarring. In this study, we used a well-characterised mouse model to investigate the hypothesis that Chlamydia can infect and damage the ovary. Chlamydial DNA was detected in ovaries at 6 and 35 days post infection (pi) using qPCR and inclusion bodies were localised within macrophages in the ovarian stroma using immunofluorescence. Chlamydial infection was associated with an increase in the expression of mRNA for CXCL16 and IFNy, suggesting the induction of a pro-inflammatory immune response within the ovary, which persists at least up to 35 days pi. Significantly greater numbers of immune cells including macrophages, NK cells and CD4+ /CD+ cells in the ovary 35 days pi, suggesting a localised ovarian inflammatory response to chlamydial infection, parallels this. Strikingly, the number of ovarian follicles was significantly reduced 35 days following a single infection compared to uninfected controls (p<0.05, n=4-5 mice/group) and the extent of follicle depletion was greater following a second infection (p<0.05, n=4-5 mice/group). Two infections was also associated with changes to the overall ovarian morphology and increased apoptosis and fibrosis in the ovary (p<0.05, n=5/group), consistent with activation of a prolonged inflammatory response. Collectively, these observations demonstrate that Chlamydia can penetrate the ovary, deplete the ovarian reserve and compromise ovarian function, and suggest that the ovary may act as a potential reservoir of infection. Ovarian follicles are essential for female fertility because they secrete hormones and contain oocytes. Follicles cannot be replaced once lost from the ovary. Thus, our data suggests that damage to the ovary caused by Chlamydia is permanent and may underlie some cases of unexplained infertility and poor IVF outcome in women.

Abstract # 2143

Abnormal Pattern Of Ca2+ Oscillations During Fertilization In Vivo Impairs Offspring Growth Trajectory In The Mouse. Virginia Savy, National Institute of Environmental Health Sciences, USA

During mammalian fertilization, the sperm triggers a series of oscillations in the egg's intracellular Ca2+ concentration ([Ca2+]i), which is the hallmark signal for egg activation. Interestingly, experimental manipulation of [Ca2+]i in vitro during or immediately after fertilization results in alterations in the blastocyst transcriptome, implantation success and offspring health. However, it remains unclear whether the findings reported from in vitro studies recapitulate the complex regulation of in vivo fertilization. Here we tested the hypothesis that, even in the highly specialized environment of the oviduct, appropriate Ca2+ signaling after fertilization is critical for proper preimplantation embryo development and offspring growth. In somatic cells, plasma membrane Ca2+ ATPase (PMCA) pumps are responsible for clearing excess Ca2+ from the cell following Ca2+ release events. We found that in mouse eggs, the most highly expressed PMCA isoform was PMCA1 (encoded by Atb2b1). To generate mouse eggs with abnormally increased [Ca2+]i exposure following fertilization, we conditionally deleted PMCA1 (cKO) in oocytes using the Zp3-cre transgene. As anticipated, in vitro fertilized cKO eggs had a much longer first Ca2+ transient than controls (mean \pm SEM: 11.3 \pm 1.0 min, N=30 vs 3.6 \pm 0.3 min, N=49; p<0.0001); however, the oscillation frequency was similar between groups. Assuming a comparable difference in Ca2+ dynamics between control and cKO eggs during in vivo fertilization, we evaluated the impact of altered Ca2+ signaling following fertilization on offspring growth trajectory. Heterozygous (Atp2b1+/-) offspring from Atb2b1-flox/flox; Cre+ females mated with wild type

males were weighed weekly for 8 weeks. Wild type (Atp2b1+/flox) offspring from Atb2b1-flox/flox females mated to wild type males served as controls. Offspring weigh at birth was similar between groups for both females and males; however, growth trajectory was different between groups by the 1st week of age. On average the experimental males were 14.7% smaller than controls at 8 weeks

(mean weight \pm SEM: 22.9 \pm 0.3 g, N=33 vs 20.4 \pm 0.3 g, N=34, males from 17 litters), whereas females were 5.9% smaller than controls (18.1 \pm 0.2 g, N=29 vs 17.0 \pm 0.2 g, N=30, females from 17 litters). Despite the altered postnatal growth rate, cKO-derived mice had normal glucose and insulin tolerance at 3 months of age. Our findings strongly support the idea that appropriate Ca2+ signaling in the first few hours following fertilization is necessary to ensure appropriate embryo "quality" and offspring health. Given the essential role of Ca2+ signaling for egg activation and embryo development, further research is necessary to decode the link between Ca2+ dynamics and long-term effects on offspring health, to ensure safe clinical practice308ring assisted reproductive procedures.

Abstract # 2186

Genetic Control Of The Uterine-Placental Interface. Ayelen Moreno, University of Kansas Medical Center, USA

The hemochorial placenta is organized into functional compartments that are situated at the uterine and fetal interfaces. At the uterine interface trophoblast cells migrate into the uterus where they effectively transform the uterine vasculature and facilitate the delivery of maternal nutrients into the placenta. An essential transport/barrier function for maternal nutrient delivery to the fetus is provided by trophoblast cells interacting with the fetal vasculature at the fetal interface. In contrast to the mouse, the uterine-placental interface is well developed in the rat and human. Trophoblast cells with invasive properties, arise from the junctional zone in the rat and a homologous structure in the human placentation site termed the extravillous trophoblast column, and migrate deep into the uterus. Thus, development of the junctional zone and the extravillous trophoblast column are vital to establishing the uterine-placental interface. Some insights into junctional zone development have arisen from mutagenesis of Plac1 and Phlda2 loci in the mouse. However, the mouse has limitations for investigating the uterine-placental interface. Consequently, in this study we examine the biology of PLAC1 and PHLDA2 in the rat. Plac1 and PhIda2 are differentially expressed in compartments of the placentation site over the course of gestation. To study the impact of PLAC1 and PHLDA2 on the uterine-placental interface we generated global loss-of-function rat models using CRISPR/Cas9 genome editing. Exon 3 of the Plac1 gene and Exon 1 of the PhIda2 gene were independently targeted in separate experiments. CRISPR/Cas9 reagents were electroporated into embryonic day 0.5 rat zygotes. Zygotes were then transferred into the oviducts of pseudopregnant female rats. Offspring were screened by PCR and mutations confirmed by genomic DNA sequencing. A mutant Plac1 rat founder was generated with a 469 bp deletion that removed >95% of the Plac1 coding sequence and a mutant PhIda2 rat founder was produced containing a 103 bp deletion in Exon 1 resulting in a frameshift and a premature stop codon. Both mutations were effectively transmitted through the germline. Plac1 is an X-chromosome linked gene and PhIda2 is situated on Chromosome 1 and is paternally imprinted. Deficits in either gene did not affect postnatal survival; however, disruptions in Plac1 and Phlda2 did affect placental development. Plac1 null or inheritance of the maternal Plac1 mutant allele yielded placentomegaly. Specifically, the enlarged placenta was characterized by an expanded junctional zone, an irregular junctional zone-labyrinth zone boundary, and a compromised uterine-placental interface. Intrauterine interstitial invasive

trophoblast cell migration was severely attenuated in Plac1 mutants. In summary, our experimentation confirms the involvement of PLAC1 and PHLDA2 in hemochorial placenta development and provides a new set of tools for investigating the roles of PLAC1 and PHLDA2 in an important model of deep placentation. PLAC1 and PHLDA2 represent important entry points into molecular pathways controlling development of the uterine-placental interface. (Supported by an ADA fellowship to JN, AHA fellowships to MM and KK, NIH grants HD020676; HD079363, HD099638, and the Sosland Foundation)

Abstract # 2197

Induced Pluripotent Stem Cell Gene-Editing Therapy In An Infertile Mouse Model To Restore In Vivo Spermatogenesis. Amanda Colvin Zielen, University of Pittsburgh, USA

Approximately 1% of men in the general population have azoospermia where sperm is absent from their ejaculate. Non-obstructive azoospermia (NOA) is more common (~85%) than obstructive azoospermia; 15% of NOA patients also have a maturation arrest phenotype (NOA-MA) where germ cells are present in the testes but fail to complete spermatogenesis, likely due to a genetic defect. Sperm recovery rates from men with NOA-MA are relatively low, severely limiting their options for having biological children. We hypothesized that if a single gene mutation is identified to cause NOA-MA in a patient, then ex vivo geneediting of germ cells will restore gene function and in vivo transplantation of gene-corrected germ cells will regenerate spermatogenesis in infertile males. To test our hypothesis, we used CRISPR/Cas9 gene-editing to produce mice with an 11 base-pair deletion in the minichromsome maintenance 8 (Mcm8) gene at a location analogous to one of our Pittsburgh patients. Mutations in MCM8 are associated with male and female infertility as well as DNA damage/repair defects and cancer in clinical and murine studies. Mcm8-11/-11 mice exhibited an NOA-MA infertility phenotype. Homozygous Mcm8(-11) male mice were unable to sire offspring when paired with wildtype females, while heterozygous Mcm8+/-11 mice sired 3.6±0.13 litters in five months with 7±0.8 pups per litter. Compared with normal littermate controls, Mcm8-11/-11 testes were significantly reduced in size (Mcm8+/+ 115±4.9mg per testis, n=10; Mcm8+/-11 were 108±4.3 mg, n=20; Mcm8-11/-11 were 20.2±1mg, n=7). No sperm were recovered from the tail of the epididymis of Mcm8-11/-11 mice, and there was not a significant difference (p=0.25, t-test) in sperm counts (Mcm8+/+ 8.9±1.4 x106 sperm; $Mcm8+/-11 6.6\pm 1.0 \times 106$ sperm) of wildtype and heterozygous mice. Hematoxylin and eosin staining of eight-week old Mcm8-11/-11 testis sections

showed tubules varying between 0-3 germ cell layers, while heterozygous and wildtype sections had tubules with complete spermatogenesis. Preliminary immunohistochemistry staining identifies undifferentiated spermatogonia (SALL4), differentiating spermatogonia (STRA8), and spermatocytes (SYCP3) in Mcm8-11/-11 testicular sections; we are currently quantifying our results. Attempts to establish spermatogonial stem cell (SSC) lines from these animals for ex vivo gene-editing were not successful. Therefore, we isolated fibroblasts from Mcm8-11/-11 mice and programmed them to become induced pluripotent stem cells (iPSCs). Three novel Mcm8-11/-11 mouse iPSC lines were generated, cloned, and characterized (alkaline phosphatase staining, immunocytochemistry staining with pluripotency markers: OCT-4, SOX-2, NANOG, and SSEA-1; along with teratoma formation and karyotype analyses). A validated Mcm8-11/-11 iPSC clone was gene-edited using CRISPR/Cas9 and an oligonucleotide template containing the wildtype Mcm8 sequence. We identified four clones with one Mcm8 allele corrected back to the wild type (Mcm8+/-11). Gene-edited (Mcm8+/-11) clone 14 was differentiated to primordial germ-cell-like cells (PGCLCs) that exhibited a SSEA1+/CD61+ phenotype. FACS sorted, gene-edited PGCLCs were transplanted into four 5week old W/Wv mice. Breeding trials are ongoing. This work was supported by NIH grants P50 HD096723 to KEO, T32 HD087194 to ACZ, and the Magee-Womens Foundation.

Abstract # 2125

Maternal Western Diet Consumption Alters Placental Lipid Composition and Apolipoprotein Gene Expression. Katie L. Bidne, University of Nebraska – Lincoln, USA

Approximately 1% of men in the general population have azoospermia where sperm is absent from their ejaculate. Non-obstructive azoospermia (NOA) is more common (~85%) than obstructive azoospermia; 15% of NOA patients also have a maturation arrest phenotype (NOA-MA) where germ cells are present in the testes but fail to complete spermatogenesis, likely due to a genetic defect. Sperm recovery rates from men with NOA-MA are relatively low, severely limiting their options for having biological children. We hypothesized that if a single gene mutation is identified to cause NOA-MA in a patient, then ex vivo geneediting of germ cells will restore gene function and in vivo transplantation of gene-corrected germ cells will regenerate spermatogenesis in infertile males. To test our hypothesis, we used CRISPR/Cas9 gene-editing to produce mice with an 11 base-pair deletion in the minichromsome maintenance 8 (Mcm8) gene at a

location analogous to one of our Pittsburgh patients. Mutations in MCM8 are associated with male and female infertility as well as DNA damage/repair defects and cancer in clinical and murine studies. Mcm8-11/-11 mice exhibited an NOA-MA infertility phenotype. Homozygous Mcm8(-11) male mice were unable to sire offspring when paired with wildtype females, while heterozygous Mcm8+/-11 mice sired 3.6±0.13 litters in five months with 7±0.8 pups per litter. Compared with normal littermate controls, Mcm8-11/-11 testes were significantly reduced in size (Mcm8+/+ 115±4.9mg per testis, n=10; Mcm8+/-11 were 108±4.3 mg, n=20; Mcm8-11/-11 were 20.2±1mg, n=7). No sperm were recovered from the tail of the epididymis of Mcm8-11/-11 mice, and there was not a significant difference (p=0.25, t-test) in sperm counts (Mcm8+/+ 8.9±1.4 x106 sperm; $Mcm8+/-11 6.6\pm 1.0 \times 106$ sperm) of wildtype and heterozygous mice. Hematoxylin and eosin staining of eight-week old Mcm8-11/-11 testis sections showed tubules varying between 0-3 germ cell layers, while heterozygous and wildtype sections had tubules with complete spermatogenesis. Preliminary immunohistochemistry staining identifies undifferentiated spermatogonia (SALL4), differentiating spermatogonia (STRA8), and spermatocytes (SYCP3) in Mcm8-11/-11 testicular sections; we are currently quantifying our results. Attempts to establish spermatogonial stem cell (SSC) lines from these animals for ex vivo gene-editing were not successful. Therefore, we isolated fibroblasts from Mcm8-11/-11 mice and programmed them to become induced pluripotent stem cells (iPSCs). Three novel Mcm8-11/-11 mouse iPSC lines were generated, cloned, and characterized (alkaline phosphatase staining, immunocytochemistry staining with pluripotency markers: OCT-4, SOX-2, NANOG, and SSEA-1; along with teratoma formation and karyotype analyses). A validated Mcm8-11/-11 iPSC clone was gene-edited using CRISPR/Cas9 and an oligonucleotide template containing the wildtype Mcm8 sequence. We identified four clones with one Mcm8 allele corrected back to the wild type (Mcm8+/-11). Gene-edited (Mcm8+/-11) clone 14 was differentiated to primordial germ-cell-like cells (PGCLCs) that exhibited a SSEA1+/CD61+ phenotype. FACS sorted, gene-edited PGCLCs were transplanted into four 5week old W/Wv mice. Breeding trials are ongoing. This work was supported by NIH grants P50 HD096723 to KEO, T32 HD087194 to ACZ, and the Magee-Womens Foundation.

Abstract # 1918

Regulatory Roles Of Zinc Fluxes In Early Murine Ovarian Follicle Development. Yu-Ying Chen, Northwestern University, USA

Zinc, an enzyme cofactor that can also be stored as a divalent ion in cellular vesicles, is emerging as an important mediator of signaling pathways. Zinc mediates cell signaling by acting both as a diffusible ionic signal, similar to calcium ions, and as a covalent modification of select proteins, similar to phosphorylation. Previous studies from our group have shown that a zinc flux, the movement of labile zinc ions (biologically available zinc) across a cell membrane, is required for terminal oocyte maturation, egg-to-zygote transition, and embryonic mitotic divisions. To test the hypothesis that zinc also regulates the development of early-staged ovarian follicles (primordial through secondary), we measured zinc concentration, distribution, expression of zinc transporters, and the effect of exogenous zinc treatment on folliculogenesis using multiple techniques, including X-ray fluorescence microscopy (XFM), radioactive zinc uptake, RNAscope hybridization, and immunofluorescent labelling.

Using XFM, we discovered zinc to be the most abundant transition metal within the oocytes of murine primordial, primary, and secondary staged follicles, and identified that total zinc levels increase throughout follicular development. Upon staining whole follicles for labile intracellular zinc, we observed different zinc concentrations between different primordial oocytes. Furthermore, zinc was located in different subcellular domains between different follicle classes. Specifically, primordial oocytes exhibited localized foci of zinc staining, while oocytes from primary and secondary follicles showed a diffuse staining pattern. We then quantitated zinc uptake into ovarian follicles using an in vitro radioactive zinc isotope assay. Zinc uptake per primordial follicle was statistically lower than primary follicles (60 million atoms vs. 4 billion atoms respectively) over a one-hour time period. To identify the transporters that mediate zinc uptake, we performed real-time PCR and RNAscope hybridization on isolated follicles and on ovarian tissue sections. We identified several zinc transporters that increase gene expression during folliculogenesis, including zinc importers ZIP1, ZIP6, ZIP10, and zinc exporters ZnT3, ZnT4, ZnT5. These results demonstrate that zinc is dynamically regulated during early follicle development.

Finally, to determine whether zinc plays an instructive role on folliculogenesis, we performed exogenous treatment of zinc on neonatal mouse ovaries in an ex vivo model. We observed that zinc treatment increased markers of follicle

progression, including cell proliferation, p-AKT expression, FOXO3a nuclear exclusion, and oocyte growth in primordial follicles. In light of these observations, we are currently examining whether in vivo zinc fluxes actively regulate early folliculogenesis. Taken together, this study has defined the major zinc physiological dynamics of early-staged follicles and postulated zinc regulation to be a novel and incompletely understood mechanism for instructing early folliculogenesis. This research is supported by R01 GM116848 National Institute of General Medical Sciences (NIGMS) and the Thomas J. Watkins Endowment.

Abstract # 2038

Global and Site-Specific Changes in Histone Acetylation During Human Placental Trophoblast Differentiation. Gargi Jaju, Western University, Canada

Placental maldevelopment causes highly prevalent pregnancy complications, which are leading causes of sickness and death of mothers and newborn babies. A better understanding of the epigenetic mechanisms that control placental development is needed to improve management and treatment options for these serious pregnancy complications. In human placenta, a syncytialized trophoblast (syncytiotrophoblast) layer forms the primary interface between maternal and fetal blood. It performs essential functions to support fetal growth and pregnancy success, including transfer of nutrients and gases between maternal and fetal blood, and production of hormones vital for pregnancy. Syncytiotrophoblast is formed by differentiation and fusion of underlying progenitor cells called cytotrophoblasts. Proper cytotrophoblast differentiation is crucial to maintain the integrity of the syncytiotrophoblast layer throughout pregnancy. Differentiation of cytotrophoblasts into syncytiotrophoblast requires precise changes in gene expression, which is mediated, in part, by regulating acetylation of lysine residues on core histone tails. In turn, changes in histone acetylation are controlled by the actions of histone acetyltransferases and histone deacetylases (HDACs). The goal of this study was to characterize histone acetylation changes during cytotrophoblast differentiation and determine the importance of specific HDACs for this process. Human cytotrophoblasts, which spontaneously form syncytiotrophoblast in culture, and BeWo cytotrophoblast-like cells, which can be induced to differentiate into syncytiotrophoblast by exposure to cyclic adenosine monophosphate (cAMP) analogs, were used to assess expression of various acetylated histone proteins during cytotrophoblast differentiation. Using western blotting, we found that differentiation of primary cytotrophoblasts and BeWo cytotrophoblasts was associated with a global decrease in acetylation of

various histones (H3K9Ac, H3K14Ac, H3K27Ac, H3K18Ac, H2BK5). Chromatin immunoprecipitation-sequencing (ChIP-seq) revealed chromosomal regions that exhibit dynamic alterations in histone H3 acetylation during BeWo cytotrophoblast differentiation. These include regions containing genes classically associated with cytotrophoblast differentiation (TEAD4, TP63, OVOL1, CGB), as well as near genes with novel regulatory roles in trophoblast development and function, such as LHX4 and SYDE1. To identify specific HDACs required for cytotrophoblast differentiation, BeWo cytotrophoblasts were induced to differentiate in the presence of various selective HDAC inhibitors: FK228 (inhibits HDAC1/2), MS275 (inhibits HDAC1/3), LMK235 (inhibits HDAC4/5), BRD4354 (inhibits HDAC5/9), CAY10683 (inhibits HDAC2/6), or RGFP966 (inhibits HDAC3); and then immunofluorescence for E-cadherin and chorionic gonadotropin was used to quantify fused cells. The only HDAC inhibitor that inhibited cytotrophoblast differentiation was the HDAC1/HDAC2 inhibitor FK228 (71% decrease, N=3, P<0.05). FK228 also prevented the differentiationassociated increase in ERVW-1 (66.9%), ERVFRD-1 (82.6%), OVOL1 (68.6%) CGB (51.9%), and HSD11B2 (73.9%; N=4, all P<0.05), as determined by quantitative RT-PCR. BeWo cytotrophoblasts efficiently differentiated following shRNA-mediated knockdown of either HDAC1 or HDAC2, but knockdown of both HDAC1 and HDAC2 abrogated cytotrophoblast differentiation (68% decreased compared to controls, N=6, P<0.05), indicating that HDAC1 and HDAC2 may have compensatory or redundant roles in promoting cytotrophoblast differentiation. Our results show that cytotrophoblast differentiation is associated with dynamic global and site-specific changes in histone acetylation, and that both HDAC1 and HDAC2 are critical for this process. These findings reveal new insights into epigenetic mechanisms underlying cytotrophoblast fusion during human placental development.

USDA-NIFA-AFRI Merit Award

Abstract # 2239

Gene Regulation by LIN28-let-7 miRNA Axis in Sheep Trophoblast Cells. Asghar Ali, Colorado State University, USA

Normal placental development is critical for fetal and maternal health in both humans and animals. Reduced conceptus elongation is a major cause of embryonic mortality and reduced fertility in domestic ruminants. Trophoblast proliferation is critical for successful placentation and establishment of pregnancy, therefore, there is a need to better understand the molecular mechanisms that regulate trophoblast proliferation. LIN28 is an RNA binding protein and has two paralogs, LIN28A and LIN28B. Its major function is to repress let-7 miRNAs biogenesis. Let-7 miRNAs are markers of cell differentiation and high let-7 levels reduce cell proliferation. We previously reported that LIN28A and LIN28B were significantly lower and let-7 miRNAs were significantly higher in term human IUGR vs normal placenta. LIN28A and LIN28B double knockout in human first trimester trophoblast (ACH-3P) cells led to a significant increase in let-7 miRNAs, significantly decreased expression of proliferation-associated genes including ARID3A, ARID3B, HMGA1, c-MYC, VEGF-A and WNT1 and significantly reduced cell proliferation. ARID3A, ARID3B and KDM4C make a triprotein complex (the ARID3B-complex) which binds to promoter regions of HMGA1, c-MYC, VEGF-A and WNT1. ARID3B knockout in ACH-3P cells disrupted the ARID3B-complex leading to a significant decrease in these proteins and cell proliferation. In this study we hypothesized that LIN28- let-7 axis regulates proliferation of ovine trophoblast cells in vivo by targeting proliferationassociated genes. To test this hypothesis, day 9 hatched sheep blastocysts were incubated with lentiviral particles to deliver shRNA targeting LIN28A or LIN28B specifically to trophectoderm (TE). At day 16, conceptus elongation was significantly reduced in LIN28A and LIN28B knockdown conceptuses compared to control, suggesting reduced proliferation of trophoblast cells. Let-7 miRNAs were significantly increased and proliferation-associated proteins IGF2BP1-3, HMGA1, ARID3B and c-MYC were significantly decreased in trophectoderm from knockdown conceptuses compared to control. This suggests that the LIN28- let-7 axis regulates proliferation of sheep trophoblast cells by targeting proliferation-associated genes. To further test this hypothesis, ovine trophoblast (OTR) cells were derived from day 16 trophectoderm. Surprisingly, after only a few passages LIN28 was significantly reduced and let-7 miRNAs significantly increased compared to day 16 TE suggesting that passaged OTR cells represent a more differentiated phenotype of trophoblast cells. To create an OTR cell line more similar to day 16 trophectoderm we overexpressed LIN28A and LIN28B,

which significantly decreased let-7 miRNAs, significantly increased IGF2BP1-3, HMGA1, ARID3B and c-MYC and significantly increased cell proliferation. These results suggest that reduced LIN28 during early placental development may decrease trophoblast proliferation at a critical period for successful establishment of pregnancy. This project was supported by Agriculture and Food Research Initiative Competitive Grant no. 2017-67015-26460 from the USDA National Institute of Food and Agriculture.

Abstract # 2207

Effect Of Bovine Trophoblast Cell Derived Extracellular Vesicles On Gene Expression Profiles Of Immune Cells. Ana C. Silva, Utah State University, USA

Placenta-derived extracellular vesicles (EVs) play a role in the communication between the placenta and maternal immune cells possibly leading to regulation of maternal T-cell signaling components. An abnormal maternal tolerance towards the conceptus has been associated to clinical conditions such as implantation failure and recurrent pregnancy loss. The specific mechanisms by which this tolerance is acquired remain unclear. The hypothesis of this study was that trophoblast-derived EVs modulate gene expression of immune cells. Ten placentas were collected at a local abattoir and enzymatically digested. Isolated trophoblast cells were cultured for approximately 10 days with their supernatants being collected every 72 hours. Extracellular vesicles were isolated by differential centrifugation and characterized by scanning electron microscopy, dynamic light scattering and Raman spectroscopy. Scanning electron microscopy and dynamic light scattering analysis confirmed the isolation of EVs. Raman spectroscopy demonstrated that trophoblast-derived EVs have a unique biochemical fingerprint compared with peripheral blood mononuclear cell-derived EVs. Peripheral blood mononuclear cells were collected from non-pregnant lactating Holstein cows. The following leukocyte populations were stained with monoclonal antibodies and sorted by flow cytometry: CD4 + CD25 + T lymphocytes, CD4 + CD25 - T lymphocytes, CD8 + T lymphocytes, gamma delta T cells, and macrophages. The isolated placental EVs were then, added on the culture of CD4 + CD25 + T lymphocytes, CD4 + CD25 - T lymphocytes, CD8 + T lymphocytes, gamma delta T cells, and macrophages for 48 hours. In order to identify the genes modulated by trophoblast-derived EVs, gene expression of immune cells cultured with and without trophoblast EVs was assessed by microfluidic chip real time RT-PCR. Messenger RNA expression data were analyzed by the Delta Delta Ct method using the average of the housekeeping genes GAPDH and ACTB for normalization using the Fluidigm Real-Time PCR Analysis Software. These experiments were replicated three times using immune cells from three different non-pregnant cows at similar stages of lactation. Gene expression data were analyzed by the mixed procedure of SAS as a randomized block design, where cow is the block, the experimental unit is the cell culture well (n=12). A strong effect of trophoblast-derived EVs on the gene expression profiles of immune cells was detected. The different immune cell populations analyzed responded differently to trophoblast EVs. Both CD4 + CD25 + and CD4 + CD25 - T cell populations had the greatest numbers of significantly regulated transcripts for GMCSF, GATA3, FOXP3, CD28, IL10, TNF among others. Treatment with trophoblast-derived EVs also caused the modulation of C D28, FOXP3 and GATA3 in CD8 + cells, while EVs changed the expression profiles of interleukin (IL) 17, IL13, IL12 and IL6 in macrophages. In conclusion, the overall gene expression profile indicates that trophoblast-derived EVs regulate immune cell activity.

Abstract # 2198

MiR-1246 Is The Most Abundant Mirna In Luteal Extracellular Vesicles And It Regulates T Cell Transcripts Associated With Their Activation. Martyna Lupicka, Pennsylvania State University, USA

Extracellular vesicles (EV) are cup-shaped, membranous structures that contain specific cargo used for cell-to-cell communication. Previously, we showed that bovine luteal EV regulate cytokine production in monocytes and T cells. We also characterized miRNA cargo of luteal EV using Next Generation Sequencing (NGS), and it revealed that miR-1246 was the most abundant miRNA regardless of the functional status of the corpus luteum (CL). Ingenuity Pathway Analysis (IPA) of 2377 predicted miR-1246 targets (determined with TargetScan algorithm) showed potential regulation of mRNA associated with NF-KB signaling and proliferation (p<0.05). Therefore, we hypothesized that miR-1246 affects T cell activation. To determine real targets of miR-1246 in bovine T cells, a miRNA pull-down assay was performed. Biotin-labeled miR-1246 mimic was transfected into cultured bovine peripheral blood T cells (n=6). Cells were then treated with PMA (phorbol 12-myristate-13-acetate) and ionomycin to increase expression of genes associated with cell activation. After treatment, miR-1246, together with its bound targets, were isolated using streptavidin-coated beads. Pulled-down targets were sequenced using NGS. Overall, the analysis revealed 37 transcripts that were different (P<0.05) or tended to be different (P<0.08) from negative control pull-down, among which 7 were also predicted miR-1246 targets. Among these identified transcripts, genes associated with cell cycle, such as

cAMP regulated phosphoprotein 19 (ARPP19), cell division cycle 27 protein (CDC27) and PWWP domain containing 2A protein (PWWP2A), and genes associated with NFKB signaling, such as nuclear receptor coactivator 3 (NCOA3) were identified. Pathway analysis of pulled-down targets showed involvement of these transcripts in pathways associated with RXR activation, which among other functions also induces cell cycle progression and proliferation. To further test the hypothesis, cell cycle progression was measured in activated T cells transfected with miR-1246 mimics (n=2). After transfection with mimic, 8% of cells progressed to S or G2/M phase, whereas, cell cycle progression occurred in 12% of control cells. In summary, miR-1246 that is shuttled via luteal EV may regulate T cell activation in the CL through inhibition of translation of mRNA associated with cell cycle regulation. In our previous studies, luteal EV induced increased production of proinflammatory cytokines by T cells, but luteal cell-induced proliferation is limited, perhaps, because miR-1246 controls cell cycle progression and resident T cell survival during their activation. This project was supported by Agriculture and Food Research Initiative Competitive Grant no. 2016-67015-24900 from the USDA National Institute of Food and Agriculture.

Abstract # 1931

Porcine Conceptuses Utilize the Polyol Pathway and Fructose-Driven Glycolysis (Fructolysis) to Support Development during the Peri-Implantation Period of Pregnancy. Avery C. Kramer, Texas A&M University, USA

During the peri-implantation period of gestation, porcine conceptuses (embryo and associated placental membranes) undergo elongation, a process requiring extensive cell proliferation and migration, and nutrients to support these events. The hexose sugars, glucose and fructose are present in the porcine conceptus and endometrium, with fructose being the most abundant hexose sugar. Our preliminary studies suggest that in response to hypoxia, the endometrium of pigs transports alucose into the uterine lumen where the conceptus trophectoderm (Tr) directs the majority of glucose carbons away from the TCA cycle and into aerobic glycolysis for use in the pentose phosphate pathway, one-carbon metabolism, and the hexosamine biosynthetic pathway to fulfill the metabolic demands for cell proliferation. This enhanced glycolytic metabolism to form lactate deprives the environment of sufficient amounts of pyruvate to support the TCA cycle. In response, Tr cells perform glutaminolysis that converts glutamine into a-ketoglutarate (a-KG), a TCA cycle intermediate, to maintain TCA cycle flux. A result of an active TCA cycle is the generation of ATP and citrate that inhibits a glycolytic enzyme phosphofructokinase (PFK) and,

therefore, inhibits continued glycolysis. This inhibition can be circumvented via activation of the polyol pathway to synthesize fructose from glucose. Fructolysis, which refers to the partial catabolism of fructose to pyruvate, lactate and ribose, can then continue to provide the glycolytic intermediates required for conceptus elongation. Therefore, we collected porcine conceptus tissues on Days 11, 13, 15, and 16 of pregnancy and performed real-time PCR, Western blot, and immunohistochemistry to determine expression of enzymes required for the polyol pathway and fructose-driven glycolysis. We also collected elongating conceptus tissues from Days 14 and 16 of pregnancy, incubated these tissues with 14C-fructose, and measured the 14CO2 released from the conceptuses to determine if porcine conceptuses directly metabolize fructose. Results demonstrated that the Tr of Day 15 conceptuses: 1) expresses aldose reductase (AKR1B1) and sorbitol dehydrogenase (SORD), enzymes required for the polyol pathway, suggesting active conversion of alucose to fructose; 2) expresses ketohexokinase (KHK), an enzyme required for fructolysis; and 3) metabolize fructose as they elongate, indicating that conceptus Tr can utilize fructolysis during the peri-implantation period. Our results demonstrate that the Tr of porcine conceptuses: 1) utilizes the polyol pathway to convert glucose into fructose; 2) directly metabolizes fructose; and 3) utilizes fructolysis to maintain pyruvate and ribose fluxes in an environment lacking active PFK. This project was supported by Agriculture and Food Research Initiative Competitive Grant no. 2018-67015-28093 from the USDA National Institute of Food and Agriculture.

Abstract # 1839

Single-Cell RNA-Seq Reveals The Diversity Of Trophoblast Subtypes And Patterns Of Differentiation In The Bovine Placenta. Eleanore V. O'Neil, University of Missouri-Columbia, USA

Establishment of pregnancy in cattle involves growth and elongation of the mononuclear trophoblast cells (MTC) that secrete interferon tau (IFNT) for pregnancy recognition on day 15, which is followed by differentiation of trophoblast giant binucleate cells (BNC) beginning on day 17 and placentation. By day 60, the bovine placenta contains vascularized placentomes formed by interdigitation of cotyledons with caruncles of the endometrium. The chorion of the cotyledonary villi contain MTC and multinucleated syncytia, which are formed by partial fusion of the LE and BNC and are supported by fetal stromal cells. Current evidence supports the hypothesis that pregnancy loss during the first month in cattle is caused by inadequate placental development. However, little is known about trophoblast differentiation and placentation in cattle.

Heifers were bred and collected on days 17, 24, 30, and 50 of gestation (n = 3-4 heifers per day). The chorioallantois was carefully removed and gently digested with enzymes (0.125% trypsin, 0.05% type IV collagenase, and 0.04% DNAse in DMEM/F12 medium) to isolate trophoblast cells. Single cells were subjected to analysis using 10x Genomics platform and sequenced (scRNA-seq). Bases with high quality (Q > 30) were estimated to be 97% of the unique molecular identity counts. After data filtration, 56,657 single cells were assigned to 22 clusters by shared nearest neighbor and t-distributed stochastic neighbor embedding (t-SNE) methods across the four timepoints. Gene expression of cell markers was used to identify cell clusters as trophoblast cells, stromal cells, BNC, blood cells, and macrophages. Interestingly, the proportion of cell identities changed across the timepoints. On days 17, 30, and 50, approximately half or more of the cells were trophoblast cells, while 72% of the day 24 placenta cells had a stromal cell identity, as indicated by their expression of vimentin (VIM), and extracellular matrix proteins including collagens, actins, and tubulins. On days 17 and 24, IFNT2 and IFNT3 was abundant in MTC, but negligible in day 30 and 50 placentae. The BNC populations, identified by expression of the marker gene chorionic somatomammotropin hormone 2 (CSH2), accounted for only 3% of the cells on day 17 but increased to 17% by day 50. Several pregnancyassociated glycoproteins (PAG) were expressed and showed differential expression in MTC and BNC. For example, PAG7 was almost exclusively expressed in BNC across all four days. Macrophages, demarcated by expression of cluster of differentiation (CD) CD14 and CD68, were almost absent on days 17 and 24 (< 0.5% total cells), but made up 3% of the cells in day 30 and 50 placentae. These results document bovine placental trophoblast differentiation at single-cell resolution and advance our understanding of bovine placentation during the establishment of pregnancy. Supported by USDA National Institute of Food and Agriculture grants 2016-67015-24741 and 2019-67015-28998.

Abstract # 1922

Unraveling The Landscape Of Mitochondrial Mtdna Methylation In Bovine Oocytes And Embryos. Camila B. de Lima, Université Laval, Canada

In several mammalian species, accumulation of thousands of mitochondria during oocyte maturation represents an investment of the cell, as it will be able to better support ATP demand until mitochondria replication is reinitiated at morulae stage. The production of ATP occurs essentially through oxidative phosphorylation, which is dependent on mitochondrial DNA. Recently, mtDNA has gained more attention as changes in its structure and sequence were associated with mitochondrial dysfunction and thereby the pathogenesis of metabolic diseases. With the improvement of detection techniques, recent studies proposed that mtDNA is subjected to cytosine methylation, which can influence mitochondrial gene expression and function. Given the relevance of mitochondria for oocyte maturation and formation of the embryo, it is important to comprehend the mtDNA epigenetic dynamics and distribution. For this purpose, GV-stage oocytes were collected from abattoir ovaries or from OPU, and then matured, fertilized and cultured in vitro up to blastocyst stage (Day 7). Methylation profile of mtDNA was characterized by WGBS. Transcription profile was obtained from RNA-Seq data (GEO Series GSE52415). Statistical analysis considered a=5%. Global methylation level of OPU-oocytes is lower when compared to abattoir occytes (10.09 vs. 16.04%; p<0.000), and this is reflected in the total methylation of derived blastocysts (20.04 vs. 23.55%, respectively; p<0.000). In terms of distribution, the highest methylation levels were found in the regions coding for respiratory chain enzymes (ND1, ND2, ND3, ND4, ND5 and ND6) and ATPases (ATP8 and ATP6) of blastocysts, especially those derived from OPU-oocytes. Further investigation revealed that total methylation level is negatively correlated with expression of mitochondrial genes in OPU samples (r= -0,71 and -0.73; oocytes and blastocysts, respectively), but this strong correlation was not maintained in vitro (r = -0.31 and -0.21, respectively). Average methylation level was also significantly increased in the light strand in all gene regions comparing to the heavy strand of mtDNA, but surprisingly, there was little strand-specific correlation with gene expression in all groups, indicating that methylation of both strands together may be essential for transcriptional machinery recognition and control. These results reinforce the existence of a specific epigenetic regulation of mitochondrial function. With a less methylated mtDNA, oocytes can better support mitochondrial biogenesis during maturation and energy demand postfertilization. On the other hand, although blastocysts have a high energy demand, ATP can be obtained from other sources, allowing for a more restrictive regulation of mitochondrial genes. The high correlation observed between methylation and transcription in OPU oocytes and the derived blastocysts is a guite unique phenomenon, but the loss of such correlation observed in abattoir samples indicates a possible dysregulation in the maturation of mitochondria during maternal-embryo transition. Finally, the comprehension of the profound interaction between mitoepigenetics and metabolism can provide a whole new set of metabolic tools for the improvement of existing culture systems and biomarkers for metabolic diseases.

Effects of Prenatal and Postnatal Nutrition on Neuropeptide Y Neuronal Projections to Kisspeptin Neurons in the Arcuate Nucleus of Beef Heifers. Sarah M. West, Texas A&M University, USA

Early life nutrition modulates the development of hypothalamic neurocircuitries controlling GnRH secretion, thus programming puberty in female mammals. Neuropeptide Y (NPY) is an orexigenic peptide involved in the metabolic control of reproduction. The inhibitory effects of NPY on GnRH secretion are mediated directly and indirectly via neurons expressing kisspeptin, a potent GnRH stimulator. Morphological changes in the NPY neurocircuitry can delay puberty and have long-term detrimental effects on reproduction. Therefore, it is critical to understand the effects of early life nutrition on the development and plasticity of the hypothalamic NPY system. Using the bovine model, objectives herein were to test the hypothesis that either maternal obesity or undernutrition during late gestation, in combination with a high or low rate of body weight (BW) gain in heifer offspring during the juvenile period, alters: 1) the expression of kisspeptin neurons in the arcuate nucleus (ARC), and 2) the magnitude of NPY neuronal projections to kisspeptin neurons. Brangus cows (n = 36) bearing female pregnancies were fed to achieve thin (L, n = 12), moderate (M, n = 12), or obese (H, n = 12) body condition (BC) by ~6 mo (second trimester) of gestation and maintained at the target BC until calving. Heifer offspring from each group were then weaned at ~3.5 mo of age and assigned randomly to be fed to achieve a low (L; 0.5 kg/d) or a high rate of BW gain (H; 1 kg/d) until 8 mo of age. This 3×2 factorial design created six combinations of maternal-postnatal nutritional treatments (LL, LH, ML, MH, HL, and HH). At ~14 mo of age, heifers were euthanized and hypothalamic tissue was dissected and processed for double-label immunofluorescence to determine the extent of NPY projections toward kisspeptin neurons. While maternal overnutrition did not impact NPY inputs to kisspeptin neurons, maternal undernutrition reduced (P<0.05) the percentage of kisspeptin neurons highly innervated $(-\geq 7 \text{ close appositions})$ by NPY projections in the heifer offspring compared to maternal M and H diets. When combining the effects of maternal and postnatal nutrition, the percentage of kisspeptin neurons highly innervated by NPY fibers was decreased in LH heifers compared to MH (P<0.05) and HH heifers (P=0.09). Moreover, reduced postnatal nutrition resulted in a trend (P=0.1) for a higher percentage of kisspeptin cells receiving NPY contact in the caudal region of the ARC. Preliminary analysis indicates that gestational undernutrition, when combined with adequate postnatal nutrition (LH heifers), results in diminished NPY (inhibitory) inputs to kisspeptin neurons in the ARC. This likely represents a

compensatory response during postnatal development to counter the effects of undernutrition in utero and to allow for the pubertal increase in GnRH pulsatile secretion. This premise is supported by the observation that LH heifers attain puberty at a similar age as MH (control) heifers. Additionally, our findings demonstrate that reduced nutrition during juvenile development increases NPY inputs to kisspeptin cells in the caudal ARC, which likely contributes to the wellestablished effects of postnatal undernutrition delaying puberty in heifers.

Abstract # 2127

Lipids Involved In Pro And Anti-Inflammatory Responses Are Altered In Follicular Fluid And Plasma Of Cows Administered A Low Dose FSH Treatment And May Be Used As Markers Of Ovulation In Beef Cows. Alexandria P. Snider, University of Nebraska-Lincoln, USA

Superovulation procedures using Follicle Stimulating Hormone (FSH) in cattle promote development of a larger cohort of follicles to increase number of oocytes collected for assisted reproductive technologies. These procedures are used if there are problems associated with ovulation since anovulation is a major factor affecting female fertility. Ovulation has been demonstrated to be an inflammatory process. Thus, our hypothesis was that treatment of cows with a low-dose-FSH protocol (35 IU FSH every 12 hours for 3.5 days plus prostaglandin at last and 12 hours after last FSH; FSHLow) would increase follicular fluid (FF) proinflammatory lipid markers compared to unstimulated controls; and blood plasma lipid markers compared to early or late luteal phase unstimulated controls. Follicular fluid from unstimulated samples was collected prior to and 24 hours after FSHLow. Blood plasma was collected from the same unstimulated cows (n=11) at D7-early luteal control, D15-late luteal control and 24 hours after FSHLow. Lipid compounds (863) were identified via UPLC-MS Analysis (CSH PhenylHexyl method) with 124 lipid compounds annotated utilizing XCMS software package in R. Analysis of variance (AOV) function was used for each lipid compound and p-values were adjusted using the Bonferroni-Hochberg method (p.adjust function) to determine differences in FF and plasma samples in non-stimulated controls and FSHLow-stimulated cows. There were 29 annotated lipid compounds different (p<0.05) in FF. Seventeen are involved in anti-inflammatory responses with ten of them decreased (p<0.05; e.g. HODE cholesteryl ester, C18-02:0 PC) FSHLow compared to control cows. Twelve of the 29 lipids are associated with pro-inflammatory responses with six of them increased (p<0.05) in FSHLow compared to Controls. Of these six lipids, LysoPC(20:4) and Glycerophosphocholine are involved in cytokine signaling;

PE(P-36:2) and SM(d18:1/16:0) stimulate macrophage recruitment; Docosahexaenoyl PAF C-16 stimulates leukocyte localization; and Sodium Glycochenodeoxycholate increases signaling through the NFKB pathway (p<0.05). In blood plasma, 16 lipid markers associated with anti-inflammatory and 16 associated with pro-inflammatory responses were altered in cows after FSHLow compared to Day 7 and 15 controls. A greater number of lipid markers associated with anti-inflammatory response were decreased (13; p<0.05; e.g. Oleamide, CE(15:2)) than increased (7; p<0.05; e.g. PC(38:2), PC(38:1)) in FSHLow compared to D15 controls indicating a shift from anti- to proinflammatory processes. Seven lipids associated with pro-inflammatory response were increased (p<0.05) in plasma after FSHLow compared to D15 controls. These pro-inflammatory lipids are involved with cytokine signaling (LysoPC(18:3) and TGs) and TLR2 receptor function (diacylalycerols). Overall, lipid markers decreased or elevated in FF were found to have a similar profile in blood plasma suggesting that collection of either would be reflective of lipid content in the ovarian follicle or circulating blood plasma. Taken together, these results indicate that FSHLow stimulation increases pro-inflammatory lipids in FF and blood plasma over that of controls and these lipids amplify different aspects of the inflammatory process. Furthermore, these lipid markers could be utilized to better understand females with anovulation or other problems with the ovulatory process resulting in female infertility.

Abstract # 2164

Artificial Intelligence Analysis of the Mammalian Sperm Zinc Signature Predicts Male-factor Subfertility. Karl Kerns, University of Missouri, USA

Analysis of both the U.S swine and bovine herds show variation in pregnancy rate is more attributable to male-factor subfertility and infertility than the dam. To date, a limited degree of correlations is observed between conventional semen analysis parameters and actual fertility after standard quality cutoffs are met. Thus, a clear ability to predict male-factor fertility is lacking. Building on our recent discovery of the sperm zinc efflux on the pathway to fertilization competency present in boar, bull, and human spermatozoa published in Nature Communications (DOI:10.1038/s41467-018-04523-y), we hypothesized in vitro capacitation-induced changes to the sperm zinc signature would be indicative of male-factor sub- and infertility. The ongoing fertility trial currently includes 108 boar ejaculates inseminated to over 1,917 sows in a single, fixed-time artificial insemination setting, with pregnancy results ranging from 56.4% - 96.8%. Each ejaculate underwent in vitro capacitation with 10,000 spermatozoa imaged at

0, 1, and 4 hours utilizing high-throughput, image-based flow cytometry. We calculated over 6,550 bioimage values for each of the time points analyzed. Mutual information analysis found 27 sperm bioimage features with scores greater than 0.1 mutually informative to the pregnancy rate. Linear regression analysis was performed on these features and tested with a nested model. ANOVA of the linear regression model identified four features significant with high fertile males within the nested model and eight features for the full model. Next the data was randomly split (4:1) into training and testing sets and classification trees were calculated to predict the pregnancy rates after being discretized into fertile (above 85% pregnancy rates) and subfertile classes (below 80% pregnancy). One tree was trained with 17 features found in traditional semen analysis related strictly to sperm morphology and computerassisted sperm analysis (CASA) motility outputs, and a separate tree was trained with 170 features related to differences in zinc signature subpopulation changes after in vitro capacitation, significant features found by mutual information analysis, and motility. The traditional semen analysis feature set yielded respective training and testing accuracies of 100% and 53.8%, whereas the later feature set yielded respective training and testing accuracies of 100% and 76.9%. Artificial neural network analysis of zinc, acrosome, and plasma membrane integrity bioimages along with litter size are currently underway. In summary we identified the ability for sperm to transition from a zinc signature 1 and 2 to a capacitated-state signature 3 and 4 along with acrosomal modification and changes to the plasma membrane integrity excels in predictive value of male factor fertility compared to traditional motility and morphology scores alone. Altogether, our findings establish a new paradigm on the role of zinc ions in sperm function and pave the way for accurate sperm biomarker identification of male-factor sub/infertility in future precision agriculture and medicine applications. Supported by the National Institute of Food and Agriculture (NIFA), U.S. Department of Agriculture (USDA) Postdoctoral Fellowship award number 2019-67012-29714 (KK), USDA NIFA grant number 2017-67015-26760 (PS), NIH BD2K Training Grant T32HG009060 (SK), and funding from the MU F21C Program (PS).

Abstract # 2183

BVDV Infection Epigenetically Alters T-Cell Transcription Factors In Persistently Infected Fetal Spleens. Hanah M. Georges, Colorado State University, USA

Maternal infection with Bovine Viral Diarrhea Virus (BVDV) has life-long negative effects on progeny. Despite current preventative measures, BVDV continues to

be an issue, costing the industry \$1.5 billion annually and producing infected calves that remain the primary reservoirs of the virus. If fetal infection occurs prior to day 120 of gestation, then the fetus becomes persistently infected (PI) and sheds the virus throughout its life. The mechanisms of persistent infection and impact on postnatal health is still not well known. Previous in vivo studies revealed a substantial activation of the PI fetal innate immune response 22 days after maternal infection. The innate immune activation was then followed by an attenuation of both the innate and adaptive immune branches 115 days after maternal infection. It was concluded that attenuation of the immune system was caused by a lack of T-cell response in the fetus, resulting in an inability for Tcells and B-cells to mature properly. In this study, it was hypothesized that T-cell activation and signaling genes were epigenetically altered after fetal infection, thus impairing the expression of key genes of the innate and adaptive immune responses Splenic tissue from PI and control fetuses were collected on day 245 of gestation, 170 days post-maternal infection. DNA was isolated and sent to Zymo Research for reduced representation bisulfite sequencing. Methylation sequencing files were aligned to the bovine ARS-UCD-1.2 genome using the Bismark package, then processed and analyzed using the methylKit R package. Differentially methylated regions (DMR) were selected based on a 25% difference in methylation compared to controls as well as a p-value cutoff of < 0.05. Within these parameters, 2,641 regions were differentially methylated: 1,951 hypermethylated and 691 hypomethylated regions. Results revealed hypermethylation of nuclear factor of activated T cells (NFAT) 1 and 4, while NFAT2 was hypomethylated. Calcium signaling components, calcium release activated calcium channel protein ORAI and calmodulin, were hypomethylated. Additionally, signal transducer guanine nucleotide exchange factor VAV1 was hypermethylated. Calcium regulated NFAT family members consist of NFAT 1,2, and 4. The NFAT family is critical in T-cell activation/anergy as well as cardiac development. NFAT 1 and 4 are associated with T helper (Th) 1 cell differentiation, while NFAT 2 is associated with Th2 cell differentiation. Hypermethylation of NFAT 1 and 4 is likely to shift the Th cell differentiation from Th1 to Th2 cells. An increase in NFAT2 and VAV1 expression due to hypomethylation would promote anergy of T-cells, further exacerbating the shift from Th1 to Th2 cells. This shift of Th cells is associated with T-cell receptor hyperreactivity and lymphoproliferative disorder. Additionally, the hypomethylation of ORAI and calmodulin may contribute to the Th2 hyper-reactivity by increasing the amount of calcium transported into a cell upon T-cell activation. The observed epigenetic modification of critical T-cell genes may help explain inability of postnatal PI calves to fight secondary infections efficiently, contributing to performance loss and continued BVDV viral shedding. This work is supported by: USDA AFRI NIFA Predoctoral Fellowship 2019-67011-29539/1019321, 2016-38420-25289 and W3112 Project.

SSR Trainee Travel Award – Continental United States

Abstract # 1833

Phosphate Regulation Pathways are Present in the Ovine Conceptus, Endometrium and Placentome. Claire Stenhouse, Texas A&M University, USA

Phosphate is the most abundant anion in humans comprising approximately 1% of total body weight. Around 80% of phosphate present in the fetal skeleton at the end of gestation crosses the placenta. Phosphate is essential for bone development and growth however, little is known regarding the mechanisms of placental phosphate transport during pregnancy. This study sought to identify phosphate regulatory pathways in the ovine endometrium and placentome throughout gestation. Suffolk ewes were bred with fertile rams upon visual detection of estrus (Day 0). On Days 9, 12, 17, 30, 70, 90, 110 and 125 of pregnancy (n=4-18/Day), ewes were euthanized and hysterectomized. On Days 9, 12 and 17, the lumen of the uterine horns were flushed with PBS to recover conceptuses. On Day 17, conceptus tissue was frozen in liquid nitrogen. On the other days of pregnancy, following separation of the endometrium from the chorioallantois, sections of placentomes and endometria were frozen in liquid nitrogen. Inorganic phosphate was detected spectrophotometrically in allantoic and amniotic fluid, and homogenised placentomes and endometria. The expression of mRNAs for sodium-dependent phosphate transporters (SLC20A1 and SLC20A2) and components of klotho signalling (FGF21, FGF23, FGFR1, KL and KLB) were quantified by qPCR. Klotho proteins are essential for fibroblast growth factor receptor action, with FGF23 as an important phosphaturic hormone. Concentrations of phosphate were greater in placentomes than endometria at Days 30 and 110 (P<0.05). In contrast, concentrations of phosphate in endometria were greater than those in placentae at Day 125 of pregnancy (P<0.001). Endometrial phosphate concentration was lower at Day 30 when compared with both Days 9 and 12 (P<0.05). Phosphate in placentomes was lowest on Day 125 (P<0.001) and total phosphate was greater in allantoic fluid associated with female compared to male fetuses at Day 125 (P<0.05). The expression of all candidate mRNAs was detected in both placentomes and endometria, except for KLB which was only expressed in placentomes. Day 17 conceptuses express SLC20A1, SLC20A2, KLB, and FGFR1 mRNAs. Endometrial expression of FGFR1 (P<0.001) and FGF21 (P<0.05) mRNAs was highest at Day 30, as was expression of KL mRNA (Days 30 and 110) (P<0.001). Stable endometrial expression of FGF23, SLC20A1 and SLC20A2 mRNAs was observed throughout gestation. Expression of KLB (P=0.06) and FGF21 (P<0.05) mRNAs increased in placentomes between Days 110 and 125. Expression of FGF23 mRNA increased with advancing gestational day (P<0.01) in placentomes. Expression of FGFR1 mRNA in placentomes was lowest at Day 90, before increasing to Day 125 (P=0.05) of

pregnancy. In contrast, SLC20A1 mRNA expression peaked at Day 30, before decreasing to Day 110 (P<0.001). These results indicate that phosphate and its transporters have dynamic expression throughout gestation, suggesting an important role for multiple phosphate regulatory pathways throughout gestation. Temporal expression profiles support a role for phosphate in sheep during the peri-implantation period and in later stages of gestation. This research was supported by Agriculture and Food Research Initiative Competitive Grant 2016-67015-24958 from the USDA National Institute of Food and Agriculture.

Abstract # 2065

The Atypical Centriole of Spermatozoa: A Molecular Basis for Basal Sliding and Asymmetric Flagellar Beating. Sushil Khanal, The University of Toledo, USA

Sperm cells have two centrioles, microtubule based sub cellular structure that form centrosomes and cilia. The centrioles are named based on their relative location: the proximal centriole and the distal centriole. We discovered in human and other mammals that the spermatozoon distal centriole (SDC) is remodeled during spermiogenesis to have an atypical structure and it functions in the zygote as expected from a centriole (Fishman et. al., 2018). The SDC in human consists of doublet microtubules splayed outward making a funnel shape structure, instead of triplet microtubules and barrel shaped structure found in the typical centriole. Importantly, the SDC consists of a unique organization of centriole lumen proteins, POC1B, POC5, and CETN1 into two main rod structures, which we refer as SDC rods. The SDC rods flank the microtubule. The mechanistic detail forming the atypical centriole and its role remains an enigma. Recently, we identified a novel SDC rod protein, FAM161A. In vitro, FAM161A binds to microtubules and SDC rod proteins (POC1B and POC5). In the spermatozoon, FAM161A appears to localize between the microtubules and POC1B or POC5, suggesting that FAM161A functions as a linker between the microtubules and rods.

In vivo, FAM161A have a unique localization during spermiogenesis. In the round spermatid stage of human, bovine, and rabbit, centriole remodeling initiates with the enrichment of POC1B, POC5, and CETN1 and their elongation in both proximal and distal centrioles. In the same stage, FAM161A localizes only in a unique plate like structure close to proximal centriole. Later, in the elongated spermatid stage, the FAM161A incorporates into the centrioles. This timing of incorporation suggests that the FAM161A function in centriole remodeling after the rods have already started to form.

In the spermatozoon, the protein organization of the SDC rod has left-right asymmetry. The position of left and right rod has distinct position in straight and curved sperm tail, suggesting that the rods are sliding up and down during flagellar beating. This is the first direct evidence that the asymmetric flagellar beating during sperm movement is accompanied with the centriole internal movement. Altogether, this study gives a novel insight to the sperm atypical centriole formation and suggests that centriole sperm are atypical to allow centriole movement which may control sperm movement. This work is supported by grant HD092700 from Eunice Kennedy Shriver National Institute of Child Health & Human Development (NICHD).

Abstract # 1951

Epididymal Basal Cells Expressing LGR5 Are Multipotent Adult Stem Cells. Laurie Pinel, University of Quebec, Canada

The epididymal epithelium is pseudostratified and comprised of various cell types including principal, clear, narrow and basal cells. Basal cells share common properties of adult stem cells. They can differentiate into principal and clear cells in vivo, form organoids, self-renew, and differentiate in vitro. The characteristics of basal cells support the notion that these serve as a stem cell population residing at the base of the epididymal epithelium. However, there is currently no method to specifically identify epididymal stem cells. The present objective is to identify a specific marker of this population of stem cells in the epididymis. Leucine-rich repeat-containing G-protein coupled receptor 5 (LGR5) is a seven-transmembrane G-coupled receptor. It shares homology with two members of the LGR family, LGR4 and LGR6; all three proteins are receptors for R-Spondin growth factors, which modulate Wnt/Spondin signaling. LGR5 is a well-established marker of adult stem cells in a variety of tissues. We developed epididymal basal cell-derived organoids as a means to investigate epididymal stem cell differentiation. LGR5 was overexpressed in isolated basal cells of the rat epididymis and localized to the plasma membrane of basal cell-derived organoids. Its expression decreased as organoids differentiated. LGR5, 4 and 6 transcripts were expressed throughout the epididymis during postnatal development. LGR5 and LGR6 mRNA levels decrease during postnatal development while LGR4 mRNA levels remained constant. LGR5 was immunolocalized to undifferentiated columnar cells of the epididymis as early as PND7. However, as the epithelium differentiated, LGR5 became associated with basal cells. In the adult epididymis, LGR5 was localized primarily to basal cells, although weak staining was observed in narrow cells. Co-localization of LGR5 with the basal cell marker TP63 in the adult epididymis indicated the existence of at least 3 basal cell subtypes: LGR5+/TP63-, LGR5+/TP63+ and LGR5-/TP63+. Together these data demonstrate that LGR5 is expressed in basal stem cells of the epididymis and that these cells have the ability to form organoids in vitro. Supported by CIHR, CIRD and the Canada Research Chairs Program.

Abstract # 2217

Spatial Dynamics Of Protein Translation In Sertoli Cells. Ana Cristina Lima, Oregon Health & Science University, United States

The Sertoli cells (SC) of the testis juggle a panoply of functions required for male germ cell development and reproductive health. To attain such fine-tuned control, SCs are

thought to compartmentalize their functions in distinct subcellular domains. We hypothesized that, similarly to neurons, this mechanism is regulated by localized translation of mRNAs and on-site production of specialized proteins.

To visually detect translation in SCs by immunofluorescence, we adapted the technique of surface sensing of translation (SUNSET) to our system. Both in vitro (TM4 cell line) and in vivo (C56BL/6J mouse testis) results indicated the presence of translation sites distally to the SC nucleus. Next, we looked for mRNAs that could potentially be locally translated at these sites, by generating transcriptome data of TM4 cells and additionally mining 3 published murine RNA-seq datasets. Among others, the tubulobulbar complex protein actin-related protein 3 (Arp3) and the blood-testis barrier Claudin 11 (Cldn11) stood out as potential targets of localized translation. Their mRNA is differentially expressed in SCs during the first-wave of spermatogenesis and the protein shows stage-specific subcellular localization. SUNSET coupled with single molecule fluorescence in situ hybridization (smFISH-IF) showed the presence of the mRNA and protein of Cldn11 and Arp3 at the sites of active translation in SCs. These can be found basally, at the blood-testis barrier, and adluminally, adjacent to elongated spermatids in a stage-specific manner (VII-VII).

We then used this approach to investigate the spatial dynamics of protein translation in SCs during the cycle of the seminiferous epithelium. Stage-specific patterns of protein translation could represent relevant biological events that when disrupted could lead to disease. Using ImageJ and R software, we developed a computational pipeline for image and data analysis of testicular sections marked for translation and/or mRNA and protein of interest. To capture the temporal information provided by the cycle of the tubules, we used the Acrv1 protein for tubule staging as previously described. This approach allowed us to collect spatial data for localization of protein translation during the 12 different stages of mouse spermatogenesis, from 5-15 tubules per stage. Concordant with the microscopy observations, general protein translation in SC changes dynamically throughout the cycle. Remarkably, the number of translation sites are significantly higher at stage 7, when these SCs are remodeling the blood-testis barrier, establishing the tubulobulbar complex and preparing for spermiation. Our results indicate that SC may indeed compartmentalize their functions by mRNA transport and localized production of specialized proteins.

This novel approach will provide a landscape of spatial regulation of mRNA translation in SCs and allow us to ask questions about how local translation is involved in different abnormal phenotypes.

A Role for the Transcription Factor SP6 Within the Primitive Syncytium at the Peri-Implanation Stage of Human Embryo Development. Yuliana C. Tan, The Jackson Laboratory for Genomic Medicine, USA

The primitive syncytium (PrSyn) is a simian-specific trophoblast cell type that mediates blastocyst attachment and invasion into the endometrium at the peri-implantation stage of development. It is at this stage that loss of human embryos is greatest. Knowledge of the PrSyn is largely based on historical morphological studies; the molecular cell biology of the PrSyn remains poorly understood. We have identified the expression of SP6 (also known as epiprofin) within the late stage human blastocyst temporally and cellular correlated with known syncytiotrophoblast markers. SP6, a three C2H2 zinc finger motifs-containing transcription factor well characterized in mouse epidermal development, is not expressed in the mouse trophoblast lineage. We hypothesized SP6 regulates simian-specific features of the peri-implantation embryo, specifically in the formation and function of the PrSyn.

To test this, we have generated SP6 knockout (SP6KO) human induced pluripotent stem cell (iPSC) lines and differentiated these into the trophoblast lineage in which SP6, in the wildtype, is first expressed at Day 3. We compared the molecular and morphological phenotype of SP6KO to wild type (SP6WT) cells through iPSC to PrSyn differentiation. Additionally, we established a trophoblast organoid culture system derived from human iPSCs and used this to test differences in invasion between SP6KO and SP6WT cells. A morphological phenotype assessment using immunofluorescence confocal imaging showed reduced syncytial cells (25% vs 34%) and increased Ki67 expression in the SP6KO line suggesting defects in fusion and cell cycle regulation. Transcriptome analysis show no significant difference at day 3, but by day 5 of differentiation revealed 223 downregulated and 24 up-regulated genes (logFC = 1.5, FDR = 0.05) within the SP6KO. Gene ontology and literature analysis indicated functions enriched in post-translational modification of proteins regulating cell cycle, cell adhesion and migration (TRPV2, DUSP9, PREX1, ZNF703, FAM65B, MYC, BCL2), cell fusion (ERVW-1, ERVFRD-1), epidermal differentiation (TGFBR2, HBEGF, NOTCH1, HEY1, ENDOU, DACT2), cytoskeletal and extracellular matrix remodeling (KRT80, CRIP2, LRRC15, CDKL5, MTSS1, MCAM, ASB2), response to hormones (PITX1, ZFHX3, NCOA3, DIO3), and immune regulation (FAM65B, IL7R, CD274, VSIR, PRDM1, SERPINB12, ERVFRD-1, ERVV-2), which are indicative of the PrSyn's important role in communication with endometrium during implantation.

We would argue SP6 has an essential role in human, but not mouse, peri-implantation biology and that components of the epidermal differentiation program have been coopted for use at this stage. This study emphasizes the utility of this PrSyn model to address questions in early human development and the molecular mechanism at play in cell type evolution.

ASCL2 is Essential for Differentiation and Function of Extravillous Trophoblast Cells during Human Placental Development. Mariyan J. Jeyarajah, Western University, Canada

The primitive syncytium (PrSyn) is a simian-specific trophoblast cell type that mediates blastocyst attachment and invasion into the endometrium at the peri-implantation stage of development. It is at this stage that loss of human embryos is greatest. Knowledge of the PrSyn is largely based on historical morphological studies; the molecular cell biology of the PrSyn remains poorly understood. We have identified the expression of SP6 (also known as epiprofin) within the late stage human blastocyst temporally and cellular correlated with known syncytiotrophoblast markers. SP6, a three C2H2 zinc finger motifs-containing transcription factor well characterized in mouse epidermal development, is not expressed in the mouse trophoblast lineage. We hypothesized SP6 regulates simian-specific features of the peri-implantation embryo, specifically in the formation and function of the PrSyn.

To test this, we have generated SP6 knockout (SP6KO) human induced pluripotent stem cell (iPSC) lines and differentiated these into the trophoblast lineage in which SP6, in the wildtype, is first expressed at Day 3. We compared the molecular and morphological phenotype of SP6KO to wild type (SP6WT) cells through iPSC to PrSyn differentiation. Additionally, we established a trophoblast organoid culture system derived from human iPSCs and used this to test differences in invasion between SP6KO and SP6WT cells. A morphological phenotype assessment using immunofluorescence confocal imaging showed reduced syncytial cells (25% vs 34%) and increased Ki67 expression in the SP6KO line suggesting defects in fusion and cell cycle regulation. Transcriptome analysis show no significant difference at day 3, but by day 5 of differentiation revealed 223 downregulated and 24 up-regulated genes (logFC = 1.5, FDR = 0.05) within the SP6KO. Gene ontology and literature analysis indicated functions enriched in post-translational modification of proteins regulating cell cycle, cell adhesion and migration (TRPV2, DUSP9, PREX1, ZNF703, FAM65B, MYC, BCL2), cell fusion (ERVW-1, ERVFRD-1), epidermal differentiation (TGFBR2, HBEGF, NOTCH1, HEY1, ENDOU, DACT2), cytoskeletal and extracellular matrix remodeling (KRT80, CRIP2, LRRC15, CDKL5, MTSS1, MCAM, ASB2), response to hormones (PITX1, ZFHX3, NCOA3, DIO3), and immune regulation (FAM65B, IL7R, CD274, VSIR, PRDM1, SERPINB12, ERVFRD-1, ERVV-2), which are indicative of the PrSyn's important role in communication with endometrium during implantation.

We would argue SP6 has an essential role in human, but not mouse, peri-implantation biology and that components of the epidermal differentiation program have been coopted for use at this stage. This study emphasizes the utility of this PrSyn model to address questions in early human development and the molecular mechanism at play in cell type evolution.

Loss Of TDP-43 In Sertoli Cells Leads To Failure Of Spermatogenesis In Mice. Helena D. Zomer, University of Illinois at Urbana Champaign, USA

Infertility affects 15% of human couples and approximately 30 to 40% of the occurrences are due to the male factor. In most cases of male infertility, the underlying pathogenesis is idiopathic. The TAR DNA binding Protein of 43 kD (TDP-43) is an evolutionarily conserved, ubiquitously expressed transcription factor and RNA-binding protein with major human health relevance. It has been previously shown to be present in Sertoli and germ cells of the testis, and its aberrant expression was reported in the sperm of infertile men. Sertoli cells play a key role in spermatogenesis by offering physical and nutritional support to the male germ cells. Thus, the aim of this study was to investigate the requirement of TDP-43 in Sertoli cells. Conditional knockout (cKO) of TDP-43 in mouse Sertoli cells using the Amh-cre deleter strain caused failure of spermatogenesis and male infertility. The cKO mice showed decreased testis weight from as early as postnatal day (PND) 12, which persisted to adult age, and a 5-fold reduction in sperm count. Histopathological analysis revealed seminiferous tubules with a decreased diameter and multiple degenerating alterations, including loss of germ cell layers, presence of vacuoles, and sloughing of round spermatids, suggesting loss of contact with Sertoli cells. Using a biotin tracer, we found that the blood-testis-barrier (BTB) was disrupted in 28.5% of tubule cross-sections at PND 24 and 42.7% at PND 90 in TDP-43 cKO mice. Investigation of the junction proteins by immunohistochemistry showed that the expression of connexin-43 (gap junction) and N-cadherin (ectoplasmic specialization) was altered in 73.7 ± 15.1 SD and $56.25\% \pm 25.6$ SD of the tubules, respectively. Quantitative real-time PCR showed overexpression of candidate genes involved in the formation and/or maintenance of Sertoli cell junctions (N-cadherin, Gja1/connexin-43, claudin-11, and occludin) as well as in the phagocytic pathway (Elmo1, Rac1, Tyro3, and Bai1). Finally, Oil Red O lipid staining showed a decrease in the number of tubule cross-sections containing lipid droplets in Sertoli cells and in the tubule lumen of cKO mice. Given that Sertoli cytoplasmic lipid droplets result from the phagocytosis of residual bodies and apoptotic germ cells, the data indicate inefficient phagocytosis. Overall, our findings suggest that TDP-43 is required in Sertoli cells for the completion of spermatogenesis, formation and maintenance of the BTB, and phagocytosis, thus indicating an essential role for TDP-43 in male fertility.

Abstract # 1768

Age-dependent Dysregulation of Hyaluronan and Collagen Matrices Alters Ovarian Biomechanical Properties. Farners Amargant, Northwestern University, USA

Female reproductive aging is associated with infertility due to decreased egg quality and quantity. We recently identified that there is an increase in collagen (fibrosis) in the ovarian stroma with advanced reproductive age, likely affecting gamete quality. Hyaluronan (HA) is an extracellular matrix glycosaminoglycan that maintains tissue homeostasis, and its loss can change tissue micromechanical properties, leading to a mechanically stiff microenvironment. Therefore, we hypothesized that reproductive aging is associated with a loss of ovarian HA, which promotes stromal stiffness and fibrosis. HA levels are dictated by the relative activities of enzymes that regulate its synthesis (hyaluronan synthases) and degradation (hyaluronidases). To investigate whether there were age-associated changes in these enzymes, we performed real time PCR to examine the expression of hyaluronan synthases (Has1, Has2, Has3) and hyaluronidases (Hyal1, Hyal2, Tmem2, Kiaa1199) in enriched ovarian stromal tissue from reproductively young (6-12 weeks) and old (14-17 months) CB6F1 mice. Of these genes, Has3 and Hyal1 were the only ones whose expression changed with age, with Has3 expression decreasing (1.45-fold change) and Hyal1 expression increasing (1.38-fold change). We further validated their stromal expression and localization using RNA in situ hybridization. These gene expression changes would predict a net loss of ovarian stromal HA with age. To investigate this, we assessed the HA content in the ovary using a hyaluronic acid binding protein (HABP) assay. HA was detected in follicles, corpora lutea (CL), and the ovarian stroma, and the total ovarian HA content was significantly reduced in reproductively old mice compared to young controls (p=0.008). This reduction in HA occurred specifically in the stroma, as HA loss in other ovarian sub-compartments was not significant between age cohorts (follicles p=0.056; CL p=0.55). To examine how advanced reproductive age affects ovarian micromechanical properties, we performed nanoindentation analysis to measure ovarian stiffness. It took more force to indent ovaries from reproductively old mice (3.57±2.4kPa) compared to young mice (1.69±2.4kPa; p<0.001). We then examined whether the increase of ovarian stiffness with age was dependent on the increase in collagen and the decrease in HA content by quantifying the micromechanical properties of collagenase-treated and Has3-/- mice ovaries, respectively. Reducing collagen content in reproductively old mouse ovaries restored the micromechanical properties to those of ovaries from young mice (reproductively young 1.98±0.42kPa; reproductively old 4.36±1.24kPa; reproductively old collagenase 2.28±0.61kPa). On the other hand, Has3-/- ovaries were stiffer than ovaries from age-matched wild-type (WT) mice (WT 2.51±0.66kPa; Has3-/- 6.67±2.00kPa; p=0.0079). These results demonstrate that both increased collagen and HA loss in the ovarian stroma contribute to the increase in ovarian stiffness observed with age. These findings are significant because the use of pharmacological approaches to prevent collagen and HA changes in the stroma with age may enhance reproductive longevity. This work was supported by the National Institute of Child Health and Human Development (R01HD093726).

Abstract # 1837

Plasma Gelsolin: A Mediator Of Ovarian Cancer Chemoresistance And An Inhibitor Of CD8+ T-Cell Function. Meshach Asare-Werehene, University of Ottawa, Canada

Ovarian Cancer (OVCA) is the leading cause of death in gynecologic cancer. Although combined surgical debulking and chemotherapy is an important treatment strategy, chemoresistance remains a major challenge for long term therapeutic success. Tumor-derived soluble factors down-regulate immune cells which influence the responsiveness of cancer cells to chemotherapy. Although exosomes are involved in cell-cell communications, their role in chemoresistance in OVCA is unclear. We have previously shown that increased gelsolin (GSN) overexpression in gynecologic cancers is significantly associated with chemoresistance, poor prognosis and cancer deaths; however, whether these effects are associated with the secreted plasma gelsolin (pGSN) or the cytosolic gelsolin (cGSN) Isoform, is unknown. Here, we hypothesize that exosomal pGSN derived from chemoresistant OVCA cells confers resistance in chemosensitive OVCA cells, regulate glutathione (GSH) production and suppresses the anti-tumor functions of CD8+ T-cells. The overall objective is to determine if and how OVCA cell-T cell interactions regulate chemosensitivity and how deregulation of these interactions modulate tumor microenvironment (TME) and tumor chemosensitivity. Clinical and in-vitro studies with OVCA cell lines of various histologic subtypes [high grade serous (HGS), endometroid and clear cell], human peripheral CD8+ T-cells, OVCA patient tissue microarray (TMA; Centre hospitalier de l'Université de Montréal; n=208), OVCA tissues (University of Fukui Hospital; n=95) and OVCA TCGA datasets (n=1,259) were used. T-cell and OVCA cells cultures/co-cultures, gain- and loss-infunctions studies, extracellular vesicle dynamics, apoptosis, cytokine and immune profiling and protein expression were assessed with standard molecular and cellular techniques to determine the mechanisms involved in pGSN-mediated immune suppression and OVCA chemoresistance. We have shown that increased expression of tissue pGSN is significantly associated with advanced tumor stage (p<0.01), poor survival (p < 0.01), chemoresistance (p < 0.01) and suboptimal residual disease (p < 0.05). Elevated pGSN levels diminish the favorable prognostic impact of infiltrated CD8+ T on patient survival (p=0.02). Our interrogation of OVCA TCGA datasets revealed that patients with increased pGSN mRNA expression had shortened progression-free and overall survival compared with patients expressing lower amount regardless of the chemotherapeutic agent. pGSN secreted and transported via exosomes, up-regulates HIF-1a-mediated pGSN expression in chemoresistant OVCA cells in an autocrine manner and confers cisplatin resistance in otherwise chemosensitive OVCA cells. Exosomal pGSN activated the Nuclear factor erythroid 2-related factor 2 (NRF2) pathway leading to increased production of GSH, a response attenuated cisplatininduced death. In chemosensitive condition, exosomal pGSN secretion is low hence allowing an optimal CD8+ T-cell function. This resulted in optimal IFNy secretion, STAT1 phosphorylation in the OVCA cells, reduced GSH production and increased CDDPinduced apoptosis. In the chemoresistant condition, increased exosomal pGSN secretion by OVCA cells induced caspase-8/3-dependent apoptosis in CD8+ T-cells. IFNy secretion was therefore reduced, a response that resulted in high GSH production and CDDP resistance in OVCA cells. These findings suggest that pGSN may play a role in immune-modulation and chemoresistance in OVCA, providing novel insights into the coldness (poor immune infiltration and function) of OVCA and suggesting an efficient alternative therapy. (Supported by grants from the Canadian Institutes of Health Research, Ovarian Cancer Canada and the Mitacs Globalink Award).

Endometrial Epithelial ARID1A Loss Causes Defects of Uterine Receptivity and Endometrial Gland Function. Ryan M.Marquardt, Michigan State University, United States

Endometrial receptivity is key to successful pregnancy establishment and is compromised in many women with endometriosis. ARID1A, a SWI/SNF chromatin remodeling complex subunit, is attenuated in the endometrium of women with endometriosis. Moreover, conditional uterine Arid1a knockout mice are infertile due to endometrial receptivity defects resulting from increased pre-implantation epithelial proliferation. We thus hypothesized that epithelial ARID1A loss compromises fertility by causing a non-receptive state in the endometrium. To examine the effects of endometrial epithelial-specific ARID1A loss, we established a conditional knockout mouse where Arid1a is ablated in the endometrial epithelium (Ltficre/+Arid1af/f). We observed severe subfertility in Ltficre/+Arid1af/f mice in a six-month breeding trial (n=6). Immunohistochemical analysis revealed a failure of embryo implantation and stromal cell decidualization at gestation day (GD) 4.5 (n=3-4), and an artificial decidualization test confirmed the compromised decidual response (n=6) caused by Arid1a loss in the endometrial epithelium. Ltficre/+Arid1af/f mice also exhibited a non-receptive endometrium at pre-implantation stage (GD 3.5) due to increased epithelial proliferation (n=3), and we found significant reduction in expression levels of endometrial gland-related genes including Foxa2 (n=5; p<0.01) and Lif (n=4-5; p<0.05), critical factors for pregnancy establishment. Furthermore, ChIP analysis indicated that ARID1A directly binds the Foxa2 promoter during early pregnancy in wild type mouse uterus (n=5), implying direct transcriptional regulation of Foxa2 by ARID1A. Previous experiments revealed that implantation and decidualization can be rescued in uterine Foxa2 knockout mice by LIF repletion at GD 3.5. However, LIF repletion did not rescue implantation in Ltficre/+Arid1af/f mice, assessed histologically at GD 5.5 (n=3). Despite the failure of LIF to rescue implantation, phospho-STAT3 and EGR1, downstream signaling targets of LIF important for implantation and decidualization, were significantly decreased around Ltficre/+Arid1af/f implantation sites at GD 4.5 based on IHC H-score (n=3; p<0.001). Taken together, these data indicate that loss of preimplantation LIF expression is disrupted by endometrial epithelial Arid1a ablation but is not the sole cause of implantation failure. Our results reveal the importance of epithelial ARID1A in promoting endometrial receptivity by allowing proper implantation and decidualization, regulating epithelial proliferation, and maintaining gland function.

Research reported in this publication was supported in part by the Eunice Kennedy Shriver National Institute of Child Health & Human Development of the National Institutes of Health under Award Number R01HD084478 to J.W.J. and T32HD087166 to R.M.M., MSU AgBio Research, and Michigan State University. The content is solely the responsibility of the authors and does not necessarily represent the official views of the National Institutes of Health.

NOTUM-Dependent Modulation Of WNT Signaling In Extravillous Trophoblast Cell Lineage Development. Vinay Shukla, University of Kansas Medical Center, USA

The hemochorial placenta develops through tightly regulated expansion and differentiation of trophoblast stem (TS) cells. Effective strategies for the isolation and propagation of human TS cells were recently determined. Human TS cells can differentiate into extravillous trophoblast (EVT) cells and syncytiotrophoblast. EVT cells are specialized cells that invade into the uterus and remodel the uterine vasculature facilitating the redirection of maternal nutrients to the developing fetus. Disruptions in EVT cell lineage determination, expansion, and differentiation are associated with numerous obstetrical complications, such as early pregnancy failure, preeclampsia, intrauterine growth restriction, preterm birth, and stillbirth. Here, we investigate canonical WNT signaling in the regulation of human TS cell differentiation into EVT cells. EVT cell differentiation is accompanied by extensive cell elongation and spreading and the upregulation of transcripts indicative of the EVT cell fate (e.g. HLAG, MMP2, etc). Initially, canonical WNT signaling was assessed by the accumulation of beta-catenin (CTNNB1) in stem cell versus EVT cell nuclei. CTNNB1 was abundant in stem cell nuclei but not in EVT nuclei, suggesting that WNT signaling was downregulated during EVT cell development. Consistent with these observations, we found that addition of a potent WNT activator, CHIR99021 (a GSK3B inhibitor), inhibited differentiation of TS cells into EVT cells. We next interrogated human TS cells in stem and EVT differentiation states for expression of components of the WNT signaling pathway with the goal of identifying potential endogenous regulators of WNT signaling. We observed the downregulation of several transcripts encoding proteins driving WNT signaling and the upregulation of other transcripts encoding proteins inhibiting WNT signaling. Among the upregulated transcripts, NOTUM expression was striking in terms of both magnitude of the increase and overall expression level. NOTUM antagonizes WNT signaling by facilitating the depalmitoleoylation of WNT proteins, which impair their binding to frizzled receptors. We hypothesized that NOTUM is required to repress WNT signaling during human EVT cell differentiation. A loss-of-function strategy using NOTUM short hairpin RNAs demonstrated that the differentiation-dependent increase in NOTUM expression was essential for EVT cell differentiation. Knockdown of NOTUM inhibited both morphological and molecular indices of EVT cell development. Disruption of NOTUM also enhanced the abundance of active CTNNB1 in the nucleus and LEF1 transcript levels. We further demonstrated that NOTUM expression is tightly controlled by WNT signaling. A role for NOTUM in regulating the invasive trophoblast cell lineage is speciesrestricted. The rat, which exhibits deep hemochorial placentation similar to the human, does not express NOTUM in any trophoblast cell lineage. Overall, our findings indicate that canonical WNT signaling is essential for maintaining human trophoblast stemness and prevention of human TS cell differentiation. NOTUM is an important contributor to the downregulation WNT signaling and is essential to human EVT cell differentiation. Although, NOTUM may not be a conserved regulator of the invasive trophoblast cell lineage, roles for WNT in trophoblast stemness and WNT repression in

trophoblast cell differentiation may be conserved. [Supported by KUMC Biomedical Research Training Program (VS); F32HD096809 (KMV), GM103418 (MK); NIH grants HD020676, HD099638; Sosland Foundation)

Abstract # 2108

miR-218-5p Promotes Endovascular Trophoblasts Differentiation In Part Via The Activation Of The NF-Kb Pathway. Yanan Shan, York University, Canada

During placenta development, the endovascular trophoblasts (enEVTs) invade into uterine spiral arteries and help to transform them into the high flow, low resistant blood vessels. Recently, we demonstrated that miR-218-5p promotes enEVT differentiation, invasion, and spiral artery remodeling (Brkic et al., 2018. Mol Ther 26: 2198-2205). Gene Ontology analysis of cDNA microarray with mir-218 (the precursor of miR-218-5p)overexpressing cells revealed that the NF-kB pathway is one of the most affected pathways. These findings suggested that the NF-kB pathway plays a role in mediating the effects of miR-218-5p on enEVT differentiation. To test this hypothesis, we first measured cytosolic and nuclear fractions of p65 and p50, two members of the NF-kB family, in control and mir-218-overexpressing HTR-8/SVneo cells. We found that miR-218-5p overexpression resulted in the accumulation of p65 and p50 in the nucleus, confirming the activation of this pathway. & nbsp; Using bioinformatics tools, we identified 3 potential binding sites of miR-218-5p in the 3'UTR of NLRC5, an inhibitor of the NF-kB pathway. Real-time PCR and Western blotting revealed that stable overexpression of mir-218 or transient transfection of miR-218-5p both reduced the mRNA and protein levels of NLRC5. Luciferase reporter assays also confirmed the interaction between miR-218-5p and the 3'UTR of NLRC5. Furthermore, knockdown of NLRC5 in HTR-8/SVneo cells increased cell migration, invasion, the formation of the endothelial-like networks, and expression of enEVT markers, VE-cadherin and NCAM. Conversely, overexpression of NLRC5 reduced the stimulatory effect of miR-218-5p on cell invasion and formation of endothelial-like networks. & nbsp; Finally, inhibition of the NF-kB pathway using ACHP strongly suppressed the ability of mir-218 to induce cell invasion and network formation. These findings suggest that miR-218-5p inhibits NLRC5, leading to the subsequent activation of NF-kB, and that activation of the NF-kB pathway mediates, in part, the stimulatory effect of miR-218-5p on enEVT differentiation (Supported by CIHR). Key Words: enEVT, miR-218-5p, NLRC5, NF-kB, invasion

Abstract # 2144

Central Spindle Formation Protects Against Incorrect Kinetochore-Microtubule Attachment And Aneuploidy In Mouse Oocytes. Jessica Kincade, University of Missouri, USA

Aneuploidy is the leading genetic cause of miscarriage and infertility in women and occurs frequently in oocytes. Therefore, it is particularly important to study the early

mechanisms of oocyte maturation in order to understand why this meiotic process is error prone. Spindle formation and positioning are two critical events that must be regulated tightly to avoid erroneous chromosome segregation. Following germinal vesicle breakdown (GVBD), the spindle is assembled centrally before migrating towards the cortex to allow the first asymmetric division. The biological significance of the primary central positioning of the spindle is unknown. Given that centromeres facing the cortex have relatively high rates of unstable microtubule (MT) attachments, we hypothesized that early central spindle positioning is required to protect against a cortical influence that may hinder correct kinetochore-MT (K-MT) attachments. Using time-lapse microscopy, we found that the spindle forms where GVBD occurs, whether positioned at the center or at the cortex of the cell. Based on this observation, fullgrown GV (prophase I) oocytes were collected from CF-1 mice (6-8 weeks old) and sorted according to the position of the GV into three groups: central, intermediate, and peripheral. Approximately 44% of the cells exhibited a central GV position, while 25% of cells showed a peripheral GV position. These proportions were similar to those obtained by histological evaluation of ovarian oocytes in 6-8-week-old mice, but not to those of 3-week-old mice, which tended to have a majority of peripherally positioned GVs, suggesting that GV positioning is a dynamic process during oocyte growth. Interestingly, when peripheral GV oocytes were matured in vitro, GVs (~ 43%) migrated towards the center and GVBD (and spindle assembly) occurred either at the center of the cell or during migration. Arresting oocytes at prophase I with milrinone (phosphodiesterase inhibitor) allowed almost all cells to complete central GV relocation, while such migration is impeded by cytochalasin D (F-actin inhibitor) and taxol (MT stabilizing agent), suggesting that both F-actin and MTs play a role in GV positioning. To understand why central spindle formation is necessary, we analyzed the phenotypes of peripheral GV oocytes following meiotic resumption. Although the percentages of GVBD and polar body (PB) extrusion did not vary significantly between groups, we found that peripheral GV oocytes underwent chromosomal alignment (~20 min) and the first PB extrusion (~30 min) earlier than central GV oocytes. Importantly, peripheral GV oocytes showed a significant increase of an euploidy at metaphase II when compared to central GV oocytes. Because abnormal K-MT attachment is a major cause of aneuploidy, we asked whether establishing K-MT attachments is perturbed when the spindle forms peripherally. Using cold-stable MT assay and confocal microscopy, we found that peripheral GV oocytes had a significant increase of abnormal K-MT attachments at metaphase I compared to central GV oocytes. These results indicate that preferential central spindle formation is an insurance mechanism to protect against incorrect K-MT attachments and aneuploidy. This research was supported by laboratory start-up funding from the University of Missouri to AZB.

Cumulus-Oocyte Interaction Is Required To Maintain Active Suppression Of Glycine Transport In The Preovulatory Mouse Oocyte. Allison K. Tscherner, Ottawa Hospital Research Institute, Canada

Oocytes and early embryos are highly sensitive to changes in cell volume. It is now understood that cell volume dysregulation was a major cause of developmental arrest that occurred in traditional embryo culture. Early (1- to 2-cell) mouse embryos use a novel mechanism to control cell volume, in which glycine is accumulated intracellularly via the GLYT1 transporter (SLC6A9 protein). While SLC6A9 is expressed and localizes to the membrane of fully-grown oocytes, transport of glycine is absent until this transporter becomes activated by an unknown mechanism. In vivo, GLYT1 activation normally occurs in parallel with release of an oocyte from meiotic arrest that precedes ovulation. It also activates in vitro shortly after oocytes are removed from antral follicles, implying active suppression within follicles. The primary aim of this research is to identify the specific factor(s) responsible for the release of suppression of GLYT1 in oocytes, which are currently not known. To evaluate this, we have established a GLYT1 activity assay based on [3H]glycine uptake and adapted it for single oocyte measurements. Oocytes were cultured within COCs for 4 hours after removal from follicles. We have found for the first time that it is possible to maintain guiescence of GLYT1 in GV oocytes within isolated COCs, in a model where COCs are cultured individually and meiotic arrest is maintained by natriuretic peptide precursor C (NPPC). This suppressive effect is reversed when NPPC is removed. NPPC acts by inducing production of cGMP, which in turn mediates suppression of the oocyte's cAMP-specific phosphodiesterase, PDE3. GLYT1 suppression is similarly maintained when oocyte meiosis is arrested with milrinone, a direct inhibitor of PDE3. However, GLYT1 suppression is maintained only in intact COCs cultured in milrinone, whereas oocytes stripped of cumulus cells maintain meiotic arrest but GLYT1 is activated. Together, these findings indicate that maintaining GLYT1 suppression requires both meiotic arrest and the presence of cumulus cells, though either factor itself is insufficient to maintain active suppression. Finally, since gap junctions between the oocyte and cumulus cells play a major role in the physical association as well as chemical communication between these cells, we impaired gap junctional coupling with specific inhibitors and observed a partial activation of GLYT1 in COCs in the presence of milrinone. Overall, we have shown that the factor maintaining GLYT1 suppression before the resumption of meiosis requires the presence of cumulus cells. GLYT1 quiescence is only maintained under conditions of oocyte meiotic arrest and appears to involve gap junctional communication between cumulus cells and the oocyte. This study highlights the conditions required for glycine transport in vitro and provides insight into the signaling mechanisms likely involved in GLYT1 suppression in ovarian follicles in vivo.

Dynamic Regulation of Apoptosis in Male Sexual Development and Cancer Therapy-Induced Infertility. Kaitlyn A. Webster, Harvard School of Public Health, USA

Due to advances in pediatric cancer therapies, long-term survival is anticipated for 80% of patients. However, radiation or chemotherapy-induced infertility is commonly observed in pediatric cancer survivors. Age at treatment, sex and pubertal status influence risk of permanent infertility, suggesting that vulnerability of reproductive tissues is dynamic and an important determinant of therapy sensitivity. Using BH3 profiling – an assay that measures a cell's propensity to induce intrinsic apoptosis in response to prodeath peptides – we previously found that apoptosis is dynamically regulated across mammalian cell types and ages, with tissues typically being highly primed for apoptosis in neonates/juveniles but resistant in adults. It is unclear how apoptosis is regulated throughout developing reproductive systems, and how this impacts cancer therapy sensitivity. Importantly, embryonic sex differentiation, pituitary morphogenesis, and germ cell attrition are known to be cell death-dependent processes. We sought to characterize the role and regulation of intrinsic apoptosis in reproductive development, and impacts of excessive or insufficient apoptosis on male fertility. We assessed death vulnerability at the single-cell level in reproductive tissues from embryos to adults, finding that germ cells in pre-pubertal mice are highly primed to undergo apoptosis and that this sensitivity is reduced after puberty in males but not females (N=3 per age; P<0.0001). To test functional relevance of these findings, we exposed pre- and postpubertal males to 6-8 Gy testicular irradiation to model clinical exposure to radiation therapy, which is known to cause infertility in patients. Testicular apoptosis was 6x greater in irradiated juveniles vs. adults (N=6, P<0.0001), as measured by an enzymatic Cleaved Caspase-3 activation assay. Surprisingly, we found that pre-pubertal irradiated males exhibited testicular regeneration by 2 months post-treatment and could sire viable offspring. In contrast, despite reduced levels of post-treatment apoptosis, postpubertally irradiated males showed testicular degeneration beginning at and continuing after 2 months, and failed to produce offspring despite making sperm (N=4). To investigate the potential for preventing radiation-induced infertility by blocking apoptosis, we studied reproductive development in male mice carrying a null mutation in the pro-apoptotic gene Bax, which were previously shown to exhibit male-specific infertility. We observed that apoptotic priming was, paradoxically, increased in Bax -/testes, which also misexpressed PLZF, a marker of undifferentiated spermatogonia. Thus, we hypothesize that differentiation state of spermatogenic cells may explain the apoptotic vulnerability or resistance characterized in our previous analyses. Furthermore, we have made the novel finding that suppression of apoptosis in the Bax -/- males also results in pituitary hormone signaling defects, abnormal Müllerian duct regression, and aberrant WNT/β-Catenin signaling, which we believe underlie male infertility in this model. Our studies reveal age-dependent dynamic regulation of apoptosis in male sex differentiation and spermatogenesis, and elucidate developmental pathways that can be modulated to prevent therapy-induced infertility. Overall, the insights gained here may inform new treatments or treatment

modulators that prevent reproductive toxicity, or restore spermatogenesis in infertile males.

Abstract # 1638

GATA2 May Regulate FSH Production In Male Mice Via The BMP Antagonist Gremlin 1. Gauthier Schang, McGill University, Canada

Mammalian reproduction is dependent on follicle-stimulating hormone (FSH) and luteinizing hormone (LH) secreted by pituitary gonadotrope cells. These dimeric glycoproteins share a common a-subunit linked to hormone-specific β -subunits. Expression of the FSHB subunit (Fshb) depends on the transcription factors FOXL2, SMAD3, and SMAD4. These proteins mediate the actions of the activins or related TGFB ligands, which stimulate Fshb transcription. Another transcription factor, GATA2, was also implicated in FSH production in male mice, although its mechanisms of action and role in females were not determined. To address these gaps in knowledge, we generated and analyzed gonadotrope-specific Gata2 knockout mice using the Cre-lox system. While conditional knockouts (cKO) males exhibited ~50% reductions in serum FSH and pituitary Fshb mRNA levels relative to controls, FSH production and fertility were normal in gonad-intact cKO females. LH production was unaltered in cKOs of both sexes. Fshb expression was also reduced in male mice in which Gata2 was ablated in adult gonadotropes, ruling out a developmental effect. The male-specific FSH phenotype was reminiscent of that observed in mutant mice expressing a stabilized form of β -catenin in their gonadotropes. In that case, FSH deficiency derived from increased expression or activity of the activin antagonists follistatin and inhibin. These mechanisms did not explain FSH deficiency in Gata2 cKO males; nor did a testicular factor, as FSH deficiency persisted post-castration. RNA-seg analysis of purified gonadotropes from cKO males revealed a profound decrease in expression of gremlin 1 (Grem1), a bone morphogenetic protein (BMP) antagonist. Grem1 is expressed in gonadotropes, but not other cell lineages, in the male mouse pituitary. Both Gata2 and Grem1 mRNA levels were significantly higher in pituitaries of wild-type males relative to females, but both increased significantly following ovariectomy in the latter. In cKO females, post-ovariectomy increases in pituitary Grem1 and Fshb expression were blocked or blunted relative to controls. This suggests that an ovarian factor, perhaps estradiol, may contribute to the sex-specific FSH deficiency in gonad-intact cKO mice. Indeed, exogenous estradiol decreased Gata2 and Grem1 expression levels in castrated wild-type males Collectively, the data suggest that GATA2 promotes Grem1 expression in gonadotropes and that the Gremlin protein potentiates FSH production. The mechanisms of Gremlin action in this context are not yet clear, but may involve potentiation of activin-like and/or attenuation of BMP signaling in gonadotropes.

Decreased Endogenous CBS-H2S in the Secretory Phase Contributes to Decidualization in Human Endometrial Stromal Cells. Qianrong Qi, University of California Irvine, United States

Introduction: Human endometrial stromal cells (ESCs) proliferate in the proliferative phase, undergo spontaneous decidualization for preparing endometrium to be receptive for embryo implantation in the secretory phase. Endogenous hydrogen sulfide (H2S) synthesized from L-cysteine by cystathionine- β -synthase (CBS) and cystathionine- γ -lyase (CSE) is a multifaceted biogas with many biological functions including stimulating cell proliferation. However, it is unknown if H2S plays a role in ESC proliferation and decidualization.

Objective: To test a hypothesis that endometrial H2S biosynthesis undergoes cyclic changes during the menstrual cycle to regulate ESC proliferation and decidualization.

Methods: Endometria from premenopausal (proliferative and secretory phase) nonpregnant and pregnant women (n=4-8/group) were collected. Primary endometrial stromal cells (ESC) were isolated and cultured. Cultured cells were treated with a H2S donor NaHS (100 μ M), estradiol (10 nM E2 β), progesterone (1 μ M P4), or P4 (1 μ M) and dibutyryl-cAMP (1 mM db-cAMP) for up to 8 days. Vehicle (0.1% ethanol) was used as a control. Endogenous CBS in ESC was knock-out by using the human CBS sgRNA CRISPR/Cas9 All-in-One Lentivector. Cells morphology was monitored and photographed every other day. Cell proliferation was determined by the CCK8 assay. Levels of mRNA were determined by qPCR and protein was determined by immunoblotting; H2S production was determined by the methylene blue assay.

Results: Levels of CBS (but not CSE) mRNA and protein and H2S production were lower in endometria from the secretory phase than that in the proliferative and pregnancy in women. Baseline CBS and CSE and decidualization markers, i.e., insulin-like growth factor binding protein 1 (IGFBP-1) and prolactin (PRL), were unchanged during culture. H2S donor NaHS and E2β promoted time-dependent ESC proliferation with elevated CBS mRNA and protein expression, without altering morphology and IGFBP1 and PRL mRNA expression. P4 and P4/db-cAMP inhibited ESC proliferation, CBS mRNA and protein expression and H2S production; however, these P4 treatments stimulated time-dependent increases in IGFBP1 and PRL mRNA and ESC transformation into an epithelial phenotype, indicative of ESC decidualization. CBS knockout attenuated E2βand H2S- stimulated ESC proliferation, but enhanced IGFBP1 and PRL expression and cell morphology transformation.

Conclusion: CBS-H2S production displays cyclic changes in the menstrual cycle, which is downregulated in the secretory phase. Decidualization of ESC in vitro is associated with decrease CBS-H2S signaling and CBS knockout promoted ESC decidualization in vitro. Endogenous CBS-H2S is important for ESC decidualization (AHA 20POST35090000, RO1 HL70562, and R21 HD097498).

Single-Cell RNA Sequencing Of Neonatal Ovaries Reveals Distinct Inhibitory Gene Signatures Of Mullerian Inhibiting Substance (MIS/AMH) In Ovarian Cell Types: A Novel Insight Into The Mechanisms Of Regulation Of The Ovarian Reserve. Marie-Charlotte Meinsohn, Massachusetts General Hospital, USA

Women are born with a limited number of primordial follicles. Their activation is an irreversible process that leads to either ovulation or atresia. The mechanisms involved in long-term primordial follicles quiescence and subsequent activation remain unclear. Mullerian inhibiting substance (MIS/AMH), produced by the granulosa cells of growing follicles, regulates ovarian reserve maintenance by providing negative feedback to primordial follicle activation. We have previously shown that administration of exogenous MIS in mice resulted in a complete arrest of folliculogenesis and loss of cyclicity. We hypothesized that MIS inhibits folliculogenesis by imposing a quiescent state on granulosa cells, thereby inhibiting their differentiation. We first confirmed expression of the MIS receptor, Misr2, in pregranulosa cells, granulosa cells, and ovarian surface epithelium (OSE) in mouse, rat, and human ovaries by in situ hybridization (RNAish). Mice and rats were injected with AAV9-MIS (or vector control) to deliver MIS continuously from postnatal day 1 (PND1) through PND6. At PND6, the MIStreated ovaries were significantly smaller, and had significantly fewer growing primary and secondary follicles. To elucidate the mechanisms of action of MIS on granulosa cells and characterize its non-cell autonomous effects on the diverse cell types of the ovary, we performed single-cell RNA sequencing (inDROP) of MIS-treated and control mice ovaries at PND6. We catalogued a single cell atlas of the normal mouse ovary along with gene expression signatures uniquely associated with cell autonomous and non-cell autonomous MIS responses. In cells with high Misr2 expression (granulosa, OSE) we identified a common canonical MIS signature (Smad6, Id3, Igfbp5), which was associated with cell-cycle repression. Furthermore, we identified unique cell-specific gene signatures induced by MIS in the OSE, ovarian stroma, oocytes, and granulosa cells. Key genes within each MIS signature were validated by RNAish and qPCR. In granulosa cells, Kctd14, Tmem184a, Slc18a2, and Nr5a2 were downregulated by MIS. In OSE, MIS regulated the expression of the progenitor markers Aldh1a1 and Lgr5, and was accompanied by an inhibition of proliferation. Finally, in stromal cells, Ptch1 and Ltbp2 were significantly downregulated and Kcnk3 upregulated by MIS, and those changes were accompanied by repression of proliferation and tissue remodeling. Conversely, oocyte transcriptome was only modestly affected by MIS treatment, suggesting the inhibition of folliculogenesis is primarily driven by inhibition of granulosa cell differentiation. By comparing gene expression in quiescent and activated follicles in the control ovaries to that of granulosa cells treated by MIS we defined a common quiescent gene signature in granulosa cells involving important pathways of stemness, immediate-early genes, and cytokine signaling. Importantly, we could recapitulate the inhibition of primordial follicle activation in ex vivo ovarian cultures, and primordial follicle in vitro cultures, by treatment with recombinant MIS. These studies support the view that MIS inhibits cell growth of multiple cell types in the ovary, and imposes a

quiescent cell state in the granulosa cells of both primordial and preantral follicles leading to inhibition of preantral follicle progression, and profound suppression of ovarian activity.

Abstract # 1690

Uncovering A TAF4b-Dependent Gene Expression Program Required For Embryonic Oocyte Differentiation. Megan A. Gura, Brown University, USA

Proper embryonic female germ cell development is critical for the healthy establishment of the adult ovarian reserve. T BP- A ssociated F actor 4b (TAF4b) is a subunit of the basal transcription factor TFIID complex, which is required for RNA Polymerase II recruitment in gonadal tissues. Taf4b -deficient female mice are infertile due to several related deficits of embryonic germ cell development including increased chromosome asynapsis, excessive germ cell death, and delayed germ cell cyst breakdown. We have previously demonstrated that Taf4b mRNA and protein expression are nearly exclusive to the germ cells of the embryonic ovary from E9.5 to E18.5 and its expression is directly regulated by STRA8 and DAZL in male meiotic germ cells. Therefore, we hypothesized that TAF4b, as part of germ cell-specific from of TFIID, regulates obgenesis and meiotic gene programs. To elucidate a TAF4b-dependent program of embryonic oocyte development, we performed low-input RNA-sequencing on GFP+ germ cells sorted from Oct4-EGFP transgenic mice that were Taf4b heterozygous or -deficient at E14.5 and E16.5. To our surprise, gene ontology analysis of our differentially expressed genes (DEGs) showed few germ cell development-related genes deregulated in the absence of TAF4b. Importantly, a few notable genes were down-regulated in the Taf4b -deficient germ cells such as Nobox . Brca2, Rhox10, and Rhox13. There were several unexpected DEGs such as Mtor, Apoe, Clock, and Igf2. Further perplexing from this RNA-seg analysis was the proportion of DEGs on the X chromosome at each time point, especially several members of the MAGE and RHOX gene families. For E14.5 DEGs in the Taf4b -deficient germ cell, there were very few down-regulated genes but many up-regulated genes located on the X chromosome. At E16.5 the trends were precisely the reverse, many down-regulated genes but no upregulated genes were on the X chromosome. These interesting results implicate an unexpected but important role of TAF4b in regulating gene expression on the X chromosome during oocyte development. We are currently performing CUT&RUN using mouse embryonic stem cells and sorted embryonic female germ cells to clarify which genes are directly bound by TAF4b. This research may add new dimensionality to the female germ cell transcriptome as we uncover new genes that participate in the healthy development of the ovarian reserve.

Adrenomedullin Is A Critical Regulator Of Placental And Fetal Development. Marija Kuna, University of Kansas Medical Center, USA

Adrenomedullin (ADM) is a peptide hormone with a broad spectrum of actions on vascular smooth muscle, endothelial cells, and immune cells. These ADM cellular targets are prominent constituents of the uterine-placental interface that undergo structural and functional transformation during the course of gestation. Trophoblast cells are viewed as primary engineers of pregnancy-dependent uterine transformation. Impaired placentation and compromised trophoblast cell function is a common denominator of the "Great Obstetrical Syndromes", such as early pregnancy loss, preeclampsia, intrauterine growth restriction, and pre-term birth. ADM is produced by trophoblast cells at the uterine-placental interface and possesses modulatory actions on the uterine vasculature and resident immune cell populations that promote fetal development. Deficits in circulating maternal ADM have been linked to preeclampsia. Animal models can be effective tools in elucidating the pathophysiology of pregnancy. Mutant Adm mouse models have provided considerable insight into the role of ADM in the biology of pregnancy. Unlike the mouse, the rat exhibits deep hemochorial placentation, which also occurs in the human. To explore the physiological role of ADM signaling at the uterine-placental interface, we generated and characterized an Adm mutant rat model using Crispr-Cas9-mediated genome editing. Crispr RNAs were designed to target Exon 2 of the Adm gene. Cas9 proteins along with an Adm targeted Crispr RNA: transactivator RNA complex were electroporated into embryonic day 0.5 rat zygotes and transferred into the oviducts of appropriately-timed pseudopregnant female rats. A founder offspring possessing a 206 bp deletion spanning part of Exon 2 (the first coding exon), the Exon 2-Intron 2 boundary, and 121 bp into Intron 2 was identified via PCR screening and confirmed by genomic DNA sequencing. The deletion resulted in an out-of-frame mutation and the appearance of a premature Stop codon and a predicted protein product containing only the first four amino acids of ADM. The founder Adm mutant rat was mated with a wild-type rat in order to confirm germline transmission and to generate heterozygous pups. Adm heterozygous males and females were fertile; however, Adm heterozygous intercrosses did not generate live Adm null rats. Timed Adm heterozygous intercrosses were euthanized at various stages of gestation to determine the onset of demise. Adm null fetal-placental sites were viable at gestation day (gd) 13.5, some were dying on gd 15.5, and all were dead and resorbing by gd 18.5. Fetal and placental growth restriction were evident on gd 13.5. On gd 15.5 some Adm null placentas exhibited prominent hemorrhagic regions, whereas both hemorrhage and edema were evident in some gd15.5 Adm null fetuses. These phenotypic observations in the Adm null rat model resemble earlier descriptions of ADM deficiency in the mouse. Our results indicate that ADM serves as a critical regulator of placental and fetal development. This new Adm mutant rat model will be used to investigate roles for ADM in the regulation of vascular smooth muscle, endothelial cells, and immune cells at the uterine-placental interface. (Supported by postdoctoral

support provided by P20 GM103418 and the American Heart Association, NIH grants: HD020676, HD060860, HD099638 and Sosland Foundation)

SSR Trainee Travel Award – International

Abstract # 1786

Metabolic Features of Hepatic Steatosis and Insulin Resistance are Alleviated by Nicotinamide Mononucleotide Treatment in a DHT-Induced PCOS Mouse Model. Ali Aflatounian, University of New South Wales, Australia

Nicotinamide adenine dinucleotide (NAD+) plays a key role in energy metabolism. Recent studies have shown that NAD+ precursors, such as nicotinamide mononucleotide (NMN), can have beneficial effects on age related sub-fertility, insulin resistance and liver damage. Polycystic ovary syndrome (PCOS) is a common and complex endocrine disorder, which is defined by the presence of key characteristic reproductive and endocrine defects. PCOS patients also suffer from metabolic features including obesity, insulin resistance, liver steatosis and an increased risk of type 2 diabetes. Although insulin sensitizing agents such as metformin are commonly administered to ameliorate PCOS metabolic traits, there is uncertainty about the effectiveness of metformin in women with PCOS. Therefore, we aimed to assess the efficacy of nicotinamide mononucleotide (NMN), a precursor of NAD+, in treating features of PCOS in a dihydrotestosterone (DHT)-induced PCOS mouse model. Peripubertal female mice were implanted s.c with blank (n=14) or DHT (n=14) implants. After 12 weeks, control and PCOS mice (8/group) were treated with NMN in drinking water while the remaining mice received normal water (NW). All mice were euthanized 8 weeks after administration of NMN/NW. NMN treatment had no beneficial effect on the PCOS reproductive traits of irregular cycles and anovulation. However, oil red O absorption, a marker of liver steatosis, was significantly lower in NMN- versus NW-treated PCOS mice (PCOS+NW: 13.4±2.3; PCOS+NMN: 2.6±1.7; P<0.01). Fasting insulin levels and homeostatic model assessment of insulin resistance (HOMA-IR) were also ameliorated in PCOS+NMN mice compared to PCOS+NW mice (fasting insulin levels: PCOS+NW, 0.85±0.1 ng/mL; PCOS+NMN, 0.52±0.1 ng/mL; P<0.05. HOMA-IR: PCOS+NW, 10.6±1.9; PCOS+NMN, 6.9±0.5; P<0.05). Furthermore, the observed DHT-induced increase in fat pad weight was not observed in inguinal or mesenteric fat pad weights of PCOS+NMN mice (inguinal fat weight: PCOS+NW, 17.1±1 mg/BW; PCOS+NMN, 12.7±1 mg/BW; P<0.001. Mesenteric fat weight: PCOS+NW, 14.1±1 mg/BW; PCOS+NMN, 11.7±1 mg/BW; P<0.041). These findings suggest that boosting NAD+ via NMN administration may represent a novel therapeutic option to target metabolic features of PCOS.

The PARP Inhibitor, Olaparib, Blocks Intrinsic DNA Repair In Oocytes And Depletes The Ovarian Reserve In Mice: Implications For Fertility. Amy Winship, Monash University, Australia

Introduction: The ovary contains a finite number of oocytes stored within primordial follicles, which give rise to all mature ovulatory oocytes. They are highly sensitive to DNA damaging insults, like cytotoxic cancer treatments. Members of the poly(ADP-ribose) polymerase (PARP) enzymes are central to the repair of single-strand DNA breaks. PARP inhibitors have shown promising clinical efficacy in reducing tumour burden, by blocking DNA repair capacity. Olaparib is a PARP1/2 inhibitor recently FDA approved for treatment of BRCA1 and BRCA2 mutation carriers with metastatic breast cancer. Despite this, there is no preclinical or clinical information regarding the potential impacts of olaparib on the ovary or female fertility. Unfortunately, it may be many years before clinical data on fertility outcomes for women treated with PARP inhibitors becomes available, highlighting the importance of rigorous preclinical research using animal models to establish the potential for new cancer therapies to affect the ovary in humans. We aimed to comprehensively determine the impact of olaparib alone, or following chemotherapy, on the ovary in mice.

Methods: On day (d)0, adult female mice (n=5-8/treatment group) were administered a single intraperitoneal dose of cyclophosphamide (75mg/kg/body weight), doxorubicin (10mg/kg), carboplatin (80mg/kg), paclitaxel (7.5mg/kg), or vehicle control. From d1-d28, mice were administered subcutaneous olaparib (50mg/kg), or vehicle control. This regimen is proven to reduce tumour burden in preclinical mouse studies and is also physiologically relevant for women. Vaginal smears were performed to monitor estrous. At 24h after final treatment, ovaries were harvested for follicle enumeration and immunohistochemical analysis of primordial follicle remnants (FOXL2 expressing granulosa cells), DNA damage (YH2AX) and analysis of apoptosis (TUNEL). Serum anti-Müllerian hormone (AMH) concentrations were measured by ELISA.

Results: Olaparib significantly depleted primordial follicles by 46% versus control (p<0.01), but had no impacts on other follicle classes, serum AMH, corpora lutea number (indicative of ovulation), or estrous cycling. Primordial follicle remnants were rarely detected in control ovaries, but were significantly elevated in ovaries from mice treated with olaparib alone (p<0.05). Similarly, DNA damage denoted by γ H2AX foci, was completely undetectable in primordial follicles of control animals, but was observed in ~11% of surviving primordial follicle oocytes in mice treated with olaparib alone.

Discussion: These observations suggest that functional PARPs are essential for primordial follicle oocyte maintenance and survival and that inhibition of intrinsic DNA repair mechanisms may be a cause of primordial follicle loss. Importantly, diminished ovarian reserve can result in premature ovarian insufficiency and infertility. Notably, the extent of follicle depletion might be enhanced in BRCA1 and BRCA2 mutation carriers, and this

is the subject of current investigations. Together, our data suggest that fertility preservation options should be considered for young women prior to olaparib treatment, and that human studies of this issue should be prioritised.

Abstract # 2004

Contraceptive use and preference of HIV infected pregnant women living with HIV negative partners in the central region of Cameroon: a cross sectional survey. Martin Kuete, Anhui Biochem United Pharmaceutical Research Institute, Cameroon

Evidences in sub-Saharan Africa including Cameroon indicate that most of HIV discordant couples want more children despite their HIV status. Investigating and establishing contraception preferences among HIV infected individuals are fundamental and crucial to provide effective reproductive healthcare. We performed a cross-sectional study using structural based questionnaire to explore HIV positive pregnant women patterns including their family planning services, their preferences and its use, and their knowledge related to HIV/AIDS. Bivariate and multivariate analyses were conducted to explore associations and predictors of contraception preference and use; all tests were two sided significant at P< 0.05. Overall, 94 HIVpositive pregnant women aged 30.70±5.50 years living with HIV negative partners were from the different areas of the central region of Cameroon. Three-fourths were aware of the effectiveness of modern contraceptives and condoms, and only 28% had experienced modern contraception. 98% preferred to use traditional methods associated with infrequent condoms use. Multiple sociodemographic factors (marital status, group age, educational level, religion, occupation) affected contraceptive method preferences and its use (P<0.05). These factors are the landmarks to predict discordant couples' behavior in HIV disclosure, discussion and decision making for contraception, preventing mother to-child transmission and HIV negative partner infection (P&It;0.05). Despite the awareness of participants related both on contraception methods and HIV/AIDS matters, participants faced societal, cultural and demographic barriers to make own decision for contraception use. Promoting effective family planning services and giving the entire range of contraception options may help women living with HIV to choose for effective ones and consequently reduce new cases of HIV infection.

Abstract # 2076

Does Maternal High Fat Diet Alter the Ovarian Reserve in Female Mouse Offspring? Meaghan J. Griffiths, Monash University, Australia

Background: Obesity contributes to adverse pregnancy events. Obese pregnant women have increased rates of early pregnancy loss and congenital abnormalities. Moreover, a high fat diet prior to conception in mice contributes to fetal growth abnormalities and developmental delay. Such abnormalities may arise from oocyte defects, including epigenetic reprogramming alterations, oxidative stress and meiotic abnormalities. Existing literature suggests a decrease in the finite ovarian reserve of primordial follicles in adult mice exposed to a high fat diet (HFD). In this study, we aimed to determine if combined maternal (preconception), gestational and lactational exposure to a HFD altered follicle number in offspring. Materials and Methods: C57BL/6 dams were fed ad libitum a normal fat diet (NFD; 6% fat, SF04-057, Specialty Feeds, WA, Australia) or high fat diet (HFD; 22% fat, SF00-219, Specialty Feeds, WA, Australia) for 6 weeks prior to mating, gestation and lactation. Pups were maintained on the mother's diet until weaning at post-natal day (PN)21, at which time they were either culled (n=6-8 animals/aroup) or placed on normal chow and subsequently culled at 4 (n=4 animals/group) or 6 weeks of age (n=3 animals/group). One ovary per mouse per litter was utilised for follicle counts using design-based stereology. Growing follicles and corpora lutea were assessed by light microscopy. In the contralateral ovary, histological markers of DNA damage (yH2AX), follicular atresia (TUNEL) and oocyte quality (Stella) were assessed (n=3-4/group). Data are mean ± standard error of the mean. Statistical analysis was performed using unpaired t-test or one-way ANOVA, with significance considered p<0.05. Results: At PN21, exposure to HFD throughout development and weaning yielded no significant differences in primordial (NFD 1968±31, HFD 1241±743), primary (NFD 691±134, HFD 594±303) or growing follicle (NFD 633±38, HFD 525±72) numbers. At 6 weeks of age, primordial (NFD 1516±308, HFD 1339±311), primary (NFD 975±127, HFD 647±139) and growing follicle (NFD 222±34, HFD 177±21) numbers remained similar in the two groups. HFD exposure led to an increased proportion of TUNEL-positive dying follicles (NFD 7.5±0.9%, HFD 27±10%, p=0.06) at PN21. At 6 weeks of age, there were no differences in follicle death between groups (NFD $32\pm11\%$, HFD 25±5%). Localisation patterns of DNA double strand breaks (yH2AX) and Stella were similar between all diet and age groups. Conclusions: Preliminary data suggest exposure to a high fat diet throughout development until weaning yields no effect on follicle numbers, but follicular atresia may be increased. Previous studies demonstrate a decrease in ovarian reserve in offspring aged 15 weeks, exposed to high fat diet throughout development. Therefore, the age groups assessed in the current study may be too early to observe any follicle number differences. Further analysis will determine if these HFD-exposed offspring are able to enter puberty as normal by assessing corpora lutea number at 4 weeks of age.

Abstract # 2088

Cystic Ovary Disease Impacts Gamete/Embryo Transport and Its Cholinergic Regulation. Deirdre Scully, Trinity College Dublin, Ireland

Cystic ovary disease (COD) is a common cause of subfertility in humans and animals. The effect of COD on the function of the oviduct – especially on the transport of the oocyte and the early embyo – is largely unknown. Therefore, the aim of this study was to investigate transport function and the influence of the cholinergic system in oviducts affected by COD. Oviducts were excised from cows affected by COD (n=29) as well as from healthy cows in mid diestrus (n=20) immediately after slaughter. A unique digital live cell imaging (LCI) system established in our lab was used to capture real time videos of ciliary beat and particle transport speed under near in vivo conditions. For ciliary beat frequency (CBF), the differences in grayscale of beating cilia were transformed into frequencies using ImageJ® and AutoSignal®. For particle transport speed (PTS), polystyrene beads were added to the buffer media and were automatically tracked using ImagePro ®. Additionally, smooth muscle contraction and epithelial ion transport were investigated using organ baths and Ussing chambers. Our results showed that PTS was significantly decreased in oviducts from cows affected by COD as compared to controls (p=0.01, Unpaired Student t-test). Further to that, in healthy control cows, PTS was consistently increased in the oviduct ipsilateral to ovulation as compared to the contralateral oviduct (p=0.03, Paired Student t-test). This was not the case in cows affected by COD (p=0.47, Paired Student t-test). Reduced PTS in oviducts from cows with COD was not due to changes in CBF. Although smooth muscle contraction was similar in oviducts from healthy and COD cows, the contractile response (mN) to the cholinomimetic drug carbachol (10 -7 -10 -4 M) was significantly reduced in COD as compared to the controls (p<0.0001, non-linear regression "best fit" analysis). Carbachol-induced active ion transport in the oviductal epithelium of COD cows, which was measured by the change in short circuit current (µA/cm 2), was significantly decreased as compared to controls (p=0.03, Unpaired t test of area under the curve (AUC)). These results suggest, for the first time, that oviductal transport is compromised in COD. Decreased cholinergic regulation of tubal contractions and fluid formation could have detrimental consequences for the transport and nutrition of the gametes and the early embryo in the oviduct. This knowledge is pivotal to establish novel therapeutic concepts for successful treatment of infertility in individuals affected by COD.

The Gates Foundation Poster Award for Research Relevant to Contraceptive Research and Development

(Made Possible by the Bill and Melinda Gates Foundation)

Abstract # 2042

Development of Anti-Follicle Stimulating Hormone Receptor Nanobody as a Contraceptive Prototype in Monkeys. Sroisuda Chotimanukul, Chulalongkorn University, Thailand

Population control of monkeys in Thailand is essential for animal welfare, zoonotic prevention and human safety in free-ranging or captive setting, especially when resources are limited. In species in which dominance rank and reproductive success are positively correlated, traits include physical strength, fighting abilities, and body mass are known to be positively related to androgen levels. Novel technique of contraception without interfering androgen level is targeting specific protein at testis that regulate spermatogenesis. Follicle stimulating hormone (FSH) is essential for normal function of Sertoli cells in males which is to support spermatogenesis. The biochemical actions on target tissues are initiated by the interaction of the FSH with FSH receptor (FSHR) in testis. This study aimed to develop anti-FSHR nanobody from the concept of targeting specific protein in monkey testis. The monkey FSHR protein purification was performed by plasmid transformation. The purified FSHR recombinant protein was analysed by Western blot analysis. Finally, the FSHR was concentrated and stored at -80°C. Selection of nanobody repertoire from phage display library was performed. Briefly, specific clones were captured by binding to FSHR and nonspecific clones were removed. Phages were amplified by infection and regrowth of phage-producing cells between selection rounds. After selection, individual colonies were tested for FSHR specific binding by enzyme-linked immnosorbent assay (ELISA). The best nanobody clone was subcultured and purified. The interaction of anti-FSHR nanobody and specific FSHR protein was characterized by surface plasmon resonance (SPR). From this study, anti-FSHR nanobody was purified with the molecular weight of 27 kDa. The result showed high affinity for binding with dissociation constant (KD) = $10.3 \times 10-6$ M. In conclusion, monkey anti-FSHR nanobody was successfully developed by the technique of phage display. Furthermore, the high-affinity binding between anti-FSHR nanobody and specific FSHR protein was found in vitro. Nevertheless, the efficacy of anti-FSHR nanobody on monkey Sertoli cells should be investigated in a further study.

Trainee Research Award Platform Competition – Pre-Doctoral

Abstract # 2144

Central Spindle Formation Protects Against Incorrect Kinetochore-Microtubule Attachment And Aneuploidy In Mouse Oocytes. Jessica Kincade, University of Missouri, Columbia, USA

Aneuploidy is the leading genetic cause of miscarriage and infertility in women and occurs frequently in oocytes. Therefore, it is particularly important to study the early mechanisms of oocyte maturation in order to understand why this meiotic process is error prone. Spindle formation and positioning are two critical events that must be regulated tightly to avoid erroneous chromosome segregation. Following germinal vesicle breakdown (GVBD), the spindle is assembled centrally before migrating towards the cortex to allow the first asymmetric division. The biological significance of the primary central positioning of the spindle is unknown. Given that centromeres facing the cortex have relatively high rates of unstable microtubule (MT) attachments, we hypothesized that early central spindle positioning is required to protect against a cortical influence that may hinder correct kinetochore-MT (K-MT) attachments. Using time-lapse microscopy, we found that the spindle forms where GVBD occurs, whether positioned at the center or at the cortex of the cell. Based on this observation, full-grown GV (prophase I) oocytes were collected from CF-1 mice (6-8 weeks old) and sorted according to the position of the GV into three groups: central, intermediate, and peripheral. Approximately 44% of the cells exhibited a central GV position, while 25% of cells showed a peripheral GV position. These proportions were similar to those obtained by histological evaluation of ovarian oocytes in 6-8-week-old mice, but not to those of 3-week-old mice, which tended to have a majority of peripherally positioned GVs, suggesting that GV positioning is a dynamic process during oocyte growth. Interestingly, when peripheral GV oocytes were matured in vitro, GVs (~ 43%) migrated towards the center and GVBD (and spindle assembly) occurred either at the center of the cell or during migration. Arresting oocytes at prophase I with milrinone (phosphodiesterase inhibitor) allowed almost all cells to complete central GV relocation, while such migration is impeded by cytochalasin D (F-actin inhibitor) and taxol (MT stabilizing agent), suggesting that both F-actin and MTs play a role in GV positioning. To understand why central spindle formation is necessary, we analyzed the phenotypes of peripheral GV oocytes following meiotic resumption. Although the percentages of GVBD and polar body (PB) extrusion did not vary significantly between groups, we found that peripheral GV oocytes underwent chromosomal alignment (~20 min) and the first PB extrusion (~30 min) earlier

than central GV oocytes. Importantly, peripheral GV oocytes showed a significant increase of aneuploidy at metaphase II when compared to central GV oocytes. Because abnormal K-MT attachment is a major cause of aneuploidy, we asked whether establishing K-MT attachments is perturbed when the spindle forms peripherally. Using cold-stable MT assay and confocal microscopy, we found that peripheral GV oocytes had a significant increase of abnormal K-MT attachments at metaphase I compared to central GV oocytes. These results indicate that preferential central spindle formation is an insurance mechanism to protect against incorrect K-MT attachments and aneuploidy. This research was supported by laboratory start-up funding from the University of Missouri to AZB.

Abstract # 2125

Maternal Western Diet Consumption Alters Placental Lipid Composition and Apolipoprotein Gene Expression. Katie L. Bidne, University of Nebraska – Lincoln, USA

Maternal obesity has deleterious effects on the long-term health of offspring, including increasing risk of metabolic and cardiovascular disease. While the causes are multi-factorial, placenta function is of particular importance as it is the site of maternal-fetal nutrient exchange. Our hypothesis was that dam consumption of a high fat, high carbohydrate western diet (WD) have increased lipid deposition in the mid-gestation placenta compared to standard chow controls (ND). Mass spectrometry imaging determined the abundance and distribution of lyso-phosphatidylcholines (LPC) and phosphatidylcholines (PC) in placentas from WD and ND dams collected at e12.5, which is the first day of a fully functional placenta. Decidua/junctional zone (D/JZ) and labyrinth (LAB) were also identified to quantitate region-specific LPC and PC levels. In WD placentas, there were increases in D/JZ LPC 16:1 (P<0.1); D/JZ (P<0.05) and LAB (P<0.10) LPC 18:1; and D/JZ and LAB PC 36:1 (P<0.05). PC 38:3 was increased in both D/JZ and LAB (P<0.05) of male placentas but only D/JZ (P<0.1) of female placentas. In female WD placentas, there were strong correlations between LPCs 16:1 and 18:1 in both LAB and DJ/Z (r<0.64), but only moderate correlations in ND placentas (r=0.46). In male placentas, there was a strong correlation between LPCs 16:1 and 18:1 (r=0.64) in the ND D/JZ. There were moderate correlations (r<0.58) in the male ND LAB and WD D/JZ and LAB. In female placentas, PC 36:1 and 38:3 had strong correlations (r<0.6) in all regions except ND LAB (r =0.46). Moderate correlations (r<0.56) were observed between PC 36:1 and 38:3 in the male LAB and D/JZ, except for a strong correlation in the ND

D/JZ (r=0.64). These data suggested increased elongation (16:1 to 18:1) and desaturation (36:1 to 38:3) in WD placenta. Therefore, expression of lipid metabolism genes in the LAB was determined. Proven breeder, female C57BL/6J mice were placed on WD or ND at twelve weeks of age. When WD females reached 25% increase in body weight, age matched ND and WD females were mated with control, age-matched males. At e12.5, pregnant dams were euthanized and fetus/placenta pairs collected. Quartile analysis of fetal weight placed 28% of ND and 31% of WD fetuses in Q1 with 16% of ND and 33% of WD fetuses in Q3 (Chi-square, P<0.05). Nanostring nCounter assays were performed using RNA from Q1 WD and Q2/3 ND LAB to identify differential expression of genes associated with metabolic processes and immunometabolism. There were no differences in genes that regulate fatty acid metabolism. However, apolipoprotein expression (ApoB, Apoa4, Apoa2, Apoam, and Apoa1) was increased (P<0.05) 10.5-26.2-fold in WD LAB. Together, these data suggest increased activity of phospholipid fatty acid elongation and desaturation enzymes within the placenta and increased lipoprotein assembly in the labyrinth. These differences at the end of placental development may impact placental function through the second half of gestation and ultimately contribute to undesirable offspring phenotypes.

Abstract # 1918

Regulatory Roles Of Zinc Fluxes In Early Murine Ovarian Follicle Development. Yu-Ying Chen, Northwestern University, USA

Zinc, an enzyme cofactor that can also be stored as a divalent ion in cellular vesicles, is emerging as an important mediator of signaling pathways. Zinc mediates cell signaling by acting both as a diffusible ionic signal, similar to calcium ions, and as a covalent modification of select proteins, similar to phosphorylation. Previous studies from our group have shown that a zinc flux, the movement of labile zinc ions (biologically available zinc) across a cell membrane, is required for terminal oocyte maturation, egg-to-zygote transition, and embryonic mitotic divisions. To test the hypothesis that zinc also regulates the development of early-staged ovarian follicles (primordial through secondary), we measured zinc concentration, distribution, expression of zinc transporters, and the effect of exogenous zinc treatment on folliculogenesis using multiple techniques, including X-ray fluorescence microscopy (XFM), radioactive zinc uptake, RNAscope hybridization, and immunofluorescent labelling. Using XFM, we discovered zinc to be the most abundant transition metal within the oocytes of murine primordial, primary, and secondary staged

follicles, and identified that total zinc levels increase throughout follicular development. Upon staining whole follicles for labile intracellular zinc, we observed different zinc concentrations between different primordial oocytes. Furthermore, zinc was located in different subcellular domains between different follicle classes. Specifically, primordial oocytes exhibited localized foci of zinc staining, while oocytes from primary and secondary follicles showed a diffuse staining pattern. We then quantitated zinc uptake into ovarian follicles using an in vitro radioactive zinc isotope assay. Zinc uptake per primordial follicle was statistically lower than primary follicles (60 million atoms vs. 4 billion atoms respectively) over a one-hour time period. To identify the transporters that mediate zinc uptake, we performed real-time PCR and RNAscope hybridization on isolated follicles and on ovarian tissue sections. We identified several zinc transporters that increase gene expression during folliculogenesis, including zinc importers ZIP1, ZIP6, ZIP10, and zinc exporters ZnT3, ZnT4, ZnT5. These results demonstrate that zinc is dynamically regulated during early follicle development. Finally, to determine whether zinc plays an instructive role on folliculogenesis, we performed exogenous treatment of zinc on neonatal mouse ovaries in an ex vivo model. We observed that zinc treatment increased markers of follicle progression, including cell proliferation, p-AKT expression, FOXO3a nuclear exclusion, and oocyte growth in primordial follicles. In light of these observations, we are currently examining whether in vivo zinc fluxes actively regulate early folliculogenesis. Taken together, this study has defined the major zinc physiological dynamics of early-staged follicles and postulated zinc regulation to be a novel and incompletely understood mechanism for instructing early folliculogenesis. This research is supported by R01 GM116848 National Institute of General Medical Sciences (NIGMS) and the Thomas J. Watkins Endowment.

Abstract # 2038

Global and Site-Specific Changes in Histone Acetylation During Human Placental Trophoblast Differentiation. Gargi Jaju, Western University, USA

Placental maldevelopment causes highly prevalent pregnancy complications, which are leading causes of sickness and death of mothers and newborn babies. A better understanding of the epigenetic mechanisms that control placental development is needed to improve management and treatment options for these serious pregnancy complications. In human placenta, a syncytialized trophoblast (syncytiotrophoblast) layer forms the primary interface between maternal and fetal blood. It performs essential functions to support fetal growth and pregnancy success, including transfer of nutrients and gases between maternal and fetal blood, and production of hormones vital for pregnancy. Syncytiotrophoblast is formed by differentiation and fusion of underlying progenitor cells called cytotrophoblasts. Proper cytotrophoblast differentiation is crucial to maintain the integrity of the syncytiotrophoblast layer throughout pregnancy. Differentiation of cytotrophoblasts into syncytiotrophoblast requires precise changes in gene expression, which is mediated, in part, by regulating acetylation of lysine residues on core histone tails. In turn, changes in histone acetylation are controlled by the actions of histone acetyltransferases and histone deacetylases (HDACs). The goal of this study was to characterize histone acetylation changes during cytotrophoblast differentiation and determine the importance of specific HDACs for this process. Human cytotrophoblasts, which spontaneously form syncytiotrophoblast in culture, and BeWo cytotrophoblast-like cells, which can be induced to differentiate into syncytiotrophoblast by exposure to cyclic adenosine monophosphate (cAMP) analogs, were used to assess expression of various acetylated histone proteins during cytotrophoblast differentiation. Using western blotting, we found that differentiation of primary cytotrophoblasts and BeWo cytotrophoblasts was associated with a global decrease in acetylation of various histones (H3K9Ac, H3K14Ac, H3K27Ac, H3K18Ac, H2BK5). Chromatin immunoprecipitation-sequencing (ChIP-seq) revealed chromosomal regions that exhibit dynamic alterations in historie H3 acetylation during BeWo cytotrophoblast differentiation. These include regions containing genes classically associated with cytotrophoblast differentiation (TEAD4, TP63, OVOL1, CGB), as well as near genes with novel regulatory roles in trophoblast development and function, such as LHX4 and SYDE1. To identify specific HDACs required for cytotrophoblast differentiation, BeWo cytotrophoblasts were induced to differentiate in the presence of various selective HDAC inhibitors: FK228 (inhibits HDAC1/2), MS275 (inhibits HDAC1/3), LMK235 (inhibits HDAC4/5), BRD4354 (inhibits HDAC5/9), CAY10683 (inhibits HDAC2/6), or RGFP966 (inhibits HDAC3); and then immunofluorescence for E-cadherin and chorionic gonadotropin was used to quantify fused cells. The only HDAC inhibitor that inhibited cytotrophoblast differentiation was the HDAC1/HDAC2 inhibitor FK228 (71% decrease, N=3, P<0.05). FK228 also prevented the differentiationassociated increase in ERVW-1 (66.9%), ERVFRD-1 (82.6%), OVOL1 (68.6%) CGB (51.9%), and HSD11B2 (73.9%; N=4, all P<0.05), as determined by quantitative RT-PCR. BeWo cytotrophoblasts efficiently differentiated following shRNA-mediated knockdown of either HDAC1 or HDAC2, but knockdown of both HDAC1 and HDAC2 abrogated cytotrophoblast differentiation (68% decreased compared to controls, N=6, P<0.05), indicating that HDAC1 and HDAC2 may have

compensatory or redundant roles in promoting cytotrophoblast differentiation. Our results show that cytotrophoblast differentiation is associated with dynamic global and site-specific changes in histone acetylation, and that both HDAC1 and HDAC2 are critical for this process. These findings reveal new insights into epigenetic mechanisms underlying cytotrophoblast fusion during human placental development.

Abstract # 2239

Gene Regulation by LIN28-let-7 miRNA Axis in Sheep Trophoblast Cells. Asghar Ali, Colorado State University, USA

Normal placental development is critical for fetal and maternal health in both humans and animals. Reduced conceptus elongation is a major cause of embryonic mortality and reduced fertility in domestic ruminants. Trophoblast proliferation is critical for successful placentation and establishment of pregnancy, therefore, there is a need to better understand the molecular mechanisms that regulate trophoblast proliferation. LIN28 is an RNA binding protein and has two paralogs, LIN28A and LIN28B. Its major function is to repress let-7 miRNAs biogenesis. Let-7 miRNAs are markers of cell differentiation and high let-7 levels reduce cell proliferation. We previously reported that LIN28A and LIN28B were significantly lower and let-7 miRNAs were significantly higher in term human IUGR vs normal placenta. LIN28A and LIN28B double knockout in human first trimester trophoblast (ACH-3P) cells led to a significant increase in let-7 miRNAs, significantly decreased expression of proliferation-associated genes including ARID3A, ARID3B, HMGA1, c-MYC, VEGF-A and WNT1 and significantly reduced cell proliferation. ARID3A, ARID3B and KDM4C make a triprotein complex (the ARID3B-complex) which binds to promoter regions of HMGA1, c-MYC, VEGF-A and WNT1. ARID3B knockout in ACH-3P cells disrupted the ARID3B-complex leading to a significant decrease in these proteins and cell proliferation. In this study we hypothesized that LIN28- let-7 axis regulates proliferation of ovine trophoblast cells in vivo by targeting proliferationassociated genes. To test this hypothesis, day 9 hatched sheep blastocysts were incubated with lentiviral particles to deliver shRNA targeting LIN28A or LIN28B specifically to trophectoderm (TE). At day 16, conceptus elongation was significantly reduced in LIN28A and LIN28B knockdown conceptuses compared to control, suggesting reduced proliferation of trophoblast cells. Let-7 miRNAs were significantly increased and proliferation-associated proteins IGF2BP1-3, HMGA1, ARID3B and c-MYC were significantly decreased in trophectoderm from knockdown conceptuses compared to control. This suggests that the

LIN28- let-7 axis regulates proliferation of sheep trophoblast cells by targeting proliferation-associated genes. To further test this hypothesis, ovine trophoblast (OTR) cells were derived from day 16 trophectoderm. Surprisingly, after only a few passages LIN28 was significantly reduced and let-7 miRNAs significantly increased compared to day 16 TE suggesting that passaged OTR cells represent a more differentiated phenotype of trophoblast cells. To create an OTR cell line more similar to day 16 trophectoderm we overexpressed LIN28A and LIN28B, which significantly decreased let-7 miRNAs, significantly increased IGF2BP1-3, HMGA1, ARID3B and c-MYC and significantly increased cell proliferation. These results suggest that reduced LIN28 during early placental development may decrease trophoblast proliferation at a critical period for successful establishment of pregnancy. This project was supported by Agriculture and Food Research Initiative Competitive Grant no. 2017-67015-26460 from the USDA National Institute of Food and Agriculture.

Trainee Research Award Platform Competition - Post Doctoral

Abstract # 2197

Induced Pluripotent Stem Cell Gene-Editing Therapy In An Infertile Mouse Model To Restore In Vivo Spermatogenesis. Amanda Colvin Zielen, University of Pittsburgh, USA

Approximately 1% of men in the general population have azoospermia where sperm is absent from their ejaculate. Non-obstructive azoospermia (NOA) is more common (~85%) than obstructive azoospermia; 15% of NOA patients also have a maturation arrest phenotype (NOA-MA) where germ cells are present in the testes but fail to complete spermatogenesis, likely due to a genetic defect. Sperm recovery rates from men with NOA-MA are relatively low, severely limiting their options for having biological children. We hypothesized that if a single gene mutation is identified to cause NOA-MA in a patient, then ex vivo geneediting of germ cells will restore gene function and in vivo transplantation of gene-corrected germ cells will regenerate spermatogenesis in infertile males. To test our hypothesis, we used CRISPR/Cas9 gene-editing to produce mice with an 11 base-pair deletion in the minichromsome maintenance 8 (Mcm8) gene at a location analogous to one of our Pittsburgh patients. Mutations in MCM8 are associated with male and female infertility as well as DNA damage/repair defects and cancer in clinical and murine studies. Mcm8-11/-11 mice exhibited an NOA-MA infertility phenotype. Homozygous Mcm8(-11) male mice were unable to sire offspring when paired with wildtype females, while heterozygous Mcm8+/-11 mice sired 3.6 ± 0.13 litters in five months with 7 ± 0.8 pups per litter. Compared with normal littermate controls, Mcm8-11/-11 testes were significantly reduced in size (Mcm8+/+ 115±4.9mg per testis, n=10; Mcm8+/-11 were 108±4.3 mg, n=20; Mcm8-11/-11 were 20.2±1mg, n=7). No sperm were recovered from the tail of the epididymis of Mcm8-11/-11 mice, and there was not a significant difference (p=0.25, t-test) in sperm counts (Mcm8+/+ 8.9±1.4 x106 sperm; $Mcm8+/-11 6.6\pm 1.0 \times 106$ sperm) of wildtype and heterozygous mice. Hematoxylin and eosin staining of eight-week old Mcm8-11/-11 testis sections showed tubules varying between 0-3 germ cell layers, while heterozygous and wildtype sections had tubules with complete spermatogenesis. Preliminary immunohistochemistry staining identifies undifferentiated spermatogonia (SALL4), differentiating spermatogonia (STRA8), and spermatocytes (SYCP3) in Mcm8-11/-11 testicular sections; we are currently quantifying our results. Attempts to establish spermatogonial stem cell (SSC) lines from these animals for ex vivo gene-editing were not successful. Therefore, we isolated fibroblasts from

Mcm8-11/-11 mice and programmed them to become induced pluripotent stem cells (iPSCs). Three novel Mcm8-11/-11 mouse iPSC lines were generated, cloned, and characterized (alkaline phosphatase staining, immunocytochemistry staining with pluripotency markers: OCT-4, SOX-2, NANOG, and SSEA-1; along with teratoma formation and karyotype analyses). A validated Mcm8-11/-11 iPSC clone was gene-edited using CRISPR/Cas9 and an oligonucleotide template containing the wildtype Mcm8 sequence. We identified four clones with one Mcm8 allele corrected back to the wild type (Mcm8+/-11). Gene-edited (Mcm8+/-11) clone 14 was differentiated to primordial germ-cell-like cells (PGCLCs) that exhibited a SSEA1+/CD61+ phenotype. FACS sorted, gene-edited PGCLCs were transplanted into four 5week old W/Wv mice. Breeding trials are ongoing. This work was supported by NIH grants P50 HD096723 to KEO, T32 HD087194 to ACZ, and the Magee-Womens Foundation.

Abstract # 1980

Somatic Cell Lineage Specification by Notch Signaling in Fetal Mouse Ovaries. Saniya Rattan, National Institute of Environmental Health Sciences

Organogenesis of the ovary is a complex process involving germ and somatic cell lineage determination. Somatic cells in the fetal ovary give rise to the supporting or granulosa cell lineage and the interstitial cell populations. After birth, interstitial cells differentiate into the theca cells and ovarian stroma. Interstitial cells not only play a critical role in steroidogenesis, but are also implicated in ovarian disorders such as polycystic ovarian syndrome, primary ovarian insufficiency, and androgen-producing tumors. Despite their role in normal ovarian functions and diseases, the developmental processes determining interstitial cell progression are not clearly defined. Here, we performed a time-course analysis of somatic cell fate progression with a focus on the interstitium by genetic lineage-tracing experiments in the mouse ovary. Before the onset of ovarian organogenesis, somatic cells are thought to be homogeneous with the expression of SF1 (Steroidogenic factor 1). To our surprise, we discovered a subpopulation of SF1 + somatic cell progenitors that expressed Hes1, a transcription factor indicative of NOTCH pathway activation. Expression of Hes1, which was absent in the supporting cell lineage, represented the earliest event that defines the interstitial cell lineage. We next investigated the importance of the interstitium-specific pattern of Hes1 expression by ectopically activating NOTCH signaling in all somatic cells in the fetal ovary. Constitutive activation of NOTCH resulted in defects of cell lineage specification and ovarian development. The steroidogenic interstitial cells and ovarian stromal cells were significantly reduced and follicular arrest occurred in neonatal ovaries that constitutively expressed NOTCH in both the supporting and the interstitial cell lineages. These results illustrate that the somatic cell pool in the undifferentiated ovary is heterogenous and not homogenous as previously thought. The interstitial cell lineage is defined earlier than the supporting cell lineage in the undifferentiated ovary by the activation of the NOTCH pathway. A properly tuned NOTCH pathway is absolutely essential for interstitial and supporting cell development and folliculogenesis. This research was supported by ---the National Institute of Environmental Health Sciences intramural research funds.

Abstract # 2217

Spatial Dynamics Of Protein Translation In Sertoli Cells. Ana Cristina Lima, Oregon Health & Science University, USA

The Sertoli cells (SC) of the testis juggle a panoply of functions required for male germ cell development and reproductive health. To attain such fine-tuned control, SCs are thought to compartmentalize their functions in distinct subcellular domains. We hypothesized that, similarly to neurons, this mechanism is regulated by localized translation of mRNAs and on-site production of specialized proteins. To visually detect translation in SCs by immunofluorescence, we adapted the technique of surface sensing of translation (SUnSET) to our system. Both in vitro (TM4 cell line) and in vivo (C56BL/6J mouse testis) results indicated the presence of translation sites distally to the SC nucleus. Next, we looked for mRNAs that could potentially be locally translated at these sites, by generating transcriptome data of TM4 cells and additionally mining 3 published murine RNA-seg datasets. Among others, the tubulobulbar complex protein actin-related protein 3 (Arp3) and the blood-testis barrier Claudin 11 (Cldn11) stood out as potential targets of localized translation. Their mRNA is differentially expressed in SCs during the first-wave of spermatogenesis and the protein shows stage-specific subcellular localization. SUnSET coupled with single molecule fluorescence in situ hybridization (smFISH-IF) showed the presence of the mRNA and protein of Cldn11 and Arp3 at the sites of active translation in SCs. These can be found basally, at the blood-testis barrier, and adluminally, adjacent to elongated spermatids in a stage-specific manner (VII-VII).

We then used this approach to investigate the spatial dynamics of protein translation in SCs during the cycle of the seminiferous epithelium. Stage-specific patterns of protein translation could represent relevant biological events that

when disrupted could lead to disease. Using ImageJ and R software, we developed a computational pipeline for image and data analysis of testicular sections marked for translation and/or mRNA and protein of interest. To capture the temporal information provided by the cycle of the tubules, we used the Acrv1 protein for tubule staging as previously described. This approach allowed us to collect spatial data for localization of protein translation during the 12 different stages of mouse spermatogenesis, from 5-15 tubules per stage. Concordant with the microscopy observations, general protein translation in SC changes dynamically throughout the cycle. Remarkably, the number of translation sites are significantly higher at stage 7, when these SCs are remodeling the blood-testis barrier, establishing the tubulobulbar complex and preparing for spermiation. Our results indicate that SC may indeed compartmentalize their functions by mRNA transport and localized production of specialized proteins. This novel approach will provide a landscape of spatial regulation of mRNA translation in SCs and allow us to ask questions about how local translation is involved in different abnormal phenotypes.

Abstract # 1768

Age-dependent Dysregulation of Hyaluronan and Collagen Matrices Alters Ovarian Biomechanical Properties. Farners Amargant, Northwestern University, USA

Female reproductive aging is associated with infertility due to decreased egg quality and quantity. We recently identified that there is an increase in collagen (fibrosis) in the ovarian stroma with advanced reproductive age, likely affecting gamete quality. Hyaluronan (HA) is an extracellular matrix glycosaminoglycan that maintains tissue homeostasis, and its loss can change tissue micromechanical properties, leading to a mechanically stiff microenvironment. Therefore, we hypothesized that reproductive aging is associated with a loss of ovarian HA, which promotes stromal stiffness and fibrosis. HA levels are dictated by the relative activities of enzymes that regulate its synthesis (hyaluronan synthases) and degradation (hyaluronidases). To investigate whether there were age-associated changes in these enzymes, we performed real time PCR to examine the expression of hyaluronan synthases (Has1, Has2, Has3) and hyaluronidases (Hyal1, Hyal2, Tmem2, Kiaa1199) in enriched ovarian stromal tissue from reproductively young (6-12 weeks) and old (14-17 months) CB6F1 mice. Of these genes, Has3 and Hyal1 were the only ones whose expression changed with age, with Has3 expression decreasing (1.45-fold change) and Hyal1 expression increasing (1.38-fold change). We further validated their

stromal expression and localization using RNA in situ hybridization. These gene expression changes would predict a net loss of ovarian stromal HA with age. To investigate this, we assessed the HA content in the ovary using a hyaluronic acid binding protein (HABP) assay. HA was detected in follicles, corpora lutea (CL), and the ovarian stroma, and the total ovarian HA content was significantly reduced in reproductively old mice compared to young controls (p=0.008). This reduction in HA occurred specifically in the stroma, as HA loss in other ovarian sub-compartments was not significant between age cohorts (follicles p=0.056; CL p=0.55). To examine how advanced reproductive age affects ovarian micromechanical properties, we performed nanoindentation analysis to measure ovarian stiffness. It took more force to indent ovaries from reproductively old mice $(3.57\pm2.4kPa)$ compared to young mice $(1.69\pm2.4kPa)$; p<0.001). We then examined whether the increase of ovarian stiffness with age was dependent on the increase in collagen and the decrease in HA content by quantifying the micromechanical properties of collagenase-treated and Has3-/- mice ovaries, respectively. Reducing collagen content in reproductively old mouse ovaries restored the micromechanical properties to those of ovaries from young mice (reproductively young 1.98±0.42kPa; reproductively old 4.36±1.24kPa; reproductively old collagenase 2.28±0.61kPa). On the other hand, Has3-/- ovaries were stiffer than ovaries from age-matched wild-type (WT) mice (WT 2.51±0.66kPa; Has3-/- 6.67±2.00kPa; p=0.0079). These results demonstrate that both increased collagen and HA loss in the ovarian stroma contribute to the increase in ovarian stiffness observed with age. These findings are significant because the use of pharmacological approaches to prevent collagen and HA changes in the stroma with age may enhance reproductive longevity. This work was supported by the National Institute of Child Health and Human Development (R01HD093726).

Abstract # 2143

Abnormal Pattern Of Ca2+ Oscillations During Fertilization In Vivo Impairs Offspring Growth Trajectory In The Mouse. Virginia Savy, National Institute of Environmental Health Sciences, USA

During mammalian fertilization, the sperm triggers a series of oscillations in the egg's intracellular Ca2+ concentration ([Ca2+]i), which is the hallmark signal for egg activation. Interestingly, experimental manipulation of [Ca2+]i in vitro during or immediately after fertilization results in alterations in the blastocyst transcriptome, implantation success and offspring health. However, it remains unclear whether the findings reported from in vitro studies recapitulate the

complex regulation of in vivo fertilization. Here we tested the hypothesis that, even in the highly specialized environment of the oviduct, appropriate Ca2+ signaling after fertilization is critical for proper preimplantation embryo development and offspring growth. In somatic cells, plasma membrane Ca2+ ATPase (PMCA) pumps are responsible for clearing excess Ca2+ from the cell following Ca2+ release events. We found that in mouse eggs, the most highly expressed PMCA isoform was PMCA1 (encoded by Atb2b1). To generate mouse eggs with abnormally increased [Ca2+]i exposure following fertilization, we conditionally deleted PMCA1 (cKO) in oocytes using the Zp3-cre transgene. As anticipated, in vitro fertilized cKO eggs had a much longer first Ca2+ transient than controls (mean \pm SEM: 11.3 \pm 1.0 min, N=30 vs 3.6 \pm 0.3 min, N=49; p<0.0001); however, the oscillation frequency was similar between groups. Assuming a comparable difference in Ca2+ dynamics between control and cKO egas during in vivo fertilization, we evaluated the impact of altered Ca2+ signaling following fertilization on offspring growth trajectory. Heterozygous (Atp2b1+/-) offspring from Atb2b1-flox/flox; Cre+ females mated with wild type males were weighed weekly for 8 weeks. Wild type (Atp2b1+/flox) offspring from Atb2b1-flox/flox females mated to wild type males served as controls. Offspring weigh at birth was similar between groups for both females and males; however, growth trajectory was different between groups by the 1st week of age. On average the experimental males were 14.7% smaller than controls at 8 weeks (mean weight \pm SEM: 22.9 \pm 0.3 g, N=33 vs 20.4 \pm 0.3 g, N=34, males from 17 litters), whereas females were 5.9% smaller than controls (18.1 \pm 0.2 g, N=29 vs 17.0 ± 0.2 g, N=30, females from 17 litters). Despite the altered postnatal growth rate, cKO-derived mice had normal glucose and insulin tolerance at 3 months of age. Our findings strongly support the idea that appropriate Ca2+ signaling in the first few hours following fertilization is necessary to ensure appropriate embryo "quality" and offspring health. Given the essential role of Ca2+ signaling for egg activation and embryo development, further research is necessary to decode the link between Ca2+ dynamics and long-term effects on offspring health, to ensure safe clinical practices during assisted reproductive procedures.

Abstract # 2186

Genetic Control Of The Uterine-Placental Interface. Ayelen Moreno, University of Kansas Medical Center, USA

The hemochorial placenta is organized into functional compartments that are situated at the uterine and fetal interfaces. At the uterine interface trophoblast cells migrate into the uterus where they effectively transform the uterine vasculature and facilitate the delivery of maternal nutrients into the placenta. An essential transport/barrier function for maternal nutrient delivery to the fetus is provided by trophoblast cells interacting with the fetal vasculature at the fetal interface. In contrast to the mouse, the uterine-placental interface is well developed in the rat and human. Trophoblast cells with invasive properties, arise from the junctional zone in the rat and a homologous structure in the human placentation site termed the extravillous trophoblast column, and migrate deep into the uterus. Thus, development of the junctional zone and the extravillous trophoblast column are vital to establishing the uterine-placental interface. Some insights into junctional zone development have arisen from mutagenesis of Plac1 and Phlda2 loci in the mouse. However, the mouse has limitations for investigating the uterine-placental interface. Consequently, in this study we examine the biology of PLAC1 and PHLDA2 in the rat. Plac1 and PhIda2 are differentially expressed in compartments of the placentation site over the course of gestation. To study the impact of PLAC1 and PHLDA2 on the uterine-placental interface we generated global loss-of-function rat models using CRISPR/Cas9 genome editing. Exon 3 of the Plac1 gene and Exon 1 of the Phlda2 gene were independently targeted in separate experiments. CRISPR/Cas9 reagents were electroporated into embryonic day 0.5 rat zygotes. Zygotes were then transferred into the oviducts of pseudopregnant female rats. Offspring were screened by PCR and mutations confirmed by genomic DNA sequencing. A mutant Plac1 rat founder was generated with a 469 bp deletion that removed >95% of the Plac1 coding sequence and a mutant PhIda2 rat founder was produced containing a 103 bp deletion in Exon 1 resulting in a frameshift and a premature stop codon. Both mutations were effectively transmitted through the germline. Plac1 is an X-chromosome linked gene and PhIda2 is situated on Chromosome 1 and is paternally imprinted. Deficits in either gene did not affect postnatal survival; however, disruptions in Plac1 and Phlda2 did affect placental development. Plac1 null or inheritance of the maternal Plac1 mutant allele yielded placentomegaly. Specifically, the enlarged placenta was characterized by an expanded junctional zone, an irregular junctional zone-labyrinth zone boundary, and a compromised uterine-placental interface. Intrauterine interstitial invasive trophoblast cell migration was severely attenuated in Plac1 mutants. In summary, our experimentation confirms the involvement of PLAC1 and PHLDA2 in hemochorial placenta development and provides a new set of tools for investigating the roles of PLAC1 and PHLDA2 in an important model of deep placentation. PLAC1 and PHLDA2 represent important entry points into molecular pathways controlling development of the uterine-placental interface. (Supported by an ADA fellowship to JN, AHA fellowships to MM and KK, NIH grants HD020676; HD079363, HD099638, and the Sosland Foundation)

Abstract # 1668

A Role for the Transcription Factor SP6 Within the Primitive Syncytium at the Peri-Implanation Stage of Human Embryo Development. Yuliana Tan, The Jackson Laboratory for Genomic Medicine, USA

The primitive syncytium (PrSyn) is a simian-specific trophoblast cell type that mediates blastocyst attachment and invasion into the endometrium at the periimplantation stage of development. It is at this stage that loss of human embryos is greatest. Knowledge of the PrSyn is largely based on historical morphological studies; the molecular cell biology of the PrSyn remains poorly understood. We have identified the expression of SP6 (also known as epiprofin) within the late stage human blastocyst temporally and cellular correlated with known syncytiotrophoblast markers. SP6, a three C2H2 zinc finger motifs-containing transcription factor well characterized in mouse epidermal development, is not expressed in the mouse trophoblast lineage. We hypothesized SP6 regulates simian-specific features of the peri-implantation embryo, specifically in the formation and function of the PrSyn.

To test this, we have generated SP6 knockout (SP6KO) human induced pluripotent stem cell (iPSC) lines and differentiated these into the trophoblast lineage in which SP6, in the wildtype, is first expressed at Day 3. We compared the molecular and morphological phenotype of SP6KO to wild type (SP6WT) cells through iPSC to PrSyn differentiation. Additionally, we established a trophoblast organoid culture system derived from human iPSCs and used this to test differences in invasion between SP6KO and SP6WT cells. A morphological phenotype assessment using immunofluorescence confocal imaging showed reduced syncytial cells (25% vs 34%) and increased Ki67 expression in the SP6KO line suggesting defects in fusion and cell cycle regulation. Transcriptome analysis show no significant difference at day 3, but by day 5 of differentiation revealed 223 down-regulated and 24 up-regulated genes (logFC = 1.5, FDR = 0.05) within the SP6KO. Gene ontology and literature analysis indicated functions enriched in post-translational modification of proteins regulating cell cycle, cell adhesion and migration (TRPV2, DUSP9, PREX1, ZNF703, FAM65B, MYC, BCL2), cell fusion (ERVW-1, ERVFRD-1), epidermal differentiation (TGFBR2, HBEGF, NOTCH1, HEY1, ENDOU, DACT2), cytoskeletal and extracellular matrix remodeling (KRT80, CRIP2, LRRC15, CDKL5, MTSS1, MCAM, ASB2), response to hormones (PITX1, ZFHX3, NCOA3, DIO3), and immune regulation (FAM65B, IL7R, CD274, VSIR, PRDM1,

SERPINB12, ERVFRD-1, ERVV-2), which are indicative of the PrSyn's important role in communication with endometrium during implantation. We would argue SP6 has an essential role in human, but not mouse, peri-implantation biology and that components of the epidermal differentiation program have been co-opted for use at this stage. This study emphasizes the utility of this PrSyn model to address questions in early human development and the molecular mechanism at play in cell type evolution.

Trainee Research Award Poster Competition – Pre-Doctoral

Abstract # 2064

Spatial and temporal dynamics of FGL2 expression reveal immunoregulatory function essential to the establishment and outcome of pregnancy. Pascale Robineau-Charette, Ottawa Hospital Research Institute

Fibrinogen-like protein 2 (FGL2) is a known immunomodulator and prothrombinase, previously suggested to be involved in the immune balance of the maternal-fetal interface that is crucial to reproductive success. The female reproductive tract is the site of several key events that require careful endocrine and immunological regulation, from ovulation to pre-implantation embryo transport and placentation. We mapped spatial and temporal dynamics of FGL2 expression through murine reproductive tissues, which revealed remarkable cell type specificity hinting at precise function. We carefully examined several parameters of reproductive performance in our Fgl2 knockout (ko) and overexpressing (tg) mouse colonies. Fgl2 ko females produced only half as many pups as their wild-type (wt) counterparts, due to smaller and less frequent litters. Interestingly, this phenotype was rescued in Fal2 ta X Fal2 ko mating pairs, despite the presence of only one overexpressing allele. We observed equal rates of embryo resorption in all three genotypes, suggesting a defect in Fgl2 ko ovarian or oviductal (pre-implantation) function. In the ovary, FGL2 is expressed in the stroma and theca cell layer of follicles, and intensity of expression peaks 8 hours after hCG injection in a superovulation cycle. Strong expression is acquired by some cumulus granulosa cells shortly before ovulation and persisting in cumulus-oocyte complexes (COCs) found in the oviduct, suggesting a role in ovulation and in luteinization. Fal2 ko and Fal2 ta animals however had a normal ovulation efficiency, as measured by the number of COCs retrieved after superovulation. Fgl2 ko and wt ovaries showed equivalent numbers of functional corpora lutea, demonstrating normal luteinization. In the oviduct, FGL2 expression is restricted to secretory cells of the epithelium, whose frequency increase from the fimbrial to the isthmal end. We detected FGL2 in the culture medium of OVE4, primary oviductal epithelial cells, confirming its secretion into oviductal fluid, where it likely contributes to the immunosuppressive environment conducive to fertilization and to tolerance of paternal/fetal antigens. Single-nuclei RNA sequencing of the ovary, ampulla and isthmus at different timepoints after superovulation will reveal differential immune dynamics between Fgl2 wt and ko animals, to identify mechanistic actions of FGL2 in these tissues. Despite being born at rates comparable to wt mice, Fgl2 tg pups are significantly smaller than their wt and ko counterparts, at birth and at weaning, indicating a probable deficient placental function.

Interestingly, we found that women with high placental FGL2 expression tend to be affected by an immunological subtype of preeclampsia, characterized by chronic inflammatory placental lesions and small for gestational age infants. Our histological examination of term placentas from Fgl2 tg animals will confirm correlative evidence, in the human placenta, of FGL2's role as an immunoregulator at the maternal-fetal interface. Overall, this work supports the hypothesis that FGL2 is secreted throughout the female reproductive tract at precise stages of the estrous cycle, and in the developing placenta, as a physiological attempt to maintain the careful immune equilibrium required for the successful establishment and maintenance of pregnancy.

Abstract # 1760

Single Cell Interrogation Of The Uterine-Placental Interface. Regan L. Scott, University of Kansas Medical Center, USA

During a healthy pregnancy, a special lineage of placental cells, referred to as invasive trophoblast cells, exit the placenta and invade into the uterus where they restructure the uterine parenchyma and facilitate remodeling of spiral arteries. Invasive trophoblast cells help anchor the placenta, modulate immune cell populations, and facilitate nutrient delivery to the fetus. These trophoblastdirected uterine modifications are essential for a healthy pregnancy. Insufficient trophoblast invasion and abnormal cross-talk at the uterine-placental interface are major contributors to obstetrical complications such as early pregnancy loss, preeclampsia, intrauterine growth restriction, and pre-term birth. In humans, these events transpire during early gestation, thus their investigation represents a significant ethical challenge. In vitro analyses can provide insights into trophoblast cell potential but fall short as tools to understand the physiology of the invasive trophoblast cell lineage. Implementation of in vivo models to test hypotheses regarding mechanisms underlying the development and function of the invasive trophoblast cell lineage are essential to advance the field. Rodents exhibit hemochorial placentation similar to humans. While the mouse displays shallow trophoblast invasion, the rat exhibits deep intrauterine trophoblast invasion and extensive uterine spiral artery remodeling, comparable to what is observed in the human. In this study, we sought to phenotype cells at the uterine-placental interface of the rat with the goal of identifying conserved candidate regulators of the invasive trophoblast cell lineage. Single-cell RNA sequencing (scRNA-seq) and single-cell assay for transposase-accessible chromatin sequencing (scATAC-seq) were used to interrogate cells at the uterine-placental interface on gestation days 15.5 and 19.5 of the Holtzman

Sprague-Dawley rat. Single cell suspensions were prepared by enzymatic digestion of the uterine-placental interface. Single cell libraries were then constructed using the 10X Genomics platform and sequenced with an Illumina NovaSeg 6000 system. Computational analysis with the Cellranger pipeline led to the identification a number of unique cell clusters defined by their transcript profiles, including invasive trophoblast cells (e.g. Prl5a1, Prl7b1, Tpbpa, Plac1, Tfap2c, Igf2, Cdkn1c, Tfpi), endothelial (e.g.Egfl7, Adgrl4, Rasip1, Sox17, Nos3), vascular smooth muscle (e.g. Acta2, Myl9, TagIn, Myh11), natural killer (e.g. Nkg7, Prf1, Gzmb, Gzmm), and macrophage (e.g. Fcgr3a, Lyz2, Aif1, Tyrobp, Cybb) cell clusters. A prominent subset of rat invasive trophoblast cell transcripts is conserved in the invasive extravillous trophoblast cell lineage of first trimester human placenta (e.g. lgf2, Cdkn1c, Tfpi, Ascl2, Mmp12, Cited2, etc). Nuclei were also isolated from the single cell preparations of the uterineplacental interface, libraries prepared, and sequenced. Analysis with the Cellranger-ATAC pipeline identified unique clusters based on chromatin accessibility, including invasive trophoblast, endothelial cell, vascular smooth muscle, natural killer cell, and macrophage clusters. ASCL2, AP1, TFAP2C, and ATF1 DNA binding motifs were most abundant in accessible regions of the invasive trophoblast cell clusters. These findings provide a foundational dataset to identify and interrogate key conserved regulatory mechanisms essential for development and function of an important compartment within the hemochorial placentation site that is essential for a healthy pregnancy. (Supported by HD020676, HD096083, HD099638; Pew Charitable Trust, Sosland Foundation)

Abstract # 1788

Chlamydia Infects The Ovary, Elicits An Immune Response And Depletes The Ovarian Reserve In Mice. Urooza C. Sarma, Monash University, Australia

Chlamydia trachomatis is the most common sexually transmitted infection worldwide and can cause severe damage to the Fallopian tubes, often resulting in complete infertility. Recent studies indicate significantly increased miscarriage rates and time to natural conception, along with poor IVF outcomes in women seropositive for Chlamydia but in the absence of tubal pathology, suggesting that that fertility may be compromised by mechanisms that extend beyond fallopian tube scarring. In this study, we used a well-characterised mouse model to investigate the hypothesis that Chlamydia can infect and damage the ovary. Chlamydial DNA was detected in ovaries at 6 and 35 days post infection (pi) using qPCR and inclusion bodies were localised within macrophages in the ovarian stroma using immunofluorescence. Chlamydial infection was associated with an increase in the expression of mRNA for CXCL16 and IFNy, suggesting the induction of a pro-inflammatory immune response within the ovary, which persists at least up to 35 days pi. Significantly greater numbers of immune cells including macrophages, NK cells and CD4+ /CD+ cells in the ovary 35 days pi, suggesting a localised ovarian inflammatory response to chlamydial infection, parallels this. Strikingly, the number of ovarian follicles was significantly reduced 35 days following a single infection compared to uninfected controls (p<0.05, n=4-5 mice/group) and the extent of follicle depletion was greater following a second infection (p<0.05, n=4-5 mice/group). Two infections was also associated with changes to the overall ovarian morphology and increased apoptosis and fibrosis in the ovary (p<0.05, n=5/group), consistent with activation of a prolonged inflammatory response. Collectively, these observations demonstrate that Chlamydia can penetrate the ovary, deplete the ovarian reserve and compromise ovarian function, and suggest that the ovary may act as a potential reservoir of infection. Ovarian follicles are essential for female fertility because they secrete hormones and contain oocytes. Follicles cannot be replaced once lost from the ovary. Thus, our data suggests that damage to the ovary caused by Chlamydia is permanent and may underlie some cases of unexplained infertility and poor IVF outcome in women.

Abstract # 1690

Uncovering A TAF4b-Dependent Gene Expression Program Required For Embryonic Oocyte Differentiation. Megan A. Gura, Brown University, USA

Proper embryonic female germ cell development is critical for the healthy establishment of the adult ovarian reserve. T BP- A ssociated F actor 4b (TAF4b) is a subunit of the basal transcription factor TFIID complex, which is required for RNA Polymerase II recruitment in gonadal tissues. Taf4b -deficient female mice are infertile due to several related deficits of embryonic germ cell development including increased chromosome asynapsis, excessive germ cell death, and delayed germ cell cyst breakdown. We have previously demonstrated that Taf4b mRNA and protein expression are nearly exclusive to the germ cells of the embryonic ovary from E9.5 to E18.5 and its expression is directly regulated by STRA8 and DAZL in male meiotic germ cells. Therefore, we hypothesized that TAF4b, as part of germ cell-specific from of TFIID, regulates oogenesis and meiotic gene programs. To elucidate a TAF4b-dependent program of embryonic oocyte development, we performed low-input RNA-sequencing on GFP+ germ cells sorted from Oct4-EGFP transgenic mice that were Taf4b -

heterozygous or -deficient at E14.5 and E16.5. To our surprise, gene ontology analysis of our differentially expressed genes (DEGs) showed few germ cell development-related genes deregulated in the absence of TAF4b. Importantly, a few notable genes were down-regulated in the Taf4b -deficient germ cells such as Nobox. Brca2, Rhox10, and Rhox13. There were several unexpected DEGs such as Mtor, Apoe, Clock, and Igf2. Further perplexing from this RNAseq analysis was the proportion of DEGs on the X chromosome at each time point, especially several members of the MAGE and RHOX gene families. For E14.5 DEGs in the Taf4b -deficient germ cell, there were very few downregulated genes but many up-regulated genes located on the X chromosome. At E16.5 the trends were precisely the reverse, many down-regulated genes but no up-regulated genes were on the X chromosome. These interesting results implicate an unexpected but important role of TAF4b in regulating gene expression on the X chromosome during oocyte development. We are currently performing CUT & RUN using mouse embryonic stem cells and sorted embryonic female germ cells to clarify which genes are directly bound by TAF4b. This research may add new dimensionality to the female germ cell transcriptome as we uncover new genes that participate in the healthy development of the ovarian reserve.

Abstract # 1857

Endometrial Epithelial ARID1A Loss Causes Defects of Uterine Receptivity and Endometrial Gland Function. Ryan M. Marquardt, Michigan State University, USA

Endometrial receptivity is key to successful pregnancy establishment and is compromised in many women with endometriosis. ARID1A, a SWI/SNF chromatin remodeling complex subunit, is attenuated in the endometrium of women with endometriosis. Moreover, conditional uterine Arid1a knockout mice are infertile due to endometrial receptivity defects resulting from increased pre-implantation epithelial proliferation. We thus hypothesized that epithelial ARID1A loss compromises fertility by causing a non-receptive state in the endometrium. To examine the effects of endometrial epithelial-specific ARID1A loss, we established a conditional knockout mouse where Arid1a is ablated in the endometrial epithelium (Ltficre/+Arid1af/f). We observed severe subfertility in Ltficre/+Arid1af/f mice in a six-month breeding trial (n=6). Immunohistochemical analysis revealed a failure of embryo implantation and stromal cell decidualization test confirmed the compromised decidual response (n=6) caused by Arid1a loss in the endometrial epithelium. Ltficre/+Arid1af/f mice also

exhibited a non-receptive endometrium at pre-implantation stage (GD 3.5) due to increased epithelial proliferation (n=3), and we found significant reduction in expression levels of endometrial gland-related genes including Foxa2 (n=5; p<0.01) and Lif (n=4-5; p<0.05), critical factors for pregnancy establishment. Furthermore, ChIP analysis indicated that ARID1A directly binds the Foxa2 promoter during early pregnancy in wild type mouse uterus (n=5), implying direct transcriptional regulation of Foxa2 by ARID1A. Previous experiments revealed that implantation and decidualization can be rescued in uterine Foxa2 knockout mice by LIF repletion at GD 3.5. However, LIF repletion did not rescue implantation in Ltficre/+Arid1af/f mice, assessed histologically at GD 5.5 (n=3). Despite the failure of LIF to rescue implantation, phospho-STAT3 and EGR1, downstream signaling targets of LIF important for implantation and decidualization, were significantly decreased around Ltficre/+Arid1af/f implantation sites at GD 4.5 based on IHC H-score (n=3; p<0.001). Taken together, these data indicate that loss of preimplantation LIF expression is disrupted by endometrial epithelial Arid1a ablation but is not the sole cause of implantation failure. Our results reveal the importance of epithelial ARID1A in promoting endometrial receptivity by allowing proper implantation and decidualization, regulating epithelial proliferation, and maintaining aland function. Research reported in this publication was supported in part by the Eunice Kennedy Shriver National Institute of Child Health & Human Development of the National Institutes of Health under Award Number R01HD084478 to J.W.J. and T32HD087166 to R.M.M., MSU AgBio Research, and Michigan State University. The content is solely the responsibility of the authors and does not necessarily represent the official views of the National Institutes of Health.

Abstract # 2183

BVDV Infection Epigenetically Alters T-Cell Transcription Factors In Persistently Infected Fetal Spleens. Hanah M. Georges, Colorado State University, USA

Maternal infection with Bovine Viral Diarrhea Virus (BVDV) has life-long negative effects on progeny. Despite current preventative measures, BVDV continues to be an issue, costing the industry \$1.5 billion annually and producing infected calves that remain the primary reservoirs of the virus. If fetal infection occurs prior to day 120 of gestation, then the fetus becomes persistently infected (PI) and sheds the virus throughout its life. The mechanisms of persistent infection and impact on postnatal health is still not well known. Previous in vivo studies revealed a substantial activation of the PI fetal innate immune response 22 days after maternal infection. The innate immune activation was then followed by an attenuation of both the innate and adaptive immune branches 115 days after maternal infection. It was concluded that attenuation of the immune system was caused by a lack of T-cell response in the fetus, resulting in an inability for Tcells and B-cells to mature properly. In this study, it was hypothesized that T-cell activation and signaling genes were epigenetically altered after fetal infection, thus impairing the expression of key genes of the innate and adaptive immune responses Splenic tissue from PI and control fetuses were collected on day 245 of gestation, 170 days post-maternal infection. DNA was isolated and sent to Zymo Research for reduced representation bisulfite sequencing. Methylation sequencing files were aligned to the bovine ARS-UCD-1.2 genome using the Bismark package, then processed and analyzed using the methylKit R package. Differentially methylated regions (DMR) were selected based on a 25% difference in methylation compared to controls as well as a p-value cutoff of < 0.05. Within these parameters, 2,641 regions were differentially methylated: 1,951 hypermethylated and 691 hypomethylated regions. Results revealed hypermethylation of nuclear factor of activated T cells (NFAT) 1 and 4, while NFAT2 was hypomethylated. Calcium signaling components, calcium release activated calcium channel protein ORAI and calmodulin, were hypomethylated. Additionally, signal transducer guanine nucleotide exchange factor VAV1 was hypermethylated. Calcium regulated NFAT family members consist of NFAT 1,2, and 4. The NFAT family is critical in T-cell activation/anergy as well as cardiac development. NFAT 1 and 4 are associated with T helper (Th) 1 cell differentiation, while NFAT 2 is associated with Th2 cell differentiation. Hypermethylation of NFAT 1 and 4 is likely to shift the Th cell differentiation from Th1 to Th2 cells. An increase in NFAT2 and VAV1 expression due to hypomethylation would promote anergy of T-cells, further exacerbating the shift from Th1 to Th2 cells. This shift of Th cells is associated with T-cell receptor hyperreactivity and lymphoproliferative disorder. Additionally, the hypomethylation of ORAI and calmodulin may contribute to the Th2 hyper-reactivity by increasing the amount of calcium transported into a cell upon T-cell activation. The observed epigenetic modification of critical T-cell genes may help explain inability of postnatal PI calves to fight secondary infections efficiently, contributing to performance loss and continued BVDV viral shedding. This work is supported by: USDA AFRI NIFA Predoctoral Fellowship 2019-67011-29539/1019321, 2016-38420-25289 and W3112 Project.

Trainee Research Award Poster Competition - Post Doctoral

Abstract # 2142

Anti-Coagulation Factor Contributions To Placental And Fetal Development. Ross McNally, University of Kansas Medical Center, USA

During gestation in many mammalian species trophoblast cells are directly bathed in maternal blood. It is this hemochorial placentation that is responsible for the intimate communication between both maternal and fetal compartments. One such placenta-mediated event involves trophoblast cell transformation of the uterus; wherein invasive trophoblast cells migrate from the placenta and restructure the maternal vasculature thus providing adequate blood flow to the developing fetus. Aberrant trophoblast cell development and function lead to obstetrical complications that are associated with coagulopathies. Trophoblast cells can regulate thrombotic activity through the production of anti-coagulation factors, including tissue factor pathway inhibitor (TFPI) and thrombomodulin (THBD). In mice, loss of TFPI or THBD results in prenatal lethality. Disruption of mouse Tfpi or Thbd genes is associated with anomalous placentation, which was viewed as a contributor to the in-utero demise. Mouse models do not adequately mirror the deep intrauterine trophoblast invasion observed in human and rat placentation. Consequently, in this study we examine the biology of TFPI and THBD in the rat. TFPI and THBD are differentially expressed in compartments of the placentation site over the course of gestation. To investigate the physiological roles of these anti-coagulation factors we utilized CRISPR/Cas9 genome editing to establish loss-of-function rat models for TFPI and THBD. Exon 4 of the Tfpi gene and Exon 1 of the Thbd gene were independently targeted in separate experiments. CRISPR/Cas9 reagents were microinjected into embryonic day 0.5 rat zygotes. The zygotes were then transferred into the oviducts of appropriately timed pseudopregnant female rats. Offspring were screened by PCR and mutations confirmed by genomic DNA sequencing. Two mutant Tfpi rat founders were generated: i) 636-bp deletion including all of Exon 4 (Tfpi-K1), which encodes Kunitz domain 1; and ii) 1-bp insertion within Exon 4 (Tfpi1bp); whereas, one mutant Thbd rat founder was produced containing a 1316 bp deletion of Exon 1. Mutations were effectively transmitted through the germline. Heterozygous males and females with any of the Tfpi or Thbd mutations were fertile. However, heterozygous intercrosses for Tfpi-K1, Tfpi1bp, or Thbd rat strains did not yield viable homozygous mutant offspring. Timed heterozygous intercrosses were euthanized at various stages of gestation to determine the onset of in-utero demise. Tfpi-K1 and Tfpi1bp phenotypes were indistinguishable. At gestation day (gd) 11.5 Tfpi null mutants were visibly growth restricted and possessed anemic yolk sacs. All homozygous

Tfpi mutants were dead by gd 13.5. Thbd null mutants exhibited growth restriction by gd 10.5 and were dead by gd 12.5. Rat TFPI deficiency exhibited a uniform prenatal death at midgestation, which contrasts with the reported heterogenous phenotypes associated with mouse TFPI deficiency. Rat and mouse THBD deficiency exhibited similar phenotypes. In summary, we have successfully generated rat models possessing global disruption of Tfpi and Thbd loci. Although, the midgestation lethality of homozygous Tfpi and Thbd rat mutants precludes examining their impact on the uterine-placental interface of late gestation, roles for TFPI and THBD in early placentation events are actively being pursued. (Supported by NIH grants HD020676, HD079363, HD099638; and the Sosland Foundation).

Abstract # 1986

The Filopodia Marker MYO10 Reveals A Novel Method For The Assessment Of Granulosa Cell Function And Quality Of Human Growing Follicles. Sofia Granados Aparici, McGill University Health Centre, Canada.

Therapeutic advances over the recent decades have dramatically increased the number of childhood cancer survivors. This success has focused attention on post-treatment quality of life, including fertility, which is frequently compromised by the therapeutic interventions. Currently, cryopreservation of ovarian tissue is the only option available to pre-pubertal girls. However, the effects of cryopreservation on subsequent oocyte and follicular growth remain little understood, due in large part to a lack of knowledge of the early stages in humans. Beginning early during growth, bi-directional signaling between the oocyte and the follicular granulosa cells that surround it regulate oocyte and follicular development. This essential signaling occurs via specialized actin-rich filopodia that project from the granulosa cells to the oocyte membrane. In view of their essential role during folliculogenesis, these intercellular bridges may be a valuable marker of granulosa cell function and follicle quality. We analyzed the morphology of granulosa cell filopodia, as well as the distribution of a protein (MYO10) implicated in the formation of canonical filopodia, in human follicles at early stages of growth. Fresh ovarian tissue was prospectively collected from patients who underwent ovarian surgery. Frozen ovarian tissue was donated by patients who underwent ovarian tissue cryopreservation due to malignant disease. Follicles from primordial to secondary stages were stained using the Factin binding protein, phalloidin, and anti-MYO10. Confocal microscopy was used to image equatorial optical sections of each follicle. MYO10 expression in the granulosa cells was quantified using Image J. 180 follicles were analyzed

and comparisons made between age range (22-30 vs 35-40 years) and fresh vs frozen-thawed follicles. In primordial follicles, actin was present in the oocyte cortex as well as in the squamous adjacent granulosa cells. However, although no filopodia were detectable, some MYO10 foci were present at the interface with the oocyte plasma membrane. As follicles transitioned to the primary stage, filopodia were seen to project from some granulosa cells to the oocyte. This was accompanied by an increase in the number of MYO10 foci. By the late primary stage, a rich network of filopodia extended from the granulosa cells to the oocyte through a visible zona pellucida, named transzonal projections (TZPs). Correspondingly, many MYO10 foci marked the TZP body. Interestingly, whereas some TZPs reached the oocyte plasma membrane others penetrated and connected each other deep into the oocyte. In follicles obtained from 22- to 30year old women but not in those of 35- 40-year old women, a positive correlation was observed between the distribution of MYO10 in aranulosa cells and oocyte diameter. In frozen-thawed follicles from 22- to 30-year old women, this correlation was no longer observed. Strikingly, large MYO10 aggregates in the oocyte cytoplasm were observed and significantly increased in frozenthawed when compared to fresh follicles. These data suggests a significant impact of age and cryopreservation on the ability of granulosa cells to modulate filopodia formation. Additionally, it identifies a method of molecularly assessing follicle function and quality that may be useful to develop and improve the existing ovarian cryopreservation methods for pre and postpubertal patients.

Abstract # 2157

Cumulus-Oocyte Interaction Is Required To Maintain Active Suppression Of Glycine Transport In The Preovulatory Mouse Oocyte. Allison K. Tscherner, Ottawa Hospital Research Institute, Canada

Oocytes and early embryos are highly sensitive to changes in cell volume. It is now understood that cell volume dysregulation was a major cause of developmental arrest that occurred in traditional embryo culture. Early (1- to 2cell) mouse embryos use a novel mechanism to control cell volume, in which glycine is accumulated intracellularly via the GLYT1 transporter (SLC6A9 protein). While SLC6A9 is expressed and localizes to the membrane of fully-grown oocytes, transport of glycine is absent until this transporter becomes activated by an unknown mechanism. In vivo, GLYT1 activation normally occurs in parallel with release of an oocyte from meiotic arrest that precedes ovulation. It also activates in vitro shortly after oocytes are removed from antral follicles, implying active suppression within follicles. The primary aim of this research is to identify the specific factor(s) responsible for the release of suppression of GLYT1 in oocytes, which are currently not known. To evaluate this, we have established a GLYT1 activity assay based on [3H]glycine uptake and adapted it for single oocyte measurements. Oocytes were cultured within COCs for 4 hours after removal from follicles. We have found for the first time that it is possible to maintain quiescence of GLYT1 in GV oocytes within isolated COCs, in a model where COCs are cultured individually and meiotic arrest is maintained by natriuretic peptide precursor C (NPPC). This suppressive effect is reversed when NPPC is removed. NPPC acts by inducing production of cGMP, which in turn mediates suppression of the oocyte's cAMP-specific phosphodiesterase, PDE3. GLYT1 suppression is similarly maintained when oocyte meiosis is arrested with milrinone, a direct inhibitor of PDE3. However, GLYT1 suppression is maintained only in intact COCs cultured in milrinone, whereas oocytes stripped of cumulus cells maintain meiotic arrest but GLYT1 is activated. Together, these findings indicate that maintaining GLYT1 suppression requires both meiotic arrest and the presence of cumulus cells, though either factor itself is insufficient to maintain active suppression. Finally, since gap junctions between the oocyte and cumulus cells play a major role in the physical association as well as chemical communication between these cells, we impaired gap junctional coupling with specific inhibitors and observed a partial activation of GLYT1 in COCs in the presence of milrinone. Overall, we have shown that the factor maintaining GLYT1 suppression before the resumption of meiosis requires the presence of cumulus cells. GLYT1 quiescence is only maintained under conditions of oocyte meiotic arrest and appears to involve gap junctional communication between cumulus cells and the oocyte. This study highlights the conditions required for glycine transport in vitro and provides insight into the signaling mechanisms likely involved in GLYT1 suppression in ovarian follicles in vivo.

Abstract # 2127

Lipids Involved In Pro And Anti-Inflammatory Responses Are Altered In Follicular Fluid And Plasma Of Cows Administered A Low Dose FSH Treatment And May Be Used As Markers Of Ovulation In Beef Cows. Alexandria P. Snider, University of Nebraska-Lincoln, USA

Superovulation procedures using Follicle Stimulating Hormone (FSH) in cattle promote development of a larger cohort of follicles to increase number of oocytes collected for assisted reproductive technologies. These procedures are used if there are problems associated with ovulation since anovulation is a major factor affecting female fertility. Ovulation has been demonstrated to be an inflammatory process. Thus, our hypothesis was that treatment of cows with a low-dose-FSH protocol (35 IU FSH every 12 hours for 3.5 days plus prostaglandin at last and 12 hours after last FSH; FSHLow) would increase follicular fluid (FF) proinflammatory lipid markers compared to unstimulated controls; and blood plasma lipid markers compared to early or late luteal phase unstimulated controls. Follicular fluid from unstimulated samples was collected prior to and 24 hours after FSHLow. Blood plasma was collected from the same unstimulated cows (n=11) at D7-early luteal control, D15-late luteal control and 24 hours after FSHLow. Lipid compounds (863) were identified via UPLC-MS Analysis (CSH PhenylHexyl method) with 124 lipid compounds annotated utilizing XCMS software package in R. Analysis of variance (AOV) function was used for each lipid compound and p-values were adjusted using the Bonferroni-Hochberg method (p.adjust function) to determine differences in FF and plasma samples in non-stimulated controls and FSHLow-stimulated cows. There were 29 annotated lipid compounds different (p<0.05) in FF. Seventeen are involved in anti-inflammatory responses with ten of them decreased (p<0.05; e.g. HODE cholesteryl ester, C18-02:0 PC) FSHLow compared to control cows. Twelve of the 29 lipids are associated with pro-inflammatory responses with six of them increased (p < 0.05) in FSHLow compared to Controls. Of these six lipids, LysoPC(20:4) and Glycerophosphocholine are involved in cytokine signaling; PE(P-36:2) and SM(d18:1/16:0) stimulate macrophage recruitment; Docosahexaenoyl PAF C-16 stimulates leukocyte localization; and Sodium Glycochenodeoxycholate increases signaling through the NFKB pathway (p<0.05). In blood plasma, 16 lipid markers associated with anti-inflammatory and 16 associated with pro-inflammatory responses were altered in cows after FSHLow compared to Day 7 and 15 controls. A greater number of lipid markers associated with anti-inflammatory response were decreased (13; p<0.05; e.g. Oleamide, CE(15:2)) than increased (7; p<0.05; e.g. PC(38:2), PC(38:1)) in FSHLow compared to D15 controls indicating a shift from anti- to proinflammatory processes. Seven lipids associated with pro-inflammatory response were increased (p<0.05) in plasma after FSHLow compared to D15 controls. These pro-inflammatory lipids are involved with cytokine signaling (LysoPC(18:3) and TGs) and TLR2 receptor function (diacylalycerols). Overall, lipid markers decreased or elevated in FF were found to have a similar profile in blood plasma suggesting that collection of either would be reflective of lipid content in the ovarian follicle or circulating blood plasma. Taken together, these results indicate that FSHLow stimulation increases pro-inflammatory lipids in FF and blood plasma over that of controls and these lipids amplify different aspects of the inflammatory process. Furthermore, these lipid markers could be utilized to better understand females with anovulation or other problems with the ovulatory process resulting in female infertility.

Abstract # 2164

Artificial Intelligence Analysis of the Mammalian Sperm Zinc Signature Predicts Male-factor Subfertility. Karl Kerns, University of Missouri, USA

Analysis of both the U.S swine and bovine herds show variation in pregnancy rate is more attributable to male-factor subfertility and infertility than the dam. To date, a limited degree of correlations is observed between conventional semen analysis parameters and actual fertility after standard quality cutoffs are met. Thus, a clear ability to predict male-factor fertility is lacking. Building on our recent discovery of the sperm zinc efflux on the pathway to fertilization competency present in boar, bull, and human spermatozoa published in Nature Communications (DOI:10.1038/s41467-018-04523-y), we hypothesized in vitro capacitation-induced changes to the sperm zinc signature would be indicative of male-factor sub- and infertility. The ongoing fertility trial currently includes 108 boar ejaculates inseminated to over 1,917 sows in a single, fixed-time artificial insemination setting, with pregnancy results ranging from 56.4% - 96.8%. Each ejaculate underwent in vitro capacitation with 10,000 spermatozoa imaged at 0, 1, and 4 hours utilizing high-throughput, image-based flow cytometry. We calculated over 6,550 bioimage values for each of the time points analyzed. Mutual information analysis found 27 sperm bioimage features with scores greater than 0.1 mutually informative to the pregnancy rate. Linear regression analysis was performed on these features and tested with a nested model. ANOVA of the linear regression model identified four features significant with high fertile males within the nested model and eight features for the full model. Next the data was randomly split (4:1) into training and testing sets and classification trees were calculated to predict the pregnancy rates after being discretized into fertile (above 85% pregnancy rates) and subfertile classes (below 80% pregnancy). One tree was trained with 17 features found in traditional semen analysis related strictly to sperm morphology and computerassisted sperm analysis (CASA) motility outputs, and a separate tree was trained with 170 features related to differences in zinc signature subpopulation changes after in vitro capacitation, significant features found by mutual information analysis, and motility. The traditional semen analysis feature set yielded respective training and testing accuracies of 100% and 53.8%, whereas the later feature set yielded respective training and testing accuracies of 100% and 76.9%. Artificial neural network analysis of zinc, acrosome, and plasma membrane integrity bioimages along with litter size are currently underway. In summary we identified the ability for sperm to transition from a zinc signature 1 and 2 to a capacitated-state signature 3 and 4 along with acrosomal modification and changes to the plasma membrane integrity excels in

predictive value of male factor fertility compared to traditional motility and morphology scores alone. Altogether, our findings establish a new paradigm on the role of zinc ions in sperm function and pave the way for accurate sperm biomarker identification of male-factor sub/infertility in future precision agriculture and medicine applications. Supported by the National Institute of Food and Agriculture (NIFA), U.S. Department of Agriculture (USDA) Postdoctoral Fellowship award number 2019-67012-29714 (KK), USDA NIFA grant number 2017-67015-26760 (PS), NIH BD2K Training Grant T32HG009060 (SK), and funding from the MU F21C Program (PS).

Best International Abstracts

Abstract # 1745

Investigating the Effects of Fipronil On Male Fertility. Jeong-Won Bae, Kyungpook National University, Republic of Korea

Fipronil (FPN) is a widely used phenylpyrazole pesticide for the control of insects and removal of veterinary pet fleas, ticks, etc. Although FPN presents moderate hazards to human health, people are readily exposed in daily life. In 2017, FPN was detected in chicken eggs in Europe and Korea. FPN acts by impairing the central nervous systems of insects by blocking gamma-aminobutyric acid (GABA) and alutamate-activated chloride (GluCI) channels. A previous study demonstrated that GABA and GABA A R are present in spermatozoa and play various roles in the process of sperm capacitation, which is required for fertilization. However, the effects of FPN on mammalian fertility are not yet fully understood. Therefore, the present study was designed to investigate the effects of FPN on spermatozoa. Herein, we treated various concentrations of FPN (0.1, 1, 10, 100, and 300 µM) or a control treatment with ICR mouse spermatozoa. Sperm motility and motion kinematics were assessed using computer-assisted sperm analysis. Capacitation status was evaluated using combined Hoechst 33258/chlortetracycline fluorescence. Intracellular ATP and LDH generation were also measured. In addition, the PKA activity, protein tyrosine phosphorylation, as well as GABA A R B-3 and GABA A R B-3 pS408/pS409 were evaluated by Western blot analysis. Finally, in vitro fertilization was performed, and the cleavage and blastocyst formation rates were determined. FPN treatment significantly reduced sperm motility and motion kinematic parameters in a dose-dependent manner, whereas the acrosome reaction was enhanced. Intracellular ATP generation was significantly decreased in all treatment groups, and LDH was similar in all treatment compared with the control. Levels of phospho-PKA substrate and phospho-tyrosine substrate were significantly decreased in a dose-dependent manner. Meanwhile, there was no difference between control and treatment groups in the level of GABA A R B-3. Only the ratio of GABA A R B-3 pS408/pS409 was significantly decreased at higher concentrations of FPN (100 and 300 μ M). Moreover, cleavage and blastocyst formation rates were also significantly decreased at 10, 100, and 300 µM FPN. Taken together, these data suggest that FPN can directly and indirectly suppress various sperm functions. Therefore, FPN can negatively affect male fertility leading to infertility. From these results, we suggest that the use of FPN as a pesticide requires robust regulation and caution. This work was supported by a

National Research Foundation of Korea (NRF) grant funded by the Korea government (Ministry of Science and ICT) (NRF- 2019R1F1A1049216).

Abstract # 1727

Cadmium Exposure Leads to Features of Polycystic Ovary in Rats. Charles Santosda Costa, Federal University of Espírito Santo, Brazil

Cadmium (Cd) is a pollutant heavy metal and Cd exposure is associated with cardiovascular and metabolic abnormalities. However, few studies have evaluated Cd's toxicologic effect on reproductive function. In this study, we assessed whether Cd exposure results in reproductive abnormalities. Cd was administered to adult female rats (100ppm in drink water for 30 days), mimicking the Cd levels found in exposed human blood, and Cd level accumulated in blood and reproductive tract were evaluated by inductively coupled plasma mass spectrometry (ICPMS). We further assessed the reproductive tract function, inflammation, oxidative stress and fibrosis. All the protocols were approved by the Ethics Committee of Animals of the Federal University of Espírito Santo. All data are reported as the mean \pm SEM. Comparisons between the aroups were performed using Student's and Mann-Whitney t-tests for Gaussian and non-Gaussian data, respectively. A value of p < 0.05 was regarded as statistically significant. Cd exposure led to increased serum, ovary and uterus Cd levels compared to control rats (784, 2018 and 8841 %, respectively, p<0.05, n=4). An irregular estrous cyclicity, with longer estrous cycle length (~76 %), high basal LH levels (~ 136%) and ovary atrophy were observed in Cd rats (p<0.05, n=5-6). A reduction in ovarian follicular reserve was observed, with low primordial and primary follicles numbers in Cd rats (36 and 39%, p<0.05, n=6). Impairment in ovarian follicular development was observed in Cd rats, with reduction in preantral, antral follicles and corpora lutea numbers (41, 48 and 39 % respectively, p<0.05, n=6). A reduction in the Cd antral follicle granulosa thickness was observed (15 %, p<0.05, n=6). Cd exposure led to uterus atrophy, reduction in the total uterine area and myometrium layer (20 and 31 %, p<0.05 and p<0.001, respectively, n=6). Cd exposure was able to increase ovary inflammation by neutrophil (MPO) and macrophage (NAG) indirect activity (45 and 22 % respectively, p<0.05, n=5). Cd uterine inflammation increased by MPO activity and mast cell number (Alcian blue staining) (10 and 128 % respectively, p<0.05, n=4). High TBARS (the thiobarbituric reactive species), DHE (superoxide anion indicator) and low GSH (reduced glutathione) levels were observed in Cd ovaries compared with control ovaries (34, 176 and 6 % respectively, p<0.05, n=5). An increase in uterine DHE levels were observed in Cd rats (207 %, p<0.05,

n=6). Ovarian and uterine fibrosis was observed in Cd rats using a Picrosirius Red staining (15 and 79 % respectively, p<0.05, n=4). Metabolic dysfunctions were observed in Cd rats, with reduction in adiposity and body weight gain (25 and 37 %, p<0.05, n=6). Interesting, an increase in the serum T4, leptin, and insulin and a reduction in the adiponectin levels were observed in Cd rats (25, 43, 37 and 10% respectively, p<0.05, n=6-7). Cd exposure impairs insulin sensitivity and glucose tolerance tests (11 and 12 % respectively, p<0.05, n=8). Thus, these data suggest that Cd exposure led to abnormal reproductive and metabolic features similar to those found in the polycystic ovary syndrome (PCOS) rat models.

Abstract # 1786

Metabolic Features of Hepatic Steatosis and Insulin Resistance Are Alleviated by Nicotinamide Mononucleotide Treatment in A DHT-Induced PCOS Mouse Model. Ali Aflatounian, University of New South Wales, Australia

Nicotinamide adenine dinucleotide (NAD+) plays a key role in energy metabolism. Recent studies have shown that NAD+ precursors, such as nicotinamide mononucleotide (NMN), can have beneficial effects on age related sub-fertility, insulin resistance and liver damage. Polycystic ovary syndrome (PCOS) is a common and complex endocrine disorder, which is defined by the presence of key characteristic reproductive and endocrine defects. PCOS patients also suffer from metabolic features including obesity, insulin resistance, liver steatosis and an increased risk of type 2 diabetes. Although insulin sensitizing agents such as metformin are commonly administered to ameliorate PCOS metabolic traits, there is uncertainty about the effectiveness of metformin in women with PCOS. Therefore, we aimed to assess the efficacy of nicotinamide mononucleotide (NMN), a precursor of NAD+, in treating features of PCOS in a dihydrotestosterone (DHT)-induced PCOS mouse model. Peripubertal female mice were implanted s.c with blank (n=14) or DHT (n=14) implants. After 12 weeks, control and PCOS mice (8/group) were treated with NMN in drinking water while the remaining mice received normal water (NW). All mice were euthanized 8 weeks after administration of NMN/NW. NMN treatment had no beneficial effect on the PCOS reproductive traits of irregular cycles and anovulation. However, oil red O absorption, a marker of liver steatosis, was significantly lower in NMN- versus NW-treated PCOS mice (PCOS+NW: 13.4±2.3; PCOS+NMN: 2.6±1.7; P<0.01). Fasting insulin levels and homeostatic model assessment of insulin resistance (HOMA-IR) were also ameliorated in PCOS+NMN mice compared to PCOS+NW mice (fasting insulin levels: PCOS+NW, 0.85±0.1 ng/mL; PCOS+NMN, 0.52±0.1 ng/mL; P<0.05. HOMA-

IR: PCOS+NW, 10.6±1.9; PCOS+NMN, 6.9±0.5; P<0.05). Furthermore, the observed DHT-induced increase in fat pad weight was not observed in inguinal or mesenteric fat pad weights of PCOS+NMN mice (inguinal fat weight: PCOS+NW, 17.1±1 mg/BW; PCOS+NMN, 12.7±1 mg/BW; P<0.001. Mesenteric fat weight: PCOS+NW, 14.1±1 mg/BW; PCOS+NMN, 11.7±1 mg/BW; P<0.041). These findings suggest that boosting NAD+ via NMN administration may represent a novel therapeutic option to target metabolic features of PCOS.

Abstract # 1788

Chlamydia Infects the Ovary Elicits an Immune Response And Depletes The Ovarian Reserve In Mice. Urooza C. Sarma, Monash University, Australia

Chlamydia trachomatis is the most common sexually transmitted infection worldwide and can cause severe damage to the Fallopian tubes, often resulting in complete infertility. Recent studies indicate significantly increased miscarriage rates and time to natural conception, along with poor IVF outcomes in women seropositive for Chlamydia but in the absence of tubal pathology, suggesting that that fertility may be compromised by mechanisms that extend beyond fallopian tube scarring. In this study, we used a well-characterised mouse model to investigate the hypothesis that Chlamydia can infect and damage the ovary. Chlamydial DNA was detected in ovaries at 6 and 35 days post infection (pi) using aPCR and inclusion bodies were localised within macrophages in the ovarian stroma using immunofluorescence. Chlamydial infection was associated with an increase in the expression of mRNA for CXCL16 and IFNy, suggesting the induction of a pro-inflammatory immune response within the ovary, which persists at least up to 35 days pi. Significantly greater numbers of immune cells including macrophages, NK cells and CD4+ /CD+ cells in the ovary 35 days pi, suggesting a localised ovarian inflammatory response to chlamydial infection, parallels this. Strikingly, the number of ovarian follicles was significantly reduced 35 days following a single infection compared to uninfected controls (p<0.05, n=4-5 mice/group) and the extent of follicle depletion was greater following a second infection (p<0.05, n=4-5 mice/group). Two infections was also associated with changes to the overall ovarian morphology and increased apoptosis and fibrosis in the ovary (p<0.05, n=5/group), consistent with activation of a prolonged inflammatory response. Collectively, these observations demonstrate that Chlamydia can penetrate the ovary, deplete the ovarian reserve and compromise ovarian function, and suggest that the ovary may act as a potential reservoir of infection. Ovarian follicles are essential for female fertility because they secrete hormones and contain oocytes. Follicles cannot be

replaced once lost from the ovary. Thus, our data suggests that damage to the ovary caused by Chlamydia is permanent and may underlie some cases of unexplained infertility and poor IVF outcome in women.

Abstract # 1789

The PARP Inhibitor, Olaparib, Blocks Intrinsic DNA Repair in Oocytes and Depletes The Ovarian Reserve In Mice: Implications For Fertility. Amy Winship, Monash University, Australia

Chlamydia trachomatis is the most common sexually transmitted infection worldwide and can cause severe damage to the Fallopian tubes, often resulting in complete infertility. Recent studies indicate significantly increased miscarriage rates and time to natural conception, along with poor IVF outcomes in women seropositive for Chlamydia but in the absence of tubal pathology, suggesting that that fertility may be compromised by mechanisms that extend beyond fallopian tube scarring. In this study, we used a well-characterised mouse model to investigate the hypothesis that Chlamydia can infect and damage the ovary. Chlamydial DNA was detected in ovaries at 6 and 35 days post infection (pi) using qPCR and inclusion bodies were localised within macrophages in the ovarian stroma using immunofluorescence. Chlamydial infection was associated with an increase in the expression of mRNA for CXCL16 and IFNy, suggesting the induction of a pro-inflammatory immune response within the ovary, which persists at least up to 35 days pi. Significantly greater numbers of immune cells including macrophages, NK cells and CD4+ /CD+ cells in the ovary 35 days pi, suggesting a localised ovarian inflammatory response to chlamydial infection, parallels this. Strikingly, the number of ovarian follicles was significantly reduced 35 days following a single infection compared to uninfected controls (p<0.05, n=4-5 mice/group) and the extent of follicle depletion was greater following a second infection (p<0.05, n=4-5 mice/group). Two infections was also associated with changes to the overall ovarian morphology and increased apoptosis and fibrosis in the ovary (p<0.05, n=5/group), consistent with activation of a prolonged inflammatory response. Collectively, these observations demonstrate that Chlamydia can penetrate the ovary, deplete the ovarian reserve and compromise ovarian function, and suggest that the ovary may act as a potential reservoir of infection. Ovarian follicles are essential for female fertility because they secrete hormones and contain oocytes. Follicles cannot be replaced once lost from the ovary. Thus, our data suggests that damage to the ovary caused by Chlamydia is permanent and may underlie some cases of unexplained infertility and poor IVF outcome in women.

Abstract # 1805

Paternal Diet Alters Pre-Implantation Embryo Development and Metabolism in Mice. Hannah L. Morgan, University of Nottingham, United Kingdom

Poor parental nutrition during pre-conception periods has been shown to impact embryonic development, fetal growth and alter disease risk of the offspring. The influence of paternal well-being on fetal development and offspring health is beginning to gain more research focus, and emerging evidence has linked sub-optimal paternal diet at the time of conception to poorer offspring outcome. However, the mechanisms that define this development trajectory are still not fully understood. This study aimed to determine how paternal diet (over- and under-nutrition) impacts early blastocyst formation and whether dietary vitamin and mineral supplementation can negate any detrimental effects. Male C57/BL6 mice were fed one of five diets; low protein diet (LPD (9% casein, 24% sugar, 10% fat)), western diet (WD (19% casein, 21% fat, 34% sugar)), diets supplemented with methyl-donors (MD-LPD) and MD-WD) or an isocaloric control diet (18% casein, 10% fat, 21% sugar) for at least 8 weeks (n=8/group). Chow fed female C57/BL6 mice (n=4-5) were mated with these males and on embryonic day 1.5, embryos were flushed from the oviduct and cultured individually (n=17-36) in EmbryoMax® KSOM media at 37°C, 5% CO2, using Embryoscope time-lapse imaging. To define the connection between paternal diet and pre-implantation development, stud male testis gene expression was examined via microarray (n=8 males per group). Paternal diet did not alter fundamental fertility, as indicated by no significant difference in the number of embryos flushed per female. Embryos from the LPD, WD, MD-LPD and MD-WD fathers displayed advanced rates of preimplantation development when compared to embryos derived from control males. WD embryos had a significantly shortened cell cycle length at the 4-cell stage (11±0.1 vs 12±0.3 hours; p<0.05), when compared to control embryos. However, there was no differences in cleavage synchronicity or in the percentage of embryos achieving successful blastulation between treatment aroups. MD-WD embryos demonstrated a significantly reduced time to the start of blastulation (42±0.7 vs 47±1.1 hours; p<0.01) and, the length of blastulation was significantly increased in embryos from WD males compared to LPD (15±0.6 vs 11±0.9; p<0.05). Male testis transcriptome data identified that WD, MD-LPD and MD-WD had a significant downregulation of biological process such as the cell cycle; with changes in cyclin-dependant kinase (Cdk6), transcription factor (E2f2) and retinoblastoma-like protein (Rbl2) gene expression, and embryonic development; which included changes to homeobox protein (Hoxb4, Hoxb7

and Hoxb13) gene expression (FDR<0.05) These findings suggest that paternal sub-optimal diet alters the trajectories of embryo development at these early stages, and this could negatively impact fetal development later in gestation. Furthermore, we have provided evidence these embryo development changes could be influenced by a dysregulation of key developmental genes originating in the testis.

Abstract # 1973

Inflammation Contributes to Follicle Depletion During Maternal Ageing in Mice. Carolina Lliberos, Monash University, Australia

Female reproductive ageing is characterised by a progressive decline in oocyte number and quality, leading to the loss of ovarian function, cycle irregularity, infertility and eventually menopause. The mechanisms that underlie the natural depletion of follicles throughout reproductive life are poorly characterised. In this study, we investigated the hypothesis that inflammation contributes to the loss of follicles as females age. We first determined follicle numbers and characterised the systemic and local ovarian inflammatory phenotype in C57/BI6 mice at 2, 6, 12 and 18-months of age. This period of time spans the onset of sexual maturity to the end of female fertility in mice. We observed that the decrease in follicle numbers over the reproductive lifespan was associated with an increase in the serum concentration and intra-ovarian mRNA and protein levels of proinflammatory cytokines IL-1a/β, TNF-a, IL-6, IL-18, and inflammasome proteins ASC and NLRP3. To gain further insight into the possible role of the NLRP3 inflammasome in follicle depletion, we compared follicle numbers in wild type (WT), nlrp3 -/- and asc -/- mice (n=3-6/genotype). We found that the primordial follicle reserves were elevated in aged asc -/- and nlrp3 -/- mice relative to agematched WT mice (WT= 191±62 vs asc -/- = 1122±493, p =0.0130; vs nlrp3 -/- = 700 ± 220 , p =0.0195). The number of primary and growing follicles, as well as corpora lutea, were also significantly higher in inflammasome-deficient mice. Consistent with follicle data, serum AMH levels were significantly increased in 12month-old asc -/- compared to WT mice (WT= 9.27±1.04 vs asc -/- = 16.08±1.33, p =0.0022). Notably, expression levels of major pro-inflammatory cytokines within the ovary (e.g. Tnfa, II1a and II1b) were significantly lower in aged asc -/- mice compared to WT (Tnfa : WT= 2.02 ± 0.14 vs asc -/- = 0.87 ± 0.23 , p = 0.0087). A significant decrease was also observed in the serum levels of several inflammatory cytokines in asc -/- mice relative to age-matched WT mice (TNF-a: WT= 10.96 \pm 5.02 vs asc -/- = 0.47 \pm 0.47, p =0.0281). These data suggest that inflammation contributes to the age-associated depletion of follicles and raises

the possibility that ovarian ageing could be delayed, and fertility prolonged, by suppressing inflammatory processes in the ovary.

Abstract # 2004

Contraceptive Use and Preference of HIV Infected Pregnant Women Living with HIV Negative Partners in The Central Region Of Cameroon: A Cross Sectional Survey. Martin Kuete, Anhui Biochem United Pharmaceutical Research Institute, Cameroon

Evidences in sub-Saharan Africa including Cameroon indicate that most of HIV discordant couples want more children despite their HIV status. Investigating and establishing contraception preferences among HIV infected individuals are fundamental and crucial to provide effective reproductive healthcare. We performed a cross-sectional study using structural based questionnaire to explore HIV positive pregnant women patterns including their family planning services, their preferences and its use, and their knowledge related to HIV/AIDS. Bivariate and multivariate analyses were conducted to explore associations and predictors of contraception preference and use; all tests were two sided significant at P < 0.05. Overall, 94 HIV-positive pregnant women aged 30.70±5.50 years living with HIV negative partners were from the different areas of the central region of Cameroon. Three-fourths were aware of the effectiveness of modern contraceptives and condoms, and only 28% had experienced modern contraception. 98% preferred to use traditional methods associated with infrequent condoms use. Multiple sociodemographic factors (marital status, group age, educational level, religion, occupation) affected contraceptive method preferences and its use (P < 0.05). These factors are the landmarks to predict discordant couples' behavior in HIV disclosure, discussion and decision making for contraception, preventing mother to-child transmission and HIV negative partner infection (P<0.05). Despite the awareness of participants related both on contraception methods and HIV/AIDS matters, participants faced societal, cultural and demographic barriers to make own decision for contraception use. Promoting effective family planning services and giving the entire range of contraception options may help women living with HIV to choose for effective ones and consequently reduce new cases of HIV infection.

Abstract # 2030

Reproductive Health and Family Planning Services Use Among Married Women in Central China: Does "One Child to Two Child Policy" Relaxation Affect The Population Behavior? Martin Kuete, Anhui Biochem United Pharmaceutical Research Institute, Cameroon

Family planning services use dramatically lowers maternal mortality and disabilities, infant mortality risk, unwanted pregnancies, birth defects, both illegal and unsafe abortions, mother-to-child transmission of human immunodeficiency virus and overall improve women and men sexual and reproductive health. Recently, the Chinese government has launched the two-child policy allowing families to have additional child. The aim of this study was to explore the population interest for family planning services, the unmet needs of reproductive health services and the populations' expectations towards male contraceptive methods. Cross-sectional study using stratified random sampling was conducted in 102 counties of Hubei province of China between august 2014 and July 2016. 17,555 randomized subjects interviewed from rural, transitional, and urban areas were included in the data analysis. Univariate and bivariate statistical analyses were applied to fit the associations between a set of sociodemographic patterns, family planning related factors and contraceptives use. In all tests, a P-value below 0.05 was considered significant. The studied population was disproportionally dominated by Han ethnic individuals (96%). Although 54% resided in rural area, 34% in urban area, and 12% in urban area; participants were enrolled in a range of prosperous activities found across the surveyed settings. The number of living children per family varied from 0-6 children. Although 81% of population recognized family planning as a shared responsibility, the contraceptive method rates excluding condom were intrauterine devices (IUDs) 76%, 16% tubal ligation, 8% vasectomy, pills 3%, vaginal ring 2%, withdrawal and female awareness based method 1%. 24% had a history of contraceptive failure and the rate of effective contraceptive used after prior failure remained lower 6% (tubal ligation and vasectomy) and 26% IUDs. Among 13% who had never practiced any form of contraceptive, 74% clearly rejected family planning services especially male contraception. Overall, age, gender, education, vulnerable living status, knowledge in family planing services, discussion and making decision with spouse, and gender discrepancies were strongly associated with family planning services use and reproductive health unmet needs (P < 0.001). The decline of contraceptive use roughly varied with sociodemographic and reproductive health features. While the family size is increasing among China's population, family planning services especially vasectomy practice rate is decreasing. More investments taking in

account population's expectations are needed to support exiting strategies for the new family planning policy and reproductive health matters in China.

Abstract # 2076

Does Maternal High Fat Diet Alter the Ovarian Reserve In Female Mouse Offspring? Meaghan J. Griffiths, Monash University, Australia

Background: Obesity contributes to adverse pregnancy events. Obese pregnant women have increased rates of early pregnancy loss and congenital abnormalities. Moreover, a high fat diet prior to conception in mice contributes to fetal growth abnormalities and developmental delay. Such abnormalities may arise from oocyte defects, including epigenetic reprogramming alterations, oxidative stress and meiotic abnormalities. Existing literature suggests a decrease in the finite ovarian reserve of primordial follicles in adult mice exposed to a high fat diet (HFD). In this study, we aimed to determine if combined maternal (preconception), gestational and lactational exposure to a HFD altered follicle number in offspring.

Materials and Methods: C57BL/6 dams were fed ad libitum a normal fat diet (NFD; 6% fat, SF04-057, Specialty Feeds, WA, Australia) or high fat diet (HFD; 22% fat, SF00-219, Specialty Feeds, WA, Australia) for 6 weeks prior to mating, gestation and lactation. Pups were maintained on the mother's diet until weaning at post-natal day (PN)21, at which time they were either culled (n=6-8 animals/group) or placed on normal chow and subsequently culled at 4 (n=4 animals/group) or 6 weeks of age (n=3 animals/group). One ovary per mouse per litter was utilised for follicle counts using design-based stereology. Growing follicles and corpora lutea were assessed by light microscopy. In the contralateral ovary, histological markers of DNA damage (yH2AX), follicular atresia (TUNEL) and oocyte quality (Stella) were assessed (n=3-4/group). Data are mean ± standard error of the mean. Statistical analysis was performed using unpaired t-test or one-way ANOVA, with significance considered p<0.05.

Results: At PN21, exposure to HFD throughout development and weaning yielded no significant differences in primordial (NFD 1968±31, HFD 1241±743), primary (NFD 691±134, HFD 594±303) or growing follicle (NFD 633±38, HFD 525±72) numbers. At 6 weeks of age, primordial (NFD 1516±308, HFD 1339±311), primary (NFD 975±127, HFD 647±139) and growing follicle (NFD 222±34, HFD 177±21) numbers remained similar in the two groups. HFD exposure led to an increased proportion of TUNEL-positive dying follicles (NFD 7.5±0.9%, HFD 27±10%, p=0.06) at PN21. At 6 weeks of age, there were no differences in follicle death between

groups (NFD 32±11%, HFD 25±5%). Localisation patterns of DNA double strand breaks (yH2AX) and Stella were similar between all diet and age groups. Conclusions: Preliminary data suggest exposure to a high fat diet throughout development until weaning yields no effect on follicle numbers, but follicular atresia may be increased. Previous studies demonstrate a decrease in ovarian reserve in offspring aged 15 weeks, exposed to high fat diet throughout development. Therefore, the age groups assessed in the current study may be too early to observe any follicle number differences. Further analysis will determine if these HFD-exposed offspring are able to enter puberty as normal by assessing corpora lutea number at 4 weeks of age.

Abstract # 2088

Cystic Ovary Disease Impacts Gamete/Embryo Transport and Its Cholinergic Regulation. Deirdre Scully, Trinity College Dublin, Ireland

Cystic ovary disease (COD) is a common cause of subfertility in humans and animals. The effect of COD on the function of the oviduct – especially on the transport of the oocyte and the early embyo – is largely unknown. Therefore, the aim of this study was to investigate transport function and the influence of the cholinergic system in oviducts affected by COD. Oviducts were excised from cows affected by COD (n=29) as well as from healthy cows in mid diestrus (n=20) immediately after slaughter. A unique digital live cell imaging (LCI) system established in our lab was used to capture real time videos of ciliary beat and particle transport speed under near in vivo conditions. For ciliary beat frequency (CBF), the differences in grayscale of beating cilia were transformed into frequencies using ImageJ® and AutoSignal®. For particle transport speed (PTS), polystyrene beads were added to the buffer media and were automatically tracked using ImagePro®. Additionally, smooth muscle contraction and epithelial ion transport were investigated using organ baths and Ussing chambers. Our results showed that PTS was significantly decreased in oviducts from cows affected by COD as compared to controls (p=0.01, Unpaired Student t-test). Further to that, in healthy control cows, PTS was consistently increased in the oviduct ipsilateral to ovulation as compared to the contralateral oviduct (p=0.03, Paired Student t-test). This was not the case in cows affected by COD (p=0.47, Paired Student t-test). Reduced PTS in oviducts from cows with COD was not due to changes in CBF. Although smooth muscle contraction was similar in oviducts from healthy and COD cows, the contractile response (mN) to the cholinomimetic drug carbachol (10-7–10-4 M) was significantly reduced in COD as compared to the controls (p<0.0001, non-linear regression "best fit" analysis).

Carbachol-induced active ion transport in the oviductal epithelium of COD cows, which was measured by the change in short circuit current (μ A/cm2), was significantly decreased as compared to controls (p=0.03, Unpaired t test of area under the curve (AUC)). These results suggest, for the first time, that oviductal transport is compromised in COD. Decreased cholinergic regulation of tubal contractions and fluid formation could have detrimental consequences for the transport and nutrition of the gametes and the early embryo in the oviduct. This knowledge is pivotal to establish novel therapeutic concepts for successful treatment of infertility in individuals affected by COD.